# U.PORTO

**FEUP FACULDADE DE ENGENHARIA**
UNIVERSIDADE DO PORTO

# Treatment Train for Mature Urban Landfill Leachate

*Thesis submitted in partial fulfilment of the requirements for the degree of*
*Doctor in Philosophy in Chemical and Biological Engineering*
*at the Faculty of Engineering, University of Porto*

## Ana Isabel de Emílio Gomes

Supervisor:                Vítor Jorge Pais Vilar, Ph.D.
Co-Supervisors:     Rui Alfredo da Rocha Boaventura, Ph.D.
                        Tânia Filomena Castro Valente Silva, Ph.D.

Laboratory of Separation and Reaction Engineering – Laboratory of Catalysis and Materials
Department of Chemical Engineering
University of Porto
July, 2020

# Acknowledgments

*With love to my son*

# Abstract

Grounded on the knowledge acquired in previous research, one of the main goals of this thesis was to investigate a treatment train for mature urban leachates able to achieve a final effluent in compliance with the limits for direct discharge into the environment, particularly for organic and nitrogen compounds. Special attention was also given to the cost-competitiveness of the explored technologies, especially of the advanced oxidation process (AOP), which is the most expensive.

First, the experimental work started at lab-scale to optimize a multistage strategy (European Patent – EP 2784031A1) that proved to be efficient for total ammonia nitrogen (TAN) and chemical oxidation demand (COD) removal up to discharge limits (according to the Portuguese legislation), but not for total nitrogen (TN). Thus, the tested optimized treatment train comprised a: (i) sequential batch reactor (SBR); (ii) coagulation/sedimentation (C/S); (iii) photo-Fenton (PF) oxidation ($Fe^{2+}/H_2O_2/UV$-Vis); and (iv) final biological oxidation. The optimized treatment train was applied to a mature urban leachate presenting high COD and TN content (3.6 g $O_2$/L and 2.0 g N/L) and low biodegradability ($BOD_5$/COD = 0.05). Legal compliance was successfully attained for COD (< 150 mg $O_2$/L), TAN (< 8 mg N/L) and TN (< 15 mg N/L), and also for total suspended solids (TSS: < 60 mg/L) and sulfate ions ($SO_4^{2-}$: < 2000 mg/L), under the operating conditions: (i) SBR operated in a 24h-cycle mode (15h aeration, ~ 0.5 mg $O_2$/L, + 8.5h anoxic, with methanol addition at COD/N mass ratio of 2.5, + 0.5h settling), with volume exchange ratios of 14.3%, 16.4% and 21.4%, for temperatures of 20, 25 and 30 ºC, respectively, to reach a final TN < 15 mg N/L and alkalinity values ~ 1.1 g $CaCO_3$/L; (ii) coagulation using $FeCl_3$ (240 mg $Fe^{3+}$/L), at pH = 3.0, to precipitate humic substances (dissolved organic carbon (DOC) decrease > 60%) and remove suspended and colloidal matter (residual turbidity ≈ 33 NTU); (iii) PF stage working at 60 mg $Fe^{2+}$/L and pH 2.8-3.0, until COD ~ 400 mg/L; (iv) final biological oxidation operated in continuous mode, with an hydraulic retention time (HRT) of 12h, to reach COD and TSS values below the legal limits.

Then, to test the flexibility of the strategy against the high variability of the leachate, the optimized treatment train was applied at full-scale for nearly one year. Located at a municipal waste landfill (nearby Porto), the facility comprised the following treatment units: (i) a first biological reactor (BR1); (ii) a coagulation and photo-treatment unit (C/P); (iii) a second biological reactor (BR2); (iv) a sludge tank (ST); (v) a filter-press system (FP); and (vi) a drainage tank. Each treatment sequence was applied to ca. 30 $m^3$ of urban leachate from an aerated lagoon, leading to global removal efficiencies of 98% for COD (from 8.30 to 0.15 g $O_2$/L), 97% for DOC (from 2.32 to 0.08 g C/L) and 85% for TN (from 2.65 to 0.41 g N/L). The sludge produced was also treated *in-situ* and complied with the legal disposal standards. Despite the efforts, achieving legal compliance for direct discharge was not accomplished for all parameters. The balance between COD and TN removal, as

well as $SO_4^{2-}$ content is a key element for the success of this strategy. To reduce the operating costs of the treatment train (i) glycerol, a by-product from biodiesel production, was used as a cost-effective external carbon source to promote biological denitrification, and (ii) an innovative artificial photoreactor (4 FluHelik reactors connected in series) was employed in the C/P unit to promote the PF oxidation reaction. Glycerol was applied in BR1 and BR2, proving its effectiveness for denitrification purposes. When compared with previous studies, where similar UV-Vis lamps were merely located inside the treatment tank, to achieve the same DOC goal, the usage of FluHelik required 2 times less radiation energy. The average total operational cost for the complete treatment sequence was 6.7 €/m$^3$, which included chemicals, energy consumption, sludge treatment and respective disposal.

The photo-Fenton process is considered the most promising of the AOPs to be driven by sunlight, due to the fact that the photoreduction of ferric species can be driven with light up to 580 nm, allowing a more efficient use of sunlight. So, as a complement to artificial light, the use of solar radiation can contribute to a decrease of operational costs (particularly, for electric power consumption). In this sense, recognizing the drawbacks that are blocking the application of solar PF at industrial scale (high investment cost, land area requirements and deterioration of the reflective surfaces with loss of photo-efficiency over time), together with the low transmissibility of leachates, solar collectors with different reflector materials - anodized aluminium with (MS) and without (R85) protective coating, soiled aluminium (R85s) and stainless steel (SS) - and geometries - flat (F), simple double parabola (SP) and traditional double parabola (DP) - were tested and their efficiency assessed (first by actinometric measurements with ferrioxalate, and later by carrying out photo-Fenton oxidation of a bio-coagulated leachate). According to the actinometry results, at lab-scale under simulated sunlight, the optical concentration ratio ($CR_O$) was determined and followed the sequence: SS-F (0.59) ≈ R85-F (0.60) < R85s-DP (0.67) ≈ SS-SP (0.70) ≈ SS-DP (0.72) < MS-DP (0.84) < R85-DP (0.93). These results agree with the ray-trace and specular reflectance analysis. The PF process efficiency was coherent with the optical efficiency of the different reflective surfaces, and the time required to achieve 60% of mineralization decreased as follows: SS-F (158') > R85-F and R85s-DP (153') > SS-SP (141') > SS-DP (127') > R85-DP (121') > MS-DP (117'). According to the cost analysis, for the same investment required to build 100 m$^2$ of an R85-DP collector, it is possible to construct 126 m$^2$ of an SS-F collector, containing 1.6 times more absorber tubes per square meter, which leads to a treatment rate increment of 51%. Moreover, the impact of 8-year of outdoor aging on the R85 aluminium reflectors was clearly shown. The reflectors performance was also validated at pilot-scale, under natural sunlight.

Finally, for the PF stage, the following disadvantages and challenges were found (i) the required acidic conditions impose restrictions to alkalinity recovery in the upstream biological denitrification

process (to ensure compliance with $SO_4^{2-}$ legal limit); (ii) on the other hand, as only partial nitritification occurs (oxidation of ammonia to nitrite), denitrification at full extent of the bio-treated effluent is desirable, as it reflects on the oxidation efficiency and oxidant-savings during the initial part of the PF stage (to oxidize nitrites to nitrates), and (iii) the production of iron sludge that proved to be difficult to settle, requiring long settling times. Therefore, the application of ozone-driven processes, normally requiring a neutral-alkaline pH and without sludge production, as an alternative AOP stage for the treatment strategy was evaluated.

First, using a bio-coagulated leachate, the best operating conditions (initial pH = 9.0 and inlet ozone dose = 18 mg $O_3$/min) were established and various system setups (bubble column (BC) reactor alone or coupled with FluHelik) and process combinations ($O_3/H_2O_2$, $O_3$/UVC and $O_3$/UVC/$H_2O_2$) were tested. The setup comprised by the FluHelik coupled with BC using a Venturi injector, led to the highest treatment efficiency, treating 50% more leachate than BC-alone using the same ozone dose and reaction time (3h). Moreover, the FluHelik/BC-Venturi was clearly the configuration that enhanced the ozone mass transfer from the gas to the liquid phase, resulting in lower amounts of $O_3$ in the off-gas, reducing the operational costs by 41% when compared to the BC-alone. The $O_3$/UVC process was the best among the $O_3$-based AOPs tested, while the addition of $H_2O_2$ was not beneficial in terms of biodegradability enhancement (especially for $O_3/H_2O_2$). Considering these results, different bio-treated (nitrified (LN) or denitrified (LD)) and bio-coagulated leachates (with iron salts and acidic conditions (LNC), and with aluminium salts without pH adjustment (LDC)) were further tested for $O_3$ and $O_3$/UVC processes. So, in view of simultaneous legal compliance for organic and nitrogen compounds, 6 possible treatment train strategies were evaluated: (1) LN + $O_3$/UVC + bio-denitrification; (2) LD + $O_3$/UVC + bio-oxidation; (3;4) LN + iron-acidic coagulation + $O_3$ or $O_3$/UVC + bio-denitrification; and (5;6) LD + aluminium-neutral coagulation + $O_3$ or $O_3$/UVC + bio-oxidation. The estimated treatment cost for a sequence combining Bio + $O_3$/UVC + Bio is not economically viable (> 30 €/m$^3$). So, the inclusion of C/S stage before the $O_3$-driven oxidation shows to be essential for the economic feasibility of the treatment train. For the different scenarios, the treatment strategy comprising: (i) a first biological stage for nitrification/denitrification (with methanol addition as an external carbon source); (ii) coagulation with 300 mg $Al^{3+}$/L and without pH adjustment; (iii) $O_3$/UVC process, with transferred ozone dose of 2.1 g $O_3$/L and 12.2 kJ$_{UVC}$/L; and (iv) a final biological oxidation, allowed to reach a final effluent able to simultaneously comply with the legal values for organic and nitrogen parameters, and not exceeding the discharge limits for other parameters affected by the addition of chemicals along the treatment train (namely, aluminium, total iron and sulfate ions). Also, the treatment cost of this strategy was estimated as 8.9 €/m$^3$, with the ozone-driven stage counting for 6.9 €/m$^3$, which is reasonable considering the costs for the current technologies in use.

# Resumo

Com base no conhecimento adquirido em trabalhos de investigação anteriores, um dos principais objetivos desta tese foi investigar uma estratégia de tratamento para lixiviados maduros de aterros urbanos, capaz de atingir um efluente final em conformidade com os limites de descarga direta no meio ambiente, particularmente em termos de compostos orgânicos e azotados. Também foi dada atenção à competitividade em termos de custo das tecnologias exploradas, principalmente para o processo de oxidação avançada (POA), que é o mais caro.

O trabalho experimental foi iniciado em escala de laboratório, a fim de otimizar uma estratégia de múltiplos estágios (patente europeia - EP 2784031A1) eficiente na remoção do azoto amoniacal total e da carência química de oxigénio (CQO) até os limites de descarga (de acordo com a legislação Portuguesa), mas não para o azoto total. Assim, foi testada a seguinte estratégia de tratamento: (i) reator sequencial de batelada (SBR); (ii) coagulação/sedimentação (C/S); (iii) oxidação por foto-Fenton (FF) ($Fe^{2+}$/$H_2O_2$/UV-Vis); e (iv) oxidação biológica final. O tratamento otimizado foi aplicado a um lixiviado urbano maduro, com alto conteúdo de CQO e azoto amoniacal (3,6 g de $O_2$/L e 2,0 g de N/L) e baixa biodegradabilidade ($CBO_5$/CQO = 0,05). A conformidade legal foi alcançada para CQO (< 150 mg $O_2$/L), azoto amoniacal (< 8 mg N/L) e azoto total (< 15 mg N/L), e também para sólidos suspensos totais (SST: < 60 mg / L ) e sulfatos ($SO_4^{2-}$: < 2000 mg/L), nas seguintes condições de operação: (i) SBR operado em ciclos de 24 horas (15h de arejamento, ~ 0,5 mg de $O_2$/L, + 8,5h anóxico, com adição de metanol numa razão mássica CQO/N de 2,5 + 0,5h de sedimentação), e com taxas de troca de volume de 14,3%, 16,4% e 21,4%, para temperaturas de 20, 25 e 30 ºC, respetivamente, para atingir um azoto total final < 15 mg N/L e valores de alcalinidade ~ 1,1 g $CaCO_3$/L; (ii) coagulação com $FeCl_3$ (240 mg $Fe^{3+}$/L), a pH = 3,0, para precipitar substâncias húmicas (diminuição de carbono orgânico dissolvido (COD) > 60%) e remover a matéria suspensa e coloidal (turbidez residual ≈ 33 NTU); (iii) etapa de FF com 60 mg $Fe^{2+}$/L e pH 2,8-3,0, até CQO ~ 400 mg/L; (iv) oxidação biológica final operada em modo contínuo, com um tempo de retenção hidráulica (TRH) de 12 h, para atingir valores de CQO e SST abaixo dos limites legais.

Em seguida, para testar a flexibilidade da estratégia relativamente à elevada variabilidade do lixiviado, a estratégia de tratamento otimizada foi aplicada em larga escala durante cerca de um ano. Localizada num aterro sanitário municipal (nas proximidades da cidade do Porto), a instalação compreendia as seguintes unidades de tratamento: (i) um primeiro reator biológico (RB1); (ii) uma unidade de coagulação e foto-tratamento (C/P); (iii) um segundo reator biológico (RB2); (iv) um tanque de lamas (TL); (v) um sistema de filtro prensa (FP); e (vi) um tanque de drenagem. Cada sequência de tratamento foi aplicada a ca. 30 $m^3$ de lixiviado urbano de uma lagoa arejada, com

eficiências globais de remoção de 98% para CQO (de 8,30 a 0,15 g $O_2$/L), 97% para COD (de 2,32 a 0,08 g C/L) e 85% para azoto total (de 2,65 a 0,41 g N/L). A lama produzida também foi tratada *in situ* e cumpriu com os valores legais para deposição. Apesar dos esforços, o cumprimento legal da descarga direta para todos os parâmetros não foi alcançado. O equilíbrio entre a remoção de CQO e azoto total, bem como o conteúdo de $SO_4^{2-}$ é um elemento essencial para o sucesso desta estratégia. Para reduzir os custos operacionais (i) o glicerol, um subproduto da produção de biodiesel, foi usado como fonte externa de carbono para promover a desnitrificação biológica e (ii) um foto-reator artificial inovador (4 reactores FluHelik em série) foi utilizado na unidade C/P para promover a reação de foto-oxidação. O glicerol foi aplicado no RB1 e RB2, comprovando sua eficácia para fins de desnitrificação. Quando comparado com estudos anteriores, onde lâmpadas UV-Vis semelhantes estavam apenas localizadas dentro do tanque de tratamento, para atingir a mesma meta de COD foi necessária 2 vezes menos energia de radiação utilizando o FluHelik. O custo operacional total médio para a sequência completa de tratamento foi de 6,7 €/m$^3$, incluindo produtos químicos, consumo de energia, tratamento de lamas e respetivo descarte.

O processo foto-Fenton é considerado o POA mais promissor a ser conduzido pela luz solar, uma vez que a foto-redução de espécies férricas pode ser conduzida com radiação até 580 nm, o que permite um uso mais eficiente da luz solar. Assim, enquanto complemento à luz artificial, o uso da radiação solar pode contribuir para uma diminuição dos custos operacionais (principalmente no consumo de energia elétrica). Nesse sentido, reconhecendo as desvantagens que estão a impedir a aplicação de FF solar em escala industrial (elevados custo de investimento e de área de implementação, deterioração das superfícies refletoras e consequente perda de foto-eficiência ao longo do tempo), juntamente com a baixa transmissibilidade de lixiviados, foram testados coletores solares com diferentes materiais refletores - alumínio anodizado com (MS) e sem revestimento protetor (R85), alumínio degradado (R85s) e aço inoxidável (SS) - e geometrias - planas (F), parábola dupla simples (SP) e dupla tradicional parábola (DP). A eficiência dos coletores foi avaliada primeiro através de medições actinométricas com ferrioxalato e, posteriormente, pela oxidação por foto-Fenton de um lixiviado bio-coagulado. De acordo com os resultados da actinometria, em escala laboratorial e sob luz solar simulada, a razão de concentração ótica ($CR_O$) foi determinada: SS-F (0,59) ≈ R85-F (0,60) < R85s-DP (0,67) ≈ SS -SP (0,70) ≈ SS-DP (0,72) < MS-DP (0,84) < R85-DP (0,93). Estes resultados foram concordantes com a análise de traçados de raios e refletância especular. A eficiência do processo FF foi coerente com a eficiência ótica das diferentes superfícies refletoras e o tempo necessário para atingir 60% de mineralização diminuiu da seguinte forma: SS-F (158') > R85-F e R85s-DP (153') > SS-SP (141') > SS-DP (127') > R85-DP (121') > MS-DP (117'). De acordo com a análise de custo, tendo o mesmo investimento necessário para construir 100 m$^2$ de um coletor R85-DP, é possível construir 126 m$^2$ de um coletor

SS-F, contendo 1,6 vezes mais tubos absorvedores por metro quadrado, o que incrementa a taxa de tratamento em 51%. Além disso, o impacto de 8 anos de exposição ao ar livre nos refletores de alumínio R85 foi claramente demonstrado. O desempenho dos refletores também foi validado em escala piloto, sob luz solar natural.

Finalmente, para a etapa de FF, foram encontradas as seguintes desvantagens e desafios: (i) as condições ácidas exigidas impõem restrições à recuperação da alcalinidade no processo de desnitrificação biológica a montante (para garantir a conformidade com o limite legal de $SO_4^{2-}$); (ii) por outro lado, como ocorre apenas nitrificação parcial (oxidação de amónia a nitrito), é desejável a total remoção do azoto no efluente biotratado, pois terá reflexos na eficiência da oxidação e na poupança do oxidante durante a parte inicial da etapa de FF (para oxidar nitritos em nitratos) e (iii) a produção de lamas de ferro que se mostrou difícil de sedimentar, exigindo longos tempos de sedimentação. Assim, normalmente exigindo pH alcalino-neutro e sem produção de lamas, foi avaliada a aplicação de processos de ozonização como etapa alternativa de POA na estratégia de tratamento.

Primeiro, usando um lixiviado bio-coagulado, foram estabelecidas as melhores condições operacionais (pH inicial = 9,0 e dose de ozono alimentada = 18 mg $O_3$/min) e testadas várias configurações do sistema (reator de coluna de bolhas (BC) sozinho ou acoplado ao FluHelik) e combinações de processos ($O_3/H_2O_2$, $O_3/UVC$ and $O_3/UVC/H_2O_2$). A configuração do FluHelik acoplada ao BC usando um injetor de Venturi, obteve a maior eficiência do tratamento, tratando 50% mais lixiviado do que usando apenas o BC, para a mesma dose de ozono e tempo de reação (3h). Além disso, o FluHelik/BC-Venturi foi claramente a configuração que promoveu a transferência de massa de ozono da fase gasosa para a líquida, resultando em menores quantidades de $O_3$ no efluente gasoso, reduzindo os custos operacionais em 41% quando comparado com a utilização apenas do BC. O processo $O_3/UVC$ foi o melhor entre os testados, enquanto a adição de $H_2O_2$ não foi benéfica em termos de melhoria da biodegradabilidade (especialmente para $O_3/H_2O_2$). Considerando estes resultados, diferentes lixiviados bio-tratados (nitrificado (LN) ou desnitrificado (LD)) e bio-coagulados (com sais de ferro e em condições ácidas (LNC) e com sais de alumínio sem ajuste de pH (LDC)) foram posteriormente testados para tratamento por $O_3$ e $O_3/UVC$. Assim, tendo em vista a conformidade legal para compostos orgânicos e de azoto, foram avaliadas 6 possíveis estratégias tratamento: (1) LN + $O_3/UVC$ + bio-desnitrificação; (2) LD + $O_3/UVC$ + bio-oxidação; (3; 4) LN + coagulação ácido-ferro + $O_3$ ou $O_3/UVC$ + bio-desnitrificação; e (5; 6) LD + coagulação neutra em alumínio + $O_3$ ou $O_3/UVC$ + bio-oxidação. O custo estimado para as sequências que combinam Bio + $O_3/UVC$ + Bio não são economicamente viáveis (> 30 €/m³). Portanto, a inclusão do estágio C/S antes da etapa de oxidação por ozono mostra-se essencial para a viabilidade económica do tratamento. A estratégia de tratamento que compreende: (i) um primeiro

estágio biológico para nitrificação/desnitrificação (com adição de metanol como fonte externa de carbono); (ii) coagulação com 300 mg de $Al^{3+}$/L e sem ajuste de pH; (iii) processo $O_3$/UVC, com dose de ozono transferida de 2,1 g $O_3$/L e 12,2 $kJ_{UVC}$/L; e (iv) uma oxidação biológica final, permite alcançar um efluente final capaz de cumprir simultaneamente os valores legais para parâmetros orgânicos e de azoto, e não exceder os limites de descarga para outros parâmetros afetados pela adição de produtos químicos ao longo do tratamento (ou seja, alumínio e sulfato). Além disso, o custo do tratamento dessa estratégia foi estimado em 8,9 €/$m^3$, com a etapa de ozono contabilizando 6,9 €/$m^3$, o que é razoável considerando os custos das tecnologias atuais em uso.

# Table of Contents

## List of Figures

# List of Tables

# 1 Motivation and outline

*Underlying the motivation and ambition of the research theme, this chapter sets out the main challenges related to landfill leachate treatment and describes the structure and content of this thesis.*

## 1.1 Theme relevance

With various European and global initiatives requiring more recycling and alternative techniques for handling urban waste, landfilling is and will continue to be in demand, as the only cost-effective disposal method. Generation of complex organic/inorganic liquids from landfilling, as so called "leachates", remains inevitable, resulting from rainwater percolation through the landfill and waste decomposition, transferring contaminants from the solid to the liquid phase. The produced landfill leachate is considered a high-strength wastewater, usually characterized as a complex mixture of organic and inorganic compounds, including humic acids, ammoniacal nitrogen, heavy metals and inorganic salts. Leachate can migrate to groundwater, or even surface water, posing a severe environmental problem, as aquifers require extensive time for rehabilitation.

Presently, landfill leachates are a major concern for the landfill management authorities, mainly due to the following factors:

(i)   Leachate production starts at the early stages of the landfill but continues several decades after closure. This means that leachate treatment facilities should also last and their effectiveness ensured over a long period of time.

(ii)   Leachate composition and quantity are highly variable, not only between landfills but also throughout the year within the same landfill, depending on several factors, such as the landfill age, type of disposed waste and climatic conditions. So, it is difficult to define a unique treatment strategy that will be efficient in any given situation.

(iii)   With the aging of the landfills, the leachate generated contains high molecular weight contaminants, i.e. biorecalcitrant organic compounds. Therefore, for mature leachates, the use of conventional biological treatment followed by traditional physicochemical methods is not enough to achieve an effluent in agreement with the discharge limits.

(iv)   The need to comply with the increasingly restrictive legislation regarding quality standards for wastewater discharge. This usually leads to higher costs for the leachate treatment, thus directly affecting landfilling costs.

For these reasons, the combination of traditional and/or innovative physicochemical techniques with biological processes is required to effectively treat mature leachates, at a reasonable cost. Earlier research work, using leachate from the same urban landfill as that used in the present thesis, began by testing treatment approaches using different advanced oxidation processes. Later, under the Advanced-LFT project (SI IDT – 33960/2012 F2), a multistage treatment system for leachates from mature municipal landfills (European Patent – EP 2784031A1) was developed. The proposed

treatment train combines an initial biological oxidation, physicochemical (coagulation/sedimentation), a photocatalytic advanced oxidation step (photo-Fenton), and a final biological oxidation, to achieve a final effluent in compliance with the legal requirements for direct discharge into the environment. This strategy was partially tested at pilot-scale and proved to be effective for total ammonia nitrogen (TAN) and chemical oxidation demand (COD) removal up to legal values (according to the Portuguese legislation, Annex XVIII from Decree-Law no. 236/98). However, the removal of the high total nitrogen (TN) content of the leachate was not accomplished, nor the final biological reactor was fully assessed. Moreover, the photo-oxidation stage presented major drawbacks when aiming at a full-scale application, particularly with respect to the land area requirements and investment costs associated with the traditional compound parabolic collectors (CPCs), even when combining solar and artificial radiation.

## 1.2 Thesis objectives and outline

Considering the above-mentioned challenges, the present thesis focuses on the continuity of the research for an effective treatment train to be applied to mature urban leachates, aiming to:

(i)     Minimize the environmental impact of this hazardous wastewater, by achieving a final effluent in legal compliance with the main parameters for direct discharge into water bodies.

(ii)    Reduce the economic impact of the treatment train, particularly at the stage with the highest associated costs, i.e. advanced oxidation stage.

To accomplish these main targets and as the research work evolved, several partial objectives were also covered:

(i)     Optimization of the formerly proposed multistage strategy by:
   a.    Including an additional denitrification step, using a batch sequential reactor (SBR) as the first treatment stage, to biologically remove the TN content, aiming to comply with its legal limit, and with glycerol as an alternative and cost-effective external carbon source to promote denitrification;
   b.    Applying novel artificial photoreactors (FluHelik) and solar collectors' optics to promote the photo-oxidation of the bio-coagulated leachate, aiming at decreasing the expectable high investment and/or operational costs and land area requirements.

(ii)    Assessment of the flexibility of the optimized treatment train strategy against the high variability of the influent leachate, under real operating conditions (full-scale facility), also covering operational costs.

(iii)   Evaluation of ozone-driven processes as an alternative for the advanced oxidation step of the treatment train strategy, testing various system setups, process combinations, and also applying at different treatment stages, with a comparison of the estimated operational costs for different scenarios.

This thesis has been organized into 4 main sections – I. Introduction, II. Materials and Methods, III. Results and Discussion, and IV. Conclusions - divided in total by 10 chapters, with the bibliographic references presented at the end of each chapter and organized according to order of appearance.

The first section of this thesis is composed of three chapters. Chapter 1 refers to the present introductory section, addressing the relevance of the proposed research theme and objectives concerning this work. Chapter 2 provides background information on landfill leachate, as also a brief overview of the problems of global magnitude related to urban solid waste and landfilling, with focus on leachate production and composition. Chapter 3 intends to present the most common treatment technologies in use, current situation regarding treatment systems for urban landfill leachate, including treatment costs. This chapter also analyses leachate treatment process combinations proposed during this last decade by several authors, main achievements and, whenever possible, cost estimation. Finally, a review on the preceding research work carried out with leachate coming from the same landfill as the one used in this thesis is presented.

The second section includes Chapter 4 that describes all chemicals, analytical determinations, experimental setups, and respective experimental procedures used within this thesis.

Section III encloses 5 chapters. Chapter 5 presents the laboratory scale studies carried out to optimize the previously proposed multistage strategy, in order to incorporate TN removal on the first biological reactor. Thus, the tested treatment train comprised a: (i) sequential batch reactor (SBR), with nitrification/denitrification cycles; (ii) coagulation using ferric salts in acidic conditions; (iii) photo-Fenton oxidation reaction ($Fe^{2+}/H_2O_2/UV$-Vis); and (iv) final biological oxidation. On the first biological reactor, the maximum daily nitrogen load that could be treated reaching the TN legal limit to be discharged into water bodies was assessed. The influence of the biological denitrification process on the following treatment stages (coagulation and photo-Fenton oxidation) was also evaluated. Finally, the minimum photo-treatment time required to achieve a

final effluent, after a subsequent biological treatment, in agreement with the discharge limits in terms of COD, was determined.

Chapter 6 reports the application of the optimized treatment train strategy, at full-scale, in a compact facility located at a municipal waste landfill (nearby Porto) and comprising the following treatment units: (i) a first biological reactor (BR1); (ii) a coagulation and photo-treatment unit (C/P); (iii) a second biological reactor (BR2); (iv) a sludge tank (ST); (v) a filter-press system (FP); and (vi) a drainage tank. The start-up and operation, during nearly one year, tested the flexibility of the treatment train strategy against the high variability of the influent leachate. Glycerol, a by-product from biodiesel production, was used as a cost-effective external carbon source to promote biological denitrification. An innovative artificial photoreactor (4 FluHelik reactors connected in series) was used in the C/P unit to promote the oxidation of the leachate by the photo-Fenton reaction. A cost analysis for the multistage treatment is presented, based on the full-scale operation, including the treatment and disposal of the produced sludge.

Chapter 7 refers to the testing of different solar collector designs to promote the photo-Fenton process applied to the treatment of mature landfill leachate. In this chapter, different reflector materials (anodized aluminium with and without protective coating; soiled aluminium and mirrored stainless steel) and geometries (traditional double-parabola; simplified double-parabola and flat) for the solar collectors' optics were tested aiming at cost reduction and durability increase of the solar collectors'. Reflectance properties of different reflector materials and geometries were characterized and the photonic flow using the different solar collectors, at lab- and pilot-scale, was determined. The impact of the different collectors' optics, including the effect of soiled aluminium reflectors, at lab- and pilot-scale, on the efficiency of the photo-Fenton treatment applied to mature urban landfill leachate was also evaluated. Finally, the investment costs for the different solar collectors were compared.

Chapter 8 reports the results of ozone-driven processes applied as an alternative for the photo-Fenton stage of the multistep treatment strategy. The best operating conditions (initial pH and ozone dose) for the ozone process applied to a pre-treated mature landfill leachate were established. In order to minimize the losses of ozone and improve the ozonation treatment efficiency, different system setups (bubble column reactor with or without FluHelik photoreactor coupled in series, using a porous diffuser or a Venturi injector) and ozone-driven processes (combining ozone with hydrogen peroxide and/or with UVC radiation) were investigated. The effect of the different ozone-based treatments on leachate biodegradability was evaluated and the operational costs of the different system setups and process combinations were compared.

Following the results obtained in the previous activity, Chapter 9 reports the tests carried out with leachate after different pre-treatments (with/without biological nitrogen removal and with/without coagulation, using aluminium or iron salts). The performance of $O_3$ and $O_3$/UVC processes on the oxidation of the organic matter, colour removal and biodegradability enhancement were evaluated. Furthermore, 3-dimension excitation-emission matrix (3D-EEM) fluorescence spectroscopy was used to examine the changes in the characteristics of dissolved organic matter of the different leachate pre-treatments before and after the application of the ozone-driven processes. Lastly, the operating costs between the different combinations of leachate pre-treatment and the ozone-driven treatment stage were estimated and compared.

The final section of this thesis presents a single chapter. Chapter 10 displays the final remarks, where the most pertinent results and conclusions of this thesis are reported, and some future research directions are proposed.

# 2 Landfill leachate: Contextualization

*This chapter provides an overlook of the problematics associated with the production and management of municipal solid wastes, with a focus on waste deposition in landfills and on the generation of landfill leachate.*

## 2.1 Municipal solid wastes

All human activities generate waste and the worldwide trend of rapid urbanization, population growth, and economic development is pushing global waste production to a continuous increase. According to the latest report promoted by the World Bank [1], in 2016 the worlds' cities generated 2.01 billion tonnes of solid waste, amounting to a footprint of 0.74 kilograms per person per day. Additionally, over the next 30 years, the report projects an increase of 70%, up to 3.40 billion tonnes of urban wastes generated in 2050. Facing this scenario, around the world there is the recognition that waste is a severe problem, either by the amount generated or by typology, as it can seriously affect public health and damage the environment [2].

Waste management originally aimed at preventing diseases by appropriate waste disposal. Early procedures had as the only requirement the disposal of wastes outside the cities, in open dumps. Over time, several techniques have been developed and practiced for solid waste management, such as landfilling, incineration, recycling, composting and anaerobic digestion (Table 2.1). However, not all countries follow sustainable waste management practices and, due to noise and odour impacts, some technical solutions are not always well accepted by populations. In 2016, at least 33% of the cities' world waste was not managed in an environmentally safe manner (open dumping or burning), while about 37% was disposed of in some type of landfill, 13.5% recycled, 11% incinerated and 5.5% composted [1].

Cities waste, commonly known as garbage or trash, which includes domestic (household), commercial and non-hazardous industrial wastes, is classified as municipal solid waste (MSW) [3]. The composition and quantity of MSW differ across the world countries', reflecting the varied patterns of consumption related to the living standards and lifestyle of their inhabitants. Generally, developing countries generate MSW with high organic content ($\geq 50\%$), when compared to those generated in industrialised ones [1, 4]. In turn, developed countries produce MSW with the largest portion of dry wastes (paper and cardboard, plastic, metal, and glass) [1, 4]. Similarly, waste management systems also vary between countries. Considering that MSW management is expensive, low-income countries generally rely on open dumping (93%), while high-income countries are decreasing landfill rates (39%) due to diversion of waste to recycling and composting (35%) and incineration (22%) [1].

**Table 2.1** – Waste management and treatment options and associated environmental impacts [5].

| Treatment | Process description | Main environmental impacts |
|---|---|---|
| Landfilling | It encompasses the management of waste disposal on land, with or without pre-treatment. | •Methane ($CH_4$) emissions from biodegradable wastes (global warming contribution).<br>•Retention of carbon compounds in the landfill.<br>•Water pollution through leachates production. |
| Incineration | Burning of waste at high temperatures, with or without pre-treatment.<br>Energy recovery may occur. | •Emissions of dioxins, fine particles and nitrogen oxides ($NO_x$), sulphur dioxide ($SO_2$) and hydrogen chloride (HCl).<br>•Carbon dioxide ($CO_2$) emissions from fossil-derived fuels (e.g. plastic) and nitrogen dioxide ($NO_2$) (global warming contribution).<br>•Replacement of fossil fuels by energy recovered. |
| Recycling | Several components of the waste stream are reused and recover. | •Lower emissions of greenhouse gases and other pollutants.<br>•Less virgin feedstock extraction resulting in energy savings and fewer impacts. |
| Composting | Decomposition of organic wastes by microorganisms under aerobic conditions. The produced compost can be used as a soil conditioner. | •$CH_4$ emissions from biodegradable wastes (global warming contribution);<br>•Water pollution through leachates production.<br>•$CO_2$ and other compounds emissions. |
| Anaerobic digestion | Like composting but the process occurs without oxygen, converting biodegradable wastes into biogas ($CO_2$ and $CH_4$), which can be used as an alternative fuel. | •$CO_2$ emissions avoided due to fossil fuels replacement and energy recovery.<br>•Sludge production. |
| Mechanical biological treatment (MBT) | Pre-treatment that couples mechanical and biological processes. MBT aims to separate biodegradable waste and reduce the amount of waste to landfill, by sorting recyclable waste. | •Waste reuse and recycling and energy recovery.<br>•Reduction of methane and leachate production.<br>•Landfills are needed for disposal of unrecovered waste. |

Regarding the European Union (EU), the latest Eurostat data [6] estimate that 488 kg of MSW per person was generated in 2018. Across the EU Member States (EU-28), the amount of MSW generated varied significantly, with Romania producing the least amount of waste (272 kg per person), while Denmark produced the highest one (766 kg per person). Overall, across EU-28, 30% of the waste was recycled, 28% incinerated, 23% landfilled and 17% composted. When compared to 2005 data (Figure 2.1), the MSW produced in EU-28 decreased by 5.5%, and landfilling has fallen 48% (from 110 to 56 million tons in 2018). This reduction can partly be attributed to the implementation of European legislation, such as Directive 62/1994 [7] (on packaging and packaging waste) and Directive 31/1999 [8] (on landfill). The first has set a recovery target of 60% for all packaging put on the EU market until 31 December 2008; the second stipulated that Member States were obliged to reduce the amount of biodegradable MSW going to landfills up to 35 % by 16 July 2016. This Directive has led countries to adopt different strategies to avoid sending the organic fraction of MSW to landfill, namely composting (including fermentation), incineration and pre-treatment, such as mechanical-biological treatment (including physical stabilization). As a result, the amount of waste recycled (material recycling and composting) rose from 81 million tonnes (163 kg per capita) in 2005 to 117 million tonnes (230 kg per capita) in 2018.
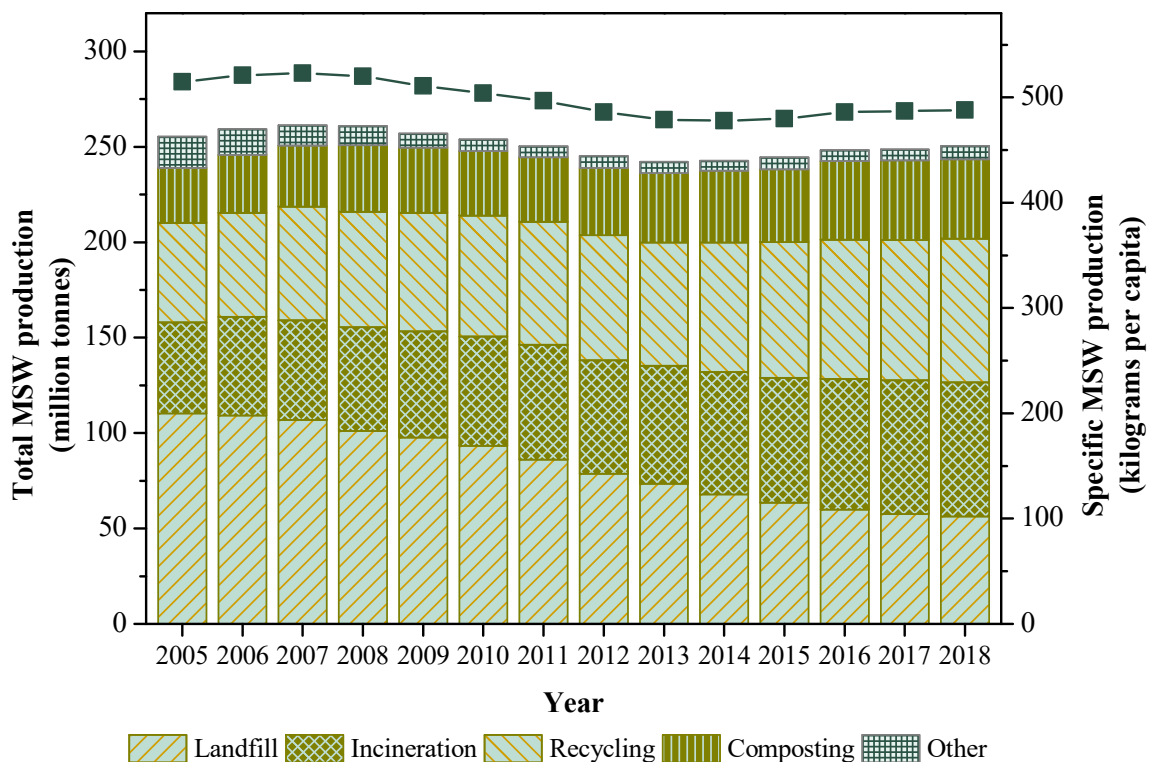


**Figure 2.1** – Evolution of the municipal solid waste (MSW) production and management operation in the European Union (left "y" axis for columns and right "y" axis for ■; source: Eurostat [6]).

In Portugal, adequate procedures and legislation concerning the collection and disposal of MSW were only established in late XX century. By 1995, urban waste disposal was rudimentary and more than 300 open dumps existed in Portugal, being the final destination of about 76% of MSW produced [9, 10]. Since then, mostly in response to European Union Directives, many efforts were devoted to MSW management, including a more rigorous control of the associated impacts. By 2002, the uncontrolled disposal in dumps was eradicated and mostly replaced by landfilling in sanitary sites [9]. In 2018, Portuguese cities produced 5.2 million tonnes of MSW, a value that is been rising since 2013 (Figure 2.2). According to the management operation, 49% of wastes were sent to landfills, 18% incinerated, 12% recycled and 17% composted (including digestion). Presently, Portugal has 23 municipal waste management systems, responsible for 32 urban waste landfills [11, 12].
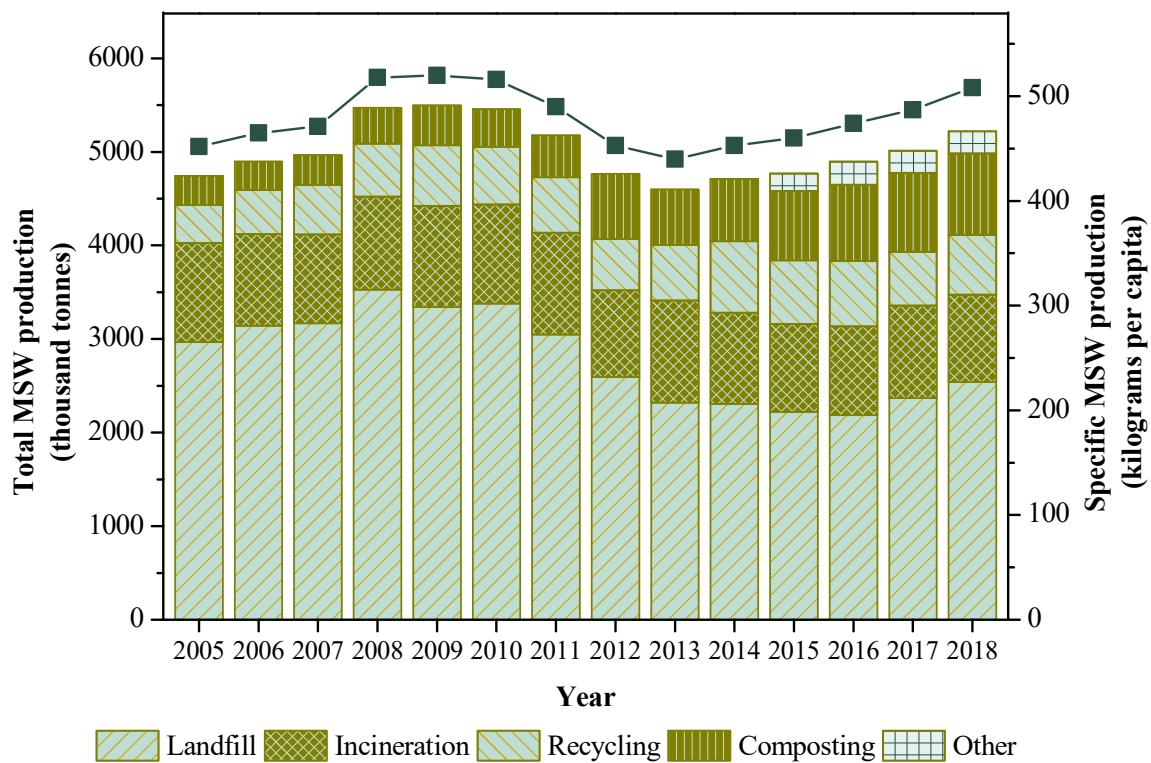


**Figure 2.2** – Evolution of the municipal solid waste (MSW) production and management operation in Portugal (left "y" axis for columns and right "y" axis for ■; source: Eurostat [6]).

## 2.2 Landfilling

Around the world, sanitary landfilling constitutes a major component of the solid waste management systems. According to the data previously presented, every year about 744 million tonnes of MSW is disposed of in a landfill and this number tends to increase. The use of sanitary landfilling, as the preferential mean of disposing MSW, is directly linked to the historical development of waste management operations and its economic advantages. In terms of capital and operating costs, landfilling is the most cost-effective option when compared to other possible means of waste elimination [13]. While not the best solution for waste management, landfills have made a significant contribution to reducing the environmental impact of waste production and are often the first step towards sustainable waste management. The use of landfills is therefore expected to increase in developing countries and decrease in developed countries by diverging wastes to recycling and composting operations.

A landfill can be overseen as a complex environment where many interacting physical, chemical, and biological processes take place. In most landfills, assuming they receive some organic wastes, microbial processes dominate the waste degradation processes and hence govern the generation and composition of the gaseous and leachate emissions (Table 2.1). Waste degradation is a long-term event, associated with highly concerning environmental effects stretching far beyond the landfill lifetime. Over the last decades, the quality of landfill design, according to technical, social and economic development has improved dramatically and has been mainly devoted towards ensuring minimal environmental impact. Nowadays, a modern landfill is an engineered method for waste disposal in specially constructed and protected cells that allows waste to decompose, under controlled conditions, until relatively inert, stabilized material [14]. Additionally, in many countries, landfill facilities are subject to extensive legal regulations but, regrettably, they often do not meet legal environmental standards and targets.

### 2.2.1 Waste degradation

The waste degradation processes inside the landfill are the key to understand and control the resulting gaseous and leachate emissions and, consequently, their environmental impacts. Numerous landfill studies [15, 16] suggest five distinct sequential stages for waste stabilization in a landfill (Figure 2.3): I. aerobic; II. hydrolysis and fermentation; III. acetogenic; IV. methanogenic; and V. maturation.
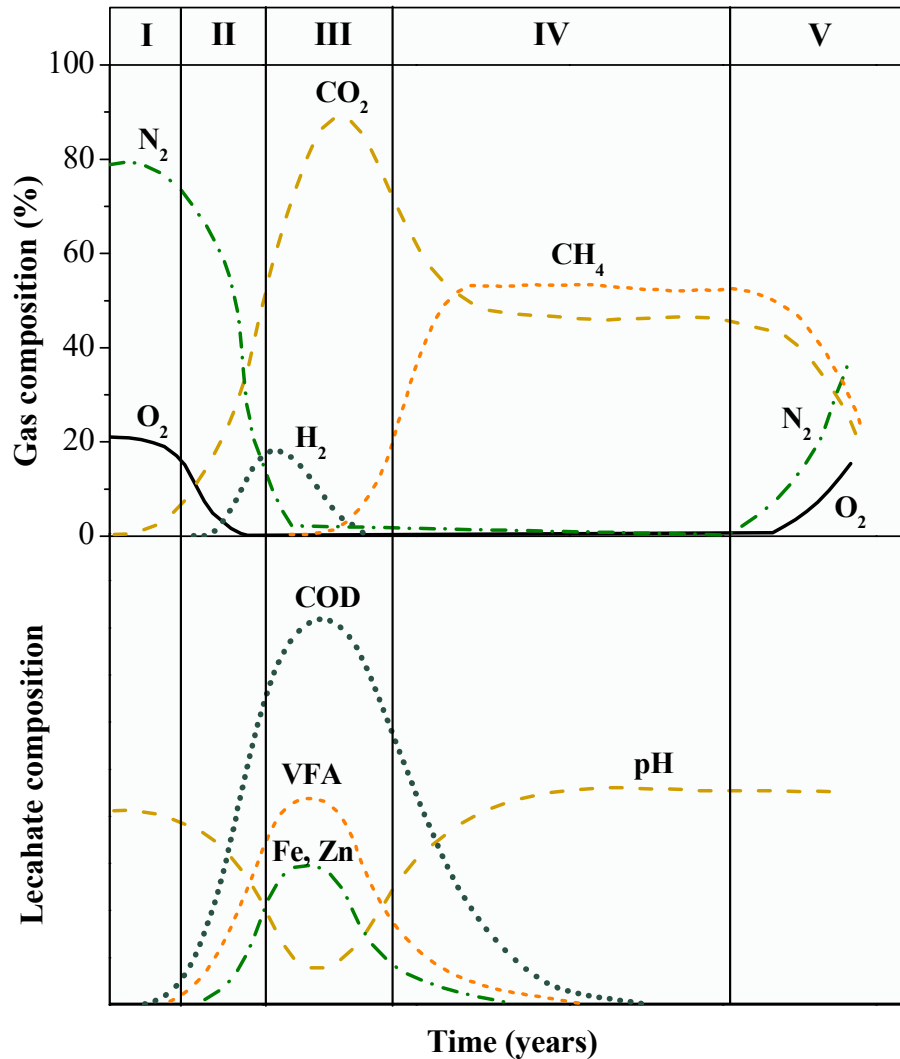
**Figure 2.3** – Stages for MSW degradation in a typical landfill (adapted from [16]).

The decomposition of wastes begins immediately after landfilling, where easily degradable organic matter is decomposed during a short aerobic stage (stage I). The duration of this stage is limited due to the rapid consumption of the available oxygen ($O_2$) in aerobic reactions (Figure 2.3). During this aerobic stage, exothermic reactions predominate, with the consequent rise in temperature. Afterward, as evidenced by the depletion of oxygen, an intermediate anaerobic stage, also called hydrolysis and fermentation (stage II), develops. A trend toward reducing conditions is established, in accordance with the shifting of electron acceptors from oxygen to nitrates ($NO_3^-$) and sulfates ($SO_4^{2-}$), and the displacement of oxygen by carbon dioxide ($CO_2$) (Figure 2.3). The hydrolysis process starts allowing the solubilisation of organic matter (carbohydrates, lipids, and proteins) into long-chain fatty acids, glucose and monoids, easily metabolised by bacteria. Hydrolysis is caused by extracellular enzymes produced by the fermenting bacteria and can be considered the overall rate-limiting step in the landfill environment [16]. The continuous hydrolysis (solubilisation) of

solid waste, followed by (or concomitant with) microbial conversion of biodegradable organic content, by fermentative acidogenic bacteria, results in the production of intermediate volatile fatty acids (VFAs) at high concentrations (Table 2.2). A significant pH reduction occurs, causing an increase in the concentration of zinc (Zn), iron (Fe) and other heavy metals (Figure 2.3). Viable biomass growth associated with acid-forming bacteria, together with rapid consumption of substrate and nutrients, are predominant features of this stage. By the end of stage II, measurable concentrations of chemical oxygen demand (COD) and VFA can be detected in the leachate [17].

**Table 2.2** – Important reactions involved in anaerobic waste biodegradation (adapted from [16]).

| Anaerobic process | Reaction[a] |
|---|---|
| Fermentative | $C_6H_{12}O_6 + 2H_2O \rightarrow 2CH_3COOH + 4H_2 + 2CO_2$ |
| | $C_6H_{12}O_6 \rightarrow CH_3C_2H_4COOH + 2H_2 + 2CO_2$ |
| | $C_6H_{12}O_6 \rightarrow 2CH_3CH_2OH + 2CO_2$ |
| Acetogenic | $CH_3CH_2COOH + 2H_2O \rightarrow CH_3COOH + 3H_2 + CO_2$ |
| | $CH_3C_2H_4COOH + 2H_2O \rightarrow 2CH_3COOH + 2H_2$ |
| | $CH_3CH_2OH + H_2O \rightarrow CH_3COOH + 2H_2$ |
| | $C_6H_5COOH + 4H_2O \rightarrow 3CH_3COOH + H_2$ |
| Methanogenic | $H_4 + CO_2 \rightarrow CH_4 + 2H_2O$ |
| | $CH_3COOH \rightarrow CH_4 + CO_2$ |
| | $HCOOH + 3H_2 \rightarrow CH_4 + 2H_2O$ |
| | $CH_3OH + H_2 \rightarrow CH_4 + H_2O$ |

[a]$C_6H_{12}O_6$: glucose; $H_2O$: water; $CH_3COOH$: acetic acid; $H_2$: hydrogen; $CO_2$: carbon dioxide; $CH_3C_2H_4COOH$: butyric acid; $CH_3CH_2OH$: ethanol; $CH_3CH_2COOH$: propionic acid; $C_6H_5COOH$: benzoic acid; $HCOOH$: formic acid; $CH_3OH$: methanol; $CH_4$: methane.

In the following stage, known as acetogenic (stage III), the acidogenesis products, i.e. the propionic acid, butyric acid and alcohols, are transformed by acetogenic or fatty acid oxidizing bacteria into $CO_2$, hydrogen ($H_2$) and acetic acid ($CH_3COOH$). The first signs of methanogenesis appear as the concentration of methane ($CH_4$) gas starts to increase while, in contrast, the concentration of $H_2$ and $CO_2$ decreases (Figure 2.3). The metabolization of VFAs leads to a reduction in their concentration, causing an increase in pH.

During the methanogenic stage (stage IV), intermediate VFAs are metabolised by methanogenic bacteria and converted into $CH_4$ and $CO_2$ (Table 2.2). The high rate of methane formation, resulting in a $CH_4$ concentration in the gas of 50-65% by volume, maintains the low concentrations of VFAs

and $H_2$ (Figure 2.3). During this stage, $SO_4^{2-}$ and $NO_3^-$ are reduced to sulphide ($S^{2-}$) and ammonium ($NH_4^+$), respectively. The pH and alkalinity values increase, supporting the growth of methanogenic bacteria and inhibiting the solubilisation of heavy metals.

The maturation stage (stage V) corresponds to the final stabilization of the waste mass in which the bacterial activity is significantly reduced, remaining mainly the refractory organic matter. As a result, $CH_4$ production decreases to such low levels that nitrogen ($N_2$) and oxygen reappear in the landfill gas due to diffusion from the atmosphere. Usually, at this stage, the leachate generated contains a higher concentration of humic (HA) and fulvic acids (FA) which translate into high molecular weight substances that are hardly reduced to less complex compounds.

### 2.2.2 Main environmental issues

As a result of waste degradation processes in the landfill, gaseous and leachate emissions pose serious threats to human health and the quality of the environment. The major components of landfill gaseous emissions are $CH_4$ and $CO_2$, with a large number of other constituents at low concentrations such as $H_2S$, ammonia ($NH_3$) and non-methane volatile organic compounds (VOCs) [18]. In theory, the biological decomposition of 1 tonne of MSW produces 442 $m^3$ of landfill gas containing 55% methane and calorific value of 15 - 21 $MJ/m^3$ [2, 19], which is approximately half that of natural gas. Landfill gas is normally controlled by installing vertical or horizontal wells within the landfill (Figure 2.4). These wells are either vented to the atmosphere or connected to a central blower system that pulls gas to a flare or treatment process. The uncaptured gas can pose an environmental threat because methane is a greenhouse gas and many of the VOCs are odorous and toxic. Global $CH_4$ emissions from landfills are estimated to be 500–800 million tonnes $CO_2$ equivalent per year [20], representing a contribution of around 20% of the global anthropogenic methane emissions [2].

Leachate is the liquid by which soluble materials of the deposited waste inside a landfill may be transported and released into the environment. About two hundred hazardous compounds have already been identified in landfill leachates, such as aromatic compounds, halogenated compounds, phenols, pesticides, heavy metals and ammonium [21]. All of these substances have a cumulative, threatening and detrimental effect on the survival of aquatic life, ecology and food chains with potential harmful consequences for public health, including carcinogenic effects, acute toxicity and genotoxicity [22, 23]. In general, landfill leachate has a profound impact on soil permeability,

groundwater, surface water, and nitrogen attenuation. The most typical harmful effect of leachate discharge into the environment is that of groundwater contamination, which poses a serious problem as aquifers require extensive time for rehabilitation [2]. Many incidents of water pollution involving leachate have been reported for different countries [24-27] and, in the 90's the United States Environmental Protection Agency (USEPA) estimated that more than 75% of the country landfills were polluting groundwater [28]. To prevent this, the first step in landfill design development is to site the landfill far from the groundwater table, abstraction wells and surface water bodies. Hydrogeological studies are also important in order to identify the best landfill location, with a preference for soils with natural low permeability. Waterproof covers, different covering liners, and drainage systems for the produced leachate are normally legal requirements for landfills design (Figure 2.4).
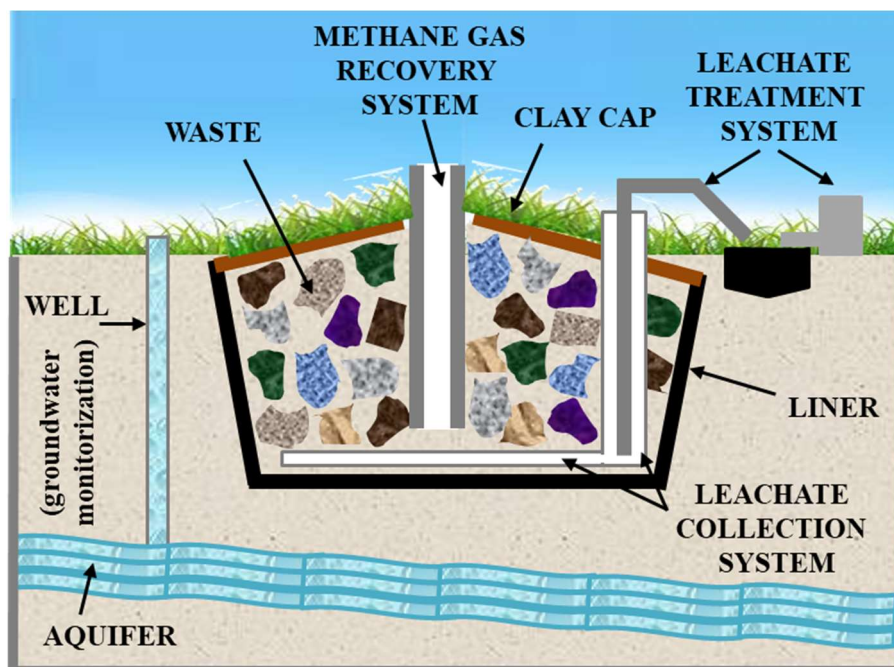


**Figure 2.4** – Simplified schematics of a modern landfill (adapted from [29]).

## 2.3 Landfill leachate

Appropriate waste and landfill management can reduce the quantity and improve the quality of the leachate but cannot eliminate it completely. As previously described, landfill leachate is a water-based solution formed during the breakdown processes of wastes, with dissolved or entrained environmentally harmful substances. Among those substances, there are several compounds classified as potentially hazardous: bio-accumulative, toxic, genotoxic, and with possible endocrine disruptive effect [22, 23]. Therefore, this hazardous and heavily polluted wastewater needs to be treated properly before discharge into the receiving bodies [30, 31]. To design an appropriate treatment system, it is required to know two main factors: the volumetric flow rate and the composition of the wastewater to be treated. In the case of leachate, these factors are closely linked and present considerable and continuous variations over time. Moreover, they also depend on the climate and characteristics of the deposited wastes.

The main parameters generally used to characterize leachate include chemical oxygen demand (COD), 5-day biochemical oxygen demand ($BOD_5$), total or dissolved organic carbon (TOC or DOC), total nitrogen (TN) and total ammoniacal nitrogen (TAN). This set of parameters is particularly relevant, as they usually present high concentrations and impose more limitations in the treatment processes due to several difficulties associated with their elimination.

### 2.3.1 Generation

In most climates, rain (and snow) is a major contributor to leachate generation, which is demonstrated by a clear pattern between precipitation and landfill leachate formation [32]. It can theoretically be assumed that the percolation of infiltrated water through the compact mass of waste resembles that which occurs in a layer of soil, similarly, having a water retention capacity. Once the maximum water retention capacity in the waste mass is reached, significant leachate production occurs at the base of the landfill, and approximately all infiltrated water becomes leachate [33]. Water balance for the determination of leachate generated in an operating landfill can be defined by Equation 2.1 [34]. The results obtained by this method are considered to be almost as accurate as those determined using more complex analysis methods [16].

$$L = P - R - ET - U_S - U_W \qquad (2.1)$$

Where $L$ is the amount of leachate produced, $P$ and $R$ are the precipitation and surface runoff, respectively, and $ET$ is the evapotranspiration (vegetated surface) or evaporative (bare soil) losses. The changes in the moisture content of the soil, $U_S$, and of the waste components, $U_W$, are also discounted.

The best estimate for precipitation is obtained using on-site measurements, however, when performing an expedite calculation it is possible to use data from meteorological stations whose area of influence covers the study site. Runoff represents the fraction of precipitation that flows to the surface of the ground, with no opportunity to infiltrate. Its occurrence depends on a number of factors, including the intensity and duration of the precipitation event, previous soil moisture conditions, cover soil permeability, terrain slope and cover vegetation type [35]. Evapotranspiration is defined as the loss of water to the atmosphere through the transpiration of vegetation, together with evaporation that occurs in the soil. Thus, it depends on soil type, vegetation type and soil moisture conditions, which in turn is influenced by climatic factors such as precipitation, temperature and humidity [33]. Usually, evapotranspiration values are obtained from measurements made at meteorological stations, near the location site. Evaporative water loss has a complex determination, so it can simply be estimated by actual evapotranspiration and soil type [8].

There are also numerous mathematical models developed to simulate the processes ruling leachate occurrence and behaviour in landfills [36]. Within the computational modelling there are some reference programs, namely: (a) Water Balance Model (WBM), proposed by Dennis G. Fenn [33], is the most commonly used; (b) Hydrologic Simulation on Solid Waste Disposal Sites (HSSWD), developed by Eugene R. Perrier and Anthony C. Gibson [37]; (c) Hydrologic Evaluation of Landfill Performance (HELP model), initially developed by Paul R. Schroeder [38].

In the absence or insufficiency of information, it is usual to consider theoretical values based on easily determined variables, such as the average annual precipitation or the amount of waste deposited in the landfill. In an expeditious calculation, it is acceptable to assume that the average annual leachate production represents between 15 and 25% of the average annual rainfall [39]. Studies assuming that approximately 13% of precipitation over a landfill becomes leachate, and based on a 20 m deep landfill and a waste density of 1 tonne per $m^3$, concluded that an acceptable value for the volume of leachate produced is 0.005 $m^3$ per day for each tonne of waste deposited [40]. A theoretical estimate that relates leachate generation to the landfill area, points to a production of 5 $m^3$ per day of leachate per hectare [41]. So, considering the data mentioned in the previous points of this thesis, and in order to have an idea of its magnitude, Table 2.3 presents an estimate for leachate that can be generated annually worldwide.

**Table 2.3** – Estimates for leachate worldwide generation per year.

| | Waste generated[a] ($\times 10^6$ tonne) | Waste landfilled[a] ($\times 10^6$ tonne) | Leachate generated ($\times 10^6$ m$^3$) |
|---|---|---|---|
| **World** | 2010 | 744 | 1357[b] <br> 744 – 3719[c] |
| **EU** | 248.7 | 57 | 104[b] <br> 57 – 286[c] |
| **Portugal** | 4.7 | 2.2 | 4.1[b] <br> 2.2 – 11[c] |

[a] According to data sources [1, 6]. [b] Assuming 0.005 m$^3$ of leachate generated per day for each tonne of waste [40].
[c] Assuming 1 m$^3$ of leachate generated per 0.2 (minimum) and 1.0 (maximum) tonne of waste [42].

The production of significant volumes of leachate occurs until at least 20 years after the final restoration has taken place [43], so typically a minimum 30-year post-closure care period is legally required. However, some authors support longer periods since a landfill site may still produce leachate with high concentrations over 50 years after filling operations have ceased [44].

## 2.3.2 Composition

Although leachate composition depends on many different factors (e.g. climatic conditions, type of waste deposited in the landfill and site operations practices), changes in the main characterization parameters (COD, BOD$_5$, pH, TAN and heavy metals) are expected according to the dynamics of the decomposition processes occurring in the landfill. As the composition of the leachate varies widely through successive stages of degradation, three types of leachate– young, intermediate, and old - depending on the age of the landfill, can be distinguished (Table 2.4).

Young leachate, resulting from the early acetogenic stage of waste degradation, is extremely variable and difficult to predict. Usually, it contains large amounts of readily biodegradable organic matter, as indicated by the high ratio BOD$_5$/COD with values up to 0.5-0.7 [13, 31, 34, 45], indicating that biological treatment processes are suitable for the treatment of the leachate generated at this stage. The concentration of VFAs can be quite significant, representing 95% of the total organic carbon (TOC), leading to low pH (around 5). Relatively high concentrations of iron (Fe), manganese (Mn), nickel (Ni) and zinc (Zn) can also be observed during this stage, as the lower pH and bonding with the VFAs increase the solubility of metals [16].

**Table 2.4** – Typical characterization of leachate according to landfill age (sources: [31, 34])

| Parameter | Young | Intermediate | Old |
|---|---|---|---|
| **Landfilling stage** | Acetogenic | Methanogenic | Maturation |
| **Age (year)** | < 5 | 5 – 10 | > 10 |
| **pH** | < 6.5 | 6.5 – 7.5 | > 7.5 |
| **COD (g/L)** | > 10 | 4 – 10 | < 4 |
| **$BOD_5$/COD** | > 0.5 | 0.1 – 0.5 | < 0.1 |
| **TOC/COD** | < 0.3 | 0.3 – 0.5 | > 0.5 |
| **TAN (mg/L)** | < 400 | 400 | > 400 |
| **Heavy metals (mg/L)** | > 2 | < 2 | < 2 |
| **Organic compounds[a] (dominant species)** | 80% VFA | 5 – 30% VFA + HA + FA | HA + FA |
| **Molecular size distribution** | Broad range of high fraction of low MW[b] organics | | Narrow range of high fraction of high MW[b] organics |
| **Biodegradability** | Important | Medium | Low |

[a] VFA – Volatile fatty acids; HA – Humic acids; FA – Fulvic acids. [b] MW – Molecular weight.

On the other side, "old" leachate, also called mature or stabilized, possesses quite more stable characteristics. As the content of VFAs and other easily biodegradable organic compounds in the leachate decreases over time, organic matter in the leachate becomes dominated by refractory compounds such as humic-like and fulvic-like substances [13, 16, 34]. Thus, a low ratio $BOD_5$/COD, often close to 0.1, is a characteristic value for mature leachate (Table 2.4). The high content of humic substances provides a dark colour to old leachate. Also, with the decrease of VFA's content there is an increase in pH, normally around 8 [3, 16] and, consequently, the concentration of metal ions is in general low. However, lead (Pb) can be an exception, since it forms very stable complexes with humic acids [34].

## 2.4 Legal framework

To minimize the potential environmental impacts, many legal authorities throughout the world have set regulations regarding maximum contaminants levels in treated leachate prior to disposal (Table 2.5).

**Table 2.5** – Legal limits in different countries for the main (organic and nitrogen) parameters applicable to leachate for discharge into water bodies.

| Country | Parameters[a] (mg/L) | | | | Reference |
|---------|------|------|------|------|-----------|
| | BOD$_5$ | COD | TAN | TN | |
| Belgium | - | 250 | 5 | - | Oloibiri, *et al.* [46] |
| Brazil | 50 | 200 | 20 | - | Scandelai, *et al.* [47] |
| China | - | 100 | 25 | - | Li, *et al.* [48] |
| USA[b] | 140 | - | 10 | - | Meeroff and Lakner [49] |
| France | 30 | 120 | 5 | 30 | Azreen and Zahrim [50] |
| Germany | 20 | 200 | - | 70 | Azreen and Zahrim [50] |
| Hong Kong | 30 | 200 | 5 | 100 | Azreen and Zahrim [50] |
| Italy | - | 160 | - | - | Pastore, *et al.* [51] |
| Malaysia | 20 | 400 | 5 | - | Azreen and Zahrim [50] |
| Poland | 25 | 125 | 10 | 15 | Kowalik and Laakkonen [52] |
| South Korea | - | 50 | 50 | 150 | Azreen and Zahrim [50] |
| Turkey | 50 | 100 | - | - | Ozturk, *et al.* [53] |

[a] BOD$_5$ – 5-day biochemical oxygen demand; COD – chemical oxygen demand; TAN – total ammonia nitrogen; TN – total nitrogen. [b] Maximum daily value.

In the case of the European Union, four major pieces of legislation govern landfilling and leachate management:

(i)   Council Directive 1999/31/EC of 26th April 1999 [8], known as Landfill Directive, regulates waste management of landfills in the EU (amended by Council Directive 2011/97/EU of 5th December and Directive 2018/850 of 30th May);

(ii)  Directive 2008/98/EC of 19th November 2008 [54], or Waste Framework Directive, provides a general framework of waste management requirements and sets the basic waste management definitions for the EU (amended by Commission Directive 2015/1127 of 10th July, Council Regulation 2017/997 of 8th June and Directive 2018/850 of 30th May);

(iii) Directive 2000/60/EC of 23rd October 2000 [55], also called Water Framework Directive, establishes a framework for the EU action in the field of water policy (amended by Directive 2008/32/EC, of 11th March, Directive 2008/105/EC of 16th December, Directive 2009/31/EC,

of 23rd April, Directive 2013/39/EU of 12th August, Council Directive 2013/64/EU of 17th December and Commission Directive 2014/101/EU of 30th October);

(iv) Council Directive 91/271/EEC of 21st May 1991 concerning urban wastewater treatment [56], aims to protect the environment from the harmful effects of urban wastewater discharges, including discharges from some industrial sectors (amended by Commission Directive 98/15/EC of 27th February, Regulation (EC) No 1882/2003 of 29th September, Regulation (EC) No. 1137/2008 of 22nd October and Council Directive 2013/64/EU of 17th December).

Landfill Directive places strict operational and technical requirements on waste management and landfills, to prevent or reduce harmful effects on the environment and human health during the whole lifecycle of the landfill [8]. According to this Directive, the presence of a geological barrier for the protection of soil and groundwater and the establishment of a basic sealing system are an absolute requirement. In turn, the Waste Framework Directive requires Member States to prioritize prevention and reduction of waste, with the disposal of waste in landfills as the last resort [54]. Together, these Directives regulate the nature of wastes that landfills can receive, but also the execution of aftercare, thus directly influencing leachate management practices. The long-term effect of the changes imposed by the Directives, namely the decreasing amount of biodegradable solid wastes, on leachate composition and treatability is currently unknown [42]. Finally, the Water Framework Directive and the Urban Wastewater Treatment Directive, aiming to protect the environment from the effects of insufficiently treated urban wastewater, have established standards on the treated wastewater discharged from urban wastewater treatment plants (WWTP) into receiving waters [56].

In Portugal, Decree-Law no. 183/2009, of 10th August [57], transposes Landfill Directive and, through a set of norms and criteria, regulates the installation, operation, closure and post-closure procedures for sanitary landfills. According to this diploma, the landfill operator is responsible for the implementation of monitoring procedures for the produced leachate, groundwater, surface water and leachate basins (the parameters and periodicity are also set) and for the treatment and appropriate final destination of the leachate produced in the landfill. Monitoring must be carried out not only during the operation phase but also before (for natural waters adjacent to the landfill) and after the closure of landfills (leachate quality must be assessed every six months). Since no legislation is directly applicable to the discharge of leachate into water bodies, Decree-Law no. 236/98, of 1st August [58], containing standards and criteria for the discharge of wastewater into water bodies, is also extended to the discharge of leachate. This legal instrument aims at promoting the quality of water resources and the protection of public health, and the emission limit values (ELV) are established for several elements (Table 2.6). Recently, the update of the Strategic Plan for Urban Waste (PERSU 2020+ [12]) was approved by ministerial ordinance (Portaria nº 241-

B/2019, of 31$^{st}$ July [59]). Based on the Circular Economy Strategy and recent revisions of the Waste Framework Directive, PERSU 2020+ establishes the general lines and aligns strategies for the fulfilment of new European targets (for 2035) [12].

**Table 2.6** – Emission limit values (ELV) in Portugal for the direct discharge of wastewaters into the environment (source: Decree-Law no. 236/98 [58]).

| Parameter | Units | ELV[a] |
|---|---|---|
| pH | Sörensen scale | 6.0 - 9.0 |
| Temperature | ºC | Increase of 3ºC[b] |
| BOD$_5$ (at 20ºC) | mg O$_2$/L | 40 |
| COD | mg O$_2$/L | 150 |
| TSS | mg/L | 60 |
| Aluminium | mg Al/L | 10 |
| Total iron | mg Fe/L | 2.0 |
| Odour | - | Not detectable at a dilution of 1:20 |
| Colour | - | Not visible at a dilution of 1:20 |
| Free residual chlorine | mg Cl$_2$/L | 0.5 |
| Total residual chlorine | mg Cl$_2$/L | 1.0 |
| Phenols | mg C$_6$H$_5$OH/L | 0.5 |
| Oil and grease | mg/L | 15 |
| Sulphides | mg S/L | 1.0 |
| Sulphites | mg SO$_3^{2-}$/L | 1.0 |
| Sulfates | mg SO$_4^{2-}$/L | 2000 |
| Total phosphorus | mg P/L | 10 / 3[c] / 0.5[d] |
| Ammonium nitrogen | mg NH$_4^+$/L | 10 |
| Total nitrogen | mg N/L | 15 |
| Nitrates | mg NO$_3^-$/L | 50 |
| Aldehydes | mg/L | 1.0 |
| Total arsenic | mg As/L | 1.0 |
| Total lead | mg Pb/L | 1.0 |
| Total cadmium | mg Cd/L | 0.2 |
| Total chromium | mg Cr/L | 2.0 |
| Hexavalent chromium | mg Cr (VI)/L | 0.1 |
| Total copper | mg Cu/L | 1.0 |
| Total nickel | mg Ni/L | 2.0 |
| Total mercury | mg Hg/L | 0.05 |
| Total cyanide | mg CN/L | 0.5 |
| Mineral oils | mg/L | 15 |
| Detergents (sodium lauryl sulfate) | mg/L | 2.0[e] |

[a] The ELV is understood as the monthly average, which is defined as the arithmetic mean of the average daily referring to the days of 1-month operation, which should not be exceeded. The daily value based on a representative sample of the wastewater discharged during a period of 24-hours, cannot exceed twice the monthly average value (the 24-hours composed sample must consider the discharge regime of the wastewater produced). [b] Temperature of the receiving water body after the wastewater discharge, measured at 30 m downstream from the discharging point. [c] In waters that feed lagoons or reservoirs. [d] In lagoons or reservoirs. [e] Value relative to the industrial plant's discharge for the HCH production and/or lindane extraction.

## 2.5 References

1.  Kaza, S., L. Yao, P. Bhada-Tata, and F. Van Woerden, *What a waste 2.0: A global snapshot of solid waste management to 2050*, ed. U.D. Series. 2018, Washington, D.C.: World Bank.

2.  Danthurebandara, M., S. Van Passel, D. Nelen, Y. Tielemans, and K. Van Acker, *Environmental and socio-economic impacts of landfills*, in *Linnaeus ECO-TECH*. 2012: Kalmar, Sweden.

3.  Vithanage, M., S.S.R.M.D.H.R. Wijesekara, A.R. Siriwardana, S.S. Mayakaduwa, and Y.S. Ok, *Management of municipal solid waste landfill leachate: A global environmental issue*, in *Environmental Deterioration and Human Health*, A.e.a. Malik, Editor. 2014, Springer Dordrecht.

4.  Diaz, L.F., G.M. Savage, and L.L. Eggerth, *Solid waste management*. United Nations Environment Programme. 2005.

5.  Smith, A., K. Brown, S. Ogilvie, K. Rushton, and J. Bales, *Waste management option and climate change*. 2001, European Commission: Luxembourg.

6.  Municipal waste statistics. EUROSTAT.

7.  European Parliament and Council Directive 94/62/EC of 20 December 1994 on packaging and packaging waste, in 94/62/EC, E. Parliament, Editor. 1994.

8.  U., E., *Council Directive 1999/31/EC, of 26 April 1999, on the landfill of waste* 1999: Available online: http://eur-lex.europa.eu/legal-content/EN/TXT/PDF/?uri=CELEX:31999L0031&from=EN p. 1-19.

9.  Pascoal, D.S.B., *Analysis of the Portuguese municipal solid waste management system*, in *Mechanical Engineering*. 2012, Faculty of Science and Technology, University of Coimbra: Coimbra.

10. Ribeiro, A., F. Castro, M. Macedo, and J. Carvalho. Waste management in Portugal and Europe – An overview of the past, present and future. in Wastes: Solutions, Treatments and Opportunities - 1st International Conference. 2011.

11. Marçal, A. and A.R. Teixeira, *Anual report on urban wastes*. 2019, Portuguese Environmental Agency: Amadora.

12. *PERSU2020+ Reflexão estratégica e ajustamentos às medidas do PERSU 2020*, M.o.E.a.E.T. Portuguese Republic, Editor. 2019, APA - Agência Portuguesa do Ambiente.

13. Renou, S., J.G. Givaudan, S. Poulain, F. Dirassouyan, and P. Moulin, *Landfill leachate treatment: review and opportunity*. Journal of Hazardous Materials, 2008. **150**: p. 468-493.

14. Allen, A., *Containment landfills: The myth of sustainability*. Engineering Geology, 2001. **60**(1-4): p. 3-19.

15. Farquhar, G.J. and F.A. Rovers, *Gas production during refuse decomposition*. Water, Air and Soil Pollution, 1973. **2**(4): p. 483-495.

16. Christensen, T., R. Cossu, and R. Stegmann, *Sanitary landfilling: Process, technology and environmental impact*. . 1989, London: Academic Press Limited.

17. Karthikeyan, O.P. and K. Joseph, *Bioreactor landfills for sustainable solid waste management*, A.U. Centre for Environmental Studies, Chennai, Editor. 2006.

18. Crowley, D., A. Staines, C. Collins, J. Bracken, M. Bruen, J. Fry, V. Hrymak, D. Malone, B. Magette, M. Ryan, and C. Thunhurst, *Health and environmental effects of landfilling and incineration of waste - a literature review*. 2003, School of Food Science and Environmental Health: Dublin.

19. Carey, P., *Landfill manuals - landfill site design*, G. Carty, Editor. 2000, Environmental Protection Agency: Ireland.

20. Bogner, J., M.A. Ahmed, C. Diaz, A. Faaij, Q. Gao, S. Hashimoto, K. Mareckova, R. Pipatti, and T. Zhang, *Waste Management*, in *Climate Change 2007: Mitigation. Fourth Assessment Report of the Intergovernmental Panel on Climate Change* B. Metz, et al., Editors. 2007: Cambridge (UK) and New York (USA).

21. Jensen, D.L., A. Ledin, and T.H. Christensen, *Speciation of heavy metals in landfill leachate polluted groundwater.* Water Research, 1999. **33**: p. 2642-2650.

22. Gajski, G., V. Orescanin, and V. Garaj-Vrhovac, *Chemical composition and genotoxicity assessment of sanitary landfill leachate from Rovinj, Croatia.* Ecotoxicology and Environmental Safety, 2012. **78**: p. 253-259.

23. Mukherjee, S., S. Mukhopadhyay, M.A. Hashim, and B.S. Gupta, *Contemporary environmental issues of landfill leachate: Assessment & remedies.* Critical Reviews in Environmental Science and Technology, 2015. **45**(5): p. 472-590.

24. Christensen, T.H., P. Kjeldsen, P.L. Bjerg, D.L. Jensen, J.B. Christensen, A. Baun, H.-J. Albrechtsen, and G. Heron, *Biogeochemistry of landfill leachate plumes. Review.* Applied Geochemistry, 2001. **16**: p. 659-718.

25. Fatta, D., A. Papadopoulos, and M. Loizidou, *A study on the landfill leachate and its impact on the groundwater qulity of the greater area.* Environmental Geochemistry and Health, 1999. **21**: p. 175-190.

26. Mor, S., K. Ravindra, R. Dahiya, and A. Chandra, *Leachate characterization and assessment of groundwater pollution near municipal solid waste landfill site.* Environmental Monitoring and Assessment, 2006. **118**: p. 435-456.

27. Vadillo, I., B. Andreo, and F. Carrasco, *Groundwater contamination by landfill leachate in a karstic aquifer.* Water, Air and Soil Pollution, 2005. **162**: p. 143-169.

28. Lee, G.F. and R.A. Jones, *Landfills and ground-water quality.* Ground Water, 1991. **29**(4): p. 482-488.

29. Ibrahim, M. and N.A.M. Mohamed, Improving sustainability concept in developing countries. Towards sustainable management of solid waste in Egypt. Procedia Environmental Sciences 2016. **34**: p. 336-347.

30. Gotvajn, A.Z. and A. Pavko, Perspectives on biological treatment of sanitary landfill leachate, in Wastewater Treatment Engineering. 2015, IntechOpen.

31. Gao, J., V. Oloibiri, M. Chys, W. Audenaert, B. Decostere, H. Yanling, H.V. Langenhove, K. Demeestere, and S.W.H.V. Hulle, *The present status of landfill leachate treatment and its development trend from a technological point of view.* Reviews in Environmental Science and Bio/Technology, 2015. **14**: p. 93-122.

32. Rafizul, I.M. and M. Alamgir, Characterization and tropical seasonal variation of leachate: results from landfill lysimeter studies. Waste Management, 2012. **32**: p. 2080-2095.

33. Fenn, D.G., K.J. Hankley, and T.V. Degeare, *Use of the water balance method for predicting leachate generation at solid waste disposal sites.* 1975, U.S. Environmental Protection Agency: Cincinnati.

34. Bhalla, B., M.S. Saini, and M.K. Jha, *Effect of age and seasonal variations on leachate characteristics of municipal solid waste landfill.* International Journal of Research in Engineering and Technology, 2013. **02**(08): p. 223-232.

35. Fenn, D.G., K.J. Hanley, and T.V. DeGeare, *Use of the water balance method for predicting leachate generation at solid waste disposal sites.* 1975, United States Environmental Protection Agency: Cincinnati.

36. El-Fadel, M., A. Findikakis, and J.O. Leckie, *Modeling leachate generation and transport in solid waste landfills.* Environmental Technology, 1997. **18**(7): p. 669-686.

37. Perrier, E.R. and A.C. Gibson, *Hydrologic simulation on solid waste disposal sites.* 1981, U.S. Environmental Protection Agency: Cincinnati.

38. Schroeder, P.R., Hydrologic evaluation of landfill performance. Report of Water Resources Engineering Group. 1983, U.S. Army Engineers Vicksburg.

39. Guidance for the treatment of landfill leachate, U.K. Environmental Agency, Editor. 2007.

40. McDougall, F., P. White, M. Franke, and P. Hindle, *Integrated solid waste management: a life cycle inventory.* 2001, Oxford: Blackwell Science.

41. Bicudo, J. and I. Pinheiro, Quantitative and qualitative characterization of the leaching waters of Loures and Vila Franca de Xira inter-municipal landfills. 1993, Portuguese National Laboratory of Civil Engineering: Lisboa.

42. Brennan, R.B., M.G. Healy, L. Morrison, S. Hynes, D. Norton, and E. Clifford, *Management of landfill leachate: The legacy of European Union Directives.* Waste Management, 2016. **55**: p. 355-363.

43. Pedroso, M.A.R., Assessment study on the leachate management options in five municipal solid waste landfill facilities. 2007, Technical University of Lisbon: Lisboa.

44. Kurniawan, T.A., W. Lo, and G. Chan, *Physicochemical treatments for removal of recalcitrant contaminants from landfill leachates.* Journal of Hazardous Materials, 2006. **129**: p. 80-100.

45. Stegmann, R., K.-U. Heyer, and R. Cossu. *Leachate treatment.* in *10th International Waste Management and Landfill Symposium.* 2005. Sardinia, Italy: CISA, Environmental Sanitary Engineering Centre.

46. Oloibiri, V., M. Chys, S. De Wandel, K. Demeestere, and S.W.H. Van Hulle, Removal of organic matter and ammonium from landfill leachate through different scenarios: Operational cost evaluation in a full-scale case study of a Flemish landfill. Environmental Management, 2017. **203**: p. 774-781.

47. Scandelai, A.P.J., L.C. Filho, D.C.C. Martins, T.K.F.S. Freitas, J.C. Garcia, and C.R.G. Tavares, *Combined processes of ozonation and supercritical water oxidation for landfill leachate degradation.* Waste Management, 2018. **77**: p. 466-476.

48. Li, H.-s., S.-q. Zhou, Y.-b. Sun, P. Feng, and J.-d. Li, *Advanced treatment of landfill leachate by a new combination process in a full-scale plant.* Journal of Hazardous Materials, 2009. **172**: p. 408-415.

49. Meeroff, D.E. and J. Lakner, *Safe discharge of landfill leachate to the environment* 2014, Center for Solid and Hazardous Waste Management, University of Florida.

50. Azreen, I. and A.Y. Zahrim, Overview of biologically digested leachate treatment using adsorption, in Anaerobic digestion processes: Applications and effluent treatment, N. Horan, A.Z. Yaser, and N. Wid, Editors. 2018, Springer Nature: Singapore.

51. Pastore, C., E. Barca, G. Del Moro, C. Di Iaconi, M. Loos, H.P. Singer, and G. Mascolo, Comparison of different types of landfill leachate treatment by employment of nontarget screening to identify residual refractory organics and principal component analysis Science of the Total Environment, 2018. **635**: p. 984-994.

52. Kowalik, P. and S. Laakkonen, Legal requirements and wastewater discharges to Polish water bodies, 1945-2003. Ambio, 2007. **36**(2-3): p. 220-228.

53. Ozturk, I., M. Altinbas, O. Koyuncu, O. Arikan, and C.G. Yangin, *Advanced physico-chemical treatment experiments on young municipal landfill leachates.* Waste Management, 2003. **23**(5): p. 441-446.

54. U., E., Directive 2008/98/EC of the European Parliament and of the Council, of 19 November 2008, on waste and repealing certain Directives. 2008: Available online: http://eur-lex.europa.eu/legal-content/EN/TXT/PDF/?uri=CELEX:32008L0098&from=EN

55. U., E., Directive 2000/60/EC of the European Parliament and of the Council, of 23rd October 2000, establishing a framework for Community action in the field of water policy. 2000: Availabe online: https://eur-lex.europa.eu/resource.html?uri=cellar:5c835afb-2ec6-4577-bdf8-756d3d694eeb.0004.02/DOC_1&format=PDF.

56. U., E., *Council Directive of 21st May 1991 concerning urban waste water treatment.* . 1991: Available online: http://eur-lex.europa.eu/legal-content/EN/TXT/PDF/?uri=CELEX:31991L0271&from=EN.

57. in *Decree-law no. 183/2009, of 10th August*, P. Republic, Editor. 2009: Republic Diary - I Series - A.

58. in *Decree-law no. 236/98, of 1st August*, P. Republic, Editor. 1998: Republic Diary - I Series - A.

59. *Portaria n.º 241-B/2019, of 31st July*, M.o.E.a.E. Transition, Editor. 2019: Republic Diary, series I.

# 3 Landfill leachate treatment: Status and research perspectives

*This chapter provides an overview on the most common treatment technologies, detailing some theoretical background regarding biological nitrogen removal and advanced oxidation processes, specifically photo-Fenton and ozone-based processes. The current situation in the world, and particularly in Portugal, regarding treatment systems for urban landfill leachate treatment and reported costs will also be addressed. The combination of treatment processes becomes mandatory when legal compliance is in view. The proposals of several authors during this last decade, as well as previous research carried out with leachate from the same landfill as the one used in the present study, are thoroughly described and analysed, including the main achievements and estimated treatment costs.*

## 3.1 Treatment technologies

It is well known that for many countries, including in Europe, the co-treatment of leachate with domestic sewage in a municipal WWTP is a quite common practice [1, 2]. This co-treatment is regarded as an economical and feasible solution, with urban wastewater providing an important source of phosphorous, which could otherwise be a limiting factor in the biological treatment of landfill leachate [3, 4]. Nonetheless, due to the identified presence of hazardous persistent compounds in the leachate, which are not removed in the conventional WWTP, this option is now becoming less favourable [5]. A recent study [6], undertaken to investigate the impact of leachate feeding strategies on WWTP, concluded that the co-treatment led to a deterioration in the quality of discharged wastewater (increasing by 12-20% the effluent quality index) and adversely affected aeration energy demand and plant maintenance and operation costs. Moreover, for the EU countries, the Water Framework Directive [7] and Urban Wastewater Treatment Directive [8] have placed tighter regulations on all discharges into receiving waters. So, for WWTPs that receive landfill leachate, plant managers are very apprehensive over its impact on a WWTP ability to meet discharge limits, particularly with respect to total ammonia nitrogen (TAN) and total nitrogen (TN), and also COD and colour. In view of this, a rising number of municipal WWTP have stopped accepting landfill leachate [9] or, at least, established maximum loads (usually for COD and TAN) and many times requiring the payment of a fee to accept the leachate. Also, this option requires the leachate to be transported from the landfill to an off-site WWTP, either via tanker truck or pumped directly through a pipe.

On-site leachate treatment is an alternative to the increasing costs associated with hauling leachate to a local WWTP. These treatment facilities are designed to meet the specific needs of each landfill allowing to treat (partially or completely) their leachate and discharge it into a sanitary sewer (partial treatment) or water body (complete treatment) without any transportation or disposal costs. Nowadays, there is a variety of operations and processes available for on-site landfill leachate treatment, which include recirculation (bioreactor landfill), natural attenuation (constructed wetlands and aerated lagoons), biological processes (aerobic, anaerobic or anoxic, with suspended or attached biomass growth), and physicochemical processes (conventional, membrane technology and advance oxidation processes) [5, 10-15]. Considering that the leachate treatment plants (LTPs), currently, in operation often consist of several of the above-mentioned treatment methods, a brief overview of the main treatment technologies follows. Also, due to their importance for the present PhD thesis, a more detailed theoretical background regarding biological nitrogen removal, coagulation, photo-Fenton and ozonation processes will be provided.

### 3.1.1 Recirculation

Leachate recirculation (or recycling) is one of the least expensive treatment techniques since a treatment plant is not required. Such a set-up is often referred to as a bioreactor landfill [12] and intends to achieve accelerated stabilization of MSW, primarily through the addition of leachate back into the landfill [16]. This involves moisture and air control to enhance the establishment of conditions for efficient biodegradation of the waste organic fractions [5]. Numerous practices have shown that whether via aerobic or anaerobic processes, leachate recirculation in landfills can potentially lead to more rapid waste decomposition, with less time required for stabilization and settlement. However, some setbacks have also been reported [10, 16], namely ponding, saturation and acidic conditions in the landfill (impairing methanogens) due to intensive leachate introduction.

### 3.1.2 Natural attenuation

The usage of constructed wetlands (CW) for leachate treatment has been practiced for many years in different countries with varying degrees of success [17]. They are designed to mimic natural wetland by using aquatic plants, soil and associated microorganisms, with consequent contaminants removal mechanisms that include plant adsorption, soil microbial degradation, chemical oxidation and precipitation, and physical sedimentation and filtration [18]. Nitrogen and some toxic contaminants in leachate can be removed through phytoremediation and effect of root zone, where plant roots supply oxygen for the nitrifying bacteria and other microorganisms growing in the rhizosphere of wetland plants. Also, the extensive root system provides a larger surface area for attached microorganisms, increasing the potential for the decomposition of organic matter [15]. The plants that are commonly used in CWs are cattail (*Typha latifolia*), willow-coppice (*Salix sp.*), reed (*Phragmites australis*), rush (*Juncus effusus*), yellow flag (*Iris pseudacorus*) and mannagrass (*Glyceria maxima*) [17, 19].

Despite its potential performance, CW use on a full-scale in developed countries has not been extensively pursued due to poor performance in winter and extensive land area requirements. However, in developing countries, with warm tropical and subtropical climates, not only a good biological activity is expected but also landfill leachate volume-saving (reducing environmental pollution and preventing the dispersion of polluted leachate). Where land is available at low-cost, systems such as constructed wetlands, are attractive alternatives for landfill leachate management.

An aerated lagoon (AL) is typically a 1-5m deep basin, with sloping sidewalls, trying to simulate a natural pond bed [12, 20, 21]. In the design of an aerated lagoon, the hydraulic retention time (HRT) is generally the parameter that determines the sizing, and is usually longer than seven days, and may range from 30 to 60 days [21, 22]. Oxygenation is normally carried out by surface aerators or by air injection to ensure an adequate concentration of dissolved oxygen.

According to the literature [21, 23, 24], the removal efficiencies of COD and $BOD_5$ vary widely and depend mainly on HRT and temperature, but also on aeration rate, organic load of the leachate and available nutrients. Ideally, HRT should be between 5 days at 20 ºC and 10 days at 10 ºC, and it is possible to obtain $BOD_5$ and COD removal percentages greater than 90% when HRT exceeds 10 days (for values of $BOD_5/COD > 0.4$) [25]. The complexity associated with nitrogen removal through the nitrification process generally occurs with low removal efficiencies when using aerated lagoons, given the difficulty in providing optimal conditions for the activity of the autotrophic bacteria responsible for oxidation of nitrogen compounds, leading to HRT greater than 60 days [23, 25].

The great advantage associated with this treatment process is the low operation and maintenance cost compared to other methods, making it very attractive. This system also allows compensating for variation in leachate production, by accommodating the excess leachate due to precipitation events, and composition, by allowing its homogenization. When these are the main purposes, then this type of process is normally called stabilization lagooning. This is an important feature concerning operational control for following treatment units (if used), as a constant flow rate can be assumed when sizing downstream stages. However, due to all the factors involved, it is difficult to achieve the satisfactory removal rates presented in the literature [10]. Besides, the high area of implantation, the release of odours (mostly, when the amount of oxygen is limited) and the high sludge production are negative aspects associated with this treatment process [22].

### 3.1.3 Biological treatment

Many biological techniques currently in use for landfill leachate treatment are adaptations of wastewater treatment methods [12]. Anaerobic or anoxic biological processes have been considered the cheapest ones to eliminate organic and nitrogenous matter from leachate [26], particularly for young leachates, i.e. when the $BOD_5/COD$ ratio has a high value ($> 0.5$), attaining up to 50% of COD removal [12, 14]. With time, the major presence of refractory compounds (mainly humic and fulvic acids) tends to limit the effectiveness of biological processes [27]. So, for old leachate with

rich nitrogen concentrations and poor $BOD_5$/COD ratios (< 0.1), such systems are less suitable, except for nitrification/denitrification (normally requiring the addition of an external carbon donor). Following, a brief description of the main biological treatment technologies applied to landfill leachate treatment is presented, including the respective advantages and drawbacks. Table 3.1 summarizes the information on the performance of the mentioned biological treatments. Considering the relevance of biological nitrogen removal for the work developed in this thesis, further information on this matter will also be provided.

### 3.1.3.1 Biological treatment technologies

*Conventional activated sludge (CAS)*

This treatment process shares the same basis as the aerated lagoons (AL), i.e. microorganisms are used to treat the leachate, but unlike the latter, it is possible to control the bacterial population through sludge recirculation, which leads to a significant reduction in HRT (between 1 to 20 days) [25]. CAS consists of a completely mixed aeration reactor where biodegradation occurs, usually a tank equipped with an aeration system, and a downstream clarifier where sludge is settled and recirculated back to the reactor. Due to its intensive aeration and large populations of acclimatized bacteria, the activated sludge process offers a more intensive treatment than AL [22]. Inadequate sludge settling, the need for long aeration times, high energy requirements and inhibition of microorganisms by high TAN concentrations are some of the disadvantages that have shifted the focus on activated sludge to other more robust technologies [10, 12].

*Sequencing batch reactor (SBR)*

SBR is a variation of the conventional activated sludge system in which biological treatment, equalization, sludge settling and clarification take place in the same tank over a time sequence [12]. Each operation cycle in the SBR generally consists of five different phases: fill, react, settle, draw, and idle. The length of each phase is based on the characteristics of the effluent to be treated, so the total cycle time is expressed as the sum of the five phases [28, 29]. This kind of operation creates a robust treatment less affected by frequent variation of organic load or TAN [30], which is an important feature when dealing with a wastewater presenting variable flow and contamination, such as landfill leachates. These systems allow aerobic and/or anoxic conditions so both nitrification and denitrification can be achieved in the same unit. Despite the good performance and flexible nature, the use of SBR's is marred by problems such as sludge bulking and poor clarification [22].

**Table 3.1** – Performance of different biological processes on the landfill leachate treatment.

| Process[a] | Initial characterization | Removal (%) | Observation[b] | Reference |
|---|---|---|---|---|
| CAS | • Anaerobically pre-treated<br>• COD = 270-1000 mg/L<br>• TAN = 53-270 mg/L | • COD: 22-55<br>• BOD$_5$: > 88<br>• TAN: 60-100 | • HRT = 3-4 d<br>• T = 5, 7 and 10 °C | Hoilijoki, *et al.* [31] |
| | • COD = 3200 mg/L<br>• BOD$_5$/COD = 0.51<br>• TAN = 1750 mg/L | • COD: 75<br>• TAN: 92 | • HRT = 5.5 d<br>• OLR = 4.5 g COD/L/d | Ellouze, *et al.* [32] |
| SBR | • COD = 528-3060 mg/L<br>• TAN = 167-1519 mg/L | • COD: 40-50<br>• TAN: > 99 | • 24h-cycle: (1-2h anoxic + 3.75-4.75h aerobic) ×4<br>• SRT = 20 d; T = 20 °C | Spagni, *et al.* [33] |
| | • COD = 1769-2623 mg/L<br>• BOD$_5$/COD ≈ 0.2<br>• TAN = 993-1406 mg/L | • COD: 20-30<br>• TAN: > 98<br>• TN: > 95 | • 24h-cycle: (2h anoxic + 3.75h aerobic) ×4<br>• SRT = 20-25 d; T = 20°C | Spagni and Marsili-Libelli [34] |
| | • COD = 3000 mg/L<br>• BOD$_5$/COD = 0.22<br>• TAN = 1200 mg/L | • COD: 76<br>• TAN: 99 | • 24h-cycle: 1h fill + 4h anoxic + 5h aerobic + 2h anoxic + 3h aerobic + 8h settle + 1h decant | Li, *et al.* [35] |
| | • COD = 680 mg/L<br>• BOD$_5$/COD = 0.16<br>• TAN = 312 mg/L | • COD: 49<br>• TAN: 100 | • 24h-cycle: 0.25h fill + 10h anoxic + 1.5h settle + 0.25h decant | Klimiuk and Kulikowska [36] |
| | • COD = 5750 mg/L<br>• TAN = 185 mg/L | • COD: 31 | • 21h-cycle: (1h anaerobic + 1h anoxic + 2h aerobic + 1h anoxic + 1h aerobic)×3 | Uygur and Kargi [37] |
| | • COD = 4357 mg/L<br>• TAN = 3772 mg/L | • COD: 25-30<br>• TAN: 10-36<br>• TN: 15-20 | • SRT = 25-39 d; T = 36 °C<br>• 24h-cycle: 14 fill anoxic events each followed by 85 min aerobic phase | Ganigué, *et al.* [38] |
| | • COD = 1674 mg/L<br>• TAN = 1268 mg/L | • COD: 29<br>• TAN: 98<br>• TN: 80 | • SRT = 29 d; T = 16-19 °C<br>• step-feed strategy and alternating anoxic-aerobic (8/12h-cycle) | Monclús, *et al.* [39] |
| | • COD = 3876 mg/L<br>• BOD$_5$/COD = 0.14<br>• TAN = 1451 mg/L | • COD: < 7<br>• TAN: > 95 | • Mixture of Annamox biomass and activated sludge (80% w/w)<br>• 12h-cycle: anaerobic-aerobic - anoxic | Xu, *et al.* [40] |
| MBR | • COD = 18,685 mg/L<br>• TN = 310 mg/L | • COD: 89<br>• TN: 85 | • 9 g/L of biomass<br>• Addition of KH$_2$PO$_4$ | Insel, *et al.* [41] |
| | • COD = 1550 mg/L<br>• TAN = 1451 mg/L | • COD: 63<br>• TAN: 98 | • HRT = 32 h; SRT = 80 d<br>• OLR = 1.3 g COD/L/d | Zolfaghari 2016 |
| | • COD = 4224 mg/L<br>• TAN = 1547 mg/L | • COD: 45 | • 1.5 bar; SRT > 45 d<br>• Tubular ceramic UF membrane (external) | Canziani, *et al.* [42] |
| RBC | • COD = 3950 – 14,000 | • COD: 52 | • HRT = 1 d<br>• OLR = 24.7 g COD/m$^2$ d | Castillo, *et al.* [43] |
| UASB | • COD = 11939 mg/L<br>• TAN = 1679 mg/L | • COD: 80<br>• TAN: no removal | • HRT = 1.6 d<br>• OLR = 7.5 g COD/L/d | Castrillón, *et al.* [44] |
| | • COD = 1770 mg/L | • COD: 40 | • HRT = 2-7 days | Kawai, *et al.* [45] |

[a] CAS – conventional activated sludge; SBR – sequencing batch reactor; MBR – membrane bioreactor; RBC – rotating biological contactor; UASB – upflow anaerobic sludge blanket. [b] HRT – hydraulic retention time; OLR – organic loading rate; SRT – sludge retention time.

*Membrane bioreactor (MBR)*

This process has gained a lot of attention for the treatment of landfill leachate [46]. MBRs are essentially composed of two parts: (i) a bioreactor, dealing with the removal of organics and (ii) a membrane module, for the separation of treated leachate from biomass [26]. MBR systems are usually designed as ultrafiltration (UF) and/or microfiltration (MF) in a hollow fibre, plate, or frame. The membrane can be fitted externally (sidestream) or within (submerged) the reactor tank. In comparison to the conventional activated sludge systems, MBRs allow for complete retention of the biomass in the system by replacing the secondary clarifier with a membrane module. The MBR can operate with long sludge age, high concentrations of biomass (up to 20 mg/L), and attain a clarified effluent [26, 46, 47]. Additional important advantages are also higher loading rates, smaller volumes, lower production of excess sludge, and easier development of microorganisms with lower growth rates. However, the presence of high concentrations of inorganic compounds in the leachate causes membrane fouling, consequently decreasing productivity and membrane lifespan [22, 46]. The main drawbacks pointed out for MBRs full-scale operations are the high membrane costs, membrane fouling (leading to increased operational and membrane replacement costs), and high energy consumption.

*Rotating biological contactor (RBC)*

RBC is an attached growth bioreactor that offers an alternative technology to the CAS process. In an RBC unit, the pollutants contained in the leachate are removed by the biofilm that is established on the entire surface area of the support material (usually flat or corrugated disks), which continually rotates [15]. For this reason, RBCs are more appropriate for the treatment of leachate from old landfills. This treatment method consumes relatively low amounts of energy and temperature effects are easier to control at RBC's, because they are compact and normally covered [48]. If the support material is completely submerged in the leachate to be treated and the reactor tightly closed to avoid air entrance, they can also be used for leachate denitrification [49]. Treating high organic polluted leachates may result in clogging by means of inorganic precipitates and/or produced biomass [48]. Other drawbacks pointed to RBCs are the slow process start-up, need of adequate primary treatment and secondary clarifier, limited process flexibility and difficulty to maintain an appropriate biofilm thickness under adverse conditions [15, 49].

*Upflow anaerobic sludge blanket (UASB)*

This is an anaerobic treatment carried out by metabolically active granular sludge with enhancing settling characteristics that ensure great biomass retention regardless the HRT [5, 15]. In this bioreactor, the wastewater flows upwards through the blanket of granular sludge that converts the organic pollutants into biogas (methane and carbon dioxide) [11]. The upward motion of the biogas bubbles promotes mixing in the sludge bed. The main disadvantage of this treatment is the high sensitivity to toxic substances and the limited TAN removal [11, 15].

### 3.1.3.2 Biological nitrogen removal

*Nitrification*

Nitrogen can trigger eutrophication in receiving watercourses and its removal from landfill leachate is not only desirable but, in many countries, legally mandatory. Nitrification is a two-step process accomplished by autotrophic bacteria where ammonia ($NH_4^+$) is oxidised to nitrite ($NO_2^-$), by ammonia-oxidizing bacteria (AOB), according to Equation 3.1. Then, the $NO_2^-$ is further on oxidised to nitrate ($NO_3^-$), by nitrite-oxidizing bacteria (NOB), as shown by Equation 3.2:

$$2NH_4^+ + 3O_2 \rightarrow 2NO_2^- + 4H^+ + 2H_2O \tag{3.1}$$

$$2NO_2^- + O_2 \rightarrow 2NO_3^- \tag{3.2}$$

Each oxidative stage is performed by different bacterial genera which use $NH_4^+$ or $NO_2^-$ as energy source and molecular oxygen ($O_2$) as electron acceptor, while carbon dioxide ($CO_2$) is used as a carbon source. The most recognized genus of bacteria that carries out ammonia oxidation is *Nitrosomonas*. However, *Nitrosococcus*, *Nitrosopira*, *Nitrosovibrio* and *Nitrosolobus* are also able to oxidize ammonium to nitrite [50]. These ammonia oxidizers are genetically diverse, but related to each other, and can be found in the beta subdivision of the *Proteobacteria*. For nitrite oxidation several genera such as *Nitrospira*, *Nitrospina*, *Nitrococcus*, and *Nitrocystis* are known to be involved. However, the most famous nitrite oxidizing genus is *Nitrobacter*, which genetically is closely related to the alpha subdivision of the *Proteobacteria* [50]. The complete oxidation reaction for nitrification is shown in Equation 3.3:

$$NH_4^+ + 2O_2 \rightarrow NO_3^- + 2H^+ + H_2O \tag{3.3}$$

Being an aerobic process, the concentration of dissolved oxygen (*DO*) should be high for nitrification to occur effectively, not less than 1 mg/L, and evenly distributed in the reactor [51]. The temperature affects the growth of nitrifying bacteria and should not be below 8°C or above 30°C to achieve an ideal growing rate. Reaction rates are typically assumed to double for every 10 °C increase in temperature (i.e. Arrhenius rate law). Present reports [52] also show that high temperature of 28-38 ºC may favour nitrogen removal via nitrite since the specific growth rate of AOB is higher than that of NOB. Some researchers also verified that nitritation start-up could be promoted and accelerated at high temperatures [53].

The optimum pH for most nitrifiers varies from 7.5 to 8.5, and since nitrification reaction will produce $H^+$ (see Equation 3.1), lowering the pH value, the alkalinity in the water should be adequate to balance the produced acidity [54]. Theoretically, 7.14 mg of alkalinity is consumed per 1 mg of $NH_4^+$-N oxidized. The pH of mature leachates is around 8.0 - 8.5 and during aeration it can increase up to pH 9 and higher. Under these circumstances, the equilibrium shifts from ammonium to free ammonia (FA) in the gas phase with potential inhibitory effect on nitrifying bacteria. Anthonisen*, et al.* [55] observed that both ammonium and nitrite oxidations are inhibited by FA; inhibition of nitrite oxidation by *Nitrobacter* began at a concentration of 0.1–1.0 mg FA/L, while ammonium oxidation by *Nitrosomonas* became inhibited at 10–150 mg FA/L, allowing selective inhibition of nitrite oxidation at a range of FA concentrations of 1.0–10 mg/L. Supporting this observation, a later study by Bae*, et al.* [56] reported that nitrite accumulation occurred at an initial FA concentration of around 4.7 mg/L, giving a high $NO_2/NO_X$ ratio (up to 77%) in a batch reactor. Chung*, et al.* [57] accomplished a long-term accumulation of nitrite in a continuous-flow reactor by maintaining the FA concentration in the reactor around 20 mg/L. Chung*, et al.* [58], however, found that a FA concentration of 5–10 mg/L was most efficient in inhibiting nitrite oxidation without slowing down the rate of ammonium oxidation.

### *Denitrification*

A subsequent process - denitrification - is generally performed by heterotrophic denitrifiers under anoxic conditions. The oxidized nitrogen compounds ($NO_2^-$ and $NO_3^-$) are reduced to gaseous nitrogen ($N_2$) by heterotrophic microorganisms that use nitrite and/or nitrate instead of $O_2$ as electron acceptors and organic matter as a carbon and energy source. Denitrifiers are common among the Gram-negative bacteria such as *Pseudomonas*, *Alcaligenes*, *Paracoccus*, and *Thiobacillus*. Some Gram-positive bacteria (such as *Bacillus*) and a few halophilic archaeal microorganisms (e.g. *Haloferax denitrificans*) are also able to denitrify [59, 60]. Denitrifying

bacteria are ubiquitous in nature [61] and numerous researchers cultivated them using mixed cultures taken from wastewater treatment plants as seeds. During the denitrification process, $NO_3^-$ is reduced to $N_2$ (Equation 3.4):

$$NO_3^- \rightarrow NO_2^- \rightarrow NO \rightarrow N_2O \rightarrow N_2 \qquad (3.4)$$

Denitrification requires anoxic environments since the process only relies on the addition of an external carbon source and presence of $NO_3^-$ and/or $NO_2^-$. Among carbon sources, the most common ones are methanol, ethanol and acetic acid [62, 63] which have been used for wastewater denitrification, as well as in full-scale plants of drinking water treatment [64]. A combined carbon source using methanol and acetic acid was found to be superior in nitrogen removal and additional benefits of this mixed carbon source included the excellent sludge settling properties compared to the use of methanol or acetic acid alone [65]. The choice of substrate depends on several considerations such as costs, capacity, and configuration of reactors and on the post-treatment process of the denitrified water. Theoretically, 2.86 g COD is required during the denitrification process to convert one gram of nitrate nitrogen ($NO_3^-$-N) into $N_2$. Nonetheless, a larger required amount of COD is almost always assumed, often an amount between 3.5–5 g COD/g N is used (Ekenberg, 2007). Also, considering methanol ($CH_3OH$) as carbon source for denitrification, the theoretically required amount is 2.47 mg $CH_3OH$ per mg $NO_3^-$ -N (Equation 3.5) [66, 67].

$$6NO_3^- + 5CH_3OH \rightarrow 3N_2 + 5CO_2 + 7H_2O + 6OH^- \qquad (3.5)$$
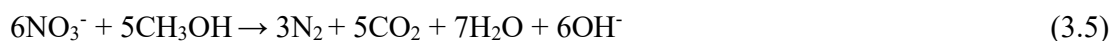
The denitrification process is not as sensitive to parameters in the effluent as nitrification. However, it requires anoxic conditions and the presence of methanol, or other carbon-based molecules [51]. The optimal temperatures have shown to be from 5 to 30°C [68]. The pH will also have an impact on denitrification, and the optimal pH has shown to be from 7 to 9. A pH below 7 can cause production of nitric oxide *NO* which is a toxic gas [54, 69]. Heterotrophic denitrification itself can increase the pH because it causes a release of hydroxyl ions and raises alkalinity. Each mg of $NO_3^-$ -N reduced to $N_2$ induces an alkalinity increase of 3.57 mg $CaCO_3$.

Oxygen and organic matter requirements involved in nitrification and denitrification contribute to the operational costs of the biological treatment. Partial nitrification is one strategy that is based on the accumulation of nitrite, which is the intermediary compound in both nitrification and denitrification [70]. In this strategy, ammonium is just partially oxidized to nitrite and the nitrite thus obtained is then denitrified to nitrogen gas. This eliminates the extra steps of oxidation to nitrate followed by reduction back to nitrite, found in the standard nitrification/denitrification designs. In this way, it is possible to save 25% of the oxygen uptakes for nitrification and 40% of the carbon

needs for denitrification (particularly interesting for low COD/N ratio effluents, such as mature landfill leachate [34, 71, 72]).

Although not explored during this thesis, another strategy for nitrogen removal that must be mentioned is the anaerobic ammonium oxidation (Anammox). In this process, under anaerobic conditions, ammonium is oxidized to nitrogen gas with nitrite as the electron acceptor. This is an autotrophic process, so $CO_2$ is used for growth of the bacteria, therefore biodegradable organic carbon is not required (cost savings with external carbon donor) [73]. Also, the biomass yield is very low, and consequently, little sludge is produced contributing to lower operational costs [73]. So, combining partial nitrification via nitrite with Anammox is also an interesting approach when dealing with leachates [74-76].

### 3.1.4 Conventional physicochemical processes

Physicochemical methods are often coupled to biological methods mainly to improve treatment efficiency or make the biological oxidation process possible when hampered by the presence of bio-refractory materials [13]. These techniques are applied for removing non-biodegradable (mostly humic and fulvic acids) and/or undesirable compounds (such as, heavy metals, halogenated organic compounds (AOXs), polychlorinated biphenyls (PCBs), among others) from the leachate. Conventional physicochemical techniques frequently applied to landfill leachates include coagulation-flocculation (C/F), chemical precipitation, air (ammonia) stripping and adsorption. Typically, these techniques are used as post-treatment for biological processes, when a municipal sewage system is intended for final discharge, or as pre-treatment for more advanced physicochemical treatment processes (i.e. pressure-driven membrane technologies and advanced oxidation processes), when aiming direct discharge into a waterbody. Table 3.2 summarizes information on the performance of the main conventional physicochemical processes applied to landfill leachate treatment. Following is a brief description for the mentioned techniques, including main advantages and drawbacks.

**Table 3.2** – Performance of conventional physicochemical processes applied to the treatment of leachate.

| Process[a] | Initial characterization | Removal (%) | Observation[b] | Reference |
|---|---|---|---|---|
| C/F | • COD = 3000-4500 mg/L<br>• $BOD_5/COD$ = 0.09-0.22<br>• TAN = 1000-1750 mg/L | • COD: 28, 32 and 24, for pH = 4, 5 and 6, respectively. | •$[Fe_2(SO_4)_3]$ = 0.6 g/L + 1mL polyacrylamide (0.1% v/v) | Guo, et al. [77] |
| | • COD = 18 352 mg/L<br>• $BOD_5/COD$ = 0.6<br>• TAN = 2445 mg/L | • COD: 28<br>• Colour: 78<br>• Turbidity: 90 | • pH = 3.8<br>•$[FeCl_3]$ = 1.2 g/L | Castrillón, et al. [44] |
| | | • COD: 27<br>• Colour: 84<br>• Turbidity: 93 | • pH = 6<br>•$[Al_2(SO_4)_3]$ = 5 g/L | |
| | | • COD: 35<br>• Colour: 91<br>• Turbidity: 90 | • pH = 6.5<br>• [PAC] = 4 g/L | |
| | • COD = 4814 mg/L<br>• $BOD_5/COD$ = 0.14<br>• TAN = 2950 mg/L | • COD: 73<br>• Colour: 98<br>• Turbidity: 100 | • pH = 5.2<br>•$[FeCl_3]$ = 1.7 g/L | |
| | | • COD: 60<br>• Colour: 95<br>• Turbidity: 92 | • pH = 6<br>•$[Al_2(SO_4)_3]$ = 3.2 g/L | |
| | | • COD: 62<br>• Colour: 97<br>• Turbidity: 98 | • pH = 7<br>• [PAC] = 6 g/L | |
| | • COD = 14 680 mg/L<br>• $BOD_5/COD$ = 0.10<br>• TAN = 381 mg/L | • COD: 18<br>• DOC: 82<br>• TAN: 36 | • pH = 3<br>•$[FeCl_3.H_2O]$ = 0.3 g/L | Vedrenne, et al. [78] |
| | • COD = 5700 mg/L<br>• $BOD_5/COD$ = 0.07<br>• Turbidity = 140 NTU | • COD: 39<br>• Turbidity: 6 | • pH = 6<br>•$[Al_2(SO_4)_3]$ = 2 g/L | Amor, et al. [79] |
| | | • COD: 63<br>• Turbidity: 83 | • pH = 5<br>•$[FeCl_3]$ = 2 g/L | |
| Chemical precipitation | • COD = 9700 mg/L<br>• $BOD_5/COD$ = 0.15<br>• TAN = 2600 mg/L | • TAN: 98 | • pH = 9<br>• Molar ratio of $Mg^{2+}$:$NH_4^+$:$PO_4^{3-}$ = 2:1:1 | Di Iaconi, et al. [80] |
| | • COD = 4295 mg/L<br>• $BOD_5/COD$ = 0.49<br>• TAN = 1750 mg/L | • COD: 9<br>• TAN: 82 | • pH = 5.3-8.4<br>• Molar ratio of $Mg^{2+}$:$NH_4^+$:$PO_4^{3-}$ = 3:1:1 | Huang, et al. [81] |
| Ammonia stripping | • COD = 3000-4500 mg/L<br>• $BOD_5/COD$ = 0.09-0.22<br>• TAN = 1000-1750 mg/L | • TAN: 97 | • pH = 11<br>• $t$ = 18 h | Guo, et al. [77] |
| | • COD = 3484 mg/L<br>• TAN = 2156 mg/L | • COD: 46<br>• TAN: 94 | • pH = 12<br>•$[Ca(OH)_2]$ = 10 g/L | Castrillón, et al. [44] |
| Adsorption | • Previously coagulated<br>• COD = 500 mg/L | • COD: 25, for GAC<br>• COD: 35, for PAC | • $t$ = 2 h<br>• GAC = 1.25 g/L (0.6 mm, BET surface area 1250 $m^2$/g)<br>• PAC = 1.25 g/L (0.15 mm, BET surface area 1250 $m^2$/g) | Papastavrou, et al. [82] |
| | • COD = 3484 mg/L<br>• TAN = 2156 mg/L | • COD: 63<br>• Colour: 45 | • $t$ = 5 h<br>• GAC = 20 g/L (0.4-1.7 mm, BET surface area 1020 $m^2$/g | Castrillón, et al. [44] |

[a] C/F – coagulation/flocculation. [b] PAC - aluminium polychloride (C/F process); GAC – granular activated carbon and PAC – powered activated carbon (Adsorption process).

### Coagulation/flocculation (C/F)

It is a relatively simple technique used to remove suspended solids, colloidal particles, colour, organic load (humic acids and halogenated organic constituents characterized by the parameters COD and AOX) and heavy metals from the leachate [83-85]. Because the removal efficiency of organic particles is directly proportional to their molecular weight, C/F is more appropriate for the treatment of old landfill leachate ($CBO_5$/COD ratio < 0.1), or for effluents coming from a previous biological treatment. Removal of suspended solids may be as high as 75%, while COD and AOX removal efficiencies may range from 40% to 75%. This treatment process is not effective in removing ammonia nitrogen [25], and the biodegradability is not affected [86]. The most used coagulants are ferric chloride ($FeCl_3$) and aluminium sulfate (alum – $Al_2(SO_4)_3$) due to their low cost and good efficiency [84, 85]. An associated disadvantage is the high sludge production, the sensitivity of the process to pH, and the increased concentration of aluminium or iron, and also of chloride and/or sulfate in the leachate effluent [20, 48].

### Chemical precipitation

This process is commonly used as a pre-treatment for leachates, mainly for the removal of ammonium nitrogen but also heavy metals [10]. During chemical precipitation, dissolved ions in the solution are converted to the insoluble solid phase (precipitates) via chemical reactions and can be separated by sedimentation or filtration [15]. Struvite (magnesium ammonium phosphate (MAP)) or lime is usually employed as the precipitant, depending on the target of the removal (TAN or heavy metals, respectively). The advantage of struvite precipitation is that the sludge produced after treatment may be utilized as a nitrogen fertilizer if the leachate does not contain any heavy metals. However, the drawbacks of chemical precipitation include the high dose of precipitant required, the sensitivity of the process to pH, the generation of sludge and the need for further disposal of the sludge [83].

### Air (ammonia) stripping

In this process a large volume of air passes through the leachate to promote mass transfer of some unwanted substances from the liquid to the gas phase [11, 12]. Air stripping is used to remove ammonium (alternatively to biological nitrification) and volatile organic compounds (VOCs)

present in the leachate. The efficiency of the process is increased significantly by increasing values of pH or temperature [22]. A major concern about air stripping is the control and destruction of exhaust air (such as ammonia gas), since its release into the atmosphere cause severe air pollution [11, 12].

*Adsorption*

Adsorption is a mass transfer process by which a substance is transferred from the liquid phase to the surface of a solid through physical and/or chemical interactions. It is a widely employed technique for the removal of recalcitrant organic compounds, colour and heavy metals from landfill leachates [11, 83]. The most used adsorbent is activated carbon (AC), either granular (GAC) or powder (PAC), due to its large surface area, microporous structure, high adsorption capacity and surface reactivity [83]. However, as leachate gets older, it contains it contains a higher fraction of high-molecular-weight complex molecules that are not able to diffuse into the microporous structure of GAC, meaning a lower degree of adsorption. A main disadvantage associated with this process is the frequent regeneration of AC columns, required to avoid clogging issues and restoration of the adsorption capacity, and the high cost of the adsorbent.

### 3.1.5 Membrane technologies

Different membrane filtration techniques (microfiltration (MF), ultrafiltration (UF), nanofiltration (NF), and reverse osmosis (RO)) are used in landfill leachate treatment. The selection of the proper membrane technique depends on several factors such as the nature and concentration of contaminants present in the leachate and pH [11]. NF and RO are considered the most efficient techniques for treating leachates, with NF removing a substantial extent of organics (60-70%), as well as some salts, while RO achieves retention rates > 98% for COD, TAN and heavy metals [15, 83]. Table 3.3 presents some examples regarding the performance of membrane technologies applied to the treatment leachates. In fact, during the last two decades, there was an increasing number of LTPs all over the world that adopted RO technologies [12], despite the requirement for high operating pressure (50–60 bar) to overcome the osmosis pressure and, therefore, high energy demand. It should also be noted that, RO membrane filtration (similarly to active carbon adsorption) only transfer the contaminants from one stream to another and do not solve the environmental problem [12, 15]. Moreover, the RO concentrate that is produced (~ 20-30% by volume) is normally

re-infiltrated back into the landfill, contributing to an influent leachate increasingly more loaded with an expected decrease in the treatment efficiency over time.

When compared to RO, NF membranes present lower operational pressure, high flux, high rejection of polyvalent ions, relatively low investment, operational and maintenance costs [87]. Nonetheless, for both membrane technologies, fouling phenomenon is considered a major demerit for the proper operation, making frequent surface cleaning processes necessary. The most commonly used pre-treatment options, to mitigate organic fouling and to improve the product water quality in the landfill leachate treatment employing NF or RO, are coagulation/flocculation (C/F) and granular activated carbon (GAC) adsorption [88]. Not so often, MF and UF are also used as pre-treatments for NF or RO processes.

**Table 3.3** – Performance of membrane technologies applied to the treatment of landfill leachate.

| Process[a] | Initial characterization | Removal (%) | Observation | Reference |
|---|---|---|---|---|
| MF + PAC | • Mature, biologically pre-treated<br>• COD = 1870 mg/L<br>• TAN = 1280 mg /L<br>• pH = 9.3 | • COD: 63<br>• TAN: 15 | • Cross-flow MF (Delrin®, DuPont, Delaware); hydrophilic cellulose nitrate membranes (0.2 and 0.45 μm)<br>• 2 bar; pH = 9.3; T = 25 ºC<br>• 8 g PAC/L | Ince, *et al.* [87] |
| NF | | • COD: 41<br>• TAN: 53 | • Polymeric membrane (FM NP030), 80 cm$^2$, cut-off 400 Da<br>• 1.1 m/s; 20 bar; pH = 9.3; T = 25 ºC<br>• Target COD value (< 700 mg/L) was no reached by NF. | |
| | • Previously coagulated<br>• TOC = 636 mg/L<br>• TN = 918 mg/L<br>• pH = 7.3 | • TOC: 90<br>• TN: 10 | • Polymeric membrane (NF 270), 21.2 cm$^2$, cut-off 300 Da<br>• 5 bar | Mariam and Nghiem [89] |
| | • COD = 56 521 mg/L<br>• TAN = 196 mg/L<br>• pH = 5 | • COD: 94<br>• TAN: 52<br>• Colour: 84<br>• Cr$^{3+}$: 98<br>• Ni$^{2+}$: 95<br>• Cu$^{2+}$: 93 | • Polymeric membrane (NF 300), 150 cm$^2$, cut-off 300 Da<br>• 900 L/h; 20 bar | Chaudhari and Murthy [90] |
| RO | • COD = 3100 mg/L<br>• TAN = 1000 mg/L<br>• pH = 6.0-6.5 | • COD: > 99<br>• TAN: 99<br>• TSS: > 99<br>• Cl$^-$ = Fe$^{2+}$: 99<br>• Cu$^{2+}$: > 99 | • Full-scale, Hanover, Germany<br>•Polymeric membrane (FT-30), open channel spiral wound, 25.6 m$^2$<br>• 8000 L/h; 20-40 bar | Li, *et al.* [91] |

[a] NF – nanofiltration, RO – reverse osmosis.

### 3.1.6 Advanced oxidation processes (AOPs)

The main objective of these type of processes is to mineralize the contaminants into $CO_2$, $H_2O$, and inorganics or, at least, transform them into harmless products and enhancing the bio-treatability of recalcitrant and/or non-biodegradable organic substances [17]. During the last decade, AOPs for leachate treatment have gained growing interest [11], applying strong oxidizing agents such as ozone ($O_3$), hydrogen peroxide ($H_2O_2$) and persulfate ($S_2O_8^{2-}$), catalysts ($TiO_2$ and $Fe^{2+}$, as most commons), as well as a combination of these oxidants and/or catalysts with radiation (mainly ultraviolet: UV, but also with visible: UV-Vis) or ultrasound (US). At the base of action of these oxidation processes is the generation of the hydroxyl free radical ($^\bullet OH$), which presents a high oxidation potential ($E^0 = 2.80$) that allows the attack of a wide range of organic compounds (phenols, hydrocarbons, acids, alcohols, aldehydes, ketones, among others) up to mineralization. Hydroxyl radicals can be generated by (i) non-photochemical methods, such as conventional Fenton process ($Fe^{2+}/H_2O_2$), ozonation ($O_3$) at high pH ($> 8.0$), and combining ozone with hydrogen peroxide ($O_3/H_2O_2$) or with a catalyst ($O_3$/catalyst), and (ii) photochemical methods, namely photocatalysis ($TiO_2/UV$), photo-Fenton ($Fe^{2+}/H_2O_2/UV$), $H_2O_2/UV$, $O_3/UV$ and $O_3/UV/H_2O_2$. The conventional Fenton process can also be modified by the combined application of electricity and even ultrasound (US). The electro-Fenton (EF) process, in which either or both oxidant and catalyst can be generated electrochemically *in situ*, is an indirect electrochemical oxidation that employs $^\bullet OH$ produced by the Fenton reaction to oxidize organic compounds.

Among various AOPs, Fenton (F) oxidation process, photo-Fenton (PF), and ozone ($O_3$) have been widely reported and are regarded as the most effective methods for landfill leachate treatment, leading to considerable depletions of COD, colour, and significant biodegradability increase (Table 3.4). These processes have been studied either applied to the raw leachate, mainly as a pre-treatment for a subsequent biological process [27, 92-97], or as a polishing step prior to discharge in the environment [98-101]. The high effectiveness demonstrated by these processes has also called attention of the scientific community as possible solutions for the treatment of the severe problem imposed by leachate concentrates coming from membrane processes [102-105]. Some authors [106, 107], also tested the combination of $O_3$ with Fenton to treat mature landfill leachate. The main drawbacks pointed out for AOPs are the high demand of electrical energy (for ozone generators and/or UV lamps), high oxidant doses (expensive reactants) required to attain complete degradation (mineralization), and the need for a control system to allow the treatment to act properly.

**Table 3.4** – Performance of advanced oxidation processes applied to the treatment of landfill leachate.

| Process[a] | Initial characterization | Removal (%) | Observation | Reference |
|---|---|---|---|---|
| F | • Mature leachate<br>• COD = 10 540 mg/L | • COD: 60 | • [$H_2O_2$] = 295 mM<br>• [$Fe^{2+}$] = 830 mg/L | Lopez, *et al.* [108] |
| | • Mix of "old" and "young" leachate<br>• COD = 2072 mg/L<br>• TOC = 769 mg/L | • COD: 70<br>• TOC: ~ 68 | • [$H_2O_2$] = 75 mM<br>• [$Fe^{2+}$] = 2790 mg/L<br>• pH = 2.5; T = 25ºC<br>• $t$ = 60 min | Hermosilla, *et al.* [109] |
| | • After SBR<br>• COD = 1396-2455 mg/L | • COD: 70-85 | • [$H_2O_2$] = 3 M<br>• [$Fe^{2+}$] = 16 750 mg/L<br>• pH = 3.0; T = 40ºC<br>• $t$ = 35 min | Cotman and Gotvajn [110] |
| | • Mature leachate before discharge to urban WWTP<br>• COD = 743 mg/L<br>• $BOD_5$ = 10 mg/L<br>• pH = 3.5<br>• N-$NO_3^-$ = 1824 mg/L | • COD: 31 | • [$H_2O_2$] = 240 mM<br>• [$Fe^{2+}$] = 220 mg/L<br>• pH = 3.0<br>• $t$ = 40 min | Cortez, *et al.* [99] |
| | • Mature leachate before discharge to urban WWTP and diluted 2 ×<br>• COD = 340 mg/L<br>• $BOD_5$/COD = 0.01 | • COD: 46<br>• $BOD_5$/COD = 0.15 | • $H_2O_2$ = 12 mM<br>• [$Fe^{2+}$] = 220 mg/L<br>• pH = 3.0<br>• $t$ = 40 min | Cortez, *et al.* [97] |
| | • After air stripping<br>• COD = 3000–4500 mg/L<br>• $BOD_5$/COD = 0.18 | • COD: 61<br>• $BOD_5$/COD = 0.38 | • [$H_2O_2$] = 20 mL/L<br>• [$Fe^{2+}$] = 4.0 g/L<br>• pH = 3.0<br>• $t$ = 60 min | Guo, *et al.* [77] |
| PF | • Mature leachate after aerated lagoon<br>• COD = 3420 mg/L<br>• DOC = 1045 mg/L<br>• $BOD_5$/COD = 0.07 | • DOC: 24 | • [$H_2O_2$] = 54 mM<br>• [$Fe^{2+}$] = 20 mg/L<br>• pH = 2.8; T = 17 – 35 ºC | Vilar, *et al.* [111] |
| | | • DOC: 86 | • [$H_2O_2$] = 366 mM<br>• [$Fe^{2+}$] = 20 mg/L<br>• $Q_{UV}$ = 206 kJ/L<br>• pH = 2.8; T = 15 – 43 ºC | |
| | • Mature leachate<br>• COD = 3300-4400 mg/L<br>• TOC = 1658-2782 mg/L<br>• $BOD_5$ = 640-780 mg/L | • COD: 86 | • Hg lamp TQ 150: 150W, photonic flow = 8.8 ×$10^{-5}$ Einstein/s<br>• [$H_2O_2$] = 295 mM ÷ 4 feedings<br>• [$Fe^{2+}$] = 2 g/L | Primo, *et al.* [112] |
| | • Mix "old" and "young" leachate<br>• COD = 2072 mg/L<br>• TOC = 769 mg/L | • COD: 70<br>• DOC: ~ 68 | • [$H_2O_2$] = 75 mM<br>• [$Fe^{2+}$] = 90 mg/L<br>• P = 400 W<br>• pH = 2.5; T = 25ºC<br>• $t$ ~ 240 min | Hermosilla, *et al.* [109] |
| | • Mature leachate after aerated lagoon<br>• COD = 3270-4575 mg/L<br>• DOC = 954-1220 mg/L<br>• $BOD_5$/COD = 0.04-0.07 | • DOC: 86 | • CPC = 2.08 $m^2$<br>• [$H_2O_2$] = 306 mM<br>• [$Fe^{2+}$] = 60 mg/L<br>• $Q_{UV}$ = 110 kJ/L<br>• pH = 2.6-2.9 | Rocha, *et al.* [113] |
| | • Mature leachate after aerated lagoon<br>• COD = 4235 mg/L<br>• DOC = 1406 mg/L | • COD: 94<br>• DOC: 86 | • CPC = 39.52 $m^2$<br>• [$H_2O_2$] = 300 mM<br>• [$Fe^{2+}$] = 80 mg/L<br>• pH = 2.8 | Silva, *et al.* [94] |

| Process[a] | Initial characterization | Removal (%) | Observation | Reference |
|---|---|---|---|---|
| EF | • COD = 2500 mg/L | • COD: 70 | • Anode: Ti/IrO$_2$-RuO$_2$-TiO$_2$<br>• Cathode: titanium<br>• [H$_2$O$_2$] = 187 mM<br>• [Fe$^0$] = 1.745 g/L<br>• Current density: 20.6 mA/cm$^2$, inter-electrode gap: 1.8 cm<br>• pH = 2.0; $t$ = 120 min | Wang, et al. [114] |
| PEF | • Mature leachate after biological nitrification and coagulation/aeration<br>• DOC = 337 – 430 mg/L<br>• COD = 1030 - 1505 mg/L<br>• pH = 2.2 – 2.9 | • DOC: 34, for [Fe$^{2+}$] = 12 mg/L<br>• DOC: 42, for [Fe$^{2+}$] = 60 mg/L | • Anode: boron doped Diamond (BDD), 10 cm$^2$<br>• Cathode: carbon-PTFE air-diffusion, 10 cm$^2$<br>• Current density: 200 mA/cm$^2$<br>• [Fe$^{2+}$] = 12 and 60 mg/L | Moreira, et al. [115] |
| | | • DOC: 72 | • [Fe$^{2+}$] = 60 mg/L<br>• pH = 2.8; T = 20ºC | |
| O$_3$ | • Raw leachate diluted 5 ×<br>• COD = 1010 mg/L<br>• BOD$_5$/COD = 0.17<br>• Colour = 2300 Pt-Co units<br>• pH = 8.0<br>• Alkalinity = 1.1 g CaCO$_3$/L | • COD: 57, for [O$_3$] = 1.5 g/h<br>• COD: 81, for [O$_3$] = 2 g/h<br>• Colour: 95 (both conditions) | • Q$_{O_3}$ = 4 L/min<br>• [O$_3$] = 1.5 – 2 g/h<br>• $t$ = 240 min | Ntampou, et al. [116] |
| O$_3$ | • COD = 5230 mg/L<br>• BOD$_5$/COD = 0.1<br>• pH = 8.7<br>• [HCO$_3^-$] = 21 750 mg/L | • COD: 27<br>• BOD$_5$/COD = 0.1 | • Q$_{O_3}$ = 0.2 L/min<br>• [O$_3$] = 80 mg/L<br>• $t$ = 60 min | Tizaoui, et al. [93] |
| O$_3$/H$_2$O$_2$ | | • COD: 48<br>• BOD$_5$/COD = 0.7 | • Similar O$_3$ conditions<br>• [H$_2$O$_2$] = 2 g/L | |
| O$_3$ | • Mature leachate before discharge to municipal WWTP<br>• COD = 743 mg/L<br>• BOD$_5$/COD = 0.01 | • COD: 23<br><br>• COD: 30<br><br>• COD: 36<br><br>• COD: 40 | • Q$_{O_3}$ = 0.83 L/min<br>• [O$_3$] = 112 mg/L<br>• $t$ = 60 min<br>• pH = 3.5, 7, 9 and 11, respectively. | Cortez, et al. [100] |
| O$_3$/H$_2$O$_2$ | | • COD: 47<br><br>• COD: 57<br><br>• COD: 63 | • Same ozonation conditions as described, but with pH = 7<br>• [H$_2$O$_2$] = 200, 400 and 600 mg/L, respectively | |
| O$_3$ | • Mature leachate before discharge to municipal WWTP and diluted 2 ×<br>• COD = 340 mg/L<br>• BOD$_5$/COD = 0.01 | • COD: 27<br>•BOD$_5$/COD = 0.15 | • Q$_{O_3}$ = 0.83 L/min<br>• [O$_3$] = 112 mg/L<br>• pH = 7.0; $t$ = 60 min | Cortez, et al. [97] |
| O$_3$/H$_2$O$_2$ | | • COD: 72<br>•BOD$_5$/COD = 0.24 | • Similar O$_3$ conditions<br>• [H$_2$O$_2$] = 400 mg/L | |
| O$_3$ | • Concentrated leachate from RO process<br>• COD = 1880 mg/L | • COD: 34<br>• Colour: 94<br>•BOD$_5$/COD = 0.33 | • Q$_{O_3}$ = 0.5 L/min<br>• [O$_3$] = 40 mg/L; 1.2 g/h;<br>• pH = 9.0; $t$ = 180 min | Amaral-Silva, et al. [98] |

| Process[a] | Initial characterization | Removal (%) | Observation | Reference |
|---|---|---|---|---|
| $O_3/H_2O_2$ | • $BOD_5/COD = 0.05$<br>• pH = 7.1 | • COD: 44<br>• Colour 87<br>• $BOD_5/COD = 0.29$ | • Similar $O_3$ conditions<br>• $[H_2O_2] = 4$ g/L | |
| F | | • COD: 55<br>• Colour: 71<br>• TAN: 7 | • $[H_2O_2] = 50$ mM<br>• $[Fe^{2+}] = 2790$ mg/L<br>• pH = 3.0; $t = 120$ min<br>• $Q_{O_3} = 0.2$ L/min<br>• $[O_3] = 80$ mg/L<br>• pH = 7.0<br>• $t = 60$ min | Amr and Aziz [107] |
| $O_3$ | • COD = 2180 mg/L<br>• $BOD_5/COD = 0.03$<br>• Colour = 4100 Pt-Co units<br>• TAN = 1065 mg/L<br>• pH = 8.5<br>• $V_L = 2$ L | • COD: 15<br>• Colour: 27<br>• TAN: 0 | | |
| $F + O_3$ | | • COD: 58<br>• Colour: 95<br>• TAN: 9 | | |
| $F/O_3$ | | • COD: 65<br>• Colour: 98<br>• TAN: 12 | • Similar conditions as described above, except:<br>• pH = 7.0; $t = 90$ min | |
| $O_3$ | | • COD: 15<br>• Colour: 25 | Experiments with $O_3$:<br>• $Q_{O_3} = 20$ L/min<br>• $[O_3] = 3.5$ g/h<br>Experiments with US:<br>• US = 100 W, 20 kHz<br>Experiments with $H_2O_2$:<br>• $[H_2O_2] = 60$ mM<br>Experiments with F:<br>• $[Fe^{2+}] = 1675$ mg/L<br>All experiments:<br>• pH = 7; $t = 180$ min | Asaithambi, et al. [92] |
| US | | • COD: 10<br>• Colour: 15 | | |
| $O_3/H_2O_2$ | • COD = 1500 mg/L | • COD: 38<br>• Colour: 47 | | |
| $US/H_2O_2$ | | • COD: 26<br>• Colour: 35 | | |
| $O_3/F$ | | • COD: 88<br>• Colour: 71 | | |
| $US/F$ | | • COD: 40<br>• Colour: 54 | | |
| $O_3/US/F$ | | • COD: 95<br>• Colour: 100 | | |

[a] Abbreviations: F – Fenton; PF – photo-Fenton; EF – electro-Fenton; PEF – photo-electro-Fenton; US - ultrasound

### 3.1.6.1 Photo-Fenton process

Before approaching the photo-Fenton process, it is necessary to review the concepts related to the classical Fenton reaction. The mechanism of free radical generation in a classical Fenton oxidation involves the following key steps (Equations 3.6 through 3.12) [117]:

$$Fe^{2+} + H_2O_2 \rightarrow Fe^{3+} + {}^{\bullet}OH + OH^- \qquad k_{3.6} \approx 70 \text{ M}^{-1} \text{ s}^{-1} \qquad (3.6)$$

$$Fe^{3+} + H_2O_2 \rightarrow Fe^{2+} + OOH^{\bullet} + H^+ \qquad k_{3.7} = 0.001 - 0.01 \text{ M}^{-1} \text{ s}^{-1} \qquad (3.7)$$

$${}^{\bullet}OH + H_2O_2 \rightarrow OOH^{\bullet} + H_2O \qquad k_{3.8} = 3.3 \times 10^7 \text{ M}^{-1} \text{ s}^{-1} \qquad (3.8)$$

$${}^{\bullet}OH + Fe^{2+} \rightarrow Fe^{3+} + OH^- \qquad k_{3.9} = 3.2 \times 10^8 \text{ M}^{-1} \text{ s}^{-1} \qquad (3.9)$$

$$Fe^{3+} + OOH^{\bullet} \rightarrow Fe^{2+} + H^+ + O_2 \qquad k_{3.10} =< 2 \times 10^3 \text{ M}^{-1} \text{ s}^{-1} \qquad (3.10)$$

$$Fe^{2+} + OOH^{\bullet} + H^+ \rightarrow Fe^{3+} + H_2O_2 \qquad k_{3.11} = 1.2 \times 10^6 \ M^{-1} \ s^{-1} \qquad (3.11)$$

$$HO_2^{\bullet} + HO_2^{\bullet} \rightarrow H_2O_2 + O_2 \qquad k_{3.12} = 8.3 \times 10^5 \ M^{-1} \ s^{-1} \qquad (3.12)$$

The above reaction sequence is known as the thermal, or classical Fenton process, as it is driven only by thermal and not photochemical energy. The above net reaction can overall be defined as the dissociation of $H_2O_2$ in the presence of iron as catalyst.

$$2Fe^{2+} + H_2O_2 + 2H^+ \rightarrow 2Fe^{3+} + 2H_2O \qquad (3.13)$$

Iron plays the role of catalyst in the above reactions by changing between $Fe^{2+}$ and $Fe^{3+}$. However, in the Fenton chain reactions, the rate constant for $k_{3.6}$ is 70 $M^{-1} \ s^{-1}$ (Equation 3.6), while that of $k_{3.7}$ is 0.001–0.01 $M^{-1} \ s^{-1}$ (Equation 3.7), meaning that the rate of $Fe^{2+}$ consumption is faster than rate of their generation. There are several reports on the reduction of $Fe^{3+}$ to $Fe^{2+}$ consuming $H_2O_2$ [117, 118], but the reduction of $Fe^{3+}$ to $Fe^{2+}$ is several orders of magnitude slower than the conversion of $Fe^{2+}$ to $Fe^{3+}$ in the presence of hydrogen peroxide ($k_{3.7} <<< k_{3.6}$) [109]. Moreover, $Fe^{3+}$ does not remain in its ionic form and tends, in the absence of other complexing substances, to form complexes with water and hydroxyl ligands. The type of ferric-aqua complex that is formed depends on the pH of the medium. When the pH is 2.3 < pH < 3.5, the complex $Fe[(H_2O)_5OH]^{2+}$ is formed, which is soluble and exhibits photoactivity in the UV-Vis part of the solar spectrum. Above pH 3.5, insoluble $[Fe(H_2O)_6]^{3+}$ begins to form, leading to iron precipitation. Maintaining the pH at acidic values is therefore vital for the Fenton process. So, Equation 3.13 implies that the reaction is completed under acidic conditions i.e. the presence of $H^+$ ions is necessary for the decomposition of $H_2O_2$. These features also result in the production of a large amount of ferric hydroxide sludge during the neutralization stage.

The primary processes involved in leachate treatment by Fenton oxidation are pH adjustment, oxidation, neutralization, coagulation, and precipitation. In the Fenton treatment of landfill leachate, both oxidation and coagulation contribute to the removal of organics [117, 119].

Fenton-like processes operated under irradiation, e.g. photo-Fenton, usually exhibit faster substrate transformation and much faster and higher DOC removals and may demand lower catalyst concentrations than corresponding thermal processes [120, 121]. Photo-Fenton presents two main features: (a) the reduction of $Fe^{3+}$ to $Fe^{2+}$ to produce more hydroxyl radicals via photolysis [117, 119];

$$(Fe-OH)^{2+} + h\upsilon \rightarrow Fe^{2+} + {}^{\bullet}OH \qquad (3.14)$$

And (b) the photo-decarboxylation of ferric carboxylates [109, 117]

$$Fe(III)(RHCO_2) + h\upsilon \rightarrow Fe^{2+} + CO_2 + RH^{\bullet} \tag{3.15}$$

In its turn, the $H_2O_2$ molecule can also be cleaved with a quantum yield of two $^{\bullet}OH$ radicals per quanta of absorbed radiation (Equation 3.16), further boosting the oxidation capacity of the reactional system:

$$H_2O_2 + h\upsilon \rightarrow {}^{\bullet}OH + {}^{\bullet}OH \qquad (\phi_{OH^{\bullet}} = 1 \text{ for UVC light, 254 nm}) \tag{3.16}$$
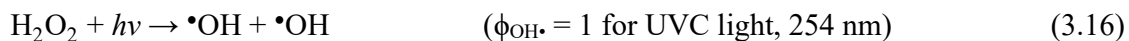
As seen, pH is one of the major factors limiting the performance of (photo-) Fenton, since it affects the speciation of iron and $H_2O_2$ decomposition [122]. Acidic pH highly favours the oxidation reaction as (i) the oxidation potential of $^{\bullet}OH$ decreases with increase in pH from $E_0 = 2.8$ V to $E_{14}$ = 1.96 V [123], (ii) the most photoactive ferric-ion water complex ($FeOH^{2+}$) predominate at pH near 3, and (iii) precipitation of ferric hydroxide ($Fe(OH)_{3\ (s)}$) for pH > 3. Above pH 4, $H_2O_2$ starts to decomposes in a different manner [122] and under alkaline conditions, $H_2O_2$ does not produce $^{\bullet}OH$ radicals [124].

Also important in terms of the process removal efficiency and overall cost is the mass ratio of $H_2O_2$ and $Fe^{2+}$. Excess or shortage of any of these reagents results in the occurrence of scavenging reactions through Equations 3.8 and 3.9 [108], so an optimal $H_2O_2/Fe^{2+}$ ratio is necessary to avoid scavenging effects and increased COD removal. This optimal ratio can greatly fluctuate according to the type of pollutants present, matrix effect in complex wastewaters and to the varying method of determining the optimal dosage [119]. The $H_2O_2/Fe^{2+}$ ratio is required to be kept as low as possible to avoid $^{\bullet}OH$ recombination and reduce final sludge volume. Furthermore, the addition of $H_2O_2$ at the beginning or during the reaction implies changes in the ratios of $H_2O_2/COD$ and $H_2O_2/Fe^{2+}$ [112] and ultimately in the removal efficiency of COD. Fenton reagent addition mode has been studied by several authors [109, 112, 119, 122]. All these studies have recognized higher removal of COD (around 10%) by continuous addition of reagents. Moreover, keeping the concentration of $H_2O_2$ by stepwise addition reduces the $^{\bullet}OH$ scavenging, thus making more hydroxyl radicals available to oxidise organic matter.

The presence of inorganic salts also influences the rates of reactions represented by Equations 3.6 to 3.12. Chloride and sulfate ions can form complexes with $Fe^{3+}$, markedly decreasing the regeneration of $Fe^{2+}$, while formation of $Cl_2^{\bullet-}$ and $SO_4^{\bullet-}$ that are less reactive than $^{\bullet}OH$, decreases the overall system efficiency. Carbonate and phosphate ions have a much stronger effect. Both can

scavenge $^{\bullet}OH$, while phosphate can also precipitate iron via the formation of insoluble iron phosphate salts.

The first photo-Fenton experiments on leachate [109, 112], demonstrated the high process efficiency over conventional Fenton, with considerably lower catalyst requirements and, consequently, lower iron sludge production. It is worth mentioning that, the effectiveness of irradiation can significantly vary for raw and pre-treated leachate due to the difference in the concentration of total dissolved solids and the level of turbidity [117]. Also, the high cost (due to electrical power consumption) expected for the photo-treatment to be effective turned the research to the field of solar photo-Fenton (sPF) [27, 78, 79, 96]. For this purpose, the most used solar photoreactor is the Compound Parabolic Collector (CPC), whose geometry allows the use of both direct and diffuse radiation, while its modular design makes it ideal for large-scale operations [118, 120]. Nonetheless, the normally high land area requirements and the investment cost associated with CPCs are major blockers for full-scale implementation of this type of photoreactor. In this sense, research efforts must be directed to develop and test new photoreactors (not only solar, but artificial too), specifically designed for photo-Fenton applications and wastewater decontamination (CPCs were designed to optimize $TiO_2$ photocatalysis). Recently, the usage of raceway pond reactors (RPR) for the photo-Fenton treatment of coloured industrial wastewaters emerged as an interesting cost-effective approach [125-127]. However, RPR performance still lacks to be tested with real industrial wastewater.

Although the photo-Fenton process has proven its potential for the treatment of wastewater, only few reports on developments at an industrial or large pilot scale may be found in the literature (e.g., [128-130]). Besides the specific problems related to the design of photochemical reactors, some inherent drawbacks of the Fenton process still persist: (i) pH range limited to mildly acidic conditions; (ii) production of sludge due to precipitation of iron hydroxides/oxides after neutralization and subsequent disposal or recycling; (iii) and decreased efficiency and additional costs of immobilized/supported iron catalysts that might be used at neutral pH and recycled.

### 3.1.6.2 Ozone-based process

During ozonation, organic contaminants are oxidized in two ways [131, 132] : (i) ozone itself can directly react with dissolved chemicals, at varying rates, and is a highly selective oxidant and, besides to direct oxidation, (ii) ozone decomposes via a chain reaction mechanism to form $^{\bullet}OH$

radicals (Equations 3.17 to 3.23), which in turn can oxidize the pollutant. The two pathways can lead to different products and display different transformation kinetics. Direct oxidation usually occurs with atoms that have a negative charge density (e.g., N, P, O) and nucleophilic carbons, and with multiple bonded constituents such as carbon-carbon and nitrogen-nitrogen [133]. The $O_3$ reacts with the carbon unsaturated bond due to its dipolar structure and leads to the splitting of the bonds, which is based on the so-called Criegee mechanism [134, 135]. The kinetics of reaction between organic compounds and ozone have been measured for several hundreds of compounds, with rate constants covering a range of more than 9 orders of magnitude [136]. A wide variation in the kinetic constants has also been observed for the direct oxidation of inorganic compounds [137]. The indirect reaction pathway, by contrast, involves radicals and particularly the $^\bullet OH$ radical.

$$O_3 + OH^- \rightarrow O_2 + HO_2^- \qquad \text{(O transfer)} \qquad k_{3.17} = 70 \ M^{-1} s^{-1} \qquad (3.17)$$

$$O_3 + HO_2^- \rightarrow O_3^{\bullet-} + HO_2^\bullet \qquad \text{(e}^-\text{ transfer)} \qquad k_{3.18} = 2.8 \times 10^6 \ M^{-1} s^{-1} \qquad (3.18)$$

$$HO_2^\bullet \leftrightarrow O_2^{\bullet-} + H^+ \qquad k_{3.19} = 3.2 \times 10^5 \ s^{-1}; \ k_{-3.19} = 2.0 \times 10^{10} \ M^{-1} s^{-1} \qquad (3.19)$$

$$O_2^{\bullet-} + O_3 \rightarrow O_3^{\bullet-} + O_2 \qquad k_{3.20} = 1.6 \times 10^9 \ M^{-1} s^{-1} \qquad (3.20)$$

$$O_3^{\bullet-} + H^+ \leftrightarrow HO_3^\bullet \qquad k_{3.21} = 5.2 \times 10^{10} \ M^{-1} s^{-1}; \ k_{-3.21} = 3.3 \times 10^2 \ s^{-1} \qquad (3.21)$$

$$HO_3^\bullet \rightarrow {}^\bullet OH + O_2 \qquad k_{3.22} = 1.1 \times 10^5 \ s^{-1} \qquad (3.22)$$

$$O_3^{\bullet-} + {}^\bullet OH \rightarrow O_3 + OH^- \qquad k_{3.23} = 2.5 \times 10^9 \ M^{-1} s^{-1} \qquad (3.23)$$
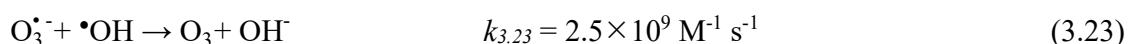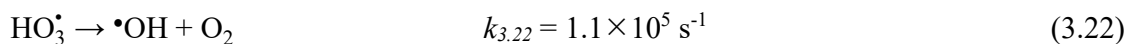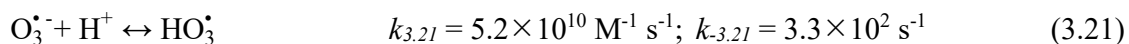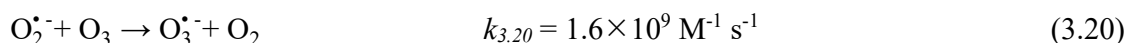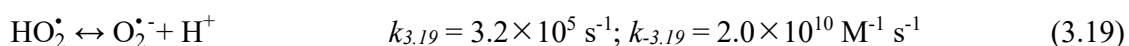
Compounds that react directly with $O_3$ to start the described reaction chains (Equations 3.17 and 3.18) are called initiators. In pure water, hydroxide anion ($OH^-$) is considered the only initiator of the reaction chain, but other initiators can be added, namely hydroperoxide anion ($HO_2^-$), UV radiation, humic substances, and solid catalysts (metals, etc.). The importance of $OH^-$ as an initiator of the chain reactions, underlies pH as a key factor in the $O_3$ process which also plays an important role in all the acid-base equilibria by influencing the concentrations of the dissociated/non-dissociated forms [132]. There is a general agreement that the higher the pH, the faster $O_3$ decays.

Substances that convert $^\bullet OH$ into superoxide radicals $O_2^{\bullet-}/HO_2^\bullet$ promote the chain reaction; they act as chain carriers, the so-called promoters (for example: $R_2$-CH-OH and aryl-(R)). Hydrogen peroxide is also a good example of a promoter. In fact, $H_2O_2$ is not only an initiating agent of ozone

decomposition (with the formed $HO_2^-$, Equation 3.24), but it also acts as a promoter of $O_3$ decomposition (Equations 3.25 and 3.26) [134].

$$H_2O_2 \leftrightarrow HO_2^- + H^+ \qquad\qquad pKa = 11.8 \qquad\qquad\qquad (3.24)$$

$$\bullet OH + H_2O_2 \rightarrow HO_2^{\bullet-} + H_2O \qquad k_{3.25} = 2.7 \times 10^7 \ M^{-1} \ s^{-1} \qquad (3.25)$$

$$\bullet OH + HO_2^- \rightarrow HO_2^{\bullet-} + OH^- \qquad k_{3.26} = 7.5 \times 10^9 \ M^{-1} \ s^{-1} \qquad (3.26)$$
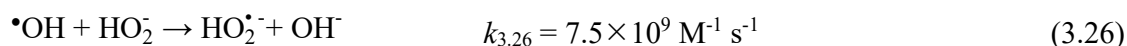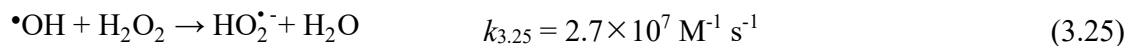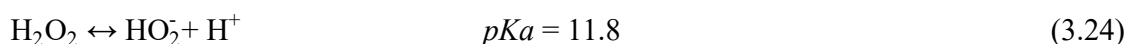
Consequently, the addition of $H_2O_2$ enhances the decomposition cycle of ozone, resulting in the formation of further $\bullet OH$ [138]. Other examples of promoters are methanol, formic acid, some humic substances and other natural organic matter (NOM). Ozonation can also be improved by readily absorbing UV radiation ($\lambda < 300$ nm), which generates $H_2O_2$ as an intermediate, and then decomposes to $\bullet OH$ (Equations 3.27 and 3.28). Again, the occurrence of $H_2O_2$ photolysis (Equation 3.16) can further promote the overall oxidation potential.

$$O_3 + H_2O + h\nu \rightarrow H_2O_2 + O_2 \qquad (h\nu < 300 \ nm) \qquad\qquad (3.27)$$

$$O_3 + H_2O_2 \rightarrow HO_2^{\bullet} + \bullet OH + O_2 \qquad k_{3.28} = 6.5 \times 10^{-2} \ M^{-1} \ s^{-1} \qquad (3.28)$$
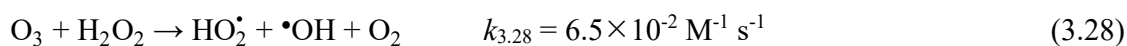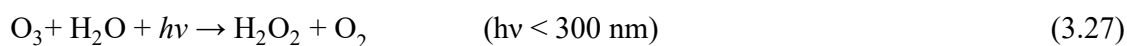
On the contrary, substances that react with $\bullet OH$ to form secondary radicals but do not produce $O_2^{\bullet-}/HO_2^{\bullet}$ are called inhibitors, or scavengers (for example: $CH_3\text{-}COO^-$ and alkyl-(R)). Carbonate and bicarbonate ions typically act as scavengers, as mentioned previously for the Fenton and photo-Fenton processes (Equations 3.29 and 3.30) [132]:

$$HCO_3^{\bullet-} + \bullet OH \rightarrow CO_3^{\bullet-} + H_2O \qquad k_{3.29} = 8.5 \times 10^6 \ M^{-1} \ s^{-1} \qquad (3.29)$$

$$CO_3^{2-} + \bullet OH \rightarrow OH^- + CO_3^{\bullet-} \qquad k_{3.30} = 4.2 \times 10^8 \ M^{-1} \ s^{-1} \qquad (3.30)$$
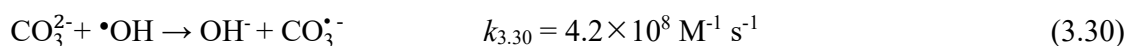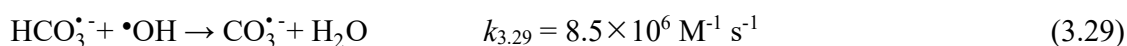
Parameters that may exert significant influence on $O_3$ decay kinetics include pH, temperature (according to Arrhenius law), hardness, alkalinity, UV wavelength, metals concentration, anions/cations concentration and solid content (or particulate matter) in water. Moreover, hydrodynamic conditions greatly affect the gas-liquid transfer of ozone, particularly when the concentration of suspended solids in water is high [139, 140], because of the interactions between the size of the solid particle and the thickness of the gas penetration in the liquid film on the bubble surface [132]. This is recognized as a cost and energy intensive process, with the main operation expenditure attributed to ozone generation. Nonetheless, the usage of AOPs with ozonation has more industrial application compared to any other AOPs in wastewater treatment [138].

## 3.2 Treatment systems: current situation

The wide variability of landfill leachate, both in quantity (volumetric flow rate) and quality (chemical composition), makes the definition of an effective treatment system a major engineering challenge. Furthermore, the leachate treatment is governed by technological options, effluent discharge alternatives, final discharge requirements and economical aspects. Also, the increasing environmental awareness accompanied by strict legal regulations, especially for ground and surface water, further pressures the existing leachate treatment systems. As previously mentioned, typically leachate treatment may be performed:

(i) Off-site at a WWTP (with or without leachate pre-treatment), which implies transport or pumping of the leachate; some WWTP may require the payment of a fee for the acceptance of the leachate.

(ii) On-site at a leachate treatment plant (LTP), for complete (or partial) treatment, which generically includes conventional physicochemical techniques followed/preceded by biological processes, concluding (or not) with further in-depth treatment for direct discharge into water bodies.

Considering the present thesis objectives, an overview on treatment systems around the world and associated costs, with specific attention to the current situation in Portugal, follows. Furthermore, focus will be given to on-site LTPs that comply with the legal values for discharge of the leachate directly into the environment.

### 3.2.1 World

Due to several practical and economic reasons, co-treatment of leachate in municipal WWTPs is the most widely applied method in different regions of the world. In Florida, USA, it was reported that 36 out of 52 landfill operators were relying on municipal WWTPs for treating their leachate [141]. In Europe, there are still many countries, such as Ireland, Italy, and Poland, where most of the leachate is co-treated with municipal wastewater in WWTPs. For instance, in the Republic of Ireland during 2013, approximately 1.1 million $m^3$ of leachate was sent to municipal WWTP, either by (i) discharge of leachate to sewer (51% by volume), or (ii) tankers (48% by volume) [2, 142]. In other European countries, like France and Germany, most landfills have on-site leachate treatment plants. In 2008, the level of co-treatment in France was reported as 21% [10], similar to Germany values in 2005 [48].

There is a worldwide lack of information related to on-site leachate treatment systems and their performance. Nonetheless, searching in specific literature it is possible to find some data which were summarized in Table 3.5. In Brazil, despite the scarce monitoring of sanitary landfills, a recent review on the status of landfill leachate treatment systems [143] reports that they are mainly treated by biological processes (aerobic and anaerobic lagoons, activated sludge, and wetlands). The sanitary landfills in large Brazilian cities located in the states of São Paulo and Rio de Janeiro, apply advanced treatment technologies, such as membrane filtration. In China, a recent survey [144] reports that, from 2004 to March 2019, there were at least 175 full-scale MBRs commissioned or under construction. The most applied treatment process was "pre-treatment + MBR + tertiary treatment", with nanofiltration (NF) and/or reverse osmosis (RO) applied as polishing stage (i.e. MBR + NF/RO) to further clarify the leachate to a recyclable standard. A study by Wang, *et al.* [145], also points out that nowadays more than 80% of LTPs in China are composed by the sequence of "physicochemical + MBR + NF" processes.

Concerning the LTPs in Europe, there is a dearth of publicly available data [142]. The main reason for this is that landfills (many of which are privately owned and operated) keep this type of information confidential, as it is commercially sensitive. It is known that during the late 90s, in the Netherlands, Germany, France, Belgium, Spain and Portugal, many leachate treatment systems were designed with an aerated lagoon in front of a 2-stages RO plant [22, 95]. Commonly, the RO concentrate is re-infiltrated in the landfill body, although very limited data on the matter are available. Steensen [146], in 1997, reported the practices of 100 LTPs operating in Germany, all using a combination of several individual processes and with more than 60% having a biological process as the first stage of the treatment. Also, in 15 plants, the chemical oxidation process was chosen for further purification. A latter study [147], in 2001, also respecting Germany, analysed 150 LTPs from which: 58 plants used a combination of biological process and activated carbon adsorption, and 49 plants combined a biological stage followed by reverse osmosis.

**Table 3.5** – Examples of landfill leachate treatment systems in different countries that comply with the respective legal values for direct discharge (sources:[13, 95, 143, 144, 148-150]).

| Location | Influent (mg/L) | Treatment system[a] | Observations |
|---|---|---|---|
| Seropédica (R.J., Brazil) | • COD = 1931 <br> • BOD$_5$ = 863 <br> • TAN = 2185 | Stabilization lagoon + air stripping + biological treatment with activated sludge + decantation + sand filtration + NF | • Operating since 2014 <br> • 10 000 tonne MSW/day |
| Gramacho (R.J., Brazil) | | Physicochemical pre-treatment + aerobic biological treatment with activated sludge + NF | • Operation 1978-2012 <br> • 9000 tonne MSW/day |
| São Gonçalo (R.J., Brazil) | | Pre-filtration + 3 stages RO <br> (mobile treatment unit-container) | • Operation 2014 <br> • 2500 tonne MSW/day |
| Campos (R.J., Brazil) | | Pre-filtration + 3 stages RO <br> (mobile treatment unit-container) | • Operation 2009 <br> • 430 tonne MSW/day |
| Hunan (China) | • COD = 3200 <br> • BOD$_5$ = 550 <br> • TAN ≤ 1300 | Pre-treatment + UABF + MBR (anaerobic/anoxic/aerobic processes × 2 and MF) + NF + RO | • Operating since 2011 <br> • $V_L$ = 300 m$^3$/d |
| | • COD = 20 000 <br> • BOD$_5$ = 10 000 <br> • TAN ≤ 1500 | Pre-treatment + MBR (anoxic/aerobic processes and external UF) + NF + RO | • Operating since 2017 <br> • $V_L$ = 200 m$^3$/d |
| Jiangsu (China) | • COD = 25 000 <br> • BOD$_5$ = 8500 <br> • TAN = 2500 | Pre-treatment + MBR (anoxic/aerobic processes and external) + RO | • Operating since 2015 <br> • $V_L$ = 400 m$^3$/d |
| Bord-Matin (France) | • COD = 1750 <br> • TAN = 850 | Nitrification and post-denitrification biological process + chemical precipitation with lime in a lamellar settling tank + O$_3$ | • Operating since 1972 <br> • $V_L$ = 12.5 m$^3$/d |
| Hersin-Coupigny (France) | | MBR + RO | • Operating since 1994 <br> • $V_L$ = 40 m$^3$/d |
| Singhöfen (Germany) | | Pre-denitrification and nitrification reactor with sedimentation tank and sand filter + O$_3$/UV stage with sand filter + aerated packed bed | • Operating since 1994 <br> • $V_L$ = 110 m$^3$/d <br> • The effectiveness of O$_3$-alone allowed to fulfil legal compliance. |

| Location | Influent (mg/L) | Treatment system[a] | Observations |
|---|---|---|---|
| Asbach (Germany) | | BIOQUINT® system: nitrification fixed-bed biofilter (45 m$^3$) and denitrification fixed-bed biofilters (2×10 m$^3$) + O$_3$ (4 kg O$_3$/h) | • Operating since 1998 <br> • V$_L$ = 70 m$^3$/d |
| Friedrichshafen (Germany) | | BIOQUINT® improved system: nitrification AS (100 m$^3$) + denitrification AS (25 m$^3$) + O$_3$ (1.5 kg O$_3$/h) merged with a fixed-bed bioreactor (10 m$^3$) | |
| "Il Fossetto" (Italy) | | Since 2006: mixing and pre-aeration + sieving + pre-filtration by cartridge filters + UF + acidification (pH ~ 5) + RO + chlorination + AC | • Operating since 1988 <br> • Until 2006: all leachate was sent to external plants <br> • V$_L$ = 60 m$^3$/d <br> • Concentrated leachate (~ 30%) is recirculated back into the landfill |
| Warminsko-Mazurskie Voivodeship (Poland) | • COD = 285-2250 <br> • BOD$_5$ = 50-1350 <br> • TAN = 94-900 | Since 2013: acidification (pH ~ 6.0-6.5) + sand filter + cartridge filter + RO (ROCHEM CD9-RO disc-tube modules, operating pressure 65 bar) | • Operating since 1983 <br> • V$_L$ = 60-90 m$^3$/d <br> • Concentrated leachate (~ 25%) is recirculated back into the landfill |
| Nonthaburi (Thailand) | • COD = 2700 <br> • TOC = 650 <br> • BOD$_5$ = 400 <br> • TAN = 112 | C/S (2×56.5 m$^3$, HRT = 160 min, [FeCl$_3$] = 1.5 g/L) + sand/carbon filtration (2×3.3 m$^2$) + MF (5 μm pore size) + RO (7 modules Hydraunautic LFC 3-LD) | • Operating since 1982 <br> • Until 2005: 300,000 m$^3$ of leachate stored in a stabilization pond |
| Odayeri (Turkey) | • COD = 16 360 <br> • TAN = 2531 <br> • Colour = 8800 Pt/Co | Equalization tanks + MBR (with external cross flow UF membranes) + NF membrane systems | • Operating since 1995 <br> • V$_L$ = 50 m$^3$/d |
| Chung-Nam (Korea) | • COD = 400-1500 <br> • BOD$_5$ = 100-500 <br> • TAN = 200-1400 <br> • NO$_3^-$ = 28-251 | Since April 2000: submerged membrane reactor (KIMAS) + RO spiral wound membrane module (Filmtec, USA) | • V$_L$ = 50 m$^3$/d <br> • Until April 2000: contact aeration + RBC + GAC adsorption, but there was not stable COD and TN removal facing the new legal standards. Also, the system suffered biomass washout and frequent replacement of GAC was needed. |

[a] NF – nanofiltration; RO – reverse osmosis; UABF – upflow anaerobic biofilm reactor; MBR – membrane biological reactor; MF – microfiltration; AS – activated sludge; C/S – coagulation/sedimentation.

### 3.2.2 Portugal

In Portugal, according to official data [151], nearly half of the currently active landfills pre-treat the leachate on-site, followed by final treatment on a WWTP (Table 3.6). The majority of these LTPs includes common physicochemical techniques, normally a coagulation/flocculation (C/F) stage, pre- or proceeded by aerobic and/or anaerobic biological processes, where aerated lagoons (AL) and conventional activated sludge (CAS) are predominant choices. In turn, all landfills whose leachate treatment allows direct discharge into water bodies use reverse osmosis (RO) as a polishing step, usually preceded by at least one biological treatment stage (again, AL and CAS are prevalent).

**Table 3.6** – Sanitary landfills management entities in Portugal, respective leachate treatment systems and final discharge (sources: [151-153])

| Entity | Landfill | Treatment system[a] | Discharge |
|---|---|---|---|
| Algar | Portimão | AL + clarifier + RO ($\downarrow$99% COD; $\downarrow$99% DOC; $\downarrow$99% TAN) | Water body |
| | Loulé | | |
| Amarsul | Seixal | AL + sedimentation ($\downarrow$29% COD; $\downarrow$11% TAN) | WWTP |
| | Palmela | Inactive LTP | |
| Ambilital | Alentejo litoral | Evaporation/condensation towers + stripping tower + scrubber + aerated tank ($\downarrow$98% COD; $\downarrow$92% TAN) | Reused for refrigeration |
| Ambisousa | Penafiel | AL + sedimentation ($\downarrow$14-24% BOD$_5$; $\downarrow$25% COD) | WWTP |
| | Lustosa | | |
| Amcal | Vila Ruiva | Anaerobic lagoon + facultative lagoon + aerated lagoons + sedimentation (+ CW) ($\downarrow$35% BOD$_5$; $\downarrow$34% COD; $\downarrow$12% DOC $\downarrow$84% TAN) | Recirculated back to landfill |
| Braval | Baixo Cávado | C/F + filtration + CAS (anoxic + aerated tanks) + AC ($\downarrow$98% COD; $\downarrow$95% DOC; $\downarrow$97% TAN) | WWTP |
| Ecobeirão | Planalto Beirão | Stabilization lagoon + clarifier + RO ($\downarrow$~100% COD; $\downarrow$~100% TAN) | Water body |
| ERSUC | Aveiro | CAS + C/F + filtration ($\downarrow$50% COD; $\downarrow$27% TSS; $\downarrow$30% TN) | WWTP |
| | Coimbra | CAS + C/F ($\downarrow$92% COD; $\downarrow$43% TSS; $\downarrow$50% TN) | |
| Gesamb | Évora | Stabilization lagoons + sand filtration + micro cartridge filtration + RO ($\downarrow$93% BOD$_5$; $\downarrow$99% COD; $\downarrow$~100% DOC) | Water body |
| Lipor | Maia | CAS + UF + RO | Water body |
| Resialentejo | Beja | Stabilization lagoon + RO ($\downarrow$~100% COD; $\downarrow$~100% DOC; $\downarrow$~100% TAN) | Water body |
| Resíduos do Nordeste | Urjais | Stabilization lagoon + RO ($\downarrow$~100% COD; $\downarrow$~100% DOC; $\downarrow$~100% TAN) | Water body |
| Resinorte | Bigorne | AL + sedimentation + RO ($\downarrow$99% COD, for Bigorne and Celorico LTPs) | Water body |
| | Boticas | | |
| | Celorico | | |
| | Vila Real | | |

| Entity | Landfill | Treatment system[a] | Discharge |
|---|---|---|---|
| Resisestrela | Fundão | Anaerobic tank + aerated tank + anoxic tank + aerated tank + ultrafiltration (↓99% COD) | WWTP |
| Resitejo | Resitejo | Stabilization lagoon + RO (↓~100% COD; ↓98% TAN) | Water body |
| Resulima | Vale do Lima e Baixo Cávado | Anaerobic lagoon + CAS + C/F (↓90% COD; ↓91% TAN) | WWTP |
| Suldouro | Gestal | AL + CAS (anoxic and aerated) + C/F + flotation (↓96% COD; ↓~ 100% TAN; ↓96% TN) | WWTP |
| | Sermonde | AL + CAS (anoxic and aerated) + C/F + flotation (↓86% COD; ↓77% TSS) | |
| Valnor | Avis | Anaerobic lagoons + AL + aerated tank + sedimentation + RO (↓~ 100% TAN) | Water body |
| | Castelo Branco | AL + CAS + filtration + RO (↓99% COD; ↓~ 100% TAN) | |
| Valorlis | Leiria | AL + clarifier + constructed wetland (↓33% COD) | WWTP |
| Valorminho | Valença | AS (anoxic/aerated) + regularization tank (↓77% BOD$_5$; ↓77% COD; ↓88% TN) | WWTP |
| Valorsul | Cadaval | C/F + AL + sedimentation | WWTP |
| | Mato da Cruz | AL + C/F (↓47% BOD$_5$; ↓46% COD) | |

[a] Abbreviations: AC – activated carbon; AL – aerated lagoon; CAS – conventional activated sludge; C/F – coagulation/flocculation; CW – constructed wetlands; RO – reverse osmosis; UF – ultrafiltration; BOD$_5$ – 5-day biochemical oxygen demand; COD – chemical oxygen demand; DOC – dissolved organic carbon; TAN – total ammonia nitrogen; TN – total nitrogen; TSS – total suspended solids.

### 3.2.3 Costs

Over the last years, increased attention has been focused on the financial risk associated with the environmental liabilities that are associated with landfill aftercare [142]. The cost of leachate treatment can be divided into operational and capital costs, and can vary significantly depending on leachate type and site-specific factors (including age of landfill, strength of leachate, required level of treatment, volume of leachate produced, climate, availability of appropriate receiving waters and proximity to sewer or WWTP).

Worldwide, the most common applied practice for leachate management is the collection and storage (usually in lagoons located on site) of the leachate, prior to transfer to WWTPs for treatment [154, 155]. Co-treatment of leachate with municipal wastewater is widely considered the lowest capital cost option but it may carry high operation costs, while alternative on-site treatments have

higher capital costs and lower operational costs. Published in 2020, a technical report [156] on the municipal landfill in Santo André (state of São Paulo, Brazil), that generates about 225 $m^3$/day of leachate, indicates a cost of around R\$ 54,000.00 per month (8500 €/month) for the transport and treatment of the leachate in a WWTP located in a nearby city. In the United Kingdom, according to the 2007 Guidance for the Treatment of Landfill Leachate [22], the estimated cost to transport leachate, without any previous treatment, to a WWTP was 17.50 £/$m^3$ (19.75 €/$m^3$). However, it is expected that this value has increased over the years as more stringent legal values were imposed. In this sense, in Italy, a 2018 study [148] points to operational costs for leachate co-treatment (off-site), including transportation, of 50-100 €/$m^3$.

For economic reasons, several LTPs incorporate a biological process as the initial treatment stage. Indeed, a survey over 166 leachate treatment plants [47] showed that 72% had a biological treatment such as aerated lagoons (AL), constructed wetlands (CW), conventional activated sludge (CAS), sequencing batch reactors (SBR), membrane bioreactor (MBR), and upflow anaerobic sludge blanket (UASB). The Guidance for the Treatment of Landfill Leachate [22] estimated in 2007 that for the treatment of 400 $m^3$/day of leachate ($COD_0$ = 6000 mg $O_2$/L), using an SBR with further disposal into a sewer, had a total cost of 4.12 £/$m^3$ (4.65 €/$m^3$). In Germany, according to Stegmann, *et al.* [48], in 1994, seven treatment plants with capacities from 11 000 up to 64 000 $m^3$/year were investigated, and total costs for investment and operation varied in the range 9-30 €/$m^3$ of leachate. In 2015, the same authors roughly estimated the costs of leachate treatment in Germany to be 10-70 €/$m^3$ of leachate. In Italy, Calabrò, *et al.* [148] indicate around 15-40 €/$m^3$ for a reverse osmosis treatment on-site. From the previously mentioned study by Zhang, *et al.* [144] regarding 175 LTPs in China combining MBR + NF + RO processes, the total investment costs for this treatment option were analysed. According to the authors, from 2015 the total capital cost is on average of 12 100 USD/$m^3$/d (11 160 €/$m^3$/d) with the tertiary treatment by NF/RO cost representing 15-20% of the total investment.

RO membrane separation units are generally adopted in Portugal to achieve an higher treatment efficiency for stabilized leachates. According to the latest official data available [151], in 2008, the usage of RO in Portuguese LTPs presented an average total cost of 8.1 €/$m^3$ (3.3 €/$m^3$ for capital costs, and 4.7 €/$m^3$ for current costs). Some examples of base values for the purchase or rental of reverse osmosis systems for leachate treatment in Portugal are presented in Table 3.7. For the treatment of 100 $m^3$/day of leachate, a total cost for the RO system over a 5-year operating period will be approximately 1.5 million euros, including membrane replacement that occurs on average every 3 years [157]. During this period, the reverse osmosis performance is effective, but the efficiency may decrease up to 50% by the end of the 5th year of operation, due to the salt increase

after the subsequent recirculation of the concentrate over the landfilled waste mass. Although the high treatment efficiencies reached by the RO process, it has the disadvantage of high treatment costs, in addition to the problems imposed for the treatment of concentrates with additional costs.

**Table 3.7** – Examples of base values for the purchase or rental of reverse osmosis systems for leachate treatment (source: [157]).

| Type of contract | Entity | Base value (€) |
|---|---|---|
| • Public tender (Portuguese Republic Diary: Part L - Public Procurement, procedure nº 2065/2010).<br>• Acquisition of a new RO system for leachate treatment, with a capacity of 100 m³/day, operation, and 3 years maintenance. | Ecolezíria | 700,000.00 |
| • Public tender (Portuguese Republic Diary: Part L - Public Procurement, procedure nº 5617/2013).<br>• Design, installation, and maintenance of a new RO system for Vila Real landfill[a]; Rehabilitation and maintenance operation for RO systems for the Boticas, Celorico de Basto and Lamego landfills. | RESINORTE | 800,000.00[a] |
| • Acquisition of a new RO system with treatment capacity of 100 m³ leachate /day. | AST, Lda. | 650,000.00 |
| • Public tender (Portuguese Republic Diary: Part L - Public Procurement, procedure nº 76/2014).<br>• Provision of services for the rental of a RO unit for wastewater treatment of the Environmental Park[b]. | RESIALENTEJO | 199,000.00 |
| • Monthly rental price of a RO unit with treatment capacity of 100 m³ leachate /day. | AST, Lda. | 25,000.00 |
| • Price paid for an exceptional rental of a RO unit (during the winter season) | GESAMB | 109,900.00 |

[a] Of this amount, approximately € 500,000.00 corresponds to the design, installation and maintenance of the reverse osmosis system for the treatment of 130 m³ of leachate per day at the Vila Real landfill. [b] For the treatment of 100 m³/day.

To update the existing information on leachate treatment systems currently operating in Portugal, at the early-stage of the work developed on this PhD thesis, in 2015, a survey was prepared and distributed to the various entities responsible for the management of Portuguese landfills (listed in Table 3.6). Despite the insistence on requesting a response, only 5 MSW landfills responded (Table 3.8). It should be noted that landfills with leachate treatment capable of complying with the limit values for discharge into water bodies reported treatment costs between 10 and 25 €/m³ of leachate.

**Table 3.8** – Main results obtained from surveys sent to landfill management entities in Portugal.

| Landfill | Characterization | Treatment system | Removal (%) | Cost (€/m³) | Advantages/Drawbacks |
|---|---|---|---|---|---|
| No. 1<br>116 000 tonne<br>MSW/year | • $V_L$ = 105 m³/day<br>• pH = 8.2<br>• COD = 11 483 mg/L<br>• TOC = 4850 mg /L<br>• TAN = 3417 mg/L<br>• Cl⁻ = 3586 mg/L<br>• $HCO_3^-$ = 157 750 mg/L<br>• Conductivity = 26.4 mS/cm | AL + sedimentation + RO<br><br>Direct discharge | • COD = 99.8 | 25 | Accumulation of concentrates that return to the landfill, worsening the characteristics of the leachate to be treated. |
| No. 2 - 3<br>150 000 tonne<br>MSW/year | • $V_L$ = 110 - 125 m³/day<br>• COD = 10 000 mg/L<br>• $CBO_5$ = 1000 mg /L<br>• TAN = 3000 mg/L<br>• Conductivity = 40 mS/cm | AL + sedimentation + RO<br><br>Direct discharge | • COD = 99.5<br>• $CBO_5$ = 99.5<br>• TAN = 99 | 10 | Advantages: high efficiency; high capacity to adapt to variations in raw water; high quality of treated effluent allowing reuse<br>Drawbacks: high cost, wear of membranes (high electrical conductivity of raw water that implies high operating pressure, in the order of 50 bar) and electronic components (due to $H_2S$); Difficulty in removing TAN at concentrations below the ELV for discharge, even with removal in the order of 99%, major problems/breakdowns due to the high conductivity of the raw leachate |
| No. 4<br>13 000 tonne<br>MSW/year | • $V_L$ = 6.7 m³/day<br>• COD = 2925 mg/L<br>• $CBO_5$ = 1245 mg /L<br>• TN = 1131 mg/L | Anaerobic lagoon + facultative lagoon + aerated lagoons + sedimentation (+ CW)<br>Recirculated back to landfill | • COD = 30<br>• $CBO_5$ = 25<br>• TAN = 75 | 3.5 | The system does not guarantee proper treatment |
| No. 5<br>119 164 tonne<br>MSW/year | • $V_L$ = 125 m³/day<br>• pH = 8.1<br>• COD = 5515 mg/L<br>• $CBO_5$ = 288 mg /L<br>• TAN = 3497 mg/L<br>• Cl⁻ = 3646 mg/L<br>• Conductivity = 29.8 mS/cm | AL + CAS (anoxic and aerated) + C/F + flotation<br><br>WWTP | - | - | - |

## 3.3 Treatment train strategies

A considerable amount of work has been done on landfill leachate treatment in the past decades. But the strict implementation of environmental legislative demands and the ageing of existing landfills put pressure on managers and operators of landfills to implement more efficient processes. So, most recent research is now targeting the combination of two or more treatment technologies as efficient and effective ways for landfill leachate treatment. It is well recognized that (i) efficiency, (ii) cost, and (iii) environmental impacts, are the three major criteria that should be considered to select a sustainable treatment technology or combination of treatment technologies for landfill leachates. Recent developments in landfill leachate treatment, especially during this last decade, focusing on the combination of biological and physicochemical processes, always including an AOP stage, in view of legal compliance for the leachate direct discharge into the environment, are presented in the following sections. In addition, Table 3.9 systematizes the main results obtained from different research works (initial concentrations and removals obtained for each treatment stage proposed), including details regarding the experimental conditions used; while Table 3.10 details information regarding the estimated operational costs for the proposed treatment combination strategies. Later, a thorough review over the research previously carried out with leachate coming from the same landfill as the one used in the present study, including cost estimations, will also be presented.

### 3.3.1 Combination of treatment processes for landfill leachate treatment

In 2011, Cassano, *et al.* [158] used medium-age landfill leachate to investigate and compare different treatment strategies. The research tested the usage of a sequencing batch biofilter granular reactor (SBBGR), with or without ozonation, followed or not by a solar photo-Fenton (sPF) polishing stage, considering two distinct target COD values, 160 mg/L and 500 mg/L (according to legal standards in Italy), to be met in the final effluent for discharging into waterbodies and sewers, respectively. According to the reported results, SBBGR allowed a complete removal (99%) of nitrogen compounds, with residual TAN and $NO_x$ of 6 and 9 mg/L, respectively, while the combination of treatment processes (SBBFR/$O_3$, SBBGR + sPF and, SBBGR/$O_3$ + sPF) were able to reach both requested COD values (Table 3.9). Operating costs for the tested treatment scenarios were also estimated (Table 3.10).

**Table 3.9** – Characterization and efficiency of treatment processes combining AOPs (research reported over the past decade).

| Treatment stage | Parameters (mg/L) and removals | | | | | Observations/Conditions[a] | Reference |
|---|---|---|---|---|---|---|---|
| | COD | BOD$_5$ | DOC | TN | TAN | | |
| Raw leachate | ~3100 | - | ~1100 | - | ~1000 | • Leachate (medium-age) collected from Apulia municipal landfill, Italy. | Cassano, *et al.* [158] 2011 |
| SBBGR | 1200 ↓54% | - | 425 ↓61% | - | 6 ↓99% | • <u>SBBGR</u>: biomass support material KMT-k1 (Kaldness, Norway); $V_T$ = 12 L; Cycle = 8h (fill 0.5h + reaction 7h, with continuous aeration at flow rate of 250 dm$^3$/h + draw 0.5h); HRT = 12 d; C source: methanol (3 g/L). | |
| SBBGR/O$_3$ | 160 | - | 141 | - | - | • <u>SBBGR/O$_3$</u>: same SBBGR conditions but with 0.5h of biological and chemical degradation during reaction phase with O$_3$; O$_3$ dose = 1.6 kg/m$^3$$_{influent}$. | |
| **Global efficiency** | **↓95%** | **-** | **↓87%** | **--** | | | |
| SBBGR + sPF | 160 | - | 70 | - | - | • <u>sPF</u>: CPC = 1 m$^2$; $V_T$ = 19 L; pH = 2.7-2.9; catalyst: [Fe$^{2+}$] = 55 mg/L; [H$_2$O$_2$]: 35 mM. | |
| **Global efficiency** | **↓95%** | | **↓93%** | | | | |
| SBBGR/O$_3$ + sPF | 144 | - | 60 | - | - | • <u>SBBGR/O$_3$ + SPF</u>: similar as described above but with O$_3$ dose = 0.4 kg/m$^3$$_{influent}$ and [H$_2$O$_2$] = 26 mM. | |
| **Global efficiency** | **↓95%** | **-** | **↓95%** | **-** | **-** | | |
| Raw leachate | ~ 2320 | - | ~ 970 | ~ 1710 | ~ 1620 | • Leachate (medium-age) collected from Apulia municipal landfill, Italy. | Del Moro [159] 2013 |
| SBBGR | 835 (↓64%) | | 378 (↓61%) | 36 (↓98%) | 7 (↓99%) | • <u>SBBGR</u>: biomass support material KMT-k1 (Kaldness, Norway); $V_T$ = 12 L; Cycle = 8h (fill 0.5h + reaction 7h, with continuous aeration + draw 0.5h); OLR ~ 1 g COD/L/d; NLR ~ 0.2 g TAN/L/d; sludge age ~ 800 d. | |
| UV/H$_2$O$_2$ | 676 (↓7%) | | 310 (↓7%) | 36 (≈) | 7 (≈) | • <u>UV/H$_2$O$_2$</u>: flow-through annular photoreactor, with low pressure mercury UV lamp (40W, MTL844-G, Helios) emitting at 254 nm; flow rate recirculation SBBGR/photoreactor = 3 L/h; [H$_2$O$_2$] = 30% (w/w) at flow rate = 0.1 mL/min; [H$_2$O$_2$] = 650 mg/L; $t$ = 7 h/L. | |
| **Global efficiency** | **↓71%** | **-** | **↓68%** | **↓98%** | **↓99%** | | |
| SBBGR/UV/H$_2$O$_2$ | 261 | - | 156 | 36 | 1 | • <u>SBBGR/ UV/H$_2$O$_2$</u>: SBBGR cycle = 8h (fill 0.5h + biological reaction only 3.5h + biological and UV/H$_2$O$_2$ 3.5h + draw 0.5h) OLR ~ 1 g COD/L/d; NLR ~ 0.2 g TAN/L/d; sludge age ~ 800 d | |
| **Global efficiency** | **↓89%** | **-** | **↓82%** | **↓99%** | **~100%** | | |
| Raw leachate | 6200 | 832 | - | 2309 | 2003 | • Leachate collected from Orís urban landfill, Osona, Catalonia, Spain. | Anfruns et al [160] 2013 |
| PN-SBR | 5241 (↓15%) | 177 (↓79%) | | 2188 (↓5%) | 1054 (↓47%) | • <u>PN-SBR</u>: 24h-cycle (14 sub-cycles of 100 min each + 20 min settle + 20 min draw); Flow = 93 ± 7 L/d; NLR = 1.78 ± 0.15 kg N/m$^3$/d; SRT = 8 d; HRT = 2d. | |
| Anammox | 4686 (↓9%) | 123 (↓6%) | | 376 (↓78%) | 144 (↓45%) | • <u>Anammox</u>: $V_L$ = 377 L; T = 30 ± 1ºC; pH$_{max}$ = 7.4; N-load = 0.4 kg N/m$^3$.d; 8h-cycle (1h × 6 reaction phase + 95 min final reaction + 20 min settle + 5 min draw). | |

| Treatment stage | Parameters (mg/L) and removals | | | | | Observations/Conditions[a] | Reference |
|---|---|---|---|---|---|---|---|
| | COD | BOD₅ | DOC | TN | TAN | | |
| C/S | 803 (↓63%) | 7 (↓14%) | - | 258 (↓5%) | 164 (≈) | • <u>C/S</u>: $V_L$ = 1L; $FeCl_3.6H_2O$ = 560 mg $Fe^{3+}$/L. | Anfruns, et al. [160] 2013 |
| O₃ | 550 (↓4%) | 0 (↓1%) | - | 266 (≈) | 188 (≈) | • <u>O₃</u>: $V_L$ = 1L; pH = 7; $O_3$ = 1.15 g $O_3$/h; $t$ = 2h; T = 25 ± 2ºC; ozone generator Anseros COM-AD-02; ceramic diffuser | |
| **Global efficiency** | **↓91%** | **~100%** | **-** | **↓88%** | **↓91%** | • Produced sludge = 5.5 kg/m³_effluent | |
| Panammox® + Acidification | 2085 (↓42%) | 6 (↓14%) | - | 291 (↓4%) | 134 (≈) | • <u>Acidification</u>: pH adjusted to 3 with 0.5 M HCl; overnight settling. | |
| **Global efficiency** | **↓66%** | **↓99%** | **-** | **↓87%** | **↓93%** | • Produced sludge = 0.62 kg/m³_effluent | |
| Panammox® + Acid. + UV/Fe²⁺ | 1740 (↓48%) | 6 (↓14%) | - | 286 (↓4%) | 162 (≈) | • <u>UV/Fe²⁺</u>: $V_L$ = 0.8 L; pH = 3; $[Fe^{2+}]$ = 150 mg/L; $t$ = 7h; low pressure mercury UV lamp (50051, Heraeus, λ = 254 nm) | |
| **Global efficiency** | **↓72%** | **↓99%** | **-** | **↓88%** | **↓92%** | • Produced sludge = 0.72 kg/m³_effluent | |
| Panammox® + Acid. + UV/H₂O₂ | 1559 (↓50%) | 8 (↓14%) | - | 308 (↓3%) | 190 (≈) | • <u>UV/H₂O₂</u>: $V_L$ = 0.8 L; pH = 3; $[H_2O_2]$ = 1 g/L; $t$ = 7h; low pressure mercury UV lamp (50051, Heraeus, λ = 254 nm). | |
| **Global efficiency** | **↓75%** | **↓99%** | **-** | **↓87%** | **↓91%** | • Produced sludge = 0.02 kg/m³_effluent | |
| Panammox® + Acid. + Fenton | 1170 (↓57%) | 0 (↓15%) | | 247 (↓6%) | 182 (≈) | • <u>Fenton</u>: $V_L$ = 0.8 L; pH = 3; $[H_2O_2]$ = 1 g/L; $[Fe^{2+}]$ = 150 mg/L; $t$ = 7h. | |
| **Global efficiency** | **↓81%** | **~100%** | **-** | **↓89%** | **↓91%** | • Produced sludge = 0.26 kg/m³_effluent | |
| Panammox® + Acid. + PF | 109 (↓74%) | 0 (↓15%) | - | 290 (↓4%) | 229 (↓%) | • <u>PF</u>: $V_L$ = 0.8 L; pH = 3; $[H_2O_2]$ = 1 g/L; $[Fe^{2+}]$ = 150 mg/L; $t$ = 7h; low pressure mercury UV lamp (50051, Heraeus, λ = 254 nm). | |
| **Global efficiency** | **↓98%** | **~100%** | **-** | **↓87%** | **↓89%** | • Produced sludge = 0.38 kg/m³_effluent | |
| Raw leachate | 2800 | 510 | 660 | 2900 | 2400 | • Leachate collected from the municipal landfill of Chang Shankou, operating since 2007, in Wuhan City, Hubei province, China. | Abood, et al. [161] 2014 |
| Agitation (stripping) | 2400 (↓14%) | 480 (↓6%) | 520 (↓21%) | | 146 (↓94%) | • <u>Agitation</u>: $V_T$ = 0.5 L; pH = 11.5; velocity gradient = 150 s⁻¹; $t$ = 5h agitation + 0.5h settle. | |
| C/F | 824 (↓56%) | 258 (↓44%) | 340 (↓27%) | | 129 (↓1%) | • <u>C/F</u>: $V_T$ = 1 L; polymeric ferric sulfate (PFS) = 1.2 kg/m³; polyacrylamide = 1 mL of 0.1% solution; pH = 5.0; settle = 1h. | |
| SBR | 126 (↓25%) | 30 (↓45%) | 161 (↓27%) | - | 45 (↓3%) | • <u>SBR</u>: mix ratio (domestic wastewater) = 1:4; pH = 7.0-8.0; 14h-cycle operation (0.5h fill + 2h anoxic + 8h aerobic + 2h anoxic + + 1h settle + 0.5h draw); Carbon source: glucose. | |
| Filtration | 72 (↓2%) | 29 (≈) | 51 (↓17%) | - | < 18 (↓1%) | • <u>Filtration</u>: column = 20 cm²; media = sand + activate carbon; rate = 1m³/m²/h. | |
| **Global efficiency** | **↓97%** | **↓98%** | **↓92%** | **-** | **↓99%** | | |

| Treatment stage | Parameters (mg/L) and removals | | | | | Observations/Conditions[a] | Reference |
|---|---|---|---|---|---|---|---|
| | COD | BOD$_5$ | DOC | TN | TAN | | |
| Raw leachate | 14 680 | - | 8089 | - | 381 | • Leachate collected from a municipal landfill in Tetlama, Morelos, Mexico.<br>• Coagulation: [FeCl$_3$.6H$_2$O] = 300 mg/L; pH = 3.0; $t_S$ = 2h.<br>• Solar PF: CPC with 16 absorber tubes; [Fe$^{2+}$] = 5.5 mg/L; Q$_{UV}$= 90 kJ/L; [H$_2$O$_2$]: 630 mg/L.<br>• Removal efficiencies for As, Hg, and Pb were 46%, 9%, and 85%, respectively. | Vedrenne, et al. [78] 2012 |
| Coagulation | 12 067 (↓18%) | - | 1464 (↓82%) | - | 243 (↓36%) | | |
| sPF | 5430 (↓39%) | - | 280 (↓15%) | - | 92 (↓42%) | | |
| **Global efficiency** | ↓57% | - | ↓96% | - | ↓78% | | |
| Raw leachate | 5700 | - | 2400 | - | - | • Leachate collected from a municipal landfill, Vila Real, Portugal.<br><br>• Coagulation: [FeCl$_2$.6H$_2$O] = 2 g/L; pH = 5.<br><br>• Solar PF: CPC = 4.16 m$^2$; [Fe$^{3+}$] = 20 mg/L; $t$ = 11.5 h; Q$_{UV}$= 110 kJ/L; [H$_2$O$_2$]: 116 mM. | Amor, et al. [79] 2015 |
| Coagulation | 3400 (↓40%) | - | 1200 (↓50%) | - | - | | |
| sPF | 980 (↓42%) | - | 420 (↓33%) | - | - | | |
| **Global efficiency** | ↓83% | - | ↓83% | - | - | | |
| Raw leachate | 43 000 | - | 15 000 | - | - | • Landfill was not identified. Presumably a young or intermediate leachate.<br>• Pre-treatment: H$_2$SO$_4$ to decrease pH from 7 to 2.8-2.9; removal of settled solids; addition of [Fe$^{3+}$] = 2 mM (as FeCl$_3$.6H$_2$O) and repeated several coagulation steps<br>• SPF: CPC photoreactor: 3 m$^2$; 12 borossilicate glass tubes; V$_T$ = 35 L; pH = 2.8-2.9; [Fe$^{2+}$] = 1 mM; [H$_2$O$_2$] = 22 g/L, added periodically throughout the tests (700-1000 mg/L); $t$ = 11.4h; Q$_{UV}$ = 117 kJ/L<br>• Indirectly tested by means of Zahn-Wellens biodegradability test | Torres-Socías, et al. [162] 2015 |
| Acidification/ Coagulation | 29 000 (↓25%) | - | 13 000 (↓25%) | - | - | | |
| sPF | 14 000 (↓25%) | - | 8200 (↓25%) | - | - | | |
| Biological oxidation | - | - | - | - | - | | |
| Raw leachate | 427-869 | - | - | - | 244-627 | • Raw leachate collected from the landfill site of IMOG in Moen, Belgium.<br>• ANR: cylindrical vessel, $V_T$ = 6 L; reactor top packed with polyurethane foam (pore size 2-3 mm); semi-continuous feed (6.5 min feed/8.5 min react). HRT = 2 d; T = 35 ± 1 ºC; $DO$ = 0.30 – 0.70 mg O$_2$/L.<br>• O$_3$: generator (Ozomat COM-AD-02, Anseros) V$_L$ = 10 L; O$_2$ flow = 1 L/min; ([O$_3$]$_{inlet}$ = 90 mg/L; [O$_3$] = 0.48 g/L of leachate; $t$ = 60 min (5.4 g O$_3$/h)<br>• GAC: glass column (internal diameter 2.54 cm and length 100 cm), packed with 50 cm (135 g) of GAC (Organosorb10®, Desotec); bed volume = 0.27 L; operated down-flow mode; flow-rate = 8.82 mL/min | Gao, et al. [163] 2015 |
| ANR + O$_3$ **Global efficiency** | ↓27% | - | - | ↓80% | - | | |
| ANR + GAC **Global efficiency** | ↓81% | - | - | ↓66% | - | | |
| ANR + O$_3$ + GAC **Global efficiency** | ↓83% | - | - | ↓78% | - | | |

| Treatment stage | Parameters (mg/L) and removals | | | | | Observations/Conditions[a] | Reference |
|---|---|---|---|---|---|---|---|
| | COD | BOD₅ | DOC | TN | TAN | | |
| ANR/O₃ **Global efficiency** | ↓91% | - | - | ↓27% | - | • <u>ANR/O₃</u>: O₃ effluent recycled to ANR was 1/10 volume ratio. | Gao, *et al.* [163] 2015 |
| | ↓84% | - | - | ↓41% | - | • <u>ANR/O₃</u>: O₃ effluent recycled to ANR was 1/4 volume ratio. | |
| | ↓83% | - | - | ↓52% | - | • <u>ANR/O₃</u>: O₃ effluent recycled to ANR was 1/2 volume ratio. | |
| Raw leachate | 1550 | - | 323 | 299 | 288 | • Leachate collected from Frampton's municipal landfill, Québec, Canada. • MBR with a submerged hollow fiber ultrafiltration (ZW-1), nominal pore size = 0.04 μm and total filtration surface area = 0.047 m². • MBR: $V_T$ = 5 L; T = 17.5 ± 1.0 ºC; DO = 7.0 ± 0.8 mg O₂/L; OLR = 1.2 g COD/L/day; HRT = 32 h; SRT = 80 day; VSS = 8.9 g/L • EOP: electrode: Ti/BDD; current intensity = 3 A; voltage = 13.2 V; *t* = 120 min; T = 21 ± 1 ºC; pH = 8.4 ± 0.2. | Zolfaghari, *et al.* [164] 2016 |
| Sequencing MBR | 568 (↓63%) | - | 209 (↓35%) | 209 (↓30%) | 5 (↓98%) | | |
| EOP | 89 (↓31%) | - | 57 (↓47%) | 410 (↑67%) | 65 (↑21%) | | |
| **Global efficiency** | ↓94% | - | ↓82% | ↑37% | ↓77% | | |
| Raw leachate | 2122 | - | 434 | 700 | 667 | • Leachate collected from the same site, at a different time period. Similar operational conditions as described above. | |
| Sequencing MBR | 993 (↓53%) | - | 333 (↓23%) | 630 (↓10%) | 5 (↓99%) | | |
| EOP | 435 (↓26%) | - | 214 (↓27%) | 607 (↓3%) | 9 (↑1%) | | |
| **Global efficiency** | ↓80% | - | ↓51% | ↓13% | ↓99% | | |
| Raw leachate | 1485 | - | 385 | 712 | 710 | • Leachate collected from the same site, at a different time period. • EOP: electrode: Ti/BDD; current intensity = 3 A; voltage = 9.8 V; *t* = 41 h; T = 20 ± 1 ºC; pH = 8.1 ± 0.2. • MBR: $V_T$ = 5 L; T = 17.5 ± 1.0 ºC; DO = 7.0 ± 0.8 mg O₂/L; HRT = 46 h; SRT = 100 d; VSS = 6.7 g/L. | |
| EOP | 639 (↓57%) | - | 248 (↓36%) | 688 (↓3%) | 623 (↓12%) | | |
| Sequencing MBR | 444 (↓13%) | - | 120 (↓33%) | 445 (↓34%) | 128 (↓70%) | | |
| **Global efficiency** | ↓70% | - | ↓69% | ↓38% | ↓82% | | |

| Treatment stage | Parameters (mg/L) and removals | | | | | Observations/Conditions[a] | Reference |
|---|---|---|---|---|---|---|---|
| | COD | BOD$_5$ | DOC | TN | TAN | | |
| Raw leachate | 6660 | - | - | - | - | • Leachate obtained from a Chilean landfill (16.7 ha total area) managing domestic waste. • US + O$_3$: pilot-plant, in batch mode, $V_L$ = 12 L, recirculated at 12 L/min, for $t$ = 2h. US system: Elamsonic E60H, 500 W, 37 kHz frequency. Ozone generator: Netech CH-KTB 3 G, 100 W and 3 g O$_3$/h. Bubble diffuser. • H$_2$O$_2$: 350 mg/L added at the beginning and every 20 min; $t$ = 2h. • Solar: CPC with illuminated area = 0.36 m$^2$; $t$ = 2h. | Poblete, et al. [165] 2017 |
| US + O$_3$ Global efficiency | ↓15% | - | - | - | - | | |
| US + O$_3$/H$_2$O$_2$ Global efficiency | ↓ 34% | - | - | - | - | | |
| Solar/O$_3$ Global efficiency | ↓ 28% | - | - | - | - | | |
| Solar/O$_3$/H$_2$O$_2$ Global efficiency | ↓ 34% | - | - | - | - | • As described above. | |
| AC + US + O$_3$ Global efficiency | ↓ 49% | - | - | - | - | • As described above, with adsorption as pre-treatment. • Adsorption: using AC from coffee waste. Mean AC size = 120 nm; mean specific surface area = 45.8253 m$^2$/g. [AC] = 1 g/L; $V_L$ = 40 L of leachate recirculated at 40 L/min, for $t_R$ = 2h. | |
| AC + US + O$_3$/H$_2$O$_2$ Global efficiency | ↓ 67% | - | - | - | - | | |
| AC + Solar/O$_3$ Global efficiency | ↓ 59% | - | - | - | - | | |
| AC + Solar/O$_3$/H$_2$O$_2$ Global efficiency | ↓ 71% | - | - | - | - | | |
| Raw leachate | 5300 | - | 1399 | 1750 | 1600 | • Leachate (medium-age) collected from Apulia municipal landfill, Italy. | Pastore, et al. [166] 2018 |
| SBBGR | 2410 ↓55% | - | 1073 ↓23% | 195 ↓89% | 173 ↓89% | • SBBGR: cylindrical reactor partially filled with biomass support material KMT-k1 (Kaldness, Norway); $V_T$ = 16 L; HRT = 12 d; Carbon source: methanol (3 g/L). | |
| SBBGR/H$_2$O$_2$ | 1750 | - | 844 | 126 | 123 | • SBBGR/H$_2$O$_2$ and SBBGR/UV+H$_2$O$_2$: flow-through annular photoreactor, with low pressure mercury UV lamp (40W, MTL844-G, Helios) emitting at 254 nm; UV$_{lamp}$ = 11.8 W (determined by actinometry); $t$ = 6.5h; flow rate recirculation SBBGR/photoreactor = 3 L/h; [H$_2$O$_2$] = 26 mL of a 3% solution | |
| Global efficiency | ↓67% | | ↓40% | ↓93% | ↓92% | | |
| SBBGR/UV+H$_2$O$_2$ | 1230 | - | 500 | 71 | 62 | | |
| Global efficiency | ↓77% | | ↓64% | ↓96% | ↓96% | | |
| SBBGR/O$_3$ | 184 | - | 77 | 41 | 22 | • SBBGR/O$_3$: $t$ = 6.5h; flow rate to ozone system = 70 L/h, and back to SBBGR by gravity; [O$_3$]$_{inlet}$ = 3.6 g/L | |
| Global efficiency | ↓97% | | ↓94% | ↓98% | ↓99% | | |

| Treatment stage | Parameters (mg/L) and removals | | | | | Observations/Conditions[a] | Reference |
|---|---|---|---|---|---|---|---|
| | COD | BOD$_5$ | DOC | TN | TAN | | |
| Raw leachate | 7184 | 220 | - | - | - | • Leachate collected from Ariyamangalam dumping site, Trichy, India. <br>• E-Fenton: electrode: TiO$_2$/Ti and graphite; voltage = 5 V; catalyst: FeMoPO; V$_L$ = 0.75 L; pH = 3.0; $t$ = 90 min. <br>• Biological oxidation: V$_L$ = 0.1 L; T = 37 ºC; agitation = 110 rpm; pH = 8.0; $t$ = 5 d. | Baiju, et al. [167] 2018 |
| Electro-Fenton | 1293 (↓82%) | 517 (↑135) | - | - | - | | |
| Biological oxidation | 192 (↓15%) | - | - | - | - | | |
| **Global efficiency** | **↓97%** | - | - | - | - | | |
| Raw leachate | 12 797 | - | - | - | 1416 | • 100 L of leachate collected from a landfill located in the western region of Paraná, Brazil. Colour = 4464 Pt-Co; BOD$_5$/COD ratio = 0.33 <br>• PF: 3 high-pressure Hg lamps (250 W, total irradiance ~ 20 W/m$^2$); V$_T$ = 0.1 L; [H$_2$O$_2$] = 3400 mg/L; [Fe$^{2+}$] = 80 mg/L; T = 35 ± 5 ºC; pH = 2.4 <br>• CAS: BIOFLO 110 reactor; V $_{(leachate + biomass)}$ = 3.5 L; T = 30 ± 1 ºC; pH = 6.5-8.5; HRT = 150 h; aeration rate: 1.57 (vvm); F/M: 4.41 mg/mg (BOD$_5$/MLSS) | Colombo, et al. [168] 2019 |
| PF | 2940 (↓77%) | - | - | - | 2280 (↑61%) | | |
| CAS | 1685 (↓10%) | - | - | - | 1119 (↓21%) | | |
| **Global efficiency** | **↓87%** | - | - | - | **↓21%** | | |

[a] NLR – nitrogen loading rate; SRT – sludge retention time; HRT – hydraulic retention time; V$_T$ – total volume of the reactors, for cases where V$_L$ – leachate volume tested, is not clearly identified; $t_s$ – settling time; vvm – volume of air under standard conditions per volume of liquid per minute; F/M – food to microorganism ratio.

**Table 3.10** – Estimated operating costs for the combination of treatment processes applied to landfill leachate (research reported over the past decade).

| Treatment stages | Parameters (mg/L) and removals | | | Energy demand, chemical consumption, and sludge production | Costs (€/m³) | | | Total cost | Reference |
|---|---|---|---|---|---|---|---|---|---|
| | $COD_0$ | $TN_0$ | $TAN_0$ | (kWh/m³ or kg/m³) | $E^a$ | $C^a$ | $S^a$ | (€/m³) | |
| SBBGR+ sPF | 3100 (↓95%) | - | ~1000 (↓99%) | • SBBGR: (i) Pumps + air supply = 12; (ii) Methanol = 3; (iii) Sludge = 0.4 | 0.84 | 2.76 | 0.53 | 4.13 | Cassano, et al. [158] 2011 |
| SBBGR/$O_3$ | | | | • $O_3$: (i) Energy[b] = 19.2 or 4.8; (ii) Oxygen[b] = 15.5 or 3.0 | 2.18 | 3.36 | 0.20 | 5.74 | |
| SBBGR/$O_3$ + sPF | | | | • sPF: (i) $H_2O_2$[c] = 2.75 or 3.12 L/m³; (ii) $Fe^{2+}$ = 0.29; (iii) Sludge[c] = 0.64 or 0.31 | 1.18 | 3.28 | 0.36 | 4.82 | |
| C/F + $O_3$ | 4686 (↓89%) | - | - | • C/F: (i) $FeCl_3.6H_2O$ = 2.7; (ii) Sludge = 5.5 • $O_3$: (i) NaOH (50%) = 0.16; (ii) Energy[d] = 3.5 | 4.04 | 0.93 | 2.75 | 7.72 | Anfruns, et al. [160] 2013 |
| PF | 4686 (↓89%) | - | - | • PF: (i) HCl (0.5 N) = 23 L/m³; (ii) $FeSO_4.7H_2O$ = 0.75; (iii) $H_2O_2$ = 2.5; (iv) NaHO (50%) = 0.16; (v) UV lamp = 0.072 kWh[d] | 0.008 | 4.15 | 0.5 | 4.66 | |
| PF | 4686 (↓98%) | - | - | • PF: (i) HCl (0.5 N) = 23 L/m³; (ii) $FeSO_4.7H_2O$ = 0.75; (iii) $H_2O_2$ = 5.8; (iv) NaHO (50%) = 0.16; (v) UV lamp = 0.168 kWh[d] | 0.02 | 6.66 | 0.5 | 7.18 | |
| Agit + C/F + SBR + Filtr. | 2800 (↓97%) | - | 2400 (↓99%) | • Agitation: (i) Energy = 20.4; (ii) NaHO = 8 • C/F: (i) Energy = 0.0018; (ii) $H_2SO_4$ = 6; (iii) PFS = 1.2; (iv) polyacrylamide = 0.1 • SBR: (i) Energy = 0.09; (ii) NaOH = 0.5; (iii) $H_2SO_4$ = 0.5; (iv) Glucose = 0.5 • Filtration: (i) Energy = 0.08 | 2.27[e] | 3.52[e] | - | 5.79[e] | Abood, et al. [161] 2014 |
| Pre-treatment + sPF | - | - | - | • sPF: (i) Energy = 1.6; (ii) $H_2SO_4$ (96%) = 6.4 L/m³; (iii) $FeCl_3.6H_2O$ = 0.9; (iv)$H_2O_2$ = 22 (73 L of 30% w/v/m³ of treated leachate) | 0.1 | 31 | - | 31.1 | Torres-Socías [162] 2015 |
| ANR + $O_3$ | 427 - 869 (↓27%) | (↓80%) | - | Details regarding the estimation of treatment costs for: • ANR pilot-scale reactor can be consulted at [169] • $O_3$ and GAC can be consulted at [170] | - | - | - | 0.23 - 0.73 | Gao, et al. [163] 2015 |
| ANR + GAC | ↓81% | (↓66%) | - | | - | - | - | 1.36 | |
| ANR + $O_3$ + GAC | (↓83%) | (↓78%) | - | | - | - | - | 1.11 – 1.75 | |
| ANR/$O_3$ | (↓91%) | (↓27%) | - | | - | - | - | 0.14 – 0.19 | |

| Treatment stages | Parameters (mg/L) and removals | | | Energy demand, chemical consumption, and sludge production | Costs (€/m³) | | | Total cost | Reference |
|---|---|---|---|---|---|---|---|---|---|
| | $COD_0$ | $TN_0$ | $TAN_0$ | (kWh/m³ or kg/m³) | $E^a$ | $C^a$ | $S^a$ | (€/m³) | |
| | (↓84%) | (↓41%) | - | | - | - | - | 0.17 – 0.29 | |
| | (↓83%) | (↓52%) | - | | - | - | - | 0.22 – 0.47 | |
| US + $O_3$ | 6600 (↓15%) | - | - | | 15.0[e] | 0 | - | 15.0[e] | Poblete, et al. [165] 2017 |
| US + $O_3$/$H_2O_2$ | (↓34%) | - | - | | 15.0[e] | 18.0[e] | - | 33.0[e] | |
| Solar/$O_3$ | (↓28%) | - | - | | 3.1[e] | 0 | - | 3.1[e] | |
| Solar/$O_3$/$H_2O_2$ | (↓34%) | - | - | | 3.1[e] | 23.9[e] | - | 27.0[e] | |
| AC + US + $O_3$ | (↓49%) | - | - | | 29.5[e] | 40.0[e] | - | 69.5[e] | |
| AC + US + $O_3$/$H_2O_2$ | (↓67%) | - | - | | 29.5[e] | 58.0[e] | - | 87.5[e] | |
| AC + Solar/$O_3$ | (↓59%) | - | - | | 11.7[e] | 40.0[e] | - | 51.7[e] | |
| AC + Solar/$O_3$/$H_2O_2$ | (↓71%) | - | - | | 17.6[e] | 63.9[e] | - | 81.5[e] | |
| SBR + GAC | 548-1846 < 250[f] | 400 | < 5[f] | Further details regarding operational conditions and the estimation of treatment cost for: <br> • ANR: can be consulted at [169] <br> • Ozonation: can be consulted at [171] <br> • Fenton: can be consulted at [170] <br> • Coagulation: can be consulted at [170, 172] | 0.09 | 1.72 | 0.09 | 1.90 | Oloibiri, et al. [173] 2017 |
| ANR + GAC | | | | | 0.04 | 1.32 | n.a. | 1.36 | |
| ANR[f] + SBR[f] + GAC | | | | | 0.07 | 1.56 | 0.05 | 1.68 | |
| SBR + $O_3$[f] + GAC | | | | | 0.23 | 1.43 | 0.09 | 1.76 | |
| SBR + F[f] + GAC | | | | | 0.09 | 1.78 | 0.09 | 1.96 | |
| SBR + C/S[f] + GAC | | | | | 0.09 | 1.30 | 0.09 | 1.48 | |
| ANR + $O_3$[f] + GAC | | | | | - | - | | 1.43 | |
| ANR + F[f] + GAC | | | | | 0.04 | 1.38 | - | 1.42 | |
| ANR + C/S[f] + GAC | | | | | 0.04 | 0.90 | | 0.94 | |

[a] Abbreviations: E – energy; C – chemicals; and S – sludge. [b] For $O_3$ dose = 1.6 kg/m³$_{inf}$ (SBBGR/$O_3$) and 0.4 kg/m³$_{inf}$ (SBBGR/$O_3$ + sPF), respectively. [c] For SBBGR + sPF and SBBGR/$O_3$ + sPF, respectively. [d] Estimated considering the electricity price in Spain and the electrical energy needed to produce $O_3$, 10 kWh/kg $O_3$, or the UV lamp power (0.024 kW) and the treatment time (7h). [e] The values shown were converted from US dollars (3rd March 2020, 1 USD = 0.89 EUR). [f] < 250 and < 65 mg/L, for COD and TN, to respect the Flemish legal limits for discharge. Integration biological processes (ANR + SBR): assuming 40% and 60% of nitrogen removal, respectively. Ozonation ($O_3$): dose = 0.14 g $O_3$/g $COD_0$, with $COD_0$ = 724 mg/L and 10% COD removal, for SBR + $O_3$ [171]; and dose = 0.48 g $O_3$/g $COD_0$, with $COD_0$ = 869 mg/L and 19% COD removal, for ANR + $O_3$ [163]; Fenton: pH = 6.0; [$Fe^{2+}$] = 1117 mg/L; [$H_2O_2$] = 1020 mg/L. Coagulation: dose = 1.3 g $FeCl_3$/g $COD_0$.

For the COD target of 500 mg/L, the investigated treatment set-ups presented comparable operating cost (3.2 €/m$^3_{infl.}$); while for COD target of 160 mg/L, combining SBBGR + sPF was economically more convenient (4.1 €/m$^3_{infl.}$), followed by SBBGR/O$_3$ + sPF and SBBFR/O$_3$ (4.8 and 5.7 €/m$^3_{infl.}$, respectively), indicating the energy savings offered by the option of using a solar photo-oxidation stage. It is worth mentioning the authors' care in presenting the amount of sludge generated (biological and chemical) and considering it in the cost estimates. However, the consumption and costs associated with the reagents required for pH adjustments have not been accounted for and may have some relevance due to the alkalinity levels of the leachate (and, in this case, its balance after a biological nitrification/denitrification stage). The authors also mention having verified the possibility of using the solar photo-Fenton as a pre-treatment (before the SBBGR), to increase the leachate's biodegradability. However, these results were set aside as the high consumption of H$_2$O$_2$ (3 to 4 g/L) would lead to increased operational costs for a limited biodegradability enhancement. As additional remark, although described that solar UV radiation was measured throughout the experiments (by a global UV radiometer), no data regarding UV energy consumption was presented for the conducted sPF tests.

Using the leachate coming from the same landfill as Cassano, *et al.* [158], in 2013, Del Moro, *et al.* [159] tested the effectiveness of the same biological treatment (SBBGR) followed by a UV/H$_2$O$_2$ process and compared it with the usage of the same AOP but integrated with the biological stage. According to the results (Table 3.9), removal efficiencies higher than 80% for COD, DOC, TAN and TN where obtained when UV/H$_2$O$_2$ was integrated with the biological treatment, thus allowing the effluent to be discharged into the sewerage system (according to Italian legislation). The higher efficiencies obtained for the integrated biological-AOP system (in this case, SBBGR/UV/H$_2$O$_2$) were related to the biological removal of the biodegradable compounds produced along the UV/H$_2$O$_2$ treatment. Contrary, no advantage was taken from AOP's ability to increase the biodegradability, when that process was used as an end treatment.

Anfruns, *et al.* [160] tested two treatment strategies by combining a partial nitritation-anammox system (Panammox®) with (i) coagulation/flocculation and ozonation (C/F + O$_3$), or (ii) photo-Fenton (PF), to assess nitrogen and carbon removal. Panammox® is a biological system consisting of a two-step autotrophic nitrogen removal, i.e. a partial nitritation sequencing batch reactor (PN-SBR), where about 50% of the influent TAN was oxidized to nitrite, followed by an anammox reactor, where ammonium was oxidized to N$_2$ using nitrite as the electron acceptor (further details can be found in Table 3.9). According to the authors, Panammox® system was able to remove total nitrogen within a range of 87-89%, without the need of any external carbon source. Nonetheless, under the experimental conditions applied, compliance with the legal limit values for total nitrogen,

or even for ammonia, were not achieved. The authors attributed heterotrophic denitrification (which occurred in the PN-SBR) as the main cause of the misadjusting of the expected effluent nitrogen species concentrations, since anammox activity was limited by the availability of nitrite (which was also reduced by heterotrophic bacteria). COD removal efficiencies were 91% for coagulation/flocculation and ozonation, and of 98% for photo-Fenton allowing, in this case, to reach a COD value below the legal limit. Furthermore, COD removal efficiencies, including the generation of sludge, for the acidification step prior to the PF oxidation reaction (Panammox® + acidification), and acidification followed by $UV/Fe^{2+}$ or $UV/H_2O_2$ or Fenton oxidation, were also presented. Operational costs considering the combination of $C/F + O_3$ stages and PF process were estimated (Table 3.10). However, the values reported should be viewed with reservations since, when carefully analysed: (i) oxygen consumption was not considered for the generation of $O_3$; (ii) the energy consumption for the photo-Fenton does not consider the volume of treated leachate, which introduces an error in its calculation and underestimates its value.

To meet COD and TAN (but not TN) discharge standards, Abood, *et al.* [161] tested, at lab-scale, a combined process of agitation, coagulation, SBR and filtration. The agitation stage was presented as a novel stripping method intended to overcome the ammonia toxicity. Within a 5h agitation time, at pH 11.5 and a velocity gradient of 150 $s^{-1}$, TAN removal of 94% was obtained. The following coagulation stage, using poly ferric sulfate (PFS) at pH 5.0, was then able to remove 56% of the total COD content. This pre-treatment (agitation + C/F) increased the biodegradability ratio $BOD_5$/COD from 0.18 to 0.31. Nonetheless, the effluent was diluted by the addition of domestic wastewater (ratio 1:4) before it was fed to the SBR, and glucose was further added as an external carbon source. Legal compliance was practically achieved at the end of the SBR stage (Table 3.9). After the filtration process (sand and carbon as a dual filter media), the final effluent concentrations of COD, BOD, SS, TAN, and TOC were all considerably inferior to the legal standards applied in different world countries (72 mg/L, 23 mg/L, 24 mg/L, 18 mg/L, and 51 mg/L, respectively). So, with a global efficiency of 97% and 99% for COD and TAN removal, respectively, the overall operating cost of the combined treatment was estimated as \$6.30/$m^3$ (5.79 €/$m^3$, energy and reagents specific consumptions can be seen in Table 3.10). Unfortunately, besides for the raw leachate characterization, total nitrogen was neglected in this study (probably because it is not a legal requirement in the country of origin of the research).

In 2015, Torres-Socías, *et al.* [162], reported the results of a combined treatment line for landfill leachate, consisting of a physicochemical pre-treatment stage followed by solar photo-Fenton and a final conventional biotreatment. According to the raw leachate characterization ($COD_0$ of 43 g/L; $DOC_0$ = 15 g/L; $[K^+]_0$ = 5.7 g/L; $[SO_4^{2-}]_0$ = 16 g/L), it seems that the authors where dealing with a

young or intermediate leachate. Aware that photo-Fenton efficiency and operating costs can greatly benefit of preliminary physicochemical treatment, the first treatment stage consisted of acidification (from pH 7 to pH 2.8-2.9), causing the coagulation of part of suspended solids and colour change, settling and removal of acidic sludge, and addition of 2 mM $Fe^{3+}$ (as $FeCl_3.6H_2O$) for secondary coagulation. The authors indicate that "*the same procedure was repeated and after several coagulation steps the final concentrations of COD, DOC and dissolved iron (56-57 mg/L) were stable*". This could be so for research purposes, but the impracticability of such procedure at full-scale should have been considered. Solar photo-Fenton was then carried out in a CPC photoreactor (irradiated surface of 3 $m^2$) and the final conventional biotreatment was indirectly evaluated by means of Zahn-Wellens biodegradability test. The authors recommended that sPF treatment should be maintained until mineralization of 27% (final DOC of 8 g/L) and elimination of 30% of COD were achieved (with associated global $H_2O_2$ consumption of 22 g/L and total accumulated UV energy required of 137 kJ/L). Taking these results as design points for the scaling up of the sPF process (leachate design flow of 40 $m^3$/day and 365 days/year of operation), a CPC collector surface of 6850 $m^2$ was necessary (with an associated cost of 349 €/$m^2$-collector, including auxiliary systems), involving treatment costs related to investment of 10 €/$m^3$ of leachate to be treated (considering a depreciation period of 15 years). Regarding operational costs, the authors included reagents used for pre-treatment (for acidification and $FeCl_3$) within the photo-Fenton reagent costs, and intentionally neglected the sludge production (as it would be recycled to the landfill) and the final conventional biological treatment (< 1 €/$m^3$). Regardless these, the total reagent costs presented in this study (31 €/$m^3$) would economically impair the proposed treatment strategy. Finally, the labour requirement for plant's operation was also estimated on 3h-man/batch (considering one batch per day and 18.8 €/h-man), this allows to add 1.4 €/$m^3$ to the operational costs presented in Table 3.10.

It makes sense the usage of a preliminary physicochemical treatment for removal of suspended solids and colour, as light penetration plays an important role in photo-oxidation processes. Due to its simplicity and ability in removing suspended solids, colloidal particles, colour, and organic load (such as, humic substances), coagulation is normally the pre-treatment of choice for photo-Fenton. Additionally, the combination of these two processes increases the removal of heavy metals and other species that are refractory to biological oxidation, as demonstrated by Vedrenne*, et al.* [78]. However, the major drawback of this treatment process combination is the great volume of sludge that may be generated. Vedrenne*, et al.* [78] pointed out that the volume of sludge amounted to more than 25% of the leachate initial value. As the previous researchers, also Amor*, et al.* [79] presented a work combining coagulation and solar photo-Fenton for the treatment of mature landfill

leachate. In this case, the authors intended to evaluate the feasibility to achieve the legal limit for COD to discharge into natural water courses. Although PF process improved the leachate's biodegradability (tested by respirometry), the authors advise not to release the coagulated-photo-treated leachate into a biological process, as in their opinion the DOC concentration was rather low when biodegradability threshold was reached. It is therefore proposed to continue PF process until reaching the legal limits for discharge into the environment or into public sewerage systems (since its COD legal limit, 1000 mg/L, was obtained under the tested conditions).

In 2015, aiming at an appropriate combination for effective and economical COD and nitrogen removal from landfill leachate, Gao, et al. [163] tested an autotrophic nitrogen removal (ANR) process followed by different post-treatment possibilities (ANR + $O_3$; ANR + GAC; ANR + $O_3$ + GAC). Ensuring a high removal of both COD and total nitrogen (Table 3.9), the best performance was obtained for an ANR post-treatment combination of ozonation and GAC. An integrated approach with continuous recirculation of ozonated ANR effluent (ANR/$O_3$) was also investigated. This approach was very successful for the removal of COD, but a decrease on total nitrogen removal was observed. The authors attributed this effect the need of a higher period for biomass adaptation or, inhibition of the autotrophic bacteria by heterotrophic competition. Also, a preliminary cost analysis is presented, based on the removal efficiency of the separated post-treatment techniques and cost factors related to full-scale installations (obtained in previous studies [169, 170]). The combination ANR + $O_3$ + GAC was considered the most cost effective due to the high COD and nitrogen removal (Table 3.10). The much lower cost presented in this study, when compared to others that applied ozone to landfill leachate, was attributed by the authors to the applied ozone dosage.

Zolfaghari, et al. [164], in 2016, combined a high performance MBR (5 L capacity), equipped with ultrafiltration, and electro-oxidation process (EOP) to treat mature landfill leachate. In this case, the tested strategy was not able to deal with the variability shown by the influent leachate, so the final COD value obtained was not always consistent to comply with legal limits. It should be mentioned that, on the contrary, many research studies apply leachate samples collected at a single time, therefore not experiencing difficulties regarding to the normally high variability of the leachate composition. Additionally, although the SBR removed TAN in the order of 99%, the value of TN only decreased slightly, indicating a low occurrence of biological denitrification. The authors also explored switching the sequence of the processes, first applying the EOP and then the sequential MBR, but no improvements on treatment efficiency were obtained. However, the energy consumption by EOP increased from 16 to 22 kWh/$m^3$, for biologically treated and raw landfill leachate, respectively.

A study by Poblete*, et al.* [165], in 2017, tested a combined coffee-waste based activated carbon (AC) with hybrid advanced oxidation processes. They compared eight treatment scenarios in terms of landfill leachate depuration (COD and colour removal were evaluated), specific energy consumption, and associated reagent and operational costs. The tested treatment scenarios were (i) ultrasound combined with ozonation (US + $O_3$), and (ii) solar/ozonation (solar/$O_3$), with or without $H_2O_2$ addition, and with or without AC pre-treatment. Under the tested experimental conditions, and in the absence of the AC pre-treatment, no combination between AOPs was able to reach a COD removal above 35%. Also, with or without AC pre-treatment, for all four scenarios with $H_2O_2$ addition, an increase of the treatment efficiency was observed (Table 3.9). Nonetheless, the estimated operational costs are not encouraging (Table 3.10). By far the lowest operational cost was presented by solar/$O_3$ combination ($3.5/m$^3$, or 3.21€/m$^3$), with a COD and colour removal of 28% and 45%, respectively. The remaining combinations, particularly those with AC pre-treatment, presented impractical costs, from $58.1 to $98.4/m$^3$ of leachate (corresponding between 53.33 to 90.32 €/m$^3$).

Pastore*, et al.* [166], in 2018, investigated the integration of three different chemical oxidation processes ($H_2O_2$, $H_2O_2$ + UV and $O_3$) after a biological treatment, run in a sequencing batch biofilter granular reactor (SBBGR), for the treatment of a medium-age urban leachate (following the works by Cassano*, et al.* [158] and Del Moro*, et al.* [159]). The SBBGR was able to remove 54% and 23% of COD and DOC, respectively, but still required a deeper treatment to comply with the discharge legal standards (in this case, Italian legislation, see Table 2.5, from chapter 2). COD removals around 50% can be expected for biological treatment applied to younger leachates such the one used in this study. The SBBGR was also able to reduce 89% of TAN and TN, due to the occurrence of simultaneous nitrification-denitrification process. Similarly to the previous studies [158, 159], the SBBGR treatment cycle did not included a planned anoxic phase, so the ability of biological nitrogen removal rely in the particular structure of the granular biomass growing in SBBGR system (i.e. with ammonia oxidizing bacteria located in the outer layers, while in the deeper layers, where oxygen cannot penetrate, denitrifying organisms prevail). Furthermore, to ensure that complete denitrification was obtained, an external carbon source (methanol at 3 g/L) was used. The integration with chemical oxidation processes improved the overall treatment efficiency for COD removal as follows: SBBGR/$H_2O_2$ (67%) < SBBGR/UV + $H_2O_2$ (77%) < SBBGR/$O_3$ (97%). Despite the efforts, only the combination of SBBGR/$O_3$ attained a COD value that allows the discharge into a sewerage system (500 mg/L), but not for direct discharge into the environment (160 mg/L). In this study, no capital or operating cost estimates were presented.

Baiju*, et al.* [167], 2018, tested a combined electro-Fenton (EF) and biological treatment for stabilized landfill leachates which resulted in an overall COD removal of 97%, bringing down the final COD from 7184 mg/L to 192 mg/L. In this case, at the end of 90 min, not only the EF process alone was responsible for 82% of COD removal but also increased $BOD_5$/COD ratio from 0.03 to 0.40. Nonetheless, the final biological oxidation was not able to reach a COD value compatible with the most stringent legal regulations (see Table 2.5, from Chapter 2). Furthermore, this study also aimed to test the efficiency of iron molybdophosphate nanoparticle as a heterogeneous catalyst in electro-Fenton process, presenting intensive material characterization work, so (regrettably) operating cost estimates were not approached.

Using a combined photo-Fenton and biological activated sludge process, with an overall removal of 98% for each parameter, in 2019 Colombo*, et al.* [168] reported results in compliance with the Brazilian legal standards for COD and $BOD_5$. While the use of both processes alone did not meet effluent discharge standards, with the combined process it was possible to treat an effluent with high organic load ($COD_0 = 12\ 797 \pm 156$ mg/L and $BOD_5 = 4251 \pm 87$ mg/L). With the combined treatment, 93-96% of the single aromatic compounds and 96% of the conjugated aromatic compounds were removed. In addition, this process removed about 98% of turbidity and colour, reaching values of $8.1 \pm 0.1$ NTU and $77 \pm 2$ Pt-Co, respectively. In turn, with PF process, the TAN concentration in the leachate increased from $1416 \pm 44$ to $2280 \pm 21$ mg/L. According to the authors, this was explained by the possible oxidation of the organic pollutants by the hydroxyl radicals, breaking the original chemical structures, and releasing nitrogenous compounds. In the biological treatment, part of this nitrogen was oxidised, obtaining a final concentration of $1119 \pm 20$ mg/L. Also, the total sulfate in the raw leachate was $85 \pm 8$ mg/L and increased to $8389 \pm 251$ mg/L after PF, and later decreased to a final concentration of $5033 \pm 151$ mg/L in the biological treatment. Both TAN and sulfate final values were considerably higher than the legal admissible for direct discharge. The authors also point out that the PF process produced $870 \pm 18$ mg/L of sludge, a considerably lower value when compared to the conventional Fenton process ($1744 \pm 34$ mg/L).

Regarding treatment costs, although only including the AOPs stage (Fenton, $O_3$ or $O_3 + H_2O_2$), the studies by Cortez*, et al.* [100] and [97] should also be mentioned. In these studies, the leachate was collected after treatment in the landfill LTP (including anaerobic lagoons, anoxic tank, aerated lagoons, and a biological decantation unit, followed by an oxidation tank and two chemical precipitators), did not meet the maximum allowable nitrogen and organic matter concentrations for direct or indirect discharge. In a first study [100], the authors tested the application of $O_3$ (at pH 3.5, 7, 9 and 11) and $O_3/H_2O_2$ (using concentrations of 200, 400 and 600 mg $H_2O_2$/L), obtaining the respective operating costs of 64.0, 49.4, 41.7, 38.2, 31.9, 26.6 and 24.7 €/m$^3$/g $COD_{removed}$. In this

case, they used the leachate as it was (i.e. $COD_0$ = 743 mg/L, respective removal efficiencies and operational conditions can be consulted at Table 3.4) and not only the final COD did not achieve the legal value under any tested condition (the authors propose to follow with biological treatment), as the estimated costs are quite discouraging. The following work [97] was applied to the leachate two times diluted (i.e. $COD_0$ = 340 mg/L, again experimental details are displayed at Table 3.4) and operating costs of 8.2, 65.5 and 25.6 €/m³/g $COD_{removed}$ were obtained for Fenton, $O_3$, and $O_3/H_2O_2$, respectively. Fenton oxidation process offered by far the lowest operating cost; however, sludge treatment and disposal were not taken into account and the final COD value was still slightly higher than the legal standard. Notwithstanding, the ozonation costs in both studies seem to be overestimated and the data provided does not allow an independent calculation (no data regarding specific energy or reagents consumption).

In 2017, an operational cost evaluation in a full-scale plant of a Flemish landfill was reported [173] using as a starting model the leachate treatment scheme applied at IMOG (Intergemeentelijke Maatschappij voor Openbare Gezondheid, i.e. nitrification-denitrification with methanol addition using SBR, followed by GAC as final polishing treatment). To estimate the biological treatment used in the IMOG landfill, a stoichiometric dosage (2.47 g $CH_3OH$/g $N-NO_3^-$) was assumed to achieve 100% of TN removal from a leachate stream with 60 kg N/d (influent concentration 0.4 kg $N/m^3$ and flow of 150 $m^3$/d). For aeration costs it was assumed that 4 kg $O_2$ were required per kg of nitrogen and given an oxygen efficiency of 1.8 kg $O_2$/kWh and an electricity cost of 0.1 €/kWh. It was also considered that 0.44 kg $COD_{biomass}$ was produced per $m^3$ of leachate and sludge disposal costs of 0.2 €/kg $COD_{biomass}$. Regarding GAC, the authors report an additional cost of 1.32 €/$m^3$, to achieve COD legal compliance (in this case, 250 mg/L) when applied after the biological process.

Furthermore, this study also considered three possible scenarios to treat stabilized landfill leachate: (1) complete or partial replacing of the classic nitrification-denitrification IMOG treatment by autotrophic nitrogen removal (ANR), while keeping the subsequent GAC stage (ANR + GAC and ANR + SBR + GAC); (2) incorporation of additional techniques into the IMOG treatment chain, namely ozonation (SBR + $O_3$ + GAC), Fenton (SBR + F + GAC) and coagulation (SBR + C/S + GAC); and (3) ANR, followed by either $O_3$ or F or C/S and with final GAC adsorption. In respect to ANR, ozonation, Fenton oxidation and coagulation processes, the data used in this study were selected from previous experimental studies performed by Gao, *et al.* [169], Chys, *et al.* [170] and [171], and Oloibiri, *et al.* [172]. For ANR process (scenario 1), lower operational costs were estimated when compared to IMOG biotreatment. Aeration requirements are considerably lower (1.71 kg $O_2$/kg N value was used), no external carbon source is required, and the sludge production was considered negligible. Nonetheless, the authors are cautious, mentioning ANR operational

problems to be a major concern, and propose as preferential option the usage of a combination between ANR (for 40% N removal) and the traditional nitrogen bio-removal (for remaining 60% N removal). Regarding scenario 2, while the effluents treated by Fenton and coagulation (both carried out at pH 6) were able to maintain the environmental discharge limit for COD (in this case, < 250 mg/L, Table 2.5 from Chapter 2) even after 36 bed volumes during GAC treatment, thus decreasing operational costs for the adsorption stage, while the ozonated effluent exceeded the legal value after only 3.5 bed volumes. Although the production of biological sludge (and associated disposal costs) was included in the traditional nitrogen removal process (and considered negligible for the ANR, as previously mentioned), it was completely disregarded for the Fenton and coagulation steps. This is an important factor, since high sludge production is expected for both processes, and should be naturally considered in a study that focuses on cost evaluation. The lowest operational cost was obtained for one of the three combinations tested for scenario 3 (ANR + C/S + GAC, see Table 3.10). Considering that the authors recognize limitations to apply ANR as a single biological treatment unit, and there is no reference to sludge production and consequent disposal costs for Fenton and coagulation processes, the estimated values should be viewed with some caution, particularly for scenario 3.

### 3.3.2 Development of a treatment train strategy

The leachate used for this work was from a sanitary landfill, closed since 2017 located in the north of Portugal, covering an area of 20.5 ha, that served a population of 446,378 inhabitants and received on average 446,378 tons of MSW per year since 1999. The landfill LTP receives ~ 150 $m^3$ of leachate per day, and includes the following treatment units: (i) an aerated lagoon (15,000 $m^3$) with pure oxygen injection; (ii) anoxic and aerobic activated sludge reactor (150 $m^3$); (iii) a clarifier (27 $m^3$), a coagulation/flocculation/flotation system and a non-aerated final retention lagoon (3000 $m^3$). According to the characterization performed to the leachate at each treatment stage of the LTP (Table 3.11), the aerated lagoon promotes biological oxidation of the leachate, achieving 85%, 70% and 57% elimination of $BOD_5$, DOC, and COD, respectively. Also, about 25% of the total nitrogen is eliminated, due to the existence of aerated and non-aerated areas on the lagoon. The biological oxidation reactor is not very efficient as regards nitrogen elimination, although it promotes some nitrification. Denitrification does not seem to occur since, at this point, the pre-treated leachate presents a low $BOD_5$/COD ratio, indicating that the remained organic carbon is recalcitrant. After sludge sedimentation in a secondary clarifier, the effluent passes through a coagulation/flocculation/flotation treatment. In this process, the removal of nitrogen is negligible but it is quite efficient at removing organics (66% and 73% decrease for COD and DOC, respectively), associated with the production of great amounts of sludge. Downstream a non-aerated lagoon is used for leachate retention. As the treated leachate does not meet the discharge limits imposed by the Portuguese legislation, it is further transport by trucks to a municipal WWTP. The biological and chemical sludge is mechanically dewatered by centrifugation and disposed of in the landfill.

The first results on the application of advanced oxidation processes in the treatment of the above-mentioned leachate date back to 2009. Initially, the application of AOPs was proposed [113] as an interesting option to improve the biodegradability of the leachate after the aerated lagoon process, since the biodegradable organic carbon fraction is almost completely removed at this stage (as revealed by the insignificant removal of organic matter in the activated sludge biological reactors). In a first approach, different heterogeneous ($TiO_2$/UV, $TiO_2$/$H_2O_2$/UV) and homogeneous ($H_2O_2$/UV, $Fe^{2+}$/$H_2O_2$/UV) photocatalytic processes were investigated [113]. The experiments were performed on a pilot-plant (CPC = 2.08 $m^2$), using 35 or 50 L of landfill leachate. For the heterogeneous photocatalytic processes (with [$TiO_2$] = 200 mg/L), low mineralization of 26% and 19% was obtained, respectively, after the consumption of 1019 $kJ_{UV}$/L and 496 $kJ_{UV}$/L plus 387 mM of $H_2O_2$. For the photo-Fenton reaction, the acidification step decreased the DOC by 20-24% and was followed by an induction period (longer or shorter on time, depending on the iron catalyst

concentration). The PF reaction (with $[Fe^{2+}] = 60$ mg/L) provided degradation rates 20 times higher than the heterogeneous photocatalytic processes, attaining 86% of DOC abatement after the consumption of 110 $kJ_{UV}/L$ and 306 mM $H_2O_2$.

Table 3.11 – Physicochemical characterization of the landfill leachate at different phases of treatment in the LTP (source:[96])

| Parameters | RL[a] | AL[a] | BO[a] | C/F[a] |
|---|---|---|---|---|
| pH | 7.6 | 7.2 | 7.5 | 5.2 |
| Temperature (ºC) | 17.1 | 17.0 | 16.8 | 17.0 |
| Conductivity (mS/cm) | 22.8 | 19.8 | 18.5 | 18.5 |
| COD (g $O_2$/L) | 14.0 | 6.1 | 6.2 | 2.1 |
| $BOD_5$ (mg $O_2$/L) | 4000 | 600 | 300 | 200 |
| $BOD_5$/COD | 0.28 | 0.10 | 0.05 | 0.09 |
| DOC (mg C/L) | 4709 | 1432 | 1410 | 379 |
| DIC (mg C/L) | 1844 | 1326 | 167 | 10 |
| Total nitrogen (g N/L) | 3.3 | 2.5 | 2.5 | 2.5 |
| Nitrate (mg $NO_3^-$-N/L) | 19 | 84 | 227 | 258 |
| Nitrite (mg $NO_2^-$-N/L) | n.d. | 181 | 441 | 423 |
| Ammonium (mg $NH_4^+$-N/L) | 761 | 714 | 632 | 506 |
| Polyphenols (mg caffeic acid/L) | 322 | 88 | 101 | 29 |
| Total iron (mg Fe/L) | 8.1 | 9.3 | 9.6 | 12.1 |
| Total dissolved iron (mg Fe/L) | 3.0 | 7.3 | 7.7 | 10.3 |
| TSS (mg/L) | 933 | 1650 | 533 | 86 |
| VSS (mg/L) | 767 | 1220 | 429 | 53 |
| Chloride (g $Cl^-$/L) | 2.3 | 2.9 | 3.0 | 3.1 |
| Sulfate (mg $SO_4^{2-}$/L) | n.a. | n.a. | n.a. | 1256 |
| Total phosphorous (mg P/L) | 19.5 | 21.7 | 11.4 | 6.8 |
| Phosphate (mg $PO_4^{3-}$/L) | 4.6 | 5.0 | 3.2 | 2.7 |
| Cadmium (mg $Cd^{2+}$/L) | 0.01 | 0.01 | 0.01 | 0.08 |
| Lead (mg $Pb^{2+}$/L) | 0.01 | 0.02 | 0.01 | 0.03 |
| Copper (mg $Cu^{2+}$/L) | 0.01 | 0.01 | 0.05 | 0.15 |
| Total chromium (mg Cr/L) | 2.2 | 2.5 | 2.5 | 0.27 |
| Zinc (mg $Zn^{2+}$/L) | 0.6 | 1.0 | 1.0 | 1.7 |

n.a. – not analyzed; n.d. – not detected. [a] RL – raw leachate; AL – leachate after aerated lagoon; BO – leachate after biological oxidation (anoxic and aerobic); C/F – leachate after coagulation/flocculation/flotation tank.

### 3.3.2.1 Aerated lagoon + Solar photo-Fenton + Biological N removal

Considering the previous research, an initial strategy was proposed [174] for the treatment of landfill leachates, after aerated lagoon, combining: (i) solar photo-Fenton, as pre-oxidation process, to degrade the most recalcitrant organic compounds and, simultaneously, to enhance the leachate biodegradability, with; (ii) a biological process, to oxidize the remaining biodegradable organic fraction and eliminate nitrogenous compounds (promoting aerobic nitrification followed by anoxic denitrification, and using methanol as an external carbon source). The initial tests were carried out at pilot-scale, using the same CPC unit as previously and an immobilized biomass reactor (IBR). The global removal efficiency of this combined system was 92%, 95% and 99%, for DOC, COD and TN contents, respectively (Table 3.12). The photo-bio-treated leachate complied with TN legal limit (< 15 mg/L), but not with COD or sulfate ions concentration (150 mg/L and 2 g/L, respectively), this later due to the addition of sulphuric acid for leachate acidification.

Normally, the leachate after aerated lagoon presents a high buffer capacity, due to high content of carbonates and bicarbonates (inorganic carbon), thus requiring a high amount of acid to decrease the pH until 2.8. Different strong acids are available for the acidification step, as mineral acids (HCl, HI, HBr, HF, $HClO_4$, $HNO_3$, $H_2SO_4$, $H_3PO_4$), organic acids (sulfonic and carboxylic acids), among others. The selection of the best acid(s) for the acidification step depends on the following factors: (i) price and commercial availability; (ii) stability in solution; (iii) degree of contamination; and (iv) possible interferences in the PF reaction. The use of HI, HBr, HF, $HClO_4$, $HNO_3$ and $H_3PO_4$ acids leads to the release of high concentrations of iodide, bromide, fluoride, perchlorate, nitrate and phosphates anions, for which the discharge limits are very low and some of them are listed as priority hazardous substances. On the other hand, $HClO_4$ is very instable in the presence of organic compounds and can cause fire or explosion [175]. HF attacks glass by reaction with silicon dioxide to form gaseous or water-soluble silicon fluorides, leading to complete rupture of the borosilicate glass of the photoreactor tubes [176]. Normally, sulphuric acid is used in the acidification process of the Fenton reaction since it is a strong acid, commercially available in a high concentration (> 96%) and at low price. In turn, hydrochloric acid is only available commercially at 37%, and presents approximately the same price as $H_2SO_4$ (98%). The major advantage of HCl is that chloride ions concentration is not limited by regulations concerning wastewater discharge into water bodies. Taking this in view, sPF tests followed [96] to evaluate possible effects of using different acid types ($H_2SO_4$ and HCl applied separately or together) keeping $SO_4^{2-}$ below the legal limit (2 g/L). It was concluded that the DOC reduction resulting from the acidification stage (due to the precipitation/retention of the organic matter, mostly humic acids) was not dependent of the type of

acid used. However, the sPF efficiency was lower when HCl was used to acidify the leachate (alone or in combination with $H_2SO_4$).

**Table 3.12** – Main results obtained for the first treatment train strategy applied to the landfill leachate (sources: [94, 174]).

| Parameter | Treatment stage[a] | | | Global efficiency |
|---|---|---|---|---|
| | AL | sPF[b] | $B_{NIT/DES}$ | |
| *Pilot-scale* | | | | |
| DOC (mg C/L) | 1098 | 470 (↓57%) | 83 (↓35%) | ↓**92%** |
| COD (mg $O_2$/L) | 4505 | 1174 (↓74%) | 227 (↓21%) | ↓**95%** |
| TN (mg N/L) | 1780 | 1280 (↓28%) | < 10 (↓71%) | ↓**99%** |
| Sulfate (mg $SO_4^{2-}$/L) | 374 | 2600 | 2600 | ↑**595%** |
| **Remarks:** | • $H_2SO_4$ addition up to pH ~ 2.8, with DOC ↓ 35% • sPF: CPC = 4.16 $m^2$; $V_L$ = 105 L; $[Fe^{3+}]$ = 80 mg/L; $Q_{UV}$= 29.2 kJ/L; $[H_2O_2]$: 90 mM • $B_{NIT/DES}$[c]: $V_L$ = 60 L; $t$ ~ 600 h; pH = 6.5 - 7.5; with $CH_3OH$ addition | | | |
| *Pre-industrial scale* | | | | |
| DOC (mg C/L) | 1406 | 195 (↓86%) | 30 (↓12%) | ↓**98%** |
| COD (mg $O_2$/L) | 4235 | 266 (↓94%) | 94 (↓4%) | ↓**98%** |
| TN (mg N/L) | 2700 | 2500 | 32 | ↓**99%** |
| Sulfate (mg $SO_4^{2-}$/L) | 100 | 12 100 | 10 800 | ↑**12 000%** |
| **Remarks:** | • $H_2SO_4$ addition up to pH ~ 2.8, with DOC ↓ 23% • sPF: CPC = 39.52 $m^2$; $V_L$ = 1 $m^3$; $t$ = 68 h; $[Fe^{3+}]$ = 80 mg/L; $[H_2O_2]$: 300 mM • $B_{NIT/DES}$[d]: $V_L$ = 1 $m^3$; $T_m$ = 26.8 ºC; pH = 7.5 – 8.5; aerobic phase ($t$ ~ 505 h; DO = 0.5 - 2.0 mg $O_2$/L) and anoxic ($t$ ~ 216 h; $CH_3OH$ addition) | | | |
| DOC (mg C/L) | 1707 | 435 (↓75%) | 170 (↓16%) | ↓**91%** |
| COD (mg $O_2$/L) | 4211 | 949 (↓77%) | 667 (↓7%) | ↓**84%** |
| TN (mg N/L) | 2900 | 2800 | 14 | ↓**~100%** |
| Sulfate (mg $SO_4^{2-}$/L) | 90 | 11 700 | 12 600 | ↑**13 900%** |
| **Remarks:** | • $H_2SO_4$ addition up to pH ~ 2.8, with DOC ↓ 27% • sPF: CPC = 39.52 $m^2$; $V_L$ = 1 $m^3$; $t$ = 29 h; $Q_{UV}$= 84 kJ/L; $[Fe^{3+}]$ = 80 mg/L; $[H_2O_2]$: 200 mM • $B_{NIT/DES}$[d]: $V_L$ = 1 $m^3$; $T_m$ = 26.8 ºC; pH = 7.5 – 8.5 (aerobic phase: $t$ ~ 91 h; DO = 0.5 - 2.0 mg $O_2$/L; and anoxic phase: $t$ ~ 167 h; with $CH_3OH$ addition). | | | |

[a] AL – aerated lagoon; sPF – solar photo-Fenton; $B_{NIT/DES}$ – biological nitrogen removal by nitrification-denitrification process. [b] Acid sludge was not removed. [c] Immobilized biomass reactor, containing 25-30 L of propylene rings colonized by activated sludge of a WWTP. [d] Activated sludge reactor with 3.5 $m^3$, equipped with air blower, mechanical stirrer, and pH control unit.

To better assess the efficiency of this treatment strategy, experiments were conducted at a pre-industrial plant, during 1-year (June 2010 to May 2011), using a photocatalytic reactor with 39.5 $m^2$ of compound parabolic collectors (CPCs) and an activated sludge reactor with 3.5 $m^3$ capacity [95]. Regarding the sPF treatment stage, the tests performed [94, 95] showed that: (i) acidification of the leachate to pH ~ 2.8 led to 54–58% of DOC abatement, mainly associated with humic acids precipitation (representing 72% of the DOC reduction); and (ii) elimination of the acid sludge was mandatory, otherwise its presence negatively affected the efficiency of the PF reaction (lower light transmission and higher $H_2O_2$ consumption due to the oxidation of particulate organic matter). With this strategy, it was again possible to remove almost 100% of the total dissolved nitrogen (TN), reaching a final value below the legal limit (< 15 mg N/L). However, even with high global efficiencies for mineralization (90%) and COD reduction (84%), simultaneous legal compliance for both nitrogen and organic compounds was not achieved by this combined system (Table 3.12). Furthermore, as mentioned, the sulfate ions concentration from these experiments greatly exceeded the legal limit. Based on the results obtained at the pre-industrial plant, and including different scenarios for the radiation source, a cost analysis for the photo-Fenton stage considering the treatment of 100 $m^3$ of leachate per day was later performed (this will be further discussed).

### 3.3.2.2 Raw leachate + Biological N removal + Solar photo-Fenton + Biological Oxidation

A different strategy [177] to treat raw leachate (i.e. collected before the aerated lagoon treatment) was tested, combining: (i) an activated sludge reactor, under aerobic and anoxic conditions, to promote the biological removal of nitrogen compounds and consumption of the biodegradable organic carbon fraction; (ii) a solar photo-Fenton oxidation process, to degrade the most recalcitrant compounds and enhance the bio-treated raw leachate biodegradability (without the interference of nitrogen species); and (iii) a final aerobic biological degradation process, for the complete removal of the remaining biodegradable organic compounds. To test this combined strategy, experiments were carried out using the same pre-industrial plant as before.

Operated for nearly 2 months (600 h aerobic + 430 h anoxic), the first biological stage was able to remove 39% of DOC, 35% of COD and 95% of TN (see Table 3.13). Because of the pH control in the biological reactor, at the end of this stage the sulfate ion concentration (~ 6.8 g/L) was already above the legal limit value. The acidification of the bio-treated raw leachate led to a further increase of $SO_4^{2-}$ (~ 14 g/L) and a decrease of 22% and 24%, for DOC and COD, respectively. The resulting acid sludge was removed, and the subsequent photo-oxidation was able to reduce 79% of DOC and

88% of COD, consuming 80.4 $kJ_{UV}$/L and 265 mM, of accumulated energy and $H_2O_2$, respectively. Afterward, the second biological oxidation obtained a final treated leachate, apart from sulfate ions, in compliance with legal discharge limits (not only for COD and TN, but also TSS and $BOD_5$).

**Table 3.13** – Main results obtained for the second treatment train strategy applied to the landfill leachate (source: [177])

| Parameter | Treatment stage[a] | | | | Global efficiency |
|---|---|---|---|---|---|
| | RL | $B_{NIT/DESN}$ | Acid. + $_sPF^b$ | BO | |
| DOC (mg C/L) | 2503 | 1534 (↓39%) | 1200 (↓13%) | 248 (↓38%) | 45 (↓8%) | ↓98% |
| COD (mg $O_2$/L) | 7426 | 4864 (↓35%) | 3720 (↓15%) | 436 (↓44%) | 117 (↓4%) | ↓98% |
| TN (mg N/L) | 4080 | 210 (↓95%) | 182 | 194 | 9 (↓5%) | ↓100% |
| Sulfate (mg $SO_4^{2-}$/L) | 42 | 6831 | 14 522 | 14 079 | 13 803 | ↑32 764% |

| Remarks: | • $B_{NIT/DES}{}^c$: $V_L$ = 2.5 m³; $T_m$ = 26.8 ºC; pH = 7.5 – 9.0; (aerobic phase: $t \sim 600$ h; DO > 0.5 mg $O_2$/L; and anoxic phase: $t \sim 430$ h; with $CH_3OH$ addition)<br>• sPF: $V_L$ = 1 m³; CPC = 39.52 m²; $t$ = 38 h; $Q_{UV}$= 80 kJ/L; [$Fe^{3+}$] = 80 mg/L; [$H_2O_2$]: 265 mM<br>• $BO^c$:$V_L$ = 0.6 m³; pH = 7.5 – 9.0; DO > 0.5 mg $O_2$/L |
|---|---|

[a] RL – raw leachate; $B_{NIT/DESN}$ – biological nitrogen removal by nitrification-denitrification process; Acid. – acidification; $_sPF$ – solar photo-Fenton; BO – biological oxidation. [b] Acid sludge removed before photo-oxidation reaction. [c] Activated sludge reactor with 3.5 m³, equipped with air blower, mechanical stirrer, and pH control unit.

### 3.3.2.3 Aerated lagoon + Biological oxidation + Coagulation/Sedimentation + Solar photo-Fenton + Biological Nitrogen removal

Considering the drawbacks found in the previous treatment strategies (and also the high treatment costs associated with the PF reaction, to be later discussed), a new approach was proposed [178] combining: (i) an initial activated sludge biological reactor, under aerobic conditions, to promote nitrification and simultaneous removal of the biodegradable organic carbon fraction and alkalinity, thus decreasing the acid dose needed in the subsequent coagulation step; (ii) a coagulation/sedimentation (C/S) stage, using ferric salts at acidic pH, to achieve the precipitation of humic acids (up to 50% of the recalcitrant organic content), resulting in a leachate with a low suspended solids content and high UV–visible transmissibility; followed by (iii) an PF oxidation reaction ($Fe^{2+}$/$H_2O_2$/UV–Vis), using artificial and/or solar radiation, to degrade the most recalcitrant organic compounds, turning them into simpler and easily biodegradable organic compounds; and (iv) a final biological oxidation step, under aerobic/anoxic conditions, to promote the removal of

the remaining nitrogen species and biodegradable organic fraction (aiming TN < 15 mg/L and COD < 150 mg $O_2$/L). The first three treatment stages were tested in the same pre-industrial plant as before, while the last biological process was evaluated by the Zahn-Wellens biodegradability test.

According to the results (Table 3.14), compliance with COD and sulfate legal discharge values was attained. For the first, the introduction of a C/S stage before PF oxidation; and for the second, the promotion of nitrification with consequent alkalinity consumption, were of most relevance. On the other hand, since the final biological treatment stage was not carried out, the strategy missed to prove its ability to reach TN legal limit simultaneously with the other parameters.

**Table 3.14** – Main results obtained for the second treatment train strategy applied to the landfill leachate (source:[178])

| Parameter | Treatment stage[a] | | | | | Global efficiency |
|---|---|---|---|---|---|---|
| | AL | $B_{NIT}$ | C/S | sPF | BO | |
| DOC (mg C/L) | 1181 | 1002 (↓15%) | 419 (↓49%) | 205 (↓18%) | 53 (↓13%) | ↓96% |
| COD (mg $O_2$/L) | 3786 | 3566 (↓6%) | 936 (↓69%) | 338 (↓16%) | 86 (↓7%) | ↓98% |
| TN (mg N/L) | 1202 | 1105 (↓8%) | - | - | - | ↓8% |
| Sulfate (mg $SO_4^{2-}$/L) | 675 | 538 | 901 | - | - | ↑33% |

| Remarks: | • $B_{NIT}$[b]: $V_L$ = 2.5 m³; $T_m$ = 15 ºC; pH not controlled; (aerobic phase: $t$ ~ 600 h; DO > 0.5 mg $O_2$/L)<br>• C/S: $V_L$ = 2.5 m³; pH = 4.2; [$Fe^{3+}$] = 240 mg/L; $t_s$ = 14h<br>• sPF: $V_L$ = 1.8 m³; CPC = 39.52 m²; $t$ = 5.7 h; $Q_{UV}$= 12.2 kJ/L; [$Fe^{3+}$] = 60 mg/L; [$H_2O_2$]: 127 mM<br>• BO: evaluated by Zhan-Wellens biodegradability test. |
|---|---|

[a] RL – raw leachate; $B_{NIT}$ – biological nitrification; C/S – coagulation/sedimentation; sPF – solar photo-Fenton; BO – biological oxidation. [b] Activated sludge reactor with 3.5 m³, equipped with air blower, mechanical stirrer, and pH control unit.

Recognized for representing the majority of treatment costs, cost analysis was carried out mainly focused on the photo-Fenton stage (only solar: with use of CPCs, only artificial: with UV-Vis lamps and, combining: solar + artificial) applied to the different strategies tested (Table 3.15). Regardless of the scenario, the usage of solar radiation source always has slightly lower costs. It is possible to infer the effect of high alkalinity on PF costs, with increasing reagents consumption for acidification, and the inclusion of a C/S stage before PF proved to be an effective approach to decrease PF costs.

**Table 3.15** – Estimated costs for the photo-Fenton stage, considering different pre-treatments and radiation source scenarios, for the treatment of 100 m$^3$ of leachate per day (sources: [178, 179]).

| Pre-treatment | Characterization[a] | Radiation source | Unitary cost[b] |
|---|---|---|---|
| Aerated lagoon + Biological TN removal | DOC = 1.5 g/L COD = 4.9 g/L Alkalinity = 7.9 g CaCO$_3$/L TN = 0.2 g/L [SO$_4^{2-}$] = 6.8 g/L | Solar: CPCs area = 13 525 m$^2$ | 16.7 €/m$^3$ |
| | | Artificial: Nº of lamps = 86 | 19.5 €/m$^3$ |
| | | Solar + Artificial: CPCs area = 8 626 m$^2$ Nº of lamps = 66 | 17.6 €/m$^3$ |
| Aerated lagoon + Biological nitrification | DOC = 1.1 g/L COD = 3.8 g/L Alkalinity = 2.4 g CaCO$_3$/L TN = 0.9 g/L [SO$_4^{2-}$] = 0.3 g/L | Solar: CPCs area = 6056 m$^2$ | 11.0 €/m$^3$ |
| | | Artificial: Nº of lamps = 39 | 11.7 €/m$^3$ |
| | | Solar + Artificial CPCs area = 3 862 m$^2$ Nº of lamps = 30 | 10.9 €/m$^3$ |
| Aerated lagoon + Biological nitrification + Coagulation/sedimentation | DOC = 0.4 g/L COD = 0.9 g/L TN = 1.1 g/L [SO$_4^{2-}$] = 0.7 g/L | Solar: CPCs area = 2099 m$^2$ | 6.4 €/m$^3$ |
| | | Artificial: Nº of lamps = 40 | 6.6 €/m$^3$ |
| | | Solar + Artificial CPCs area = 1339 m$^2$ Nº of lamps = 31 | 6.4 €/m$^3$ |

[a] Characterization of the leachate used in the PF reactions, except for "Aerated lagoon + biological TN treatment", since acidic sludge produced during acidification for PF was removed before the photo-oxidation process. [b] Considers the accumulated UV energy and amount of H$_2$O$_2$ required to obtain an effluent that, according to Zahn-Wellens biodegradability tests, meets the COD value < 150 mg/L after final biological oxidation.

It should be noted that the amount of land required for the implementation of the CPCs needs to be further calculated [179], on the basis of the total CPCs area required and on the distance between the various CPCs parallel rows, to minimize the shadowing between collectors. A CPCs row separation value of 3.94 m was determined [179], considering CPCs tilted 41º (local altitude, Porto, Portugal), so a 2.04 m$^2$ CPC module occupies 5.55 m$^2$ of land. Taking this, for a CPC area of 13 525 m$^2$, a land area of 40 175 m$^2$ can be estimated, which is equivalent to 8.0 soccer fields (50 m × 100 m).

## 3.4 Final remarks

As final remarks, nowadays the main challenges in the treatment of leachate are as follows:

(i)   Selecting a reasonable, economical, and efficient treatment train strategy, combining biological and physicochemical processes, able to deal with both organic and nitrogen content in the leachate. Process combination is mandatory when aiming to comply with the legal discharge standards.

(ii)  Improving the efficiency of TN removal by biological treatment process, since TAN levels are normally high and may inhibited successful TN removal.

(iii) Identify a suitable combination of available technologies and how to use them to ensure a stable operation is another challenge in leachate treatment. The significant changes in leachate quality and quantity intensify the difficulty of identifying a stable treatment train methodology.

(iv)  To achieve discharge standards, leachate treatment plants often use nanofiltration and reverse osmosis which makes treatment costs high. Reducing costs in leachate treatment is another priority.

To summarize, it is necessary to identify the appropriate combination of biochemical and physicochemical treatments, particularly with advanced oxidation processes, to dispose of landfill leachate. In addition, maximizing the potential of the biological treatment process, by improving the TN removal, and reducing the total costs are the main challenges associated in the development of a leachate treatment train strategy.

## 3.5 References

1. Gierlich, H.H. and J. Kolbach, *Treating landfill leachate in European countries.* Pollution Engineering, 1998. **3**: p. 10-14.

2. Brennan, R.B., M.G. Healy, L. Morrison, S. Hynes, D. Norton, and E. Clifford, *Management of landfill leachate: The legacy of European Union Directives.* Waste Management, 2016. **55**: p. 355-363.

3. Diamadopoulos, E., P. Samaras, X. Dabou, and G.P. Sakellarpoulos, *Combined tretment of leachate and domestic sewage in a sequencing bath reactor.* Water Science and Technology, 1997. **36**: p. 61-68.

4. Del-Borghi, A., L. Binaghi, A. Converti, and M. Del-Borghi, *Combined treatment of leachate from sanitary landfill and municipal wastewater by activated sludge.* Chemical and Biochemical Engineering, 2003. **17**(4): p. 277-283.

5. Gotvajn, A.Z. and A. Pavko, Perspectives on biological treatment of sanitary landfill leachate, in Wastewater Treatment Engineering. 2015, IntechOpen.

6. Dereli, R.K., M. Giberti, Q. Liu, and E. Casey, Benchmarking leachate co-treatment strategies in municipal wastewater treatment plants under dynamic conditions and energy prices. Journal of Environmental Management, 2020. **260**: p. 110129.

7. U., E., Directive 2000/60/EC of the European Parliament and of the Council, of 23$^{rd}$ October 2000, establishing a framework for Community action in the field of water policy. 2000: Availabe online: https://eur-lex.europa.eu/resource.html?uri=cellar:5c835afb-2ec6-4577-bdf8-756d3d694eeb.0004.02/DOC_1&format=PDF.

8. U., E., *Council Directive of 21$^{st}$ May 1991 concerning urban waste water treatment.* . 1991: Available online: http://eur-lex.europa.eu/legal-content/EN/TXT/PDF/?uri=CELEX:31991L0271&from=EN.

9. Webler, A.D., F.C. Moreira, M.W.C. Dezotti, C.F. Mahler, I.D.B. Segundo, R.A.R. Boaventura, and V.J.P. Vilar, *Development of an integrated treatment strategy for a leather tannery landfill leachate.* Waste Management, 2019. **89**: p. 114-128.

10. Renou, S., J.G. Givaudan, S. Poulain, F. Dirassouyan, and P. Moulin, *Landfill leachate treatment: review and opportunity.* Journal of Hazardous Materials, 2008. **150**: p. 468-493.

11. Luo, H., Y. Zeng, Y. Cheng, D. He, and X. Pan, Recent advances in municipal landfill leachate: A review focusing on its characteristics, treatment, and toxicity assessment. Science of the Total Environment, 2020. **703**: p. 135468.

12. Gao, J., V. Oloibiri, M. Chys, W. Audenaert, B. Decostere, H. Yanling, H.V. Langenhove, K. Demeestere, and S.W.H.V. Hulle, *The present status of landfill leachate treatment and its development trend from a technological point of view.* Reviews in Environmental Science and Bio/Technology, 2015. **14**: p. 93-122.

13. Wiszniowski, J., D. Robert, J. Surmacz-Gorska, K. Miksch, and J.V. Weber, *Landfill leachate treatment methods: A review.* Environmental Chemistry Letters, 2006. **4**: p. 51-61.

14. Yao, P., *Perspectives on technology for landfill leachate treatment.* Arabian Journal of Chemistry, 2017. **10**: p. 2567-2574.

15. Torreta, V., N. Ferronato, I.A. Katsoyiannis, A.K. Tolkou, and M. Airoldi, *Novel and conventional technologies for landfill leachates treatment: a review.* Sustainability, 2017. **9**(9): p. 1-39.

16. Warith, M. and H. Jin, *Bioreactor landfills: State-of-the-art review.* Emirates Journal of Engineering Research, 2005. **10**(1): p. 1-14.

17. Mukherjee, S., S. Mukhopadhyay, M.A. Hashim, and B.S. Gupta, *Contemporary environmental issues of landfill leachate: Assessment & remedies.* Critical Reviews in Environmental Science and Technology, 2015. **45**(5): p. 472-590.

18. Yang, L. and K.-Y. Tsai, *Treatment of landfill leachate with high level of ammonia by constructed wetland systems.* Journal of Environmental Science and Health A, 2011. **46**(7): p. 736-741.

19. Yalcuk, A. and A. Ugurlu, Comparison of horizontal and vertical constructed wetland systems for landfill leachate treatment. Bioresource Technology, 2009. **100**: p. 2521-2526.

20. Qasim, S.R. and W. Chiang, Sanitary landfill leachate: Generation, control and treatment. 1994, New York: Routledge.

21. Crawford, J. and P. Smith, *Landfill technology.* 1985, London: Butterworths.

22. Guidance for the treatment of landfill leachate, U.K. Environmental Agency, Editor. 2007.

23. Mehmood, M.K., E. Adetutu, D.B. Nedwell, and A.S. Ball, *In situ microbial treatment of landfill leachate using aerated lagoons. .* Bioresource Technology, 2009. **100**: p. 2741-2744.

24. Fernandes, H., A. Viancelli, C.L. Martins, R.V. Antonio, and R.H.R. Costa, *Microbial and chemical profile of a ponds system for the treatment of landfill leachate.* Waste Management, 2012. **33**(10): p. 2123-2128.

25. Christensen, T., R. Cossu, and R. Stegmann, *Sanitary landfilling: Process, technology and environmental impact. .* 1989, London: Academic Press Limited.

26. Talalaj, I.A., P. Biedka, and I. Bartkowska, *Treatment of landfill leachates with biological pretreatments and reverse osmosis.* Environmental Chemistry Letters, 2019. **17**(3): p. 1177-1193.

27. Vilar, V.J.P., S.M.S. Capelo, T.F.C.V. Silva, and R.A.R. Boaventura, *Solar photo-Fenton as a pre-oxidation step for biological treatment of landfill leachate in a pilot plant with CPCs.* Catalysis Today, 2011. **161**(1): p. 228-234.

28. Mojiri, A., H.A. Aziz, S.Q. Aziz, and N.Q. Zaman, *Review on municipal landfill leachate and sequencing batch reactor (SBR) technique.* Archives Des Sciences, 2012. **65**(7): p. 22-31.

29. Aziz, A.Q., H.A. Aziz, A. Mojiri, M.J.K. Bashir, and S.S.A. Amr, *Landfill leachate treatment using sequencing batch recator (SBR) process: Limitation of operational parameters and performance.* International Journal of Scientific Research in Knowledge, 2013: p. 34-42.

30. Laitinen, N., A. Luonsi, and J. Vilen, Landfill leachate treatment with sequencing batch reactor and membrane bioreactor. Desalination, 2006. **191**: p. 86-91.

31. Hoilijoki, T.H., R.H. Kettunen, and J.A. Rintala, *Nitrification of anaerobically pretreated municipal landfill leachate at low temperature.* Water Research, 2000. **34**: p. 1435-1446.

32. Ellouze, M., F. Aloui, and S. Sayadi, *Performance of biological treatment of high-level ammonia landfill leachate.* Environmental Technology, 2008. **29**: p. 1169-1178.

33. Spagni, A., M.C. Lavagnolo, C. Scarpa, P. Vendrame, A. Rizzo, and L. Luccarini, *Nitrogen removal optimization in a sequencing batch reactor treating sanitary landfill leachate.* Journal of Environmental Science and Health A, 2007: p. 757-765.

34. Spagni, A. and S. Marsili-Libelli, Nitrogen removal via nitrite in a sequencing batch reactor treating sanitary landfill leachate. Bioresource Technology, 2009. **100**(2): p. 609-614.

35. Li, H.-s., S.-q. Zhou, Y.-b. Sun, P. Feng, and J.-d. Li, *Advanced treatment of landfill leachate by a new combination process in a full-scale plant.* Journal of Hazardous Materials, 2009. **172**: p. 408-415.

36. Klimiuk, E. and D. Kulikowska, Effectiveness of organics and nitrogen removal from municipal landfill leachate in single- and two-stage SBR systems. Polish Journal of Environmental Studies, 2004. **13**: p. 525-532.

37. Uygur, A. and F. Kargi, Biological nutrient removal from pre-treated landfill leachate in a sequencing batch reactor. Journal of Environmental Management, 2004. **71**: p. 9-14.

38. Ganigué, R., J. Gabarró, A.S. Melsió, M. Ruscalleda, H. López, X. Vila, J. Colprim, and M.D. Balaguer, Long-term operation of a partial nitritation pilot plant treating leachate with extremely high ammonium concentration prior to an anammox process. Bioresource Technology, 2009. **100**: p. 5624-5632.

39. Monclús, H., S. Puig, M. Coma, A. Bosch, M.D. Balaguer, and J. Colprim, *Nitrogen removal from landfill leachates using the SBR technology.* Environmental Technology, 2009. **30**(3): p. 283-290.

40. Xu, Z., G. Zeng, Z. Yang, Y. Xiao, M. Cao, and H. Sun, Biological treatment of landfill leachate with the integration of partial nitrification, anaerobic ammonium oxidation and heterotrophic denitrification. Bioresource Technology, 2010. **101**: p. 79-86.

41. Insel, G., M. Dagdar, S. Dogruel, N. Dizge, E.U. Cogkor, and B. Keskinler, *Biodegradation characteristics and size fractionation of landfill leachate for integrated membrane treatment.* Journal of Hazardous Materials, 2013. **260**: p. 825-832.

42. Canziani, R., V. Emondi, M. Garavaglia, F. Malpei, E. Pasinetti, and G. Buttiglieri, Effect of oxygen concentration on biological nitrification and microbial kinetics in a cross-flow membrane bioreactor (MBR) and moving-bed biofilm reactor (MBBR) treating old landfill leachate. Journal of Membrane Science, 2006. **286**: p. 202-212.

43. Castillo, E., M. Vergara, and Y. Moreno, Landfill leachate treatment using a rotating biological contactor and an upward-flow anaerobic sludge bed reactor. Waste Management, 2007. **27**: p. 720-726.

44. Castrillón, L., Y. Fernández-Nava, M. Ulmanu, I. Anger, and E. Maraños, *Physicochemical and biological treatment of MSW landfill leachate.* Waste Management, 2010. **30**: p. 228-235.

45. Kawai, M., I.F. Purwanti, N. Nagao, A. Slamet, J. Hermana, and T. Tod, Seasonal variation in chemical properties and degradability by anaerobic digestion of landfill leachate at Benowo in Surabaya, Indonesia. . Journal of Environmental Management, 2012. **110**: p. 267-275.

46. Ahmed, F.N. and C.Q. Lan, Treatment of landfill leachate using membrane bioreactors: A review. Desalination, 2012. **287**: p. 41-54.

47. Alvarez-Vasquez, B., B. Jefferson, and S.J. Judd, *Membrane bioreactors vs. conventional biological treatment of landfill leachate: A brief review* Journal of Chemical Technology & Biotechnology, 2004. **79**: p. 1043-1049.

48. Stegmann, R., K.-U. Heyer, and R. Cossu. *Leachate treatment.* in *10th International Waste Management and Landfill Symposium.* 2005. Sardinia, Italy: CISA, Environmental Sanitary Engineering Centre.

49. Cortez, S., P. Teixeira, R. Oliveira, and M. Mota, *Rotating biological contactors: a review on main factots affecting performance.* Reviews in Environmental Science and Bio/Technology, 2008. **7**(2): p. 155-172.

50. Rittmann, B.E. and P.L. McCarty, *Environmental biotechnology: principles and applications.* 2001, New York: McGraw-Hill.

51. Bitton, G., *Wastewater microbiology.* 3rd ed. 2005, New Jersey: John Wiley & Sons Inc.

52. M., B., M.C.M. van Loosdrecht, and J.J. Heijinen, *One reactor system for ammonium removal via nitrite*, in *STOWA*. 1996: Utrecht, The Netherlands.

53. Zeng, W., Y.Z. Peng, S.Y. Wang, and C.Y. Peng, Process control of an alternating aerobic-anoxic sequencing batch reactor for nitrogen removal via nitrite. . Chemical Engineering & Technology, 2008. **31**: p. 582-587.

54. Rusten, B., B. Eikebrokk, Y. Ulgenes, and E. Lygren, *Design and operations of the Kaldnes moving bed biofilm reactors.* Aquacultural Engineering, 2006. **34**: p. 322-331.

55. Anthonisen, A.C., R.C. Loehr, T.B.S. Prakasam, and E.G. Srinath, *Inhibition of nitrification by ammonia and nitrous acid.* Journal Water Pollution Control Federation, 1976. **48**: p. 835-852.

56. Bae, W., S. Baek, J. Chung, and Y. Lee, *Optimal operational factors for nitrite accumulation in batch reactors.* Biodegradation, 2001. **12**: p. 359-366.

57. Chung, J., W. Bae, Y.W. Lee, and B.E. Rittmann, *Shortcut biological nitrogen removal in hybrid biofilm/suspended growth reactors.* Process Biochemistry, 2007. **42**(3): p. 320-328.

58. Chung, J., H. Shim, S. Park, S.J. Kim, and W. Bae, *Optimization of free ammonia concentration for nitrite accumulation in shortcut biological nitrogen removal process.* Bioprocess and Biosystems Engineering, 2006. **28**(4): p. 275-282.

59. Kim, J.K., K.J. Park, K.S. Cho, S. Nam, T. Park, and R. Bajpai, *Aerobic nitrification–denitrification by heterotrophic Bacillus strains.* Bioresource Technology, 2005. **6**: p. 1897-1906.

60. Cyplik, P., W. Grajek, R. Marecik, and P. Kroliczak, Effect of macro/micro nutrients and carbon source over the denitrification rate of Haloferax denitrificans archaeon. Enzyme and Microbial Technology, 2007. **40**(2): p. 212-220.

61. Szekeres, S., I. Kiss, T.T. Bejerano, and M.I.M. Soares, *Hydrogen-dependent denitrification in a two-reactor bio-electrochemical system.* Water Research, 2001. **35**: p. 715-719.

62. Gomez, M.A., J.M. Galvez, E. Hontoria, and J. Gonzalez-Lopez, Influence of concentration on biofilm bacterial composition from a denitrifying submerged filter used for contaminated groundwater. Journal of Bioscience and Bioengineering, 2003. **95**(3): p. 245-251.

63. Osaka, T., K. Shirotani, S. Yoshie, and S. Tsuneda, Effects of carbon source on denitrification efficiency and microbial community structure in a saline wastewater treatment process. Water Research, 2008. **42**: p. 3709-3718.

64. Feleke, Z. and Y. Sakakibara, A bio-electrochemical reactor coupled with adsorber for the removal of nitrate and inhibitory pesticide. Water Research, 2002. **36**: p. 3092-3102.

65. Cho, E. and A. Molof, Effect of sequentially combining methanol and acetic acid on the performance of biological nitrogen and phosphorus removal. Journal of Environmental Management, 2004. **73**: p. 183-187.

66. Tchobanoglous, G., F. Burton, and H. Stensel, *Wastewater engineering: Treatment and reuse.* 2003: McGraw-Hill.

67. Ahn., Y.-H., *Sustainable nitrogen elimination biotechnologies: A review.* Process Biochemistry, 2006. **41**: p. 1709-1721.

68. Carrera, J., T. Vicent, and F.J. Lafuente, Influence of temperature on denitrification of an industrial high-strenght nitrogen wastewater in a two-sludge system. Water S.A., 2003. **29**(1): p. 11-16.

69. Henze, M., P. Harremoës, J.l.C. Jansen, and E. Arvin, *Wastewater Treatment: Biological and chemical processes.* . 3rd ed. 2002, Heidelberg, Berlin Springer-Verlag.

70. Peng, Y. and G. Zhu, Biological nitrogen removal with nitrification and denitrification via nitrite pathway. Applied Microbiolgy and Biotechnology, 2006. **73**: p. 15-26.

71. Yabroudi, S.C., D.M. Morita, and P. Alem, Landfill leachate treatment over nitritation/denitritation in an activated sludge sequencing batch reactor. APCBEE procedia, 2013. **5**: p. 163-168.

72. Nhat, P.T., H.N. Biec, T.T.T. Van, D.V. Tuan, N.L.H. Trung, V.T.K. Nghi, and N.P. Dan, *Satbility of partial nitrification in a sequencing batch reactor fed with high ammonium strenght old urban landfill leachate.* International Biodeterioriation & Biodegradation, 2017. **124**: p. 56-61.

73. Breisha, G.Z., *Bio-removal of nitrogen from wastewaters - A review.* Nature and Science, 2010. **8**(12): p. 210-228.

74. Zhang, F.Z., Y. Peng, L. Miao, Z. Wang, S. Wang, and L. Baikun, A novel simultaneous partial nitrification Anammox and denitrification (SNAD) with intermittent aeration for cost-effective nitrogen removal from mature landfill leachate. Chemical Engineering Journal, 2017. **313**: p. 619-628.

75. Li, X., M.-y. Lu, Q.-c. Qiu, Y. Huang, B.-l. Li, and Y. Yuan, The effect of different denitrification and partial nitrification-Anammox coupling forms on nitrogen removal from mature landfill leachate at the pilot-scale. Bioresource Technology, 2020. **297**: p. 122430.

76. Wang, Z., L. Zhang, F. Zhang, H. Jiang, S. Ren, W. Wang, and Y. Peng, A continuous-flow combined process based on partial nitrification-Anammox and partial denitrification-Anammox (PN/A + PD/A) for enhanced nitrogen removal from mature landfill leachate. Bioresource Technology, 2020. **297**: p. 122483.

77. Guo, J., A.A. Abbas, Y. Chen, Z. Liu, F. Fang, and P. Chen, *Treatment of landfill leachate using a combined stripping, Fenton, SBR and coagulation process.* Journal of Hazardous Materials, 2010. **178**: p. 699-705.

78. Vedrenne, M., R. Vasquez-Medrano, D. Prato-Garcia, B.A. Frontana-Uribe, and J.G. Ibanez, Characterization and detoxification of a mature landfill leachate using combined coagulation-flocculation/photo-Fenton treatment. Journal of Hazardous Materials, 2012. **205-206**: p. 208-215.

79. Amor, C., E. Torres-Socías, J.A. Peres, M.I. Maldonado, I. Oller, S. Malato, and M.S. Lucas, *Mature landfill leachate treatment by coagulation/flocculation combined with Fenton and solar photo-Fenton processes.* Journal of Hazardous Materials, 2015. **286**: p. 261-268.

80. Di Iaconi, C., M. Pagano, R. Ramadori, and A. Lopez, *Nitrogen recovery from a stabilized municipal landfill leachate.* Bioresource Technology, 2010. **101**(6): p. 1732-1736.

81. Huang, H., D. Xiao, Q. Zhang, and L. Ding, Removal of ammonia from landfill leachate by struvite precipitation with the use of low-cost phosphate and magnesium sources. Journal of Environmental Management, 2014. **145**: p. 191-198.

82. Papastavrou, C., D. Mantzavinos, and E. Diamadopoulos, A comparative treatment of stabilized landfill leachate: Coagulation and activated carbon adsorption vs. electrochemical oxidation. Environmental Technology, 2009. **30**: p. 1547-1553.

83. Kurniawan, T.A., W. Lo, and G. Chan, *Physicochemical treatments for removal of recalcitrant contaminants from landfill leachates.* Journal of Hazardous Materials, 2006. **129**: p. 80-100.

84. Rui, L.M., Z. Daud, and A.A.A. Latij, *Treatment of leachate by coagulation-flocculation using different coagulants and polymer: A review.* International Journal on Advanced Science Engineering and Information Technology, 2012. **2**(2).

85. Mao, L., Z. Daud, and A.A.A. Latif, *Treatment of leachate by coagulation-flocculation using different coagulants and polymer: A review.* International Journal on Advanced Science Engineering and Information Technology, 2012. **2**(2): p. 1-4.

86. Tejera, J., R. Miranda, D. Hermosilla, I. Urra, C. Negro, and A. Blanco, Treatment of a mature landfill leachate: Comparison between homogeneous and heterogeneous photo-Fenton with different pretreatments. Water, 2019. **11**(9): p. 1849.

87. Ince, M., E. Senturk, G.O. Engin, and B. Keskinler, Further treatment of landfill leachate by nanofiltration and microfiltration-PAC hybrid process. Desalination, 2010. **255**: p. 52-60.

88. Aftab, B., J. Cho, H.S. Shin, and J. Hur, Using EEM-PARAFAC to probe NF membrane fouling potential of stabilized landfill leachate pretreated by various options. Waste Management, 2020. **102**: p. 260-269.

89. Mariam, T. and L.D. Nghiem, Landfill leachate treatment using hybrid coagulation-nanofiltration processes. Desalination, 2010. **250**: p. 677-681.

90. Chaudhari, L.B. and Z. Murthy, *Treatment of landfill leachates by nanofiltration.* Journal of Environmental Management, 2010. **91**: p. 1209-1217.

91. Li, F., K. Wichmann, and W. Heine, Treatment of the methanogenic landfill leachate with thin open channel reverse osmosis membrane modules. Waste Management, 2009. **29**: p. 960-964.

92. Asaithambi, P., B. Sajjadi, A.R.A. Aziz, and W.M.A.B.W. Daud, Ozone ($O_3$) and sono (US) based advanced oxidation processes for the removal of color, COD and determination of electrical energy from landfill leachate. Separation and Purification Technology, 2017. **172**: p. 442-449.

93. Tizaoui, C., L. Bouselmi, L. Mansouri, and A. Ghrabi, *Landfill leachate treatment with ozone and ozone/hydrogen peroxide systems.* Journal of Hazardous Materials, 2007. **140**: p. 316-324.

94. Silva, T.F.C.V., A. Fonseca, I. Saraiva, R.A.R. Boaventura, and V.J.P. Vilar, Biodegradability enhancement of a leachate after biological lagooning using a solar driven photo-Fenton reaction, and further combination with an activated sludge biological process, at pre-industrial scale Water Research, 2013. **47**: p. 3543-3557.

95. Silva, T.F.C.V., M.E.F. Silva, A.C. Cunha-Queda, A. Fonseca, I. Saraiva, R.A.R. Boaventura, and V.J.P. Vilar, Sanitary landfill leachate treatment using combined solar photo-Fenton and biological oxidation processes at pre-inductrial scale. Chemical Engineering Journal, 2013. **228**: p. 850-866.

96. Vilar, V.J.P., T.F.C.V. Silva, M.A.N. Santos, A. Fonseca, I. Saraiva, and R.A.R. Boaventura, *Evaluation of solar photo-Fenton parameters on the pre-oxidation of leachates from a sanitary landfill.* Solar Energy, 2012. **86**: p. 3301-3315.

97. Cortez, S., P. Teixeira, R. Oliveira, and M. Mota, *Evaluation of Fenton and ozone-based advanced oxidation processes as mature landfill leachate pre-treatments.* Journal of Environmental Management, 2011. **92**: p. 749-755.

98. Amaral-Silva, N., R.C. Martins, S. Castro-Silva, and R.M. Quinta-Ferreira, *Ozonation and perozonation on the biodegradability improvement of a landfill leachate.* Journal of Environmental Chemical Engineering, 2016. **4**: p. 527-533.

99. Cortez, S., P. Teixeira, R. Oliveira, and M. Mota, *Fenton's oxidation as post-treatment of a mature landfill leachate.* International Journal of Civil and Environmental Engineering, 2010. **2**(1): p. 40-43.

100. Cortez, S., P. Teixeira, R. Oliveira, and M. Mota, *Ozonation as polishing treatment of mature landfill leachate.* Journal of Hazardous Materials, 2010. **182**(1-3): p. 730-734.

101. Poznyak, T., G.L. Bautista, I. Chaírez, R.I. Córdova, and L.E. Ríos, *Decomposition of toxic pollutants in landfill leachate by ozone after coagulation.* Journal of Hazardous Materials, 2008. **152**: p. 1108-1114.

102. Xu, J., Y. Long, D. Shen, and H. Feng, Optimization of Fenton treatment process for degradation of refractory organics in pre-coagulated leachate membrane concentrates. Journal of Hazardous Materials, 2017. **323**: p. 674-680.

103. Guvenc, S.Y., K. Dincer, and G. Varank, Performance of electrocoagulation and electro-Fenton processes for treatment of nanofiltration concentrate of biologically stabilized landfill leachate. Journal of Water Process Engineering, 2019. **31**: p. 100863.

104. Fernandes, A., L. Labiadh, L. Ciríaco, M.J. Pacheco, A. Gadri, S. Ammar, and A. Lopes, *Electro-Fenton oxidation of reverse osmosis concentrate from sanitary landfill leachate: Evaluation of operational parameters.* Chemosphere, 2017. **184**: p. 1223-1229.

105. Wang, Y., X. Li, L. Zhen, H. Zhang, Y.-J. Zhang, and C. Wang, *Electro-Fenon treatment of concentrates generated in nanofiltration of biologically pretreated landfill leachate.* Journal of Hazardous Materials, 2012. **229-230**: p. 115-121.

106. Goi, A., Y. Veressinina, and M. Trapido, Combination of ozonation and the Fenton processes for landfill leachate treatment: Evaluation of treatment efficiency. Ozone: Science and Engineering, 2009. **31**(1): p. 28-36.

107. Amr, S.S.A. and H.A. Aziz, New treatment of stabilized leachate by ozone/Fenton in the advanced oxidation process. Waste Management, 2012. **32**: p. 1693-1698.

108. Lopez, A., M. Pagano, A. Volpe, and A.C. Di Pinto, *Fenton's pre-treatment of mature landfill leachate.* Chemosphere, 2004. **54**: p. 1005-1010.

109. Hermosilla, D., M. Cortijo, and C.P. Huang, *Optimizing the treatment of landfill leachate by conventional Fenton and photo-Fenton processes.* Science of the Total Environment, 2009. **407**: p. 3473-3481.

110. Cotman, M. and A.Z. Gotvajn, Comparison of different physico-chemical methods for the removal of toxicants from landfill leachate. Journal of Hazardous Materials, 2010. **178**: p. 298-305.

111. Vilar, V.J.P., J.M.S. Moreira, A. Fonseca, I. Saraiva, and R.A.R. Boaventura, Application of Fenton and solar photo-Fenton processes to the treatment of a sanitary landfill leachate in a pilot plant with CPCs. Journal of Advanced Oxidation Technologies, 2012. **15**: p. 107-116.

112. Primo, O., M.J. Rivero, and I. Ortiz, *Photo-Fenton process as an efficient alternative to the treatment of landfill leachates.* Journal of Hazardous Materials, 2008. **153**: p. 834-842.

113. Rocha, E.M.R., V.J.P. Vilar, A. Fonseca, I. Saraiva, and R.A.R. Boaventura, *Landfill leachate treatment by solar-driven AOPs.* Solar Energy, 2011. **85**(1): p. 46-56.

114. Wang, Z., J. Li, T. Weihu, X. Wu, H. Lin, and H. Zhang, *Removal of COD from landfill leachate by advanced Fenton process combined with electrolysis.* Separation and Purification Technology, 2019. **208**: p. 3-11.

115. Moreira, F.C., J. Soler, A. Fonseca, I. Saraiva, R.A.R. Boaventura, E. Brillas, and V.J.P. Vilar, *Incorporation of electrochemical advanced oxidation processes in a multistage treatment system for sanitary landfill leachate.* Water Research, 2015. **81**: p. 375-387.

116. Ntampou, X., A.I. Zouboulis, and P. Samaras, Appropriate combination of physicochemical methods (coagulation/flocculation and ozonation) for the efficient treatment of landfill leachates. Chemosphere, 2006. **62**: p. 722-730.

117. Umar, M., H.A. Aziz, and M.S. Yusoff, Trends in the use of Fenton, electro-Fenton and photo-Fenton for the treatment of landfill leachate. Waste Management, 2010. **30**: p. 2113-2121.

118. Pignatello, J.J., E. Oliveros, and A. Mackay, *Advanced oxidation processes for organic contaminant destruction based on the Fenton reaction and related chemistry.* Critical Reviews in Environmental Science and Technology, 2006. **36**: p. 1-84.

119. Deng, Y. and J.D. Englehardt, *Treatment of landfill leachate by the Fenton process.* Water Research, 2006. **40**: p. 118-124.

120. Malato, S., P. Fernández-Ibáñez, M.I. Maldonado, J. Blanco, and W. Gernjak, *Decontamination and disinfection of water by solar photocatalysis: recent overview and trends.* Catalysis Today, 2009. **147**: p. 1-59.

121. Einschlag, F.S.G., A.M. Braun, and E. Oliveros, Fundamentals and applications of the photo-Fenton process to water treatment, in Handbook of Environmental Chemistry: Environmental Photochemistry Part III, D.W. Bahnemann and P.K.J. Robertson, Editors. 2015, Springer: Heidelberg.

122. Zhang, H., H.J. Choi, and C.P. Huang, *Optimization of Fenton process for the treatment of landfill leachate.* Journal of Hazardous Materials, 2005. **125**: p. 166-174.

123. Kim, S. and A. Vogelpohl, *Degradation of organic pollutants by the photo-Fenton process.* Chemical Engineering & Technology, 1998. **21**: p. 187-191.

124. Rivas, F.J., F.J. Beltrán, O. Gimeno, and F. Carvalho, *Fenton-like oxidation of landfill leachate.* Journal of Environmental Science and Health A, 2003. **38**: p. 371-379.

125. Belalcázar-Saldarriaga, A., D. Prato-Garcia, and R. Vasquez-Medrano, Photo-Fenton processes in raceway reactors: technical, economical, and environmental implications during treatment of colored wastewaters. Journal of Cleaner Production, 2018. **182**: p. 818-829.

126. Prato-Garcia, D. and A. Robayo-Avendaño, Treatment of a synthetic colored effluent in raceway reactors: The role of operational conditions on the environmental performance of a photo-Fenton process. Science of the Total Environment, 2019. **697**: p. 134182.

127. Cabrera-Reina, A., S. Miralles-Cuevas, G. Rivas, and J.A. Sánchez-Pérez, Comparison of different detoxification pilot plants for the treatment of industrial wastewater by solar photo-Fenton: Are raceway pond reactors a feasible option? Science of the Total Environment, 2019. **648**: p. 601-608.

128. Bassam, A., I. Salgado-Transito, I. Oller, E. Santoyo, A.E. Jimenez, J.A. Hernandez, A. Zapata, and S. Malato, Optimal performance assessment for a photo-Fenton degradation pilot plant driven by solar energy using artificial neural networks. International Journal of Energy Research, 2012. **36**(14): p. 1314-1324.

129. Oliveros, E., O. Legrini, M. Hohl, T. Müller, and A.M. Braun, *Industrial waste water treatment: large scale development of a light-enhanced Fenton reaction.* Chemical Engineering and Processing, 1997. **36**: p. 397-405.

130. Malato, S., J. Blanco, M.I. Maldonado, I. Oller, W. Gernjak, and L. Pérez-Estrada, *Coupling solar photo-Fenton and biotreatment at industrial scale: main results of a demonstration plant.* Journal of Hazardous Materials, 2007. **146**: p. 440-446.

131. Rosenfeldt, E.J., K.G. Linden, S. Canonica, and U. Von Gunten, Comparison of the efficiency of ·OH radical formation during ozonation and the advanced oxidation processes $O_3/H_2O_2$ and $UV/H_2O_2$. Water Research, 2006. **40**: p. 3695-3704.

132. Gardoni, D., A. Vailati, and R. Canziani, *Decay of ozone in water: A review.* Ozone: Science and Engineering, 2012. **34**(4): p. 233-242.

133. Khadhraoui, M., H. Trabelsi, M. Ksibi, S. Bouguerra, and B. Elleuch, *Discoloration and detoxification of a Congo Red dye solution by means of ozone treatment for a possible water reuse.* Journal of Hazardous Materials, 2009. **161**: p. 974-981.

134. Beltrán, F.J., *Ozone reaction kinetics for water and wastewater systems*. 2003, Boca Raton: Lewis Publishers.

135. Criegee, R., *Mechanism of Ozonolysis.* Angewandte Chemie International Edition, 1975. **14**: p. 745-752.

136. Dowideit, P. and C. von Sonntag, Reaction of ozone with ethene and its methyl- and chlorine-substituted derivates in aqueous solution. Environmental Science & Technology, 1998. **32**: p. 1112-1119.

137. von Gunten, U., Ozonation of drinking water: Part I. Oxidation kinetics and product formation. Water Research, 2003. **37**: p. 1443-1467.

138. Krishnan, S., H. Rawindran, C.M. Sinnathambi, and J.W. Lim, Comparison of various advanced oxidation processes used in remediation of industrial wastewater laden with recalcitrant pollutants, in 29th Symposium of Malasian Chemical Engineers (SOMChE). 2017, IOP Publishing.

139. Chu, L.-B., S.-T. Yan, A.-F. Xing, X.-L. Sun, and B. Jurcik, *Enhanced sludge solubilization by microbubble ozonation.* Chemosphere, 2008. **72**: p. 205-212.

140. Paul, E. and H. Debellefontaine, Reduction of excess sludge production by biological treatment process: Effect of ozonation on biomass and on sludge. Ozone: Science and Engineering, 2007. **29**: p. 415-427.

141. Meeroff, D.E. and R. Teegavarapu, *Interactive decision support tool for leachate management.* 2010, Hinkley Center for Solid and Hazardous Waste Management, University of Florida.

142. Brennan, R.B., M.G. Healy, L. Morrison, S. Hynes, D. Norton, and E. Clifford, *Suitability of municipal wastewater treatment plants for the treatment of landfill leachate.* 2017, Environmental Protection Agency: Ireland.

143. Costa, A.M., R.G.S.M. Alfaia, and J.C. Campos, *Landfill leachate treatment in Brazil - An overview.* Journal of Environmental Management, 2019. **232**: p. 110-116.

144. Zhang, J., K. Xiao, and X. Huang, Full-scale MBR applications for leachate treatment in China: Practical, technical, and economic features. Journal of Hazardous Materials, 2020. **389**: p. 122138.

145. Wang, H., Z. Cheng, Z. Sun, N. Zhu, H. Yuan, Z. Lou, and X. Chen, Molecular insight into variations of dissolved organic matters in leachates along China's largest A/O-MBR-NF process to improve the removal efficiency. Chemosphere, 2020. **243**: p. 125354.

146. Steensen, M., Chemical oxidation for the treatment of leachate process comparison and results from full-scale plants. Water Science and Technology, 1997. **35**(4): p. 249-256.

147. Witz, U. and H.-J. Ehrig, Leachate treatment in Germany: Leachate and wastewater treatment with high-tech and natural systems, in KALMAR ECO-TEC. 2001: Kalmar, Sweden.

148. Calabrò, P.S., E. Gentili, C. Meoni, S. Orsi, and D. Komilis, Effect of the recirculation of a reverse osmosis concentrate on leachate generation: A case study in an Italian landfill. Waste Management, 2018. **76**: p. 643-651.

149. Campagna, M., M. Çakmakci, F.B. yaman, and B. Özkaya, Molecular weight distribution of a full-scale landfill leachate treatment by membrane bioreactor and nanofiltration membrane. Waste Management, 2013. **33**(4): p. 866-870.

150. Theepharaksapan, S., C. Chiemchaisri, W. Chiemchaisri, and K. Yamamoto, Removal of pollutants and reduction of bio-toxicity in a full scale chemical coagulation and reverse osmosis leachate treatment system. Bioresource Technology, 2011. **102**(9): p. 5381-5388.

151. Martinho, G., F. Santana, J. Santos, A. Brandão, and I. Santos, *Management and treatment of leachates produced by urban waste landfills.* 2008, Department of Sciences and Environmental Engineering, Faculty of Sciences and Technology, Nova de Lisboa University

152. Costa, T.J.S., Leachate treatment from municipal solid waste landfills in Portugal, in Civil Engineering. 2015, Técnico de Lisboa. p. 138.

153. *List of active landfills*. Waste Department - Portuguese Environmental Agency.

154. Kalka, J., Landfill leachate toxicity removal in combined treatment with municipal wastewater. Scientific World Journal, 2012: p. 1-7.

155. Kurniawan, T.A., W. Lo, G. Chan, and M.E.T. Sillanpaa, *Biological processes for treatment of landfill leachate.* Journal of Environmental Monitoring, 2010. **12**(11): p. 2032-2047.

156. Junior, R.A.B., L.S.V. Castro, G.C.X. Esteves, R.R. Silva, and G.C. Rocha, Viabilidade da implantação de sistemas de lagoas para tratamento do chorume do aterro sanitário de Santo André, in 30º Congresso Brasileiro de Engenharia Sanitária e Ambiental. 2020, ABES.

157. Capela, F.S.S., Contribution to the study of nitrogen removal in leachate from municipal waste, in Environmental Engineering. 2014, Universidade Nova de Lisboa: Faculdade de Ciências e Tecnologia.

158. Cassano, D., A. Zapata, G. Brunetti, G. Del Moro, C. Di Iaconi, I. Oller, S. Malato, and G. Mascolo, Comparison of several combined/integrated/biological-AOPs setups for the treatment of municipal landfill leachate: Minimization of operating costs and effluent toxicity. Chemical Engineering Journal, 2011. **172**: p. 250-257.

159. Del Moro, G., A. Mancini, G. Mascolo, and C. Di Iaconi, Comparison of UV/H2O2 based AOP as an end treatment or integrated with biological degradation for treating landfill leachates. Chemical engineering Journal, 2013. **218**: p. 133-137.

160. Anfruns, A., J. Gabarró, R. Gonzalez-Olmos, S. Puig, M.D. Balaguer, and J. Colprim, *Coupling anammox and advanced oxidation-based technologies for mature landfill leachate treatment.* Journal of Hazardous Materials, 2013. **258-259**: p. 27-34.

161. Abood, A.R., J. Bao, J. Du, D. Zheng, and Y. Luo, Non-biodegradable landfill leachate treatment by combined process of agitation, coagulation, SBR and filtration. Waste Management, 2014. **34**: p. 439-447.

162. Torres-Socías, E., L. Prieto-Rodríguez, A. Zapata, I. Fernández-Calderero, I. Oller, and S. Malato, *Detailed treatment line for a specific landfill leachate remediation: Brief economic assessment.* Chemical Engineering Journal, 2015. **261**: p. 60-66.

163. Gao, J., V. Oloibiri, M. Chys, S. De Wandel, B. Decostere, W. Audernaert, Y.L. He, and S.W.H. Van Hulle, *Integration of autotrophic nitrogen removal, ozonation and activated carbon filtration for treatment of landfill leachate.* Chemical Engineering Journal, 2015. **275**: p. 281-287.

164. Zolfaghari, M., K. Jardak, P. Drogui, S.K. Brar, G. Buelna, and R. Dubé, *Landfill leachate treatment by sequential membrane bioreactor and electro-oxidation processes,.* Journal of Environmental Management, 2016. **184**: p. 318-326.

165. Poblete, R., I. Oller, M.I. Maldonado, Y. Luna, and E. Cortes, Cost estimation of COD and color removal from landfill leachate using combined coffee-waste based activated carbon with advanced oxidation processes. Journal of Environmental Chemical Engineering, 2017. **5**: p. 114-121.

166. Pastore, C., E. Barca, G. Del Moro, C. Di Iaconi, M. Loos, H.P. Singer, and G. Mascolo, Comparison of different types of landfill leachate treatment by employment of nontarget screening to identify residual refractory organics and principal component analysis Science of the Total Environment, 2018. **635**: p. 984-994.

167. Baiju, A., R. Gandhimathi, S.T. Ramesh, and P.V. Nidheesh, *Combined heterogeneous electro-Fenton and biological process for the treatment of stabilized landfill leachate.* Journal of Environmental Management, 2018. **210**: p. 328-337.

168. Colombo, A., A.N. Módenes, D.E.G. Trigueros, S.I.G. Costa, F.H. Borba, and F.R. Espinoza-Quiñones, *Treatment of danitary landfill leachate by the combination of photo-Fenton and biological processes.* Journal of Cleaner Production, 2019. **214**: p. 145-153.

169. Gao, J., Y. He, M. Chys, B. Decostere, W. Audernaert, and S.W.H. Van Hulle, *Autotrophic nitrogen removal of landfill leachate at lab-scale and pilot-scale: feasibility and cost evaluation.* Journal of Chemical Technology & Biotechnology, 2015. **90**(12): p. 2152-2160.

170. Chys, M., W. Declerck, W. Audenaert, and S.W.H. Van Hulle, UV/$H_2O_2$, $O_3$ and (photo-)Fenton as treatment prior to granular activated carbon filtration of biologically stabilized landfill leachate. Journal of Chemical Technology & Biotechnology, 2015. **90**(3): p. 525-533.

171. Chys, M., V.A. Oloibiri, W.T.M. Audenaert, K. Demeestere, and S.W.H. Van Hulle, *Ozonation of biologically treated landfill leachate: Efficiency and insights in organic conversions.* Chemical Engineering Journal, 2015. **277**: p. 104-111.

172. Oloibiri, V., I. Ufomba, M. Chys, W.T.M. Audenaert, K. Demeestere, and S.W.H. van Hulle, A comparative study on the efficiency of ozonation and coagulation-flocculation as pretreatment to activated carbon adsorption of biologically stabilized landfill leachate. Waste Management, 2015. **43**: p. 335-342.

173. Oloibiri, V., M. Chys, S. De Wandel, K. Demeestere, and S.W.H. Van Hulle, Removal of organic matter and ammonium from landfill leachate through different scenarios: Operational cost evaluation in a full-scale case study of a Flemish landfill. Environmental Management, 2017. **203**: p. 774-781.

174. Vilar, V.J.P., E.M.R. Rocha, F.S. Mota, A. Fonseca, I. Saraiva, and R.A.R. Boaventura, Treatment of a sanitary landfill leachate using combined solar photo-Fenton and biological immobilized biomass reactor at pilot scale. Water Research, 2011. **45**: p. 2647-2658.

175. Sellers, K., K. Weeks, W.R. Alsop, S.R. Clough, M. Hoyt, and B. Pugh, *Perchlorate: Environmental problems and solutions*. 2006: CPC Press - Taylor & Francis Group.

176. Matsuno, K., *The treatment of hydrofluoric acid burns.* Occupational Medicine, 1996. **46**: p. 313-317.

177. Silva, T.F.C.V., M.E.F. Silva, A.C. Cunha-Queda, A. Fonseca, I. Saraiva, M.A. Sousa, C. Gonçalves, M.F. Alpendurada, R.A.R. Boaventura, and V.J.P. Vilar, *Multistage treatment system for raw leachate from sanitary landfill combining biological nitrification-denitrification/solar photo-Fenton/biological processes, at a scale close to industrial.* Water Research, 2013. **47**: p. 6167-6186.

178. Silva, T.F.C.V., P.A. Soares, D.R. Manenti, A. Fonseca, I. Saraiva, R.A.R. Boaventura, and V.J.P. Vilar, *An innovative multistage treatment system for sanitary landfill leachate depuration: Studies at pilot-scale.* Science of the Total Environment, 2017. **576**: p. 99-117.

179. Silva, T.F.C.V., A. Fonseca, I. Saraiva, R.A.R. Boaventura, and V.J.P. Vilar, *Scale-up and cost analysis of a photo-Fenton system for sanitary landfill leachate treatment.* Chemical Engineering Journal, 2016. **283**: p. 76-88.

# 4 Materials and methods

*A detailed description of all chemical reagents, analytical determinations, and experimental setups used throughout this thesis, as well as of the experimental procedures implemented to meet the proposed objectives, is presented within this chapter.*

*The experimental work was mostly developed in the Associate Laboratory LSRE-LCM (Laboratory of Separation and Reaction Engineering – Laboratory of Catalysis and Materials (LSRE-LCM), at the Department of Chemical Engineering (DEQ), Faculty of Engineering University of Porto (FEUP), except for the treatment train tests performed at full-scale, whose facility was located in a Municipal Solid Waste Sanitary Landfill, in northern Portugal.*

## 4.1 Chemical reagents

Table 4.1 presents the chemicals employed in the experimental work, either for the treatment processes (biological, coagulation, photo-Fenton and ozone) or for the various analytical determinations carried out in the course of the experiments. Ultrapure and pure water, required for the preparation of solutions and sample dilutions, were obtained from a Millipore Direct-Q® system (resistivity of 18.2 MΩ cm, at 25 ºC) and a reverse osmosis system (Panice®), respectively.

**Table 4.1** – List of chemicals employed on the experiments and analyses.

| Reagent | MF[a] | % (w/w) | $\rho^b$ (kg/L) | MW[c] (g/mol) | Supplier | Purpose |
|---|---|---|---|---|---|---|
| Methanol | $CH_3OH$ | - | 0.79 | 32.04 | Quimitécnica | Biological denitrification |
| Glycerol | $C_3H_8O_3$ | 88 | 1.26 | 92.09 | | |
| Sulphuric acid | $H_2SO_4$ | 96 | 1.84 | 98.08 | Quimitécnica | Coagulation process |
| Ferric chloride | $FeCl_3$ | 40 | 1.44 | 162.20 | | |
| Aluminium sulfate | $Al_2(SO_4)_3$ | - | 1.32 | 342.15 | Rivaz Química | |
| Ferrous chloride | $FeCl_2$ | 27 | 1.27 | 126.75 | Quimitécnica | Photo-Fenton process |
| Hydrogen peroxide | $H_2O_2$ | 50[d] | 1.10 | 34.02 | | |
| Ferrous sulfate heptahydrate | $FeSO_4.7H_2O$ | 98[e] | 1.90 | 278.05 | Panreac | |
| Sodium hydroxide | NaHO | 30 | 1.33 | 40.00 | Merck | |
| Oxygen | $O_2$ | > 99.9[e] | - | 32.00 | Linde | Ozone process |
| Ferric chloride hexahydrate | $FeCl_3.6H_2O$ | ≥ 98[e] | 1.82 | 270.33 | Merck | Actinometry analysis |
| Oxalic acid dihydrate | $C_2H_2O_4.2H_2O$ | ≥ 99[e] | 1.65 | 126.07 | VWR | |
| Ammonium monovanadate | $NH_4VO_3$ | - | - | 116.97 | Merck | Hydrogen peroxide analysis |
| Sulphuric acid | $H_2SO_4$ | 96 | 1.84 | 98.08 | Pronoloab | |
| 1,10-phenanthroline 1-hydrate | $C_{12}H_8N_2.H_2O$ | - | - | 198.23 | Panreac | Total dissolved iron (TDI) analysis |
| Acetic acid | $CH_3COOH$ | 100 | 1.05 | 60.05 | Fisher | |
| Ammonium acetate | $NH_4C_2H_3O_2$ | - | - | 77.08 | | |
| L-ascorbic acid | $C_6H_8O_6$ | - | - | 176.12 | Acrós | |
| Potassium dichromate | $K_2Cr_2O_7$ | - | - | 294.19 | Merk | COD analysis |
| Potassium hydrogen phthalate | $C_8H_5KO_4$ | - | - | 204.22 | | |
| Silver sulfate | $Ag_2SO_4$ | - | - | 311.80 | | |
| Mercury sulfate | $HgSO_4$ | ≥ 98[e] | - | 296.65 | Panreac | |
| Sulphuric acid | $H_2SO_4$ | 96 | 1.84 | 98.08 | Pronolab | |

| Reagent | MF[a] | % (w/w) | $\rho$[b] (kg/L) | MW[c] (g/mol) | Supplier | Purpose |
|---|---|---|---|---|---|---|
| N-Allylthiourea | $C_4H_8N_2S$ | - | - | 116.19 | Merck | BOD5 analysis |
| Sodium hydroxide pellets | NaOH | - | - | 40.00 | | |
| Alpha-D-glucose | $C_6H_{12}O_6$ | - | - | 180.16 | Fisher | Reference and mineral medium for Zahn-Wellens test and BOD5 analysis |
| Ammonium chloride | $NH_4Cl$ | - | - | 53.49 | VWR | |
| Calcium chloride dihydrate | $CaCl_2.2H_2O$ | - | - | 147.02 | | |
| Dipotassium hydrogen phosphate | $K_2HPO_4$ | - | - | 174.20 | Merck | |
| Disodium hydrogen phosphate dihydrate | $Na_2HPO_4.2H_2O$ | - | - | 178.00 | | |
| Ferric chloride hexahydrate | $FeCl_3.6H_2O$ | $\geq 98$[e] | 1.82 | 270.33 | | |
| Magnesium sulfate heptahydrate | $MgSO_4.7H_2O$ | - | - | 246.47 | Panreac | |
| Potassium dihydrogen phosphate | $KH_2PO_4$ | - | - | 163.09 | VWR | |
| Potassium hydrogen phthalate | $C_8H_5KO_4$ | - | - | 204.22 | IZASA | Standard solutions for TC-TOC-TN analyser calibration |
| Hydrogen carbonate | $HCO_3^-$ | - | - | 61.02 | | |
| Sodium carbonate | $Na_2CO_3$ | - | - | 105.99 | | |
| Potassium nitrate | $KNO_3$ | - | - | 101.10 | | |
| Sodium hydroxide 1N | NaHO | | | 40.00 | VWR | Elution and Standards for ionic chromatography |
| Methanesulfonic acid | $CH_4O_3S$ | $\geq 99$[e] | 1.48 | 96.10 | Merk | |
| Ammonium standard 1000 mg/L | $NH_4Cl$ | $> 99.9$[e] | 1.00 | 53.49 | | |
| Chloride, nitrate and sulfate standard 1000 mg/L | NaCl NaNO_3 Na_2SO_4 | $> 99.9$[e] | 1.00 | 58.44 84.99 142.04 | | |
| Nitrite standard 1000 mg/L | $NaNO_2$ | $> 99.9$[e] | 1.00 | 68.98 | | |

[a]Molecular formula. [b]Density. [c]Molecular weight. [d]Concentration in weight/volume percentage. [e] Purity.

## 4.2 Analytical determinations

The analytical determinations used throughout the experimental work are listed and briefly described below (Table 4.2).

**Table 4.2** – Physicochemical parameters and respective analytical methods.

| Parameter | Methodology |
|---|---|
| Anions[a,b] | Chloride ($Cl^-$), nitrite ($NO_2^-$), sulfate ($SO_4^{2-}$), nitrate ($NO_3^-$) and phosphate ($PO_4^{3-}$) were quantified by ion chromatography using a Dionex ICS-2100 apparatus, equipped with a IonPac® AS11-HC (4 × 250 mm) column at 30 ºC and an anion self-regenerating suppressor (ASRS® 300, 4 mm), under isocratic elution of 30 mM NaOH at a flow rate of 1.5 mL/min, during 12 minutes. |
| Biodegradability | A 28-days Zahn-Wellens biodegradability test was performed according to the OECD protocol [1]. Control and blank experiments were prepared using glucose and pure water, respectively, instead of sample. The percentage of biodegradation ($D_t$) was calculated through Equation 4.1: <br><br> $$D_t = \left[1 - \frac{C_T - C_B}{C_A - C_{BA}}\right] \times 100 \qquad (4.1)$$ <br><br> where $C_T$ and $C_B$ are the sample and blank DOC concentrations (in mg L$^{-1}$) determined at the sampling time $t$, respectively, and $C_A$ and $C_{BA}$ are the corresponding sample and blank DOC concentrations measured 3 h after beginning the test. |
| BOD$_5$ | Biochemical oxygen demand at 5 days (BOD$_5$) was determined according to Standard Methods for the Examination of Water and Wastewater [2], 5210-B test, using an OxiTop® (manometric respirometry). |
| Cations[a,b] | Ammonium ($NH_4^+$) was determined by ion chromatography using a Dionex DX-120 device equipped with a IonPac® CS12A (4 × 250 mm) column at ambient temperature and a cation self-regenerating (CSRS® Ultra II, 4 mm) suppressor, under isocratic elution of 20 mM methanesulfonic acid at a flow rate of 1.0 mL/min, during 12 minutes. Sodium ($Na^+$), potassium ($K^+$), magnesium ($Mg^{2+}$) and calcium ($Ca^{2+}$) were also measured for monitoring purposes. |
| COD | Chemical oxygen demand (COD) was quantified by Merck® Spectroquant kits (ref: 1.14541.0001) or according to Standard Methods for the Examination of Water and Wastewater [2], 5220-D (dichromate closed reflux method). |
| Colour and Turbidity | Colour (expressed in terms of Pt-Co units) and turbidity were measured in a spectrophotometer (Hach, model DR 2010). Colour was also measured according to the NP-627 (1972) [3]. |
| DM | Dry matter (DM) content of sludge was determined by gravimetry, drying the solid residue at 105 °C, according to Standard Methods for the Examination of Water and Wastewater [2], 2540-G test. |
| DO | Dissolved oxygen (DO) was measured by the multiparameter meter HI9828, from Hanna Instruments (sensor HI769828, Hanna Instruments). |

| Parameter | Methodology |
|---|---|
| DOC/DIC[a,b] | Dissolved organic carbon (DOC) was determined by NDIR spectrometry in a TC-TOC-TN analyser equipped with ASI-V autosampler (Shimadzu, model TOC-$V_{CSN}$). DOC was given by the difference between TDC (Total Dissolved Carbon) and DIC (Dissolved Inorganic Carbon). |
| Fluorescence spectra | Fluorescence spectra were measured using a Horiba Aqualog fluorometer. Fluorescence was scanned with excitation wavelengths from 225 to 450 nm in 5 nm increments and emission wavelengths from 250 to 580 nm in 1 nm increments. The normalized methods for total fluorescence (TF) and regional integration were performed as described by Chen, et al. [4]. |
| Heavy metals | Heavy metals (Al, Cr, Cu, Fe, Ni, Pb) were determined by inductively coupled plasma optical emission spectrometry (ICP-OES), using a Thermo iCAP 7000 equipment, after sample digestion with nitric acid. |
| $H_2O_2$[a,b,c] | The hydrogen peroxide ($H_2O_2$) concentration was determined by the vanadate method [5], based on the reaction of $H_2O_2$ with ammonium metavanadate in acidic medium, which results in the formation of a red-orange colour peroxovanadium cation, with maximum absorbance at 450 nm, using a spectrophotometer (Merck, model Spectroquant® Pharo 100 or Hach, model DR 2010). At full-scale facility, an $H_2O_2$ controller and sensor were used (Grundfos, model Conex DIA-1-A PA/HP) |
| $C_{O_3,D}$ [a,b,c] | Dissolved ozone ($C_{O_3,D}$) was determined using Spectroquant® photometric ozone test (ref: 1.00607.0001) |
| $C_{O_3,In}$/$C_{O_3,Out}$ | Inlet and outlet ozone gas was measured by means of a UV-based ozone analyzer (BMT 964) |
| Optical efficiency | Ray-trace analysis was performed for different reflector geometries, considering incident ray angles of 45º and 90º, using the TracePro-4.1.2 release program. |
| pH | pH was measured by a multiparameter meter HI9828, from Hanna Instruments (sensor HI769828, Hanna Instruments) or a pH meter VWR symphony - SB90M5. |
| Radiant power (RP) | The radiant power incident ($RP_i$) on the actinometric solution was determined by ferrioxalate actinometry ($Fe^{3+}_{aq}$, $6.0 \times 10^{-3}$ M; oxalic acid, $3.0 \times 10^{-2}$ M). The quantity of ferrous ions formed during the irradiation period was monitored by the conversion to the coloured tris-phenanthroline complex ($\varepsilon = 11100$ L mol$^{-1}$ cm$^{-1}$ at $\lambda_{max} = 510$ nm), according to ISO 6332 [6]. |
| Reflectance properties | Total reflectance ($\rho_T$) and diffuse reflectance ($\rho_D$) were experimentally determined by a Shimadzu UV-3600/UV-Vis-NIR spectrophotometer, equipped with a 150 mm integrating sphere, using $BaSO_4$ as 100% reflectance standard. Samples were geometrically flat, to fit into the spectrophotometer sample holder. Average values of specular reflectance ($\rho_S$) were calculated considering that the total reflectance is the sum of diffuse and specular reflectance. |
| $SSV_{30-min}$ | 30-min settled sludge volume ($SSV_{30-min}$) was measured according to Standard Methods for the Examination of Water and Wastewater [2], 2710-C test. |

| Parameter | Methodology |
|---|---|
| SVI | Sludge volume index (SVI) was determined according to Standard Methods for the Examination of Water and Wastewater [2], 2710 D test, which uses 30-min settled sludge volume (SSV30) and TSS values. |
| T | Temperature (T) was measured by a multiparameter meter HI9828, from Hanna Instruments (sensor HI769828, Hanna Instruments) or a pH meter VWR symphony - SB90M5. |
| TDI[a,b,c] ($Fe^{2+}$/$Fe^{3+}$) | Colorimetric determination of total dissolved iron (TDI) content was done with 1,10-phenantroline according to ISO 6332 [6] using a spectrophotometer (Merck, model Spectroquant® Pharo 100 or Hach, model DR 2010) at 510 nm. |
| TN[a,b] | Total dissolved nitrogen (TN) was measured in a TC-TOC-TN analyser coupled with a TNM-1 unit (Shimadzu, model TOC-VCSN), by thermal decomposition and NO detection by chemiluminescence method. |
| TSS | Total suspended solids (TSS) were measured by gravimetry, drying the solid residue at 105 °C, according to Standard Methods for the Examination of Water and Wastewater [2], 2540-D test. |
| UV-Vis spectrum[a,b] | UV-Vis spectrum was determined in a scan range of 200-600 nm (interval = 1 nm), using an UV-Vis spectrometer (VWR, UV-6300PC) and 1 cm quartz cuvette. |
| VSS | Volatile suspended solids (VSS) were determined by gravimetry, after TSS calcination at 550 °C, according to Standard Methods for the Examination of Water and Wastewater [2], 2540-E test. |

[a] All samples were filtered through 0.45 μm Nylon membrane filters before analysis.
[b] Ultrapure and pure water used for the analytical determinations were produced by a Millipore Direct-Q® system and a reverse osmosis system (Panice®), respectively.
[c] Due to the leachate's absorption at the selected wavelengths, a blank/control sample (diluted as for the colorimetric analyses) was always prepared, and the absorbance measured at the same wavelength for correction.

## 4.3 Experimental setups and procedures

Different experimental setups were used along the experimental work to test the various treatment processes (Table 4.3).

Table 4.3 – Identification of experimental setups used in this thesis.

| Treatment process | Experimental setup | Chapter |
|---|---|---|
| Biological nitrogen removal | Lab-scale SBR | 5 |
| | Full-scale SBR | 6 |
| Coagulation | "*Jar-test*" apparatus | 5, 9 |
| | Full-scale unit | 6 |
| Advanced oxidation | Lab-scale CPC | 5, 7 |
| | Full-scale FluHelik photoreactor | 6 |
| | Pilot-scale CPC: unit A | 7 |
| | Pilot-scale CPC: unit B | 7 |
| | Pilot-scale CPC: unit C | 7 |
| | Bubble column reactor | 8 |
| | FluHelik coupled with bubble column | 8, 9 |
| Biological oxidation (Post-AOP) | Lab-scale: batch mode | 5 |
| | Lab-scale: continuous mode | 5 |
| | Full-scale SBR | 6 |

The experimental units, as well as the respective procedures adopted, are sequentially described below according to the following chapters.

### 4.3.1 Treatment train system: lab-scale

#### 4.3.1.1 Sequential batch reactor (SBR)

*Description*

The SBR (10 L) was equipped with a mechanical stirrer (Ingenieurbüro CAT, model R50D), to ensure homogeneity, and an air compressor (Aqua Medic, model Mistral 4000, version 2.0) connected to two air diffusers placed at the reactor bottom, for oxygen supply during the aerobic cycle (Figure 4.1). The reactor was also coupled to a thermostatic bath (Nüve, model BS402 (S)),

allowing the tests to be conducted at different temperatures. Measurements of pH, dissolved oxygen, temperature, conductivity and reduction oxidation potential were recorded by means of a multiparameter probe (HI 9828).
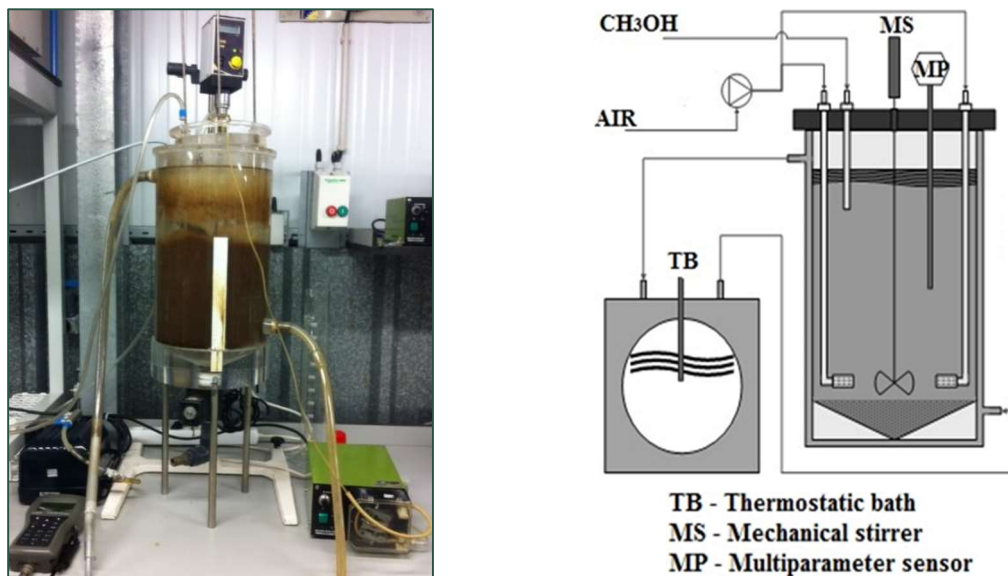


**Figure 4.1** – Photograph and schematics for lab-scale SBR, at FEUP.

*Experimental procedure*

For the start-up, the reactor was fed with 6 L of leachate and inoculated with 1 L of biomass (previously acclimated to this leachate under aerobic/anoxic conditions), and operated to promote nitrification/denitrification reactions until nearly all nitrogen content removal (2 weeks, 22 ºC < T (not controlled) < 28 ºC, 7.6 < pH (not controlled) < 9.1, 0.3 mg/L < DO (during nitrification period) < 0.8 mg/L, addition of methanol with a COD/N ratio = 2.5, during denitrification period). After that, the 24h-tests started, according to the traditional operating scheme: (i) fill phase, where a pre-determined amount of leachate was added, maintaining a total volume of 7 L; (ii) react phase, starting with an aerobic period followed by an anoxic period (total time = 23.5 h); (iii) settle phase (0.5 h); and (iv) draw phase, with the removal of a pre-established volume of treated leachate. In view of the sequential nature of the treatment strategy, and taking advantage from the knowledge acquired in previous research, the cycle time of 24 h was selected since it was considered suitable to carry out the following physicochemical treatment stages. The SBR-24h-tests were performed at 20, 25 and 30 ºC. For each temperature, the maximum nitrogen load that could be biologically removed in a 24h-cycle was determined by varying the volume exchange ratio (*VER*). This was accomplished by adjusting the leachate feeding volume while the total working volume of the reactor (7 L) was maintained. Thus, the HRT varied between 4.7 and 7 days. Methanol was added

at the beginning of each anoxic period (COD/N ratio = 2.5), as an external carbon donor for the denitrification reaction. To maintain a stable biomass concentration in the reactor (VSS = $4.0 \pm 0.1$ g/L), small amounts of sludge were periodically removed, yielding a mean sludge retention time (SRT) of 20 days. The bio-treated leachate, with final TN content below the legal limit, was collected to be used in the following coagulation tests. Also, since the coagulation tests would require a nitrified leachate, a final batch of 6 L of leachate was treated under aerated conditions (DO ~ 0.5 mg/L, 26 < T (ºC) < 28, pH not controlled) until complete ammonia removal.

### 4.3.1.2 *"Jar-test"* apparatus

*Description*

The coagulation experiments were performed using a *jar-test* apparatus (Model JLT6, Velp Scientifica, Italy) with 6 positions for 1 L beakers (Figure 4.2). The rotational speed could be adjusted from 10 to 300 rpm, with 1 rpm intervals, and the time set to hours or minutes.



**Figure 4.2** – Photograph of the *jar-test* apparatus, at FEUP.

*Experimental procedure*

To assess the influence of the biological pre-treatment on a downstream coagulation stage (Chapter 5), different coagulant dosages (160, 200 and 240 mg $Fe^{3+}$/L, at pH = 4.5) and pH values (3.0, 4.0 and 4.5, with 240 mg $Fe^{3+}$/L), using nitrified ($L_{NIT}$) and nitrified/denitrified leachate ($L_{N/D}$), were tested in the *jar-test* apparatus. $FeCl_3$ was chosen as coagulant, since in the following treatment stage iron would be used as a catalyst. Also, this coagulant is widely suggested as the best choice for leachate treatment and normally recognized to be more effective than aluminium salt coagulants [7-9]. The coagulant concentrations were selected based on previous work [10] and the pH values

are within the range reported as the optimum by different authors [10-13]. Each test was performed with 0.75 L of bio-treated leachate. After the coagulant addition and pH adjustment, a rapid stirring was applied (150 rpm for 3 min), followed by slow stirring (20 rpm for 20 min) and a sedimentation period (4 hours). Dissolved organic carbon (DOC), total suspended solids (TSS), turbidity and sulfate content were analysed in the supernatant.

Jar-test was also used (Chapter 9) to test the coagulation of a nitrified/denitrified leachate, using aluminium salt coagulant and in view of near-neutral pH conditions, to proceed with a following ozone-driven oxidation. The same procedure as described for $FeCl_3$ was applied, but in this case, different coagulant dosages (100, 200, 300, 400, 600 and 800 mg $Al^{3+}$/L) were used, without pH adjustment (bio-treated leachate pH = 9.1).

### 4.3.1.3 Sunlight simulator and CPC photoreactor

*Description*

The lab-scale photocatalytic system comprises (Figure 4.3): (i) a sunlight simulator (ATLAS, model SUNTEST XLS+) with an exposition area of 1100 $cm^2$, an air-cooled 1700 W Xenon lamp, a daylight filter and a filter quartz with infrared coating; (ii) a compound parabolic collector (CPC) of 0.025 $m^2$ illuminated area with anodized aluminium reflector and borosilicate tube (Schott-Duran, type 3.3, Germany, cut-off at 280 nm, internal diameter 46.4 mm, length 200 mm and thickness 1.8 mm); (iii) a glass vessel (1.5 L capacity) with a cooling jacket coupled to a thermostatic bath (Lab. Companion, model RW-0525G) to maintain a constant temperature during the tests; (iv) a magnetic stirrer (Velp Scientifica, model ARE) to ensure complete homogenization of the solution within the reactor; (v) a peristaltic pump (Ismatec, model Ecoline VC-380 II, with a maximum flow rate of 0.63 L /min) to promote effluent recirculation between the CPC and the glass vessel; vi) a pH and temperature meter (VWR symphony - SB90M5). All systems are connected by Teflon tubing.

*Experimental procedure*

The lab-scale PF tests were performed with 1 L of bio-coagulated-leachate, obtained under the best operating conditions regarding each previous stage. Different temperatures (15, 20, 30, 40 and 50 ºC), catalyst doses (20, 40, 60, 80 and 100 mg $Fe^{2+}$/L) and radiation intensities (22, 33 and 44 $W_{UV}/m^2$) were tested. Moreover, to evaluate the effect of the iron that remained after coagulation,

a PF trial without the addition of catalyst was carried out. Each test was started by filling the recirculation vessel with the pre-treated leachate, which was homogenized (by magnetic stirrer) and recirculated, in darkness, to the photoreactor during ca. 15 min. Meantime, the thermostatic bath was programmed to maintain the leachate at the desired temperature. Then, the sunlight simulator was turned on (with the photoreactor covered with an aluminium foil) and the irradiance was set at 250, 350 and 500 $W/m^2$ (corresponding to 22, 33 and 44 $W_{UV}/m^2$). Afterward, the catalyst was added, according to the intended concentration, and after 10 min a sample was collected for total dissolved iron (TDI) concentration control. Lastly, the photoreactor was uncovered and the first dose of hydrogen peroxide was added to start the PF reaction. The photo-treatment was conducted at pH 2.8-3.0, since it is considered the optimum pH for the PF reaction [14]. Samples were collected at pre-set intervals over the 3 h of total reaction time. During the photo-treatment, $H_2O_2$ was gradually added to maintain its concentration between 100-500 mg/L. In the end, the photo-treated leachate was neutralized with NaOH to pH 7, for iron precipitation, and the resulting sludge was able to settle for 2-4 hours.



(a)  (b)  (c)



(d)
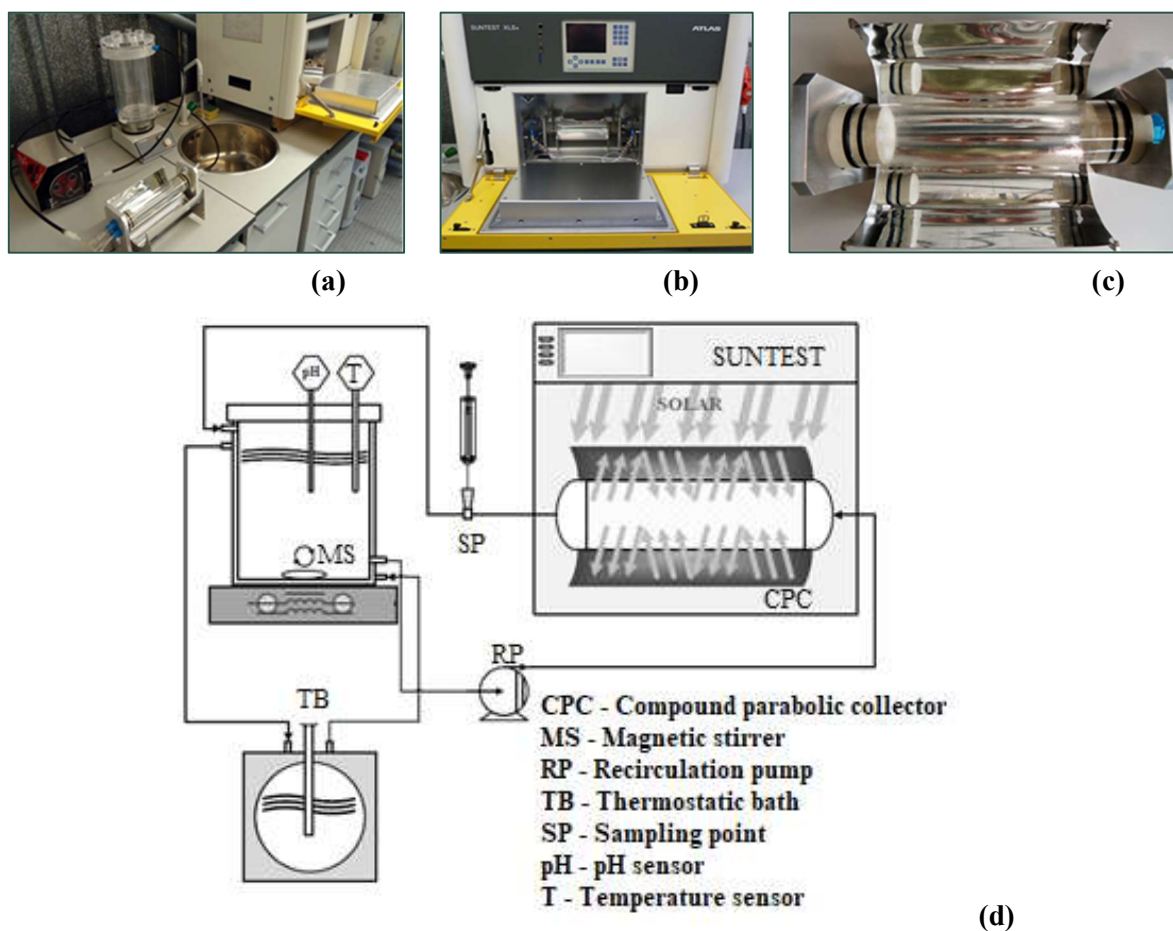
**Figure 4.3** – Lab-scale setup for photo-oxidation tests: (a) overall view, (b) sunlight simulator, (c) compound parabolic collector photo-reactor, and (d) setup schematics.

### 4.3.1.4 Biological reactor: batch and continuous mode

*Description*

The batch tests were conducted in a flask (1 L), with magnetic stirring (Heidolph MR 300) and aeration by means of a diffuser connected to an air compressor (Horizon, Bio-Oxidation Console model), according to Figure 4.4-a. The continuous mode tests were performed in a conventional activated sludge reactor (Figure 4.4-b) equipped with: (i) a feed tank, containing the photo-treated leachate; (ii) a cylindrical biological reactor (9 L), with diffusers placed at the bottom of the tank to ensure the supply of oxygen (Horizon compressor, Bio-Oxidation Console model) and to promote the stirring of the mixed liquor; (iii) a secondary clarifier (6 L) with sludge recirculation; and (iv) a final effluent storage tank. Two peristaltic pumps (Watson Marlow, model 120S) were used to feed the reactor with photo-treated-leachate and to recycle the sludge back to the reactor, respectively. For both experiments, the dissolved oxygen, pH and temperature were monitored daily (Hanna Instruments HI 9828 meter and HI 769828 probe). For the continuous mode tests, the same parameters were analysed inside the aerated reactor and at the outlet of the settler.



(a)                                (b)
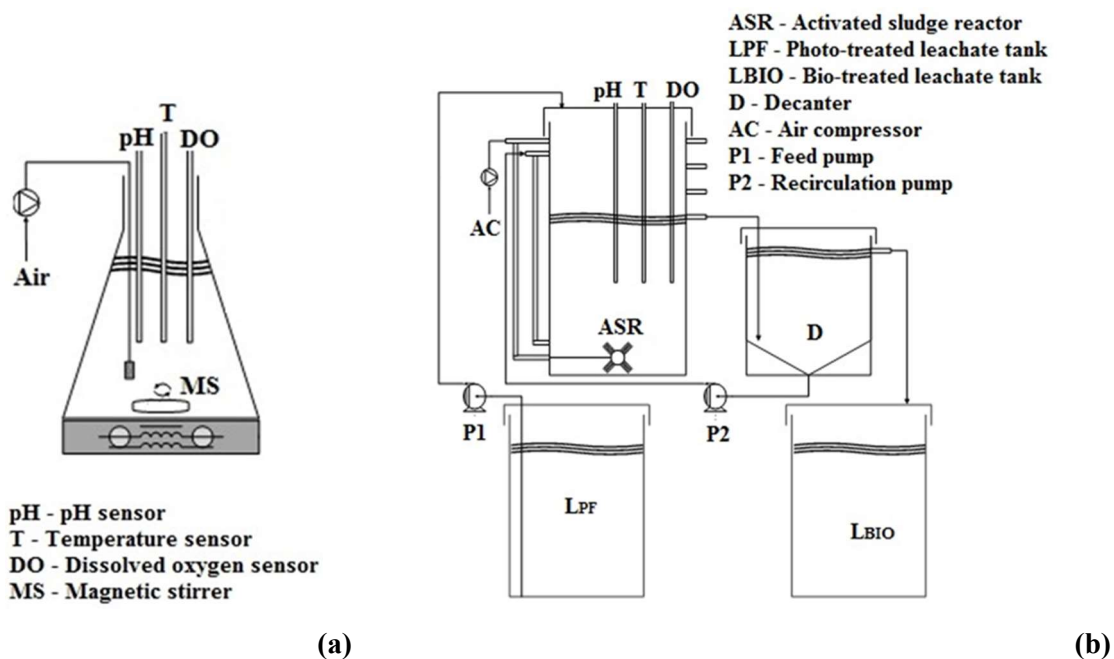
**Figure 4.4** – Schematic representation of the lab-scale biological reactors: (a) batch mode; and (b) continuous mode activated sludge reactor.

*Experimental procedure*

The final biological oxidation tests were performed using an aerobic activated sludge system, operated in batch and continuous mode. For the batch mode tests, 300 mL of biological sludge (collected from a municipal WWTP) was added to 700 mL of photo-treated leachate and the mixture was stirred with air for 24 hours. After 1 h sedimentation, the supernatant was withdrawn and replenished by an equal volume of photo-treated leachate. During the experimental period, the biomass concentration measured as VSS content was 1.5 ± 0.1 g/L. Three experiments were performed (L, M and H), in which the biological reactor was fed with photo-treated leachate presenting different mineralization levels: low (L, DOC = 237 mg/L and COD = 566 mg/L); medium (M, DOC = 189 and COD = 446 mg/L); and high (H, DOC = 118 and COD = 316 mg/L). To obtain the photo-treated leachate for the batch tests, PF reactions were carried out under the best experimental conditions (pH 2.8, 30 °C, 33 $W_{UV}/m^2$ and 60 mg $Fe^{2+}/L$), until reaching different values of accumulated energy (3.3, 5.5 and 8.9 $kJ_{UV}/L$, with corresponding $H_2O_2$ consumption of 8.9, 34.4 and 74.6 mM, for the experiments L, M and H, respectively).

For the continuous mode tests, the reactor was inoculated with 3 L of biological sludge and continuously supplied with the photo-treated leachate. The biological reactor was operated at HRT of 24 and 12 h (flow rates of 0.25 or 0.50 L/h, respectively). The mixed liquor was transferred to the settler by gravity. The sludge was recycled back to the biological reactor, at a flow rate of 1.7 L/h. During the tests, pH and temperature remained in the ranges 7.0-7.2 and 15-20 °C. The TSS and VSS concentrations inside the reactor remained virtually constant, with average values of 2.9 ± 0.1 and 2.3 ± 0.1 g/L, respectively. The leachate used in the continuous mode tests was previously treated, using the best operating conditions established for each treatment step, in a pilot plant whose description for the biological system can be consulted at Vilar, *et al.* [15], while the photocatalytic system will be described in 4.3.3.2 (pilot-plant C).

## 4.3.2 Treatment train system: full-scale

The full-scale experiments were held at a mature urban waste landfill, located in Oporto metropolitan area, North of Portugal. The compact multistage treatment facility (Figure 4.5) consisted in the following treatment units: (i) a first biological reactor (BR1), (ii) a coagulation and photo-treatment unit (C/P); (iii) a second biological reactor (BR2); (iv) a sludge tank (ST); (v) a filter-press system (FP); and (vi) a drainage tank (DT).

**(a)**



BR1 – BIOLOGICAL REACTOR 1
BR2 – BIOLOGICAL REACTOR 2
C/P – COAGULATION/PHOTO-TREATMENT UNIT
RUV1 – FLUHELIK REACTOR 1
RUV2 - FLUHELIK REACTOR 2
RUV3 - FLUHELIK REACTOR 3
RUV4 - FLUHELIK REACTOR 4
F - FLOWMETER
RLM – RADAR LEVEL METER
$H_2O_2$ – HYDROGEN PEROXID METER
DO – DISSOLVED OXYGEN METER
pH – pH METER
AC1 – AIR COMPRESSOR 1 (BR1)
AC2 – AIR COMPRESSOR 2 (BR2)
MS1 – MECHANICAL STIRRER 1 (BR1)
MS2 – MECHANICAL STIRRER 2 (C/P)
MS3 - MECHANICAL STIRRER 2 (BR2)

EV1 – ELECTROVALVE BR1 DISCHARGE
EV2 – ELECTROVALVE BR1 SLUDGE DISCHARGE
EV3 – ELECTROVALVE C/P FEEDING
EV4 – ELECTROVALVE C/P RECIRCULATION (BOTTOM)
EV5 – ELECTROVALVE C/P DISCHARGE
EV6 – ELECTROVALVE C/P SLUDGE DISCHARGE
EV7 – ELECTROVALVE BR2 FEEDING
EV8 – ELECTROVALVE BR2 DISCHARGE (FINAL)
EV9 – ELECTROVALVE BR2 SLUDGE DISCHARGE
EV10 – ELECTROVALVE C/P RECIRCULATION (TOP)
P1 – FEED PUMP
P2 – DISTRIBUTION PUMP (C/P)
P3 – RECIRCULATION PUMP (C/P)
P8 – $H_2O_2$ DOSING PUMP
P9 – $H_2SO_4$ DOSING PUMP
P10 – NaHO DOSING PUMP
P11 – $C_3H_8O_3$ DOSING PUMP
P12 – $FeCl_3$ DOSING PUMP

**(b)**



ST – SLUDGE TANK
DT – DRAINAGE TANK
PT – POLYMER TANK
FP – FILTER PRESS
MS4 – MECHANICAL STIRRER (ST)
MS5 - MECHANICAL STIRRER (PT)
MS6 - MECHANICAL STIRRER (DT)
P4 – SLUDGE PUMP (ST)
P5 – SLUDGE ADMISSION PUMP (FP)
P6 – POLYMER ADMISSION PUMP (FP)
P7 – DRAINAGE PUMP (DT)

**Figure 4.5** – Flow diagram of the full-scale facility for the treatment of leachate: (a) liquid-phase stream and (b) solid-phase stream.

The full-scale facility was also equipped with a Programmable Logic Controller (PLC) to command the opening and closing of electrovalves, start-up and shutdown of air compressors, pumps, stirrers, and lamps (Figure 4.6).
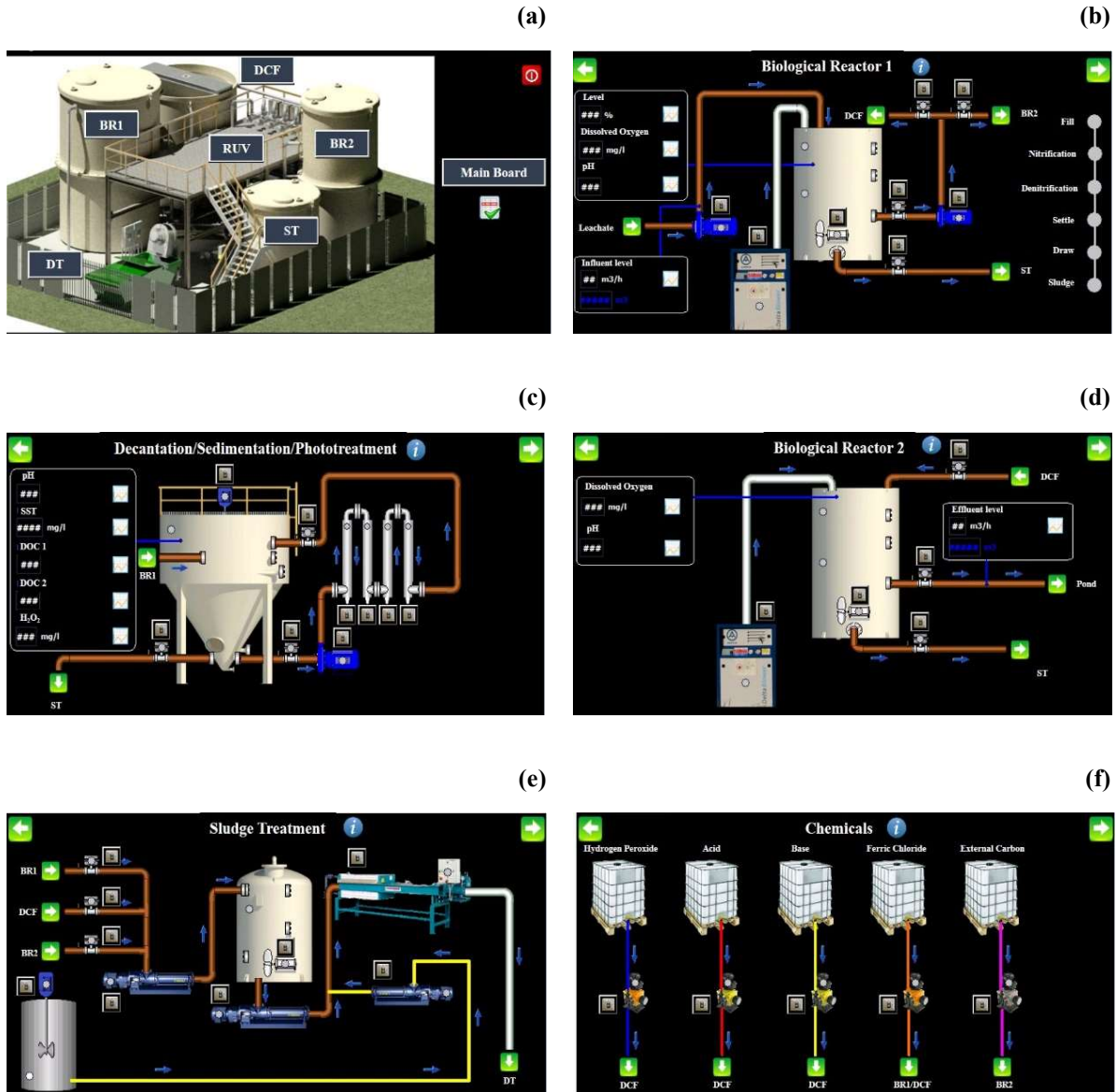


**Figure 4.6** – Programmable logic controller screen: (a) main board, (b) BR1, (c) C/P unit, (d) BR2, (e) sludge treatment and (f) chemicals.

The unit constituents of the full-scale facility are listed in the Table 4.4.

**Table 4.4** – Description of the full-scale unit constituents.

| Element | Acronym | Brand | Model | Characteristics |
|---|---|---|---|---|
| Feed pump | P1 | | | $Q = 50$ m$^3$/h |
| Distribution pump | P2 | Lowara | FHE, FHS, SHE, SHS, SHO series | Single-stage centrifugal $P_{max} = 12$ bar $Q = 50$ m$^3$/h |
| Recirculation pump | P3 | GemmeCotti | HCM PP-PVDF | Thermoplastic centrifugal $Q = 0$ to 65 m$^3$/h |
| Sludge pump | P4 | | RF 40/2 | $Q = 2$ m$^3$/h |
| Sludge admission pump | P5 | Seenex | BN 5-12 | Progressive cavity |
| Polymer admission pump | P6 | | RF 40/1 | |
| Drainage pump | P7 | Pan World | NH-250PS | |
| | P8 | ProMinent | Vario, VAMc | $Q = 64$ L/h |
| | P9 | Milton Roy | GA45D4T3 | $Q = 15$ L/h |
| Dosing pump | P10 | | | $Q = 15$ L/h |
| | P11 | Colberge | MP643-552 | $Q = 15$ L/h |
| | P12 | ProMinent | Vario, VAMc | $Q = 15$ L/h |
| | MS1 | Flygt | SR 4610, SR 4620 | Submersible |
| | MS2 | Milton Roy | Helisem | |
| Mechanical stirrer | MS3 | Flygt | SR 4610, SR 4620 | Submersible |
| | MS4 | | SR 4620 SJ | Submersible |
| | MS5 | SDM | VR4A | |
| | MS6 | Colberge | | |
| Air compressor | AC1 | Aerzen | GM 10S | 0 to 400 m$^3$/h |
| | AC2 | | GM 3S | 0 to 251 m$^3$/h |
| Filter press | FP | Diemme | KE 630N | Side beam |
| Main Electric Board | n.a. | Power Logic | Power Meter 200 and 200P | |
| OD and temperature sensor | n.a. | Lange | LDO Sensor | |
| pH sensor | n.a | | | |
| SST sensor | n.a | | | |
| H$_2$O$_2$ controller and sensor | | GRUNDFOS | Conex DIA-1-A PA/HP | |
| Console | | HACH-LANGE | SC1000 | |
| Flowmeters | F | Krohne | | |
| UV+Vis lamps | RUV1 RUV2 RUV3 RUV4 | Uv-technik | UVH 10019 F-2 | Doping: Iron Rated power = 4.2/4.5 kW L = 1125 mm UV-C, UV-B, UV-A and Vis light Sealing temperature = 350 ºC Useful lifetime: 750 – 1250 h Quartz sleeves: D$_{ext.}$ = 45 mm; Thickness = 2 mm; $\Delta T = 700 – 900$ ºC |

### 4.3.2.1 First biological reactor (BR1)

*Description*

The first biological reactor (BR1) was a cylindrical flat-bottom tank with a total volume of 70 m$^3$, equipped with a mechanical stirrer (MS1) and a hot air compressor (AC1), with variable air debt supply, and fine bubble aeration, which was achieved by means of 56 diffusers placed at the bottom of the reactor (Figure 4.7). The reactor was equipped with a dissolved oxygen concentration control system, a pH sensor, a flowmeter (F) and a radar level meter to prevent overflow from the fill stage. The fill stage of the reactor was accomplished by means of a pump (P1), located next to the aerated lagoon. The draw of BR1 to C/P was performed by means of a distribution pump (P2), with previous opening of electrovalves (EV1 and EV3).
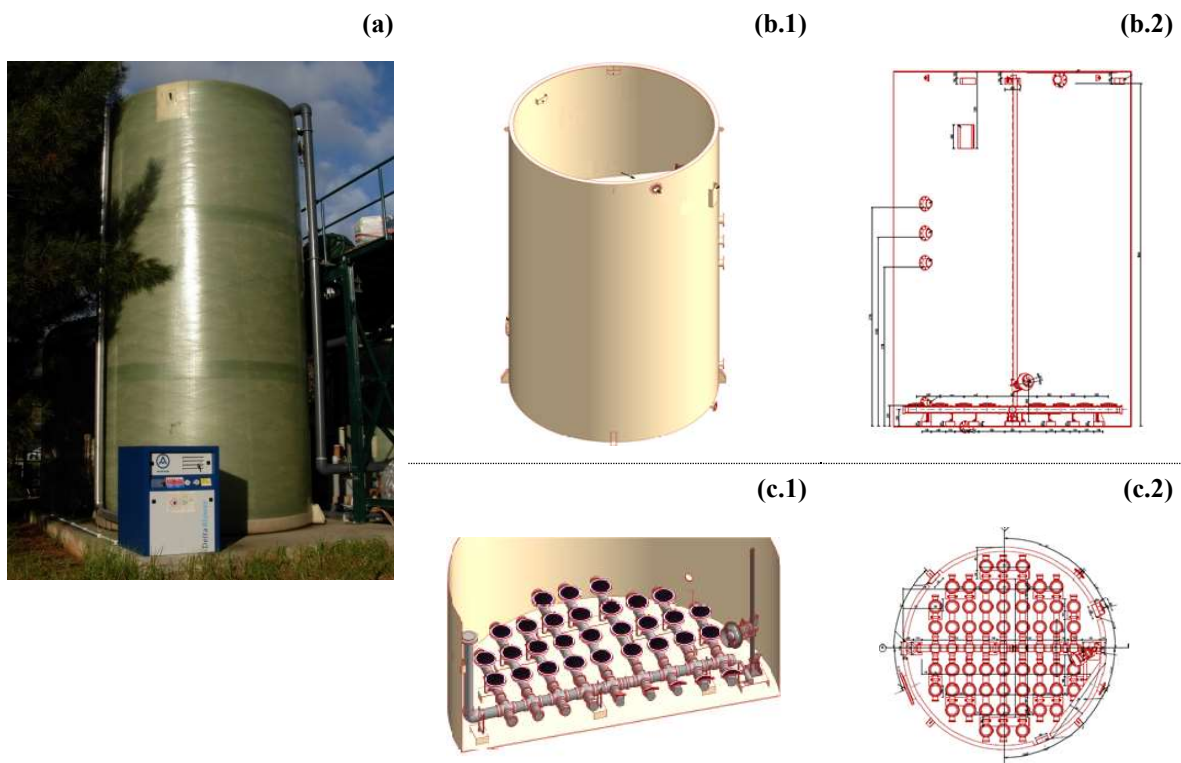


**Figure 4.7** – BR1 (a) photograph, (.1) 3D and (.2) 2D schematic images of (b) biological reactor unit and (c) bottom diffusers.

*Experimental procedure*

BR1 was inoculated with biomass from the biological reactor of the landfill treatment plant (LTP) and fed with leachate from the landfill aerated lagoon. Adaptation and growth of biomass were monitored, and the first leachate treatment trial started 97 days after the inoculation. The reactor was operated according to the traditional SBR phases: (i) fill; (ii) react; (iii) settle; and (iv) draw.

Fill phase was static (no mixing or aeration) and the react phase started with the aerators and/or stirrer, to promote the nitrification or denitrification cycles, respectively. Temperature and pH were monitored but not controlled during the react phase. The external carbon source was added when required for the denitrification process. Settle phase begun by turning off the stirrer and aerators. After 2-4 hours, the bio-treated leachate was withdrawn to C/P unit. At this point, BR1 was ready to restart the fill phase. Samples were collected at (i) fill phase (influent leachate), (ii) beginning and during react phase, and (iii) after sludge settling.

### 4.3.2.2 Coagulation unit

*Description*

Coagulation/sedimentation stage occurred at the C/P unit (Figure 4.8), a conical tank with total volume of 35 m$^3$, equipped with a slow mixture stirrer (MS2) and pH sensor. The addition of ferric chloride (FeCl$_3$) was carried out by means of a dosing pump (P12) and pH adjustment was made by adding sulfuric acid also using a dosing pump (P9). Sludge was removed to the sludge tank (ST) by opening the C/P sludge valve (EV6) and activating the sludge pump (P4).

**(a)**  **(b)**  **(c)**
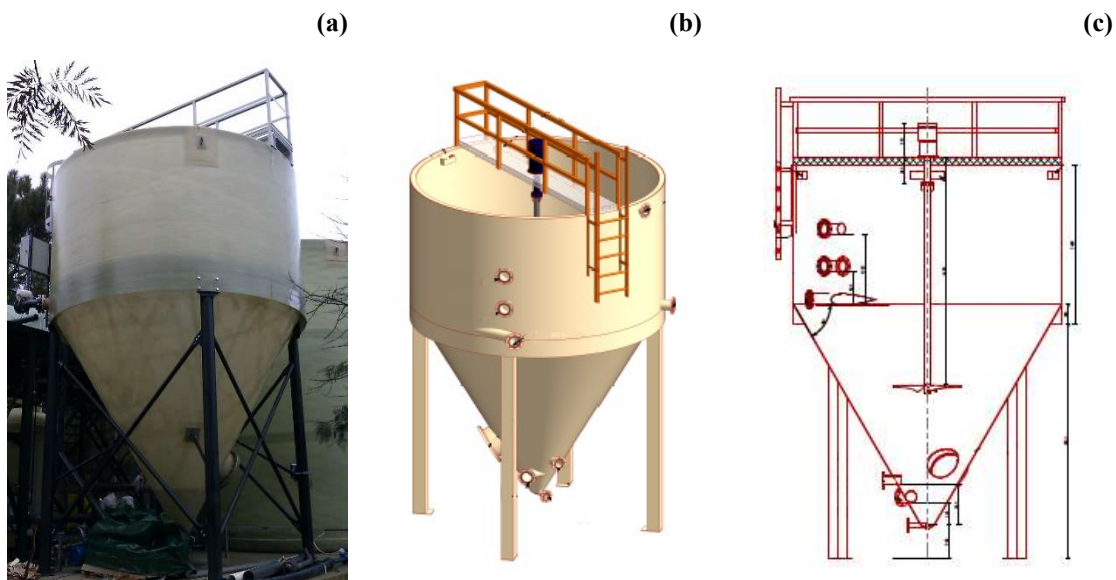


**Figure 4.8** – C/P unit (a) photograph, (b) 3D and (c) 2D schematic images.

*Experimental procedure*

The addition of ferric chloride (FeCl$_3$) was carried out simultaneously and in line with the bio-treated-leachate pumping to the C/P unit. pH adjustment was made by adding sulfuric acid using a

dosing pump. After sedimentation (usually overnight), sludge was pumped to the ST unit and a sample of bio-coagulated-leachate was collected.

### 4.3.2.3 FluHelik photoreactor

*Description*

Photo-Fenton was conducted in 4 FluHelik photoreactors, comprising UV+Vis lamps (RUV1, RUV2, RUV3 and RUV4), connected to the C/P unit by DN100 tubes for the reactor inlet and outlet. The FluHelik reactor is an annular channel reactor consisting of (i) a cylindrical shell of polished stainless steel with inlet and outlet pipes located perpendicularly to the fluid flow and tangentially to the shell in horizontal plane and at the top in opposite sides, and (ii) a concentric inner quartz tube to be filled with an UV-Vis lamp. The tangential inputs promote a helical movement of the fluid around the artificial radiation source (Figure 4.9-a). To recirculate the leachate from C/P tank through the photoreactors it was necessary to open the initial and final recirculation electrovalves (EV4 and EV10) and activate the recirculation pump (P3). Hydrogen peroxide was added by a dosing pump (P8) and monitored by a $H_2O_2$ sensor. At the end of photo-treatment, sodium hydroxide was added also by means of a dosing pump (P10). Sludge removal was performed as described for coagulation sludge. The photo-treated-leachate was transferred to the next treatment unit (BR2) by opening of valves for leachate discharge from C/P (EV5) and BR2 fill (EV7) and activating the distribution pump (P2).

The amount of radiation energy provided by the lamps, $Q_{Lamp}$ (kJ/L) is given by Equation 4.2.

$$Q_{Lamp} = N \times P_{Lamp} \times \frac{t}{V_t} \qquad (4.2)$$

where $N$ is the number of lamps, $P_{Lamp}$ is the useful lamp power (kW), indicated by the supplier and considering a wavelength range from 200 to 600 nm, $t$ is the lamp operating time (expressed in s) and $V_t$ is the total volume of leachate under treatment (L).
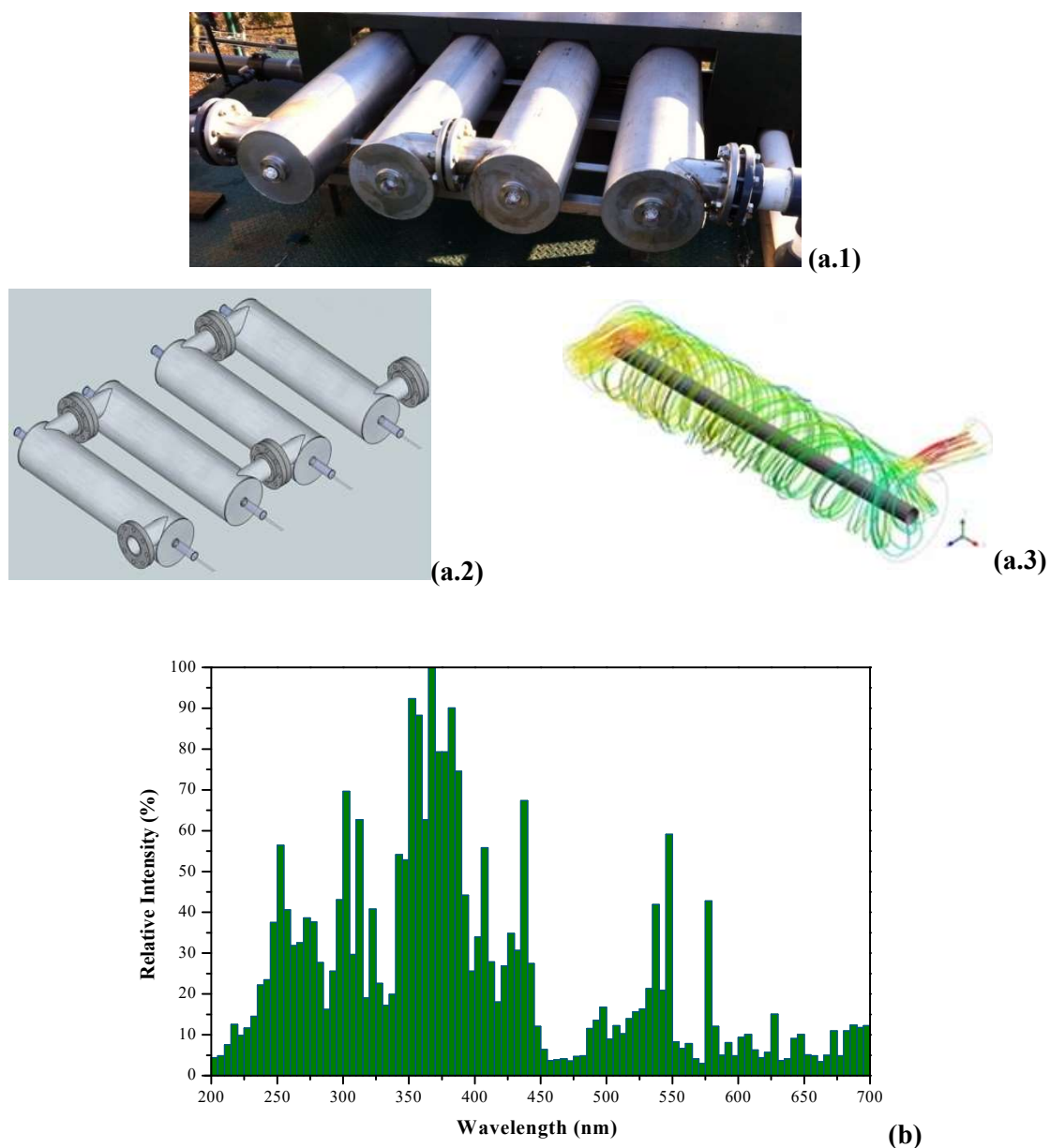
**Figure 4.9** – FluHelik photoreactors (a.1) photograph, (a.2) 3D schematic image and (a.3) CFD simulation image; and (b) UV-Vis lamp spectrum (provided by supplier UV-Technik).

*Experimental procedure*

Photo-treatment was initiated by adding the catalyst (FeCl$_2$), dosed at a concentration of approximately 60 mg Fe$^{2+}$/L. Photo-Fenton was carried out in the FluHelik reactors, using artificial light (4 UV+Vis lamps, UV-Technik, model UVH 10019 F-2 with iron doping, set at 4.2 kW each, lamp spectrum can be seen at Figure 4.9) and H$_2$O$_2$ was added intermittently, i.e., as it was being consumed during the reaction. H$_2$O$_2$ was pumped in line before the leachate entered the

photoreactors. No acid addition was required to adjust pH at 2.8. During the PF process, samples were taken periodically to monitor the catalyst concentration and subsequent organic carbon content determination at the laboratory. At the end, sodium hydroxide was added, by means of a dosing pump, to raise the pH for iron precipitation. After a settling period (2-4 hours or overnight) the iron sludge was removed, and the photo-treated-leachate was pumped to the final biological reactor.

### 4.3.2.4 Final biological reactor (BR2)

*Description*

BR2 was a cylindrical flat-bottom tank with a total volume of 40 m$^3$ equipped with a mechanical stirrer (MS3) and a hot air compressor (AC2), with variable air debt supply. Fine bubble aeration was performed by means of 16 diffusers placed at the bottom of the reactor (Figure 4.10). The reactor was equipped with a dissolved oxygen concentration control system and a pH sensor. A discharge flowmeter (F) measured the multistage system gravity discharge from BR2 to the LTP final pond by opening the discharge valve (EV8).
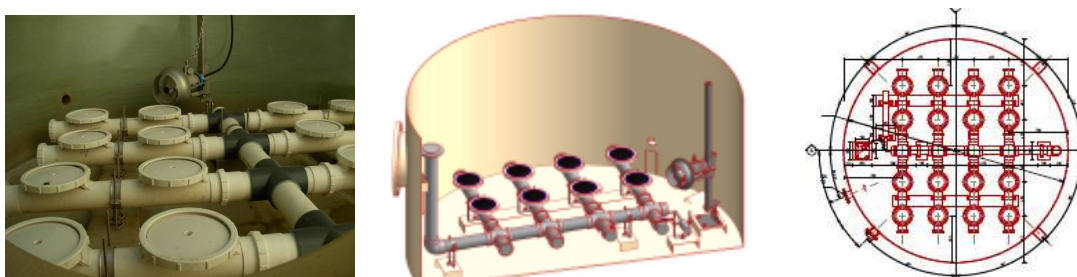


**Figure 4.10** – Photograph, 2D and 3D schematic images of BR2 bottom diffusers.

*Experimental procedure*

For the BR2 start-up, leachate and biomass were pumped from the BR1. BR2 was also operated as an SBR. Fill phase was static, i.e. with no mixing or aeration. The react phase started with the aerators and/or stirrer, to promote the removal of remaining carbonaceous and nitrogenous matter. During the react phase, external carbon addition for denitrification was provided on some occasions. The settling phase (3-6 hours) began by turning off the stirrer and aerators and the final treated leachate was discharged to the LTP final pond. Samples were collected at (i) fill phase (photo-treated-leachate), (ii) beginning and during react phase, and (iii) after sludge settling.

**4.3.2.5 Sludge treatment unit**

*Description*

Sludge tank (ST), polymer tank (PT) and drainage tank (DT) were all equipped with mechanical stirrers (MS4, MS5 and MS6, respectively). Filter-press system (FP) was a side beam compact filter, with 32 plates (630 x 630 mm) and a working pressure ranging 12-30 bar (Figure 4.11). The sludge and polymer were transferred to the FP system by activating the sludge and polymer admission pumps (P5 and P6). The closing and opening of the FP plates pack was automatically done by means of a hydraulic piston.

**(a)**



**(b)**



**Figure 4.11** – Photograph and 3D schematic images of (a) sludge tank and (b) filter-press system.

*Experimental procedure*

The produced sludge was treated in a filter press system with polymer addition. Drainage liquid from sludge treatment was stored and, when suitable, reintroduced back into the liquid phase treatment. Sludge samples from coagulation and PF stages were collected for dry matter analysis. Also, samples of the dewatered sludge were collected for characterization.

### 4.3.3 Solar collectors

To compare different photochemical reactors or their components, such as different reflective surfaces geometries and materials, actinometric tests can be used as a performance indicator. Chemical actinometry is a simple and accurate method to measure radiation, providing measurements of total light dose inside a reactor [16]. Ferrioxalate actinometry, introduced by Hatchard and Parker [17], has been a standard tool of photochemical investigations for more than half a century and is also recommended by IUPAC. The quantum yield of iron (II), $\Phi$ Fe(II), which is partially complexed, has been measured between 254 and 587 nm, and increases with the decreasing wavelength up to $1.24 \pm 0.04$ below 365 nm [17]. So, measuring UV and visible radiation up to 580 nm, makes ferrioxalate an appropriate actinometer to evaluate photoreactors performance aiming to work with the photo-Fenton process.

### 4.3.3.1 Lab-scale photoreactors

*Description*

A tubular lab-scale photoreactor (Schott-Duran, type 3.3, Germany, cut-off at 280 nm, internal diameter 46.4 mm, length 200 mm and thickness 1.8 mm) was used to test different collector optics. The collector's optics tested were composed of distinct reflective surface materials and geometries (Table 4.5).

**Table 4.5** – General characteristics of the reflective surfaces tested.

| Material | Geometry | Reflective Surface | Observation |
|---|---|---|---|
| Anodized Aluminium Reflective 85 | Traditional Double Parabola | R85-DP | New |
| | | R85s-DP | Soiled: 8 years outdoor exposure |
| | Flat | R85-F | New |
| Anodized Aluminium MiroSun | Traditional Double Parabola | MS-DP | With protective coating |
| Mirrored Stainless Steel 304L | Traditional Double Parabola | SS-DP | New |
| | Simple Double Parabola | SS-SP | New |
| | Flat | SS-F | New |

The lab-scale experiments were carried out in the sunlight simulator described in 4.3.1.3. The spectral irradiance of the sunlight simulator xenon lamp and the transmittance of the borosilicate absorber tube are presented in Figure 4.12.
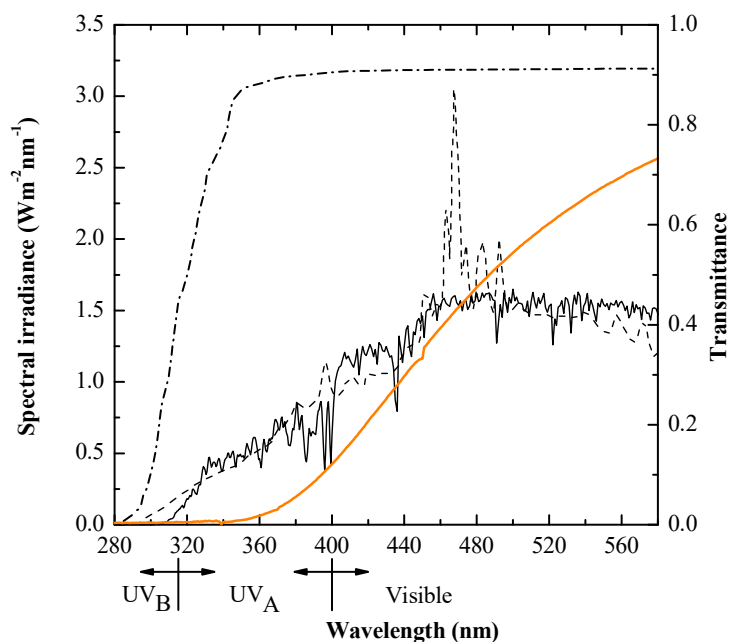


**Figure 4.12** – Spectral irradiance of (- -) xenon lamp (ATLAS technical data), (—) natural sunlight (ASTM G-173-03 AM1.5G reference spectrum [18]); and transmittance for (- ·-) Duran glass transmittance (Duran technical data) and (—) pre-treated leachate (used in photo-Fenton tests), both express from 0 to 1.

*Experimental procedure*

For lab-scale experiments, 1 L of the actinometric solution was prepared for each test. Samples were taken every 30 seconds during the first 5 minutes and then every 60 seconds for the remaining 25 minutes of irradiation. During the tests, the recirculation flow was set at 1.25 L/min.

Photo-Fenton reactions were performed at pH $2.8 \pm 0.1$ and temperature of $25 \pm 1$ºC. Initially, with the leachate recirculating in obscurity, a control sample was taken, and afterwards, iron sulfate (60 mg $Fe^{2+}$ $L^{-1}$) and the $H_2O_2$ first dose (500 mg $L^{-1}$) were added. $H_2O_2$ was gradually added along the treatment to ensure a concentration between 100-500 mg $L^{-1}$. To evaluate the degradation process, samples were collected at pre-defined times along 180 minutes.

### 4.3.3.2 Pilot-scale photoreactors

*Description*

Three different solar pilot-plants (A, B and C) were used to perform the actinometric and photo-Fenton experiments. All of them were installed on the roof of the Chemical Engineering Department, at FEUP, oriented to the south and tilted 41º (local latitude).

The pilot-plant A (Figure 4.13-a), with 0.88 $m^2$ collector area, is composed by four borosilicate glass tubes (Schott-Duran type 3.3, Germany, cut-off at 280 nm, length 1500 mm, internal diameter 46.4 mm and thickness 1.8 mm), two 20 L conical tanks and two magnetic centrifugal pumps for recirculation (Grundfos, model CM5-5 A-R-G-V-AQQV, experimental flow rate set at 1.2 $m^3$/h). All the system is connected by polypropylene tubes. This pilot-plant has two independent fluid lines, each one connected to 2 absorber tubes (0.44 $m^2$), making possible to carry out two different tests simultaneously under the same solar irradiation conditions or use the whole reflecting area. Pilot-plant A also allows the removal and exchange of the reflecting surfaces, namely traditional double-parabola and flat mirrors (Table 4.5).

Pilot-plant B (Figure 4.13-b) comprises a 2.42 $m^2$ solar collector, consisting of 13 stainless steel simple double-parabola reflectors and 13 borosilicate glass tubes (with the same characteristics as those used in pilot-plant A) arranged horizontally and connected by couplings and tees of polypropylene, adductor pipes, so that the fluid circulates in parallel (horizontal flow). A magnetic centrifugal pump (Gemmecotti, model HTM15PP, flow rate set to attain 1.2 $m^3$/h per borosilicate tube) was used to promote the leachate recirculation between the collector and the recirculation tank (140 L capacity). A flowmeter connected to a polypropylene diaphragm valve was used to control the flow rate. Pilot-plant B also has a $H_2O_2$ metering/control system, comprising a dosing pump (Grundfos Alldos), a level deposit (10 L capacity) and a $H_2O_2$ sensor/controller (WP7/Grundfos Alldos, Conex DIA-1). Additionally, it includes an artificial FluHelik photoreactor, making it possible the use of natural and/or artificial light, by adjusting the polypropylene three-way valves.

The pilot-plant C (Figure 4.13-c) consists of a 2.08 $m^2$ solar collector with 10 borosilicate glass tubes (with the same characteristics as those used in pilot-plant A) connected in series (serpentine flow) by polypropylene junctions, with CPC double truncated parabola mirrors in anodized aluminium. Since this pilot-plant can be operated using the total (4.16 $m^2$) or only half of the area, it has two storage conic tanks (50 and 100 L), two magnetic centrifugal pumps for recirculation (TMB, model 65-WR-V-N1, experimental flow rate set at 1.2 $m^3$ $h^{-1}$) and two flowmeters. This

collector has been used in several research studies over the past 8-years, and the degradation of the reflective surface due to outdoor exposure is noticeable.

**a)**



CP - Centrifugal pump
F - Flowmeter
NRV - Non-return valve
pH - pH sensor
TM - Temperature sensor
RT - Recirculation tank
UV-R - UV radiometer

V1, V2 - Recirculation/Discharge valves
V3, V4 - Flow rate control valves
V5 - RT feeding valve
V6 - Solar collector valve
——— - Main path
- - - - Alternative path

**b)**



MP - H₂O₂ measuring pump
RP - Recirculation pump
SC - Solar collector
PR - Photo-reactor
H₂O₂-MC - H₂O₂ measuring and control
L - Lamp

pH - pH sensor
T - Temperature sensor
TC - Temperature control
F - Flowmeter
V₁ - Flow distribution valve
V₂ - Recirculation valve
V₃ - PR admission valve
V₄ - PR outflow valve
V₅ - SC admission valve
V₆ - H₂O₂-MC admission valve
V₇ - Outflow valve

**c)**



CP – Centrifugal pump
CPC – Compound parabolic collector
F – Flowmeter
HR – Heating resistance
NRV – Non-return Valve

pH – pH-sensor
RS – Refrigerator system
RT – Recirculation tank
TM – Temperature sensor
UV-R – UV radiometer

V1 – Outflow/recirculation valve
V2 – Outflow valve
V3, V4 – Temperature control feeding valves
V5, V6 – RS/HR feeding valves
V7, V8 – RS exit valves

V9, V10 – HR exit valves
V11, V12 – Flow control valves
V13, V14 – R bypass valves
V15 – CPC valve
V16 – RT feeding valves

Solar UV irradiance was measured by a global UV-radiometer (CUV4, Kipp&Zonen) mounted on the solar collectors at the same angle, which provided data in terms of incident $W_{UV}$ $m^{-2}$ (spectral response: 280-400 nm). The total amount of accumulated UV energy ($Q_{UV,n}$ kJ/L) per litre of water inside the reactor, in the time interval $t$, was calculated using Equation 4.3 [19].

$$Q_{UV,n} = Q_{UV,n-1} + \Delta t_n \overline{UV}_{G,n} \frac{A_r}{1000 \times V_t}; \quad \Delta t_n = t_n - t_{n-1} \qquad (4.3)$$

where, $t_n$ is the time corresponding to $n$-water sample (s), $V_t$ is the total volume of water in the reactor (L), $A_r$ is the illuminated collector surface area ($m^2$) and $\overline{UV}_{G,n}$ is the average solar ultraviolet radiation ($W/m^2$) measured during the period $\varDelta t_n$ (s).

*Experimental procedure*

For the pilot-plants, under natural sunlight, actinometric tests were performed under three solar radiation intensities (low, medium and high). For each test, the pilot-plants were previously covered with a black cloth, and then filled with 15 L (pilot-plant A) or 80 L (pilot-plants B/C) of actinometric solution. Initially, the solution was recirculated for 15 minutes in the dark, then the black cloth was removed to begin the irradiation of the actinometer solution. Samples were taken every 30/60 seconds for 30 minutes and stored in the dark until analysis.

Photo-Fenton reactions were performed using similar procedure as described for the lab-scale experiments, except for temperature control.

### 4.3.3.3 Calculations

The different reflective surfaces were characterized in terms of the Geometric Concentration Ratio ($CR_G$) and the Optical Concentration Ratio ($CR_O$):

$$CR_G = \frac{A_a}{A_r} \qquad (4.4)$$

$$CR_O = \frac{\frac{1}{A_r} \int RP_i dA_r}{I_0} \qquad (4.5)$$

To determine $CR_G$ it is required to know the aperture area ($A_a$), defined as the plane area through which the incident solar radiation is accepted, and the receiver area ($A_r = \pi \times ED \times L$, where $ED$ (m) and $L$ (m) are the absorber tube external diameter and length) [20, 21]. To calculate $CR_O$ it is necessary to know the radiant power incident on the photoreactor tube ($RP_i$) and the insolation incident on the collector aperture ($I_O$) [20]. Therefore, the optical efficiency depends on the radiant power absorbed by the reaction system and, consequently, on the incident radiant power arriving on the absorber [22]. By means of the ferrioxalate actinometry it is possible to determine $RP_i$, using Equation 4.6 [22, 23]:

$$\frac{dn_{Ac}}{dt} = RP_i \sum_\lambda \left[ \frac{S_{e,\lambda} T_{D,\lambda} \phi_\lambda}{E_{ph,\lambda}} \left( 1 - 10^{-A_\lambda} \right) \right] \tag{4.6}$$

For the determination of $RP_i$ (W), besides the (i) rate of $Fe^{2+}$ production under polychromatic irradiation ($dn_{Ac}/dt$), obtained experimentally (i.e. number of actinometer ions formed during the irradiation time ($s^{-1}$)), it is required to know the (ii) relative spectral distribution of the incident radiation ($S_{e,\lambda}$) (Figure 4.12), (iii) Duran glass transmission spectrum ($T_{D,\lambda}$) (Figure 4.12), (iv) average absorption spectra of the actinometric solution ($A_\lambda = \varepsilon_\lambda \times C_{Ac} \times l$, where $\varepsilon_\lambda$, $C_{Ac}$ and $l$ are the actinometer molar absorptivity at wavelength $\lambda$ (L mol$^{-1}$ cm$^{-1}$), actinometer molar concentration (mol L$^{-1}$) and optical pathlength (cm), respectively), (v) $Fe^{2+}$ formation quantum yield at wavelength $\lambda$ ($\Phi_\lambda$) and (vi) photon energy at wavelength $\lambda$ ($E_{ph,\lambda} = h \times c / \lambda$, where $h$, $c$ and $\lambda$ are the Planck's constant ($6.63 \times 10^{-34}$ J s), light velocity ($3.00 \times 10^8$ m s$^{-1}$) and wavelength (m), respectively).

To compare the photo-Fenton efficiencies a pseudo-first-order kinetic model was fitted to the experimental data according to Equation 4.7:

$$DOC_t = DOC_0 \times e^{-k_{DOC} \times t} \tag{4.7}$$

where $DOC_t$ and $DOC_0$ are, respectively, the values of DOC concentration (mg C/L) after $t$ time (min) or accumulated radiation energy ($Q$, kJ/L) and at time or accumulated radiation energy of 0.

The accumulated energy per unit of water volume ($V_t$, L), in a time interval ($t_n - t_{n-1}$), was calculated through the radiant power ($RP$) that reaches the reaction medium, as follows:

$$Q_n = Q_{n-1} + \frac{RP \times (t_n - t_{n-1})}{V_t} \tag{4.8}$$

The $RP$ is determined in the same way than the $RP_i$, despising only the term relating to the Duran glass transmission from Equation 4.6.

For discussion purposes, time and energy required to achieve 60% of mineralization were calculated once, according to previous studies [13], it represents the approximate DOC removal that is favourable to the application of a final biological treatment stage to the leachate.

To allow a better comparison between the PF treatments performed under natural sunlight, at pilot-scale, a "constant irradiation theoretical time", $t_{44W}$, was also determined, according to Equation 4.9:

$$t_{44W,n} = t_{44W,n-1} + \frac{V_t}{RP_{44W}} \times \left(Q_n - Q_{n-1}\right) \tag{4.9}$$

Additionally, the pseudo-first-order rate constants ($k$) obtained under natural sunlight were corrected for a temperature of 25ºC, using the Arrhenius equation. For the experimental determination of the activation energy ($E_a$) required for the pseudo-first-order rate constant correction, five photo-Fenton trials were performed with the leachate in the Suntest® chamber, under the same experimental conditions except for the temperature. The tested temperatures (Kelvin) were as followed: 288, 293, 298, 313 and 323 - and the respective calculated $k$ values (min$^{-1}$): $5.3 \times 10^{-2}$, $6.6 \times 10^{-2}$, $7.6 \times 10^{-2}$, $1.5 \times 10^{-1}$ and $2.1 \times 10^{-1}$. Therefore, an Arrhenius plot was obtained by a linear fit of the logarithm of Arrhenius' equation:

$$k = Ae^{-E_a/RT} \tag{4.10}$$

where, $k$ is the pseudo-first-order rate constant, $T$ is the absolute temperature (in Kelvin), $A$ is the pre-exponential factor, $E_a$ is the activation energy for the reaction (J mol$^{-1}$), and $R$ is the universal gas constant (8.3145 J mol$^{-1}$ K$^{-1}$). Taking the natural logarithm of Arrhenius' equation yields:

$$\ln k = \ln A - \frac{E_a}{R} \times \frac{1}{T} \tag{4.11}$$

The slope of the Arrhenius plot (Figure 4.14), equal to the negative activation energy divided by the gas constant ($-E_a/R$) can be used to find the activation energy:

$$E_a = -(3.7 \pm 0.3) \times 10^3 \times 8.3145 = (3.1 \pm 0.2) \times 10^4 \text{ J mol}^{-1}$$

The Arrhenius plot can also be used to obtain the pre-exponential factor, $A$, by extrapolating the line back to the y-intercept. However, constant $A$ is eliminated when using two known temperatures and integrating the equation, as follows:

$$\ln k_1 = \ln A - \frac{E_a}{RT_1} \; ; \; \ln k_2 = \ln A - \frac{E_a}{RT_2} \tag{4.12}$$
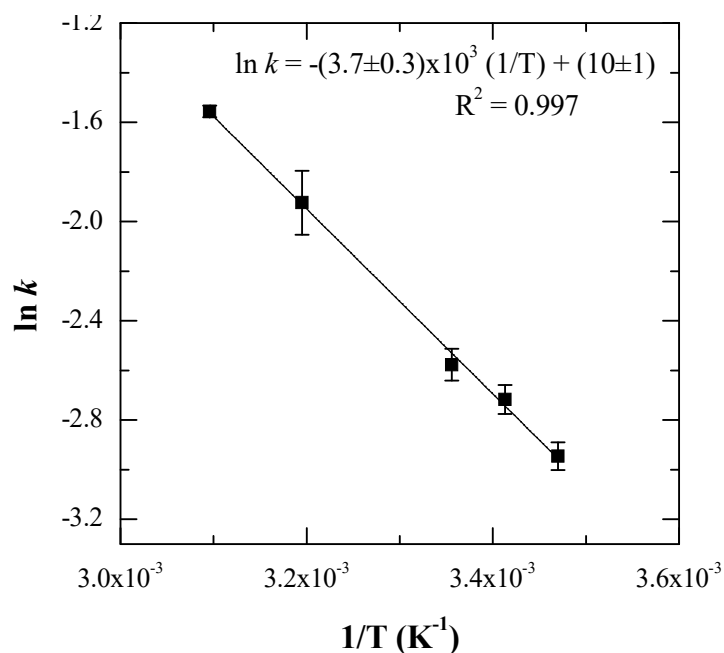
**Figure 4.14** – Arrhenius plot: linear relation between the logarithm of the rate constant, *k*, and the inverse of temperature, 1/*T*.

By rewriting the second equation:

$$\ln A = \ln k_2 + \frac{E_a}{RT_2} \tag{4.13}$$

and substituting for *ln A* into the first equation:

$$\ln k_1 = \ln k_2 + \frac{E_a}{RT_2} - \frac{E_a}{RT_1} \tag{4.14}$$

which means

$$\ln k_1 - \ln k_2 = - \frac{E_a}{RT_1} + \frac{E_a}{RT_2} \tag{4.15}$$

or

$$\ln \frac{k_1}{k_2} = - \frac{E_a}{R} \left( \frac{1}{T_1} - \frac{1}{T_2} \right) \tag{4.16}$$

where, $k_1$ is the pseudo-first order rate constant (min$^{-1}$) obtained experimentally at $T_1$ (in Kelvin), and $k_2$ is the pseudo-first order rate constant to be determined at a defined $T_2$ (in this case 298 K, i.e. 25ºC).

## 4.3.4 Ozonation systems

For all ozonation setups tested, ozone was generated from pure and dry oxygen using an ozone generator (BMT 802N), capable of producing up to 4 g $O_3$/h. The oxygen flow rate was controlled with the aid of a digital mass flow meter (Alicat Scientific). Both inlet and outlet gaseous ozone concentrations were monitored by means of a UV-based ozone analyser (BMT 964), after passing through a sample gas dehumidifier (BMT DH3b). The residual gas was vented through a catalytic ozone destruction unit (Heated Catalyst BMT) and bubbled into Woulff bottles containing 2% KI solution.

### 4.3.4.1 Bubble column reactor

*Description*

One of the lab-scale setups was a bubble column reactor (BMT bubble column 4.1, with internal diameter of 73 mm and maximum fluid column height of 370 mm), with magnetic stirring and no recirculation of the leachate (Figure 4.15). A constant flow of an ozone/oxygen-gas mixture was applied through a ceramic porous diffuser, placed at the bottom of the bubble column (BC).
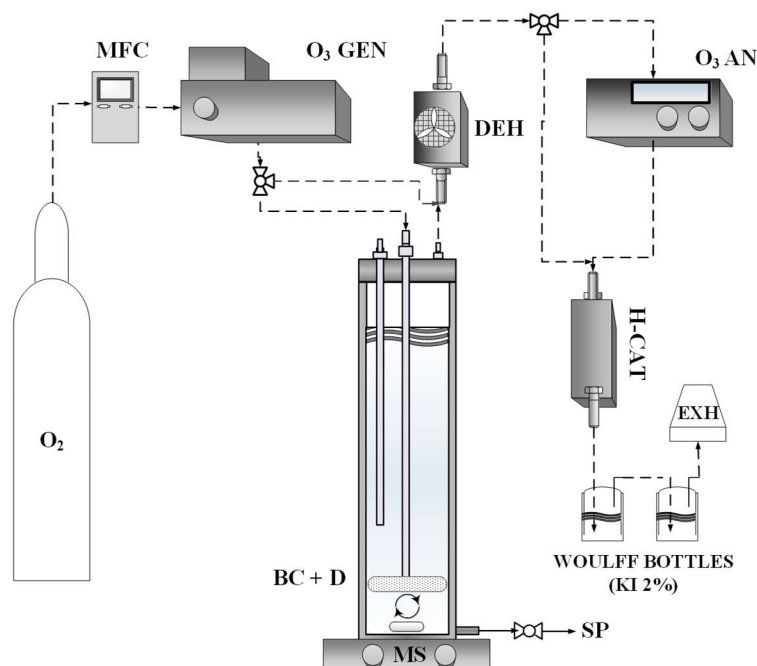


**Figure 4.15** – Schematics for the ozonation system using the bubble column reactor with a porous diffuser (MFC – mass flow controller; $O_3$ GEN – ozone generator; BC – bubble column; D – diffuser; MS – magnetic stirrer; SP – sampling point; DEH – dehumidifier; $O_3$ AN – ozone analyser; H-CAT - catalytic ozone destruction unit; EXH – exhaustion).

*Experimental procedure*

The BC reactor was filled with 1.0 L of a bio-coagulated leachate (fluid column height of 240 mm) and a total treatment time of 3h was adopted. Effluent samples were taken periodically ($t$ = 0, 20, 40, 60, 90, 120, 150 and 180 min) at the bottom of the BC. Leachate pH was adjusted using a diluted NaOH solution. For the experiments at different initial pH values (3.7, 7.0 and 9.0), the inlet ozone concentration and ozone gas flow were set at 90 mg $O_3$/L and 0.10 NL/min (9 mg $O_3$/min), respectively. Afterwards, using the best initial pH, different inlet ozone doses (9, 18 and 27 mg $O_3$/min) were tested by: (i) doubling the inlet ozone concentration (from 90 to 180 mg $O_3$/L), while maintaining the gas flow (0.10 NL/min); and (ii) maintaining the inlet ozone concentration (180 mg $O_3$/L) but increasing the gas flow rate (from 0.10 to 0.15 NL/min).

### 4.3.4.2 FluHelik coupled with bubble column

*Description*

Another ozonation lab-scale setup was tested by coupling a FluHelik photoreactor in series with a bubble column reactor, with leachate recirculation (ISMATEC BVP-Z pump, flow rate ($Q_l$) of 75 L/h) between the reactors. Under this configuration, two gas-liquid injection devices were tested: (i) a porous diffuser, placed at the bottom of the bubble column (FluHelik/BC-Diffuser system, Figure 4.16-a); and (ii) a Venturi injector, placed at the inlet of the FluHelik (FluHelik/BC-Venturi system, Figure 4.16-b). For the ozone-based AOPs experiments using radiation, a UVC lamp (Philips TUV 11W or 6W, G6 T5, respectively, for bio-treated or bio-coagulated leachates) was placed inside the FluHelik.

*Experimental procedure*

Under this configuration, a leachate volume of 1.5 L was used to maintain a water column height in the BC reactor of 240 mm. The ozone gas flow and inlet concentration were set at 0.10 NL/min and 180 mg $O_3$/L, respectively. For tests combining ozone with: (i) hydrogen peroxide, a predetermined amount of $H_2O_2$ was injected in a single-step into the column at time zero; and/or (ii) UVC radiation, a UVC lamp was placed inside the FluHelik photoreactor.

For the experiments using a bio-coagulated leachate, a treatment time of 3 h was adopted, with periodic sample collection ($t$ = 0, 15, 30, 45, 60, 75, 90, 120, 150 and 180 min) for analytical characterization. For the experiments carried out with a bio-treated leachate (without coagulation

stage), the treatment time was extended to 10 h and 12 h, for tests using $O_3$/UVC and only $O_3$, respectively.
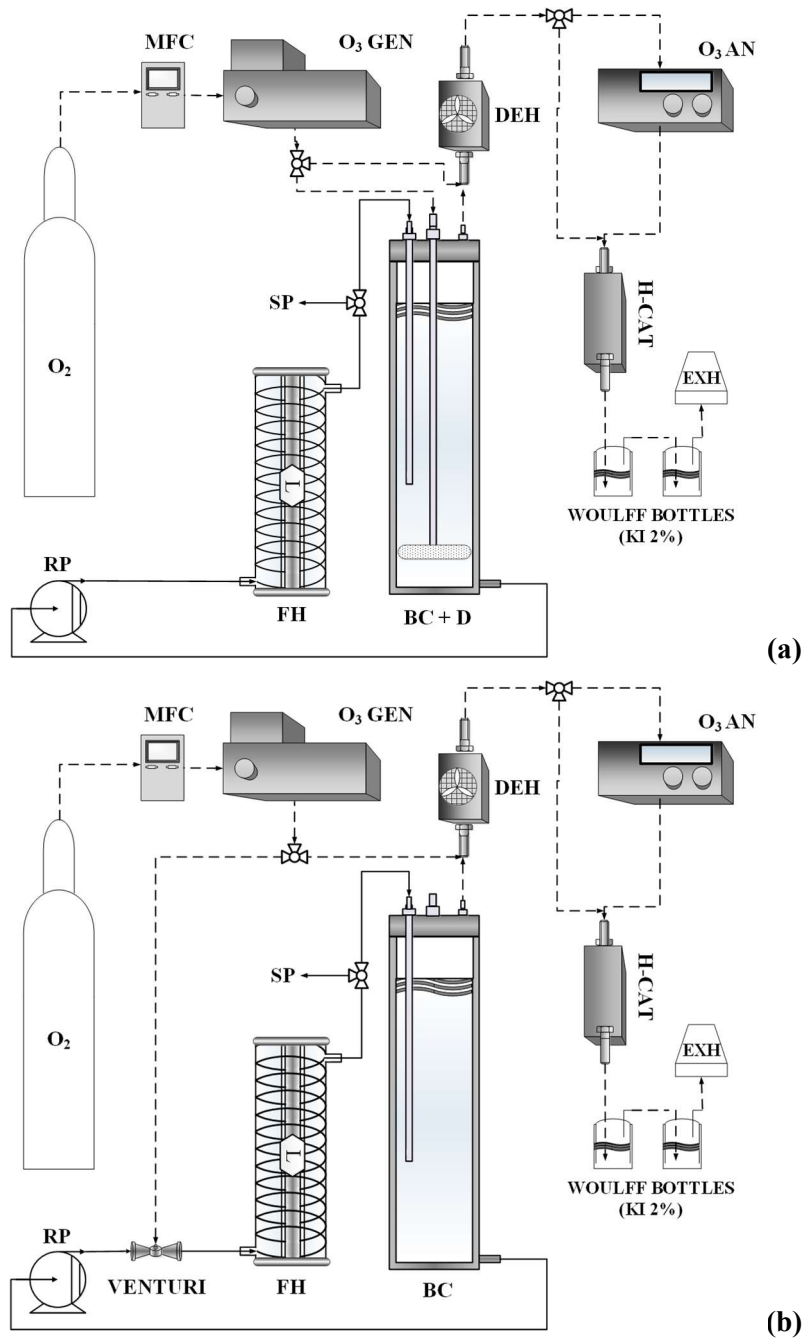


**Figure 4.16** – Schematics for the ozonation systems using the FluHelik photoreactor coupled in series with the bubble column reactor with a (a) porous diffuser and (b) Venturi injector (MFC – mass flow controller; $O_3$ GEN – ozone generator; RP – recirculation pump; FH – FluHelik photoreactor; BC – bubble column; D – diffuser; MS – magnetic stirrer; SP – sampling point; DEH – dehumidifier; $O_3$ AN – ozone analyser; H-CAT - catalytic ozone destruction unit; EXH – exhaustion).

### 4.3.4.3 Calculations

To assess and compare the efficiency of the different ozone-driven processes, DOC and COD removals were evaluated as a function of: (i) treatment time, by fitting a pseudo-first order kinetic model to the experimental data (as described in 4.3.3.3); and (ii) ozone consumption, considering the transferred ozone dose. The transferred ozone dose ($OD_T$) was estimated through mass balance calculations of ozone in the gas phase following Equation 4.17:

$$OD_T = \frac{Q_g}{V_L} \int_0^t \left( C_{O_3,\text{I-g}} - C_{O_3,\text{O-g}} \right) dt \tag{4.17}$$

with $OD_T$ (mg $O_3$/L effluent), calculated by integrating the difference between the constant inlet ozone concentration ($C_{O_3,\text{I-g}}$) and the outlet/off-gas concentration ($C_{O_3,\text{O-g}}$) during the applied time interval. $Q_g$ (L/min) is the applied gas flow rate and $V_L$ (L) is the volume of leachate in the reactor.

Additionally, considering the kinetic constants ($k$, min$^{-1}$), for DOC and COD removal, calculated for the $O_3$-based AOPs tests, the synergy effect was calculated as follows:

$$\left( k_{O_3\text{-based AOP}} / \left( k_{O_3\text{-only}} + k_{H_2O_2 \text{ or } H_2O_2/\text{UVC}} \right) - 1 \right) \times 100 \tag{4.18}$$

## 4.4 References

1.  OECD Guideline for Testing of Chemicals, Test No. 302B: Inherent Biodegrdability: Zahn-Wellens/EMPA test. 1992, Organisation for Economic Co-operation and Development (OECD).

2.  Clesceri, L.S., Greenberg, A.E., Eaton, A.D., *Standard Methods for Examination of Water & Wastewater*. 2005, American Public Health Association (APHA), American Water Works Association (AWWA) & Water Environment Federation (WEF).

3.  (IPQ), I.P.d.Q., Water: Determination of true colour, in NP 627:1972. 1972.

4.  Chen, W., P. Westerhoff, J.A. Leenheer, and K. Booksh, *Fluorescence Excitation-Emission matrix regional integration to quantify spectra for dissolved organic matter.* Environmental Science & Technology, 2003. **37**: p. 5701-5710.

5.  Nogueira, R.F.P., M.C. Oliveira, and W.C. Paterlini, Simple and fast spectrophotometric determination of H2O2 in photo-Fenton reactions using metavanadate. Talanta, 2005. **66**: p. 86-91.

6.  ISO 6332:1998 - Water quality - Determination of iron - Spectrometric method using 1,10-phenanthroline. 1998, International Organization for Standardization (ISO).

7.  Amor, C., E. Torres-Socías, J.A. Peres, M.I. Maldonado, I. Oller, S. Malato, and M.S. Lucas, *Mature landfill leachate treatment by coagulation/flocculation combined with Fenton and solar photo-Fenton processes.* Journal of Hazardous Materials, 2015. **286**: p. 261-268.

8.  Daud, Z., A.A.A. Latif, and L.M. Rui, *Coagulation-flocculation in leachate treatment by using ferric chloride and alum as coagulant.* International Journal of Engineering Research and Applications, 2012. **2**(4): p. 1929-1934.

9.  Rui, L.M., Z. Daud, and A.A.A. Latij, *Treatment of leachate by coagulation-flocculation using different coagulants and polymer: A review.* International Journal on Advanced Science Engineering and Information Technology, 2012. **2**(2).

10. Silva, T.F.C.V., P.A. Soares, D.R. Manenti, A. Fonseca, I. Saraiva, R.A.R. Boaventura, and V.J.P. Vilar, *An innovative multistage treatment system for sanitary landfill leachate depuration: Studies at pilot-scale.* Science of the Total Environment, 2017. **576**: p. 99-117.

11. Ntampou, X., A.I. Zouboulis, and P. Samaras, Appropriate combination of physicochemical methods (coagulation/flocculation and ozonation) for the efficient treatment of landfill leachates. Chemosphere, 2006. **62**: p. 722-730.

12. Vedrenne, M., R. Vasquez-Medrano, D. Prato-Garcia, B.A. Frontana-Uribe, and J.G. Ibanez, Characterization and detoxification of a mature landfill leachate using combined coagulation-flocculation/photo-Fenton treatment. Journal of Hazardous Materials, 2012. **205-206**: p. 208-215.

13. Moreira, F.C., J. Soler, A. Fonseca, I. Saraiva, R.A.R. Boaventura, E. Brillas, and V.J.P. Vilar, *Incorporation of electrochemical advanced oxidation processes in a multistage treatment system for sanitary landfill leachate.* Water Research, 2015. **81**: p. 375-387.

14. Pignatello, J.J., E. Oliveros, and A. Mackay, *Advanced oxidation processes for organic contaminant destruction based on the Fenton reaction and related chemistry.* Critical Reviews in Environmental Science and Technology, 2006. **36**: p. 1-84.

15. Vilar, V.J.P., E.M.R. Rocha, F.S. Mota, A. Fonseca, I. Saraiva, and R.A.R. Boaventura, Treatment of a sanitary landfill leachate using combined solar photo-Fenton and biological immobilized biomass reactor at pilot scale. Water Research, 2011. **45**: p. 2647-2658.

16. Goldstein, S., D.A.Y. Diamant, and Y. Rabani, *Photolosys of aqueous $H_2O_2$: Quantum yield and applications for polychromatic UV actinometry in photoreactors.* Environmental Science and Technology, 2007. **41**: p. 7486-7490.

17. Hatchard, C.G. and C.A. Parker, *A new sensitive chemical actinometer. II. Potassium ferrioxalate as a standard chemical actinometer.* Proceedings of the Royal Society of London A, 1956. **235**: p. 518-536.

18. ASTM, Standard tables for reference solar spectral irradiances: direct normal and hemispherical on 37º tilted surface. 2003.

19. Malato, S., J. Blanco, A. Vidal, and C. Richter, *Photocatalysis with solar energy at a pilot-plant scale: an overview.* Applied Catalysis B, 2002. **37**: p. 1-15.

20. Ochieng, R.M. and F.N. Onyango, Some techniques in configurational geometry as applied to solar collectors and concentrators, in Solar Collectors and Panels, Theory and Application, R.M. Ochieng, Editor. 2010, InTech: Rijeka, Croatia.

21. Malato, S., Solar photocalatytic decomposition of pentachlorophenol dissolved in water, in Chemical Engineering Department. 1999, Universidad de Almeria: Almeria, Spain.

22. Rios-Enriquez, M., N. Shahin, C. Durán-de-Bazúa, J. Lang, E. Oliveros, S.H. Bossmann, and A.M. Braun, Optimization of the heterogeneous Fenton-oxidation of the model pollutant 2,4-xylidine using the optimal experimental design methodology. Solar Energy, 2004. **77**: p. 491-501.

23. Bossmann, S.H., E. Oliveros, S. Göb, S. Siegwart, E.P. Dahlen, L. Payawan, M. Straub, M. Wörner, and A.M. Braun, *New evidence against hydroxyl radicals as reactive intermediates in the thermal and photochemical enhanced fenton reactions.* Journal of Physical Chemistry A, 1998. **102**: p. 5542-5550.

# 5 Treatment train for mature landfill leachates: Optimization studies at laboratory scale

*In view of simultaneous legal compliance with the discharge limits for organic and nitrogen parameters, the treatment train strategy for urban mature leachates outlined in previous research work was optimized at lab-scale. The leachate under test, collected at the aerated lagoon of the landfill treatment plant, presented a high organic and total nitrogen (TN) content (DOC = 1.1 g C/L; COD = 3.6 g $O_2$/L; TN = 2.0 g N/L) and low biodegradability ($BOD_5$/COD = 0.05). The treatment train comprised a: (i) sequential batch reactor (SBR), operated in a 24h-cycle mode with nitrification/denitrification cycles (using methanol as external carbon source); (ii) coagulation using ferric salts in acidic conditions; (iii) photo-Fenton oxidation reaction ($Fe^{2+}$/$H_2O_2$/UV-Vis); and (iv) final biological oxidation.*

*In the first stage, the SBR was tested for total nitrogen removal and assessment of the maximum daily TN load that could be treated, reaching the legal limit (< 15 mg N/L), which increased by 50% with the rise in temperature from 20 to 30 °C. For the coagulation stage, the highest dissolved organic carbon (DOC) removal (64%) and lower final turbidity (33 NTU) were obtained using 240 mg $Fe^{3+}$/L, at pH 3.0. The jar-tests, comparing nitrified ($L_{NIT}$) and nitrified/denitrified ($L_{N/D}$) leachate, stressed the effect of the leachate alkalinity, generated during the denitrification reaction, on process efficiency. For the coagulated $L_{N/D}$, with alkalinity of 1.1 g $CaCO_3$/L, the final concentration of sulfate was only slightly below the legal limit (< 2 g/L). The photo-Fenton (PF) oxidation process (pH range of 2.8-3.0, 60 mg $Fe^{2+}$/L), as third treatment step, promoted a significant enhancement on leachate biodegradability, consuming 75 mM of $H_2O_2$ and 8.9 kJ/L of accumulated UV energy, to achieve an effluent that can be further biologically treated in compliance with the COD discharge limit (150 mg $O_2$/L) into environment. Biological continuous mode tests by the conventional activated sludge process, with a hydraulic retention time (HRT) of 12h, allowed to obtain COD and TSS values (107 ± 3 and 50 ± 2 mg/L, respectively) below the legal limit.*

This Chapter is based on the following research article: "Gomes, A.I., Santos, S.G.S., Silva, T.F.C.V., Boaventura, R.A.R., Vilar, V.J.P. *Treatment train for mature landfill leachates: Optimization studies.* Science of the Total Environment 673 (2019) 470-479

## 5.1 Introduction

Currently, solid waste disposal in sanitary landfills is the most common method used worldwide for waste management [1, 2]. The produced landfill leachate is usually characterized as a complex mixture of recalcitrant organic and inorganic compounds depending on several factors, such as the landfill age, type of disposed waste and climatic conditions [3, 4]. The leachate varies in terms of composition and quantity, throughout the year and among landfills. So, it is difficult to define an unique treatment strategy to be efficient in any given situation [1]. Additionally, to minimize the potential environmental impacts, legal authorities throughout the world have imposed maximum contaminants' levels in treated leachate prior to disposal (Table 2.5 of Chapter 2).

To meet the increasingly strict quality standards for the direct discharge of leachate into waterbodies, the combination of traditional and/or innovative physicochemical methods with biological processes is indispensable [5, 6]. In this sense, advanced oxidation processes emerge due to their ability to mineralize refractory organic matter, decrease toxicity and increase biodegradability, making them suitable to combine with a downstream biological process [7-9]. Hence, over the last years, different treatment combinations have been tested and proposed by several researchers, namely Cassano, *et al.* [10], Moreira, *et al.* [11], Silva, *et al.* [12], Oloibiri, *et al.* [13], Baiju, *et al.* [14], among others (further details in Table 3.9 of Chapter 3). Silva et al. [2, 8, 12] tested different treatment approaches at pilot- and pre-industrial scale (as described in section 3.3.2 of Chapter 3), whose efforts culminated in a multistage treatment system for leachates from mature municipal landfills (European Patent – EP 2784031A1). The proposed methodology combined biological and physicochemical processes, including a photocatalytic advanced oxidation step (photo-Fenton), in order to achieve a final effluent in compliance with the legal discharge requirements. This strategy was partially tested at pilot-scale and proved to be effective for total ammonia nitrogen (TAN) and COD removal up to legal values for direct discharge into waterbodies (according to Portuguese legislation, see Table 2.6 of Chapter 2). However, the removal of the high total nitrogen (TN) content of the leachate was not accomplished, and the final biological reactor performance was indirectly assessed by means of the Zahn-Wellens biodegradability test results.

In this context, aiming at a treatment train strategy capable of reducing both COD and TN contents up to the legal levels, the present work adapted the proposed multistage strategy [12], and tested the operational conditions required to ensure the simultaneous fulfilment of the legal limits for organic and nitrogen parameters. Besides the COD, TAN and TN, the legal compliance of other parameters, namely total suspended solids (TSS), iron and sulfate, was also assessed (again according to the Portuguese legislation, Table 2.6 of Chapter 2). For the first treatment stage, an SBR was tested for

the TN removal by nitrification/denitrification reactions, using 24h-cycles. Then, coagulation followed by photo-Fenton (PF) oxidation and a final biological oxidation (HRT of 12 and 24 hours) were applied for the COD removal. Using the knowledge acquired in prior research [12, 15, 16], this work also assessed: (i) the maximum nitrogen load that could be biologically removed within 24 hours; (ii) the influence of the biological pre-treatment (nitrification or nitrification/denitrification) in the coagulation; (iii) the effect of the operational parameters (catalyst concentration, temperature and irradiance) in the PF reaction; and (iv) the efficiency of the final biological oxidation, in batch and continuous mode.

## 5.2 Materials and methods

The mature urban leachate used in this work was collected after the aerated lagoon at an LTP, from an MSW landfill located in northern Portugal and stored at 4°C. The main physicochemical characteristics of the leachate, at each treatment stage, are presented in Table 5.1.

**Table 5.1** – Physicochemical characterization of the landfill leachate at each treatment step.

| Parameters | RL[c] | L$_{NIT}$[c] | L$_{N/D}$[c] | CL[c] | PL[c] | TL[c] | ELV[c] |
|---|---|---|---|---|---|---|---|
| **pH** | 8.1 | 7.0 | 8.2 | 3.0 | 7.2 | 7.1 | 6 - 9 |
| **BOD$_5$[a] (mg O$_2$/L)** | 190 | n.d. | n.d. | 80 | 205 | 13 | 40 |
| **COD[a] (mg O$_2$/L)** | 3581 | 3308 | 3386 | 1184 | 390 | 105 | 150 |
| **DOC[a] (mg C/L)** | 1136 | 981 | 993 | 380 | 137 | 62 | - |
| **DIC[a] (mg C/L)** | 1026 | 10 | 263 | 5 | 12 | 46 | - |
| **Alkalinity[b] (g CaCO$_3$/L)** | 4.2 | < 0.1 | 1.1 | < 0.1 | < 0.1 | 0.2 | - |
| **TN[a] (mg N/L)** | 2050 | 1616 | 14 | 12 | 12 | 7 | 15[d] |
| **TAN[a] (mg NH$_4^+$-N/L)** | 1771 | 4 | < 0.1 | n.d. | n.d. | n.d. | 8 |
| **Nitrite (mg NO$_2^-$-N/L)** | 56 | 1502 | 7 | n.d. | n.d. | n.d. | - |
| **Nitrate (mg NO$_3^-$ - N/L)** | 8 | 7 | 3 | n.d. | n.d. | n.d. | 11 |
| **Sulfate (mg SO$_4^{2-}$/L)** | 100 | 110 | 110 | 1870 | 1895 | 1888 | 2000 |
| **TDI[a] (mg (Fe$^{2+}$+Fe$^{3+}$)/L)** | 4.8 | 3.9 | 4.2 | 10.4 | 0.5 | 0.4 | 2[d] |
| **TSS[a] (mg/L)** | 620 | 407 | 387 | 148 | 37 | 48 | 60 |
| **VSS[a] (mg/L)** | 404 | 265 | 244 | 37 | 23 | 35 | - |

n.d. – not determined. [a] BOD$_5$ - 5-day biochemical oxygen demand; COD - Chemical oxygen demand; DOC - Dissolved organic carbon; DIC - Dissolved inorganic carbon; TN – Total dissolved nitrogen; TAN - Total ammonia nitrogen; TDI - Total dissolved iron; TSS - Total suspended solids; VSS - Volatile suspended solids. [b] Alkalinity values considering that, for pH < 11, the inorganic carbon was in the form of carbonates/bicarbonates [17]. [c] RL – Raw leachate; L$_{NIT}$ – Nitrified leachate; L$_{N/D}$ – Nitrified and denitrified leachate; CL – Coagulated leachate; PL – Photo-treated leachate; TL – Treated leachate for discharge; and ELV – Emission limit values, according to Portuguese legislation [18]. [d] Emission value for total nitrogen and total iron.

All the chemicals used in this work, the detailed description of the experimental units and respective procedures, as well as the analytical methods employed, can be consulted, respectively, in sections 4.1, 4.3.1 and 4.2 of Chapter 4. Furthermore, specific operating conditions for the SBR-24h-tests are shown in Table 5.2.

**Table 5.2** – Operating conditions and performance of the SBR-24h-tests.

| Parameters | 1.1 | 1.2 | 1.3[a] | 2.1 | 2.2 | 2.3 | 2.4[a] | 3.1 | 3.2 | 3.3 | 3.4[a] |
|---|---|---|---|---|---|---|---|---|---|---|---|
| $T_m$ (ºC) | 20.6 | 21.1 | 21.2 | 24.3 | 24.3 | 25.1 | 25.0 | 28.2 | 28.0 | 28.1 | 28.6 |
| $V^b$ (L) | 1.00 | 1.00 | 1.00 | 1.00 | 1.25 | 1.15 | 1.15 | 1.15 | 1.25 | 1.50 | 1.50 |
| $VER^b$ (%) | 14.3 | 14.3 | 14.3 | 14.3 | 17.9 | 16.4 | 16.4 | 16.4 | 17.9 | 21.4 | 21.4 |
| VSS (g/L) | 4.11 | 4.17 | 4.05 | 3.88 | 4.07 | 3.94 | 4.08 | 4.03 | 4.08 | 4.15 | 4.26 |
| $t_{NIT}^c$ (h) | 12.5 | 15.0 | 15.0 | 15.0 | 15.0 | 15.0 | 15.0 | 15.0 | 15.0 | 15.0 | 15.0 |
| $TAN^d$ (mg/L) | 253 | 287 | 266 | 307 | 368 | 325 | 306 | 295 | 388 | 427 | 451 |
| IC/TAN ratio | 1.7 | 1.3 | 1.4 | 1.4 | 1.2 | 1.2 | 1.3 | 1.8 | 1.2 | 1.2 | 1.2 |
| $FA^e$ (mg $NH_3$-N/L) | 59.6 | 31.6 | 26.9 | 31.5 | 44 | 37.2 | 35.6 | 31.9 | 55.4 | 76.1 | 41.3 |
| TAN removal (%) | 69.6 | 99.9 | 99.3 | 99.1 | 87.6 | 98.9 | 99.9 | 98.3 | 98.5 | 99.5 | 99.3 |
| $t_{DESN}^f$ (h) | 11 | 8.5 | 8.5 | 8.5 | 8.5 | 8.5 | 8.5 | 8.5 | 8.5 | 8.5 | 8.5 |
| Nitrite$^g$ (mg N/L) | 170 | 258 | 255 | 273 | 299 | 301 | 301 | 276 | 283 | 306 | 409 |
| Nitrite removal (%) | 97.6 | 97.1 | 97.2 | 97.8 | 94 | 97.4 | 97.7 | 97.3 | 96.8 | 98.2 | 97.9 |

[a] Experiments used for the determination of the kinetic parameters regarding nitritation and denitritation reactions. [b] $V$ - volume of leachate substituted at the beginning of the trial and corresponding $VER$ – volume exchange ratio. [c] Nitritation reaction time, i.e. aeration phase. [d] Total ammonia nitrogen content at the beginning of the aerated phase. [e] Concentration of free ammonia (FA) at the beginning of the aerated phase (calculated according to $\left(TAN \times 10^{pH}\right)/\left(e^{6344/(273+T)}+10^{pH}\right)$, with T in Celsius degrees). [f] Denitritation reaction time, i.e. anoxic phase. [g] Nitrite content at the beginning of the anoxic phase.

## 5.3 Results and discussion

### 5.3.1 Biological nitrogen removal

#### 5.3.1.1 General remarks

The leachate used in this work (Table 5.1) presented the typical characteristics of a mature landfill leachate (as detailed in Chapter 2), namely: (i) a high content of total ammonia nitrogen, corresponding to ~ 86% of the total dissolved nitrogen, and (ii) a low biodegradable organic fraction ($BOD_5/COD = 0.05$). These characteristics, together with the high temporal variability, are the major challenges in treating mature landfill leachates. In this case, the variability of the leachate was not a problem, since the same sample was used in all tests. However, in view of a full-scale application, the influent variability must be taken into account. Therefore, an SBR reactor was selected as the first treatment unit, since (i) it is a flexible activated sludge process designed to operate under non-steady state flow conditions, and (ii) it provides a dilution effect that enables to decrease the leachate toxic load and to mitigate the variability of the influent composition. Also, the SBR process can be operated under different conditions, such as aerobic/anoxic cycles, so both nitrification and denitrification reactions can be achieved in the same unit.

During all the SBR-24h-tests, only partial nitrification or "*nitritation*", i.e. oxidation of ammonium to nitrite, was attained whereas complete oxidation to nitrate was never detected ($< 7$ mg $NO_3^-$-N/L). This was also observed in other studies [2, 11, 20] and may be explained by: (i) nitrite-oxidizing bacteria inhibition by the free ammonia content (Table 5.2), that presented values above the inhibition threshold (between 0.1-1.0 mg $NH_3$-N/L [19] and up to 20 mg $NH_3$-N/L [21]); and (ii) relatively low concentration of oxygen in the aeration period (~ 0.5 mg $O_2$/L). Also, during the first hours (~ 4 h) of the aeration phase, it was detected that, the amount of TAN removed was slightly higher than of nitrite formed, with subsequent decrease on the TN content (Figure 5.1). This was attributed to the ammonia stripping phenomenon since part of the TAN was present in its highly volatile molecular form ($NH_3$) (mean pH $8.50 \pm 0.07$ at the beginning of the react phase) (see Table 5.2). As expected, the amount of TAN lost by air stripping was raised with increasing temperature and initial concentration of TAN (Table 5.3). After this period, the pH began to decrease, and the TN content remained approximately constant. Consequently, the TAN removal rates were 3-7 % higher than the nitrite production rates.
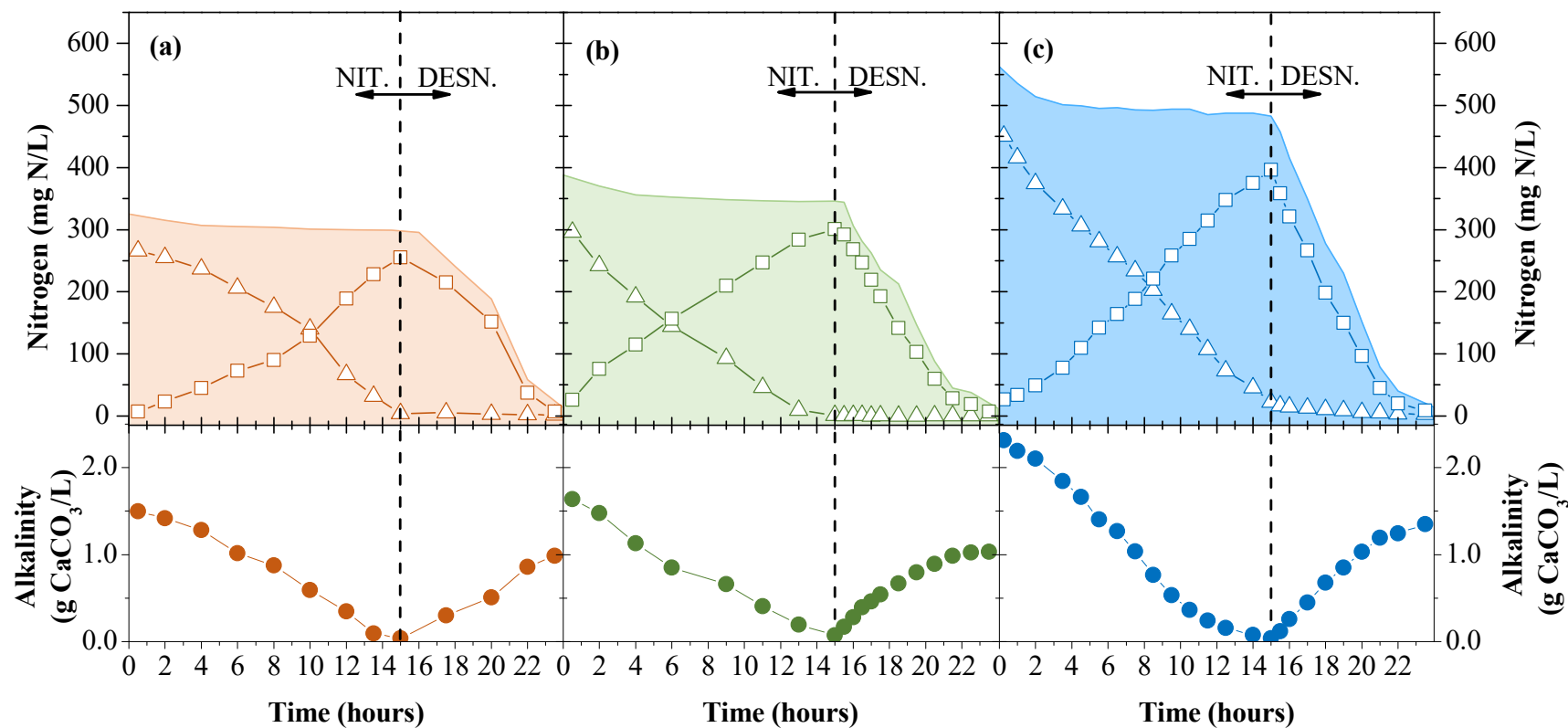
**Figure 5.1** – Evolution of (▨, ▨, ▨) total nitrogen, (△, △, △), total ammonia nitrogen, (□, □, □) nitrite-nitrogen, and (●, ●, ●) alkalinity, during the 24 h-SBR cycles, at (a) 20 ºC, (b) 25 ºC and (c) 30 ºC.

### 5.3.1.2 Nitritation-denitritation reactions

Several SBR-24h-tests were performed at different temperatures (Table 5.2) and, for each one, (i) the maximum daily nitrogen load that could be treated, reaching the TN legal limit, and (ii) the nitrification and denitrification kinetic parameters, were determined. Initially, from the tests 1.1 and 1.2, performed at 20 ºC, the time for the aerobic and anoxic periods were established at 15 and 8.5h, respectively, based on the results for the TAN and nitrite removals. For the following tests, it was verified that, with the increase in temperature (from 20 to 30 °C), it was possible to raise the daily load of nitrogen that could be biologically treated (Table 5.3). Therefore, with a TAN removal > 99%, a nitrite reduction > 97% and a final TN < 15 mg N/L, the maximum volume of leachate fed daily to the SBR was of 1.00, 1.15 and 1.50 L, for 20, 25 and 30 ºC, respectively (corresponding to a volume exchange ratio of 14.3%, 16.4% and 21.4%, for tests 1.3, 2.4 and 3.4, respectively).

**Table 5.3** – Kinetic parameters of the nitritation and denitritation reactions for the SBR-24h-tests.

| Parameters | 1.3 | 2.4 | 3.4 |
|---|---|---|---|
| $T_m$ (ºC) | $21.1 \pm 0.5$ | $25.0 \pm 0.3$ | $28.6 \pm 0.3$ |
| *Aerated period* | | | |
| pH | $8.4 – 7.9$ | $8.4 – 7.6$ | $8.5 – 7.8$ |
| $TAN_{initial}$ (mg $NH_4^+$-N/L) | 266 | 306 | 451 |
| $TAN_{final}$ (mg $NH_4^+$-N/L) | 2 | < 1 | 3 |
| $TAN_{AS}$[a] (%) | 5.0 | 7.8 | 12.9 |
| $r_{TAN}$[b] (mg $NH_4^+$-N/g VSS/h) | $17.4 \pm 0.7$ | $20.2 \pm 0.6$ | $29.2 \pm 0.2$ |
| $k_N$[c] (mg $NO_2^-$-N/g VSS/h) | $4.1 \pm 0.6$ | $4.8 \pm 0.3$ | $6.4 \pm 0.3$ |
| Alkalinity[d] (mg $CaCO_3$/mg $NH_4^+$-N) | $5.9 \pm 0.7$ | $5.7 \pm 0.4$ | $6.0 \pm 0.5$ |
| *Anoxic period* | | | |
| pH | $7.9 – 8.4$ | $7.6 – 8.3$ | $7.8 – 9.2$ |
| $Nitrite_{initial}$ (mg $NO_2^-$-N/L) | 255 | 301 | 409 |
| $Nitrite_{final}$ (mg $NO_2^-$-N/L) | 7 | 7 | 9 |
| $TN_{final}$ (mg/L) | 13 | 12 | 15 |
| $k_D$[e] (mg $NO_2^-$-N/g VSS/h) | $8.2 \pm 0.9$ | $10.9 \pm 0.6$ | $12.3 \pm 0.9$ |
| Methanol[f] (mg $CH_3OH$/mg $NO_2^-$-N) | $2 \pm 1$ | $2.2 \pm 0.2$ | $1.6 \pm 0.2$ |
| Alkalinity[g] (mg $CaCO_3$/mg $NO_2^-$-N) | $3.7 \pm 0.8$ | $3.0 \pm 0.3$ | $3.4 \pm 0.1$ |

[a] TAN fraction removed by air stripping $((A_1-A_2) \times VSS/(t_N \times TAN_i) \times 100$, where $A_1$ and $A_2$ are the areas below the curves of Figure 5.2 related to (a.1) TAN and (a.2) nitrite, respectively; $t_N$ is the nitritation reaction time and $TAN_i$ is the total ammonia nitrogen content at the beginning of the aeration time (Table 5.2)). [b] TAN removal rate ($m \times VSS$, where $m$ corresponds to the slopes of Figure 5.2-a.1). [c] Nitritation reaction rate, expressed in terms of nitrite formation (values correspond to the slopes of Figure 5.2-a.2). [d] Alkalinity consumption during the aerated phase (values correspond to the slopes of Figure 5.2-a.3). [e] Denitritation reaction rate, expressed in terms of nitrite reduction (values correspond to the slopes of Figure 5.2-b.1). [f] Methanol consumption during the anoxic phase (values correspond to the slopes of Figure 5.2-b.2). [g] Alkalinity production during the anoxic phase (values correspond to the slopes of Figure 5.2-b.3).
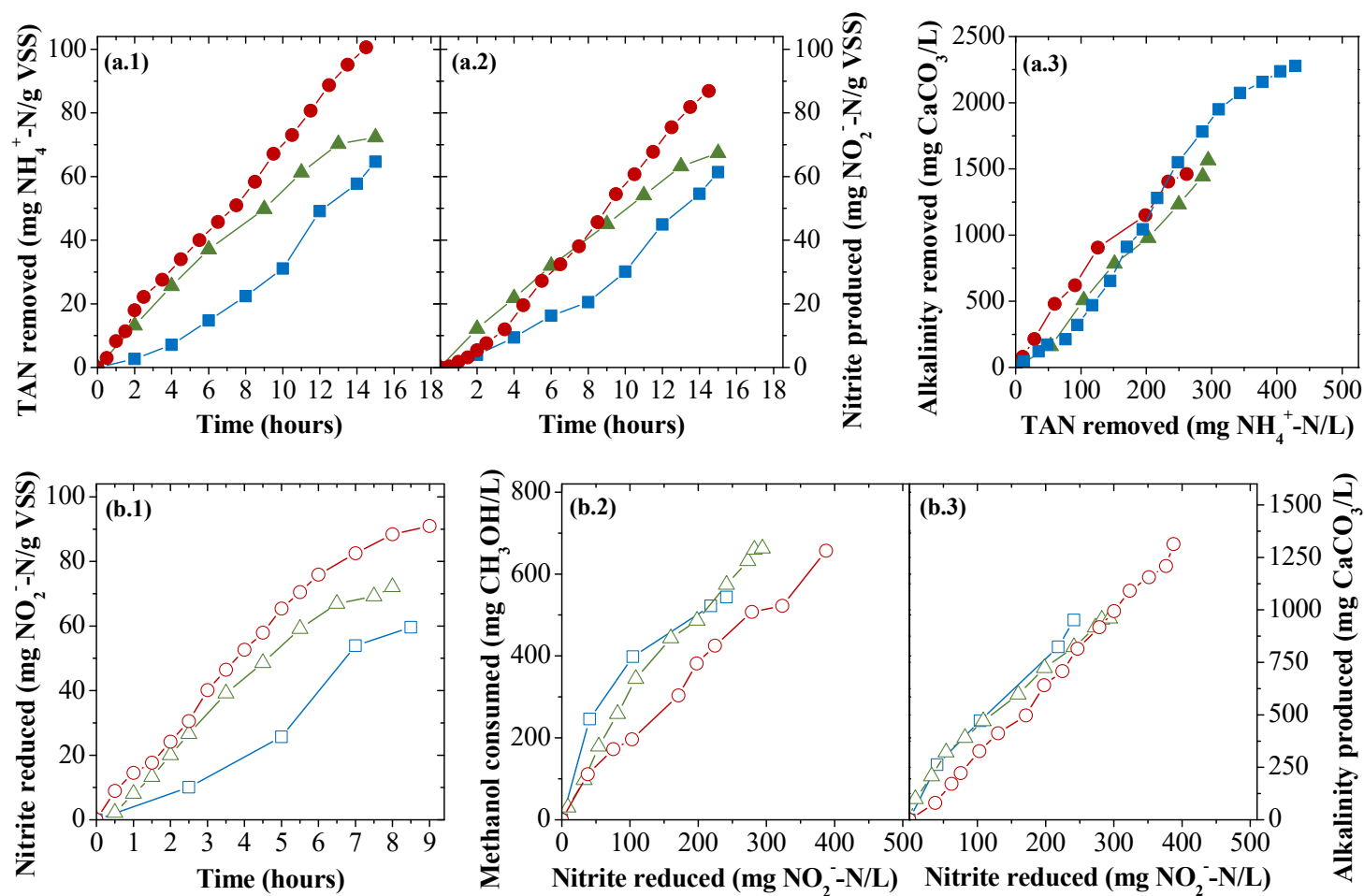
**Figure 5.2** – Representation of the (a.1) TAN removed/VSS ratio, and (a.2) nitrite produced/VSS ratio, as a function of time, and the (a.3) alkalinity removed, as a function of TAN removed, along the nitrification period (close symbols); (b.1) nitrite reduced/VSS ratio, as a function of time, and the (b.2) methanol consumed and (b.3) alkalinity produced, as a function of nitrite reduced, along the denitrification period (open symbols), at different temperatures (20 ºC - ■, □; 25 ºC - ▲, △ and 30º C - ●, ○).

For many reacting biological systems, the temperature effect on the kinetics of the degradation processes is commonly described by an Arrhenius-type equation (denoted Modified Arrhenius Function or MAF) given by Equation 5.1:

$$k_{T1} = k_{T2} \times \theta^{(T1-T2)} \qquad (5.1)$$

where $k$ is the reaction rate at the temperature *T1* and *T2* (ºC), respectively, and $\theta$ is the temperature coefficient. In this case, the increment of the nitritation and denitritation rates as temperature increased was satisfactorily described by MAF (Figure 5.3), and the temperature coefficients obtained ($\theta = 1.06$, for both reactions) are in agreement with those found in literature ($\theta_{NIT.} = 1.062$, for 20 to 35ºC [22]) and $\theta_{DEN.} = 1.06$ [23]).
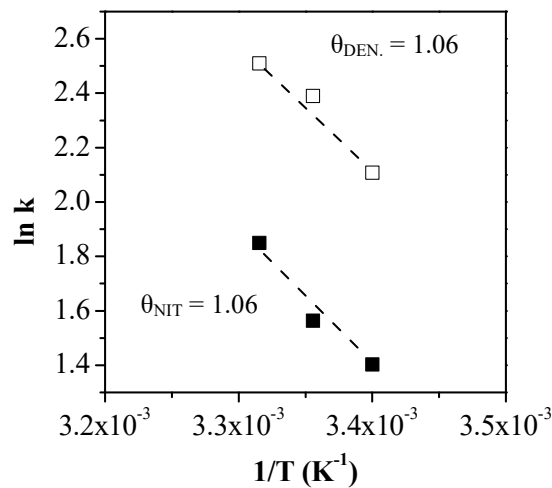


**Figure 5.3** – Modified Arrhenius plot: linear relation between the logarithm of the rate constant, $k$, and the temperature, $T$, for (■) nitritation and (□) denitritation reaction rates.

Regarding the nitritation rates (Table 5.3), similar values have been reported for mature leachate treatment using an SBR (6.3 mg $NH_4^+$-N/g VSS/h, at 28-32 ºC [24] and 2.1-6.5 mg $NH_4^+$-N/g VSS/h, at 20 ºC [25]), and an ASBO (6.3 mg $NH_4^+$-N/g VSS/h, at 26 ºC [12]). However, other studies report considerably higher specific nitritation rates (4.9 to 12.6 mg N/g VSS/h, at 20 ºC, with an SBR [26]; 8.2 and 13.6 mg $NH_4^+$-N/g VSS/h, at 26 ºC, using an ASBO [2, 11]; and 6.7 mg $NH_4^+$-N/g VSS/h, at 25ºC, with a lab-scale suspended carrier biofilm process [27]). While developing and calibrating an SBR model for a landfill leachate nitritation/denitritation process, Wett and Rauch [21] demonstrated that the limitation of the inorganic carbon (IC) had a significant effect on the process performance. According to these authors, the optimization of bicarbonate concentrations could enhance the nitritation rate up to 100 mg $NH_4^+$-N/L/h. Considering this, it is possible that the nitrification efficiencies may have been limited by the lower IC content (average value of $1.4 \pm 0.1$

mg IC/mg $NH_4^+$-N) when compared to the theoretically required (stoichiometric value of 1.71 mg IC/mg $NH_4^+$-N). Throughout the tests, at the end of the aerated phase, the average alkalinity concentration was of $0.15 \pm 0.08$ g $CaCO_3$/L and the alkalinity consumed was 15-25% lesser than the stoichiometric ratio (7.1 mg $CaCO_3$/mg $NH_4^+$-N). This lower alkalinity consumption has been previously reported for the nitrification of urban leachate [2, 15]. It should be noticed that, for the SBR-24h-tests, a simple operating mode was intended, and a straightforward aerobic/anoxic scheme was applied, but the SBR reactor offers great operational versatility that can be further explored. It is possible to alternate more between aerobic/anoxic phases, which can potentially contribute to boost the nitritation rate, by using the alkalinity produced in the anoxic phase for the following aerobic phase.

In respect to the denitritation, the reaction was ~ 2 times faster than that of the nitritation (Table 5.3). Earlier studies using old leachate reported similar denitritation rates (11.1 and between 13.5-19.4 mg N/g VSS/h, at 25 and 30 ºC, respectively [15]), and methanol consumption (1.6-2.2 mg $CH_3OH$/mg N [15] and 2.4 mg $CH_3OH$/mg N [2]). Different external carbon donors, with similar reaction rates, have also been applied using an SBR for denitrification of leachates, such as acetate (14.6 mg N/g VSS/h, at 20ºC [25]) and glycerol (9.45 mg N/g VSS/h, at 20-22 ºC [28]).

Since the following treatment stages require acidification, an important aspect to consider is the alkalinity at the end of the biological treatment. As mentioned, alkalinity was nearly all consumed during the aerobic phase, but it was afterward partially recovered during denitritation. Attention was given to this issue in a previous study [2], where 2.5 m$^3$ of raw leachate (initial TAN = 3.9 g $NH_4^+$-N/L and alkalinity = 17.1 g $CaCO_3$/L) were biologically nitrified and denitrified in an ASBO reactor (HRT > 50 days, final TN = 0.2 g N/L and alkalinity = 8.0 g $CaCO_3$/L). The amount of acid that was later required to neutralize the alkalinity, to lower the pH to apply a solar PF, corresponded to 77% of the total acid used. Also, at the end of the treatment, the sulfate concentration was ~ 7 times higher than the legal limit (2 g/L) [18]. In our case, considerably lower alkalinity values (1.0-1.5 g $CaCO_3$/L) were obtained at the end of the SBR 24 h-cycle, which is promising when legal compliance for sulfate is expected.

Considering the treatment of 150 m$^3$ of leachate/day, in a simplified scale-up scenario (Table 5.4), an SBR with a total operation volume of 1180 m$^3$ would be required. Moreover, for denitrification purposes, a cost of 1.87 €/m$^3$ for methanol consumption (assuming a price of 0.48 €/kg) can be expected.

**Table 5.4 –** Operation data for the SBR stage to treat 150 m³ per day of urban mature landfill leachate.

| Parameter | Units | Value |
|---|---|---|
| Initial-final **TN**[a] | mg N/L | 301 - 13 |
| Average operating temperature – $T_m$[a] | ºC | 20 |
| Volatile suspended solids – **VSS**[a] | g/L | 4 |
| Average DO during aerobic period – **DO**[a] | mg/L | 0.5 |
| Methanol consumption during anoxic period – $C_S$[a] | kg/m³ | 0.5 |
| Volume exchange ratio – **VER**[a] | m³/m³/day | 0.14 |
| Fill volume – $V_F$ | m³/day | 150 |
| Total volume - $V_T$[b] | m³ | 1180 |
| Depth of the reactor – $D$[c] | m | 6.0 |
| Width to depth ratio – $W/D$[c] | | 1.5:1 |
| Hydraulic retention time – **HRT**[d] | days | 7.9 |
| Total cycle time - $t_T$[e] | hours | 24 |
| Fill (with react) phase – $t_F$ | hours | 1-2 |
| React phase – $t_R$ | hours | |
| Aerobic period – $t_A$ | hours | 15 |
| Anoxic period – $t_{AX}$ | hours | 8.5 |
| Settle phase – $t_S$ | hours | 0.5 |
| Draw phase - $t_D$ | hours | 0.5-1 |

[a] Data obtained from SBR-24h-tests performed at 20 ºC. [b] $V_T = V_F/VER \times S_F$, considering a safety factor ($S_F$), of 10%. [c] Values proposed by Metcalf and Eddy [29]. [d] HRT = $V_T/V_F$. [e] $t_T = t_R + t_S$, assuming a fill phase with reaction ($t_R = t_F + t_A + t_{AX}$).

## 5.3.2 Coagulation

Chemical coagulation applied to landfill leachate has been widely studied and has proven to achieve a considerable high removal of COD, colour and solids [30-33]. In this case, coagulation is intended to remove humic substances (HS), suspended and colloidal particles that may act as photon absorbers (light-filtering species) in the following photo-Fenton stage. Most of the organic components in the leachate are HS, which are responsible by the leachate's dark colour and are considered to be hydroxyl scavengers [32]. Suspended matter can also affect light transmission by either scattering or absorbing it. To trigger the PF reaction, light needs to penetrate through the solution, so anything that prevents the light from reaching the catalyst will obviously affect the removal efficiency. Therefore, a coagulation stage prior to the PF is needed to attain a deep level of organics removal.

For the coagulant dosage tests, it is possible to verify that both $L_{NIT.}$ and $L_{N/D.}$ presented similar profiles, with DOC removal efficiencies decreasing (Figure 5.4-a.1) and turbidity increasing (Figure 5.4-a.2) as the coagulant dosage diminished. So, with a DOC removal above 40% and a reasonably low turbidity, the higher coagulant concentration tested (240 mg $Fe^{3+}$/L) was considered suitable for both bio-treated leachates. The effect of the acidic properties of the coagulant was observed, since the decrease of its dosage led to the increase of the amount of sulfuric acid added and, consequently, the increase of the sulfate concentration in the coagulated leachate (Figure 5.4-a.3). Also, the effect of the different alkalinity values, presented by the bio-treated leachates, on the coagulation efficiency was very clear. For the $L_{NIT}$, where alkalinity is virtually absent, the solely addition of the highest coagulant dosage was sufficient to lower the pH to 4.5 and no acid was added. On the contrary, the higher alkalinity of the $L_{N/D}$ implied that the amount of acid required, when the lowest coagulant dosage was tested, exceeded the sulfate legal value. The use of HCl for acidification could be an alternative, since it is equally cheap and commercially available and, beyond that, there is no legal limit for the chloride ion. However, earlier studies have demonstrated that a leachate with high chloride content negatively affects the PF reaction more than with high sulfate content [16].

Regarding the effect of leachate pH, it is possible to verify that although a decrease on the pH value favours the DOC removal (Figure 5.4-b.1) and turbidity (Figure 5.4-b.2). This trend was valid for both bio-treated leachates, but it seemed to have a greater effect on $L_{N/D}$. So, in view of the best operational performance conditions, coagulation should be performed at pH 3.0. However, at this pH, previous studies with coagulated $L_{NIT}$ [12, 15] have shown that the high nitrite content affected the following PF reaction (over-consumption of $H_2O_2$ and a significant decrease of pH, due to the indirect oxidation of nitrite into nitrate, requiring the addition of an alkaline solution). Also, to achieve a pH value of 3.0, both bio-treated leachates required a higher amount of acid, thus the sulfate ion content increased (Figure 5.4-b.3). This arouses as an important issue for the $L_{N/D}$, since its alkalinity implies an additional amount of acid, which may easily exceed the sulfate limit value. In this case, with alkalinity of 1.1 g $CaCO_3$/L, the final concentration of sulfate for the coagulated $L_{N/D.}$ was still below the legal limit. Therefore, with the coagulation performed at pH 3.0, employing a coagulant dosage of 240 mg $Fe^{3+}$/L, the $L_{N/D}$ attained a DOC and COD reduction above 60% (Table 5.1). Therefore, coagulated $L_{N/D}$ was chosen to pursue treatment.
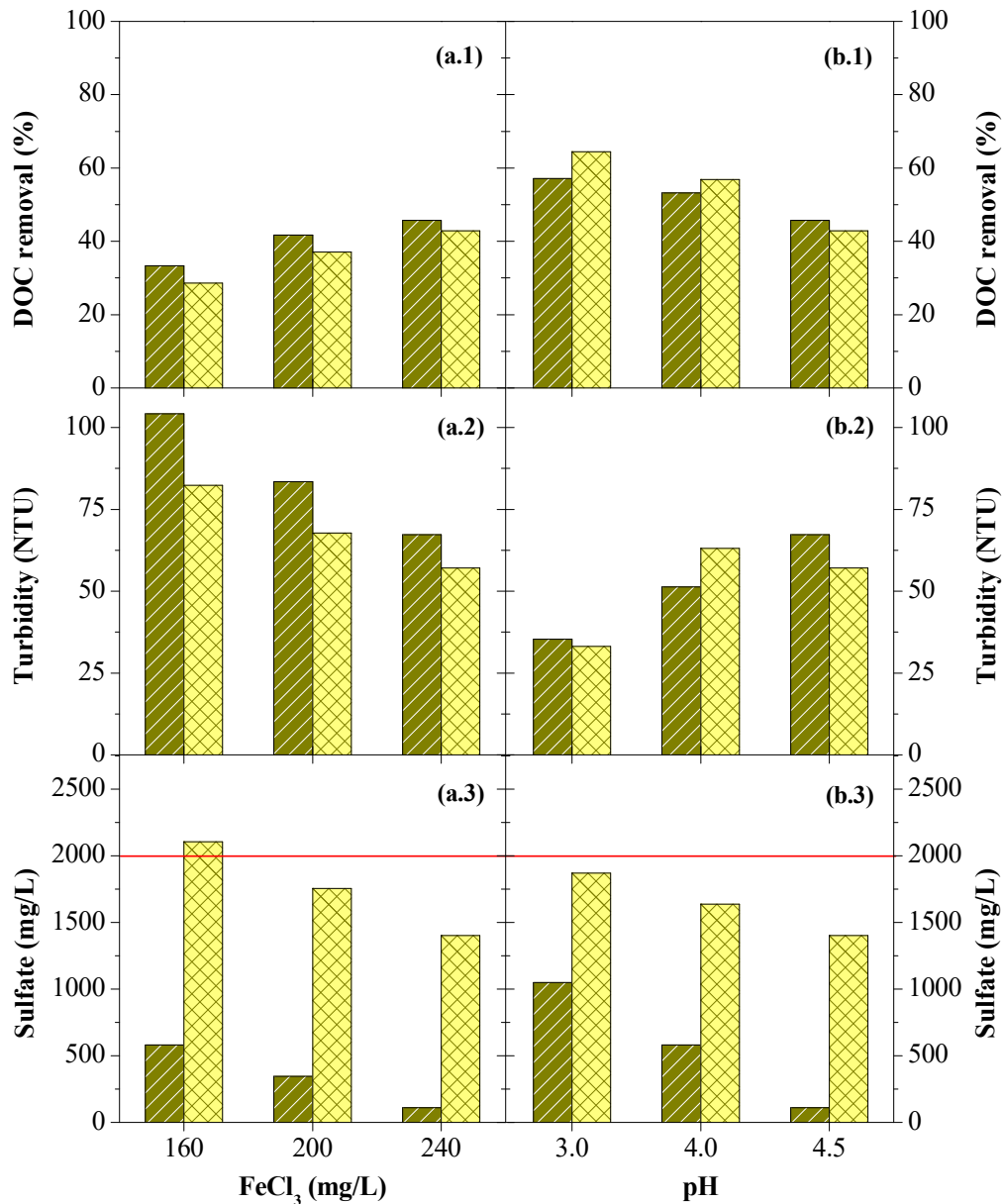
**Figure 5.4** – Effect of (a.) coagulant dosage (at pH 4.5) and (b.) pH (using 240 mg $Fe^{3+}$/L) in (.1) DOC removal, (.2) turbidity and (.3) sulfate content, during the coagulation tests of the bio-treated leachate by (▨) nitrification and (▨) nitrification/denitrification.

### 5.3.3 Photo-Fenton oxidation

Based on previous research [15, 16], the photo-Fenton reaction was applied to the bio-coagulated-leachate and the influence of different operational parameters (catalyst dosage, temperature and irradiance) was evaluated. In respect to the catalyst dosage optimization, by analysing the DOC degradation profiles (Figure 5.5-a.1), a small reduction of the organic content was always verified

after the catalyst addition (in the absence of light). This initial DOC abatement was (i) related to the precipitation of some organic matter that was not removed in the previous coagulation step, and (ii) higher with the increment of the catalyst dosage (< 5%, for $20 \leq [Fe^{2+}] \leq 40$ mg/L, and 10-15% for $[Fe^{2+}] > 40$ mg/L). As expected, the DOC removal rate and $H_2O_2$ consumption also increased with the increment of the iron-catalyst concentration (Table 5.5). Except for the test with the highest iron dose, a reasonable correlation ($R^2 = 0.992$, Figure 5.6-a) exists between the reaction rate ($k$, L/kJ$_{UV}$) and the catalyst dosage. This indicates that to overcome the inner filter effects and photonic competition by other light-absorbing species present in the leachate (e.g. fulvic acids), an iron concentration between 60 to 80 mg $Fe^{2+}$/L is required. Considering that with 60 mg $Fe^{2+}$/L, the DOC removal after 3-h reaction was only slightly lower (6.3 %) than with 80 mg $Fe^{2+}$/L, and also in a cost reduction perspective, 60 mg $Fe^{2+}$/L was defined as the most efficient catalyst dosage.

The temperature effect on the PF reaction was assessed between 15 and 50 ºC, considering that temperatures within this range were reported as minimum (winter) and maximum (summer) values during solar PF experiments [16, 34]. From the DOC degradation profile (Figure 5.5-a.2) it is possible to observe that the variation of the temperature displayed a significant impact, particularly for the three highest temperatures. For the experiments between 30-50 ºC, the DOC profile showed: (i) an initial period, characterized by a slow mineralization, followed by (ii) a fast-reaction period. The slow-reaction period was shorter as the temperature increased, indicating the importance of the thermal reactions involved (reduction of the ferric ion and thermal oxidation). The $H_2O_2$ consumption also increased with the temperature increment, and more $H_2O_2$ was spent to achieve the same mineralization level (Figure 5.5-b.2 and Table 5.5). This can be related to two main factors: (i) the thermal ferric ion reduction reactions and (ii) $H_2O_2$ decomposition at high temperatures (the rate of $H_2O_2$ decomposition doubles as the temperature rises 10 ºC). Also, for the PF reactions performed at 40 and 50 ºC, a significant decrease of the TDI concentrations was observed (Table 5.5). This trend is justifiable by the lower solubility of the ferric and ferrous ions with increasing solution temperature. However, this did not hinder the increment on the reaction rates for those temperatures and a good relation ($R^2 = 0.991$) was established between the kinetic constants ($k$, L/kJ$_{UV}$) and all temperatures tested (Figure 5.6-b). The relationship between the temperature and the PF reaction rate can be expressed by the Arrhenius law (as mentioned in Chapter 4).
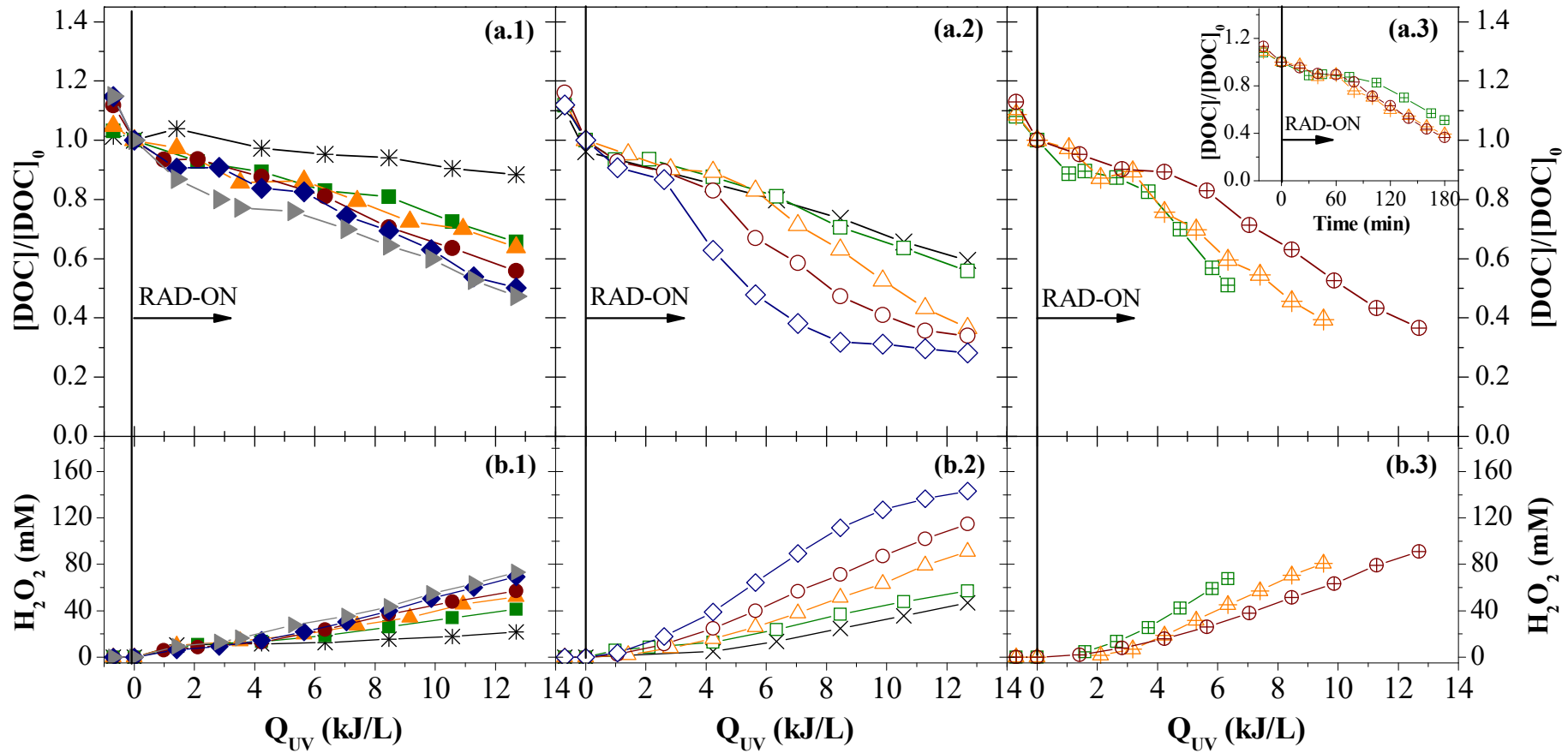
**Figure 5.5** – Evaluation of the (a) DOC and (b) $H_2O_2$ concentration, during the photo-Fenton reaction for different (.1) iron concentrations ((✱) – No catalyst added; (■) – $[Fe^{2+}]$ = 20 mg/L; (▲) – $[Fe^{2+}]$ = 40 mg/L; (●) – $[Fe^{2+}]$ = 60 mg/L; (◆) – $[Fe^{2+}]$ = 80 mg/L; (▶) – $[Fe^{2+}]$ = 100 mg/L), (.2) temperatures ((✕) 15 °C; (□) 20 °C; (△) 30 °C; (○) 40 °C; (◇) 50 °C), and (.3) radiation intensity ((⊞) 22 $W_{UV}/m^2$; (⊕) 33 $W_{UV}/m^2$; (⊕) 44 $W_{UV}/m^2$). Operating conditions: (.1) – pH = 2.8, T = 20 °C, $I$ = 44 $W_{UV}/m^2$; (.2) – pH = 2.8, $[Fe^{2+}]$ = 60 mg/L, $I$ = 44 $W_{UV}/m^2$; (.3) – pH = 2.8, T = 30 °C, $[Fe^{2+}]$ = 60 mg/L.

**Table 5.5** – Variables and kinetic parameters of the photo-Fenton process for all experiments.

| Changed parameter | $T_m{}^a$ (ºC) | $pH_m{}^a$ | $TDI_m{}^a$ (mg/L) | $DOC_F{}^b$ (mg/L) | $Red._{DOC}{}^c$ (%) | $H_2O_2/C^d$ (mg/mg) | COD degradation $k^e$ (×10⁻² L/kJ_UV) | | COD degradation $r_0{}^f$ (mg/kJ_UV) | | $R^{2,g}$ | H₂O₂ consumption $k_H{}^h$ (mmol/kJ_UV) | | $R^{2,g}$ | $Q_{UV}{}^i$ (kJ_UV/L) |
|---|---|---|---|---|---|---|---|---|---|---|---|---|---|---|---|
| TDI = 0 mg/L | 20.8 | 2.97 | 10.7 | 311 | 19.6 | 11.0 | 1.2 ± | 0.2 | 4.2 ± | 0.6 | 0.994 | 1.8 ± | 0.2 | 0.996 | > 4 |
| TDI = 20 mg/L | 20.3 | 2.87 | 24.1 | 230 | 39.6 | 10.8 | 3.0 ± | 0.7 | 11 ± | 3 | 0.987 | 3.2 ± | 0.1 | 0.999 | > 2 |
| TDI = 40 mg/L | 20.0 | 2.91 | 41.6 | 199 | 44.8 | 15.8 | 4.2 ± | 0.9 | 14 ± | 3 | 0.984 | 4.0 ± | 0.3 | 0.996 | > 5 |
| TDI = 60 mg/L | 20.0 | 2.84 | 58.3 | 163 | 57.4 | 16.1 | 5.3 ± | 0.9 | 17 ± | 3 | 0.994 | 4.3 ± | 0.5 | 0.991 | > 4 |
| TDI = 80 mg/L | 20.5 | 2.82 | 76.4 | 136 | 63.7 | 18.4 | 7 ± | 1 | 24 ± | 4 | 0.989 | 5.1 ± | 0.5 | 0.990 | > 5 |
| TDI = 100 mg/L | 19.9 | 2.80 | 93.0 | 134 | 63.6 | 19.0 | 6.8 ± | 0.8 | 22 ± | 4 | 0.993 | 5.5 ± | 0.3 | 0.997 | > 5 |
| T = 15ºC | 15.2 | 2.87 | 51.9 | 157 | 58.1 | 16.5 | 4.3 ± | 0.4 | 12 ± | 1 | 0.994 | 3.8 ± | 0.9 | 0.981 | > 2 |
| T = 20ºC | 20.0 | 2.94 | 58.3 | 163 | 57.4 | 16.1 | 5.3 ± | 0.9 | 17 ± | 3 | 0.994 | 4.3 ± | 0.5 | 0.991 | > 4 |
| T = 30ºC | 30.2 | 2.87 | 62.4 | 104 | 72.2 | 16.7 | 10 ± | 1 | 41 ± | 8 | 0.995 | 6.5 ± | 0.9 | 0.985 | > 5 |
| T = 40ºC | 40.0 | 2.90 | 53.7 | 105 | 73.1 | 18.1 | 13 ± | 1 | 53 ± | 7 | 0.994 | 8.4 ± | 0.9 | 0.990 | 4 – 11 |
| T = 50ºC | 50.0 | 2.91 | 45.9 | 88 | 76.9 | 18.6 | 18 ± | 2 | 78 ± | 14 | 0.993 | 12 ± | 2 | 0.978 | 2 - 9 |
| $I$ = 22 W_UV/m² | 30.1 | 2.90 | 59.1 | 145 | 61.0 | 16.0 | 18 ± | 3 | 83 ± | 20 | 0.997 | 10 ± | 2 | 0.978 | > 3 |
| $I$ = 33 W_UV/m² | 30.0 | 2.94 | 56.9 | 109 | 70.7 | 18.1 | 14 ± | 1 | 51 ± | 6 | 0.993 | 7.5 ± | 0.8 | 0.987 | > 3 |
| $I$ = 44 W_UV/m² | 30.2 | 2.87 | 62.4 | 104 | 72.2 | 16.7 | 10 ± | 1 | 41 ± | 8 | 0.995 | 6.5 ± | 0.9 | 0.985 | > 5 |

[a] Average values of temperature, pH and total dissolved iron observed during the photo-Fenton experiments. [b] Final DOC. [c] DOC total reduction (1-$DOC_F$/$DOC_I$, %). [d] Ratio between the H₂O₂ (mol/L) consumed and DOC (mg/L) oxidized $([H_2O_2]/(DOC_i-DOC_f) \times 34.02)$. [e] Pseudo-first-order kinetic constant for DOC degradation. [f] Initial DOC reaction rate. [g] Coefficient of determination. [h] H₂O₂ consumption rate. [i] Value or interval of energy from which the kinetic parameters were calculated.
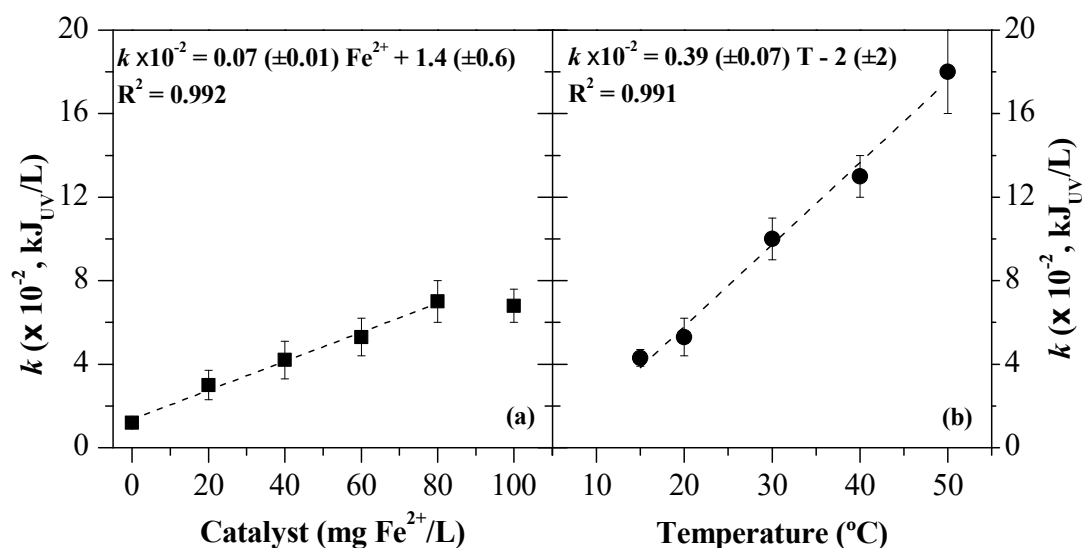
**Figure 5.6** – Relation between the pseudo-first-order kinetic constants for DOC degradation and the (a) catalyst dosage and (b) temperature.

From the Arrhenius-type plot (Figure 5.7), the values of $A$ and $E_a$ were determined as $2.2 \times 10^4$ L/kJ and $32.4 \pm 8$ kJ/mol. A very close activation energy value was also attained, only 5% higher (34.1 $\pm$ 6 kJ/mol), considering the kinetics reported for a similar PF treatment applied to an urban leachate collected at the outlet of a LTP [16]. The proximity between the $E_a$ values, i.e. the minimum energy that was required for the photochemical oxidation reaction to occur, may be due to the similarity of the oxidation state of the carbonaceous matter (COD/TOC = 3.1 and 3.2, for the bio-coagulated leachate used in the present work and for the leachate at the outlet of the LTP, respectively). Also, for similar operating conditions, the kinetic constant ($k$, L/kJ$_{UV}$) and hydrogen peroxide consumption (mmol/kJ) obtained in this work were very close to those previously reported for the photo-Fenton reaction applied to a denitrified-coagulated-leachate [15].

Considering that the irradiance varies throughout the day, due to climatic and seasonal conditions, experiments were carried out under different irradiance conditions (22, 33 and 44 W$_{UV}$/m$^2$) to evaluate its influence on the PF reaction. The results show that with the increasing of the irradiance from 22 to 33 W$_{UV}$/m$^2$, the DOC degradation over the accumulated UV energy was initially quite similar, but over time it was considerably faster (Figure 5.5-a.3). At the end of the same photo-treatment time (3 hours), the mineralization level increased from 61.0% to 70.7%, respectively, for $I = 22$ and 33 W$_{UV}$/m$^2$. In turn, when the irradiation increased from 33 to 44 W$_{UV}$/m$^2$, the final DOC mineralization was approximately the same (Table 5.5). The slightly higher consumption of UV energy observed for $I = 44$ W$_{UV}$/m$^2$, suggests a loss of photons, which means that more iron would be necessary to absorb all photons. This is in accordance with the results above, where the catalyst dosage (optimized at 44 W$_{UV}$/m$^2$) that yielded the highest DOC abatement and the best PF

performance was of 80 mg $Fe^{2+}$/L. In this way, for the conditions tested, we conclude that a moderate irradiance of 33 $W_{UV}$/m$^2$ is sufficient for an effective photo-treatment of the bio-coagulated-leachate.
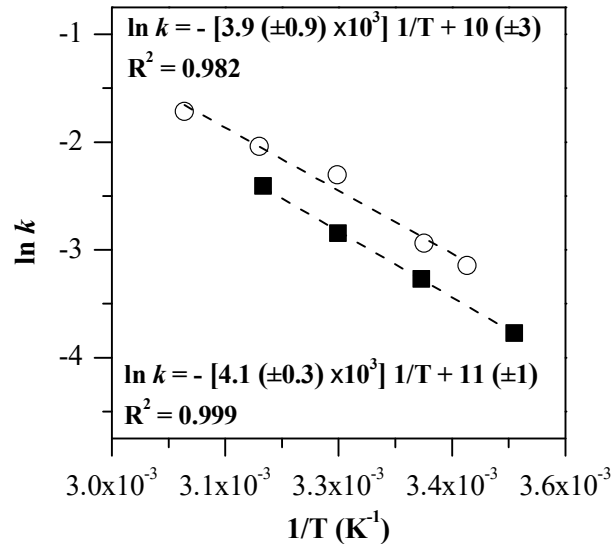


**Figure 5.7** – Arrhenius plot: linear relation between the logarithm of the photo-Fenton rate constants, $k$, and the temperature, $T$, obtained in the (○) current work and (■) in a previous research [16].

From a scale-up perspective, assuming that 150 m$^3$ of leachate is generated per day and a scenario that combines natural sunlight with artificial radiation, an area of 1182 m$^2$ for the compound parabolic collector (CPC) reactor and the use up to 27 UV lamps were estimated (Table 5.6). In this scenario, the CPCs area is the minimum required considering the month with higher average UV irradiation. This means that, during that month, if the estimated CPCs area was installed, the PF stage would be fully performed with natural solar light. In turn, the number of UV lamps relates to the month with the lowest average radiation intensity (December), meaning that 27 UV lamps (in continuous operation during 8 h) would be required to compensate the lack of natural sunlight. This approach is a good option to reduce costs related with (i) the investment for the CPCs, and (ii) the electrical energy for the lamps. Moreover, in view of further cost savings and also a compact treatment facility, it would be possible to use the same conical tank (with 150 m$^3$ of operating volume) for coagulation, PF recirculation and neutralization, thus performing both treatment stages within a 24 h time frame.

**Table 5.6** – Operation data for the treatment of 150 m$^3$ per day of landfill leachate, CPCs area and number of UV lamps required for each month of the year, for the photo-Fenton stage.

| ΔDOC[a] | ΔCOD[a] | H$_2$O$_2$[a] | T$_m$[a] | Q$_{UV}$[a] | Q$_{PF}$[b] |
|---|---|---|---|---|---|
| (mg C/L) | (mg O$_2$/L) | (mM) | (°C) | (kJ/L) | (m$^3$/day) |
| 380 - 137 | 1184 - 390 | 79 | 30 | 9 | 102 |

| Month | V$_M$[c] | E$_M$[d] | A$_{CPC}$[e] | E$_{CPC}$[f] | E$_L$[g] | N$_L$[h] |
|---|---|---|---|---|---|---|
| | (m$^3$) | (kJ$_{UV}$/m$^2$) | (m$^2$) | (kJ) | (kJ) | |
| Jan. | 3162 | 6597 | 4314 | $7.80 \times 10^6$ | $2.07 \times 10^7$ | 25 |
| Feb. | 2856 | 10194 | 2521 | $1.20 \times 10^7$ | $1.37 \times 10^7$ | 18 |
| Mar. | 3162 | 14226 | 2000 | $1.68 \times 10^7$ | $1.16 \times 10^7$ | 14 |
| Apr. | 3060 | 19774 | 1393 | $2.34 \times 10^7$ | $4.17 \times 10^6$ | 5 |
| **May** | **3162** | **24078** | **1182** | **$2.85 \times 10^7$** | **0.00** | **0** |
| Jun. | 3060 | 17309 | 1591 | $2.05 \times 10^7$ | $7.08 \times 10^6$ | 8 |
| Jul. | 3162 | 20241 | 1406 | $2.39 \times 10^7$ | $4.53 \times 10^6$ | 5 |
| Aug. | 3162 | 20554 | 1385 | $2.43 \times 10^7$ | $4.17 \times 10^6$ | 5 |
| Set. | 3060 | 19971 | 1379 | $2.36 \times 10^7$ | $3.94 \times 10^6$ | 4 |
| Oct. | 3162 | 13995 | 2033 | $1.65 \times 10^7$ | $1.19 \times 10^7$ | 14 |
| Nov. | 3060 | 8648 | 3185 | $1.02 \times 10^7$ | $1.73 \times 10^7$ | 21 |
| Dec. | 3162 | 5456 | 5216 | $6.45 \times 10^6$ | $2.20 \times 10^7$ | 27 |

[a] Data obtained from the PF experiments ($I$ = 33 W$_{UV}$/m$^2$, T = 30 °C, TDI = 60 mg/L, pH = 2.9). [b] $Q_{PF}=Q_C-Q_S$, where $Q_C$ is the daily operating volume for coagulation stage and $Q_S$ is the daily sludge volume generated in coagulation ($Q_S$ of 320 mL/L was assumed based on experimental observations). [c] $V_M = D_M \times Q_{PF}$, where $V_M$ is the volume of leachate for each month; $D_M$ is the number of days for a particular month. [d] $E_M$ – average accumulated solar UV energy for each month, data extracted from [35]. [e] CPCs area that would be required if PF reaction was mediated only by solar radiation: $A_{CPC}= Q_{UV} \times V_M \times 1000/E_M$. [f] Monthly energy that would be captured by the CPCs, if the minimum required area (corresponding to the month with higher average irradiation, in this case, May) was implemented: $E_{CPC} = E_M \times A_{CPC,May}$. [g] Electric energy required to complement the solar PF, where $E_L = Q_{UV} \times V_M \times 1000 - E_{CPC}$. [h] Number of UV lamps ($N_L$) that would be required to complement the solar PF: $N_L = \frac{N_{UV}}{\varphi \times t_{LO}}$, where $N_{UV}$ is the required number of photons, $N_{UV} = N_{ph} \times E_L \times 1000/3600$, $\varphi$ is the lamp photonic flux and $t_{LO}$ is the lamp operation time ($\varphi = 5.29 \times 10^{24}$ photons/h, with 4kW, in continuous operation during 8 h [12, 35].

## 5.3.4 Final biological oxidation

Three biological oxidation experiments were performed in batch mode (tests L, M and H) to determine the level of mineralization required for the photo-treated leachate, to ensure that the final effluent meets the COD discharge limit (COD < 150 mg/L [18]). According to the results (Figure 5.8), the batch tests L and M, fed with photo-treated leachate with COD of 566 and 446 mg/L (consumption of 8.9 and 34.4 mM of H$_2$O$_2$ and 3.3 and 5.5 kJ/L of accumulated UV energy),

respectively, did not reach the target COD value. In turn, experiment H reached the desired COD right after the second batch (H2) and for the batches H3 to H5 final COD values $\sim$ 120 mg/L were maintained. This represents an average COD removal of 54 % and consumption of 97 $\pm$ 5 mg COD/g VSS/d. This means that the prior PF stage should be performed until a COD value ~ 320 mg/L is reached, which is in accordance with the results from the Zahn-Wellens biodegradability test [12]. In this case, for experiment H, the photo-treatment was performed at T = 30 ºC, 60 mg $Fe^{2+}$/L, 74.6 mM $H_2O_2$, consuming an accumulated radiation energy of 8.9 kJ/L.
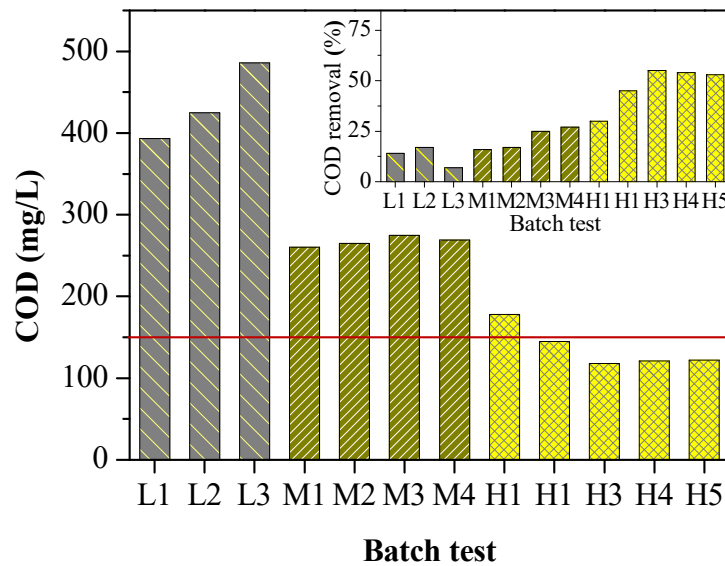


**Figure 5.8** – Evolution of the final COD concentrations and respective removal efficiencies (inner plot), for the biological oxidation batch experiments carried out with photo-treated leachate presenting different mineralization levels (▨) low: L1-L3, (▨) medium: M1-M4 and (▨) high: H1-H5.

Given the results obtained for the batch experiments, a biological oxidation in continuous mode was tested using a leachate previously treated by PF with 75 mM of $H_2O_2$. The photo-treated leachate used in these tests, presented a COD value of 390 mg/L, which is slightly higher than the one used for the batch experiment H, but lower than the batch experiment M. Notwithstanding, analysing the COD and TSS values of the overflow of the settling tank (Figure 5.9), it is possible to observe that the legal compliance was also attained. The average final COD and TSS concentrations were (i) 114 $\pm$ 9 and 51 $\pm$ 2 mg/L, respectively, for HRT = 24 h, and (ii) 107 $\pm$ 3 and 50 $\pm$ 2 mg/L, for HRT = 12 h. Therefore, operating the final biological oxidation at an HRT = 12 h, COD and TSS values were 24 and 28% below the legal limit, respectively. Moreover, the absence of inhibitory effects in the continuous flow biological reactor demonstrates that, under the correct operation of the previous treatment stages, the disposal of the pre-treated leachate in conventional

sewage system can be permitted. This is a pertinent issue for landfill and wastewater management, since a growing number of WWTPs have stopped accepting landfill leachate.
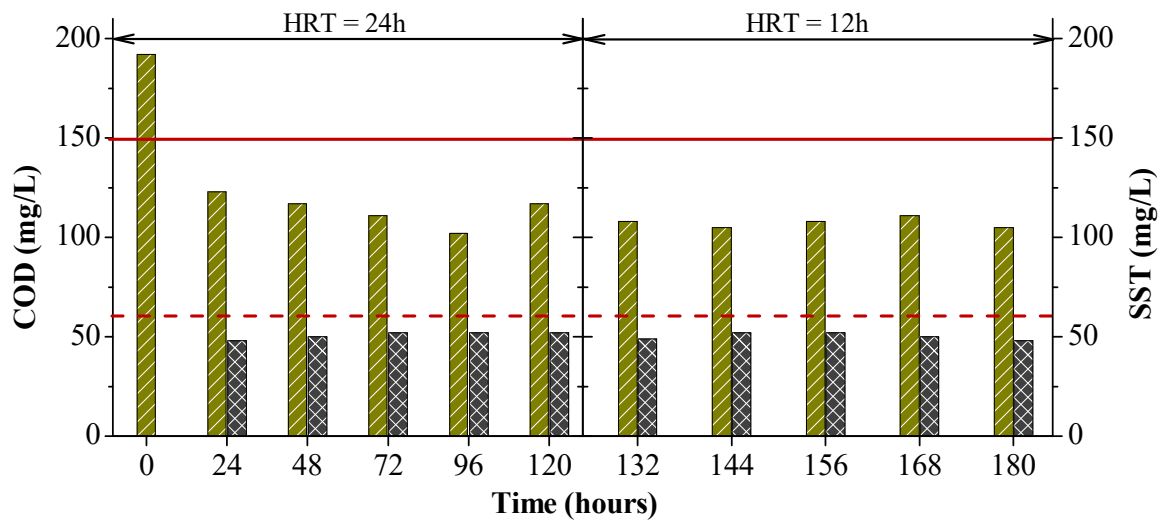


**Figure 5.9** – Evolution of (▨) COD and (▨ ) SST concentrations as a function of time, during the final biological oxidation in continuous mode, and representation of the legal limits for (▬) COD and (- - -) SST.

## 5.4 Conclusions

Legal compliance for mature landfill leachate direct discharge into waterbodies was successfully attained, using a treatment train combining biological with conventional and advanced physicochemical processes. From the present work, it was possible to conclude that, a leachate presenting high COD and TN content (3.6 g $O_2$/L and 2.0 g N/L) and low biodegradability ($BOD_5$/COD = 0.05) could be treated until simultaneously meeting the emission limit values (according to Portuguese legislation) for COD, TN, TSS and $SO_4^{2-}$, if the following steps/conditions were assured:

(i)     SBR operated in a 24h-cycle mode with a simple operational scheme (15h aeration, with ~ 0.5 mg $O_2$/L + 8.5h anoxic, with addition of methanol at COD/N ratio of 2.5 + 0.5h settling), and with volume exchange ratios of 14.3%, 16.4% and 21.4%, for operating temperatures of 20, 25 and 30 ºC, respectively, to reach a final TN < 15 mg N/L and low alkalinity values (1.1 g $CaCO_3$/L);

(ii)    Coagulation using $FeCl_3$ as the coagulant, dosed at 240 mg $Fe^{3+}$/L, with pH set at 3.0, to precipitate humic substances (DOC decrease > 60%) and remove suspended and colloidal matter (residual turbidity ≈ 33 NTU), to increase the efficiency of the following photo-treatment stage;

(iii)   Photo-Fenton performed with a catalyst dosage of 60 mg $Fe^{2+}$/ L and pH 2.8-3.0, until achieving a photo-treated leachate whose level of mineralization (COD ~ 400 mg/L) ensures compliance with the legal limit for COD after final biological oxidation;

(iv)    Biological oxidation operated in continuous mode, with an HRT of 12 h, to reach COD and TSS values below the legal limit.

## 5.5 References

1.  Renou, S., J.G. Givaudan, S. Poulain, F. Dirassouyan, and P. Moulin, *Landfill leachate treatment: review and opportunity.* Journal of Hazardous Materials, 2008. **150**: p. 468-493.

2.  Silva, T.F.C.V., M.E.F. Silva, A.C. Cunha-Queda, A. Fonseca, I. Saraiva, M.A. Sousa, C. Gonçalves, M.F. Alpendurada, R.A.R. Boaventura, and V.J.P. Vilar, *Multistage treatment system for raw leachate from sanitary landfill combining biological nitrification-denitrification/solar photo-Fenton/biological processes, at a scale close to industrial.* Water Research, 2013. **47**: p. 6167-6186.

3.  Christensen, T.H., P. Kjeldsen, P.L. Bjerg, D.L. Jensen, J.B. Christensen, A. Baun, H.-J. Albrechtsen, and G. Heron, *Biogeochemistry of landfill leachate plumes. Review.* Applied Geochemistry, 2001. **16**: p. 659-718.

4.  Rocha, E.M.R., V.J.P. Vilar, A. Fonseca, I. Saraiva, and R.A.R. Boaventura, *Landfill leachate treatment by solar-driven AOPs.* Solar Energy, 2011. **85**(1): p. 46-56.

5.  Li, H.-s., S.-q. Zhou, Y.-b. Sun, P. Feng, and J.-d. Li, *Advanced treatment of landfill leachate by a new combination process in a full-scale plant.* Journal of Hazardous Materials, 2009. **172**: p. 408-415.

6.  Oloibiri, V., M. Chys, S. De Wandel, K. Demeestere, and S.W.H. Van Hulle, Removal of organic matter and ammonium from landfill leachate through different scenarios: Operational cost evaluation in a full-scale case study of a Flemish landfill. Environmental Management, 2017. **203**: p. 774-781.

7.  Vilar, V.J.P., S.M.S. Capelo, T.F.C.V. Silva, and R.A.R. Boaventura, Solar photo-Fenton as a pre-oxidation step for biological treatment of landfill leachate in a pilot plant with CPCs. Catalysis Today, 2011. **161**(1): p. 228-234.

8.  Silva, T.F.C.V., A. Fonseca, I. Saraiva, R.A.R. Boaventura, and V.J.P. Vilar, Biodegradability enhancement of a leachate after biological lagooning using a solar driven photo-Fenton reaction, and further combination with an activated sludge biological process, at pre-industrial scale Water Research, 2013. **47**: p. 3543-3557.

9.  Silva, T.F.C.V., M.E.F. Silva, A.C. Cunha-Queda, A. Fonseca, I. Saraiva, R.A.R. Boaventura, and V.J.P. Vilar, Sanitary landfill leachate treatment using combined solar photo-Fenton and biological oxidation processes at pre-inductrial scale. Chemical Engineering Journal, 2013. **228**: p. 850-866.

10. Cassano, D., A. Zapata, G. Brunetti, G. Del Moro, C. Di Iaconi, I. Oller, S. Malato, and G. Mascolo, Comparison of several combined/integrated/biological-AOPs setups for the treatment of municipal landfill leachate: Minimization of operating costs and effluent toxicity. Chemical Engineering Journal, 2011. **172**: p. 250-257.

11. Moreira, F.C., J. Soler, A. Fonseca, I. Saraiva, R.A.R. Boaventura, E. Brillas, and V.J.P. Vilar, *Incorporation of electrochemical advanced oxidation processes in a multistage treatment system for sanitary landfill leachate.* Water Research, 2015. **81**: p. 375-387.

12. Silva, T.F.C.V., P.A. Soares, D.R. Manenti, A. Fonseca, I. Saraiva, R.A.R. Boaventura, and V.J.P. Vilar, *An innovative multistage treatment system for sanitary landfill leachate depuration: Studies at pilot-scale.* Science of the Total Environment, 2017. **576**: p. 99-117.

13. Oloibiri, V., I. Ufomba, M. Chys, W.T.M. Audenaert, K. Demeestere, and S.W.H. van Hulle, A comparative study on the efficiency of ozonation and coagulation-flocculation as pretreatment to activated carbon adsorption of biologically stabilized landfill leachate. Waste Management, 2015. **43**: p. 335-342.

14. Baiju, A., R. Gandhimathi, S.T. Ramesh, and P.V. Nidheesh, *Combined heterogeneous electro-Fenton and biological process for the treatment of stabilized landfill leachate.* Journal of Environmental Management, 2018. **210**: p. 328-337.

15. Silva, T.F.C.V., E. Vieira, A.R. Lopes, O.C. Nunes, A. Fonseca, I. Saraiva, R.A.R. Boaventura, and V.J.P. Vilar, How the performance of a biological pre-oxidation step can affect a downstream photo-Fenton process on the remediation of mature landfill leachates: Assessment of kinetic parameters and characterization of the bacterial communities. Separation and Purification Technology, 2017. **175**: p. 274-286.

16. Silva, T.F.C.V., R. Ferreira, P.A. Soares, D.R. Manenti, A. Fonseca, I. Saraiva, R.A.R. Boaventura, and V.J.P. Vilar, *Insights into solar photo-Fenton reaction parameters in the oxidation of a sanitary landfill leachate at lab-scale.* Journal of Environmental Management, 2015. **164**: p. 32-40.

17. Sawyer, C., P. McCarty, and G. Parkin, *Chemistry for Environmental Engineering ans Science.* 2003: McGraw-Hill Education.

18. in *Decree-law no. 236/98, of 1ˢᵗ August*, P. Republic, Editor. 1998: Republic Diary - I Series - A.

19. Anthonisen, A.C., R.C. Loehr, T.B.S. Prakasam, and E.G. Srinath, *Inhibition of nitrification by ammonia and nitrous acid.* Journal Water Pollution Control Federation, 1976. **48**: p. 835-852.

20. Ganigué, R., J. Gabarró, A.S. Melsió, M. Ruscalleda, H. López, X. Vila, J. Colprim, and M.D. Balaguer, Long-term operation of a partial nitritation pilot plant treating leachate with extremely high ammonium concentration prior to an anammox process. Bioresource Technology, 2009. **100**: p. 5624-5632.

21. Wett, B. and W. Rauch, The role of inorganic carbon limitation in biological nitrogen removal of extremely ammonia concentrated wastewater. Water Research, 2003. **37**: p. 1100-1110.

22. Guo, J., A.A. Abbas, Y. Chen, Z. Liu, F. Fang, and P. Chen, *Treatment of landfill leachate using a combined stripping, Fenton, SBR and coagulation process.* Journal of Hazardous Materials, 2010. **178**: p. 699-705.

23. Nyberg, U., B. Andersson, and H. Aspergren, *Long-term experiences witj external carbon sources for nitrogen removal.* Water Science and Technology, 1996. **33**(12): p. 109-116.

24. Nhat, P.T., H.N. Biec, T.T.T. Van, D.V. Tuan, N.L.H. Trung, V.T.K. Nghi, and N.P. Dan, *Satbility of partial nitrification in a sequencing batch reactor fed with high ammonium strenght old urban landfill leachate.* International Biodeterioriation & Biodegradation, 2017. **124**: p. 56-61.

25. Spagni, A., M.C. Lavagnolo, C. Scarpa, P. Vendrame, A. Rizzo, and L. Luccarini, *Nitrogen removal optimization in a sequencing batch reactor treating sanitary landfill leachate.* Journal of Environmental Science and Health A, 2007: p. 757-765.

26. Spagni, A. and S. Marsili-Libelli, Nitrogen removal via nitrite in a sequencing batch reactor treating sanitary landfill leachate. Bioresource Technology, 2009. **100**(2): p. 609-614.

27. Jokela, J.P.Y., R.H. Kettunen, K.M. Sormunen, and J.A. Rintala, Biological nitrogen removal from municipal landfill leachate: low-cost nitrification in biofilters and laboratory scale in-situ denitrification. Water Research, 2002. **36**: p. 4079-4087.

28. Kulikowska, D. and K. Bernat, *Nitritation-denitritation in landfill leachate with glycerine as a carbon source.* Bioresource Technology, 2013. **142**: p. 297-303.

29. Metcalf and Eddy, Wastewater engineering, treatment and reuse. 2003: McGraw-Hill.

30. Daud, Z., A.A.A. Latif, and L.M. Rui, *Coagulation-flocculation in leachate treatment by using ferric chloride and alum as coagulant.* International Journal of Engineering Research and Applications, 2012. **2**(4): p. 1929-1934.

31. Rui, L.M., Z. Daud, and A.A.A. Latij, *Treatment of leachate by coagulation-flocculation using different coagulants and polymer: A review.* International Journal on Advanced Science Engineering and Information Technology, 2012. **2**(2).

32. Vedrenne, M., R. Vasquez-Medrano, D. Prato-Garcia, B.A. Frontana-Uribe, and J.G. Ibanez, Characterization and detoxification of a mature landfill leachate using combined coagulation-flocculation/photo-Fenton treatment. Journal of Hazardous Materials, 2012. **205-206**: p. 208-215.

33. Amor, C., E. Torres-Socías, J.A. Peres, M.I. Maldonado, I. Oller, S. Malato, and M.S. Lucas, *Mature landfill leachate treatment by coagulation/flocculation combined with Fenton and solar photo-Fenton processes.* Journal of Hazardous Materials, 2015. **286**: p. 261-268.

34. Soares, P.A., T.F.C.V. Silva, D.R. Manenti, S.M.A.G.U. Souza, R.A.R. Boaventura, and V.J.P. Vilar, *Insights into real cotton-textile dyeing wastewater treatment using solar advanced oxidation processes.* Environmental Science and Pollution Research, 2014. **21**: p. 932-945.

35. Silva, T.F.C.V., A. Fonseca, I. Saraiva, R.A.R. Boaventura, and V.J.P. Vilar, *Scale-up and cost analysis of a photo-Fenton system for sanitary landfill leachate treatment.* Chemical Engineering Journal, 2016. **283**: p. 76-88.

# 6 Treatment train technology for leachate from mature urban landfill: Full-scale operation performance and challenges

*This chapter presents the application of the treatment train strategy, at full-scale, in a compact facility located at a municipal urban waste landfill comprising the following treatment units: (i) a first biological reactor (BR1); (ii) a coagulation and photo-treatment unit (C/P) and (iii) a final biological reactor (BR2). The treatment train facility also includes a sludge tank (ST), a filter-press system and a drainage tank for the treatment of the produced sludge.*

*Glycerol, a waste-product from biodiesel production, was successfully employed as an external carbon source for denitrification purposes. The coagulation sedimentation (C/S) and photo-Fenton (PF) stages were conducted in the same tank, which was coupled to an innovative artificial photoreactor (4 FluHelik connected in series), thus enabling a compact solution for the multistage facility. The major operational difficulties were found in the: (i) C/S stage, due to the production of dense foam that trapped the sludge; and (ii) PF stage, for iron precipitation. These problems were overcome, respectively, with: (i) sludge removal after nitrite oxidation with hydrogen peroxide (intermediate step prior to PF); and (ii) maintenance of a residual amount of $H_2O_2$ before neutralization step.*

*Each treatment sequence was applied to ca. 30 $m^3$ of urban leachate after an aerated lagoon, leading to global removal efficiencies of 98% for COD (from 8.30 to 0.15 g $O_2$/L), 97% for DOC (from 2.32 to 0.08 g C/L) and 85% for TN (from 2.65 to 0.41 g N/L). The sludge produced was also treated in-situ and compliance with legal disposal standards was achieved. The average total operational cost for the complete treatment sequence was 6.7 €/$m^3$, including chemicals, energy consumption, sludge treatment and respective disposal.*

This Chapter is based on the following research article: "Gomes, A.I., Foco, M.L.R., Vieira, E., Cassidy, J., Silva, T.F.C.V., Fonseca, A., Isabel, S. Boaventura, R.A.R., Vilar, V.J.P. *Multistage treatment technology for leachate from mature urban landfill: Full scale operation performance and challenges.* Chemical Engineering Journal 376 (2019) 120573

## 6.1 Introduction

In 2017, Silva*, et al.* [1] proposed a multistage treatment system for leachates from mature municipal landfills (European Patent – EP 2784031A1), combining biological and physicochemical processes, including a photocatalytic advanced oxidation step (photo-Fenton), in order to achieve a final effluent in compliance with the legal discharge requirements. As mentioned in previous chapters, this strategy was partially tested at pilot-scale and proved to be effective for TAN and COD removal up to values below the legal standards for direct discharge. However, the removal of the high TN content of the leachate was not undertaken, nor the final biological reactor was fully assessed. Furthermore, the photo-oxidation stage presented major drawbacks when aiming at a full-scale application, particularly with respect to the land area requirements and investment costs associated with the traditional compound parabolic collectors, even when combining solar and artificial radiation. Therefore, some improvements were suggested [1], namely, to (i) include a denitrification step in the biological reactor and (ii) optimize the artificial photoreactor. Considering the first, optimization studies for the complete treatment train strategy were carried out at lab-scale (described in Chapter 5) and established, for each treatment stage, the operational conditions required to ensure the fulfilment of both COD and TN contents up to the legal levels for direct discharge into waterbodies (according to the Portuguese legislation, Table 2.6 of Chapter 2). Regarding the second, Vilar and co-workers [2-4] developed an annular channel photoreactor, named FluHelik, to promote photochemical ($UVC/H_2O_2$) and photocatalytic ($Fe^{2+}/H_2O_2/UV$-$Vis$) processes. The FluHelik photoreactor comprises a cylindrical shell of stainless steel, internally polished, with inlet and outlet pipes located perpendicularly to the fluid flow and tangentially to the shell in horizontal plane and at the top in opposite sides. A concentric inner quartz sleeve houses an UV or UV-Vis lamp, according to the intended treatment process. This configuration promotes a helical motion of fluid around the lamp, inducing: (i) intense dynamics of macromixing because of larger velocity gradients and turbulent intensities and (ii) a homogeneous radiation distribution [3]. The FluHelik reactor design also favours the implementation of various reactors in series, promoting its application at industrial scale.

In the present work, the complete treatment train for a mature urban landfill leachate was operated at full-scale, using an innovative artificial photoreactor for photo-Fenton stage, which enabled a compact and modular solution. The treatment train strategy was similar as described for Chapter 5: a first biological reactor (BR1), a coagulation and photo-treatment unit (C/P) and a final biological reactor (BR2). However the following differences must be pointed out: (i) in a cost-saving perspective, glycerol was used as external carbon source and, to the best of our knowledge, it is the first time that it is tested at full-scale for the denitrification of a high-strength wastewater such as

leachate; (ii) C/S and PF stages occurred in the same treatment tank, which was coupled to 4 FluHelik photoreactors connected in series. In addition, the dewatering of the produced sludge during the treatment was evaluated using pressure filtration. Finally, based on the full-scale operational conditions, a cost analysis for the treatment train of the leachate, including the treatment and disposal of the produced sludge, is presented.

## 6.2 Materials and methods

All the chemicals used in this work, the detailed description of the experimental units and respective procedures, as well as the analytical methods employed, can be consulted, respectively, in sections 4.1, 4.3.2 and 4.2 of Chapter 4. Some determinations were carried out *in situ* (treatment monitoring), such as $SSV_{30}$, turbidity (860 nm), concentration of total dissolved iron (TDI) and $H_2O_2$. Remaining analytical characterization was conducted at the laboratory.

A total of 19 trials were performed using the complete treatment train sequence. The operational time scheme applied to BR1 and BR2 are displayed in Table 6.1. The most relevant operational and technical problems that occurred during the trials are listed in Table 6.2.

**Table 6.1 –** Operational time scheme applied to BR1 and BR2.

| BR1 | | | | | | | | | | BR2 | | | | | | | | |
|---|---|---|---|---|---|---|---|---|---|---|---|---|---|---|---|---|---|---|
| **Trial** | **Time scheme aerobic/anoxic phase (days)** | | | | | | | | | **Trial** | **Time scheme aerobic/anoxic phase (days)** | | | | | | | |
| | **1** | **2** | **3** | **4** | **5** | **6** | **7** | **8** | | | **1** | **2** | **3** | **4** | **5** | **6** | **7** | **8** |
| 1 | | | | | | | | | | 1 | | | | | | | | |
| 2 | | | | | | | | | | 2 | | | | | | | | |
| 3 | | | | | | | | | | 3 | | | | | | | | |
| 4 | | | | | | | | | | 4 | | | | | | | | |
| 5 | | | | | | | | | | 5 | | | | | | | | |
| 6 | | | | | | | | | | 6 | | | | | | | | |
| 7 | | | | | | | | | | 7 | | | | | | | | |
| 8 | | | | | | | | | | 8 | | | | | | | | |
| 9 | | | | | | | | | | 9 | | | | | | | | |
| 10 | | | | | | | | | | 10 | | | | | | | | |
| 11 | | | | | | | | | | 11 | | | | | | | | |
| 12 | | | | | | | | | | 12 | | | | | | | | |
| 13 | | | | | | | | | | 13 | | | | | | | | |
| 14 | | | | | | | | | | 14 | | | | | | | | |
| 15 | | | | | | | | | | 15 | | | | | | | | |
| 16 | | | | | | | | | | 16 | | | | | | | | |
| 17 | | | | | | | | | | 17 | | | | | | | | |
| 18 | | | | | | | | | | 18 | | | | | | | | |
| 19 | | | | | | | | | | 19 | | | | | | | | |

☐ Aerobic period ▨ Anoxic period * Glycerol addition
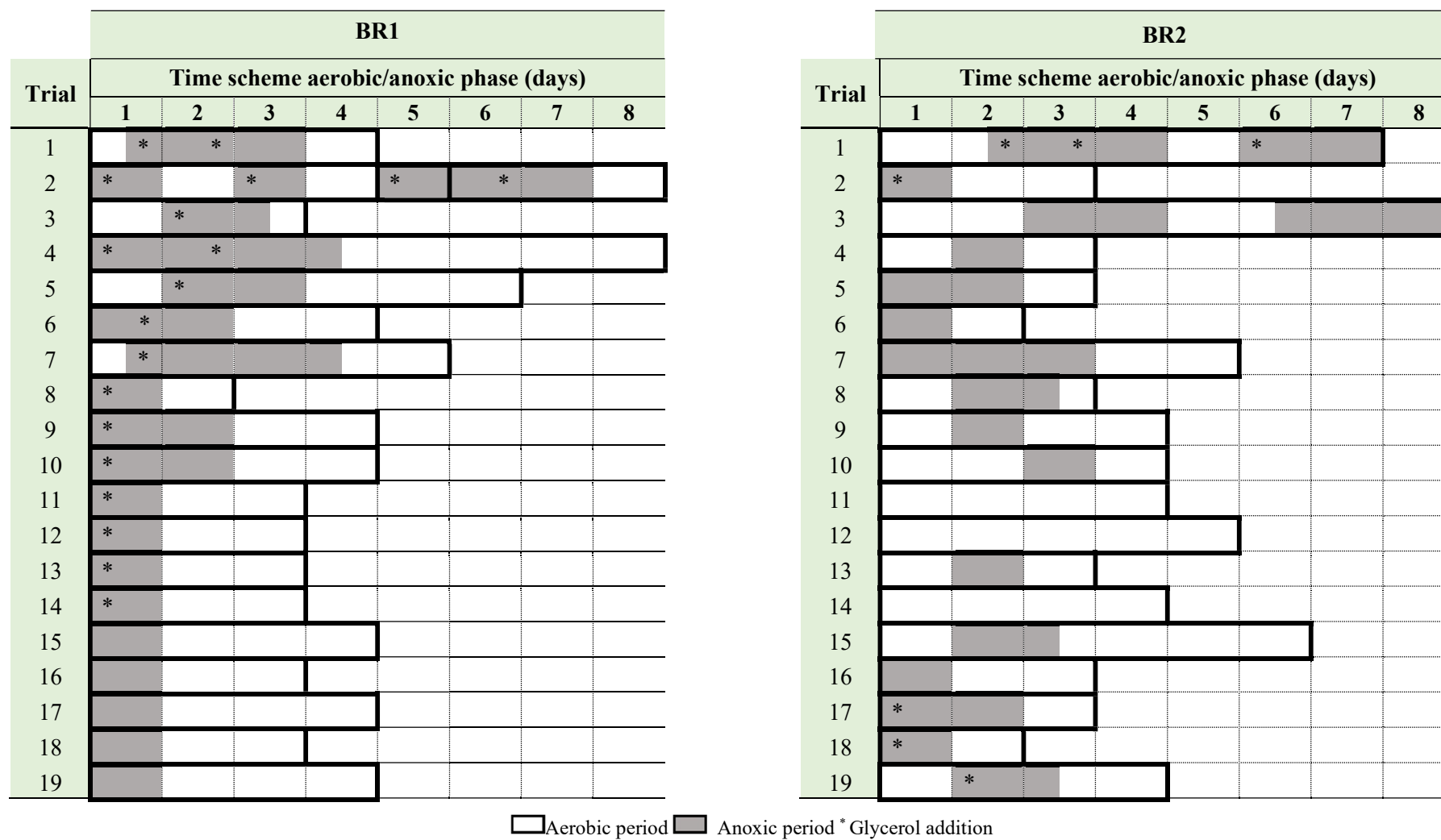
**Table 6.2** – List of operational problems and technical constrains for each treatment unit, at full-scale facility.

| Treatment unit | Trial(s) | Operational problems and technical constrains |
|---|---|---|
| BR1 | Start-up | Spill of reactor during the night, due to intense foam production during aeration (day 22). Solution: anti-foaming addition prior to aeration period.<br>Drawn of leachate without previous sedimentation (day 55). |
| | 1 | Due to glycerol viscosity it was required to install a progressive cavity pump. |
| | 4, 6-9 | Occurrence of electrical failure that led to the shutdown of the entire facility for periods longer than 12h (during the night or weekends). |
| | 5 | Floating sludge resulting from the addition of filtrate coming from the sludge treatment containing high polymer dosage. From this point forward the filtrate from the sludge filter press was only reintroduced at the coagulation unit. |
| C/P | All trials | Time-limited coagulant addition, once the coagulant inlet was located at the C/P feeding tube, therefore, it was necessarily carried out simultaneously with the transference of bio-treated-leachate to C/P unit. Moreover, variations of coagulant dosage were due to occasional air pockets within the hose that connected the dosing pump and the coagulant inlet, thus creating variable resistance to coagulant passage.<br><br>Turbulence created with the transference of the bio-treated-leachate led to a high dense foam production at the surface, trapping the particulate matter. |
| | 1-2 | Problem with acid dosing pump: (i) no acidification at trial 1, (ii) long acidification time at trial 2. |
| | 2-4; 16-18 | Problems with sludge treatment system (partial clogging of the filter plates and sludge admission pump failure) led to a long coagulation/sedimentation time, due to the impossibility to remove the sludge. |
| | 16 | pH probe malfunctioning. |
| BR2 | 2-3 | After the discharge of trial 2, BR2 was 69 h working with minimum volume, since the problems with sludge treatment led to a longer coagulation stage period due to the impossibility to remove the sludge. |
| | 4, 6 | Occurrence of electrical failure, during the night or weekend, which led to the shutdown of the entire facility for periods longer than 12h. |
| | 7 | Failure of mechanical stirrer. The reactor had to be completely emptied for removal of the mechanical stirrer which was subsequently replaced with a new. |
| Filter Press | | Excessive polymer addition led to partial clogging of the filter plates. High pressure jet cleaning was required and the sludge treatment stopped for a few days. |
| | | Sludge admission pump failure. Treatment was restarted after substitution of pump rotor. |

## 6.3 Results and discussion

### 6.3.1 Influent leachate characterization

During the treatment period, the influent leachate, coming from the aerated lagoon, presented great variability (Table 6.3). One of the main variations was biodegradability: (i) $BOD_5/COD$ ratio < 0.2, for trials 1-14 and, (ii) $BOD_5/COD$ ratio > 0.3, from trial 15 forward. Also, from trial 10, a gradual increase in both total ammonia nitrogen ($NH_4^+$-N) and dissolved inorganic carbon (DIC) concentrations, and a decrease of nitrite ($NO_2^-$-N) concentration was observed. These differences could be related to the [5]: (i) variability of raw leachate coming to the aerated lagoon; (ii) seasonality (influence of temperature and precipitation); and (iii) aerated lagoon treatment efficiency. Indeed, problems were detected in the lagoon aerators during trials 10-14, which stopped working during trials 15-19. Consequently, the oxidation of biodegradable organic matter and ammonia was conditioned when the aeration problems occurred.

### 6.3.2 Biological reactor 1

#### 6.3.2.1 Start-up period

BR1 was inoculated with biomass from the activated sludge tank of the landfill LTP and periodically fed with leachate from the aerated lagoon. During this start-up period, the influent leachate presented high concentration of TAN (1.2 to 1.8 g $NH_4^+$-N/L, corresponding to 85-96% of the total nitrogen, high COD content (2.4 to 4.6 g $O_2$/L) and low biodegradability ($BOD_5/COD$ ratio < 0.2). BR1 was firstly operated to promote nitrification and the oxidation of ammonia to nitrite was detected 11 days after inoculation (Figure 6.1). From this point forward, nitrification presented an average rate of 0.17 kg $NH_4^+$-N/kg VSS/day and an estimated alkalinity consumption of 6.1-7.4 kg $CaCO_3$/kg $NH_4^+$-N oxidized, which is in agreement with the stoichiometric requirement (7.1 kg $CaCO_3$/kg $NH_4^+$-N). Consequently, nitrite concentration in BR1 increased. Given the leachate's low biodegradability, associated with the presence of recalcitrant organic compounds, methanol was added to promote denitrification. The denitrification attained an average rate of 0.07 kg N/kg VSS/day and an estimated consumption of 1.7-2.1 kg COD/kg N removed (stoichiometric ratio of 1.72 kg COD/kg $NO_2^-$-N). With the establishment of both nitrification and denitrification processes, and a biomass concentration of 1.5 g VSS/L (growth rate of $0.014 \pm 0.003$ g VSS/day, Figure 6.1), the BR1 start-up period was completed.

**Table 6.3** – Physicochemical characterization of the BR1 influent leachate.

| Trial | $V_F$[a] (m³) | VER[a] (%) | DOC (mg/L) | DIC (mg/L) | Alkalinity[b] (g CaCO₃/L) | BOD₅ (mg/L) | COD (mg/L) | $\frac{BOD_5}{COD}$ | TN[c] (mg/L) | $NH_4^+$-N (mg/L) | $NO_2^-$-N (mg/L) | $NO_3^-$-N (mg/L) | $SO_4^{2-}$ (mg/L) | TSS (mg/L) | VSS (mg/L) |
|---|---|---|---|---|---|---|---|---|---|---|---|---|---|---|---|
| 1 | 28.0 | 42.3 | 1122 | 1318 | 5.5 | 300 | 3596 | 0.08 | 1607 | 1219 | 366 | 12 | 193 | 765 | 455 |
| 2 | 28.0 | 40.6 | 1083 | 1174 | 4.9 | 240 | 3466 | 0.07 | 1680 | 1058 | 566 | 26 | 241 | 553 | 372 |
| 3 | 21.0 | 31.4 | 1077 | 871 | 3.7 | 480 | 3549 | 0.14 | 1740 | 962 | 730 | 11 | 140 | 340 | 288 |
| 4 | 22.0 | 34.8 | 1153 | 625 | 2.6 | 340 | 3154 | 0.11 | 1827 | 858 | 949 | 8 | 131 | 784 | 550 |
| 5 | 28.0 | 41.9 | 1416 | 650 | 2.7 | 240 | 3469 | 0.07 | 2116 | 1103 | 932 | 14 | 344 | 405 | 290 |
| 6 | 30.0 | 44.8 | 1489 | 810 | 3.4 | 300 | 3923 | 0.08 | 2258 | 1228 | 877 | 15 | 246 | 775 | 405 |
| 7 | 30.0 | 44.8 | 1632 | 865 | 3.6 | 240 | 3949 | 0.06 | 2275 | 1336 | 896 | 20 | 249 | 810 | 440 |
| 8 | 30.0 | 44.5 | 1597 | 750 | 3.1 | 180 | 4536 | 0.04 | 1980 | 1384 | 490 | 7 | 286 | 800 | 425 |
| 9 | 30.0 | 45.6 | 1494 | 999 | 4.2 | 220 | 4328 | 0.05 | 1997 | 1443 | 511 | 16 | 297 | 690 | 377 |
| 10 | 30.0 | 45.6 | 1565 | 1393 | 5.8 | 420 | 4152 | 0.10 | 1830 | 1707 | 15 | 42 | 337 | 489 | 398 |
| 11 | 30.0 | 45.6 | 1588 | 1448 | 6.1 | 460 | 4288 | 0.11 | 1843 | 1726 | 96 | 10 | 413 | 452 | 343 |
| 12 | 30.0 | 45.6 | 1603 | 1466 | 6.1 | 520 | 4088 | 0.13 | 1925 | 1805 | 84 | 8 | 613 | 412 | 327 |
| 13 | 30.0 | 45.6 | 1618 | 1484 | 6.2 | 580 | 3991 | 0.15 | 1992 | 1884 | 72 | 6 | 812 | 372 | 310 |
| 14 | 30.0 | 45.6 | 1630 | 1406 | 5.9 | 600 | 3834 | 0.16 | 2093 | 1980 | 41 | 4 | 999 | 374 | 317 |
| 15 | 30.0 | 45.6 | 2210 | 1373 | 5.8 | 2150 | 6317 | 0.34 | 2127 | 1945 | 45 | < 1 | 753 | 694 | 577 |
| 16 | 30.0 | 45.6 | 2359 | 1389 | 5.8 | 3000 | 7013 | 0.43 | 2121 | 1969 | 39 | 5 | 761 | 506 | 394 |
| 17 | 30.0 | 45.6 | 2464 | 1467 | 6.1 | 3100 | 7451 | 0.42 | 2164 | 2064 | 35 | 3 | 703 | 860 | 667 |
| 18 | 30.0 | 45.6 | 2402 | 2119 | 8.9 | 3700 | 7923 | 0.47 | 2514 | 2433 | 39 | 3 | 677 | 1340 | 990 |
| 19 | 30.0 | 45.6 | 2325 | 2207 | 9.2 | 3900 | 8302 | 0.47 | 2648 | 2480 | 40 | 2 | 652 | 1294 | 963 |

[a] VF - Filling volume to BR1; VER – volume exchange ratio. [b] Alkalinity values considering that at pH < 11 the inorganic carbon was in the form of carbonates and bicarbonates [6]; [c] Total dissolved nitrogen.
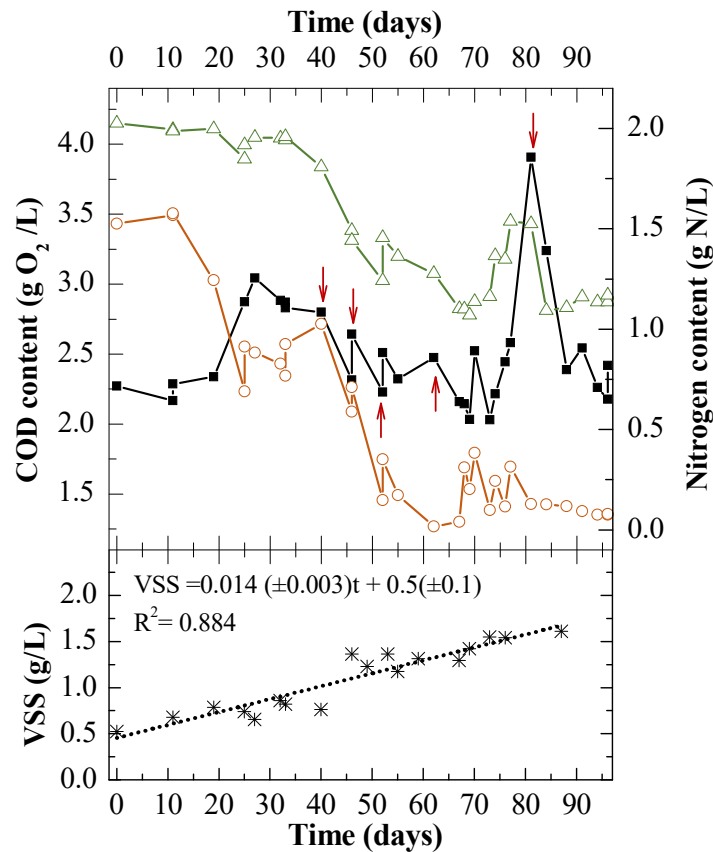
**Figure 6.1** – BR1 start-up period evolution profile for COD (■), methanol addition (↑), total nitrogen (△), ammonium nitrogen (○) and VSS content (✳).

### 6.3.2.2 Treatment period

In accordance with the treatment train strategy, the main objectives of BR1 were to (i) oxidize the existing biodegradable organic matter, (ii) remove nitrogen, by promoting nitrification and denitrification through aeration/anoxic cycles (Table 6.1), and (iii) guarantee the lowest alkalinity possible, in view of acidification requirements for the following stage. It should be mention that, at the beginning of BR1 trials (Table 6.4), the nitrogen and organic contents were lower than those of the influent leachate. There was an average decrease of (i) $65 \pm 1\%$ and $44 \pm 3\%$, respectively, for ammonia and TN (Figure 6.2-a -b), and (ii) $22 \pm 2\%$ and $24 \pm 3\%$, for DOC and COD (Figure 6.2-d -e). With a fill/discharge volume of 30 m$^3$, for a total react volume of ca. 66 m$^3$ (Table 6.5), the dilution effect provided by the SBR type reactor makes it a suitable choice to be used as the first unit for the leachate treatment, as it: (i) decreases the influent toxic load; and (ii) enables, to some extent, the mitigation of the influent's high variability. Another advantage is the occurrence of both nitrification and denitrification processes in a single treatment unit, which is an optimized smart

technical approach to achieve a compact facility. It is worth to notice that, when the influent presented low biodegradability (trials 1-14), there was an average decrease of $16 \pm 1\%$, for both DOC and COD (Figure 6.2-d -e), whereas for trials 15-19 (influent $BOD_5/COD > 0.3$) these values were $38 \pm 2\%$ and $45 \pm 3\%$, respectively. Thus, the organic matter consumption during BR1 was dependent on the biodegradability of the influent. Throughout all trials, the BR1 temperature ranged from 20-28 ºC and the biomass presented a good settleability, with an SVI always lower than 100 mL/g (data not shown) and a concentration between 1.4-5.9 g VSS/L (Table 6.5).
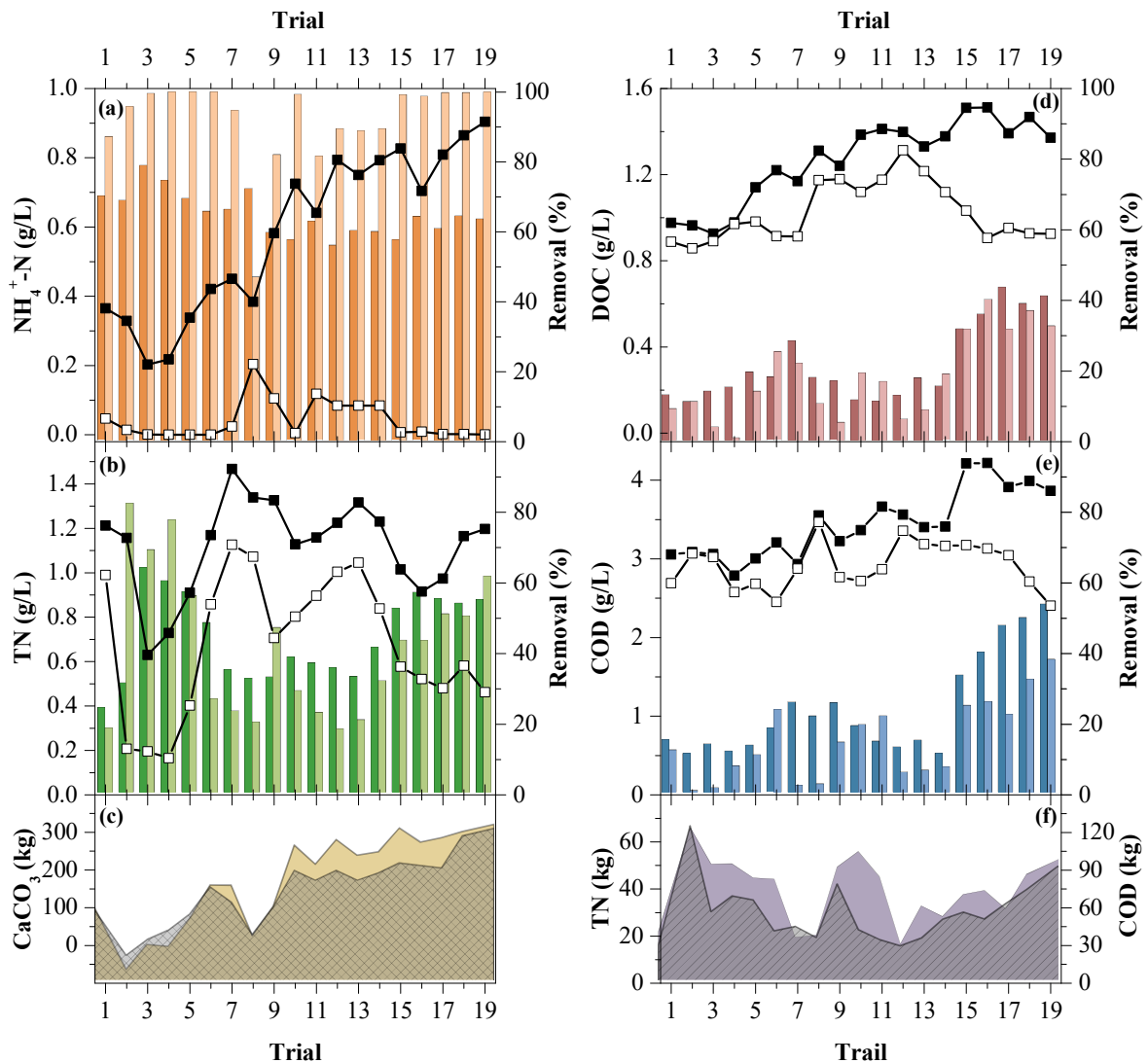


**Figure 6.2** – Evolution profile of (a) $NH_4^+$-N, (b) TN, (d) DOC and (e) COD concentrations of the leachate at the beginning (■) and at the end (□) of BR1 stage, including initial decrease (▨, ▨, ▨, ▨) and treatment removal (▨, ▨, ▨, ▨); and comparison between the balance of the amount of (c) measured (▨) and theoretical $CaCO_3$ (▨), (f) TN removed (▨) and COD consumed (▨).

**Table 6.4** – Physicochemical characterization of the leachate at the beginning of BR1.

| Trial | pH | DOC (mg/L) | DIC (mg/L) | Alkalinity[a] (g CaCO$_3$/L) | BOD$_5$ (mg/L) | COD (mg/L) | $\dfrac{BOD_5}{COD}$ | TN (mg/L) | NH$_4^+$-N (mg/L) | NO$_2^-$-N (mg/L) | NO$_3^-$-N (mg/L) | SO$_4^{2-}$ (mg/L) | TSS (mg/L) | VSS (mg/L) |
|---|---|---|---|---|---|---|---|---|---|---|---|---|---|---|
| 1 | 7.8 | 797 | 336 | 1.4 | n.d. | 2231 | n.d. | 1212 | 365 | 831 | 16 | 154 | 2130 | 1430 |
| 2 | 7.5 | 857 | 458 | 1.9 | n.d. | 2725 | n.d. | 1157 | 329 | 720 | 35 | 209 | 2475 | 1718 |
| 3 | 7.9 | 861 | 453 | 1.9 | 250 | 3062 | 0.08 | 630 | 203 | 417 | 9 | 223 | 3179 | 1988 |
| 4 | 7.9 | 978 | 522 | 2.1 | 290 | 2786 | 0.10 | 729 | 218 | 411 | 6 | 237 | 3908 | 2420 |
| 5 | 7.6 | 1141 | 499 | 2.1 | 380 | 3005 | 0.13 | 910 | 338 | 473 | 14 | 352 | 3495 | 2190 |
| 6 | 7.8 | 1221 | 530 | 2.2 | 300 | 3208 | 0.09 | 1169 | 421 | 575 | 8 | 266 | 3220 | 2230 |
| 7 | 7.7 | 1170 | 397 | 1.7 | 130 | 2934 | 0.04 | 1467 | 450 | 806 | 11 | 275 | 3695 | 2340 |
| 8 | 8.2 | 1311 | 379 | 1.6 | 120 | 3553 | 0.03 | 1339 | 384 | 947 | 7 | 286 | 4040 | 2620 |
| 9 | 8.2 | 1546 | 588 | 2.5 | 380 | 4139 | 0.09 | 1326 | 582 | 612 | 2 | 252 | 4204 | 2840 |
| 10 | 8.3 | 1385 | 784 | 3.3 | 160 | 3366 | 0.05 | 1128 | 725 | 333 | 5 | 254 | 4368 | 3062 |
| 11 | 8.1 | 1412 | 758 | 3.2 | 470 | 3665 | 0.13 | 1158 | 641 | 282 | < 1 | 325 | 4480 | 3130 |
| 12 | 8.0 | 1398 | 723 | 3.0 | 470 | 3563 | 0.13 | 1225 | 794 | 429 | 0 | 458 | 4430 | 3300 |
| 13 | 7.8 | 1331 | 630 | 2.6 | 490 | 3402 | 0.14 | 1316 | 750 | 498 | 18 | 604 | 4330 | 3430 |
| 14 | 8.1 | 1378 | 682 | 2.8 | 320 | 3411 | 0.09 | 1230 | 793 | 436 | 1 | 815 | 4641 | 3620 |
| 15 | 8.1 | 1510 | 815 | 3.4 | 420 | 4215 | 0.10 | 1015 | 827 | 81 | < 1 | 804 | 5300 | 4030 |
| 16 | 8.1 | 1512 | 843 | 3.5 | 2450 | 4220 | 0.58 | 915 | 704 | 24 | 6 | 752 | 5800 | 4260 |
| 17 | 8.5 | 1392 | 896 | 3.7 | 2100 | 3912 | 0.54 | 974 | 809 | 76 | < 1 | 795 | 6040 | 4570 |
| 18 | 7.9 | 1468 | 1156 | 4.8 | 1700 | 3992 | 0.43 | 1165 | 865 | 166 | 2 | 721 | 7467 | 5450 |
| 19 | 8.3 | 1371 | 1290 | 5.4 | 2100 | 3864 | 0.54 | 1197 | 904 | 24 | 1 | 738 | 7830 | 5860 |

[a] Alkalinity values considering that at pH < 11 the inorganic carbon was in the form of carbonates and bicarbonates [7].

n.d. – not determined.

**Table 6.5** – Operating conditions for BR1 and physicochemical characterization of the bio-treated leachate.

| Trial | $V_T{}^a$ (m³) | $V_{SD}{}^b$ (m³) | $V_D{}^c$ (m³) | $t_R{}^d$ (d) | $t_S{}^e$ (h) | $O_2{}^f$ (kg) | $C_3H_8O_3{}^g$ (mg O₂/L) | VSS (mg/L) | pH | DOC (mg/L) | DIC (mg/L) | Alkalinity[h] (g CaCO₃/L) | COD (mg/L) | TN (mg/L) | $NH_4^+$-N (mg/L) | $NO_2^-$-N (mg/L) | $NO_3^-$-N (mg/L) | $SO_4^{2-}$ (mg/L) | TSS (mg/L) | VSS (mg/L) |
|---|---|---|---|---|---|---|---|---|---|---|---|---|---|---|---|---|---|---|---|---|
| | | | | | | | | | | | | | | | | | | | | |
| 1 | 66.2 | 3.4 | 30.0 | 4 | 4 | 149 | 1040 | 1430 | 7.0 | 888 | 32 | 0.1 | 2690 | 990 | 47 | 903 | 40 | 195 | 543 | 365 |
| 2 | 69.0 | 4.8 | 25.8 | 8 | 5 | 242 | 2110 | 1718 | 9.2 | 858 | 489 | 2.2 | 3069 | 207 | 14 | 119 | 8 | 199 | 174 | 157 |
| 3 | 66.8 | 2.6 | 30.0 | 3 | 4 | 116 | 1350 | 1988 | 8.9 | 891 | 430 | 1.8 | 3023 | 196 | 1 | 193 | 2 | 202 | 414 | 312 |
| 4 | 63.3 | 4.5 | 26.4 | 4 | 20* | 446 | 1260 | 2420 | 8.3 | 971 | 378 | 1.6 | 2577 | 165 | < 1 | 147 | 17 | 261 | 369 | 220 |
| 5 | 66.9 | 2.0 | 30.0 | 6 | 4 | 274 | 900 | 2190 | 8.5 | 982 | 249 | 1.0 | 2684 | 402 | < 1 | 397 | 5 | 295 | 253 | 163 |
| 6 | 66.9 | n.a. | 30.0 | 4 | 20* | 111 | 450 | 2230 | 7.9 | 914 | 8 | < 0.1 | 2454 | 858 | < 1 | 792 | 9 | 302 | 650 | 305 |
| 7 | 66.9 | n.a. | 29.5 | 5 | 20* | 123 | 450 | 2340 | 7.0 | 913 | 13 | < 0.1 | 2876 | 1126 | 24 | 1017 | 11 | 308 | 255 | 160 |
| 8 | 67.4 | n.a. | 31.7 | 2 | 75* | 58 | 450 | 2620 | 7.3 | 1174 | 314 | 1.2 | 3468 | 1072 | 204 | 842 | 26 | 290 | 233 | 200 |
| 9 | 65.8 | n.a. | 30.0 | 4 | 20* | 158 | 915 | 2840 | 8.7 | 1179 | 267 | 1.1 | 2768 | 706 | 105 | 544 | 10 | 219 | 650 | 498 |
| 10 | 65.8 | n.a. | 30.0 | 4 | 2 | 276 | 915 | 3062 | 7.9 | 1120 | 83 | 0.3 | 2718 | 802 | 5 | 715 | 8 | 276 | 572 | 390 |
| 11 | 65.8 | n.a. | 30.0 | 3 | 4 | 149 | 460 | 3130 | 7.5 | 1176 | 161 | 0.6 | 2868 | 896 | 118 | 664 | 18 | 352 | 580 | 385 |
| 12 | 65.8 | n.a. | 30.0 | 3 | 3 | 162 | 230 | 3300 | 6.6 | 1313 | 12 | < 0.1 | 3358 | 1004 | 84 | 883 | 7 | 420 | 775 | 598 |
| 13 | 65.8 | n.a. | 30.0 | 3 | 3 | 202 | 685 | 3430 | 6.8 | 1216 | 10 | < 0.1 | 3188 | 1045 | 84 | 819 | 4 | 602 | 668 | 475 |
| 14 | 65.8 | n.a. | 30.0 | 3 | 4 | 202 | 525 | 3620 | 6.7 | 1119 | 8 | < 0.1 | 3165 | 839 | 84 | 754 | 1 | 784 | 560 | 440 |
| 15 | 65.8 | n.a. | 30.0 | 4 | 2 | 353 | n.a. | 4030 | 7.8 | 1033 | 42 | 0.2 | 3176 | 577 | 7 | 557 | 13 | 776 | 370 | 294 |
| 16 | 65.8 | n.a. | 30.0 | 3 | 2 | 322 | n.a. | 4260 | 7.6 | 906 | 91 | 0.4 | 3132 | 521 | 9 | 465 | 4 | 803 | 213 | 174 |
| 17 | 65.8 | n.a. | 30.0 | 4 | 3 | 337 | n.a. | 4570 | 8.1 | 952 | 172 | 0.7 | 3046 | 480 | 2 | 455 | 5 | 821 | 306 | 253 |
| 18 | 65.8 | n.a. | 30.0 | 3 | 3 | 251 | n.a. | 5450 | 7.8 | 927 | 119 | 0.5 | 2710 | 581 | 2 | 560 | 4 | 799 | 282 | 180 |
| 19 | 65.8 | n.a. | 30.0 | 4 | 3 | 278 | n.a. | 5860 | 8.0 | 925 | 195 | 0.8 | 2404 | 462 | 1 | 459 | 3 | 769 | 236 | 170 |

[a] Total volume. [b] Drainage from sludge treatment fed to BR1. [c] Discharged volume. [d] SBR react time. [e] Sedimentation time. [f] Amount of oxygen supplied during the aerobic phase.

[g] Glycerol provided in terms of COD for the anoxic phase. [h] Alkalinity values considering that at pH < 11 the inorganic carbon was in the form of carbonates and bicarbonates [7].

* Long sedimentation periods due to the occurrence of operational/technical problems (see Table 6.2). n.a. - not applied.

During the treatment period, BR1 attained an average removal of 92 ± 3% for TAN (Figure 6.2-a). The lowest value, observed in trial 8 (46.9%), is explained by the low oxygen supply due to an electrical failure that occurred during the aeration period (Table 6.5 and Table 6.2). Similarly to previous studies [1, 8, 9], partial nitrification, i.e. nitritation, was successfully achieved whereas complete oxidation to nitrate was never detected. In the present case, ammonia partial oxidation reduces operational costs involved in biological nitrogen removal. This approach makes it possible to save up to 25% of the oxygen uptake for nitrification (Equations 6.1 and 6.2) and 40% of the carbon required for denitrification (Equations 6.3-a and 6.3-b, using methanol; and Equations 6.4-a) and 6.4-b, with glycerol as external carbon donor), which is particularly interesting for effluents with low COD/N ratio [8, 10, 11].

$$NH_4^+ + \frac{3}{2}O_2 \rightarrow NO_2^- + 2H^+ + H_2O \qquad\qquad \text{(nitritation)} \qquad (6.1)$$

$$NO_2^- + \frac{1}{2}O_2 \rightarrow NO_3^- \qquad\qquad \text{(nitratation)} \qquad (6.2)$$

$$6\,NO_3^- + 5\,CH_3OH + 6\,H^+ \rightarrow 3\,N_2 + 13\,H_2O + 5\,CO_2 \qquad \text{(denitrification - methanol)} \qquad (6.3\text{-}a)$$

$$6\,NO_2^- + 3\,CH_3OH + 6\,H^+ \rightarrow 3\,N_2 + 9\,H_2O + 3\,CO_2 \qquad \text{(denitritation - methanol)} \qquad (6.3\text{-}b)$$

$$14\,NO_3^- + 5\,C_3H_8O_3 + 14\,H^+ \rightarrow 7\,N_2 + 27\,H_2O + 15\,CO_2 \quad \text{(denitrification - glycerol)} \qquad (6.4\text{-}a)$$

$$14\,NO_2^- + 3\,C_3H_8O_3 + 14\,H^+ \rightarrow 7\,N_2 + 19\,H_2O + 9\,CO_2 \quad \text{(denitritation - glycerol)} \qquad (6.4\text{-}b)$$
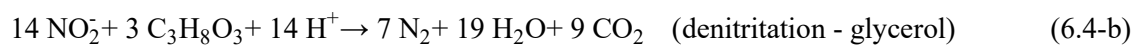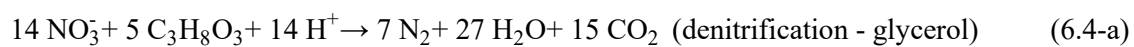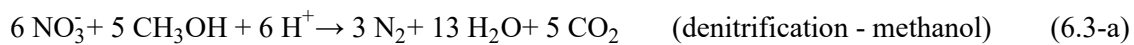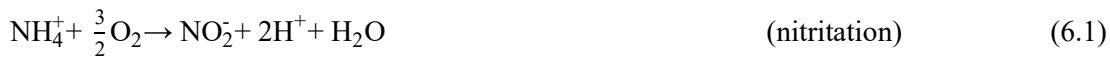
Intermediate samples collected during BR1 trials allowed to determine a nitritation specific rate between 0.11-0.16 kg $NH_4^+$-N/kg VSS/day, with an alkalinity consumption of 6.6-7.4 kg $CaCO_3$/kg $NH_4^+$-N. These results are in agreement with the lab-scale studies reported in Chapter 5 (0.10-0.15 kg $NO_2^-$-$N_{formed}$/kg VSS/day), with a previous pilot-scale work that used leachate coming from the same landfill (0.15 kg $NH_4^+$-N/kg VSS/day [1]), and also with lab-scale studies carried out by different researchers using activated sludge SBR to treat landfill leachate (0.04 to 0.15 kg $NH_4^+$-N/kg VSS/day [10]), and 0.05 to 0.16 kg $NH_4^+$-N/kg VSS/day [12]).

Considering denitritation, a mean TN removal of 42 ± 5% was achieved in BR1, with a minimum of 18% (trial 12) and a maximum of 82% (trial 2) (Figure 6.2-b), which corresponded to the lowest and highest addition of the external carbon source, respectively (Table 6.5). Methanol, one of the most popular and commercially available carbon source, was used during the start-up period. However, as the addition of an external carbon donor implies additional treatment costs, the use of glycerol, a waste-product from biodiesel production, may be a possible cost-saving solution. Moreover, glycerol is noncorrosive and, most importantly, it is non-flammable, which makes it an

appealing alternative to methanol [13]. As such, glycerol was added in trials 1-14 to promote denitritation. Nonetheless, making this change also presented a drawback since a suitable pump was required to deal with glycerol's high viscosity (Table 6.2). Samples collected immediately after glycerol addition and at the end of the anoxic period allowed to estimate (i) a nitrogen removal rate in the range of 0.05-0.12 kg N/kg VSS/day, (ii) an organic matter consumption of 1.3-2.8 kg COD/kg N removed and (iii) an alkalinity production of 2.5-4.7 kg $CaCO_3$/kg N removed. These denitritation rates were higher than those reported by Spagni, et al. [12], using a lab-scale SBR to remove nitrogen from a mature landfill leachate without addition of an external carbon source (0.025 kg N/kg VSS/day), but considerably lower than those achieved when acetate was added (0.35 kg N/kg VSS/day). Considering that polyalcohols, like glycerol, are less readily available for the denitrifying biomass, higher process rates can be expected when a commercially pure short-chain fatty acid, like acetate, is used. Nevertheless, our denitritation rates were also lower than those obtained when glycerol was used for nitrite removal of synthetic high-strength nitrite wastewaters (0.22 to 0.45 kg N/kg VSS/day [14] and 0.25 kg N/kg VSS/day [15]), yet similar when glycerol was used in a 2.8 $m^3$ SBR treating supernatants of an anaerobic co-digestion (0.11 kg N/kg VSS/day [16]). With the increment of the influent's biodegradability, from trial 15 onwards, nitrogen removal occurred with no glycerol addition (Table 6.5 and Figure 6.2-b). During these trials, denitritation was even detected during BR1 fill phase, at a rate of 0.7-2.0 kg N/kg VSS/day and consuming 1.4 to 5.0 kg COD/kg N removed. To our knowledge, only Yabroudi, et al. [10] reported similar high denitritation rates (0.4-4.6 kg N/kg VSS/day), when using a 70 L SBR treating leachate without external carbon source addition and with an anoxic phase of 1 hour (the same time used in our fill phase).

In respect to the organic content (Figure 6.2-d -e), BR1 attained a DOC and COD removal of (i) 12 ± 2% and 10 ± 2%, respectively, for trials 1-14, and (ii) 35 ± 2% and 28 ± 3%, for trials 15-19. The lower organic matter removal detected within the first trials was due to the low biodegradability of the influent leachate and glycerol addition. Generically, COD consumption was closely related to nitrogen removal (Figure 6.2-f). In terms of alkalinity, an important issue for the next treatment stage, it is possible to verify that trials with higher nitrogen removal resulted in higher final alkalinity values (Table 6.5), except for trial 8 due to the low ammonia oxidation and, consequently, low alkalinity consumption. Since alkalinity is consumed during nitritation and produced during denitritation, a good match is obtained when comparing the balance of the measured and theoretical alkalinity for each trial (Figure 6.2-c). Moreover, when considering the alkalinity at the beginning of each treatment and the alkalinity produced during denitritation, it was sufficient to totally oxidize the ammonia content for most trials.

### 6.3.3 Coagulation/sedimentation

A coagulation stage is necessary to decrease total suspended solids (TSS) concentration, organic content (DOC and COD) and colour, in order to improve the efficiency of the subsequent photo-oxidation stage [1, 17, 18]. Previous studies with leachate from the same landfill where the present work was developed, allowed to establish optimal coagulation conditions considering different extensions of the previous biological treatment (nitrified leachate ($L_{NIT}$) and nitrified/denitrified leachate ($L_{N/D}$)). At lab-scale (Chapter 5), an optimum concentration of 240 mg/L of $Fe^{3+}$, using ferric chloride, at pH 3.0, was determined (for both $L_{NIT}$ and $L_{N/D}$); at pilot-scale [1], the same $Fe^{3+}$ dose, at pH 4.2 and with a sedimentation period of 14 hours, was recommended. Considering the pilot-scale results, those conditions resulted in DOC and COD removal efficiencies over 40% and a TSS concentration in the supernatants below 250 mg/L. In the present study, lower coagulant dosages (trials 5-7) and sedimentation times (trials 12-15) were also tested to further reduce costs and treatment times.

Regardless of the operational conditions, and similarly to the pilot study [1] coagulation stage led to DOC and COD mean removal efficiencies over 40% (Table 6.6). However, the large dimension of the plant caused several effects that were not observed at pilot-scale, and high TSS values at the end of this stage were generically obtained. The high TSS concentrations may be explained by the abundant sludge flotation detected in most of the trials (Table 6.2). This was probably caused by air entrapment at the bottom of the C/P unit, which was created by the turbulence generated during the transfer of the bio-treated-leachate from BR1. Moreover, the turbulence allied to acidification, with carbon dioxide bubbles being released during pH adjustment [17, 19], also led to a dense foam production in which the floating sludge was retained (Figure 6.3). Therefore, even when coagulation conditions were close to the optimum (trials 9-11 and 19), the final TSS concentration was substantially higher than those obtained at the pilot-plant [1].



**Figure 6.3** – Foam with sludge at the C/P unit surface (coagulation/sedimentation stage).

**Table 6.6** – Operating conditions of the coagulation/sedimentation stage and physicochemical characterization of the coagulated leachate.

| Trial | Operational conditions | | | | Coagulated leachate | | | | | | | | | |
|---|---|---|---|---|---|---|---|---|---|---|---|---|---|---|
| | $V$ (m³) | $[Fe^{3+}]$ (mg/L) | $H_2SO_4$ (mM) | $t_S^a$ (h) | $V_S^b$ (m³) | pH | DOC (mg/L) | COD (mg/L) | $NH_4^+$-N (mg/L) | $NO_2^-$-N (mg/L) | $NO_3^-$-N (mg/L) | $SO_4^{2-}$ (mg/L) | TSS (mg/L) | DOC (%) |
| 1 | 30.0 | 204 | 0.0 | 16 | 6.0 | 4.5 | 537 | 1593 | 60 | 382 | 458 | 198 | 450 | 39.5 |
| 2 | 30.1 | 219 | 20.4 | 48* | 5.0 | 3.2 | 368 | 1196 | 21 | 4 | 179 | 2692 | 549 | 57.1 |
| 3 | 30.0 | 193 | 17.0 | 63* | 4.6 | 3.2 | 362 | 1293 | 5 | 2 | 186 | 2246 | 430 | 59.4 |
| 4 | 28.1 | 206 | 25.5 | 48* | 5.5 | 3.5 | 358 | 1060 | < 1 | 5 | 162 | 3449 | 388 | 63.1 |
| 5 | 30.0 | 116 | 20.2 | 16 | 7.5 | 3.2 | 447 | 1296 | < 1 | 17 | 385 | 2772 | 617 | 54.5 |
| 6 | 30.0 | 116 | 10.0 | 16 | 4.7 | 3.9 | 460 | 1390 | < 1 | 86 | 705 | 1391 | 890 | 49.7 |
| 7 | 29.5 | 118 | 4.0 | 16 | 5.3 | 4.2 | 533 | 1071 | 18 | 399 | 716 | 577 | 1070 | 41.6 |
| 8 | 31.6 | 183 | 20.4 | 4 | 4.5 | 4.5 | 541 | 1498 | 298 | 356 | 344 | 2582 | 905 | 53.9 |
| 9 | 30.0 | 176 | 16.5 | 16 | 3.9 | 4.2 | 586 | 1556 | 106 | 440 | 67 | 2335 | 673 | 50.3 |
| 10 | 30.0 | 187 | 8.5 | 16 | 6.4 | 4.2 | 573 | 1597 | 4 | 517 | 223 | 1257 | 670 | 48.8 |
| 11 | 30.0 | 179 | 12.0 | 16 | 3.3 | 4.2 | 584 | 1579 | 102 | 551 | 155 | 1802 | 713 | 50.3 |
| 12 | 30.0 | 203 | 6.8 | 2 | 7.0 | 4.2 | 593 | n.d. | 74 | 742 | 130 | 901 | 940 | 54.8 |
| 13 | 30.0 | 175 | 5.5 | 2 | 6.1 | 4.2 | 637 | n.d. | 82 | 586 | 287 | 1138 | 952 | 47.6 |
| 14 | 32.0 | 194 | 4.5 | 1 | 8.9 | 4.2 | 541 | n.d. | 78 | 549 | 95 | 1239 | 1460 | 51.7 |
| 15 | 30.0 | 186 | 6.1 | 2 | 7.2 | 4.2 | 483 | n.d. | 5 | 384 | 123 | 1248 | 1185 | 53.2 |
| 16 | 30.0 | 196 | 8.8 | 63* | 5.0 | 3.9 | 407 | n.d. | 7 | 270 | 154 | 1763 | 237 | 55.1 |
| 17 | 33.1 | 194 | 9.4 | 38* | 4.1 | 4.2 | 444 | n.d. | 4 | 226 | 134 | 1882 | 470 | 53.4 |
| 18 | 30.0 | 200 | 8.9 | 63* | 4.5 | 4.2 | 448 | n.d. | 3 | 378 | 80 | 1715 | 358 | 51.7 |
| 19 | 32.0 | 195 | 11.9 | 16 | 5.0 | 4.2 | 461 | n.d. | 2 | 313 | 81 | 2121 | 710 | 50.2 |

[a] Sedimentation times. [b] Sludge volume. * Long sedimentation periods due to the occurrence of operational/technical problems (see Table 6.2). n.d. – not determined.

As mentioned, some trials were performed to assess the process efficiency using lower coagulant dosages, pH values and sedimentation times. Using a lower coagulant dose (118 mg $Fe^{3+}$/L), while maintaining optimum pH and sedimentation time (4.2 and 16 hours), trial 7 resulted in an even higher TSS value (Table 6.6). In turn, with the same low dosage, trials 5 and 6 showed that decreasing the pH resulted in a lower final TSS content (17% and 42% less at a pH of 3.9 and 3.2, respectively). Aiming at shorter sedimentation times, trials 12-15 were performed with coagulant dosages close to the optimum and pH of 4.2, resulting in final TSS values and sludge production above 0.94 kg TSS/$m^3$ of leachate and 0.20 $m^3$ of sludge/$m^3$ of leachate, respectively. Also, with only 1 hour of sedimentation, but with the addition of 0.2 mg/L of polymer, trial 14 presented the highest final TSS concentration and amount of sludge produced (0.28 $m^3$ of sludge/$m^3$ of leachate). On the other hand, using a combination of high coagulant dosage (193-219 mg $Fe^{3+}$/L) and high sedimentation time (48-63 hours), trials 2-4 and 16-18 led to the lowest TSS values (Table 6.6). Moreover, the highest DOC removals (57 to 63%) were achieved in trials 2-4.

Another aspect that must be taken into consideration is the sulfate concentration since there is a limit of 2 g/L for discharge imposed by the Portuguese legislation [20]. During trials 2-5, with a pH of 3.2 and 3.5, the amount of sulfates exceeded the legal limit (Table 6.6). Similarly, for trials 8 and 9, with pH to 4.5 and 4.2, the minimum allowable concentration of sulfate was exceeded since the bio-treated-leachate presented high alkalinity values ($\geq$ 1.0 kg $CaCO_3$/$m^3$). It should be noted that promoting denitritation in BR1 results in higher alkalinity values and, consequently, more acid is required to achieve a final pH of 4.2 (Figure 6.4). Moreover, the initial leachate collected from the aerated lagoon presents a sulfate average concentration of (i) $(28 \pm 2) \times 10^1$ mg/L, for trials 1-12, and (ii) $(77 \pm 3) \times 10^1$ mg/L, for trials 13-19.
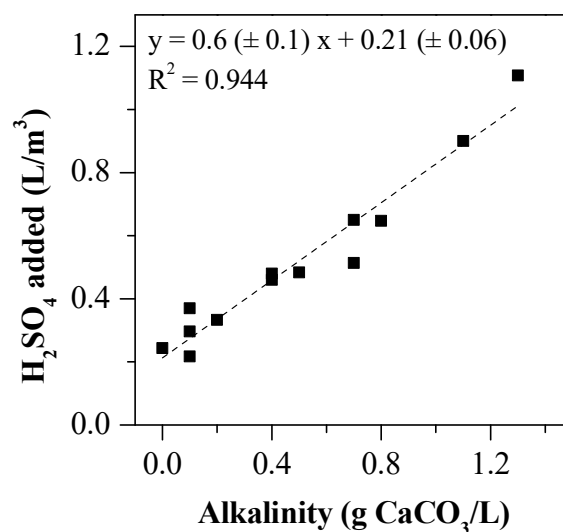


**Figure 6.4** – Relation between the alkalinity of the bio-treated effluent and the amount of sulfuric acid required to drop the pH to 4.2.

## 6.3.4 Photo-oxidation

### 6.3.4.1 Nitrite oxidation step

A photo-Fenton process was applied to pre-treated leachate aiming at the degradation of recalcitrant organic matter and the enhancement of biodegradability. Similarly to the pilot-scale study [1], at the beginning of some PF tests, a fast $H_2O_2$ consumption was observed, accompanied by a pH decrease. This is related to the oxidation of nitrites to nitrates, with intermediate formation of peroxynitrous acid (ONOOH) which, in acidic medium, rapidly decomposes releasing $H^+$ [1]. Consequently, for trials with high nitrite concentration at the beginning of the PF treatment, an initial steeper slope of the $H_2O_2$ consumption profile with a corresponding pH decrease was observed (e.g. Figure 6.5-a, trial 1). In turn, for trials with lower nitrite concentration, the rapid initial $H_2O_2$ consumption was not detected (e.g. Figure 6.5-a, trial 3). In addition, during the nitrite oxidation phase, most of the foam at the C/P surface disappeared and the trapped sludge settled. Consequently, from trial 9 forward, $H_2O_2$ was added to promote nitrite oxidation as a pre-step of PF, i.e. without photocatalyst, with lamps turned off (as a cost-saving measure), and including a new sedimentation stage followed by sludge removal (Table 6.7).
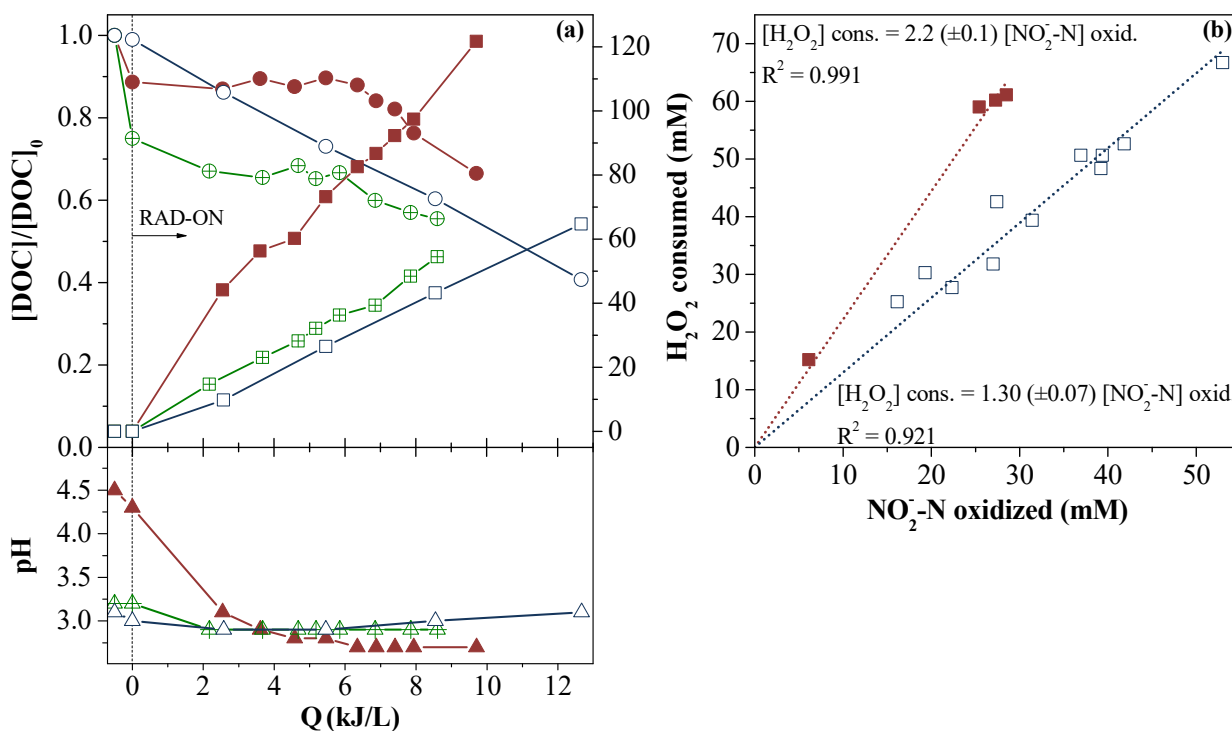


**Figure 6.5** – (a) Evolution profile of DOC degradation (circles), $H_2O_2$ consumed (squares) and pH (triangles), during photo-Fenton reaction for trial 1 (●,■,▲), trial 3 (⊕,⊞,⊬), and trial 15 (○,□,⬚); and (b) relation between nitrite ion concentration at the end of coagulation stage and hydrogen peroxide consumption for nitrite oxidation for group A1 (■) and group B (□).

**Table 6.7** – Operating conditions of the nitrite oxidation stage, including the respective physicochemical characterization of the landfill leachate.

| Trial | V (m³) | pH initial | pH final | $H_2O_2$ (mM) | $t_S$[a] (h) | $V_S$[b] (m³) | DOC (mg/L) | COD (mg/L) | $NH_4^+$-N (mg/L) | $NO_2^-$-N (mg/L) | $NO_3^-$-N (mg/L) | TSS (mg/L) |
|---|---|---|---|---|---|---|---|---|---|---|---|---|
| 9 | 26.1 | 4.2 | 3.3 | 39.4 | 1 | 4.3 | 580 | n.d. | 115 | < 1 | 540 | n.d. |
| 10 | 23.6 | 4.2 | 3.1 | 50.6 | 2 | 3.2 | 527 | n.d. | 14 | < 1 | 713 | n.d. |
| 11 | 26.7 | 4.2 | 3.1 | 50.6 | 2 | 5.3 | 555 | n.d. | 123 | < 1 | 707 | n.d. |
| 12 | 23.0 | 4.2 | 3.0 | 66.7 | 16 | 3.0 | 528 | 1480 | 74 | < 1 | 892 | 179 |
| 13 | 23.9 | 4.2 | 3.0 | 52.6 | 16 | 3.7 | 523 | 1370 | 100 | < 1 | 756 | 98 |
| 14 | 23.1 | 4.2 | 3.0 | 48.3 | 16 | 2.9 | 491 | 1316 | 95 | < 1 | 662 | 190 |
| 15 | 22.8 | 4.2 | 3.1 | 42.6 | 16 | 2.2 | 403 | 1056 | 15 | < 1 | 495 | 170 |
| 16 | 25.0 | 3.9 | 2.8 | 30.3 | 2 | 0.4 | 402 | 1201 | 13 | < 1 | 537 | 128 |
| 17 | 29.0 | 4.2 | 3.2 | 25.2 | 2 | 1.2 | 400 | 1156 | 7 | < 1 | 379 | 364 |
| 18 | 25.5 | 4.2 | 3.0 | 31.8 | 1 | 0.6 | 431 | 1301 | 5 | < 1 | 455 | 129 |
| 19 | 27.0 | 4.2 | 3.1 | 27.7 | 3 | 0.8 | 446 | 1431 | 4 | < 1 | 382 | 298 |

[a] Sedimentation times. [b] Sludge volume. n.d. – not determined.

In this way, PF trials can be divided into two groups: (i) group A, trials 1-8, with PF stage starting immediately after coagulation, and (ii) group B, trials 9-19, with nitrite oxidation as an intermediate step between coagulation and PF. Regarding group A, it is possible to further divide it into two sub-groups: (i) A1, comprising trials 1 and 6-8, with nitrite concentration ranging between 86-399 mg N/L, and (ii) A2, including trials 2-5, with no nitrite content at the end of the coagulation stage.

Whether included or separated from the PF process, a good correlation was obtained ($R^2 = 0.991$ and 0.921, for groups A1 and B, respectively) between the nitrite content at the end of coagulation and the $H_2O_2$ consumed for its oxidation (Figure 6.5-b). Moreover, it was possible to verify that the amount of $H_2O_2$ required for group A1 was higher than for group B, which may be due to the occurrence of $H_2O_2$ photolysis. Considering the above, performing the nitrite oxidation as a distinct step seemed to be advantageous, since it allowed to (i) obtain lower TSS content at the beginning of PF process (Table 6.7), (ii) save energy, since the oxidation is performed with the lamps turned off, and (iii) save $H_2O_2$.

### 6.3.4.2 Photo-Fenton efficiency

Globally, group A presented an inferior PF efficiency than group B (average DOC removal of 33 ± 6% and 48 ± 3%, respectively) (Table 6.8), which may be mostly attributed to the high TSS content during photo-treatment (Table 6.6 and Figure 6.6-a). The presence of suspended solids can negatively affect the PF reaction, by reducing the light penetration and competing with $H_2O_2$ and iron species as photon absorbers [18]. Also, the simultaneous oxidation of soluble and particulate organic matter increases the consumption of energy and reactants. Group A presented an initial DOC decay (11-25%) after catalyst addition (Figure 6.7-a -b), probably related to an additional precipitation of organic matter with $Fe^{3+}$. Beyond that, it showed intermittences in DOC degradation profiles (Figure 6.7-a -b), where after the initial decrease, there was an induction period with occasional DOC increase as the photo-treatment proceeded. This can be associated with the foam disappearance, with consequent release of the retained sludge and dissolution of the respective organic matter content.

**Table 6.8** – Operating conditions and performance of the photo-Fenton stage.

| Trial | Group | Pretreatment[a] | V (m³) | t (h) | pH[b] | T[b] (ºC) | Q (kJ/L) | $[Fe^{2+}]$ (mg/L) | $[H_2O_2]$ (mM) | DOC[c] (mg/L) | Min.[d] (%) | $H_2O_2/C$[e] $\left(\frac{mg\ H_2O_2}{mg\ DOC}\right)$ |
|---|---|---|---|---|---|---|---|---|---|---|---|---|
| 1 | A1 | BT + Coag. | 24.0 | 9.2 | 2.9 | 34.2 | 9.8 | 67.2 | 121.7 | 364 | 32.2 | 22.5 |
| 2 | | BT + Coag. | 25.1 | 7.0 | 2.8 | 29.5 | 7.1 | 67.2 | 35.1 | 301 | 18.2 | 17.8 |
| 3 | A2 | BT + Coag. | 25.4 | 8.6 | 2.9 | 29.5 | 8.6 | 63.2 | 55.8 | 201 | 44.5 | 11.8 |
| 4 | | BT + Coag. | 22.6 | 15.2 | 3.0 | 29.9 | 17.1 | 66.1 | 67.8 | 120 | 66.5 | 9.7 |
| 5 | | BT + Coag. | 22.5 | 15.0 | 2.8 | 31.4 | 17.0 | 66.4 | 56.7 | 267 | 40.3 | 10.7 |
| 6 | | BT + Coag. | 25.3 | 14.0 | 2.7 | 33.5 | 14.1 | 59.1 | 75.4 | 393 | 14.5 | 26.2 |
| 7 | A1 | BT + Coag. | 24.2 | 15.6 | 3.0 | 32.7 | 16.4 | 61.7 | 108.6 | 382 | 28.3 | 24.5 |
| 8 | | BT + Coag. | 27.1 | 13.5 | 3.2 | 28.3 | 12.7 | 55.0 | 91.0 | 427 | 21.1 | 27.2 |
| 9 | | BT + Coag. + NO₂⁻oxid. | 21.8 | 7.3 | 2.9 | 26.3 | 8.5 | 61.7 | 38.1 | 336 | 42.1 | 5.3 |
| 10 | | BT + Coag. + NO₂⁻oxid. | 20.4 | 11.7 | 2.8 | 28.1 | 14.6 | 70.3 | 52.7 | 346 | 34.3 | 9.9 |
| 11 | | BT + Coag. + NO₂⁻oxid. | 21.4 | 15.5 | 3.0 | 28.1 | 18.4 | 68.4 | 47.5 | 376 | 32.3 | 9.0 |
| 12 | | BT + Coag. + NO₂⁻oxid. | 20.0 | 13.9 | 2.8 | 26.7 | 17.7 | 62.5 | 52.0 | 291 | 44.9 | 8.3 |
| 13 | | BT + Coag. + NO₂⁻oxid. | 20.2 | 14.0 | 2.8 | 24.9 | 17.6 | 68.8 | 56.5 | 270 | 48.4 | 7.6 |
| 14 | B | BT + Coag. + NO₂⁻oxid. | 20.2 | 14.2 | 2.8 | 26.8 | 17.8 | 76.9 | 70.7 | 270 | 45.0 | 10.9 |
| 15 | | BT + Coag. + NO₂⁻oxid. | 20.6 | 10.3 | 3.0 | 28.8 | 12.7 | 66.7 | 64.7 | 166 | 58.8 | 9.3 |
| 16 | | BT + Coag. + NO₂⁻oxid. | 24.6 | 14.0 | 2.9 | 25.7 | 14.5 | 68.0 | 79.7 | 169 | 58.0 | 11.6 |
| 17 | | BT + Coag. + NO₂⁻oxid. | 27.8 | 14.4 | 3.0 | 26.4 | 13.2 | 67.7 | 82.4 | 174 | 56.5 | 12.4 |
| 18 | | BT + Coag. + NO₂⁻oxid. | 24.9 | 15.0 | 2.9 | 24.0 | 15.3 | 67.2 | 80.3 | 202 | 53.1 | 11.9 |
| 19 | | BT + Coag. + NO₂⁻oxid. | 26.2 | 14.3 | 3.0 | 26.5 | 13.9 | 67.3 | 73.2 | 212 | 52.5 | 10.6 |

[a] BT – biological treatment, Coag. – Coagulation/sedimentation, NO₂⁻oxid. – Nitrite oxidation. [b] Average pH and temperature during the photo-Fenton process. [c] DOC concentration at the end of the photo-Fenton. [d] Mineralization $((1-DOC_f/DOC_i)\times100)$. [e] Ratio between the $H_2O_2$ (mol/L) consumed and DOC (mg/L) oxidized $\left([H_2O_2]/(DOC_i-DOC_f)\times34.02\right)$.
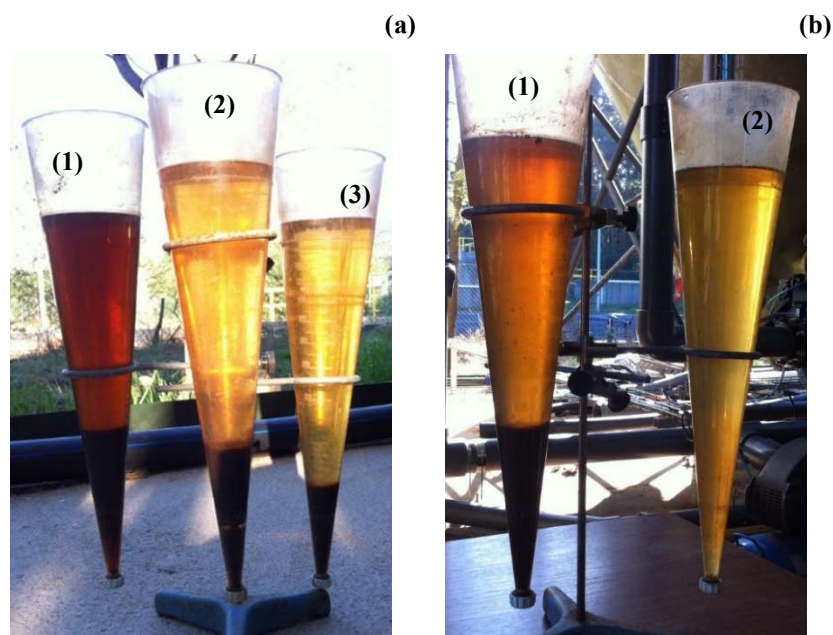
**Figure 6.6** – Photographs taken to the Imhoff cones of: (a) trial 8, from group A1, (1) after the addition of catalyst and $H_2O_2$ with consequent pH dropping from 4.5 to 3.2 (nitrite oxidation), (2) after 5 hours of PF process, and (3) after 10 hours of PF process; and (b) trial 9, from group B, (1) after the nitrite oxidation and before the sludge removal, and (2) after 5 hours of PF process.

Considering the above, for A1 trials, it seems that the DOC reduction was not actually due to the PF process but related to the precipitation of organic matter. Moreover, due to the high TSS content and consequent dissolution of the particulate matter organic content, the induction period seemed to have lasted throughout the entire PF. Within A1 group, only test 1 presented a shorter induction period, until approximately 6 kJ/L, followed by a DOC degradation showing a pseudo-first-order kinetic behaviour (Figure 6.7-a). However, trial 1 had some unique characteristics that may have favoured the PF reaction, like (i) considerably lower TSS content within A1 group, and (ii) lowest $SO_4^{2-}$ concentration from all trials, due to lack of acid addition in the coagulation stage.

For A2 trials, it is also possible to observe an induction period until approximately 4-6 kJ/L, for trials 3-5, followed by DOC mineralization according to a pseudo-first-order kinetic behaviour (Figure 6.7-b). In test 2, an induction period until 6 kJ/L was also observed, but due to the very short photo-treatment it is not possible to mark it clearly. Trial 4 achieved the highest DOC removal from all trials, which may have been attributed to the combination of a higher treatment time, and consequently higher radiation dose, and $H_2O_2$ availability to be used in photo-oxidation reactions (Table 6.8). Furthermore, the lowest DOC concentration at the beginning of PF (but quite similar to trials 2-3) was observed in trial 4 and, within A group, it presented the lowest TSS content (Table 6.6). Also, due to the absence of $NO_2^-$, A2 trials showed an $H_2O_2$ consumption 1.8 times (on average) lower than for A1 trials.
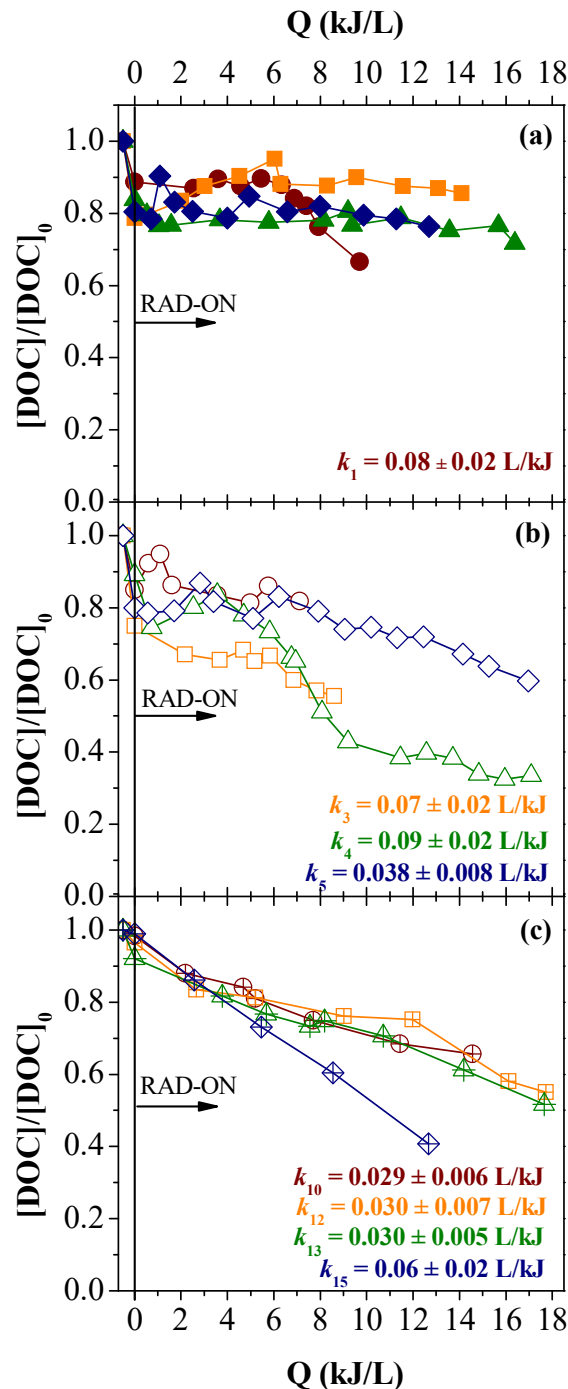
**Figure 6.7** – Evolution profile of DOC degradation during photo-Fenton reaction for: (a) A1 trials (1 - ●; 6 - ■; 7 - ▲; 8 - ◆); (b) A2 trials (2 - ○; 3 - □; 4 - △; 5 - ◇); (c) B trials (10 - ⊕; 12 – ⊞; 13 – △; 15 - ⬦)

For group B trials, it was clear that performing nitrite oxidation followed by a new sedimentation period and sludge removal, greatly improved the leachate clarification (Table 6.7 and Figure 6.6-b). It is worth to notice that the DOC content also decreased after (i) nitrite oxidation and sludge removal (average decay of $8 \pm 2\%$), and (ii) catalyst addition (mean decay of $5 \pm 1\%$). Adding both DOC drops, a quite similar DOC decay when compared to group A trials was observed. When

removing the sludge after nitrite oxidation, the induction period in group B appeared to be negligible and a continuous reduction on DOC was observed (Figure 6.7-c). Therefore, trial 13 (with the lowest TSS content) presenting similar initial DOC as trial 7 (A1 group, and with the highest TSS content), attained 20% higher DOC abatement with nearly 50% less $H_2O_2$ and with only 1.2 kJ/L more of accumulated radiation energy. Also, if the $H_2O_2$ amount spent during nitrite oxidation is considered, then the consumption was approximately equal. However, trial 13 presented 1.3 times higher nitrite content.

With close initial DOC values, the photo-treatment performance of trial 19 can be compared with trials 6 (A1) and 5 (A2). It is possible to verify that for trial 19 a 38% higher DOC removal was observed, consuming similar radiation energy and $H_2O_2$ as for trial 6. In turn, trial 19 achieved 16% higher DOC mineralization, using 1.2 times less radiation energy but 1.3 times more $H_2O_2$ than trial 5. In this case, if the amount of $H_2O_2$ used in nitrite oxidation is considered, then the consumption increases up to 1.8 times when compared with trial 5. In summary, in the presence of nitrite, performing the oxidation as a separate step of the PF stage means a cost-saving measure, especially in terms of radiation usage. In turn, having a bio-coagulated-leachate without nitrite decreases considerably the amount of $H_2O_2$ required.

A final aspect to be considered is the photo-Fenton efficiency taking into account the next treatment stage, in this case, the final biological treatment. According to Silva *et al.* [1, 21] to obtain a final COD that complies with the legal discharge limit for the disposal directly into waterbodies (< 150 mg $O_2$/L), DOC value at the end of PF stage must not exceed 250 mg/L. In the present case, a suitable value was obtained in trials 3-4 and 15-19. However, as photo-Fenton was performed during the night, data obtained from trials 16-19 were not enough to obtain the degradation kinetic constants and calculate the amount of $H_2O_2$ and energy required to achieve a DOC of 250 mg/L. In respect to trials 3 and 4, to obtain a DOC of 250 mg/L, 5.1 and 5.7 kJ/L of accumulated energy, and 30.8 and 26.7 mM of $H_2O_2$ were consumed, respectively. For trial 15, 7.7 kJ/L of accumulated energy and 81.4 mM of $H_2O_2$ were consumed (42.6 mM spent in the nitrites oxidation and 38.8 mM in the PF reaction). These values are considerably lower than those reported in the pilot-plant studies [1] where 1.6 $m^3$ of a bio-coagulated leachate, with an initial DOC of 388 mg/L and a TSS of 72 mg/L, was photo-treated using 4 UV+Vis lamps (set at 1000 W each and with same spectrum as the lamps used in the present study), consuming 15.7 $kJ_{UV}$/L and 105 mM of $H_2O_2$. The higher consumptions at pilot-scale may be mainly explained by (i) the non-optimization of the photoreactor, where the lamps were simply located inside the recirculation tank, and (ii) the presence of nitrite at the beginning of the PF. In the present study, the usage of the FluHelik photoreactors was shown to be advantageous and considerably less radiation energy was consumed.

The FluHelik configuration (section 4.3.2.3 of Chapter 4), providing a helical movement of the fluid around the radiation source, generates (i) high velocities through the reactor but lower velocities near the lamp, (ii) high turbulent intensity, thus a high degree of mixing, and (iii) uniform radiation fluence inside the reactor.

### 6.3.4.3 Neutralization step

Absent in most research papers, the neutralization step is commonly referred to as a disadvantage due to the addition of one more reagent, with consequent cost, and iron-sludge production. Very scarce information is found about (i) operational conditions such as the amount of reagent required, final pH and settling period, (ii) amount of iron-sludge produced and (iii) final effluent characterization, in terms of iron and $H_2O_2$ concentration. However, it is a crucial step for the success of the PF treatment, since iron must be removed in order to achieve the legal discharge limit (total iron content below 2.0 mg/L [20]). In addition, it must be ensured that possible residual $H_2O_2$ has no toxic effect, whether to discharge directly into a waterbody or, as in this case, to be followed by biological treatment stage.

It should be noted that for A group trials (except trial 3), due to the considerable amount of TSS during PF, it was decided to remove the acid sludge prior to neutralization. The acid sludge was settled overnight (16 h), except for trials 5 and 7 where a 2-hour sedimentation period resulted in nearly the double volume of acid sludge (Table 6.9). In respect to neutralization conditions, a final pH of 7.0 and a sedimentation period of 16 hours were defined for most trials. However, in a cost and time-saving perspective, lower final pH and sedimentation periods were also attempted, and, in a general way, the amount of neutral sludge formed did not seem to be affected. On the other hand, the analysis performed to the sludge from trials 15-19 showed that higher sedimentation time tendentially led to a higher dry matter content (Table 6.10).

**Table 6.9** – Operating conditions and physicochemical characterization of the photo-treated-neutralized landfill leachate at the outlet.

| Trial | V (m³) | $t_s$[a] (h) | $V_s$[b] (m³) | $H_2O_2$[c] (mM) | NaHO (mM) | pH[d] | $t_s$[a] (h) | $V_s$[e] (m³) | DOC[f] (mg/L) | COD[f] (mg/L) | TDI[g] (mg/L) | TSS[f] (mg/L) |
|---|---|---|---|---|---|---|---|---|---|---|---|---|
| 1 | 24.0 | 16 | 0.8 | 0.5 | 6.7 | 5.5 | 2 | 0.6 | 381 | 895 | n.d. | 187 |
| 2 | 25.1 | 16 | 0.7 | 2.1 | 22.7 | 7.0 | 2 | 0.6 | 325 | 598 | n.d. | 208 |
| 3 | 25.4 | n.a. | n.a. | 1.9 | 19.2 | 7.0 | 16 | 0.7 | 250 | 495 | n.d. | 294 |
| 4 | 22.6 | 16 | 0.4 | 3.1 | 8.8 | 5.7 | 2 | 0.7 | 115 | 325 | n.d. | 75 |
| 5 | 22.5 | 2 | 1.5 | 1.6 | 14.3 | 5.5 | 2 | 0.4 | 237 | 377 | n.d. | 269 |
| 6 | 25.3 | 16 | 0.9 | 4.4 | 20.4 | 5.5 | 2 | 0.4 | 385 | 590 | n.d. | 518 |
| 7 | 24.2 | 2 | 1.4 | 0.1 | 19.3 | 6.0 | 2 | 0.6 | 392 | 774 | n.d. | n.d. |
| 8 | 27.1 | 16 | 0.9 | 0.3 | 21.1 | 7.0 | 16 | 0.2 | 388 | 994 | 21.6 | 337 |
| 9 | 21.8 | n.a. | n.a. | 1.9 | 23.4 | 7.1 | 16 | 0.3 | 380 | 851 | 4.8 | 152 |
| 10 | 20.4 | n.a. | n.a. | 1.5 | 23.6 | 7.0 | 16 | 0.5 | 371 | 685 | 9.0 | 282 |
| 11 | 21.4 | n.a. | n.a. | 0.9 | 20.5 | 7.0 | 16 | 0.4 | 422 | 685 | 11.3 | 169 |
| 12 | 20.0 | n.a. | n.a. | 2.9 | 18.1 | 7.0 | 16 | 0.9 | 309 | 580 | 2.1 | 110 |
| 13 | 20.2 | n.a. | n.a. | 0.9 | 22.5 | 7.0 | 16 | 0.7 | 325 | 662 | 13.7 | 292 |
| 14 | 20.2 | n.a. | n.a. | 0.4 | 21.9 | 7.0 | 16 | 1.0 | 326 | 644 | 18.4 | 281 |
| 15 | 20.6 | n.a. | n.a. | 3.0 | 18.0 | 7.0 | 3 | 0.7 | 196 | 337 | 0.9 | 191 |
| 16 | 24.6 | n.a. | n.a. | 3.5 | 22.1 | 7.0 | 4 | 0.8 | 184 | 323 | 0.3 | 99 |
| 17 | 27.8 | n.a. | n.a. | 2.5 | 19.6 | 7.0 | 3 | 0.8 | 186 | 359 | 0.8 | 133 |
| 18 | 24.9 | n.a. | n.a. | 3.0 | 18.7 | 7.0 | 4 | 0.8 | 222 | 415 | 1.1 | 98 |
| 19 | 26.2 | n.a. | n.a. | 3.0 | 18.6 | 7.0 | 16 | 0.7 | 203 | 394 | 0.7 | 155 |

[a] Sedimentation times. [b] Acidic sludge volume. [c] Hydrogen peroxide residual concentration at the beginning of neutralization. [d] pH after sodium hydroxide addition. [e] Neutral sludge volume. [f] DOC, COD and TSS content after neutralization and respective sludge removal. [g] Total dissolved iron. n.a. – not applied. n.d. – not determined.

**Table 6.10** – Dry matter content in the sludge produced at neutralization step within trials 15-19.

| Trial | $t_S$ (h) | Sludge produced (L/m$^3$) | Dry matter (g/L) |
|---|---|---|---|
| 15 | 3 | 34.0 | 10.2 |
| 16 | 4 | 32.5 | 14.2 |
| 17 | 3 | 28.8 | 10.5 |
| 18 | 4 | 30.1 | 8.2 |
| 19 | 16 | 24.8 | 22.3 |

After neutralization, slight DOC differences, whether increase or decrease, were observed between the last PF and the neutralized-leachate samples (Table 6.8 and Table 6.9). However, trial 3 showed the most significant increase (20%), which can be explained by the re-dissolution of particulate organic matter present in the acid sludge. In respect to iron removal, it was more difficult than expected and the neutralized-leachate presented an intense orange colour indicating the presence of soluble iron (Figure 6.8-a). So, from trial 8 onwards, TDI after iron-sludge removal was also measured and until trial 14 it was always above 2 mg/L. Moreover, it was possible to observe that lower TDI values were obtained when the photo-treated-leachate presented higher $H_2O_2$ residual concentrations (Table 6.9). In this way, from trial 15 forward, an $H_2O_2$ residual concentration of 2.5-3.5 mM was intended to promote ferric ions as the main iron species, thus leading to higher precipitation. In these conditions, values of TDI below legal limit were attained (Table 6.9). Furthermore, the orange colour of the neutralized-leachate was no longer observed (Figure 6.8-b).

(a)                                                     (b)
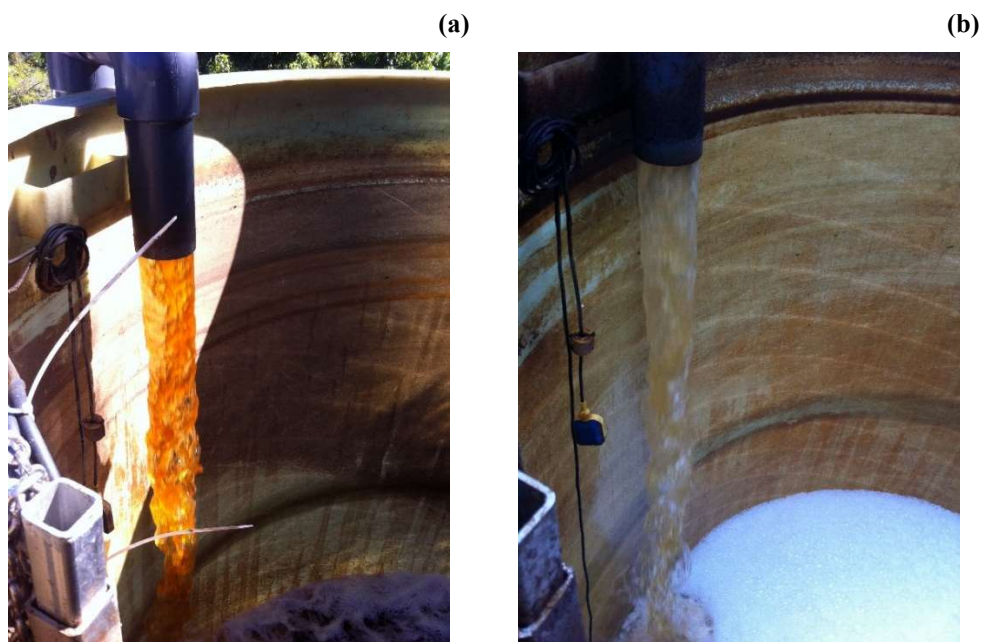


**Figure 6.8** – Photographs taken during the transference of neutralized-leachate to BR2 at (a) trial 8 and (b) trial 17.

To improve iron precipitation and clarification, samples from trial 14 were further subjected to polymer addition in a *jar-test* (Table 6.11). Promising results with the addition of 0.30 mg/L of polymer were found but, as iron precipitation improved from trial 15 forward, it was not applied at full-scale. Furthermore, biodegradability tests (Zahn-Wellens) were made, using BR2 biomass, to assess the eventual impact on the next biological treatment stage of (i) polymer addition and, simultaneously, (ii) $H_2O_2$ residual concentration (Figure 6.9). Results showed no significant differences between samples (i) without and with 0.30 mg/L of polymer addition, making it also possible to infer that residual amounts of dissolved iron do not seem to affect the biomass, and (ii) without and with 1.5 mM of $H_2O_2$ added as a single dose or 0.3 mM of daily additions. These findings are in the agreement with a study performed by Mosteo *et al.* [22] using a coupled photo-Fenton/packed-bed bioreactor, where the presence of 20 mg $Fe^{2+}$/L and residual $H_2O_2$ up to 4.6 mM had no inhibitory or negative effects on the biological activity.

**Table 6.11** – Jar-tests performed with neutralized leachate from trial 14.

| | | | | | |
|---|---|---|---|---|---|
| **Conditions** | **Polymer** | mg/L | 0.00 | 0.15 | 0.30 |
| | **Mixing** | min. | 15 | 15 | 15 |
| | **Sedimentation** | | 30 | 30 | 30 |
| **Characterization** | **DOC** | mg/L | 326 | 242 (↓26%) | 223 (↓32%) |
| | **IC** | | 6 | 19 | 26 |
| | **TDI** | | 18.4 | 7.5 (↓59%) | 1.3 (↓93%) |
| | **TSS** | | 281 | 187 (↓33%) | 143 (↓49%) |
| | **VSS** | | 75 | 73 | 74 |
| | **Turbidity** | FAU | 60 | 24 (↓60%) | 11 (↓82%) |
| | **Colour (1:20)** | Pt/Co | 35 | 14 (↓60%) | 6 (↓83%) |
| | **Visual comparison** | |  |  |  |
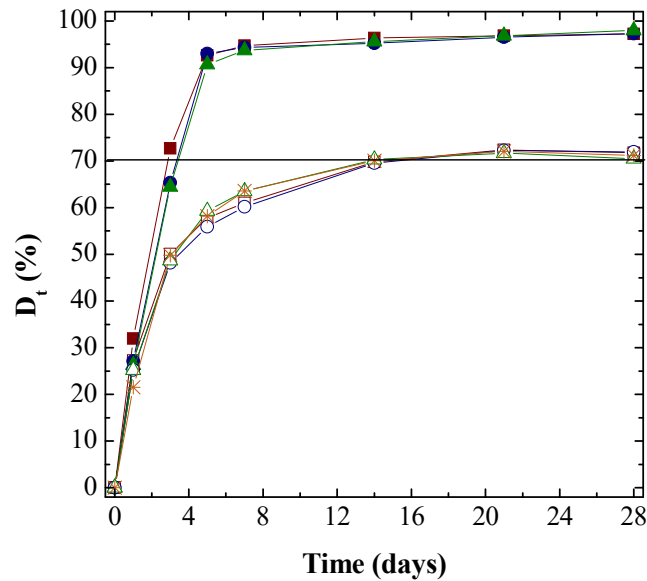
**Figure 6.9** – Zahn-Wellens test results for neutralized-leachate samples: without polymer ([TDI] = 2.4 mg/L) and $H_2O_2$ ($\ast$) and with 0.30 mg/L of polymer ([TDI] = 0.8 mg/L) without $H_2O_2$ ($\square$), with single addition of [$H_2O_2$] = 1.5 mM ($\circ$) and daily addition of [$H_2O_2$] = 0.3 mM ($\triangle$); and respective references: without polymer and without $H_2O_2$ ($\blacksquare$), single addition of [$H_2O_2$] = 1.5 mM ($\bullet$) and daily addition of [$H_2O_2$] = 0.3 mM ($\blacktriangle$).

## 6.3.5 Biological reactor 2

### 6.3.5.1 Start-up period

BR2 was initially fed with leachate and biomass from BR1 and during the start-up period (2 months), small amounts of leachate (2 to 3 m$^3$), sometimes including biomass, were also pumped from BR1. Similarly to BR1, an alternate aerobic/anoxic scheme was applied to BR2 (methanol was added a few times). Therefore, during BR2 start-up, nitrititation and denitritation rates were quite like those obtained in BR1 (mean rates of 0.20 kg $NH_4^+$-N/kg VSS/day and 0.06 kg N/kg VSS/day). It should be noted that the leachate characteristics at this point were considerably different from those expected to feed BR2 during the treatment period.

### 6.3.5.2 Treatment period

Being the final treatment stage, BR2 main objectives were to (i) oxidize the remaining organic matter, with enhanced biodegradability after PF process, and (ii) remove the remaining nitrogen,

with aerobic/anoxic cycles (Table 6.1). Since it was intended to discharge the effluent directly into waterbodies, to comply with legal requirements, BR2 performance should ensure a final COD < 150 mg $O_2$/L and TN < 15 mg/L [20].

In respect to organic matter (Figure 6.10-a -b), BR2 attained average removals of $29 \pm 3\%$ and $28 \pm 3\%$ for DOC and COD, respectively. The highest and lowest reduction of COD was observed in trials 4 and 6 (53% and 7%), respectively, and coincided with the highest and lowest mineralization obtained at the PF stage (see Table 6.8). This reveals the influence of the photo-treatment efficiency on the performance of BR2. There was also a low COD removal (9%) in trial 2, due to glycerol addition and the small amount of nitrate (79 mg N/L, Table 6.12) that was insufficient to consume the added COD. During trial 7, a failure of the mechanical stirrer obliged to empty the reactor and new leachate and biomass was pumped from BR1 to BR2 (see Table 6.2). So, a notorious increase of DOC and COD content (and ammonia nitrogen and nitrites) was observed in the final discharge of trial 8 (Table 6.13).

As mentioned above, according to biodegradability assays from the pilot-scale study [1], a maximum DOC concentration around 250 mg/L at the end of PF stage was required to achieve a leachate able to be biologically oxidized to comply the COD discharge limit. Also, considering the optimization studies at lab-scale (Chapter 5), a COD ~ 400 mg/L would be the target value to attain a biodegradable effluent after photo-oxidation. In our case, even though trials 3-5 and 15-19 met this requirement, the desired COD value was not reached (Table 6.13). However, it was possible to observe that when BR2 was consecutively fed with photo-treated-leachate presenting DOC < 250 mg/L and COD $\leq$ 400 mg/L (trials 15-19), the final COD tended to comply with the legal discharge limit.
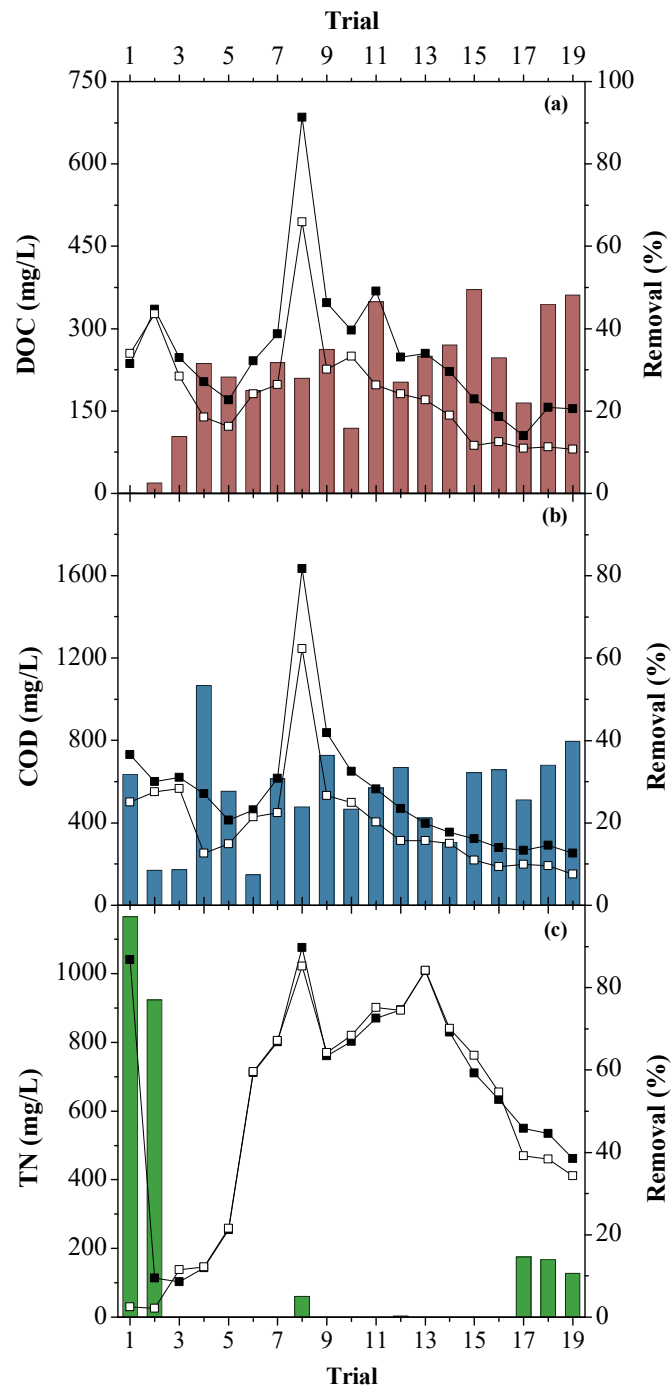
**Figure 6.10** – Evolution profile of (a) DOC, (b) COD and (c) TN concentrations of photo-treated leachate at beginning of BR2 (■) and of discharge (□), with respective removals (▬, ▬, ▬).

**Table 6.12** – Physicochemical characterization of the bio-coagulated-photo-treated-leachate at the beginning of BR2.

| Trial | pH | DOC (mg/L) | DIC (mg/L) | BOD$_5$ (mg/L) | COD (mg/L) | $\dfrac{BOD_5}{COD}$ | TN (mg/L) | NH$_4^+$-N (mg/L) | NO$_2^-$-N (mg/L) | NO$_3^-$-N (mg/L) | SO$_4^{2-}$ (mg/L) | TSS (mg/L) | VSS (mg/L) |
|---|---|---|---|---|---|---|---|---|---|---|---|---|---|
| 1 | 6.8 | 236 | 69 | 170 | 732 | 0.23 | 1041 | 31 | 14 | 996 | 373 | 1445 | 763 |
| 2 | 7.2 | 335 | 344 | 320 | 601 | 0.53 | 113 | 9 | 11 | 79 | 1308 | 2351 | 1345 |
| 3 | 7.1 | 247 | 222 | 400 | 620 | 0.65 | 103 | 3 | 9 | 80 | 1983 | 2341 | 1280 |
| 4 | 6.6 | 203 | 112 | 440 | 541 | 0.81 | 143 | 6 | 18 | 118 | 2436 | 1965 | 905 |
| 5 | 6.7 | 170 | 69 | 90 | 412 | 0.22 | 255 | 15 | 5 | 235 | 2681 | 2690 | 1160 |
| 6 | 7.1 | 241 | 64 | 100 | 462 | 0.22 | 712 | 10 | 2 | 700 | 2297 | 2280 | 983 |
| 7 | 6.2 | 290 | 61 | n.d. | 616 | n.d. | 801 | n.d. | n.d. | n.d. | n.d. | 1465 | 800 |
| 8 | 7.1 | 685 | 249 | 230 | 1634 | 0.14 | 1076 | 418 | 75 | 610 | 1950 | 1310 | 750 |
| 9 | 6.7 | 347 | 183 | 150 | 837 | 0.18 | 885 | 118 | 26 | 626 | 2010 | 1655 | 915 |
| 10 | 7.3 | 297 | 48 | 170 | 650 | 0.26 | 803 | 31 | 68 | 702 | 1632 | 2085 | 1095 |
| 11 | 6.4 | 368 | 100 | 225 | 565 | 0.40 | 870 | 72 | 39 | 722 | 1677 | 2020 | 1420 |
| 12 | 6.6 | 248 | 87 | 150 | 470 | 0.32 | 895 | 74 | 18 | 803 | 1318 | 2576 | 1619 |
| 13 | 6.9 | 255 | 82 | 100 | 397 | 0.25 | 1008 | 90 | 8 | 905 | 1205 | 2930 | 1750 |
| 14 | 7.4 | 222 | 83 | 150 | 355 | 0.42 | 945 | 87 | 5 | 746 | 1229 | 2335 | 1355 |
| 15 | 7.3 | 172 | 74 | 170 | 323 | 0.53 | 762 | n.d. | n.d. | n.d. | n.d. | 2227 | 1270 |
| 16 | 6.9 | 140 | 56 | 150 | 280 | 0.54 | 634 | 25 | 23 | 517 | 1558 | 2100 | 1185 |
| 17 | 7.1 | 105 | 106 | 170 | 267 | 0.64 | 550 | 29 | 4 | 427 | 1738 | 2075 | 1100 |
| 18 | 7.5 | 157 | 128 | 160 | 252 | 0.63 | 534 | 18 | 1 | 411 | 1704 | 1760 | 930 |
| 19 | 7.4 | 154 | 178 | 70 | 291 | 0.24 | 461 | 1 | < 1 | 366 | 1976 | 1750 | 985 |

n.d. – not determined.

**Table 6.13** – Operating conditions for BR2 and chemical characterization of the final discharge.

| Trial | Operational conditions[a] | | | | | | | Final discharge characterization | | | | | | | | | | | |
|---|---|---|---|---|---|---|---|---|---|---|---|---|---|---|---|---|---|---|---|
| | $V_T$ (m³) | $V_D$ (m³) | $t_R$ (d) | $t_S$ (h) | $O_2$[b] (kg) | $C_3H_8O_3$[c] (mg $O_2$/L) | VSS (mg/L) | pH | DOC (mg/L) | DIC (mg/L) | COD (mg/L) | $BOD_5$ (mg/L) | TN (mg/L) | $NH_4^+$-N (mg/L) | $NO_2^-$-N (mg/L) | $NO_3^-$-N (mg/L) | $SO_4^{2-}$ (mg/L) | TDI[g] (mg/L) | TSS (mg/L) |
| 1 | 39.5 | 21 | 7 | 6 | 73 | 3420 | 763 | 7.5 | 255 | 599 | 500 | 90 | 30 | <1 | 21 | 9 | 237 | 1.5 | 150 |
| 2 | 39.8 | 21 | 3 | 20* | 54 | 1500 | 1345 | 7.5 | 327 | 357 | 550 | 165 | 26 | <1 | 14 | 2 | 1273 | 1.8 | 79 |
| 3 | 39.6 | 21 | 8 | 5 | 91 | n.a. | 1280 | 7.2 | 213 | 221 | 567 | 250 | 138 | 4 | 40 | 94 | 1904 | 0.4 | 680 |
| 4 | 38.2 | 20 | 3 | 20* | 64 | n.a. | 905 | 7.4 | 139 | 130 | 253 | 15 | 146 | 14 | 16 | 112 | 2464 | 0.3 | 199 |
| 5 | 36.8 | 20 | 3 | 20* | 35 | n.a. | 1160 | 7.8 | 122 | 108 | 298 | 25 | 258 | 14 | 3 | 241 | 2335 | 0.5 | 436 |
| 6 | 39.3 | 21 | 2 | 75* | 39 | n.a. | 983 | 7.3 | 181 | 92 | 428 | 30 | 715 | 11 | 2 | 702 | 2317 | 1.1 | 189 |
| 7 | 38.6 | 20 | 5 | 20* | 58 | n.a. | 800 | 7.2 | 198 | 108 | 449 | 25 | 805 | 71 | 14 | 566 | 1998 | 1.8 | 368 |
| 8 | 37.5 | 19 | 3 | 4 | 58 | n.a. | 750 | 7.0 | 494 | 196 | 1245 | 30 | 1022 | 305 | 174 | 612 | 1994 | 1.7 | 103 |
| 9 | 38.5 | 19 | 4 | 4 | 113 | n.a. | 915 | 6.7 | 226 | 18 | 533 | 30 | 784 | 48 | 92 | 620 | 2017 | 1.8 | 156 |
| 10 | 37.5 | 19 | 4 | 6 | 73 | n.a. | 1095 | 7.0 | 250 | 107 | 499 | 50 | 820 | 28 | 84 | 707 | 1667 | 2.0 | 95 |
| 11 | 36.7 | 20 | 4 | 6 | 175 | n.a. | 1420 | 7.2 | 197 | 105 | 404 | 45 | 901 | 76 | 42 | 731 | 1708 | 1.9 | 121 |
| 12 | 36.8 | 19 | 5 | 6 | 186 | n.a. | 1619 | 7.4 | 181 | 103 | 313 | 22 | 893 | 93 | 17 | 783 | 1254 | 1.6 | 216 |
| 13 | 37.3 | 20 | 3 | 5 | 98 | n.a. | 1750 | 7.9 | 170 | 109 | 313 | 28 | 1010 | 96 | 10 | 905 | 1192 | 1.8 | 364 |
| 14 | 37.1 | 19 | 4 | 3 | 82 | n.a. | 1355 | 7.6 | 142 | 92 | 301 | 14 | 856 | 98 | 21 | 721 | 1208 | 0.8 | 488 |
| 15 | 37.6 | 20 | 6 | 4 | 31 | n.a. | 1270 | 6.7 | 87 | 54 | 219 | 19 | 762 | 33 | 51 | 621 | 1293 | 0.3 | 360 |
| 16 | 39.9 | 21 | 3 | 3 | 9 | n.a. | 1185 | 7.1 | 94 | 109 | 188 | 18 | 655 | 29 | 19 | 497 | 1576 | 0.6 | 324 |
| 17 | 39.0 | 21 | 3 | 3 | 5 | 240 | 1100 | 8.1 | 82 | 182 | 199 | 28 | 470 | 28 | 11 | 356 | 1729 | 0.3 | 278 |
| 18 | 38.7 | 22 | 2 | 4 | 29 | 390 | 930 | 7.7 | 85 | 258 | 192 | 24 | 460 | 15 | 2 | 365 | 1789 | 0.4 | 197 |
| 19 | 38.8 | 21 | 4 | 4 | 60 | 390 | 985 | 7.6 | 80 | 157 | 152 | 11 | 412 | 2 | 25 | 327 | 1929 | 0.2 | 175 |
| Emission Limit Value | | | | | | | | 6.0-9.0 | - | - | 150 | 40 | 15 | 8 | - | 11 | 2000 | 2.0 | 60 |

[a] $V_T$ - total volume; $V_D$ - discharged volume; $t_R$ - SBR react time; $t_S$ - sedimentation time. [b] Amount of oxygen supplied during the aerobic phase. [c] Glycerol provided (expressed as COD) for the anoxic phase. [d] Total dissolved iron. * Long sedimentation periods due to the occurrence of operational/technical problems (see Table 6.2). n.a. – not applied. n.d. – not determined.

Regarding TN removal, denitrification occurred only for trials with glycerol addition (1-2 and 17-19, Table 6.13), all of the others showed a negligible nitrogen removal (Figure 6.10-c). The most expressive removals were attained in trials 1 and 2, thus values close to discharge legal limit were achieved. Samples collected during trials 1 and 17-19, allowed to estimate a denitrification rate between 0.07-0.10 kg N/kg VSS/day, a consumption of 3.0-5.3 kg COD/kg N removed (stoichiometric required 2.86 kg COD/kg $NO_3^-$-N) and alkalinity production of 2.5-3.4 kg $CaCO_3$/kg N removed.

### 6.3.6 Treatment train overall analysis

#### 6.3.6.1 Treatment assessment

During the treatment period, a total of 547 $m^3$ of leachate from the LTP aerated lagoon was fed to BR1 and 384 $m^3$ was discharged after going through all the treatment train stages. Also, a total of 150.5 $m^3$ of sludge was produced: (i) 104.5 $m^3$ from C/S stage; (ii) 27.6 $m^3$ from nitrite oxidation step (trials 9-19); (iii) 6.6 $m^3$ of PF acid sludge (trials 1-2 and 4-8); (iv) 11.8 $m^3$ of iron sludge. In the course of the treatments, no biological sludge was removed from BRs.

Considering the influent and final discharge, the overall treatment allowed to attain DOC and COD mean removals of $87 \pm 2\%$ and $90 \pm 1\%$, respectively (Figure 6.11-a and -b). The worst performance registered on trial 8 was mainly due to the restart of BR2, where fresh biomass and leachate was pumped from BR1, thus increasing DOC and COD values at discharge. It is worth to notice that the highest DOC and COD removals were obtained in trials 15-19 (abatements over 96% for both), coinciding with (i) influent leachate $BOD_5$/COD ratio above 0.3 and (ii) mineralization at PF stage above 50%. Also, until trial 15, the coagulation stage was the main contributor to the decrease of organic matter but, due to the increase of influent biodegradability, from trial 15 forward it was BR1 (DOC and COD reductions above 50%).

In respect to TN, the multistage yielded an average removal of $71 \pm 4\%$, with BR1 being the stage were most TN was removed (Figure 6.11-c). It was possible to verify that TN global removal was above 98% for trials 1-2, since denitrification was promoted in both BRs. It remained above 90%, for trials 3-4, when glycerol was added at BR1 with a COD/N ratio above 1.5, and then dropped in the following trials with the reduction of glycerol amount. Once again, due to the BR2 restart, the lowest TN global removal (48.4%) was achieved in trial 8 and it remained under 60% until trial 15. Following the influent biodegradability increment, and later with the promotion of denitrification

also at BR2 (even with low amount of glycerol addition, COD/N ratio < 1.0), TN global removal started to increase up to nearly 84%.
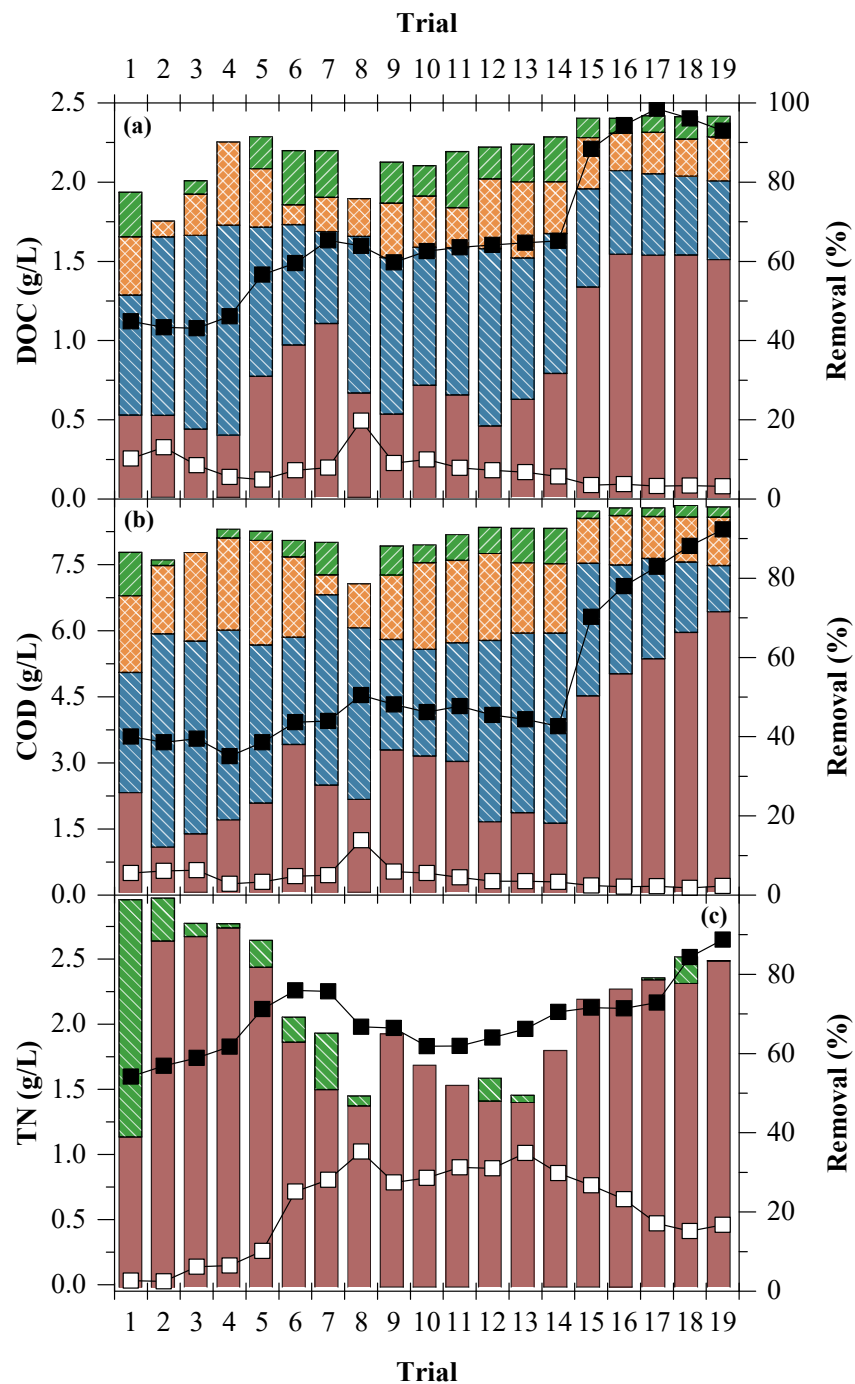


**Figure 6.11** – Evolution profile of (a) DOC, (b) COD, and (c) TN concentrations of the influent leachate (■) and discharged (□) and respective removal percentage for each treatment stage ( BR1, C/S, PF and BR2).

For legal compliance, it is also important to consider iron and sulfate contents since their concentration was increased by the addition of chemicals throughout the treatment. TDI final

concentration, at discharge (Table 6.13), was always below the legal limit despite some operational difficulties at neutralization step. For most trials, sulfate ion concentration was in accordance with discharge limits, except for trials 4-6 and 9 due to greater sulfuric acid addition in the coagulation stage: (i) to achieve a pH lower than 4.2, and (ii) when the bio-treated leachate drawn from BR1 presented alkalinity above 1.0 g $CaCO_3$/L (high TN removal).

Finally, considering the sludge treatment step, generated sludge was dewatered using a filter-press and an average of 8.9 kg of dry sludge/$m^3$ of treated leachate was obtained. The liquid side stream from filter-press was reintroduced back into the leachate treatment at BR1 and coagulation/sedimentation stage. The dried sludge was characterized and followed the legal requirements for landfill disposal (Table 6.14). The occurrence of operational and technical problems (see Table 6.2), making it impossible to remove sludge, led on some occasions to higher treatment times.

**Table 6.14** – Characterization of dried sludge (Leaching limit values calculated at L/S=10 L/kg).

| Parameter | Units | Value | Legal limit[b] |
|---|---|---|---|
| pH | | 5.3 | - |
| Conductivity | mS/cm | 4.84 | - |
| DOC | | 8780 | 1000[c] |
| Arsenic | | 0.42 | 5 |
| Lead | | 3.8 | 10 |
| Cadmium | | 0.028 | 2 |
| Total chromium | | 9.0 | 20 |
| Copper | | 4.0 | 50 |
| Nickel | | 3.4 | 10 |
| Mercury | mg/kg dry matter | <0.004[a] | 0.5 |
| Zinc | | 16 | 50 |
| Barium | | 0.94 | 100 |
| Molybdenum | | 0.14 | 10 |
| Antimony | | 0.42 | 0.7 |
| Selenium | | <0.04[a] | 0.5 |
| Chloride | | 22000 | 50000 |
| Fluoride | | 56 | 250 |
| Sulfate | | 5000 | 20000 |

[a] Quantification limits. [b] Limit values for admission at non-hazardous waste landfill, according to Decree-Law no. 183/2009, Table 4, Annex IV. [c] This value may be exceeded if the landfill is specifically intended for the admission of organic waste or when it is a non-fermentable residue.

Taking into account the experience acquired throughout the trials, and assuming that the upstream lagoon was being operated at minimum oxygen levels, some fundamental conditions for a regular and successful operation of the compact multistage facility are displayed in Table 6.15. Under those

operational key-conditions, it is expectable to obtain an effluent with suitable quality to be directly discharged into waterbodies.

**Table 6.15** – Key-conditions for a consistent and effective operation.

| Stage | Objectives | Key-conditions |
|---|---|---|
| BR1 | **Biodegradable organic matter oxidation** **Total ammonia oxidation** **Partial nitrite reduction** **Alkalinity control** | The following operation scheme should be applied:<br>1 – <u>Anoxic</u>: to take advantage of potential biodegradable organic matter from the influent for denitritation process and, consequently, to produce the alkalinity required for the next phase.<br>2 – <u>Aerobic</u>: to oxidize the total ammonia content, thus consuming all alkalinity (of the influent plus the generated in the previous anoxic phase);<br>3 – <u>Anoxic</u>: to partially reduce the nitrite concentration, resulting from the prior aerobic phase, not exceeding an alkalinity of 1.0 g $CaCO_3$/L (to minimize the addition of $H_2SO_4$ in the following stage, thus keeping $[SO_4^{2-}]$ < 2 g/L). This could be attained by restraining the amount of external carbon donor added. |
| C/S | **40-50% decrease of DOC and COD content** | C/S stage should be performed at pH 4.2, to comply with sulfate legal limits, and with a coagulant dosage of 200-240 mg $Fe^{3+}$/L. With acidification, part of the nitrites formed at BR1, are oxidized to nitrates.<br>A relatively short sedimentation time (2-4 hours) could be applied, as another sludge removal occurs at the following nitrite oxidation step. |
| PF | **Nitrites oxidation** | Nitrite oxidation with hydrogen peroxide as a distinct step prior to the PF reaction (i.e. without catalyst addition and with lamps turned-off) and further acidic sludge removal.<br>Technical Note: As a cost-saving solution, $H_2O_2$ could be replaced by air, making a bypass from the BR1 (or 2) air compressor to the C/P unit. |
| | **Recalcitrant organic matter degradation** **Biodegradability enhancement** | The PF reaction would stop when the DOC value is under 250 mg/L, e.g. by indication of a SUVA sensor.<br>Technical Note: As a time-saving solution, the number of lamps could be increased, since the assemblage of FluHelik photoreactors in series is easy and it does not compromise the compact size of the facility. |
| | **Neutralization** **Iron removal** | For an effective iron precipitation, and to attain the legal requirements (total iron < 2 mg/L), a residual amount of 3.0-3.5 mM of $H_2O_2$ must be ensured at the end of the PF reaction. |
| RB2 | **Carbon and nitrogen removal** | The following operation scheme should be applied:<br>1 – <u>Anoxic</u>: to promote denitrification up to TN < 15 mg/L, using the biodegradable organic matter from the photo-treated leachate and an external carbon source.<br>2 – <u>Aerobic</u>: to ensure that no biodegradable carbonaceous matter remains in the effluent, thus complying BOD and COD legal discharge limits. |

### 6.3.6.2 Treatment costs

Treatment cost, for each trial, was calculated considering (i) chemicals used for leachate and sludge treatment, (ii) energy spent during PF stage and overall processes, (iii) UV-Vis lamps replacement, and (iv) treated sludge disposal in a sanitary landfill. All the costs were calculated based on the volume of treated leachate ($m^3$) and dry matter content of produced and treated sludge (kg). Further details are shown in Table 6.16 to Table 6.18. On average, the total cost of the treatment train was ~ 6.7 €/$m^3$, with PF stage as the major contributor (Figure 6.12), mainly due to $H_2O_2$ consumption (Table 6.18). An exception occurs for trial 2, where the biological treatment overcomes PF stage costs, due to (i) denitrification promotion, with significant glycerol addition on both biological reactors, and (ii) the shortest photo-treatment time, thus presenting the lowest energy and hydrogen peroxide consumption. The average treatment cost calculated in this work is slightly higher than the estimated in the pilot-scale studies (~5.1 €/$m^3$ [1]), being the differences related to the incorporation of the energy consumption for the facility equipment, except PF lamps, and also the sludge treatment and disposal costs. If the same components were excluded in the present assessment, the average operational costs would lower, from 6.7 to 4.8 €/$m^3$.



| | 1 | 2 | 3 | 4 | 5 | 6 | 7 | 8 | 9 | 10 | 11 | 12 | 13 | 14 | 15 | 16 | 17 | 18 | 19 |
|---|---|---|---|---|---|---|---|---|---|---|---|---|---|---|---|---|---|---|---|
| BRs (€/$m^3$) | 2.9 | 3.3 | 1.6 | 1.6 | 1.3 | 0.9 | 0.9 | 0.9 | 1.3 | 1.3 | 0.9 | 0.7 | 1.1 | 1.0 | 0.6 | 0.6 | 0.7 | 0.7 | 0.7 |
| C/S (€/$m^3$) | 0.6 | 0.9 | 0.7 | 0.9 | 0.7 | 0.6 | 0.5 | 0.8 | 0.7 | 0.6 | 0.7 | 0.6 | 0.6 | 0.6 | 0.6 | 0.7 | 0.7 | 0.7 | 0.7 |
| PF (€/$m^3$) | 4.2 | 2.5 | 2.9 | 3.7 | 3.1 | 3.8 | 4.6 | 4.2 | 3.2 | 4.0 | 4.3 | 4.3 | 4.3 | 4.4 | 4.1 | 4.7 | 5.1 | 4.8 | 4.6 |
| Sludge (€/$m^3$) | 0.7 | 0.7 | 0.6 | 0.7 | 0.8 | 0.6 | 0.7 | 0.6 | 0.8 | 0.9 | 0.8 | 0.9 | 0.9 | 1.1 | 0.9 | 0.7 | 0.7 | 0.6 | 0.7 |
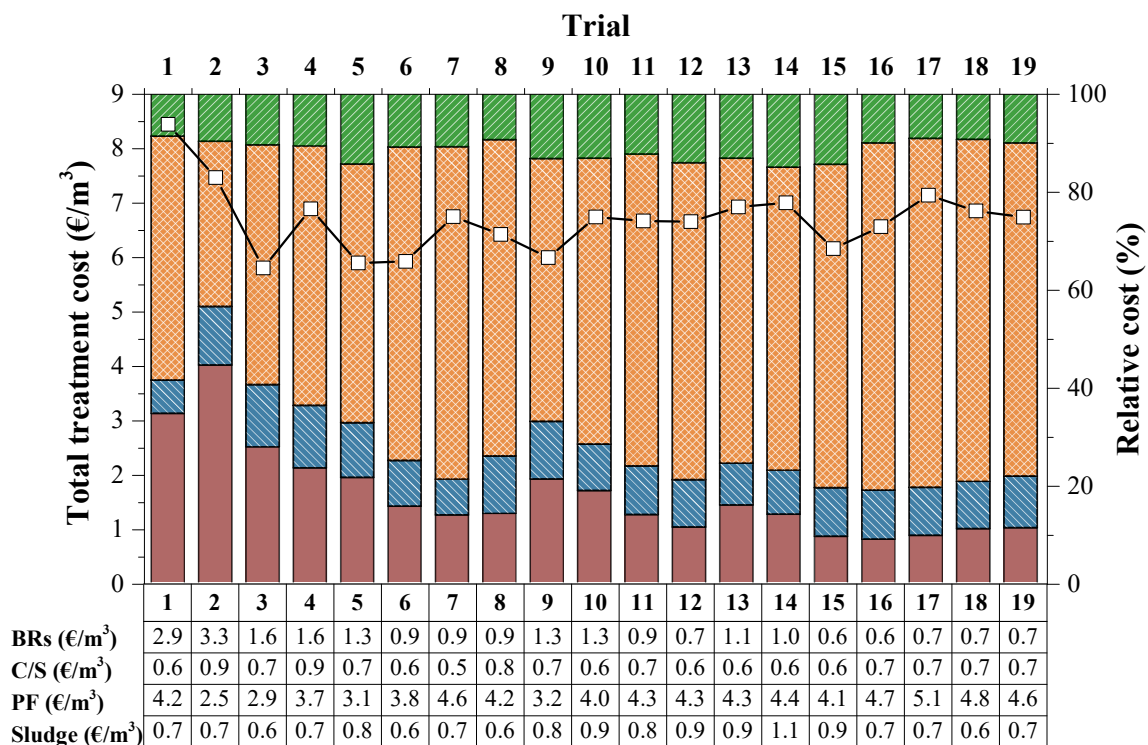
**Figure 6.12** – Multistage total treatment cost for each trial (□) and respective relative cost for the biological processes (�), coagulation (▥), photo-Fenton (▦) and sludge treatment (▨).

Considering other leachate decontamination strategies that combine different treatment processes with photo-Fenton, it is possible to find a range of operational costs reported in literature (see Table 3.10 of Chapter 3). An operating cost of 4.1 €/m$^3$, that includes equipment's energy consumption and sludge disposal costs, was presented by Cassano *et al.* [23] for a treatment of a medium-age landfill leachate, to achieve a COD target of 160 mg/L (initial COD of 2.8-3.6 g/L), combining a sequencing batch biofilter granular reactor with solar photo-Fenton. This value highlights the potential of energy savings when applying the solar photo-Fenton process. However, this study does not consider the land area requirements and the investment cost associated with the compound parabolic collectors (CPCs), which are the major drawbacks when aiming a full-scale application. In this sense, Torres-Socías *et al.* [24] estimated a CPC surface area of 6850 m$^2$, with an investment cost of 10.5 €/m$^3$ (corresponding to 24% of the estimated operating cost), to treat 40 m$^3$/day of leachate combining coagulation and solar PF. Another study by Silva *et al.* [25], projected a CPC surface area of 6056 m$^2$ and a total photo-Fenton cost of 11 €/m$^3$, to achieve a target COD of 150 mg/L, for the treatment of 100 m$^3$/day of a leachate previously oxidized by a biological system. To overcome the constraints presented by the CPC collectors for full-scale solar photocatalytic applications, recent research efforts are being made towards design simplification and low-cost solutions [26, 27]. Meanwhile, the usage of artificial photoreactors, such as FluHelik, presents a compact, modular and effective solution for the PF treatment at full-scale.

**Table 6.16** – Reagents and consumables price list.

| Reagents and consumables | Prices[a] | |
|---|---|---|
| Glycerol (88%, 1.26 g/cm$^3$) | | 0.410 |
| Sulfuric acid (98%, 1.84 g/cm$^3$) | | 0.104 |
| Ferric chloride (40%, 1.44 g/cm$^3$) | | 0.190 |
| Ferrous chloride (26.7%, 1.27 g/cm$^3$) | €/kg | 0.220 |
| Hydrogen peroxide (50% (w/v), 1.10 g/cm$^3$) | | 0.375 |
| Sodium hydroxide (30%, 1.33 g/cm$^3$) | | 0.159 |
| Polymer (Ambifloc® C58) | | 3.00 |
| Energy | €/kWh | 0.12 |
| UV-Vis lamps (hours of service = 20000) | €/lamp | 500 |
| Landfill sludge deposition | €/ton | 50 |

[a] Prices in august of 2015.

**Table 6.17 – Leachate and produced sludge data for treatment cost analysis.**

| Test Data | Un | 1 | 2 | 3 | 4 | 5 | 6 | 7 | 8 | 9 | 10 | 11 | 12 | 13 | 14 | 15 | 16 | 17 | 18 | 19 |
|---|---|---|---|---|---|---|---|---|---|---|---|---|---|---|---|---|---|---|---|---|
| Fed to C/P | $m^3$ | 30 | 25.8 | 30 | 26.4 | 30 | 30 | 29.5 | 31.7 | 30 | 30 | 30 | 30 | 30 | 30 | 30 | 30 | 30 | 30 | 30 |
| Coag. sludge[a] | $m^3$ | 6 | 5 | 4.6 | 5.5 | 7.5 | 4.7 | 5.3 | 4.5 | 8.2 | 9.6 | 8.6 | 10 | 9.8 | 11.8 | 9.4 | 5.4 | 5.3 | 5.1 | 5.8 |
| TS[a] | kg | 54 | 45 | 41 | 91 | 36 | 35 | 37 | 75 | 74 | 86 | 77 | 90 | 88 | 106 | 38 | 57 | 50 | 53 | 71 |
| PF sludge | $m^3$ | 1.4 | 1.3 | 0.7 | 1.1 | 1.9 | 1.3 | 2 | 1.1 | 0.3 | 0.5 | 0.4 | 0.9 | 0.7 | 1 | 0.7 | 0.8 | 0.8 | 0.8 | 0.7 |
| TS[b] | kg | 14 | 13 | 7 | 11 | 19 | 13 | 20 | 27 | 3 | 5 | 4 | 9 | 7 | 15 | 7 | 11 | 8 | 7 | 7 |
| Treated | $m^3$ | 22.6 | 19.5 | 24.7 | 19.8 | 20.6 | 24 | 22.2 | 26.1 | 21.5 | 19.9 | 21 | 19.1 | 19.5 | 17.2 | 19.9 | 23.8 | 23.9 | 24.1 | 23.5 |

[a] Sludge produced from nitrite oxidation (trials 9-19) was included. [b] TS as total solids, considering dry matter content and produced sludge volume.

**Table 6.18** – Treatment costs of the treatment train applied to an urban mature landfill leachate, at full-scale, for each trial.

| | | Un | MULTISTAGE TREATMENT TRIALS | | | | | | | | | | | | | | | | | |
|---|---|---|---|---|---|---|---|---|---|---|---|---|---|---|---|---|---|---|---|---|
| | | | **1** | **2** | **3** | **4** | **5** | **6** | **7** | **8** | **9** | **10** | **11** | **12** | **13** | **14** | **15** | **16** | **17** | **18** | **19** |
| **CHEMICALS** | Glycerol | L | 136 | 137 | 60 | 53 | 40 | 20 | 20 | 20 | 40 | 40 | 20 | 10 | 30 | 23 | 0 | 0 | 6.2 | 10 | 10 |
| | Specific cost[a] | €/m³ | **2.34** | **2.74** | **1.03** | **1.04** | **0.69** | **0.34** | **0.35** | **0.33** | **0.69** | **0.69** | **0.34** | **0.17** | **0.52** | **0.40** | **0.00** | **0.00** | **0.11** | **0.17** | **0.17** |
| | H₂SO₄ | L | 0.0 | 33.3 | 27.8 | 38.9 | 33.0 | 16.3 | 6.4 | 35.0 | 27.0 | 13.8 | 19.5 | 11.1 | 8.9 | 7.8 | 10.0 | 14.4 | 17.0 | 14.5 | 20.7 |
| | Specific cost[a] | €/m³ | **0.00** | **0.25** | **0.18** | **0.28** | **0.21** | **0.10** | **0.04** | **0.21** | **0.17** | **0.09** | **0.12** | **0.07** | **0.06** | **0.05** | **0.06** | **0.09** | **0.11** | **0.09** | **0.13** |
| | FeCl₃ | L | 31.8 | 34.0 | 30.0 | 30.0 | 18.0 | 18.0 | 18.0 | 30.0 | 27.4 | 29.1 | 27.8 | 31.6 | 27.2 | 32.2 | 28.9 | 30.5 | 33.3 | 31.1 | 32.3 |
| | Specific cost[a] | €/m³ | **0.29** | **0.36** | **0.27** | **0.31** | **0.16** | **0.16** | **0.17** | **0.26** | **0.25** | **0.27** | **0.25** | **0.29** | **0.25** | **0.29** | **0.26** | **0.28** | **0.30** | **0.28** | **0.29** |
| | FeCl₂ | L | 10.8 | 11.3 | 11.0 | 10.0 | 10.0 | 10.0 | 10.0 | 10.0 | 9.0 | 9.6 | 9.8 | 9.2 | 9.3 | 10.4 | 9.2 | 11.2 | 12.6 | 11.2 | 11.8 |
| | Specific cost[a] | €/m³ | **0.10** | **0.12** | **0.10** | **0.11** | **0.09** | **0.09** | **0.09** | **0.09** | **0.08** | **0.09** | **0.09** | **0.09** | **0.09** | **0.10** | **0.09** | **0.10** | **0.12** | **0.10** | **0.11** |
| | H₂O₂ | L | 186 | 59 | 93 | 101 | 90 | 128 | 166 | 162 | 122 | 147 | 151 | 164 | 161 | 161 | 165 | 178 | 201 | 184 | 174 |
| | Specific cost[a] | €/m³ | **3.09** | **1.13** | **1.54** | **1.91** | **1.50** | **2.12** | **2.81** | **2.55** | **2.02** | **2.44** | **2.51** | **2.72** | **2.68** | **2.68** | **2.75** | **2.95** | **3.34** | **3.06** | **2.89** |
| | NaHO | L | 15.5 | 55.6 | 50.0 | 19.6 | 30.0 | 50.0 | 44.0 | 55.5 | 51.1 | 48.3 | 43.9 | 40.0 | 45.6 | 44.4 | 37.2 | 54.4 | 54.5 | 46.7 | 48.9 |
| | Specific cost[a] | €/m³ | **0.10** | **0.41** | **0.32** | **0.14** | **0.19** | **0.32** | **0.28** | **0.33** | **0.32** | **0.31** | **0.28** | **0.25** | **0.29** | **0.28** | **0.24** | **0.35** | **0.35** | **0.30** | **0.31** |
| | **(1) TOTAL** | €/m³ | **5.92** | **5.02** | **3.45** | **3.79** | **2.85** | **3.15** | **3.75** | **3.77** | **3.54** | **3.88** | **3.60** | **3.59** | **3.88** | **3.80** | **3.40** | **3.77** | **4.33** | **4.01** | **3.91** |
| **ENERGY** | PFconsumption | kwh | 155 | 118 | 144 | 255 | 252 | 235 | 262 | 227 | 123 | 197 | 260 | 234 | 235 | 239 | 173 | 235 | 242 | 252 | 240 |
| | Specific cost[a,b] | €/m³ | **0.65** | **0.58** | **0.61** | **1.22** | **1.06** | **0.99** | **1.12** | **0.90** | **0.51** | **0.83** | **1.09** | **0.98** | **0.99** | **1.00** | **0.72** | **0.99** | **1.02** | **1.06** | **1.01** |
| | Others | €/m³ | **1.44** | **1.44** | **1.44** | **1.44** | **1.44** | **1.44** | **1.44** | **1.44** | **1.44** | **1.44** | **1.44** | **1.44** | **1.44** | **1.44** | **1.44** | **1.44** | **1.44** | **1.44** | **1.44** |
| | **(2) TOTAL** | €/m³ | **2.09** | **2.02** | **2.05** | **2.66** | **2.50** | **2.43** | **2.56** | **2.34** | **1.95** | **2.27** | **2.53** | **2.42** | **2.43** | **2.44** | **2.16** | **2.43** | **2.46** | **2.50** | **2.45** |
| **SLUDGE** | Polymer | kg | 0.27 | 0.23 | 0.19 | 0.41 | 0.22 | 0.19 | 0.23 | 0.41 | 0.31 | 0.37 | 0.33 | 0.40 | 0.38 | 0.48 | 0.18 | 0.27 | 0.23 | 0.24 | 0.31 |
| | Specific cost[c] | €/m³ | **0.03** | **0.03** | **0.02** | **0.03** | **0.04** | **0.02** | **0.03** | **0.02** | **0.03** | **0.04** | **0.04** | **0.04** | **0.04** | **0.05** | **0.04** | **0.02** | **0.02** | **0.02** | **0.03** |
| | Treated sludge | kg/m³ | 10.0 | 9.9 | 6.5 | 17.2 | 8.9 | 6.6 | 8.6 | 12.9 | 11.9 | 15.3 | 12.9 | 17.3 | 16.3 | 23.4 | 7.6 | 9.5 | 8.1 | 8.3 | 11.1 |
| | Specific cost[d] | €/m³ | **0.41** | **0.41** | **0.29** | **0.42** | **0.52** | **0.33** | **0.41** | **0.29** | **0.47** | **0.56** | **0.50** | **0.61** | **0.58** | **0.71** | **0.56** | **0.34** | **0.34** | **0.33** | **0.36** |
| | **(3) TOTAL** | €/m³ | **0.44** | **0.44** | **0.32** | **0.45** | **0.56** | **0.36** | **0.44** | **0.32** | **0.51** | **0.60** | **0.54** | **0.65** | **0.63** | **0.76** | **0.60** | **0.37** | **0.36** | **0.35** | **0.39** |
| | **(1) + (2) + (3)** | | **8.45** | **7.48** | **5.82** | **6.9** | **5.91** | **5.94** | **6.75** | **6.43** | **6** | **6.75** | **6.67** | **6.66** | **6.94** | **7.00** | **6.16** | **6.57** | **7.15** | **6.86** | **6.75** |

[a] Calculated based on the treated leachate volume. [b] Considering PF stage time and service time of lamps. [c] Calculated based on dry matter content of coagulated and iron sludge. [d] Calculated based on dry matter content of treated sludge.

## 6.4 Conclusions

The treatment train strategy applied to an urban mature landfill leachate, at full-scale, demonstrated its ability to achieve high removals of both organic and nitrogen compounds, obtaining maximum reductions of ~98% for both COD and TN. Glycerol was successfully used as external carbon source to promote biological denitrification and the efficiency of the FluHelik photoreactor for leachate decontamination was demonstrated. When compared with previous studies, where similar UV-Vis lamps were merely located inside the treatment tank, to achieve the same DOC goal, PF process required 2 times less radiation energy.

Despite the efforts, achieving legal compliance for all parameters to direct discharge into waterbodies was not completely accomplished. The balance between COD and TN removal, as well as sulfate content, revealed a challenge during operation and is a key element for the success of this strategy. TN removal in BR1 is advantageous for hydrogen peroxide saving during PF, however, it must be ensured that alkalinity is lower than 1.0 g $CaCO_3$/L so that the sulfate ion discharge limit is not exceeded. Moreover, some factors influenced the treatment efficiency, namely: (i) intense variations of the influent leachate; (ii) occurrence of operational/technical problems that were not observed at pilot-scale; and (iii) difficulties to anticipate operational adjustments required as the treatment proceeded. Nevertheless, when consecutive treatment trials occurred under regular conditions, the overall efficiency of the system tended to increase.

## 6.5 References

1.  Silva, T.F.C.V., P.A. Soares, D.R. Manenti, A. Fonseca, I. Saraiva, R.A.R. Boaventura, and V.J.P. Vilar, *An innovative multistage treatment system for sanitary landfill leachate depuration: Studies at pilot-scale.* Science of the Total Environment, 2017. **576**: p. 99-117.

2.  Webler, A.D., F.C. Moreira, M.W.C. Dezotti, C.F. Mahler, I.D.B. Segundo, R.A.R. Boaventura, and V.J.P. Vilar, *Development of an integrated treatment strategy for a leather tannery landfill leachate.* Waste Management, 2019. **89**: p. 114-128.

3.  Moreira, F.C., E. Bocos, A.G.F. Faria, J.B.L. Pereira, C.P. Fonte, R.J. Santos, J.C.B. Lopes, M.M. Dias, M.A. Sanromán, M. Pazos, R.A.R. Boaventura, and V.J.P. Vilar, *Selecting the best piping arrangement for scaling up an annular channel reactor: An experimental and computational fluid dynamics study.* Science of the Total Environment, 2019. **667**: p. 821-832.

4.  Espíndola, J.C., R.O. Cristóvão, S.R.F. Araújo, T. Neuparth, M.M. Santos, R. Montes, J.B. Quintana, R. Rodil, R.A.R. Boaventura, and V.J.P. Vilar, *An innovative photoreactor, FluHelik, to promote UVC/$H_2O_2$ photochemical reactions: tertiary treatment of an urban wastewater.* Science of the Total Environment, 2019. **667**: p. 197-207.

5.  Silva, T.F.C.V., M.E.F. Silva, A.C. Cunha-Queda, A. Fonseca, I. Saraiva, R.A.R. Boaventura, and V.J.P. Vilar, Sanitary landfill leachate treatment using combined solar photo-Fenton and biological oxidation processes at pre-industrial scale. Chemical Engineering Journal, 2013. **228**: p. 850-866.

6.  Sawyer, C., McCarty, P., Parkin, G., *Chemistry for Environmental Engineering and Science.* 2003: McGraw-Hill Educacion.

7.  Sawyer, C., P. McCarty, and G. Parkin, *Chemistry for Environmental Engineering ans Science.* 2003: McGraw-Hill Education.

8.  Silva, T.F.C.V., M.E.F. Silva, A.C. Cunha-Queda, A. Fonseca, I. Saraiva, M.A. Sousa, C. Gonçalves, M.F. Alpendurada, R.A.R. Boaventura, and V.J.P. Vilar, *Multistage treatment system for raw leachate from sanitary landfill combining biological nitrification-denitrification/solar photo-Fenton/biological processes, at a scale close to industrial.* Water Research, 2013. **47**: p. 6167-6186.

9.  Moreira, F.C., J. Soler, A. Fonseca, I. Saraiva, R.A.R. Boaventura, E. Brillas, and V.J.P. Vilar, *Incorporation of electrochemical advanced oxidation processes in a multistage treatment system for sanitary landfill leachate.* Water Research, 2015. **81**: p. 375-387.

10. Yabroudi, S.C., D.M. Morita, and P. Alem, Landfill leachate treatment over nitritation/denitritation in an activated sludge sequencing batch reactor. APCBEE procedia, 2013. **5**: p. 163-168.

11. Wett, B. and W. Rauch, The role of inorganic carbon limitation in biological nitrogen removal of extremely ammonia concentrated wastewater. Water Research, 2003. **37**: p. 1100-1110.

12. Spagni, A., M.C. Lavagnolo, C. Scarpa, P. Vendrame, A. Rizzo, and L. Luccarini, *Nitrogen removal optimization in a sequencing batch reactor treating sanitary landfill leachate.* Journal of Environmental Science and Health A, 2007: p. 757-765.

13. Tsuchihashi, R., G. Bowden, K. Beckmann, A. Deur, and B. Bodniewicz, Evaluation of crude glycerin as a supplemental carbon source for a high rate step-feed BNR process, in Water Environment Federation Technical Exhibition and Conference, W.E. Federation, Editor. 2008: Chicago, Illinois, USA. p. 202-219.

14. Katarzyna, B., K. Dorota, and Z. Karo, *Glycerine as a carbon source in nitrite removal and sludge production.* Chemical Engineering Journal, 2015. **267**: p. 324-331.

15. Torà, J.A., J.A. Baeza, J. Carrera, and J.A. Oleszkiewicz, Denitritation of a high-strength nitrite wastewater in a sequencing batch reactor using different organic carbon sources. Chemical Engineering Journal, 2011. **172**: p. 994-998.

16. Frison, N., S. Di Fabio, C. Cavinato, P. Pavan, and F. Fatone, Best available carbon sources to enhance the via-nitrite biological nutrients removal from supernatants of anaerobic co-digestion. Chemical Engineering Journal, 2013. **215**: p. 15-22.

17. Amor, C., E. Torres-Socías, J.A. Peres, M.I. Maldonado, I. Oller, S. Malato, and M.S. Lucas, *Mature landfill leachate treatment by coagulation/flocculation combined with Fenton and solar photo-Fenton processes.* Journal of Hazardous Materials, 2015. **286**: p. 261-268.

18. Silva, T.F.C.V., R. Ferreira, P.A. Soares, D.R. Manenti, A. Fonseca, I. Saraiva, R.A.R. Boaventura, and V.J.P. Vilar, *Insights into solar photo-Fenton reaction parameters in the oxidation of a sanitary landfill leachate at lab-scale.* Journal of Environmental Management, 2015. **164**: p. 32-40.

19. Malato, S., J. Blanco, M.I. Maldonado, I. Oller, W. Gernjak, and L. Pérez-Estrada, *Coupling solar photo-Fenton and biotreatment at industrial scale: main results of a demonstration plant.* Journal of Hazardous Materials, 2007. **146**: p. 440-446.

20. in *Decree-law no. 236/98, of 1ˢᵗ August*, P. Republic, Editor. 1998: Republic Diary - I Series - A.

21. Silva, T.F.C.V., A. Fonseca, I. Saraiva, R.A.R. Boaventura, and V.J.P. Vilar, Biodegradability enhancement of a leachate after biological lagooning using a solar driven photo-Fenton reaction, and further combination with an activated sludge biological process, at pre-industrial scale Water Research, 2013. **47**: p. 3543-3557.

22. Mosteo, R., D. Gumy, and C. Pulgarin, Coupled photo-Fenton-biological system: effect of the Fenton parameters such as residual H2O2, Fe2+ and pH on the efficiency of biological process. Water Science and Technology, 2008. **58**(8): p. 1679-1685.

23. Cassano, D., A. Zapata, G. Brunetti, G. Del Moro, C. Di Iaconi, I. Oller, S. Malato, and G. Mascolo, Comparison of several combined/integrated/biological-AOPs setups for the treatment of municipal landfill leachate: Minimization of operating costs and effluent toxicity. Chemical Engineering Journal, 2011. **172**: p. 250-257.

24. Torres-Socías, E., L. Prieto-Rodríguez, A. Zapata, I. Fernández-Calderero, I. Oller, and S. Malato, *Detailed treatment line for a specific landfill leachate remediation: Brief economic assessment.* Chemical Engineering Journal, 2015. **261**: p. 60-66.

25. Silva, T.F.C.V., A. Fonseca, I. Saraiva, R.A.R. Boaventura, and V.J.P. Vilar, *Scale-up and cost analysis of a photo-Fenton system for sanitary landfill leachate treatment.* Chemical Engineering Journal, 2016. **283**: p. 76-88.

26. Ochoa-Gutiérrez, K.S., E. Tabares-Aguilar, M.A. Mueses, F. Machuca-Martínez, and G. Li Puma, *A novel prototype offset multi tubular photoreactor (OMTP) for solar photocatalytic degradation of water contaminants.* Chemical Engineering Journal, 2018. **341**: p. 628-638.

27. Cabrera-Reina, A., S. Miralles-Cuevas, G. Rivas, and J.A. Sánchez-Pérez, Comparison of different detoxification pilot plants for the treatment of industrial wastewater by solar photo-Fenton: Are raceway pond reactors a feasible option? Science of the Total Environment, 2019. **648**: p. 601-608.

# 7 Cost-effective solar collector to promote photo-Fenton reactions: A case study on the treatment of mature urban leachates

*Some drawbacks associated with solar collectors' high investment cost, land area requirements, and loss of the photo-treatment efficiency over time (due to the soiled of the reflective surface) are blocking the application of solar photo-Fenton at industrial scale. In this work, aiming at cost reduction and durability increase of the solar collectors, different reflector materials (anodized aluminium with (MS) and without (R85) protective coating, soiled aluminium (R85s) and stainless steel (SS)) and geometries (flat (F), simple double parabola (SP) and traditional double parabola (DP)) were tested and their efficiency assessed.*

*Ferrioxalate actinometry was performed, at lab-scale under simulated sunlight, and the optical concentration ratio ($CR_O$) followed the sequence: SS-F (0.59) ≈ R85-F (0.60) < R85s-DP (0.67) ≈ SS-SP (0.70) ≈ SS-DP (0.72) < MS-DP (0.84) < R85-DP (0.93). These results agree with the ray-trace and specular reflectance analysis. The impact of 8-year of outdoor aging on the R85 aluminium reflectors was clearly shown. For the photo-Fenton lab-trials using an urban mature leachate, the time to achieve 60% mineralization decreased as follows: SS-F (158') > R85-F and R85s-DP (153') > SS-SP (141') > SS-DP (127') > R85-DP (121') > MS-DP (117').*

*According to the cost analysis, for the same investment required to build 100 $m^2$ of an R85-DP collector, it is possible to construct 126 $m^2$ of an SS-F collector, containing 1.6 times more absorber tubes per square meter, which leads to a treatment rate increment of 51%. The reflectors performance was also validated at pilot-scale, under natural sunlight.*

## 7.1 Introduction

Advanced oxidation processes, which include chemical ($O_3/H_2O_2$, $H_2O_2/Fe^{2+}$), photochemical ($UV/O_3$, $UV/H_2O_2$), photocatalytic ($TiO_2/UV$, $UV/H_2O_2/Fe^{2+}$) and electrochemical methods, are considered as a promising technique for the removal of toxic and bio-recalcitrant pollutants from different types of wastewaters [1-3]. Regardless the efficiency of these technologies, they can be quite expensive, essentially due to the high energy demand and chemicals consumption [2, 4, 5]. The use of renewable energy sources, i.e., natural sunlight as the irradiation source, can make photocatalytic methods more economically attractive [2, 5, 6]. In this sense, compound parabolic collectors (CPCs) have proven to be a good option for solar photochemical applications [5, 7], whether applied to homogeneous (i.e. photo-Fenton) or heterogeneous ($TiO_2$) photocatalysis. However, some issues are being recognized as drawbacks to the effective implementation of a full-scale photocatalytic treatment, among others, there are: (i) the cost of the solar reactors [3, 8]; and (ii) the efficiency decreasing over time due to the soiling of the reflective surface [9]. These disadvantages entail operational planning constraints and additional costs for the mirror's replacement.

The CPCs reflective surface, responsible for 15 to 25% of the solar collector cost, is traditionally composed by a truncated double parabola (requiring two separate pieces to constitute a single reflector) and made of electropolished anodized aluminium (presenting poor long-term stability). Considering that the first studies of solar photocatalysis started by using $TiO_2$, the CPCs reflectors were developed to maximize the (i) light reflection over the absorber tube wall and (ii) capture of the solar light UV fraction (3-5% of solar spectrum) [2]. These factors are crucial for $TiO_2$-based photocatalytic processes, since all reactions are light-dependent, and the effective wavelength range is under 390 nm. Conversely, in the case of the photo-Fenton (PF) process these requirements may not be so important. PF process is considered to be the most promising to be driven by sunlight, once it is able to absorb the light spectrum up to 580 nm [1, 2, 10], depending on the presence of iron-organic complexes. Beyond that, the PF presents further features besides the light mediated reactions, like the occurrence of Fenton process in the dark zones and thermally induced reactions [1, 10, 11], that contributes to the overall process performance. The UV reflectance requirements of the CPC reflective surface may also be lower, when the objective is the decontamination of wastewaters with low UV transmissibility and containing light-absorbing species that act as an inner-filter, which are overcome by higher wavelengths [1, 12].

Taking the above considerations into account, and with a focus on the cost reduction and durability increase of the solar collectors, there is an opportunity to explore different reflective surface designs

and materials considering the type of: (i) oxidation process to be employed (photon wavelengths required to promote the photocatalytic reaction) and (ii) wastewater to be treated (UV transmissibility and inner-filters effects). Therefore, it is possible that a simpler reflective surface design with a material presenting higher durability under outdoor conditions, but eventually with lower UV reflectance properties, could be successfully applied in solar collectors to promote photo-Fenton oxidation process for decontamination of wastewater, such as urban landfill leachates. To our best knowledge, no research was yet performed using different reflectors materials for solar photocatalytic purposes, while different reflectors geometry was only studied for $TiO_2$ photocatalysis [13]. Also, despite the deterioration of aluminium reflectors surface is recognized as a problem, there are no studies that evaluate its effect on photocatalytic processes [1, 9].

In this way, the present work aims to compare the efficiency of solar collectors with different reflective surface materials (anodized aluminium with (MS) and without (R85) protective coating, soiled aluminium (R85s) and stainless steel (SS)) and reflector geometries (flat (F), simple double-parabola (SP) and traditional double-parabola (DP)) for photo-Fenton applications. The reflective surfaces performance will be compared through the determination of the: (i) optical efficiencies using ray-trace analysis (for geometry) and specular reflectance (for material); (ii) optical concentration ratio ($CR_O$), by means of ferrioxalate actinometry; and (iii) mineralization rate of a mature landfill leachate. Moreover, a cost analysis for the different solar collectors applied in the leachate treatment using PF reaction will also be presented.

## 7.2 Materials and methods

All the chemicals used in this work, the detailed description of the different reflective materials and geometries, experimental units and respective procedures, as well as the analytical methods employed, can be consulted, respectively, in sections 4.1, 4.3.3 and 4.2 of Chapter 4. Further details on the photoreactors and light sources are found in Table 7.1.

The PF experiments carried out in this work used a pre-treated leachate (after biological and coagulation/sedimentation stages) collected at the full-scale treatment train facility. The values of the leachate's spectral transmittance are presented in Figure 4.12 (Chapter 4) and main characterization parameters in Table 7.2.

**Table 7.1** – Characterization of lab- and pilot-scale photoreactors and identification of light sources.

| Photoreactor | Reflective Surface | | Absorber Tube | | | | Irradiation | | Test[f] |
| | Type | $A_a$ (m²) | Tubes (no.) | $L$ (mm) | $V_i$[b] (L) | $d$[c] (mm) | Source[d] | Intensity[e] (W m⁻²) | |
|---|---|---|---|---|---|---|---|---|---|
| Lab-scale | No-RS[a] | - | 1 | 160 | 0.27 | - | XeL | 500 | Act. & PF |
| | R85-DP | 0.025 | 1 | 160 | 0.27 | - | XeL | 275, 350, 500 & 625 | Act. & PF[g] |
| | R85s-DP | 0.025 | 1 | 160 | 0.27 | - | XeL | 500 | Act. & PF |
| | MS-DP | 0.025 | 1 | 160 | 0.27 | - | XeL | 500 | Act. & PF |
| | SS-DP | 0.025 | 1 | 160 | 0.27 | - | XeL | 500 | Act. & PF |
| | SS-SP | 0.020 | 1 | 160 | 0.27 | - | XeL | 275, 350, 500 & 625 | Act. & PF[g] |
| | R85-F | 0.025 | 1 | 160 | 0.27 | - | XeL | 500 | Act. & PF |
| | SS-F | 0.025 | 1 | 160 | 0.27 | - | XeL | 500 | Act. & PF |
| | No-RS[a] | - | 2 | 160 | 0.54 | 50 | XeL | 500 | Act. & PF |
| | R85-F | 0.020 | 2 | 160 | 0.54 | 12.5 | XeL | 500 | Act. |
| | R85-F | 0.024 | 2 | 160 | 0.54 | 25 | XeL | 500 | Act. |
| | R85-F | 0.032 | 2 | 160 | 0.54 | 50 | XeL | 500 | Act. & PF |
| | R85-F | 0.040 | 2 | 160 | 0.54 | 75 | XeL | 500 | Act. |
| | R85-F | 0.048 | 2 | 160 | 0.54 | 100 | XeL | 500 | Act. |
| | SS-F | 0.020 | 2 | 160 | 0.54 | 12.5 | XeL | 500 | Act. |
| | SS-F | 0.024 | 2 | 160 | 0.54 | 25 | XeL | 500 | Act. |
| | SS-F | 0.032 | 2 | 160 | 0.54 | 50 | XeL | 500 | Act. & PF |
| | SS-F | 0.040 | 2 | 160 | 0.54 | 75 | XeL | 500 | Act. |
| | SS-F | 0.048 | 2 | 160 | 0.54 | 100 | XeL | 500 | Act. |
| Pilot-scale | No-RS[a] | 0.44 | 2 | 1500 | 4.7 | 107.1 | NS | - | Act. & PF |
| | MS-DP | 0.44 | 2 | 1500 | 4.7 | 107.1 | NS | - | Act. & PF |
| | SS-F | 0.44 | 2 | 1500 | 4.7 | 107.1 | NS | - | Act. & PF |
| | R85s-DP | 2.20 | 10 | 1500 | 23.7 | 107.1 | NS | - | Act. & PF |
| | SS-SP | 2.42 | 13 | 1500 | 31.9 | 78.2 | NS | - | Act. & PF |

[a] No reflective surface. [b] Illuminated volume. [c] Distance between the absorber tubes. [d] NS: Natural Sunlight, XeL: Xenon Lamp [e] Values only for Xe lamp. [f] Act.: Actinometry, PF: Photo-Fenton. [g] PF tests were only performed for 500 W/m².

**Table 7.2** – Physicochemical characterization of pre-treated landfill leachate.

| Parameter | Unit | Value |
|---|---|---|
| pH | Sorensen scale | 2.8 |
| Abs$_{254}$ (1:25 dilution) | | 0.35 |
| DOC | mg/L | 454 |
| SUVA | L/mg/m | 1.9 |
| COD | mg O$_2$/L | 1289 |
| TDI | mg Fe/L | 25.4 |
| TN | mg N/L | 820 |
| N-NO$_3^-$ | mg/L | 776 |
| N-NO$_2^-$ | mg/L | 7 |
| N-NH$_4^+$ | mg/L | 10 |
| H$_2$O$_2$ | mg/L | < 0.2 |

## 7.3 Results and discussion

### 7.3.1 Reflective surfaces characterization

Regarding the solar collector optics, with a focus on cost reduction and increasing the collector's durability under outdoor conditions, different materials and geometries for the reflective surface were taken into consideration. The materials used as reflective surface (see Table 4.4 of Chapter 4) were analysed in respect to the total ($\rho_T$) and diffuse ($\rho_D$) reflectance (Figure 7.1). It is possible to verify that R85 presented the higher $\rho_T$ values, while the R85s revealed a considerable decrease. The MS aluminium, due to the protective coating, presented the lower $\rho_T$ values until approximately 350 nm, but from this point forward the $\rho_T$ arises reaching values like R85. The SS generically presented the lower $\rho_T$ values, except when comparing to MS in the 280 to 350 nm range (UV$_B$ and part of UV$_A$). In respect to diffuse reflectance, it is worth noticing that the R85s had a considerably higher $\rho_D$ when compared to all the other materials (Figure 7.1). This may be due to the corrosion of the material leading to variations in the normals of the rays reflected along the surface, thus reflecting them in random directions.

The reflectors optical performance must also be compared in terms of specular reflectance ($\rho_S$), i.e. the degree to which a mirror is capable of transferring direct radiation to a target receiver surface [14]. To simplify the comparison, the average $\rho_S$ values from the ranges of 280-315 nm (UV$_B$), 315-400 nm (UV$_A$) and 400-580 nm (Vis) were used (Figure 7.1). In general, the R85 anodized aluminium presented a higher $\rho_S$, when compared to any other material tested, followed by the MS

coated aluminium, then the SS and lastly the R85s had the lowest $\rho_S$ values. In this way, although the $\rho_T$ values of the stainless steel were considerably lower than of the soiled R85, the $\rho_S$ values for the UV$_A$ and visible range were 19.4% and 30.2% higher, respectively. The difference obtained in specular reflectance for the new and soiled R85, an average decrease of 38.7%, is in accordance with a comparative degradation study, conducted by Sutter *et al.* [15]. These authors reported that after 10-year of outdoor exposure, a sample of an uncoated aluminium reflector presented an estimated corroded surface of 93.1% and a specular reflectance loss of 41.7%. The same study also reported considerably lower values for coated aluminium samples, estimating 1.6-7.1% for the corroded surface and 0.7-3.0% for specular reflectance loss. In respect to SS, a 60-year's exposure study showed that the mirrored SS type 304, due to the content of chromium element and surface finish, not only maintained a high gloss value but also a very low surface roughness [16]. Moreover, several studies have proven the remarkable corrosion resistance under different atmospheric conditions for austenitic SS, such as type 304 and 316 [17-19], so it is expected that virtually no decrease of the reflectance properties will occur in a 10-year period.



| Average Specular Reflectance | | | |
|---|---|---|---|
| Material | UVB | UVA | Visible |
| R85 | 59.4 | 67.1 | 72.9 |
| R85s | 20.9 | 27.1 | 35.9 |
| MS | 18.8 | 49.7 | 73.4 |
| SS | 21.9 | 32.4 | 46.8 |
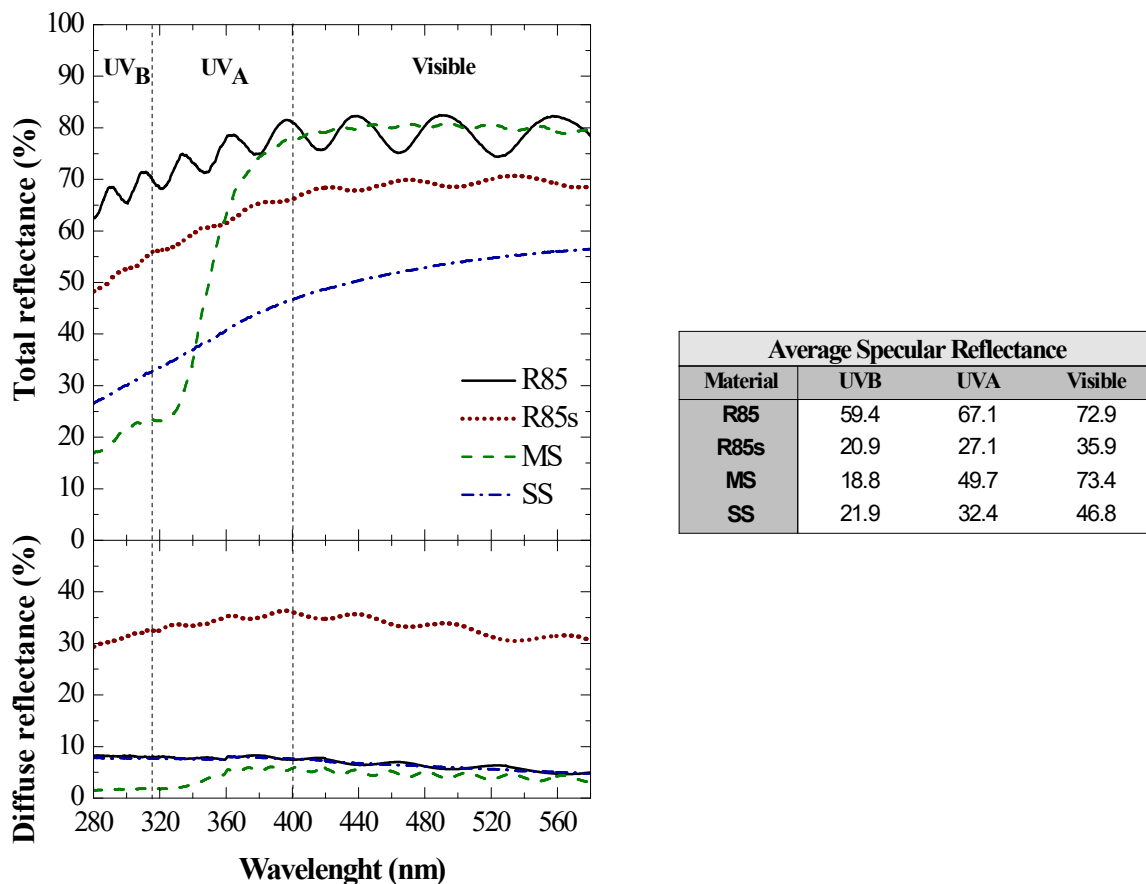
**Figure 7.1** – Total and diffuse reflectance, as a function of wavelength, and average values of specular reflectance for UV$_B$, UV$_A$ and Visible ranges, for the reflective surface materials: (—) new anodized aluminium Reflective 85 (R85), (⋯) soiled anodized aluminium Reflective 85 (R85s), (- -) coated anodized aluminium MiroSun (MS) and (- · -) mirrored stainless steel (SS).

In respect to the reflective surface geometries (Figure 7.2), considering the reflectors aperture and absorber tube diameters for the parabolic geometries (A to D), the geometric concentration ratio ($CR_G$) is as follows: A - $CR_G$ = 1.00; B and C - $CR_G$ = 0.82; and D - $CR_G$ = 0.9. Geometry A is the reflector traditionally used in CPCs, which commonly implies the moulding of two separate pieces to constitute one mirror. Geometries B-D are in fact the same but with variations in the reflector size and tube diameter. These geometries from the manufacturing point of view allow the reflective surface to be moulded in a single piece, and its execution is simpler than A, being predictable a lower final cost. Likewise, the mirror structural support for geometry B will be simpler (Figure 7.3) and, consequently, it is expected to be more cost-effective.
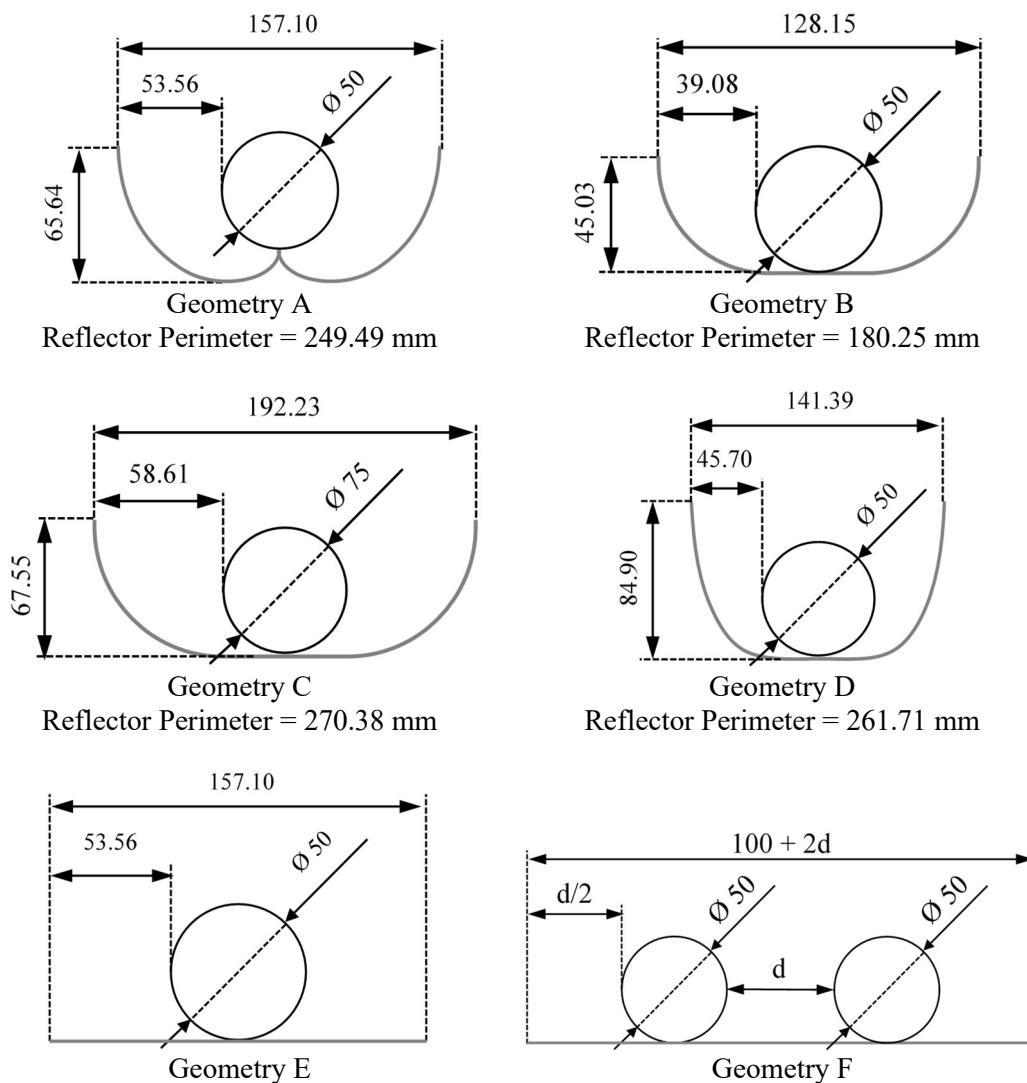
Figure 7.2 – Different geometries considered for the collectors' optics.

Also, in view of the cost reduction, within the parabolic surface designs, geometry B is the one that uses a minor amount of material and due to the smaller aperture it also allows a higher number of absorber tubes per square meter. A flat geometry, such as geometry E, would increase, to the most, the simplicity of the reflector manufacture and also of the collector structure. However, a considerable decrease of the absorber tube illuminated area is expected when compared to the parabolic geometries. A potential advantage of the flat geometry would be the reduction of the distance between the absorber tubes (geometry F), thus allowing to further increase the number of tubes and, depending on the reaction performance, it may translate into a higher volumetric treatment capacity per square meter (lower land requirements).



(a)

(b)
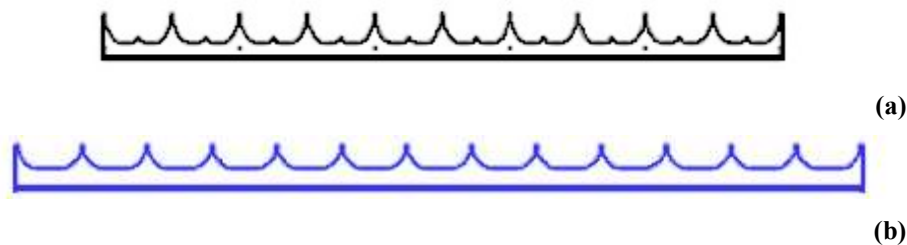
**Figure 7.3** – Reflective surface structural support for (a) two-pieces and (b) one-piece double parabola.

The traditional double-parabola (DP), simple double-parabola (SP) and flat (F) geometries were analysed by means of ray-trace, for incident radiation angles of 45º and 90º (Figure 7.4 and Figure 7.5), allowing the visualization of the light paths into the absorber tube and the number of reflections in the mirror. For the F geometry, the ray-trace was also performed considering two tubes with 50 mm between them. For the incident ray angles of 45º and 90º, the estimated illuminated area for the absorber tube is of (i) 86% and 100% for DP, (ii) 74% and 92% for SP and (iii) 57% and 50% for F reflector, in this case regardless the number of tubes. It should be noted that the ray-trace analysis was performed with the following assumptions: (i) only direct radiation is considered; (ii) the tube is a perfect absorber; and (iii) the reflecting surface is a perfect mirror. However, if an anodized aluminium (with reflectance properties like the R85) would be considered when performing the ray-trace for the F reflector (Figure 7.5), it is possible to infer a higher illuminated perimeter.

a.1)

a.2)



a.1')

a.2')



b.1)

b.2)



b.1')

b.2')
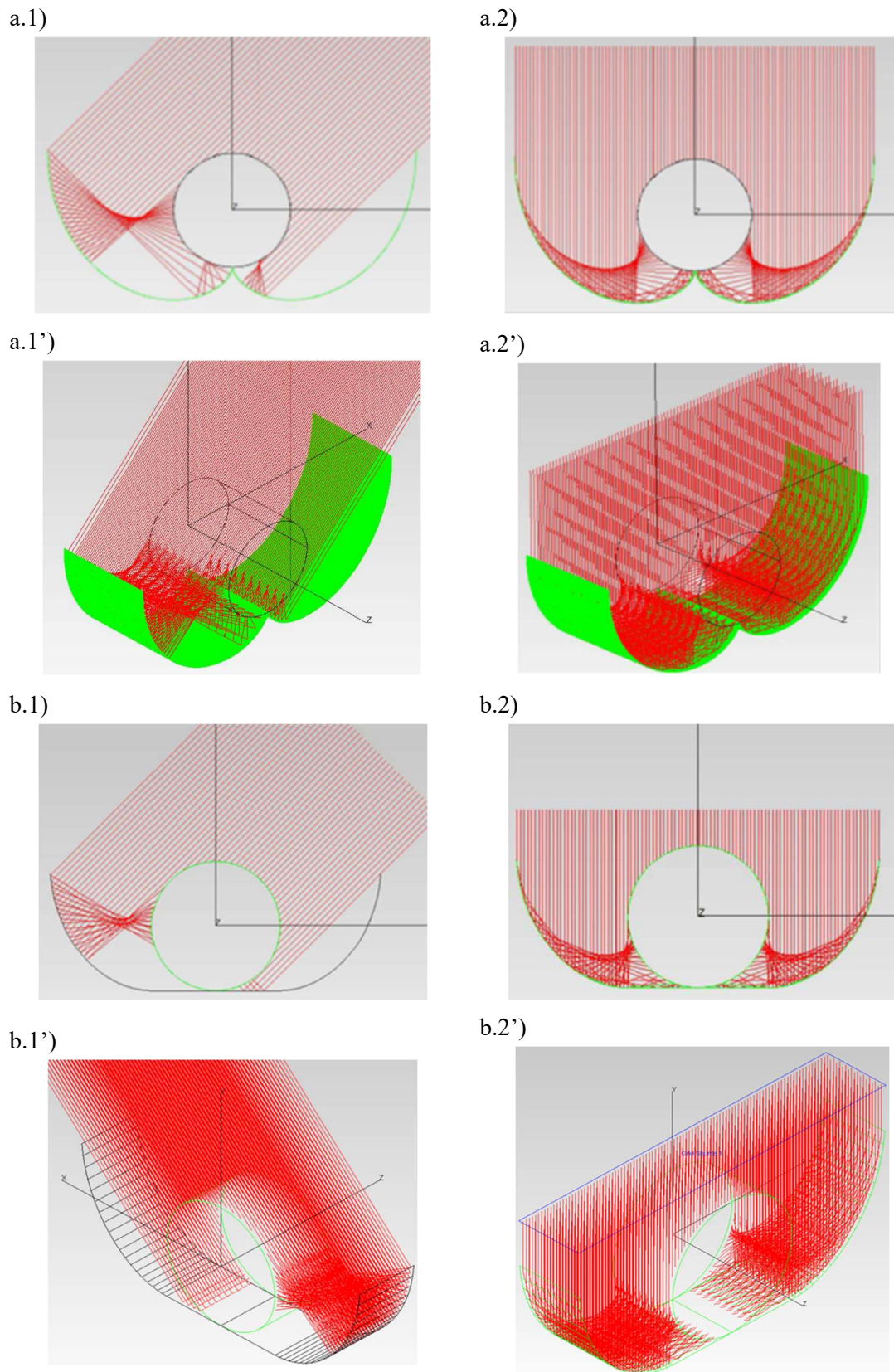


**Figure 7.4** – 2D ray-trace analysis for incident angles of (.1) 45º and (.2) 90º, and respective 3D ray-trace (.1' and 2'), considering a perfect mirror as reflective surface, for the double parabola geometries (a) traditional; and (b) simple.

a.1)

a.2)

a.1')

a.2')

b.1)

b.2)

b.1')

b.2')
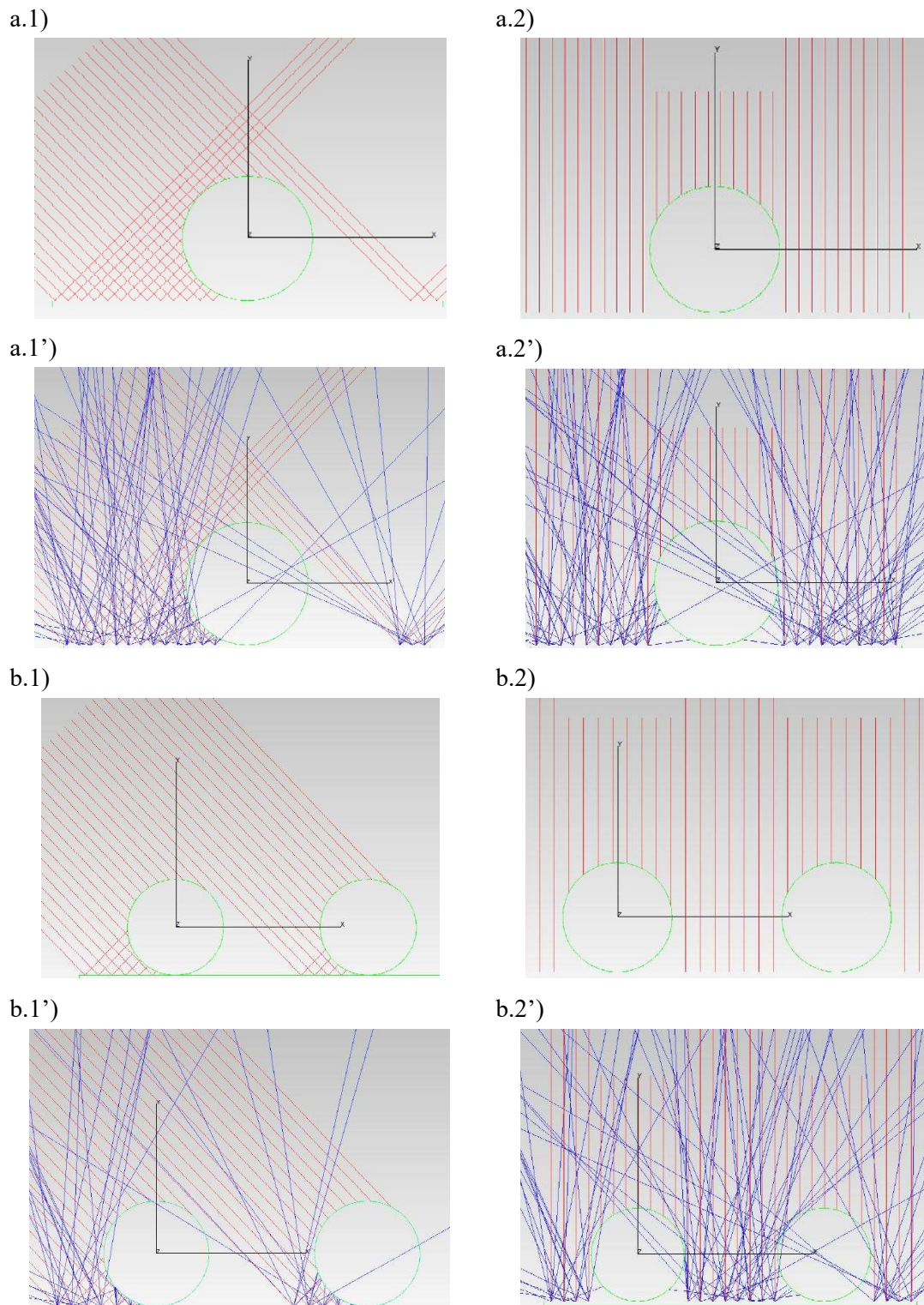
**Figure 7.5** – Ray-trace analysis, considering incident angles of (.1) 45º and (.2) 90º with a perfect mirror as reflective surface and (.1' and .2') with an anodized aluminium reflective surface, for a flat geometry mirror with (a) one and (b) two absorber tubes at 50 mm distance; red and blue traces represent the direct and reflected radiation, respectively.

### 7.3.2 Lab-scale experiments: simulated sunlight

### 7.3.2.1 Actinometric measurements

*One absorber tube*

Actinometric measurements for the different reflectors materials and geometries were performed under the same experimental conditions using simulated sunlight (44 $W_{UV}/m^2$; 328 $W_{280-580nm}/m^2$). It is expected that a more efficient reflective surface will increase the radiant power incident on the photoreactor tube ($RP_i$), resulting in a higher optical concentration ratio ($CR_O$). With this in mind and analysing the $RP_i$ values (Table 7.3), it is possible to verify that the lowest value was obtained for the photoreactor with no reflector (No-RS). In turn, the photoreactor with the R85-DP presented the highest value, followed by the MS-DP > SS-DP > SS-SP, with $RP_i$ 2.2, 2.0, 1.7 and 1.6 times higher than with No-RS, respectively. Among the parabolic reflectors, the soiled R85-DP presented the lowest $RP_i$, only 1.6 times higher than No-RS and, therefore, exhibited a considerable decrease when compared with the same aluminium reflector in good conditions. For the flat geometry reflectors, with R85 and SS materials, the obtained $RP_i$ values were considerably lower than for the parabolic, nevertheless they were 1.4 times higher when compared with the No-RS. Beyond that, the similarity between the $RP_i$ values for R85-F and SS-F means that the flat geometry overcomes the difference of the materials reflectance.

For the same reflector geometry, a solid correlation was found between the $RP_i$ and the average specular reflectance (range 280-580 nm) of the different materials tested (Figure 7.6-a). On the other hand, considering the different geometries with the same reflective material, a strong correlation was also obtained between the $RP_i$ and the absorber tube illuminated area (Figure 7.6-b). In view of the foregoing, it is plausible to state that the reflectance scanning and the ray-trace analysis can be good predictive tools for the reflective surfaces' performance.

Knowing the irradiance emitted by the lamp for the wavelength range of interest ($I_0 = 328$ $W_{280-580nm}/m^2$), it is possible to compare it with the irradiance incident on the absorber tube calculated from the actinometric measurements (Table 7.3). Hence, the calculated irradiance for the photoreactor with the R85-DP reflector corresponds to 93% of the emitted irradiance by the xenon lamp ($CR_O = 0.93 \pm 0.05$). On the other hand, the photoreactor without any reflective surface has a calculated irradiance that represents 42% ($CR_O = 0.42 \pm 0.03$) of the emitted irradiance, which makes sense since it is expected that only the superior half part of the absorber tube is effectively irradiated [20].

**Table 7.3** – Results of ferrioxalate actinometric measurements, at lab-scale, under simulated sunlight.

| No. Tubes | Reflective Surface | $I_0$[a] (W/m$^2$) | $d$[b] (mm) | $RP_i$[c] (W) | $CR_O$ | $RP$[d] (W) | $R^2$ |
|---|---|---|---|---|---|---|---|
| **1 Absorber Tube** | No-RS | 328 | n.a. | 3.5 ± 0.2 | 0.42 ± 0.03 | 3.1 ± 0.2 | 0.997 |
| | R85-DP | 164 | n.a. | 3.9 ± 0.4 | 0.94 ± 0.09 | 3.4 ± 0.3 | 0.995 |
| | | 246 | n.a. | 5.5 ± 0.9 | 0.9 ± 0.1 | 4.9 ± 0.7 | 0.993 |
| | | 328 | n.a. | 7.6 ± 0.4 | 0.93 ± 0.05 | 6.7 ± 0.3 | 0.998 |
| | | 410 | n.a. | 9.8 ± 0.9 | 0.95 ± 0.09 | 8.6 ± 0.9 | 0.997 |
| | R85s-DP | 328 | n.a. | 5.5 ± 0.3 | 0.67 ± 0.03 | 4.9 ± 0.3 | 0.997 |
| | MS-DP | 328 | n.a. | 7.0 ± 0.5 | 0.84 ± 0.06 | 6.1 ± 0.4 | 0.997 |
| | SS-DP | 328 | n.a. | 5.9 ± 0.2 | 0.72 ± 0.02 | 5.2 ± 0.2 | 0.999 |
| | SS-SP | 164 | n.a. | 3.2 ± 0.5 | 0.8 ± 0.1 | 2.8 ± 0.4 | 0.997 |
| | | 246 | n.a. | 4.4 ± 0.2 | 0.71 ± 0.03 | 3.9 ± 0.2 | 1.000 |
| | | 328 | n.a. | 5.7 ± 0.4 | 0.70 ± 0.04 | 5.1 ± 0.3 | 0.996 |
| | | 410 | n.a. | 7.5 ± 0.4 | 0.73 ± 0.04 | 6.6 ± 0.3 | 0.999 |
| | R85-F | 328 | n.a. | 5.0 ± 0.4 | 0.60 ± 0.04 | 4.4 ± 0.3 | 0.997 |
| | SS-F | 328 | n.a. | 4.8 ± 0.3 | 0.59 ± 0.04 | 4.3 ± 0.3 | 0.998 |
| **2 Absorber Tubes** | No-RS | 328 | 50 | 6.0 ± 0.5 | 0.36 ± 0.03 | 5.3 ± 0.4 | 0.994 |
| | R85-F | | 12.5 | 8.0 ± 0.8 | 0.49 ± 0.05 | 7.1 ± 0.7 | 0.995 |
| | R85-F | | 25 | 8.5 ± 0.9 | 0.51 ± 0.05 | 7.5 ± 0.8 | 0.997 |
| | R85-F | 328 | 50 | 9.0 ± 0.8 | 0.55 ± 0.05 | 7.9 ± 0.7 | 0.998 |
| | R85-F | | 75 | 8.5 ± 0.7 | 0.51 ± 0.07 | 7.5 ± 0.6 | 0.997 |
| | R85-F | | 100 | 8.0 ± 0.3 | 0.49 ± 0.02 | 7.1 ± 0.3 | 0.999 |
| | SS-F | | 12.5 | 7.3 ± 0.7 | 0.44 ± 0.04 | 6.4 ± 0.7 | 0.997 |
| | SS-F | | 25 | 7.7 ± 0.8 | 0.47 ± 0.05 | 6.8 ± 0.7 | 0.997 |
| | SS-F | 328 | 50 | 8.1 ± 0.7 | 0.49 ± 0.04 | 7.2 ± 0.6 | 0.996 |
| | SS-F | | 75 | 7.9 ± 0.9 | 0.46 ± 0.07 | 7.0 ± 0.8 | 0.993 |
| | SS-F | | 100 | 7.1 ± 0.6 | 0.43 ± 0.03 | 6.3 ± 0.5 | 0.997 |

[a] Lamp irradiance in the range of 280 to 580 nm. [b] Distance between the absorber tubes. [c] Radiant power incident on the photoreactor tube. [d] Radiant power that reaches the reaction medium. n.a. – not applicable.
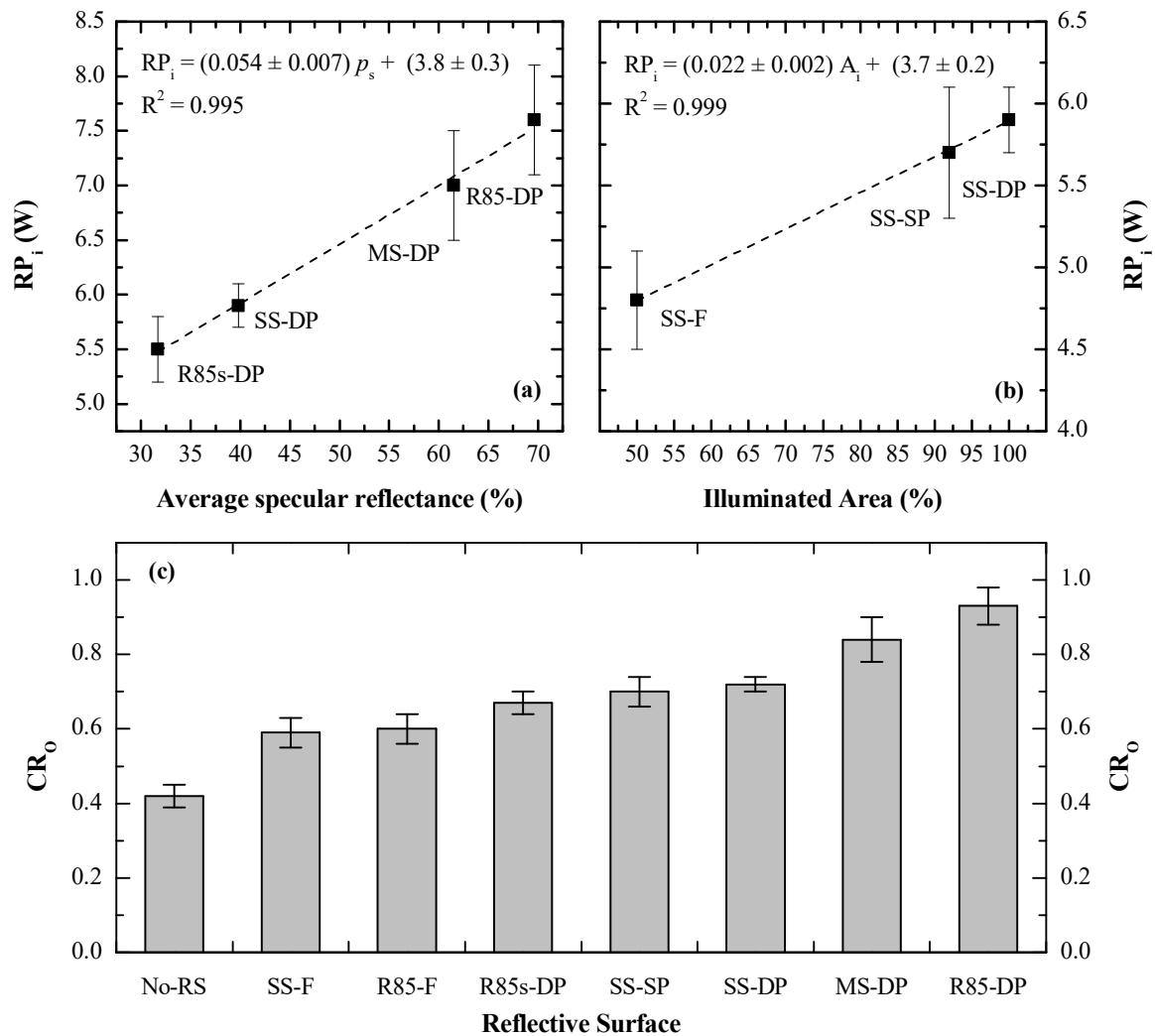
**Figure 7.6** – Variation of the radiant power incident on the photoreactor as a function of the (a) average specular reflectance, between 280-580 nm, for the different reflectors materials, and (b) illuminated area of the absorber tube for different reflectors geometries; and (c) optical concentration ratio for all reflective surface configurations.

Considering the above, the efficiency of light reflection by the reflective surfaces tested increases in the following sequence: SS-F $\approx$ R85-F < R85s-DP $\approx$ SS-SP $\approx$ SS-DP < MS-DP < R85-DP (Figure 7.6-c). Additional actinometric measurements with lamp irradiances of 275, 350 and 625 W/m$^2$, corresponding to 164, 246 and 410 W$_{280-580nm}$/m$^2$, were also performed for the R85-DP and SS-SP. A clear linear relation was obtained between the $RP_i$ and the lamp emitted irradiance (Figure 7.7). The efficiency in terms of the $CR_O$ was also coherent for the different lamp irradiances (Table 7.3).
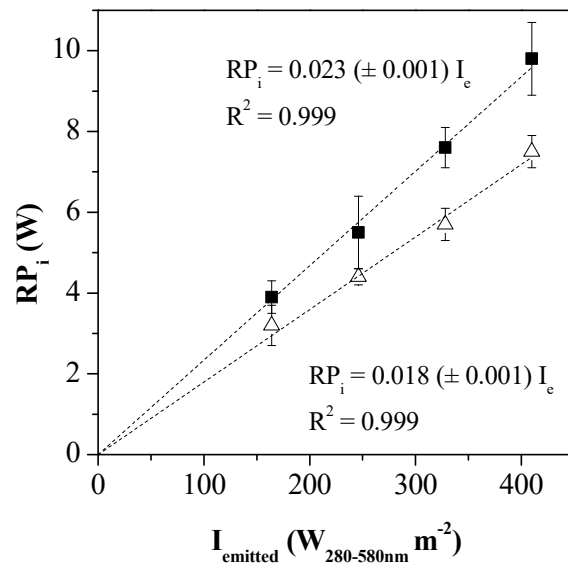
**Figure 7.7** – Relation between the radiant power incident on the photoreactor and the xenon lamp irradiance between 280 and 580 nm, for the reflective surfaces (■) R85-DP and (△) SS-SP.


*Two absorber tubes*

Actinometric tests were performed for the R85 and SS flat reflectors using two absorber tubes. For both reflectors it was observed (Table 7.3 and Figure 7.8) that the *RP* value (i) increased as the distance between the tubes increased from 12.5-50 mm (with reflective areas from 0.020-0.032 $m^2$) and, (ii) decreased for the distances of 75 and 100 mm (reflective areas of 0.040 and 0.048 $m^2$). At a first glance, these results may seem awkward, since it would be expected that the *RP* values would increase, as the reflective area lengthens, up to a given point and then stabilize. However, this apparent trend may be explained due to the occurrence of two different phenomena. For distances < 50 mm, a shadow effect may occur between the tubes, consequently as the distance between the tubes increases the shadow effect diminishes (until it is null). Additionally, the increment of the reflective area as the absorber tubes distance increases may also positively contribute to the *RP* value. Meanwhile, for distances > 50 mm, the fix position of the lamp inside the Suntest® chamber may influence the measurements, according to the inverse square law, where light irradiance decreases inversely with the distance from the source to the reflector surface, and the cosine law related to the incident angle [21]. The overlapping of these phenomena may also explain why the highest *RP* value obtained with the 2 tubes (in this case, 50 mm of distance), either with the No-RS, R85 or SS flat reflectors, did not double but it was only 1.7 or 1.8 fold higher when compared to the same reflector using only one tube Table 7.3).
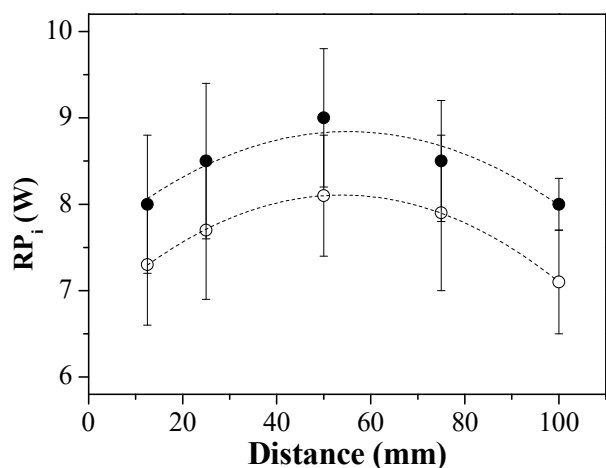
**Figure 7.8** – Radiant power incident on the photoreactor using 2 absorber tubes, at different distances, for the reflective surfaces R85-F and SS-F.

### 7.3.2.2 Photo-Fenton treatment performance

*Reflective surface effect*

To assess and compare the photo-Fenton efficiency using the different reflective surfaces, the leachate mineralization was evaluated under the same illumination conditions using the sunlight simulator (Table 7.4). An enhancement of the photo-Fenton efficiency over time was observed with the increasing of the $CR_O$ of the reflective surface (Figure 7.9 and Figure 7.10). Therefore, the photo-treatment conducted with the No-RS photoreactor was the slowest, followed by the F geometries and the R85s-DP reflector. From these results it is clear the impact in the PF efficiency of the uncoated anodized aluminum after 8-year of outdoor exposure, which largely overcomes the advantage of the DP geometry, presenting a DOC abatement rate similar to an F reflector.

**Table 7.4** – Variables and kinetic parameters of photo-Fenton experiments, at lab-scale, under simulated sunlight.

| Reflective Surface | $T^d$ (ºC) | $pH^d$ | $[TDI]^d$ (mg/L) | $k_{DOC,t}^e$ (×10⁻³ min⁻¹) | $r_{0,t}^f$ (mg/L·min) | $k_{DOC,Q}^g$ (×10⁻² L/kJ) | $r_{0,Q}^f$ (mg kJ⁻¹) | $R^2$ | $\Delta Q_{280-580n}^h$ (kJ/L) | $t^i$ (min) | $Q_{280-580nm}^i$ (kJ/L) |
|---|---|---|---|---|---|---|---|---|---|---|---|
| **1 tube** | | | | | | | | | | | |
| **No-RS$^a$** | 25.2 | 2.9 | 72.7 | 3.7 ± 0.4 | 1.6 ± 0.1 | 1.8 ± 0.1 | 7.7 ± 0.6 | 0.991 | 4 - 38 | 248 | 52 |
| **R85-DP$^b$** | 25.1 | 2.8 | 74.9 | 5.3 ± 0.3 | 2.3 ± 0.2 | 1.8 ± 0.1 | 7.9 ± 0.6 | 0.995 | 6 – 53 | 173 | 51 |
| **R85-DP$^a$** | 25.2 | 2.9 | 71.1 | 7.6 ± 0.5 | 3.4 ± 0.3 | 1.7 ± 0.1 | 7.6 ± 0.6 | 0.995 | 9 – 81 | 121 | 54 |
| **R85-DP$^c$** | 25.3 | 2.9 | 71.3 | 7.6 ± 0.3 | 3.3 ± 0.2 | 1.30 ± 0.06 | 5.6 ± 0.3 | 0.998 | 12 – 104 | 121 | 70 |
| **R85s-DP$^a$** | 25.2 | 2.9 | 70.1 | 6.0 ± 0.4 | 2.5 ± 0.2 | 1.9 ± 0.1 | 7.8 ± 0.6 | 0.994 | 7 – 59 | 153 | 49 |
| **MS-DP$^a$** | 25.6 | 3.0 | 68.5 | 7.8 ± 0.5 | 3.1 ± 0.2 | 1.8 ± 0.1 | 7.4 ± 0.5 | 0.996 | 8 – 76 | 117 | 50 |
| **SS-DP$^a$** | 25.0 | 2.9 | 66.0 | 7.2 ± 0.3 | 2.7 ± 0.1 | 1.95 ± 0.08 | 7.3 ± 0.3 | 0.998 | 7 – 66 | 127 | 47 |
| **SS-SP$^b$** | 25.3 | 2.8 | 72.0 | 4.1 ± 0.4 | 1.5 ± 0.2 | 1.8 ± 0.2 | 6.8 ± 0.8 | 0.985 | 5 – 41 | 223 | 51 |
| **SS-SP$^a$** | 25.5 | 2.9 | 76.4 | 6.5 ± 0.3 | 2.7 ± 0.1 | 1.88 ± 0.08 | 7.7 ± 0.4 | 0.998 | 7 – 62 | 141 | 49 |
| **SS-SP$^c$** | 25.1 | 2.9 | 72.0 | 6.6 ± 0.4 | 2.5 ± 0.2 | 1.47 ± 0.08 | 5.7 ± 0.4 | 0.996 | 9 - 81 | 139 | 62 |
| **R85-F$^a$** | 25.4 | 2.9 | 70.5 | 5.5 ± 0.6 | 2.3 ± 0.1 | 1.8 ± 0.2 | 7.6 ± 0.9 | 0.986 | 6 - 54 | 168 | 50 |
| **SS-F$^a$** | 25.6 | 2.9 | 70.7 | 5.8 ± 0.8 | 2.3 ± 0.1 | 2.0 ± 0.3 | 8 ± 1 | 0.977 | 6 - 53 | 158 | 46 |
| **2 tubes** | | | | | | | | | | | |
| **No-RS$^a$** | 25.0 | 2.9 | 72.9 | 4.1 ± 0.3 | 1.7 ± 0.1 | 2.3 ± 0.2 | 9.2 ± 0.7 | 0.993 | 4 - 32 | 223 | 40 |
| **R85-F$^a$** | 26.4 | 3.0 | 68.5 | 6.0 ± 0.6 | 2.3 ± 0.1 | 2.2 ± 0.2 | 8.7 ± 0.9 | 0.986 | 5 - 48 | 153 | 41 |
| **SS-F$^a$** | 25.0 | 2.9 | 71.4 | 5.8 ± 0.4 | 2.1 ± 0.1 | 2.3 ± 0.2 | 8.6 ± 0.7 | 0.993 | 5 - 45 | 158 | 39 |

[a] $V_i/V_t$ ratio = 0.3 [b] $V_i/V_t$ ratio = 0.2 [c] $V_i/V_t$ ratio = 0.4 [d] Average values for the temperature (T), pH and total dissolved iron concentration ([TDI]) during the photo-Fenton treatment.
[e] Pseudo-first-order kinetic constant for DOC degradation as a function of irradiation time. [f] Initial DOC reaction rate. [g] Pseudo-first-order kinetic constant for DOC degradation as a function of accumulated energy. [h] Interval of energy from which the kinetic parameters were calculated. [i] Time (t) and energy (Q) required to achieve 60% of mineralization.
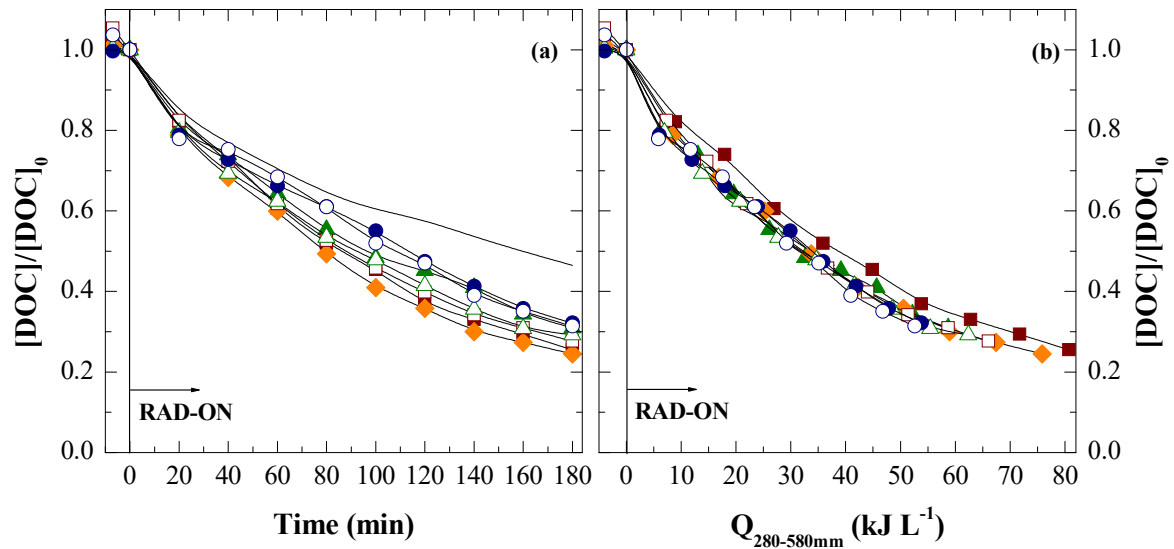
**Figure 7.9** – Evolution of normalized DOC removal as a function of (a) time and (b) accumulated energy in the range of 280-580 nm, during the photo-Fenton treatment of the pre-treated landfill leachate, under simulated sunlight (xenon lamp set for 500 W/m$^2$, $[DOC]_0 = 454$ mg/L, $[TDI] = 60$ mg/L, Flow rate = 1.25 L/min, pH = 2.8, T = 25 ºC), using one absorber tube and the different reflective surfaces: (——) No-RS; (♦) MS-DP; (■) R85-DP; (▲) R85s-DP; (●) R85-F; (□) SS-DP; (△) SS-SP; and (○) SS-F.
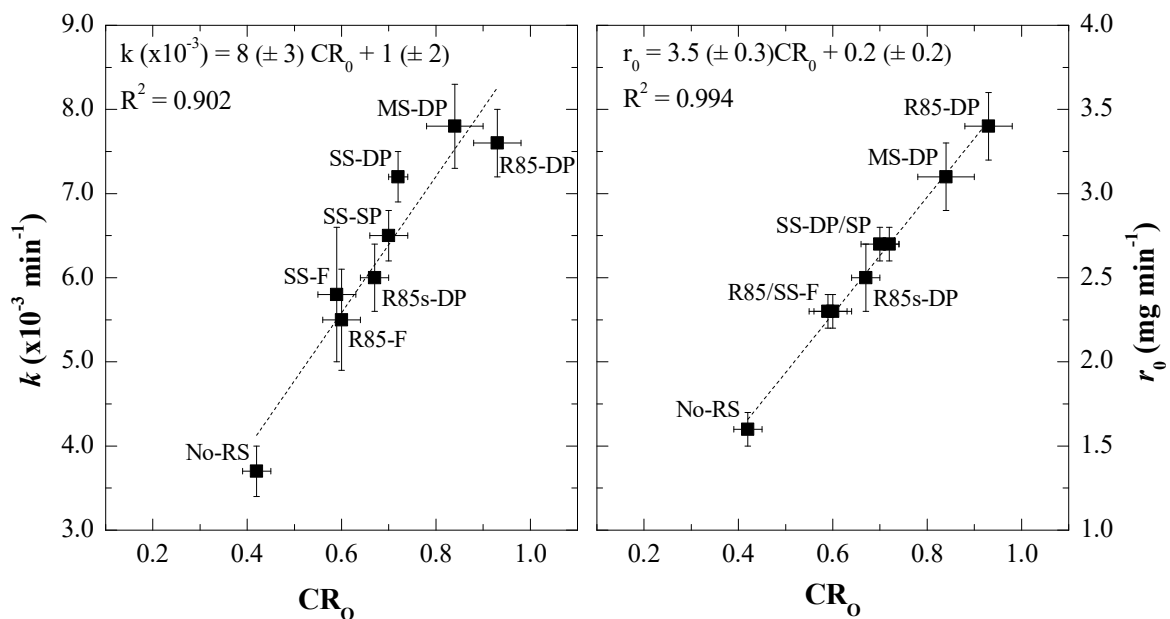


**Figure 7.10** – Representation of the DOC degradation (a) kinetic constant and (b) initial rate as a function of the optical concentration ratio, for the photo-Fenton trials in the Suntest® chamber using the different reflective surfaces.

Interestingly, the fastest DOC reduction was not obtained for the photoreactor presenting the highest $CR_O$ (R85-DP), as could be expected, but for the MS-DP reflector. Considering the materials reflectance (Figure 7.1), this indicates that for the leachate photo-treatment, the radiation in the higher $UV_A$ and visible region may be more significant than the radiation under 350 nm. In this sense, the positive effect of irradiation on the pollutants degradation rate depends not only on the intensity of the radiation source, i.e. the degradation rate increases with the radiation intensity up to a given value, but also on the wavelength, due to the different reaction mechanisms that can occur in the reaction medium: (i) pollutants direct photolysis, which takes place when the light source emits radiation at the same wavelength range as the contaminants can absorb radiation efficiently; (ii) generation of hydroxyl radicals by the photoreduction of ferric-hydroxyl complexes (Equation 7.1) [22] and (iii) direct photolysis of ferricarboxylates complexes (Equation 7.2).

$$[Fe^{3+}(OH)^-]^{2+} \rightarrow Fe^{2+} + HO^\bullet, \text{ at } \lambda < 400 \text{ nm} \tag{7.1}$$

$$[Fe^{3+}(RCOO)]^{2+} \rightarrow Fe^{2+} + CO_2 + R^\bullet, \text{ at } \lambda < 600 \text{ nm} \tag{7.2}$$
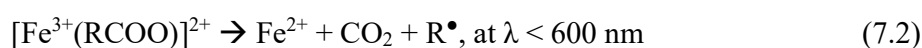
In respect to the photolysis of the leachate, preliminary trials upon $UV_A$ and $UV_A$+Vis artificial radiation [23], resulted in a mineralization decay of only 4 to 8%, thus suggesting the presence of highly recalcitrant compounds that were not easily photoreduced. Furthermore, it was proposed from previous studies [12] that the use of higher wavelengths besides UV contributes to better overcome the inner-filter effect of the leachate. This may occur since along the PF treatment, due to the degradation of the humic substances (which have a high content of carboxylic groups, about 9 meq. of carboxylic acids per gram of carbon) there is the formation of low-molecular-weight carboxylic acids that possibly form soluble iron-organic complexes. In this way, ferricarboxylates $[Fe^{3+}(RCO)^-]^{2+}$ may be present in the reaction medium and are able to participate in photo-reduction reactions at wavelengths up to 580 nm, presenting larger quantum yields (around unity) than the ferric-hydroxyl complexes $[Fe^{3+}(OH)^-]^{2+}$ [24]. Consequently, considering the above and the results obtained, a high UV reflectance of the reflective surface is not a requirement to the photo-Fenton treatment when applied to the decontamination of a mature leachate.

### $V_i/V_t$ ratio effect

To assess the influence of the illuminated volume on the leachate photo-Fenton treatment, trials using $V_i/V_t$ of 0.2 to 0.4 were performed in the sunlight simulator with the R85-DP and SS-SP reflectors. Interestingly, when varying the volumes of leachate under treatment, the same trend was

presented regardless the reflective surface (Table 7.4 and Figure 7.11). In respect to the results for $V_i/V_t$ of 0.2, when comparing with $V_i/V_t$ of 0.3, it was clear that with the increasing of the leachate volume the DOC abatement was slower. Conversely, and also for both reflective surfaces, when decreasing the leachate volume for a $V_i/V_t$ of 0.4, the DOC abatement rate remained approximately the same as for $V_i/V_t$ of 0.3, while the kinetic constant, in terms of accumulated energy, decreased revealing a loss of photonic efficiency ($\approx 20\%$). Considering that, when the volume decreased, the ratio between dark and illuminated time was reduced (from 2.3 to 1.5), it is possible to infer that a significant part of the reactions were being thermally induced in the dark. The importance of dark precursor species in photo-Fenton was demonstrated by Herrera, *et al.* [25], having verified a reduction of the required illumination time when performing degradation studies using alternate dark/light cycles. Also, Gernjak, *et al.* [26], observed that less photons were required when the dark volume increased, thus proposing that: (i) intermediates formed under the illuminated period boost the reaction further during the dark period, maintaining the catalytic iron cycle; and (ii) in the dark period there is the formation of important intermediates, like organic acids forming photo-active complexes with ferric iron, that rapidly react under light. Therefore, for both reflectors tested, an energy saving during the mineralization was observed when the leachate volume increased from a $V_i/V_t$ of 0.4 to 0.3.
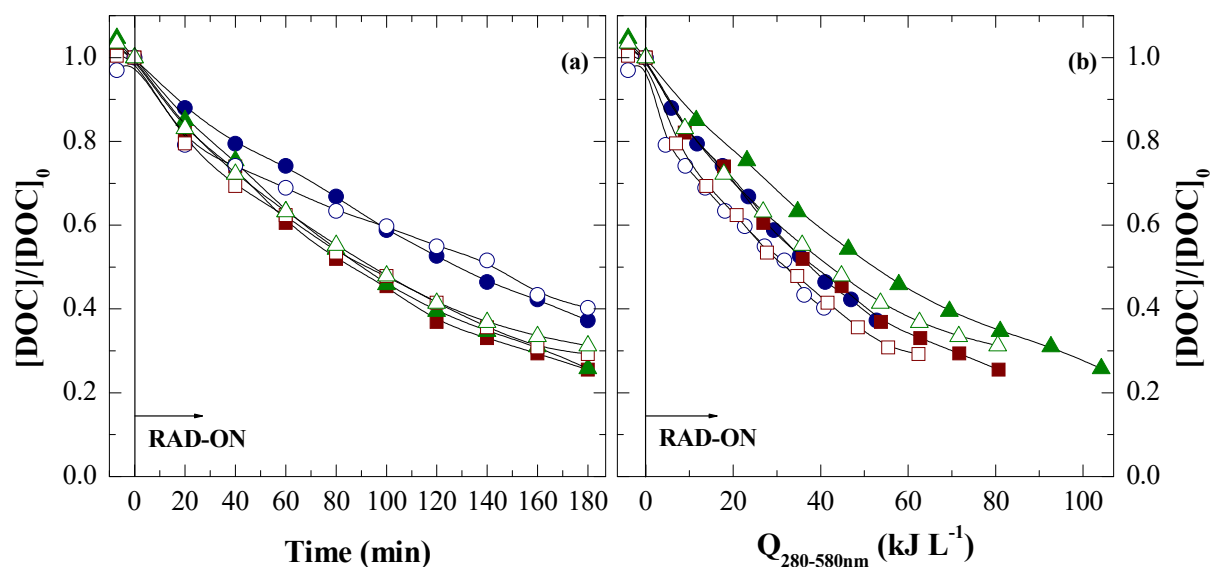


**Figure 7.11** – Evolution of normalized DOC removal as a function of (a) time and (b) accumulated energy in the range of 280-580 nm, during the photo-Fenton treatment of the pre-treated leachate, under simulated sunlight (xenon lamp set for 500 W/m$^2$, [DOC]$_0$ = 454 mg/L, [TDI] = 60 mg/L, Flow rate = 1.25 L/min, pH = 2.8, T = 25 ºC): ($\bullet$) R85-DP $V_i/V_t$ = 0.2; ($\blacksquare$) R85-DP $V_i/V_t$ = 0.3; ($\blacktriangle$) R85-DP $V_i/V_t$ = 0.4; ($\circ$) SS-SP $V_i/V_t$ = 0.2; ($\square$) SS-SP $V_i/V_t$ = 0.3; and ($\triangle$) SS-SP $V_i/V_t$ = 0.4.

*Effect of the absorber tubes number*

Under simulated sunlight, the PF treatment of the leachate was tested for the No-RS, R85-F and SS-F reflectors, using two absorber tubes 50 mm apart (distance that provided the higher *RP*, as described in 7.3.2.1.2). For comparison purposes, the photo-treatments were performed under the same experimental conditions as the tests with one tube, including the $V_i/V_t$ ratio of 0.3, by doubling the leachate volume.

When comparing the DOC degradation profile and kinetic constants over time (Table 7.4 and Figure 7.12), there was no significant difference between using one or two absorber tubes. For the kinetic constants regarding the accumulated energy (*k*, L/kJ) slightly higher values ($\approx 22\%$) were obtained for the two tubes, thus suggesting a greater efficiency in the usage of the photonic energy reaching the photoreactor. Considering that one of the drawbacks for the implementation of the full-scale solar plants is associated with the land area requirements, these results suggest that the usage of flat reflectors may be a possible solution. Its use allows to increment the number of absorber tubes per square meter of solar collector and therefore the treatment volume, eventually compensating the longer treatment time required to achieve 60% mineralization (c.a. more 32-37 min, when comparing with the traditional CPCs). This possibility will be further discussed in the cost analysis section.
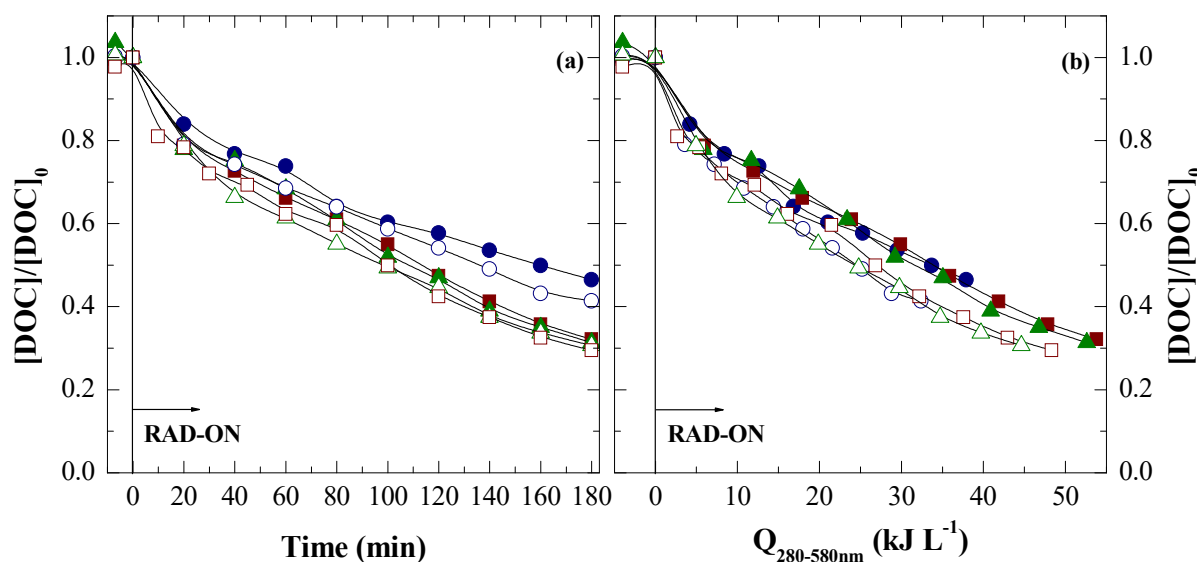


**Figure 7.12** – Evolution of normalized DOC removal as a function of (a) time and (b) accumulated energy in the range of 280-580 nm, during the photo-Fenton treatment of the pre-treated landfill leachate, under simulated sunlight (xenon lamp set for 500 W/m², [DOC]$_0$ = 454 mg/L, [TDI] = 60 mg/L, Flow rate = 1.25 L/min, pH = 2.8, T = 25 ºC): ($\bullet$) No-RS_1 tube; ($\blacksquare$) R85-F_1 tube; ($\blacktriangle$) SS-F_1 tube; ($\circ$) No-RS_2 tubes; ($\square$) R85-F_2 tubes; and ($\triangle$) SS-F_2 tubes.

### 7.3.3 Pilot-scale experiments: natural sunlight

### 7.3.3.1 Actinometric measurements

After the lab-scale trials, some reflective surfaces were chosen to be tested under natural sunlight, at pilot-scale: (i) No-RS, to be used as a "blank" for comparison purposes (pilot A); (ii) MS-DP, since it provided the best photo-Fenton treatment time in the sunlight simulator (pilot A); (iii) SS-F, due to the possibility to increase the treatment volume by increasing the number of absorber tubes and using a resistant material (pilot A); (iv) SS-SP, also using a more resistant material and a new double-parabola with a more cost-effective design (pilot B); and (v) R85s-DP, as a traditional CPC reflective surface with 8-year of outdoor exposure, to further investigate the influence of the soiled reflector (pilot C). It should be noticed that for the trials performed in pilot-plant A, with No-RS and SS-F reflectors, the distance between the tubes was the same as for a DP reflector, since it was not possible to change their position. Nevertheless, it is not expected that under sunlight the distance increment between the absorber tubes would negatively affect the photonic flux, as verified for Suntest® chamber where the light source presents a fixed position. Due to differences on solar radiation intensity between the trials, as well as the pilot-plants dimensions, the average $CR_O$ value for each reflective surface will be used for comparison instead of $RP_i$.

For the pilot-plants actinometric measurements (Table 7.5), it is possible to verify that the general trend is similar to the lab-scale results. However, the $CR_O$ values obtained at pilot-scale, for all solar intensities and reflectors tested, excepting MS-DP, were lower than at lab-scale. This seems to suggest that the increment on the reflective surface area makes it more noticeable the effect of the material low reflectance (R85s or SS) or the simpler reflector geometry (F). Therefore, the reflectors presenting $CR_O \leq 0.8$ at lab-scale, had a further decrease at pilot-scale. Conversely, regardless the scale, the MS-DP reflector maintains its high optical efficiency ($CR_O \geq 0.8$). It should also be noted that the actinometric measurements carried out under outdoor conditions presented greater variability than under controlled circumstances, which can be observed by the lower correlation constants ($R^2$), and may be related to variations of solar radiation along the trials. Some variability was also detected between trials using the same reflector but performed under different solar irradiances (Table 7.5). This can be possibly explained by differences on the sun position (azimuth and elevation angle) and diffuse radiation component (sunny vs. cloudy days). Further research would be required to assess the influence of these elements on the photonic efficiency of each collector.

**Table 7.5 –** Results of ferrioxalate actinometric measurements, at pilot-scale, under natural sunlight.

| Reflective Surface | $\overline{I_{UV}}$ [a] $(W_{UV}/m^2)$ | $\overline{I_{280-580}}$ [b] $(W/m^2)$ | $RP_i$ (W) | $CR_O$ | $RP$ (W) | $R^2$ |
|---|---|---|---|---|---|---|
| **No-RS (Pilot-plant A)** | 6.2 | 42 | $6.6 \pm 0.3$ | $0.35 \pm 0.3$ | $5.9 \pm 0.3$ | 0.990 |
| | 17.8 | 118 | $17 \pm 2$ | $0.34 \pm 0.03$ | $15 \pm 2$ | 0.997 |
| | 45.2 | 302 | $39 \pm 5$ | $0.29 \pm 0.03$ | $34 \pm 4$ | 0.998 |
| **MS-DP (Pilot-plant A)** | 13.8 | 92 | $31 \pm 2$ | $0.81 \pm 0.04$ | $28 \pm 2$ | 0.997 |
| | 39.4 | 263 | $(9 \pm 2) \times 10^1$ | $0.8 \pm 0.2$ | $(8 \pm 2) \times 10^1$ | 0.995 |
| | 50.1 | 334 | $(1.2 \pm 0.2) \times 10^2$ | $0.8 \pm 0.1$ | $(1.1 \pm 0.2) \times 10^2$ | 0.997 |
| **SS-F (Pilot-plant A)** | 18.1 | 121 | $29 \pm 7$ | $0.54 \pm 0.09$ | $24 \pm 4$ | 0.985 |
| | 43.9 | 292 | $(6 \pm 1) \times 10^1$ | $0.46 \pm 0.09$ | $(5 \pm 1) \times 10^1$ | 0.993 |
| | 47.5 | 317 | $58 \pm 9$ | $0.44 \pm 0.04$ | $51 \pm 8$ | 0.997 |
| **SS-SP (Pilot-plant B)** | 12.1 | 80 | $(1.2 \pm 0.2) \times 10^2$ | $0.61 \pm 0.02$ | $(1.1 \pm 0.1) \times 10^2$ | 0.994 |
| | 24.4 | 163 | $(2.6 \pm 0.4) \times 10^2$ | $0.60 \pm 0.09$ | $(2.3 \pm 0.4) \times 10^2$ | 0.982 |
| | 45.5 | 303 | $(4.8 \pm 0.6) \times 10^2$ | $0.53 \pm 0.07$ | $(4.3 \pm 0.5) \times 10^2$ | 0.992 |
| **R85s-DP (Pilot-plant C)** | 11.8 | 79 | $(1.0 \pm 0.1) \times 10^2$ | $0.50 \pm 0.02$ | $(0.9 \pm 0.1) \times 10^2$ | 0.990 |
| | 24.1 | 160 | $(1.9 \pm 0.2) \times 10^2$ | $0.57 \pm 0.05$ | $(1.7 \pm 0.2) \times 10^2$ | 0.990 |
| | 45.2 | 302 | $(3.4 \pm 0.2) \times 10^2$ | $0.50 \pm 0.03$ | $(3.0 \pm 0.2) \times 10^2$ | 0.997 |

[a] Average solar $UV_A$ irradiance measured by a UV radiometer. [b] Average solar irradiance between 280 and 580 nm, considering $\overline{I_{UV}} \times 0.15$, being 0.15 the fraction of UV radiation as regards the solar spectrum in the range of 280-580 nm.

## 7.3.3.2 Photo-Fenton treatment performance

An overview on the experimental kinetic constants ($k_{44W;25°C}$, $min^{-1}$) and mineralization profiles obtained for trials at the pilot-plants (Table 7.6 and Figure 7.13-a), makes it possible to verify a good agreement with the actinometric measurements and the reflectors $CR_O$ (Figure 7.14-b). Moreover, the PF efficiency obtained in the pilot-plants were quite similar to those obtained in the sunlight simulator (Table 7.4 and Table 7.6). However, the photo-treatment conducted in pilot-plant B (SS-SP) presented a considerable better performance at pilot-scale. Since this photo-oxidation was performed in simultaneous with pilot-plant C (soiled aluminium), and both reflectors presented a very close $CR_O$, a more detailed analysis will follow for these trails.

**Table 7.6** – Variables and kinetic parameters of photo-Fenton experiments, at pilot-scale, under natural sunlight.

| | Pilot-plant A | | | Pilot-plant B | Pilot-plant C |
|---|---|---|---|---|---|
| | No-RS | MS-DP | SS-F | SS-SP | R85s-DP |
| $T^a$ (ºC) | 29.4 | 37.6 | 35.1 | 30.3 | 25.2 |
| pH$^a$ | 2.8 | 2.9 | 3.0 | 2.8 | 2.8 |
| [TDI] $^a$ (mg/L) | 61.6 | 49.7 | 44.0 | 57.6 | 67.0 |
| $\overline{I_{UV}}$ ($W_{UV}/m^2$)$^a$ | 45.4 | 48.6 | 29.7 | 40.9 | 40.9 |
| $\overline{I_{280-580}}$ ($W/m^2$)$^b$ | 301.7 | 323.8 | 198.1 | 272.7 | 272.7 |
| *DOC degradation* | | | | | |
| $k_{DOC,t}^c$ ($\times 10^{-3}$ min$^{-1}$) | $5.7 \pm 0.2$ | $14 \pm 2$ | $6.5 \pm 0.8$ | $8.1 \pm 0.8$ | $5.4 \pm 0.7$ |
| $r_0$ (mg/L min$^{-1}$) | $1.98 \pm 0.07$ | $5.2 \pm 0.9$ | $2.2 \pm 0.3$ | $2.6 \pm 0.3$ | $1.8 \pm 0.2$ |
| $R^2$ | 0.999 | 0.986 | 0.986 | 0.992 | 0.984 |
| $k_{DOC,Q}^c$ ($\times 10^{-2}$ L/kJ) | $2.6 \pm 0.1$ | $2.2 \pm 0.4$ | $3.2 \pm 0.2$ | $2.9 \pm 0.3$ | $2.7 \pm 0.2$ |
| $r_0$ (mg kJ$^{-1}$) | $9.3 \pm 0.4$ | $8 \pm 2$ | $10.4 \pm 0.6$ | $9 \pm 1$ | $8.9 \pm 0.6$ |
| $R^2$ | 0.997 | 0.987 | 0.997 | 0.990 | 0.994 |
| $\Delta Q_{280\text{-}580nm}^d$ (kJ/L) | 0 - 38 | 0 – 76 | 0 – 37 | 0 – 50 | 0 - 35 |
| $t^e$ (min) | 162 | 65 | 142 | 113 | 168 |
| $Q_{280\text{-}580nm}$ $^e$ (kJ/L) | 35 | 41 | 29 | 31 | 34 |
| $t_{44W;\,25ºC}$ | | | | | |
| $k_{44W;\,25ºC}^f$ ($\times 10^{-3}$ min$^{-1}$) | $4.4 \pm 0.4$ | $8 \pm 2$ | $6.1 \pm 0.5$ | $7.1 \pm 0.9$ | $6.0 \pm 0.4$ |
| $R^2$ | 0.997 | 0.987 | 0.997 | 0.997 | 0.994 |
| $t_{44W;\,25ºC}^g$ (min) | 208 | 115 | 150 | 129 | 153 |

[a] Average values for the temperature (T), pH, total dissolved iron concentration ([TDI]) and UV intensity measured by UV radiometer during the photo-Fenton treatment. [b] Average solar irradiance between 280 and 580 nm, considering $\overline{I_{UV}} \times 0.15$. [c] Pseudo-first-order kinetic constant for DOC degradation considering experimental values. [d] Interval of energy from which the kinetic parameters were calculated. [e] Energy (Q) and time (t) required to achieve 60% of mineralization. [f] Pseudo-first-order kinetic constant for DOC degradation over time considering the "theoretical time" ($k_{44W;\,25ºC}$) with constant UV radiation intensity of 44 $W_{UV}$ m$^{-2}$ and a temperature of 25ºC. [g] Time required to achieve 60% of mineralization considering the "theoretical time" ($t_{44W;\,25ºC}$).

When comparing pilots B and C, the best PF performance was obtained in the first. In fact, after 180 minutes, the leachate final DOC in pilot-plant B was of 76 mg C/L, while in pilot-plant C a 58% higher DOC concentration was reached (120 mg C/L). Nevertheless, and as mentioned, the $CR_O$ determined for the SS-SP and R85s-DP reflectors were very close (Table 7.3 and Table 7.5), and do not justify the differences obtained. Beyond that, when comparing the PF efficiency using those reflectors under the Suntest® controlled conditions, the DOC abatement rate was only slightly better for the SS-SP. Once the reactions were executed under the same irradiance conditions, the higher number of absorber tubes of pilot B explains its superior performance, thus resulting in a (i) greater area directly exposed to the sunlight and (ii) higher temperature along the trial.
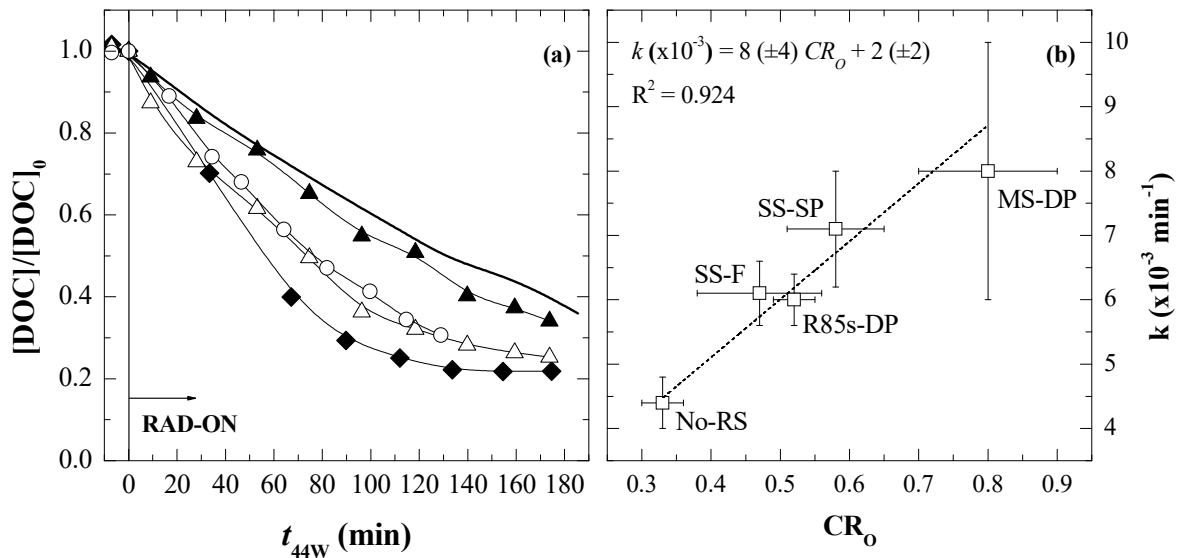
**Figure 7.13** – Photo-Fenton treatment of the pre-treated landfill leachate, under natural sunlight at pilot-scale: (a) evolution of the normalized DOC removal as a function of "theoretical time" $t_{44W}$ (—— No-RS, ♦ MS-DP, ▲ R85s-DP, △ SS-SP, ○ SS-F); and (b) relation between DOC degradation kinetic constant over time and the optical concentration ratio.

It should be noted that the collector's area of pilot B and C is quite similar, but the smaller aperture of the reflector geometry allows the increment of the absorber tubes number. This reveals as an advantage, in the case of the PF treatment since the higher temperature increase will promote the occurrence of further thermally induced reactions. Moreover, even correcting the temperature effect ($k_{44W;25°C}$), the photo-treatment in pilot-plant B was still better, suggesting that other factors may be contributing to the improvement of the treatment. In this case, with the fluid circulating in parallel, pilot B required a flow rate 13 times higher (equal to the number of tubes) during the dark phase, in order to obtain the same flow rate of the pilot C inside the absorber tubes, i.e. during the illuminated phase. The positive impact in the photo-Fenton reaction of a high mixture in the recirculation tank, as occurred in pilot B, was demonstrated by Soares, *et al.* [27]. These authors concluded that along with the hydrodynamic regime inside the tubular photoreactors, also the mixing during the dark phase should be considered in the CPCs design. Therefore, due to the parallel flow, the higher mixture of the leachate in the recirculation tank of pilot B presented as an additional advantage for the PF treatment. Beyond that, pilot B configuration enables other features that may be beneficial when the objective is the collectors scale-up, namely: (i) it ensures an efficient filling, purging and easy discharge; and (ii) it presents adductor tubes, which may be useful when the option is to incorporate the solar collector in the treatment of high wastewater volumes.

### 7.3.4 Cost analysis

Nowadays, an important aspect on the assessment of a treatment system efficiency is its economic evaluation. This evaluation is of outmost interest when the focus is the application of a treatment process in real industrial facilities. In solar-driven systems, the main investment cost is the CPC plant, with the optical components (reflective surface and absorber tubes) being responsible for approximately 35-40% of the hardware cost. Considering this, a cost analysis was performed regarding the hardware required for the construction of solar collectors, using the different reflector materials and geometries tested in this work. The analysis was based on constructive components that represent 97% of total contribution in the final cost of a traditional collector (R85-DP). To allow a better comparison between the different optics configurations, the number of modules, for approximately the same collector's area, was considered to be equal, while the number of absorber tubes varies according to the reflector geometry (Table 7.7).

**Table 7.7** – Summary of the main differences between the reflective surfaces considering a collector's area of approximately 100 m$^2$.

| | DP | SP | F | No-RS |
|---|---|---|---|---|
| **No. modules** | 45 | 45 | 45 | 45 |
| **No. tubes/module** | 10 | 13 | 16 | 16 |
| **Total no. tubes** | 450 | 585 | 720 | 720 |
| **Reflective surface** | | | | |
| **Length (m)** | 0.1571 | 0.12815 | 0.1 | n.a. |
| **Width (m)** | 1.45 | 1.45 | 1.45 | n.a. |
| **Perimeter (m)** | 0.2495 | 0.18025 | 0.1 | n.a. |
| **Material area (m$^2$)** | 163 | 153 | 104 | n.a. |
| **Collectors' area (m$^2$)** | **103** | **109** | **104** | **104** |

n.a. – not applicable.

The constructive components were then divided in three major groups: (i) structural components, taken as a fixed cost for all the collectors, since the same number of modules is being considered; (ii) reflective surface and respective hardware accessories, the cost of which will depend on the material and the geometry of the mirrors; and (iii) absorber tubes and related components, that will depend on the geometry of the reflective surface. Considering all the above, the cost per square meter of solar collector was then determined based on a market research (Table 7.**8** and Table 7.9).

**Table 7.8** – Materials price for solar collector's optics components.

| Reflective surface materials and absorber tubes | | Prices |
|---|---|---|
| Anodized aluminium Reflective 85[a] | | 16.0 |
| Anodized aluminium with protective coating MiroSun[a] | €/m² | 29.0 |
| Mirrored stainless steel 304L[b] | | 23.2 |
| Absorber tubes[c] | €/pack | 177.4 |

[a] Prices in 2010, provided by Ecosystem S.A. [b] Prices in 2016, provided by Neves e Neves Metalworking, Ltd. [c] Prices in 2011 for a 12-tube pack, provided by Glass Solutions, Ltd.

**Table 7.9** – Summary of the constructive components analysed within the three groups and respective costs.

| Components | DP | SP | F | No-RS |
|---|---|---|---|---|
| **1- Structural** | | | | |
| **Sub-total (1)** | **€ 6 348** | **€ 6 348** | **€ 6 348** | **€ 6 348** |
| **2- Reflective surface & components** | | | | |
| Reflective surface | € 4 405[a] | | € 1 670[a] | € 0 |
| (material + moulding) | € 6 521[b] | € 4 725[c] | € 2 427[c] | |
| | € 5 585[c] | | | |
| Other components | € 8 955 | € 7 256 | € 0 | € 0 |
| **Sub-total (2)** | **€ 13 360[a]** **€ 15 476[b]** **€ 14 540[c]** | **€ 11 981[c]** | **€ 1 670[a]** **€ 2 427[c]** | **€ 0** |
| **3- Absorber tubes & components** | | | | |
| Absorber tubes[d] | € 6 490 | € 8 437 | € 10 384 | € 10 384 |
| Other components | € 2 590 | € 3 367 | € 4 144 | € 4 144 |
| **Sub-total (3)** | **€ 9 080** | **€ 11 804** | **€ 14 528** | **€ 14 528** |
| **Total = (1) + (2) + (3)** | **€ 28 788[a]** **€ 30 904[b]** **€ 29 968[c]** | **€ 30 133[c]** | **€ 22 546[a]** **€ 23 303[c]** | **€ 20 876** |
| **€/m²** | **281[a]** **302[b]** **292[c]** | **277[c]** | **216[a]** **223[c]** | **200** |

[a] Anodized aluminium Reflective 85. [b] Anodized aluminium with protective coating MiroSun. [c] Mirrored stainless steel 304L. [d] Absorber tubes.

When comparing the cost variation of the collectors using the DP geometry, it is possible to observe that using R85 aluminium will be more economical when compared to using MS or SS material (7.4 and 4.1% more expensive, respectively). In fact, MS aluminium, due to protective coating,

presents nearly the double of price per square meter when compared to R85 aluminium, while the SS has an intermediate price (Table 7.8). In turn, when comparing collectors with different geometries, the overall cost will reflect three major factors: (i) amount of reflective material required; (ii) cost of mirrors moulding and respective structural support; and (iii) number of absorber tubes per square meter. In this way, the mirror structural support (Figure 7.3) and moulding costs decrease from DP to SP and are null for F and No-RS. The quantity of reflective material required per square meter also decreases from DP to SP (lower mirror perimeter, see Figure 7.2 and Table 7.8) and then to F, being null for No-RS. Also, when comparing to a collector using the traditional DP geometry, the number of absorber tubes increases 1.3-fold for the SP (smaller aperture area) and 1.6-fold for the F and No-RS geometry (if considering a distance of 50 mm between tubes). Therefore, the unitary cost associated with the tubes increases from DP to SP and then to F and No-RS. Crossing all factors with implications on the collector's cost, it is possible to conclude that increasing the number of tubes, while diminishing the costs associated with the reflectors, seems to be advantageous. This statement may be contrary to the expected when looking at the prices of the absorber tube and the reflector sheet found in the literature [3], which may lead to the assumption that, for a cost-effective solution, the number of tubes should be minimized. However, this will only be true if the (i) price of the uncoated aluminium material is considered (with protective coating it is considerably more expensive) and, (ii) cost of the mirror support structures is ignored (usually made in stainless steel and requiring laser cut). When the price of the support structures is added then the overall cost of the mirror greatly increases (Table 7.9). Accordingly, the No-RS and F reflective surfaces resulted as the best cost solution, whereas the collectors using the DP geometry are more expensive, especially if using the MS material. Interestingly, the SS-SP collector has practically the same cost as an R85-DP collector, with the advantage of presenting a more resistant and durable material.

At this point, for a decision-making process, it is pertinent to know which reflective surface tested in this work allows the highest photo-treatment capacity, considering the same collectors' cost. For comparison purposes, the cost variation of the collectors is presented as a percentage over the cost of a traditional collector using R85-DP and an equivalent area ($A_{eq}$) was calculated on the basis of the same optics cost of 100 $m^2$ of collector also using the R85-DP reflector (Table 7.10). A volumetric treatment factor ($T_{fv}$, in $m^3$/day/$m^2$) was also calculated taking into account the experimental data obtained for each experiment, at lab- and pilot-scale, namely: (i) leachate volume used; (ii) reflective surface aperture area; and (iii) time required to achieve 60% mineralization, $t_{60\%}$ (values of $t$ and $t_{44W,25°C}$ from Table 7.4 and Table 7.6, respectively). In other words, $T_{fv}$ may be defined as the volume of leachate that the system is able to treat per unit of time and surface of solar

collectors, to obtain 60% of DOC degradation. The highest $T_{fv}$ was attained for collectors using the F geometry, then SP, followed by DP (MS-DP < R85-DP < SS-DP) and finally for No-RS and R85s-DP. These results show that, for F and SP reflectors, the increment on the number of absorber tubes per square meter of collector is advantageous. In turn, despite an equal increase in the tubes number as the F reflectors, the absence of reflecting surface (No-RS) is clearly an unfavourable condition. Moreover, the effect of the soiled aluminium is demonstrated with a decrease of 20% of the $T_{fv}$ when compared to R85-DP. This loss of the photo-treatment efficiency over time, involves obvious constraints on the operational planning of an industrial treatment facility. Additionally, in a 10-year period a collector using R85-DP mirrors would require its substitution, representing a considerable increase on the maintenance costs (not considered in the present analysis).

**Table 7.10** – Cost analysis for the solar collectors presenting the different reflective surface materials and geometries.

| | DP | | | | SP | F | | No-RS |
|---|---|---|---|---|---|---|---|---|
| | R85 | R85s | MS | SS | SS | R85 | SS | |
| **Collectors' cost (%)[a]** | 0.0 | 0.0 | + 7.4 | + 4.1 | - 1.3 | - 23.1 | - 20.5 | -28.8 |
| $A_{eq}$ **(m²)[b]** | 100 | 100 | 93 | 96 | 101 | 130 | 126 | 140 |
| **Sunlight simulator** | | | | | | | | |
| $T_{fv}$ **(m³/day/m²)[c]** | 0.43 | 0.34 | 0.44 | 0.41 | 0.46 | 0.48 | 0.51 | 0.33 |
| $T_r$ **(m³/day)[d]** | 42.8 | 33.9 | 41.3 | 39.2 | 46.6 | 62.7 | 64.5 | 45.9 |
| **Natural sunlight** | | | | | | | | |
| $T_{fv}$ **(m³/day/m²)[c]** | n.d.[e] | 0.33 | 0.43 | n.d.[e] | 0.46 | n.d.[e] | 0.50 | 0.36 |
| $T_r$ **(m³/day)[d]** | n.d.[e] | 33.2 | 39.8 | n.d.[e] | 46.7 | n.d.[e] | 62.5 | 50.3 |

[a] Percentage variation of the unitary cost associated with about 100 m² of each solar collector configuration compared to a traditional R85-DP. [b] Solar collectors' equivalent area considering the same collectors' cost as an installation of 100 m² using R85-DP reflectors. [c] Experimental volumetric treatment factor. [d] Treatment rate considering the same collectors' cost ($T_r = T_{fv} \times A_{eq}$). n.d - not determined.

Knowing the experimental values of $T_{fv}$ and $A_{eq}$, it is also possible to determine the leachate treatment rate ($T_r$) that each system would be able to treat at the same cost as a facility composed by 100 m² of R85-DP reflectors (Table 7.10). In the case of F collectors, the higher $A_{eq}$ (130 and 126 m²) contributes for a $T_r$ of 46.7 m³/day and 51% superior when comparing to 100 m² of R85-DP collector. Regarding a collector using SS-SP reflector, it presents approximately the same cost and consequently similar area of an R85-DP collector, and enables a $T_r$ increment of 9%. In view of the foregoing, the SS-F reflector seems to be the best choice for the leachate used in this work, combining the simplicity and the use of a recognized durable material with the highest volumetric treatment factor.

## 7.4 Conclusions

Aiming the application of the photo-Fenton process for the treatment of wastewaters with low transmissibility, e.g. sanitary landfill leachates, in a scale-up and cost saving perspective, different collectors' optics presenting the traditional and alternative reflective materials and geometries were tested in this work. In respect to the reflectors optical efficiency it was possible to conclude: (i) the major influence of the reflector geometry and specular reflectance of the materials; (ii) the impact of 8-year of outdoor exposure of the R85 anodized aluminium (loss of 38.7% of specular reflectance and a decrease of 26% in the optical efficiency); (iii) for flat geometry the difference in the material reflectance has a negligible influence on the optical efficiency; (iv) the inclusion of a simple reflective surface, such as SS-F, increases the optical efficiency up to 17% when compared to the absence of reflector.

The photo-Fenton applied to an urban leachate showed that the process efficiency over time was mostly coherent with the optical efficiency of the different reflective surfaces. Beyond that, at pilot-scale, the SS-SP reflector presented a better performance, mainly due to the higher number of absorber tubes, i.e. higher illuminated volume. The SP geometry enables an increase of 30% of absorber tubes for approximately the same area as a collector using the DP traditional reflector, and further promotes thermally induced reactions by a higher temperature increment.

The cost analysis performed for the solar collectors showed that the F reflector would be the best option, presenting the highest volumetric treatment factor. For the same investment cost that would be required to build 100 $m^2$ of a collector using the R85-DP reflector, it is possible to construct 126 $m^2$ of a collector using an SS-F reflector, whose geometry allows to increase 1.6-fold the number of absorber tubes per square meter, corresponding to a treatment rate increment of 51%. Considering that higher illuminated surface to volume ratios reduce the reactor dimensions and thereby, capital and operating costs, the flat geometry reflectors using a resistant material, such as the stainless steel, may be a cost-saving and effective solution in the treatment of wastewater with low transmissibility and presenting UV inner-filter effects, such as leachates, by the photo-Fenton process.

## 7.5 References

1. Malato, S., P. Fernández-Ibáñez, M.I. Maldonado, J. Blanco, and W. Gernjak, *Decontamination and disinfection of water by solar photocatalysis: recent overview and trends.* Catalysis Today, 2009. **147**: p. 1-59.

2. Robert, D. and S. Malato, *Solar photocatalysis: A clean process for water detoxification.* Science of the Total Environment, 2002. **291**: p. 85-97.

3. Spasiano, D., R. Marotta, S. Malato, P. Fernández-Ibáñez, and I. Di Somma, *Solar photocatalysis: materials, reactors, some commercial, and pre-industrialized applications. A comprehensive approach.* Applied Catalysis B, 2015. **170-171**: p. 90-123.

4. Primo, O., M.J. Rivero, and I. Ortiz, *Photo-Fenton process as an efficient alternative to the treatment of landfill leachates.* Journal of Hazardous Materials, 2008. **153**: p. 834-842.

5. Silva, T.F.C.V., M.E.F. Silva, A.C. Cunha-Queda, A. Fonseca, I. Saraiva, R.A.R. Boaventura, and V.J.P. Vilar, Sanitary landfill leachate treatment using combined solar photo-Fenton and biological oxidation processes at pre-inductrial scale. Chemical Engineering Journal, 2013. **228**: p. 850-866.

6. Rocha, E.M.R., V.J.P. Vilar, A. Fonseca, I. Saraiva, and R.A.R. Boaventura, *Landfill leachate treatment by solar-driven AOPs.* Solar Energy, 2011. **85**(1): p. 46-56.

7. Lopez, A., C. Di Iaconi, G. Mascolo, and A. Pollice, Innovative and integrated technologies for the treatment of industrial wastewater. 2011: IWA Publishing.

8. Carra, I., L. Santos-Juanes, F.G.A. Fernández, S. Malato, and J.A. Sánchez-Pérez, *New approach to solar photo-Fenton operation, raceway ponds as tertiary treatment technology.* Journal of Hazardous Materials, 2014. **279**: p. 322-329.

9. Belalcázar-Saldarriaga, A., D. Prato-Garcia, and R. Vasquez-Medrano, Photo-Fenton processes in raceway reactors: technical, economical, and environmental implications during treatment of colored wastewaters. Journal of Cleaner Production, 2018. **182**: p. 818-829.

10. Rodríguez, M., S. Malato, C. Pulgarin, S. Contreras, D. Curcó, J. Giménez, and S. Esplugas, Optimizing the solar photo-Fenton process in the treatment of contaminated water. Determination of intrinsic kinetic constants for scale-up. Solar Energy, 2005. **79**(4): p. 360-368.

11. Farias, J., E.D. Albizzati, and O.M. Alfano, *New pilot-plant photo-Fenton solar reactor for water decontamination.* Industrial & Engineering Chemistry Research, 2010. **49**(3): p. 1265-1273.

12. Silva, T.F.C.V., R. Ferreira, P.A. Soares, D.R. Manenti, A. Fonseca, I. Saraiva, R.A.R. Boaventura, and V.J.P. Vilar, *Insights into solar photo-Fenton reaction parameters in the oxidation of a sanitary landfill leachate at lab-scale.* Journal of Environmental Management, 2015. **164**: p. 32-40.

13. Bandala, E.R., C.A. Arancibia-Bulnes, S.L. Orozco, and C.A. Estrada, *Solar photoreactors comparison based on oxalic acid photocatalytic degradation.* Solar Energy, 2004. **77**: p. 503-512.

14. Ennaceri, H., H. El Alami, H. Brik, O. Mokssit, and A. Khaldoun, Lotus effect and super-hydrophobic coatings for concentrated solar power systems (CSP), in International Conference on Composite Materials & Renewable Energy Applications. 2014, IEEE: Sousse, Tunisia.

15. Sutter, F., P. Heller, A. Fernandez-García, C. Kennedy, R. López-Martín, S. Meyen, and R. Pitz-Paal. Methods for service life time estimation of aluminum reflectors. in International Conference on Solar Energy for Buildings and Industry. 2010.

16. Kain, R., B. Phul, and S. Pikul, 1940 'Til now — Long-term marine atmospheric corrosion resistance of stainless steel and other nickel containing alloys. Outdoor Atmospheric Corrosion, 2002: p. 343-357.

17. Baker, E.A. and W.W. Kirk, Long-term atmospheric corrosion behaviour of various grades of stainless steel in rural, industrial, and marine environments., in Corrosion Testing and Evaluation, R. Baboian and S.W. Dean, Editors. 1990, ASTM. p. 445.

18. Cabrini, M., S. Lorenzi, T. Pastore, S. Pellegrini, M. Burattini, and R. Miglio, *Study of the corrosion resistence of austenitic stainless steels during conversion of waste to biofuel.* Materials, 2017. **10**.

19. Luo, H., X. Ii, C. Dong, and K. Xiao, *Degradation of austenite stainless steel by atmospheric exposure in tropical marine environment.* Corrosion Engineering, Science and Technology, 2013. **48**(3): p. 221-229.

20. Colina-Márquez, J., F. Machuca-Martínez, and G. Li Puma, *Radiation absorption and optimization of solar photocatalytic reactors for environmental applications.* Environmental Science & Technology, 2010. **44**(13): p. 5112-5120.

21. Taylor, A.E.F., *Illumination Fundamentals*. 2000, Lighting research Center/Renssenlaer Polytechnic Institute.

22. Molkenthin, M., T. Olmez-Hanci, M.R. Jekel, and I. Arslan-Alaton, Photo-Fenton like treatment of BPA:effect of UV light source and water matrix on toxicity and transformation products. Water Research, 2013. **47**: p. 5052-5064.

23. Moreira, F.C., Electrochemical advanced oxidation processes: Application to de degradation of synthetic and real wastewaters, in Chemical Department. 2016, Faculty of Engineering, University of Porto: Porto.

24. Clemente, A.R., E. Chica, and G.A. Peñuela, *Petrochemical wastewater treatment by photo-Fenton process.* Water, Air & Soil Pollution, 2015. **62**.

25. Herrera, F., C. Pulgarin, V. Nadtochenko, and J. Kiwi, Accelerated photo-oxidation of concentrated p-coumaric acid in homogeneous solution. Mechanistic studies, intermediates and precursors formed in the dark. Applied Catalysis B, 1998. **17**: p. 141-156.

26. Gernjak, W., M. Fuerhacker, P. Fernández-Ibañez, J. Blanco, and S. Malato, *Solar photo-fenton treatment - process parameters and process control.* Applied Catalysis B, 2006. **64**: p. 121-130.

27. Soares, P.A., M. Batalha, S.M.A.G.U. Souza, R.A.R. Boaventura, and V.J.P. Vilar, Enhancement of a solar photo-Fenton reaction with ferric-organic ligands for the treatment of acrylic-textile dyeing wastewater. Journal of Environmental Management, 2015. **152**: p. 120-131.

# 8 Ozone-driven processes for mature urban landfill leachate treatment: Organic matter degradation, biodegradability enhancement and treatment costs for different reactors configurations

*In this chapter, the application of ozone-driven processes for the treatment of mature landfill leachate was investigated by testing different system setups. As a first approach, ozonation (O₃-only) was tested, using a porous ceramic diffuser combined with a bubble column (BC), and the best operational conditions were established for leachate treatment (initial pH = 9.0; inlet ozone dose = 18 mg O₃/min). Then, the novel FluHelik photoreactor was coupled in series with the bubble column, using a diffuser or a Venturi to inject ozone into the fluid stream. The FluHelik/BC-Venturi setup led to the highest efficiency, treating 50% more leachate than BC-alone using the same ozone dose and reaction time (3h). Following, the oxidation ability of ozone combined with $H_2O_2$ and/or UVC for leachate treatment was assessed. The highest synergistic effect was obtained for the $O_3$/UVC process, with pseudo-first-order rate constant for DOC and COD removal, 2.0 and 1.4 times higher than for the $O_3$-only, respectively. Ozone-driven processes considerably enhanced the leachate biodegradability from 17% to 79% ($O_3$/$H_2O_2$), 81% ($O_3$-only), 85% ($O_3$/$H_2O_2$/UVC) and 91% ($O_3$/UVC), after a 3h reaction period.*

*With FluHelik/BC-Venturi system, the $O_3$/UVC process stands out as the most efficient and cost-effective (6.0 €/m³), ensuring an effluent that meets discharge legal limit for COD (150 mg/L) after further biological oxidation.*

## 8.1 Introduction

The main component of the leachate organic content is humic substances, which are structurally complex refractory anionic macromolecules (e.g. humic and fulvic acids) [1], responsible for more than 50% of dissolved organic matter [2]. Ozone is a strong oxidative agent ($E^0 = 2.07$ V), particularly effective in colour removal [3] and has high reactivity and selectivity towards organic pollutants containing electron rich moieties, such as humic substances [4, 5]. The application of ozone-driven processes in the treatment of landfill leachates has attracted attention, whether applied to the raw effluent as pre-treatment [3, 6] or as a polishing step [1, 4, 7, 8]. Ozone instability dictates the need for on-site generation, usually by applying Corona process to pure oxygen streams [9]. One major obstacle to a general wider use of ozone technology is the high associated ozone generation cost (15-20 kWh/kg $O_3$ when produced from pure $O_2$), stemming from the fact that only a small fraction of the initial high-purity oxygen feed (10-15 wt-%) is converted into ozone [10]. A major limitation of current ozonation technologies is the high ozone supply demands, the extended contacting time required in the reactor and the bulky size of the equipment. These disadvantages are associated with low mass transfer rates from gas to liquid phase (from 30-40%) [10], when using conventional gas-liquid contactors such as bubble columns [11], air-lift reactors [12], packed columns [13], stirred-tank reactors [14] or static mixers [15, 16], or Venturi injectors systems usually combined with very bulky gas–liquid holding tanks [17]. Enhancing the mixing rate can improve mass transfer, which can be improved through the use of microreactors [18, 19], oscillatory baffled columns (OBCs) [20] or rotating packed contactors (RPCs) [21].

The above limitations can, at some extent, be overcome by: (i) optimization of operational conditions (e.g. pH of the effluent and inlet ozone dose); (ii) equipment design (reactor configuration, multiple reactors systems and gas-liquid contact devices); and (iii) combination of different advanced oxidation processes (e.g. ozone with $H_2O_2$ and/or UVC radiation, i.e. $O_3$-based AOPs). At alkaline pH conditions ($O_3/OH^-$), ozone easily decomposes into the highly reactive hydroxyl radical ($E^0 = 2.80$ V), enhancing its oxidation ability [4, 7, 22, 23]. Finally, the production of hydroxyl radicals ($^\bullet OH$) is favoured by combining $O_3$ with $H_2O_2$ and/or UVC radiation, and a synergistic effect for the removal of organic matter can be expected [20].

In view of the above, aiming at an efficient and cost-effective ozone-driven treatment step for mature landfill leachates, this work tested different ozone system setups. To achieve these goals, using a pre-treated leachate (biologically nitrified and coagulated), experiments were carried out with: (i) ozone ($O_3$-only), to determine the best experimental conditions in terms of leachate initial pH and inlet ozone dose; (ii) $O_3$-only, to assess the effect of system setup, by coupling reactors in

series (bubble column reactor and FluHelik photoreactor) and testing different ozone injection techniques (porous ceramic diffuser or Venturi); and (iii) $O_3/H_2O_2$, $O_3/UVC$ and $O_3/UVC/H_2O_2$, to evaluate the treatment efficiency and synergetic effects, according to the pseudo-first-order rate constants determined experimentally for DOC and COD removals. Additionally, Zahn-Wellens tests were carried out to evaluate the biodegradability of the leachate after each ozone-driven treatment. Finally, operation costs were estimated to assess the feasibility of the ozone-driven processes for leachate treatment.

## 8.2 Materials and methods

The experiments carried out along this work used a pre-treated leachate (after biological and coagulation/sedimentation stages) collected at a full-scale treatment facility. The leachate was transported to the laboratory and aerated, until full nitrite conversion to nitrates (to eliminate interference of the presence of nitrites in the oxidation reactions, as observed for the photo-Fenton oxidation) and stored at 4ºC until use. The values of the leachate's main physicochemical characterization parameters are presented in Table 8.1.

**Table 8.1** – Physicochemical characterization of pre-treated landfill leachate.

| Parameter | Unit | Value |
|---|---|---|
| pH | Sorensen scale | 3.7 |
| DOC | mg/L | 395 |
| COD | mg $O_2$/L | 1073 |
| $SUVA_{254}$ | L/mg/m | 2.3 |
| Colour (1:20 dilution) | Pt-Co | 43 |
| TN | mg N/L | 560 |
| $N-NO_3^-$ | mg/L | 523 |
| $N-NO_2^-$ | mg/L | < 0.1 |
| $N-NH_4^+$ | mg/L | < 0.1 |
| $Cl^-$ | g/L | 2.6 |
| $SO_4^{2-}$ | g/L | 1.7 |
| TSS | mg/L | 170 |

All the chemicals used in this work, experimental units and respective procedures, as well as the analytical methods employed, can be consulted, respectively, in sections 4.1, 4.3.4 and 4.2 of Chapter 4. In this work, to better compare and understand the transformations of the organic matter during the treatment by the different ozone-driven processes, a comparative analysis of the evolution of the UV-Vis spectra and parameters recognized to characterize the organic matter of leachates [24] (such as, mean oxidation state (*MOS*), specific UV absorbance at 254 nm (*SUVA₂₅₄*) and ratio of UV absorbance at 300 to 400 nm (*Abs₃₀₀/Abs₄₀₀*)) were also assessed.

## 8.3 Results and discussion

### 8.3.1 Ozone-only experiments: effect of operational parameters

#### 8.3.1.1 Initial pH of the leachate

DOC and COD removal efficiency raised with leachate pH (Table 8.2), as reported in the literature [4, 23]. The overall ozone oxidation consists of: (i) direct reaction of $O_3$, which is very specific but reacting at a relatively low rate due to the selective attack of unsaturated electron-rich bonds contained in specific functional groups (e.g. aromatics and amines); and (ii) indirect reaction of secondary oxidizers, such as hydroxyl radicals (generated by $O_3$ decomposition), which are non-selective and present high oxidation rates [25, 26]. Considering that $O_3$ reacts with $HO^-$ to start the reaction chains that involve $^\bullet OH$ formation (Equations 3.17 to 3.23, section 3.1.6.2 of Chapter 3), at high pH levels the indirect oxidation reactions predominate, while at low pH levels the $O_3$ direct reactions prevail. Thus, alkaline pH conditions favoured the generation of $^\bullet OH$, boosting the oxidation of the recalcitrant organic matter. As a result, showing similar $OD_T$ values throughout the treatment time, the amount of DOC removed per gram of ozone increased 1.7 times, from pH 3.7 to 7.0, and also from pH 7.0 to 9.0 (Table 8.2). Regardless the pH value, the degree of organic carbon mineralization (DOC) was lower than COD removal (this is valid for all tests in this study), which was probably related to the oxidation of particulate organic matter and the formation and accumulation of carboxylic acids and aldehydes as final products, rather than $CO_2$ [4].

**Table 8.2** – Kinetic parameters of the $O_3$-only experiments carried out under different initial pH values.

| Parameters | Leachate initial pH[a] | | |
|---|---|---|---|
| | 3.7 | 7.0 | 9.0 |
| $OD_I$[b] (g $O_3$/L) | 1.6 | 1.6 | 1.6 |
| $OD_T$[b] (g $O_3$/L) | 1.1 | 1.1 | 1.1 |
| DOC removal (%) | 8.0 | 13.0 | 22.3 |
| COD removal (%) | 13.5 | 24.1 | 30.3 |
| | *DOC Degradation Kinetics* | | |
| $k$[c]$\times 10^4$ (min$^{-1}$) | 5.4 ± 0.8 | 8 ± 1 | 15 ± 2 |
| $R^{2,d}$ | 0.982 | 0.987 | 0.991 |
| $t$[e] (min) | 20-180 | 0-180 | 20-180 |
| $k$[f]$\times 10^{-1}$ (mg DOC/g $OD_T$) | 2.5 ± 0.3 | 4.3 ± 0.4 | 7.5 ± 0.5 |
| $R^{2,d}$ | 0.983 | 0.992 | 0.996 |
| $OD_T$[e] (g $O_3$/L) | > 0 | > 0 | > 0 |

[a] Experimental conditions: BC-alone system; $t$ = 180 min; $V_L$ = 1.0 L; $Q_g$ = 0.1 NL/min; $C_{O_3,l\text{-}g}$ = 90 mg $O_3$/L. [b] Inlet ($OD_I$) and transferred ($OD_T$) ozone dose per litre of leachate. [c] Pseudo-first-order rate constant for DOC degradation in terms of reaction time. [d] Coefficient of determination. [e] Value or interval of time ($t$, min) or transferred ozone dose ($OD_T$), from which the kinetic parameters were calculated. [f] DOC degradation reaction rates, expressed in terms of the transferred ozone dose ($OD_T$), whose values correspond to the slopes of Figure 8.1.
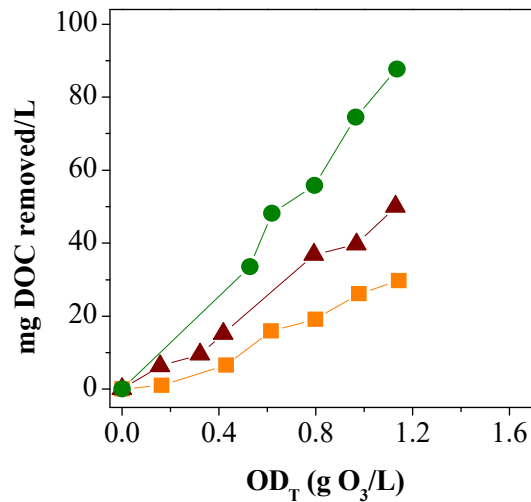
**Figure 8.1** – Representation of the amount of DOC removed, as a function of the transferred ozone dose ($OD_T$), for experiments carried out under different initial pH values: ■ - 3.7; ▲ - 7.0 ; ● - 9.0

In terms of colour (Figure 8.2-b), removals of 34%, 39% and 40%, after 20 minutes of treatment, and of 57%, 70% and 72%, at the end (180 min), were observed for pH 3.7, 7.0 and 9.0, respectively. Therefore, colour removal was improved when the initial pH increased to 7.0, but there was no significant effect when the pH further increased. Additionally, the effective colour reduction at acidic conditions indicates that ozone can easily oxidize the chromophore groups in macromolecular weight organic matter.

It should be mentioned that in the experiment performed at the natural pH of the pre-treated leachate, a slight decrease in pH from 3.7 to 3.2 was observed (Figure 8.2-c). In turn, at initial pH values of 7.0 and 9.0, a significant pH drop was registered (final pH of 4.0 and 4.9, respectively), indicating that a strong oxidation took place. This pH reduction can be attributed to the formation of carboxylic acids and low molecular weight organic acids, as well as $CO_2$ and carbonic acids from total mineralization of the organic matter. Taking into account the higher efficiency of the ozone process under basic conditions, the initial pH 9.0 was selected for the following tests.
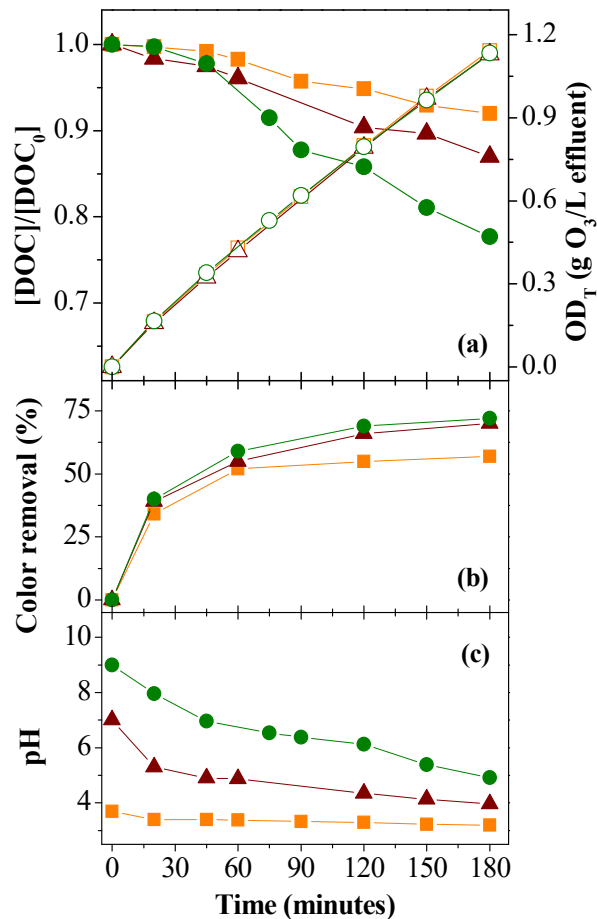
**Figure 8.2** – Evolution of the (a) DOC removal and $OD_T$, (b) colour removal and (c) pH, as a function of treatment time, for the ozone experiments under different initial pH values: ■,□ - pH 3.7; ▲,△ - pH 7.0; ●,○ - pH 9.0 closed symbols - left y axis; open symbols - right y axis.

### 8.3.1.2 Inlet ozone dose

Figure 8.3-a shows an increment on DOC and COD removal for higher inlet ozone doses (and consequently higher $OD_T$). Furthermore, it was possible to verify that the pseudo-first-order rate constants ($k$, min$^{-1}$) for DOC and COD removal were reasonably proportional to the ozone dose fed to the system (Table 8.3). However, an increase of the off-gas ozone concentration was also observed Figure 8.3-b), representing 30%, 43% and 51% of the total ozone fed to the system, for tests using 9, 18 and 27 mg O$_3$/min, respectively. This is an important parameter to consider, because the greater the amount of unused ozone, the greater the operational cost of the process [27]. Due to the generation of high amounts of foam during the test with the highest ozone dose, the assay was terminated after 150 minutes of treatment. Slower reaction rates were observed after an $OD_T$ of ~ 1.4 g O$_3$/L, corresponding to 120 and 90 minutes of treatment, respectively, for tests with 18 and 27 mg O$_3$/min. From this point on, both tests showed an increase of the off-gas and dissolved ozone concentrations (Figure 8.3-b and -c). These features together with the acidic pH conditions

(Figure 8.3-e), suggest the presence of low molecular weight acids with low affinity for ozone direct attack, after 120 and 90 minutes of treatment, for tests with 18 and 27 mg $O_3$/min, respectively.
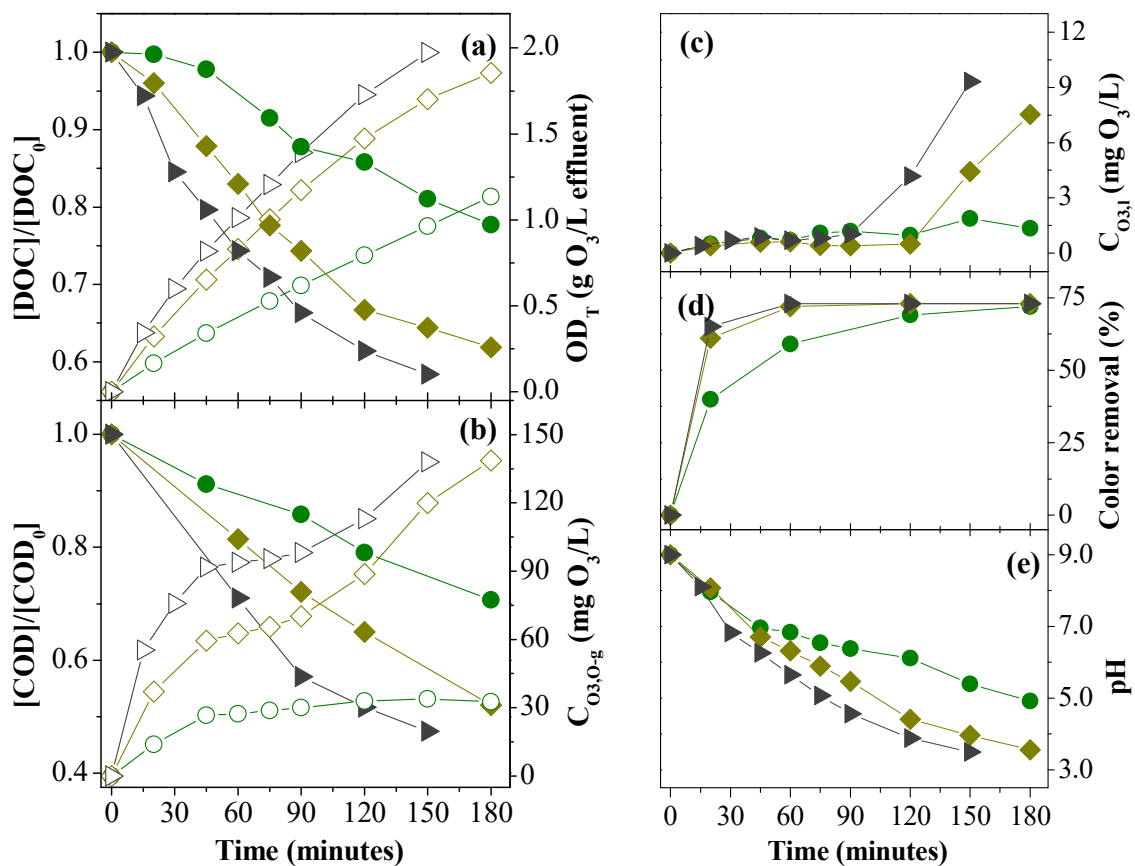


**Figure 8.3** – Evolution of the (a) DOC removal and $OD_T$, (b) COD removal and $C_{O_3,O-g}$, (c) dissolved ozone concentration ($C_{O_3,l}$), (d) colour removal and (e) pH, as a function of treatment time, for the ozone experiments with different inlet ozone doses: (●,○) 9 mg $O_3$/min; (◆,◇) 18 mg $O_3$/min; and (▶,▷) 27 mg $O_3$/min; (closed symbols) left y axis and (open symbols) right y axis.

Concerning colour removal (Figure 8.3-d), a positive impact was verified when the ozone dose increased from 9 to 18 mg $O_3$/min, but no significant improvements were detected when it was further increased to 27 mg $O_3$/min. It was observed that for $OD_T > 1$ g $O_3$/L, all tests presented 72% of colour removal, which was maintained until the end. So, considering all results, the chosen ozone dose to proceed with the following tests was 18 mg $O_3$/min ($C_{O_3,I-g} = 180$ mg $O_3$/L and $Q_g = 0.10$ L/min).

**Table 8.3** – Kinetic parameters of the ozone-only experiments carried out under different $O_3$ inlet doses.

| Parameters | Ozone inlet dose (mg $O_3$/min)[a] | | |
|---|---|---|---|
| | 9 | 18 | 27 |
| $OD_I$[b] (g $O_3$/L) | 1.6 | 3.2 | 4.1 |
| $OD_T$[b] (g $O_3$/L) | 1.1 | 1.9 | 2.0 |
| DOC removal (%) | 22.3 | 38.1 | 41.6 |
| COD removal (%) | 30.3 | 48.0 | 52.5 |
| | *DOC Degradation Kinetics* | | |
| $k$[c]$\times 10^3$ (min$^{-1}$) | $1.5 \pm 0.2$ | $3.5 \pm 0.3$ | $4.8 \pm 0.5$ |
| $R^{2,d}$ | 0.991 | 0.995 | 0.994 |
| $t$ [e] (min) | 20-180 | < 120 | < 90 |
| $k$[f]$\times 10^{-1}$ (mg DOC/g $OD_T$) | $7.5 \pm 0.5$ | $8.4 \pm 0.4$ | $9.3 \pm 0.6$ |
| $R^{2,d}$ | 0.996 | 0.996 | 0.994 |
| $OD_T$ [e] (g $O_3$/L) | > 0 | > 0 | > 0 |
| | *COD Degradation Kinetics* | | |
| $k$[c]$\times 10^3$ (min$^{-1}$) | $1.9 \pm 0.3$ | $3.6 \pm 0.1$ | $6 \pm 1$ |
| $R^{2,d}$ | 0.994 | 0.999 | 0.989 |
| $t$ [e] (min) | > 0 | > 0 | < 120 |
| $k$[f]$\times 10^{-2}$ (mg COD/g $OD_T$) | $2.6 \pm 0.2$ | $2.7 \pm 0.2$ | $3.1 \pm 0.2$ |
| $R^{2,d}$ | 0.997 | 0.997 | 0.996 |
| $OD_T$ [e] (g $O_3$/L) | > 0 | > 0 | > 0 |

[a] Experimental conditions: BC-alone system; $t = 180$ min, except for test with highest dose (150 min); leachate initial pH = 9.0; $V_L = 1.0$ L. [b] Inlet ($OD_I$) and transferred ($OD_T$) ozone dose per litre of leachate. [c] Pseudo-first-order rate constant for DOC and COD degradation in terms of reaction time. [d] Coefficient of determination. [e] Value or interval of time ($t$, min) or transferred $O_3$ dose ($OD_T$), from which the kinetic parameters were calculated. [f] DOC and COD degradation reaction rates, expressed in terms of the transferred ozone dose ($OD_T$), whose values correspond to the slopes of Figure 8.4 -a.1) and -b.1), respectively.
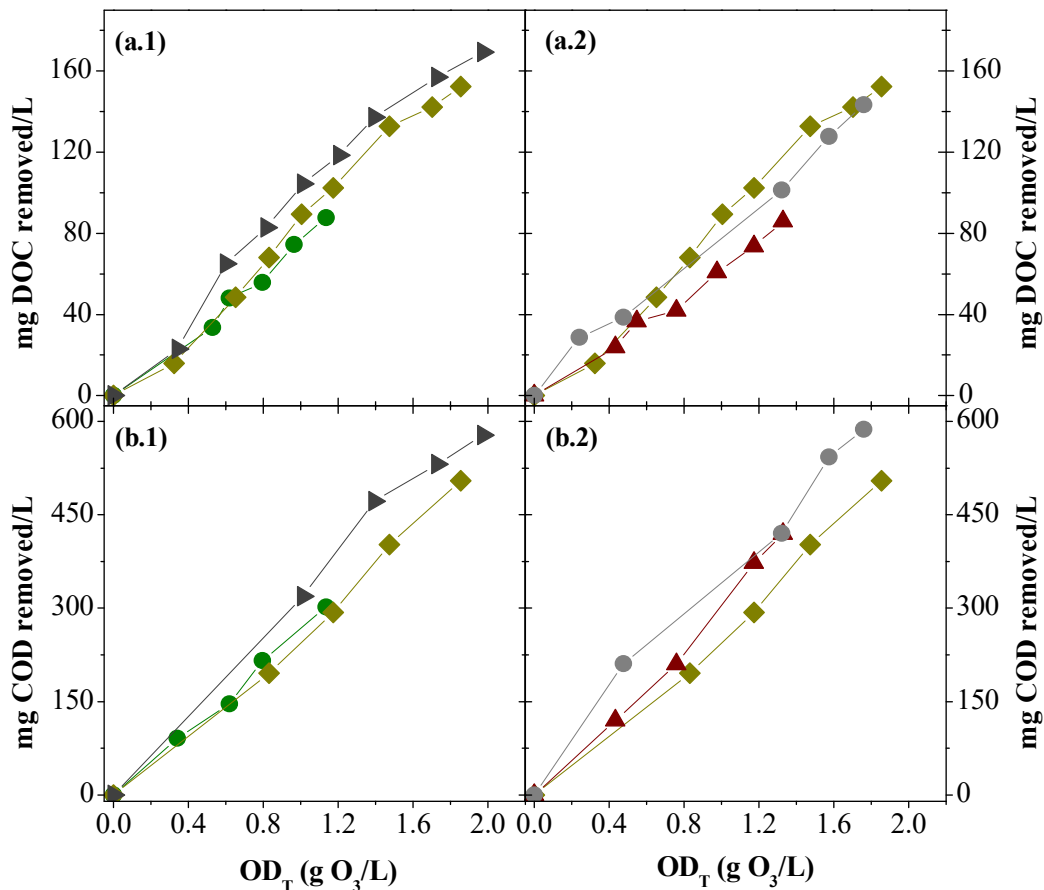
**Figure 8.4** – Representation of the amount of (a) DOC and (b) COD removed, as a function of the transferred ozone dose ($OD_T$), for the ozone experiments carried out with different: (.1) inlet ozone dosage (● - 9 mg $O_3$/min; ◆ - 18 mg $O_3$/min and – ▶ 27 mg $O_3$/min); and (.2) system configuration (◆ - BC-alone; ▲ - FluHelik/BC-Diffuser and ● – FluHelik/BC-Venturi).

### 8.3.2 Ozone-only experiments: system setup assessment

In a first approach, the ozone was injected through the porous ceramic diffuser located at the bottom of the BC and the leachate was recirculated between the BC and the FluHelik reactor (FluHelik/BC-Diffuser system). Figure 8.5-a) and -b) shows a decrease on DOC and COD removals for the FluHelik/BC-Diffuser setup when compared to the BC-alone system. This is explained by the increase of the leachate volume under treatment (from 1.0 to 1.5 L), to maintain a water column height in the BC reactor similar to the previous tests using BC-alone system, while the ozone dose was maintained, which consequently led to a decrease of the $OD_T$ values (Figure 8.5-b). Then, a second approach was attempted, where a Venturi injector was introduced at the inlet of the FluHelik (FluHelik/BC-Venturi system). In the FluHelik/BC-Diffuser setup, higher amounts of $O_3$ in the off-

gas were observed mainly in the first 120 minutes of reaction, when compared with FluHelik/BC-Venturi configuration. As the ozone was injected through the porous ceramic diffuser located at the bottom of the BC (FluHelik/BC-Diffuser), most of the ozone bubbles rose in the column and were not pumped to the FluHelik reactor. Therefore, the FluHelik/BC-Venturi configuration led to an increase of the $OD_T$ and, consequently, DOC and COD removals, since this approach enabled a higher contact time between the ozone and the leachate in both reactors. Also, this configuration was more efficient for $O_3$-only treatment when compared to the BC-alone. Both systems presented similar DOC and COD removals (Figure 8.5 and Table 8.4), but the FluHelik/BC-Venturi system was able to treat 50% more leachate volume using the same ozone dose and reaction time.

Although the ozone injection techniques used in this work, porous diffuser and Venturi, promote a high transfer of ozone from gas to liquid phase (> 90%), the ozone transfer efficiency using porous diffusers can decrease significantly over time (< 80%) due to gasket failure or diffuser fouling [17]. Beyond that, placing the Venturi injector at the inlet of FluHelik, allowed to take advantage of the particular hydrodynamic conditions provided by this reactor [28], with an expected strong radial mixing. Therefore, the FluHelik/BC-Venturi was the configuration that enhanced the ozone mass transfer from the gas phase to the liquid phase, resulting in lower amounts of $O_3$ in the off-gas (Figure 8.5-b).
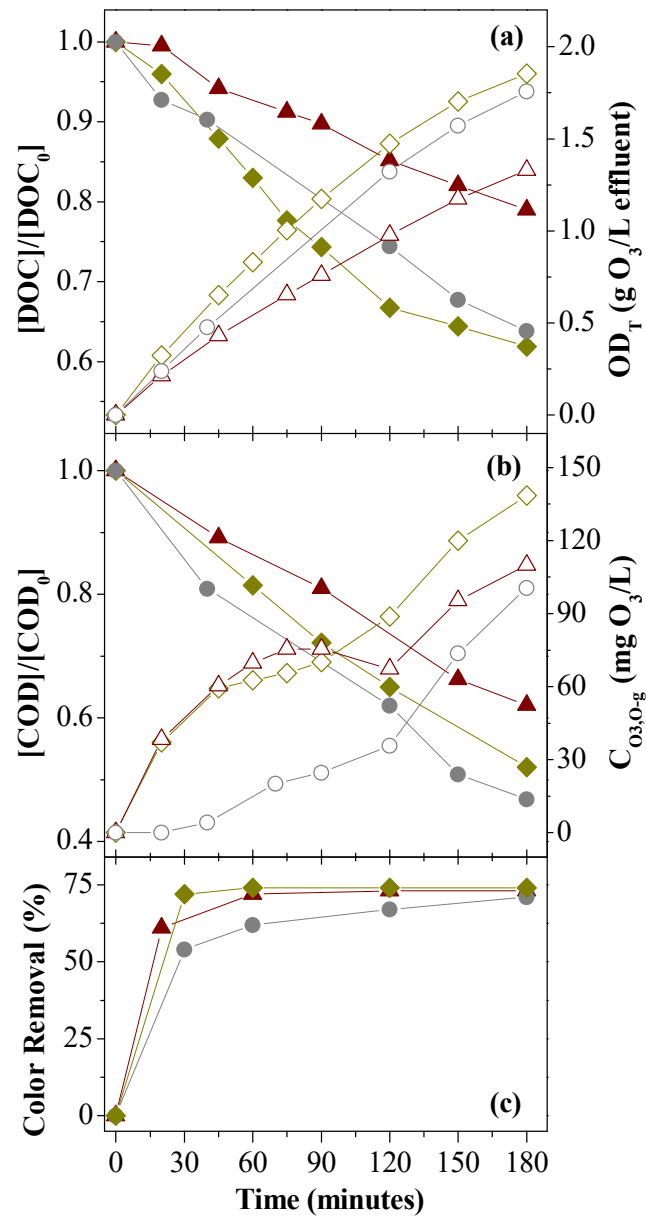
**Figure 8.5** – Evolution of the (a) DOC removal and $OD_T$, (b) COD removal and $C_{O3,O-g}$, and (c) colour removal, as a function of treatment time, for the ozone experiments with different system setups: ◆,◇ - BC-alone; ▲,△ - FluHelik/BC-Diffuser; ●,○ - FluHelik/BC-Venturi closed symbols - left y axis; open symbols - right y axis

**Table 8.4 –** Kinetic parameters of the $O_3$-only experiments carried out with different system setups.

| Parameters | System setup[a] | | |
|---|---|---|---|
| | BC | FluHelik/BC-Diffuser | FluHelik/BC-Venturi |
| $OD_I$[b] (g $O_3$/L) | 3.2 | 2.2 | 2.2 |
| $OD_T$[b] (g $O_3$/L) | 1.9 | 1.3 | 1.8 |
| DOC removal (%) | 38.1 | 21.0 | 36.2 |
| COD removal (%) | 48.0 | 38.0 | 53.1 |
| *DOC Degradation Kinetics* | | | |
| $k$[c]$\times 10^3$ (min$^{-1}$) | $3.5 \pm 0.3$ | $1.4 \pm 0.1$ | $2.5 \pm 0.2$ |
| $R^{2,d}$ | 0.995 | 0.995 | 0.996 |
| $t$[e] (min) | < 120 | 20-180 | 0-180 |
| $k$[f]$\times 10^{-1}$ (mg DOC/g $OD_T$) | $8.4 \pm 0.4$ | $6.2 \pm 0.3$ | $8.1 \pm 0.5$ |
| $R^{2,d}$ | 0.996 | 0.998 | 0.997 |
| $OD_T$[e] (g $O_3$/L) | > 0 | > 0 | > 0 |
| *COD Degradation Kinetics* | | | |
| $k$[c]$\times 10^3$ (min$^{-1}$) | $3.6 \pm 0.1$ | $2.7 \pm 0.4$ | $4.2 \pm 0.8$ |
| $R^{2,d}$ | 0.999 | 0.995 | 0.990 |
| $t$[e] (min) | > 0 | > 0 | > 0 |
| $k$[f]$\times 10^{-2}$ (mg COD/g $OD_T$) | $2.7 \pm 0.2$ | $3.1 \pm 0.2$ | $3.3 \pm 0.2$ |
| $R^{2,d}$ | 0.997 | 0.997 | 0.999 |
| $OD_T$[e] (g $O_3$/L) | > 0 | > 0 | > 0 |

[a] Experimental conditions: $t$ = 180 min; leachate initial pH = 9.0; $Q_g$ = 0.1 L/min; $C_{O_3,I\text{-}g}$ = 180 mg $O_3$/L; $V_L$ = 1.0 L, for BC system, and $V_L$ = 1.5 L, for FluHelik/BC system. [b] Inlet ($OD_I$) and transferred ($OD_T$) ozone dose per litre of leachate. [c] Pseudo-first-order rate constant for DOC and COD degradation in terms of reaction time. [d] Coefficient of determination. [e] Value or interval of time ($t$, min) or transferred $O_3$ dose ($OD_T$), from which the kinetic parameters were calculated. [f] DOC and COD degradation reaction rates, expressed in terms of the transferred ozone dose ($OD_T$), whose values correspond to the slopes of Figure 8.4-a.2) and -b.2), respectively.

### 8.3.3 Ozone-based AOPs

#### 8.3.3.1 Organic matter removal

Ozone-based AOPs ($O_3$/$H_2O_2$, $O_3$/UVC and $O_3$/UVC/$H_2O_2$) were evaluated using the FluHelik/BC-Venturi setup. When compared to $O_3$-only, the addition of 500 mg/L of $H_2O_2$ enhanced the oxidation reaction rate, particularly in terms of mineralization (Figure 8.6-a and -b). Considering the pseudo-first-order rate constants over time (displayed in Table **8.5**), the combination of $O_3$ with $H_2O_2$ led to a synergistic effect of 49% and 10%, for DOC and COD removals, respectively. In the presence of $H_2O_2$ (process also known as peroxonation) the generation of $^{\bullet}$OH is accelerated, since

H2O2 acts both as an initiating and promoter agent of the ozone decomposition reaction chain (Equations 3.25 to 3.27, section 3.1.6.2 of Chapter 3) [26]. With more $^{\bullet}$OH available to react, the indirect oxidation reaction pathway is expected to predominate, thus increasing the treatment efficiency. It should be noted that in the presence of H2O2 (for $0 < t$ (min) $< 120$, Figure 8.6-d) there was virtually no ozone loss ($C_{O3,g} < 0.1$ mg/L, Figure 8.6-b), which contributed to a higher $OD_T$ at the final of the treatment time. Also, the pH profile (Figure 8.6-e) showed a slower decay rate, with pH $> 6$ while H2O2 was present in the reaction medium. Together, these features suggest that: (i) in the presence of H2O2, the oxidative reactions occurred preferentially by $^{\bullet}$OH attack and the O3 oxidation reactions were hindered; and (ii) after H2O2 consumption, the remaining organic matter had low affinity for the ozone direct oxidation.
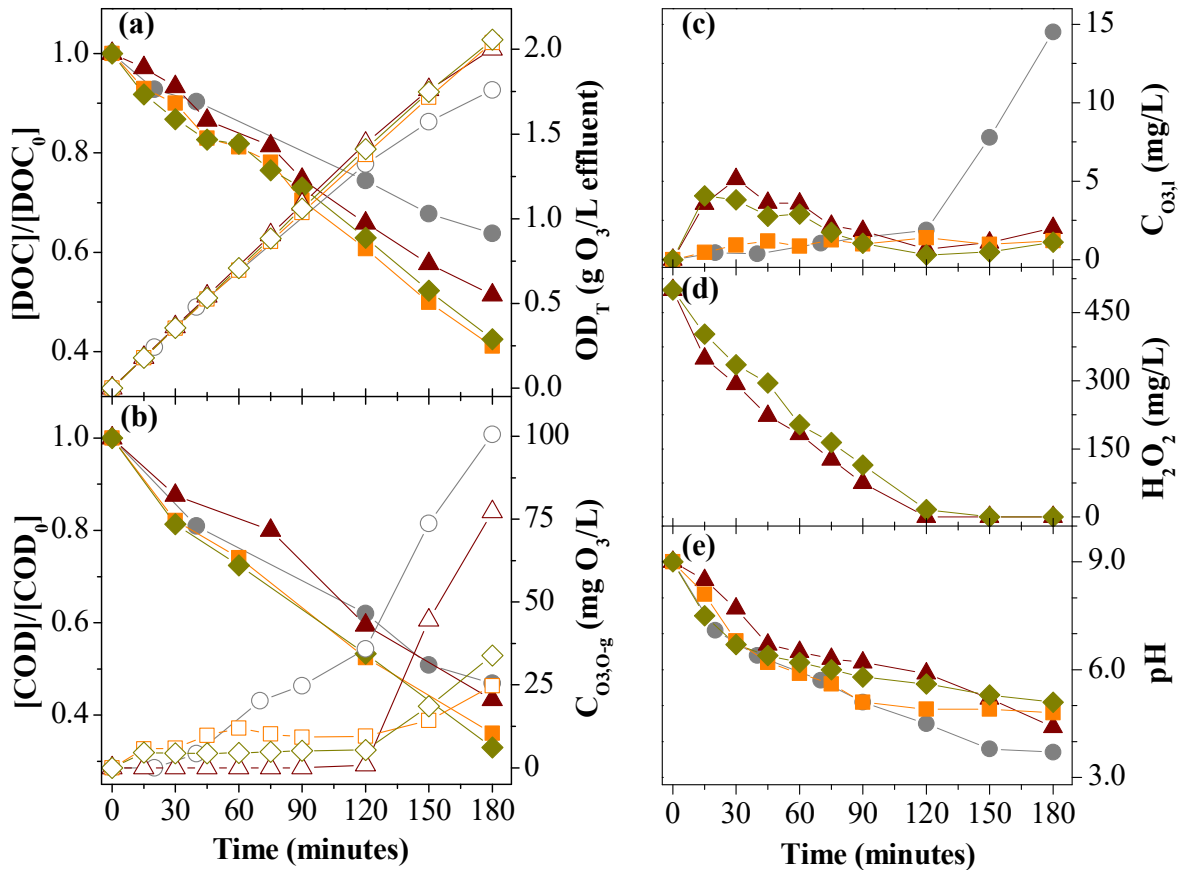


**Figure 8.6** – Evolution of the (a) DOC removal and $OD_T$, (b) COD removal and $C_{O3,O-g}$, (c) dissolved ozone concentration ($C_{O3,l}$), (d) H2O2 concentration and (e) pH, as a function of treatment time, for the experiments: (●,○) O3-only; (▲,△) O3/H2O2; (■,□) O3/UVC; and (◆,◇) O3/UVC/H2O2; (closed symbols) left y axis and (open symbols) right y axis.

**Table 8.5** – Main results and kinetic parameters, for DOC and COD degradation, of the ozone-based AOPs experiments.

| Parameters | Ozone-driven process[a] | | | |
|---|---|---|---|---|
| | $O_3$ | $O_3/H_2O_2$ | $O_3/UVC$ | $O_3/UVC/H_2O_2$ |
| $OD_I$[b] (g $O_3$/L) | 2.2 | 2.2 | 2.2 | 2.2 |
| $OD_T$[b] (g $O_3$/L) | 1.8 | 2.0 | 2.0 | 2.1 |
| DOC removal (%) | 36.2 | 48.6 | 58.4 | 57.5 |
| COD removal (%) | 53.1 | 56.6 | 66.2 | 67.1 |
| *DOC Degradation Kinetics* | | | | |
| $k$[c]$\times 10^3$ (min$^{-1}$) | $2.5 \pm 0.2$ | $3.9 \pm 0.3$ | $4.9 \pm 0.6$ | $4.6 \pm 0.4$ |
| $R^2$[d] | 0.996 | 0.993 | 0.990 | 0.995 |
| $t$[e] (min) | $> 0$ | $> 15$ | $> 0$ | $> 0$ |
| $k$[f]$\times 10^{-1}$ (mg DOC/g $OD_T$) | $8.1 \pm 0.5$ | $9.1 \pm 0.4$ | $12.0 \pm 0.5$ | $10.9 \pm 0.3$ |
| $R^2$[d] | 0.997 | 0.997 | 0.996 | 0.999 |
| $OD_T$[e] (g $O_3$/L) | $> 0$ | $> 0$ | $> 0$ | $> 0$ |
| *COD Degradation Kinetics* | | | | |
| $k$[c]$\times 10^3$ (min$^{-1}$) | $4.2 \pm 0.8$ | $4.6 \pm 0.6$ | $6 \pm 1$ | $6 \pm 1$ |
| $R^2$[d] | 0.990 | 0.998 | 0.995 | 0.997 |
| $t$[e] (min) | $> 0$ | $> 0$ | $> 0$ | $> 0$ |
| $k$[f]$\times 10^{-2}$ (mg COD/g $OD_T$) | $3.3 \pm 0.2$ | $2.9 \pm 0.2$ | $3.8 \pm 0.3$ | $3.6 \pm 0.3$ |
| $R^2$[d] | 0.999 | 0.999 | 0.997 | 0.997 |
| $OD_T$[e] (g $O_3$/L) | $> 0$ | $> 0$ | $> 0$ | $> 0$ |

[a] Experimental conditions: FluHelik/BC-Venturi system, $t$ = 180 min; leachate initial pH = 9.0; $V_L$ = 1.5 L, $Q_g$ = 0.1 L/min; $C_{O_3,l-g}$ = 180 mg $O_3$/L. [b] Inlet ($OD_I$) and transferred ($OD_T$) ozone dose per litre of leachate. [c] Pseudo-first-order rate constant for DOC and COD degradation in terms of reaction time. [d] Coefficient of determination. [e] Value or interval of time ($t$, min) or transferred $O_3$ dose ($OD_T$), from which the kinetic parameters were calculated. [f] DOC and COD degradation reaction rates, expressed in terms of the transferred ozone dose ($OD_T$), whose values correspond to the slopes of Figure 8.7.

The combination of $O_3$ with UVC radiation ($O_3$/UVC) showed the best performance, boosting DOC and COD removals (Table 8.**5**). Comparing with $O_3$-only and $O_3/H_2O_2$ tests, respectively, the pseudo-first-order rate constant ($k$, min$^{-1}$) for $O_3$/UVC increased 2.0 and 1.3-times, for DOC abatement, and 1.4 and 1.3-times, for COD removal. Therefore, the synergy obtained by combining $O_3$ and UVC was of 86% and 43%, respectively, for DOC and COD removals (Table 8.**5**). Beyond that, for the same amount of $OD_T$, the $O_3$/UVC process was able to remove more 48% and 32% of DOC, and 15% and 31% of COD, than $O_3$ and $O_3/H_2O_2$, respectively. It is known that the photodecomposition of ozone by UVC light increases the generation of HO$^\bullet$ and can also form $H_2O_2$ [29], which can further contribute to HO$^\bullet$ production by UVC photolysis (Equations 3.28 and 3.29, section 3.1.6.2 of Chapter 3). Once again, the indirect oxidation reactions are expected to predominate for the $O_3$/UVC process. Regarding the ozone concentration in the off-gas for $O_3$/UVC

system (Figure 8.6-b), it was possible to observe: (i) considerably lower values for $60 < t$ (min) $< 180$ than for $O_3$-only; and (ii) higher concentrations for $0 < t$ (min) $< 120$ than for $O_3/H_2O_2$, but much lower from $t = 120$ min until the end of the test. In terms of dissolved ozone (Figure 8.6-c), the $O_3$/UVC test allowed low concentrations during the entire treatment time, in contrast to: (i) $O_3$-only, which led to a significant increase over the last hour of the test; and (ii) $O_3/H_2O_2$ with higher values for the period $0 < t$ (min) $< 120$. The pH decay profile was similar to the $O_3$-only test until 90 min of treatment and, from this point on, remained without significant changes until de end. These results not only suggest a more effective use of the ozone supplied during the entire treatment time, but also imply the simultaneous occurrence of both direct and indirect oxidation pathways. Moreover, the FluHelik photoreactor design may have also positively contributed to the high performance of $O_3$/UVC process, since the helical motion of the fluid around the UVC lamp, enables a longer contact time between UVC photons and $O_3$ molecules and an homogeneous UV radiation distribution [28]. Also, the FluHelik photoreactor has already given proofs of high performance, including at full-scale, when applied to low transmissibility effluents, such as leachates (Chapter 6).
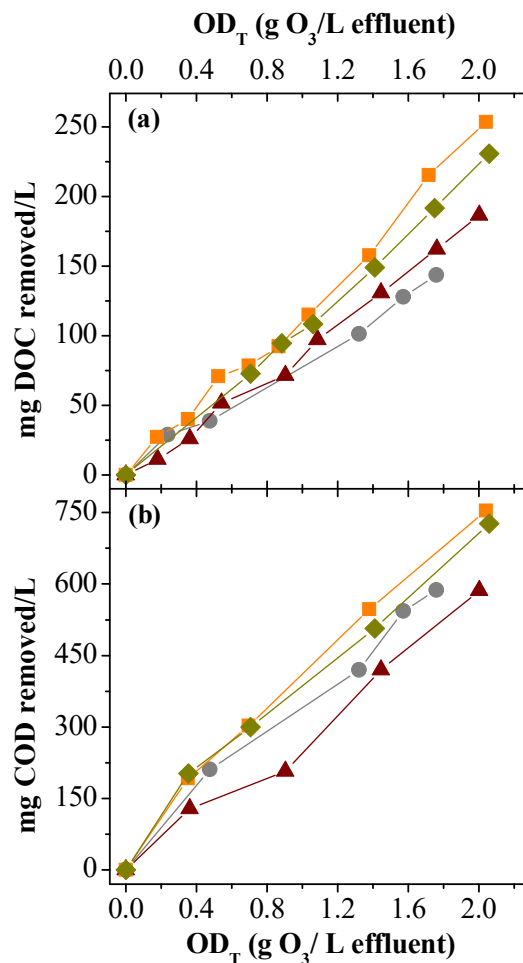


**Figure 8.7** – Representation of the amount of (a) DOC and (b) COD removed as a function of the transferred ozone dose ($OD_T$), for the experiments: (●) $O_3$-only; (▲) $O_3/H_2O_2$; (■) $O_3$/UVC; and (◆) $O_3$/UVC/$H_2O_2$.

For the $O_3$/UVC/$H_2O_2$ test, the presence of $H_2O_2$ did not lead to any improvement, in terms of DOC and COD removal over time, when compared to $O_3$/UVC (Table 8.5). Moreover, a slight decrease of efficiency over ozone consumption for DOC and COD degradation occurred (9% and 6%, respectively). These features may indicate $HO^\bullet$ scavenging effects due to eventual excess of peroxide. For the $O_3$/UVC/$H_2O_2$ system, at alkaline conditions, the $HO^\bullet$ can be generated by: (i) decomposition of $O_3$ by direct reaction with $HO^-$; (ii) decomposition of $O_3$ by direct reaction with $H_2O_2$ (either added or formed); (iii) photodecomposition of $O_3$ by UVC photons; and (iv) photolysis of $H_2O_2$ (either added or formed) by UVC photons. Interestingly, the ozone concentration profile in the off-gas was very similar to $O_3$/UVC (Figure 8.6-b), while for the dissolved ozone it was alike $O_3$/$H_2O_2$ test (Figure 8.6-c). The evolution profile for $H_2O_2$ concentration was also similar to that obtained in the $O_3$/$H_2O_2$ test (Figure 8.6-d). The pH presented a significant drop during the first hour of reaction, similar to the $O_3$-only and $O_3$/UVC tests, and from that point on the pH slowly decreased until the end of the experiment. In this case, the synergistic effect amounted to 67% and 45%, for DOC and COD removal, respectively.

Table 8.6 compares the treatment efficiency of ozone-driven processes applied to pre-treated leachate. The above-mentioned results show that, the treatment efficiency of ozone-driven processes is highly dependent on many factors, such as experimental conditions, system setup and landfill leachate characteristics. One can concluded that in general the ozonation setup used in this work allowed higher COD and DOC removals using lower $OD_T$ amounts (allows for higher ozone utilization rates).

**Table 8.6** – Comparison between results reported for $O_3$-driven processes applied to pre-treated leachates.

| Pre-treatment and characterization | System setup / Operating conditions | Main Results | | | Reference |
|---|---|---|---|---|---|
| | | $OD_T$ (g $O_3$/L) | COD (%) | DOC (%) | |
| Anaerobic/aerated ponds and chemical precipitation<br><br>pH: 3.5<br>COD: 743 mg/L<br>TOC: 284 mg/L | Acrylic column reactor with porous diffuser<br>Leachate: pH = 9; $V_L$ = 1.0 L<br>$O_3$-only process: $t$ = 60 min; $Q_g$ = 0.83 L/min; $C_{O3,l\text{-}g}$ = 112 mg/L | 4.9 | 30 | 21 | Cortez, et al. [4] |
| | $O_3$/$H_2O_2$ process:<br>Same conditions, except: $H_2O_2$ = 200 mg/L | 5.2 | 47 | 38 | |
| | Same conditions, except: $H_2O_2$ = 400 mg/L | 5.3 | 57 | 50 | |
| | Same conditions, except: $H_2O_2$ = 600 mg/L | 5.4 | 63 | 53 | |
| Biologically treated<br>pH: 8.2-8.5<br>COD: 1392 mg/L | Batch reactor with diffusion plate<br>Leachate: pH = 10; $V_L$ = 10 L<br>$O_3$-only process: $t$ = 60 min; $Q_g$ = 1 L/min; $C_{O3,l\text{-}g}$ = 80 - 90 mg/L | 0.27 | 16 | - | Chys, et al. [23] |
| Permeate of reverse osmosis<br> pH: 7.1<br>COD: 1880 mg/L | Stirred reactor with two porous diffusers<br>Leachate: pH = 9; $V_L$ = 0.5 L<br>$O_3$-only process: $t$ = 180 min; $Q_g$ = 0.5 L/min; $OD$ = 10 mg $O_3$/min | - | 33 | - | Amaral-Silva, et al. [7] |
| | Same conditions, except: $OD$ = 15 mg $O_3$/min | - | 40 | - | |
| | Same conditions, except: $OD$ = 20 mg $O_3$/min | - | 43 | - | |
| | $O_3$/$H_2O_2$ process:<br>Same conditions, except: $OD$ = 10 mg $O_3$/min and $H_2O_2$ = 2, 3 or 4 g/L | - | 43 | - | |
| Biological nitrification and coagulation with iron salts<br><br>pH = 3.7<br>DOC = 395 mg/L<br>COD = 1073 mg/L | Bubble column reactor with porous diffuser<br>Leachate: pH = 9; $V_L$ = 1.0 L<br>$O_3$-only process: $t$ = 180 min; $Q_g$ = 0.1 L/min; $C_{O3,l\text{-}g}$ = 180 mg/L | 1.9 | 48 | 38 | This work |
| | FluHelik in series with bubble column reactor and Venturi injector<br>Same conditions, except: $V_L$ = 1.5 L | 1.8 | 53 | 36 | |
| | $O_3$/$H_2O_2$ process:<br>Same conditions, except: $H_2O_2$ = 500 mg/L | 2.0 | 57 | 49 | |
| | $O_3$/UVC process:<br>Same conditions, except: UVC = 6 W | 2.0 | 66 | 58 | |
| | $O_3$/UVC/$H_2O_2$ process:<br>Same conditions, except: $H_2O_2$ = 500 mg/L and UVC = 6 W | 2.1 | 67 | 58 | |

### 8.3.3.2 Biodegradability

Change in biodegradability is one of the indicators that can be considered to evaluate the efficacy of ozone-driven processes [22]. In this sense, the leachate biodegradability was evaluated by means of the Zahn-Wellens test, before and after the application of the different ozone-driven treatments. In this screening test, a sample is considered biodegradable if the organic carbon content decreases by 70% after 28 days [30, 31]. Before ozone-driven treatment the leachate biodegradability was of 17% and afterward, according to the mineralization level obtained, it increased as follows (Figure 8.8-a): $O_3/H_2O_2$ (79%) $\approx$ $O_3$-only (81%) < $O_3/H_2O_2/UVC$ (85%) < $O_3/UVC$ (91%). Therefore, all the ozone-driven treatments were able to yield a treated leachate classified as biodegradable. However, having in mind the COD legal compliance to direct discharge into water bodies and on land (Portuguese Decree-Law no. 236/98 [32]), the leachate sample treated by $O_3/H_2O_2$ process did not reach a COD value below 150 mg/L, at the end of the biodegradability test (Figure 8.8-b). In turn, the leachate treated by $O_3/UVC$ process presented by far the lowest COD value at the end of the Zahn-Wellens test, suggesting that a shorter treatment time (i.e. < 3 h) could also be suitable to ensure legal compliance as regards this parameter. Taking these results, while $O_3/UVC$ treatment was the best (higher mineralization and lower COD), the $O_3$-only oxidized leachate also reached the COD discharge limit after the subsequent biological oxidation. These results also highlighted the differences between the mechanisms and oxidation pathways of the ozone-driven processes and insinuated that, in this case, there may be some advantages for ozone selective attack.
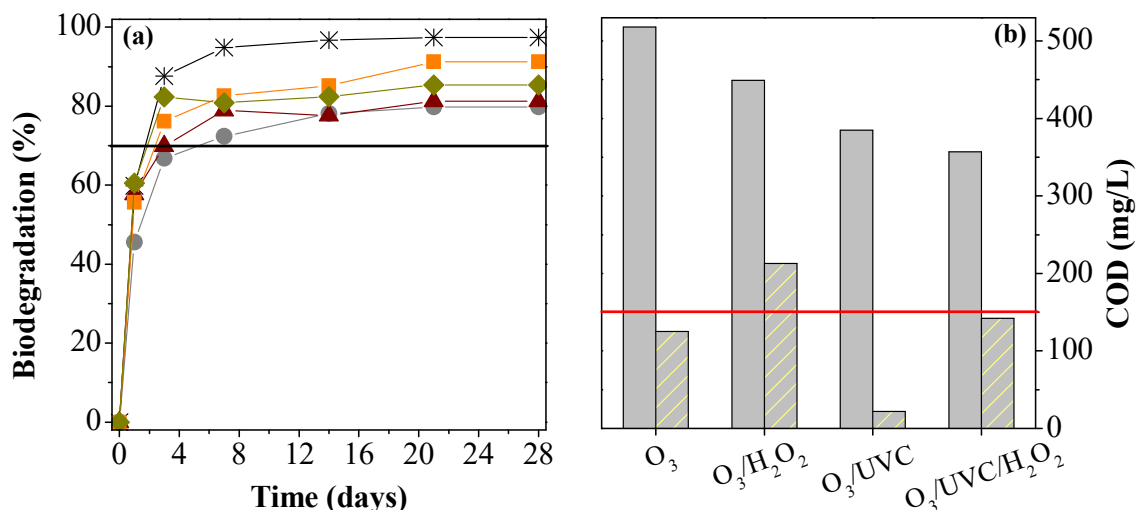


**Figure 8.8** – Biodegradability test results considering (a) the mineralization level during the Zahn Wellens test for the (✳) reference compound (glucose) and leachate samples after treatment with: (●) $O_3$-only; (▲) $O_3/H_2O_2$; (■) $O_3/UVC$; and (◆) $O_3/UVC/H_2O_2$; and (b) (▭) initial and (▨) final COD.

### 8.3.3.3 Organic matter characterization parameters

To better understand the organic matter oxidation mechanism using the different ozone-driven processes, a comparative analysis of the UV-Vis spectra was made. The absorbance in the UV-Vis range is affected by unsaturated bonds, aromatic structure and complexity of the dissolved organic matter (DOM) in the effluent [22] Before ozonation treatment, the leachate exhibited a strong absorbance in the UV region and a relative low absorption in the visible region (Figure 8.9), thus revealing a high aromaticity degree of the organic compounds. In this case, and considering that the raw leachate was pre-treated (by biological nitrification and coagulation), it is expected that the DOM content of the leachate will be mostly composed by fulvic acids, since the humic acids were precipitated and removed in the coagulation step.

Regarding the evolution of the UV-Vis spectra during the tests, dissimilarities between the different ozone-driven processes can be observed. All treatments led to a decrease of absorbance values in the UV range (Figure 8.9-a). However, while for the $O_3$-only and $O_3$/UV tests, the decrease for $t = 30$ min was quite similar, for the treatments with $H_2O_2$ addition (especially for $O_3$/$H_2O_2$ test) this decrease was by far more accentuated. Ozone has a preferential affinity toward the organic matter moieties absorbing at wavelengths within the range of 260-280 nm [23] and the rapid drop of UV absorbance, at the beginning of the treatments with $H_2O_2$, may have impaired the $O_3$ attack (with consequent high concentrations of dissolved ozone, as discussed in section 9.3.3.1). In the visible range (Figure 8.9-b), the $O_3$-only treatment led to two major decreases of absorbance, at $t = 30$ min and 60 min, and afterward, low absorbance values were maintained, with minor changes, until the end. This agrees with the high affinity of ozone to chromophore groups in the organic matter, which is consistent with the colour removal results at acidic conditions. For the $O_3$/UVC test (Figure 8.9-b.3), a significant decrease of the absorbance after 30 min of reaction was also observed, but then it only gradually decreased until the end of the treatment (similarly to the UV range). In turn, for the ozone-driven processes with $H_2O_2$ addition (Figure 8.9-b.2 and -b.4), after an initial decrease of the absorbance, large oscillations along the treatment were verified. This might indicate that some transformation products absorb radiation in this range of wavelengths, contrary to $O_3$-only and $O_3$/UVC processes.
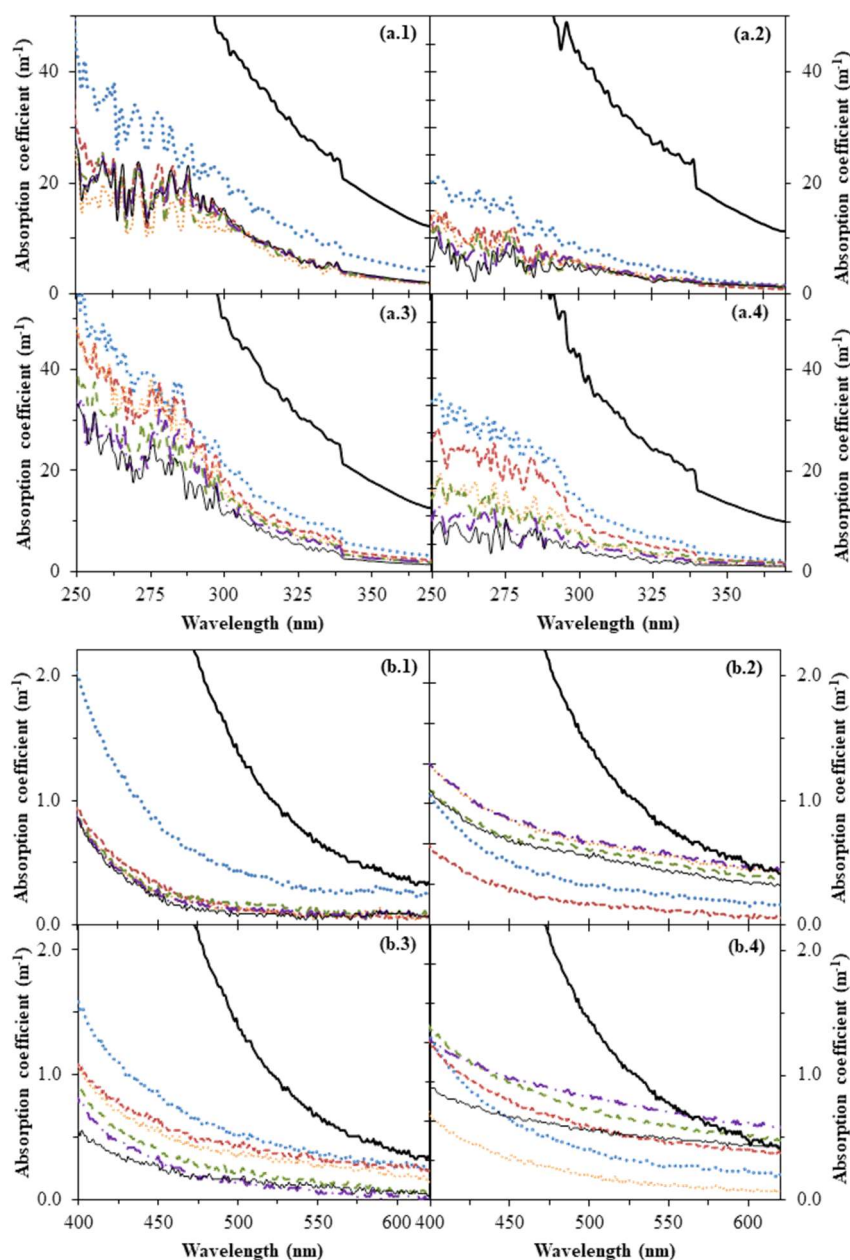
**Figure 8.9** – Evolution of the UV-Vis spectrum for (a) 250-370 nm range and (b) 400-600 nm range, during the treatment of leachate with: (.1) $O_3$-only; (.2) $O_3/H_2O_2$; (.3) $O_3/UVC$; and (.4) $O_3/UVC/H_2O_2$; for treatment times of (——) 0 min; (••••) 30 min; (— —) 60 min; (·····) 90 min; (— —) 120 min; (— · —) 150 min; and (——) 180 min.

To further characterize the effect of the different ozone-driven processes in the oxidation of the organic matter, the following parameters were also determined: (i) mean oxidation state (*MOS*), calculated according to Vogel*, et al.* [33]; ii) specific ultraviolet absorbance at 254 nm (*SUVA$_{254}$*) [34-36]; and (iii) ratio of UV absorbance at 250 to 365 nm (*Abs$_{250}$/Abs$_{365}$*) [34, 35, 37]. These parameters are useful to characterize the DOM content of landfill leachates [24], being correlated to the presence of oxygen containing functional groups (*MOS*), aromatic carbon content (*SUVA$_{254}$*)

and degree of humification or molecular weight ($Abs_{250}/Abs_{365}$). The *MOS* value for the leachate before the ozonation treatment was slightly negative or zero (Table 8.7). The more negative the MOS, the higher the expected content for polycyclic aromatics or humic substances [38]. In turn, the more positive, the higher the presence of oxygen containing functional groups. The increase of hydroxyl groups have been reported to increase after ozone oxidation, due to the substitution of functional groups of the organic intermediates related with the electrophilic reaction by ozone [8]. From all the processes applied, the $O_3/H_2O_2$ combination showed the lower *MOS* value at the end of the treatment. The initial leachate also presented a $SUVA_{254}$ value above 2 L/mg/m, indicating a predominantly aromatic organic structure. At the end of the ozone-driven treatments, $SUVA_{254}$ decreased below 1 L/mg/m, except for the test using $O_3/H_2O_2$. The absorbance ratio $Abs_{250}/Abs_{365}$ greatly increased for the leachate after treatment with $O_3$-only and $O_3/UVC$, contrary to the treatments with peroxide addition. This ratio has been shown to be inversely correlated with aromaticity and molecular weight for various water samples [34], including water humic substances [37]. This means that the initial compounds were transformed into compounds with a lower fraction of aromatic functional groups, which can be related to a greater bioavailability [39].

**Table 8.7** – Evolution of parameters for characterization of the organic matter during the different ozone-driven experiments.

| Parameters | Time (min) | Ozone-driven process[a] | | | |
|---|---|---|---|---|---|
| | | $O_3$ | $O_3/H_2O_2$ | $O_3/UVC$ | $O_3/UVC/H_2O_2$ |
| **MOS[b]** | 0 | -0.1 | 0.0 | 0.0 | 0.0 |
| | 30 | 0.0 | 0.2 | 0.4 | 0.2 |
| | 60 | 0.2 | 0.0 | 0.5 | 0.4 |
| | 120 | 0.2 | 0.3 | 0.8 | 0.6 |
| | 180 | 0.9 | 0.6 | 0.8 | 0.9 |
| **$SUVA_{254}$[b]** | 0 | 2.2 | 2.3 | 2.3 | 2.2 |
| **(L/mg/m)** | 30 | 1.1 | 1.4 | 1.1 | 1.7 |
| | 60 | 0.7 | 1.4 | 0.8 | 1.4 |
| | 90 | 0.5 | 1.6 | 0.9 | 1.1 |
| | 120 | 0.7 | 1.4 | 0.9 | 1.2 |
| | 150 | 0.8 | 1.4 | 0.8 | 0.9 |
| | 180 | 0.8 | 1.4 | 0.9 | 0.8 |
| **$Abs_{250}/Abs_{365}$** | 0 | 6.9 | 7.0 | 7.3 | 7.1 |
| | 30 | 10.2 | 11.5 | 17.1 | 13.9 |
| | 60 | 14.3 | 14.0 | 19.7 | 13.3 |
| | 90 | 12.1 | 8.1 | 24.5 | 12.8 |
| | 120 | 11.6 | 8.3 | 20.8 | 7.8 |
| | 150 | 11.8 | 8.3 | 16.5 | 6.2 |
| | 180 | 11.9 | 4.3 | 22.8 | 5.8 |

[a] Experimental conditions: FluHelik/BC-Venturi system, $t = 180$ min; leachate initial pH = 9.0; $V_L = 1.5$ L, $Q_g = 0.1$ L/min; $C_{O_3,I} = 180$ mg $O_3$/L. [b] MOS = 4 - 1.5 (COD/DOC) [33]; $SUVA_{254}$ = $Abs_{254}$/DOC [36].

### 8.3.4 Treatment costs evaluation

To assess the feasibility of the application of the ozone-driven treatments, the operating costs were determined for each system setup and oxidation process tested. The treatment costs were calculated taking into account the experimental conditions and data obtained, namely: (i) gas flow rate and ozone concentration ($Q_g$ = 0.1 NL/min; $C_{O3,I}$ = 180 mg $O_3$/L); (ii) volume of leachate treated ($V_L$ = 1.0 L, for BC-alone system and $V_L$ = 1.5 L, for FH/BC-D and -V systems); and (iii) time required to achieve 60% of COD reduction (stipulated as the minimum required to obtain a biodegradable leachate able to reach a final COD < 150 mg/L). The following energy and reagents prices were considered: (i) 0.1276 €/kWh, energy market price in Portugal for industrial applications; (ii) 15 kWh/kg $O_3$, for ozone energy consumption; (iii) 6 W for UVC lamp; (iv) 0.08 €/m$^3$ for $O_2$; (v) 0.375 €/kg for $H_2O_2$ 50% (w/v); and (vi) 0.16 €/kg for NaOH 30% (w/w).

In respect to the different setups, for the treatment of leachate using $O_3$-only process, the BC-alone system presented the highest cost (Table 8.8). When compared to BC-alone, cost reduction was only slightly lower (11%) for the FluHelik/BC-Diffuser system (eventually due to some positive effect of the hydrodynamic regime induced by the FluHelik reactor), while a very significant cost-saving of 41% was provided by the FluHelik/BC-Venturi. This highlights the importance of system design setup when aiming the application at larger scale of ozone-driven processes. Regarding the different ozone-driven oxidation processes, it is expected that the addition of components to the process ($H_2O_2$ and/or UVC) will lead to increased overall operational costs. However, this foreseeable cost increase was virtually not reflected for the treatments combining $O_3$ with $H_2O_2$ and/or UVC (only $O_3$/$H_2O_2$ treatment presented a slight cost increase). The higher oxidation efficiency demonstrated by those processes, when compared to $O_3$-only (thus requiring shorter treatment time to achieve the same oxidation level), outweighs the expected additional costs. In fact, for $O_3$/UVC process the treatment costs decreased by 10% (comparing with $O_3$-only using the same system) and stands out as the most cost-effective approach to treat leachate.

**Table 8.8 –** Cost analysis for the different ozone-driven processes applied to the leachate treatment.

| Ozone-driven process | System setup | Reagents (€/m$^3$) | Energy (€/m$^3$) | Total €/m$^3$ |
|---|---|---|---|---|
| $O_3$-only | BC-alone | 2.5 | 8.8 | 11.3 |
| $O_3$-only | FluHelik/BC-Diffuser | 2.3 | 7.8 | 10.1 |
| $O_3$-only | FluHelik/BC-Venturi | 1.6 | 5.0 | 6.6 |
| $O_3$/$H_2O_2$ | FluHelik/BC-Venturi | 2.2 | 4.6 | 6.8 |
| $O_3$/UVC | FluHelik/BC-Venturi | 1.2 | 4.8 | 6.0 |
| $O_3$/UVC/$H_2O_2$ | FluHelik/BC-Venturi | 1.8 | 4.8 | 6.6 |

## 8.4 Conclusions

In this work, a novel approach for boosting ozone-driven processes applied to mature landfill leachate treatment is presented based on the efficient and compact FluHelik photoreactor. The helical motion of the fluid around the light source, promotes an intense radial mixing, enhancing ozone dissolution and the contact between ozone molecules and UVC photons. The FluHelik/BC-Venturi was clearly the configuration that enhanced the ozone mass transfer from the gas phase to the liquid phase, resulting in lower amounts of $O_3$ in the off-gas, allowing for operational costs reduction of 41% when compared to the BC-alone.

The $O_3$/UVC oxidation process was the best among the ozone-based AOPs processes tested ($O_3$/$H_2O_2$, $O_3$/UVC and $O_3$/$H_2O_2$/UVC), leading to the highest synergistic effect (86% and 43%, for DOC and COD removals, respectively) and biodegradability enhancement (91%). Beyond that, the biodegradability tests have also emphasized that different oxidation mechanisms were involved, which was supported by UV-Vis spectra analysis and *MOS*, *SUVA$_{254}$* and *Abs$_{250}$/Abs$_{365}$* results. In this case, the addition of $H_2O_2$ was not beneficial in terms of biodegradability enhancement (especially for $O_3$/$H_2O_2$). At the end of 3-hour of reaction, all ozone-based treatments, except $O_3$/$H_2O_2$, ensured an effluent that, after further biological treatment, meets the discharge legal limit for COD (< 150 mg/L). To deal with this type of effluent, using a FluHelik/BC-Venturi system, the $O_3$/UVC oxidation process stands out as the most efficient and cost-effective, with an estimated operational cost of 6.0 €/m$^3$.

## 8.5 References

1. Poznyak, T., G.L. Bautista, I. Chaírez, R.I. Córdova, and L.E. Ríos, *Decomposition of toxic pollutants in landfill leachate by ozone after coagulation.* Journal of Hazardous Materials, 2008. **152**: p. 1108-1114.

2. Silva, T.F.C.V., M.E.F. Silva, A.C. Cunha-Queda, A. Fonseca, I. Saraiva, M.A. Sousa, C. Gonçalves, M.F. Alpendurada, R.A.R. Boaventura, and V.J.P. Vilar, *Multistage treatment system for raw leachate from sanitary landfill combining biological nitrification-denitrification/solar photo-Fenton/biological processes, at a scale close to industrial.* Water Research, 2013. **47**: p. 6167-6186.

3. Tizaoui, C., L. Bouselmi, L. Mansouri, and A. Ghrabi, *Landfill leachate treatment with ozone and ozone/hydrogen peroxide systems.* Journal of Hazardous Materials, 2007. **140**: p. 316-324.

4. Cortez, S., P. Teixeira, R. Oliveira, and M. Mota, *Ozonation as polishing treatment of mature landfill leachate.* Journal of Hazardous Materials, 2010. **182**(1-3): p. 730-734.

5. Chaturapruek, A., C. Visvanathan, and K.H. Ahn, *Ozonation of membrane biorector effluent for landfill leachate treatment.* Environmental Technology, 2005. **26**: p. 65-73.

6. Asaithambi, P., B. Sajjadi, A.R.A. Aziz, and W.M.A.B.W. Daud, Ozone ($O_3$) and sono (US) based advanced oxidation processes for the removal of color, COD and determination of electrical energy from landfill leachate. Separation and Purification Technology, 2017. **172**: p. 442-449.

7. Amaral-Silva, N., R.C. Martins, S. Castro-Silva, and R.M. Quinta-Ferreira, *Ozonation and perozonation on the biodegradability improvement of a landfill leachate.* Journal of Environmental Chemical Engineering, 2016. **4**: p. 527-533.

8. Wu, J.J., C.-C. Wu, H.-W. Ma, and C.-C. Chang, *Treatment of landfill leachate by ozone-based advanced oxidation processes.* Chemosphere, 2004. **54**: p. 997-1003.

9. Eliasson, B., M. Hirth, and U. Kogelschatz, *Ozone synthesis from oxygen in dielectric barrier discharges.* Journal of Physics D: Applied Physics, 1987. **20**: p. 1421.

10. Gottschalk, C., J.A. Libra, and A. Saupe, *Ozonation of Water and Waste Water: A Practical Guide to Undestanding Ozone and Its Applications*. 2010, Germany: Wiley-VCH Verlag GmbH & Co. kGaA.

11. Zimmermann, S.G., M. Wittenwiler, J. Hollender, M. Krauss, C. Ort, H. Siegrist, and U. von Gunten, Kinetic assessment and modelling of an ozonation step for full-scale municipal wastewater treatment: micropollutant oxidation, by-product formation and disinfection. Water Research, 2011. **45**: p. 605-617.

12. Wang, Y., H. Zhang, L. Chen, S. Wang, and D. Zhang, *Ozonation combined with ultrasound for the degradation of tetracycline in a rectangular air-lift reactor.* Separation and Purification Technology, 2012. **84**: p. 138-146.

13. Farines, V., S. Baig, J. Albet, J. Molinier, and C. Legay, *Ozone transfer from gas to water in a co-current upflow packed bed reactor containing silica gel.* Chemical Engineering Journal, 2003. **91**: p. 67-73.

14. Qiu, Y., C.-H. Kuo, and M.E. Zappi, *Performance and simulation of ozone absorption and reactions in a sitterd-tank reactor.* Environmental Science & Technology, 2001. **35**: p. 209-215.

15. Gao, M.-T., M. Hirata, H. Takanashi, and T. Hano, *Ozone mass transfer in a new gas-liquid contactor-Karman contactor.* Separation and Purification Technology, 2005. **42**: p. 145-149.

16. Tizaoui, C. and Y. Zhang, *The modelling of ozone mass transfer in static mixers using Back Flow Cell model.* Chemical Engineering Journal, 2010. **162**: p. 557-564.

17. Rakness, K.L., G. Hunter, J. Lew, B. Mundy, and E.C. Wert, *Design considerations for cos-effective ozone mass transfer in sidestream systems.* Ozone: Science and Engineering, 2018. **40**(3-4): p. 159-172.

18. Shirke, A., S. Li, D. Ebeling, M.T. Carter, and J.R. Stetter, *Integrated ozone microractor technology for water treatment.* ECS Transactions, 2014. **58**: p. 11-20.

19. Wada, Y., M.A. Schmidt, and K.F. Jensen, *Flow distribution and ozonolysis in gas-liquid multichannel microreactors.* Industrial & Engineering Chemistry Research, 2006. **45**: p. 8036-8042.

20. Lucas, M.S., N.M. Reis, and G. Li Puma, Intensification of ozonation processes in a novel, compact, multi-orifice oscillatory baffled column. Chemical Engineering Journal, 2016. **296**: p. 335-339.

21. Ku, Y., Y.-J. Huang, H.-W. Chen, and W.-M. Hou, *Decomposition of acetone by hydrogen peroxide/ozone process in a rotating packed contactor.* Water Environmental Research, 2011. **83**(7): p. 588-593.

22. Chen, W., Z. Gu, P. Wen, and Q. Li, Degradation of refractory organic contaminants in membrane concentrates from landfill leachate by a combined coagulation-ozonation process. Chemosphere, 2019. **217**: p. 411-422.

23. Chys, M., V.A. Oloibiri, W.T.M. Audenaert, K. Demeestere, and S.W.H. Van Hulle, *Ozonation of biologically treated landfill leachate: Efficiency and insights in organic conversions.* Chemical Engineering Journal, 2015. **277**: p. 104-111.

24. Miklos, D.B., C. Remy, M. Jekel, K.G. Linden, J.E. Drewes, and U. Hübner, *Evaluation of advanced oxidation processes for water and wastewater treatment - a critical review.* Water Research, 2018. **139**: p. 118-131.

25. Chiang, Y.-P., Y.-Y. Liang, C.-N. Chang, and A.C. Chao, *Differentiating ozone direct and indirect reactions on decompositioon of humic substances.* Chemosphere, 2006. **65**(11): p. 2395-2400.

26. Gardoni, D., A. Vailati, and R. Canziani, *Decay of ozone in water: A review.* Ozone: Science and Engineering, 2012. **34**(4): p. 233-242.

27. Khuntia, S., M.K. Sinha, and B. Saini, *An approach to minimize the ozone loss in a series reactor: A case of peroxone process.* Journal of Environmental Chemical Engineering, 2018. **6**: p. 6916-6922.

28. Moreira, F.C., E. Bocos, A.G.F. Faria, J.B.L. Pereira, C.P. Fonte, R.J. Santos, J.C.B. Lopes, M.M. Dias, M.A. Sanromán, M. Pazos, R.A.R. Boaventura, and V.J.P. Vilar, *Selecting the best piping arrangement for scaling up an annular channel reactor: An experimental and computational fluid dynamics study.* Science of the Total Environment, 2019. **667**: p. 821-832.

29. Kusic, H., N. Koprivanac, and A.L. Bozic, Minimization of organic pollutant content in aqueous solutions by means of AOPs: UV- and ozone-based technologies. Chemical Engineering Journal, 2006. **123**(3): p. 127-137.

30. Pluciennik-Koropczuk, E. and S. Myszograj, *Zahn-Wellens test in industrial wastewater biodegradability assessment.* Civil and Environmental Engineering Reports, 2018. **28**(1): p. 77-86.

31. Silva, T.F.C.V., A. Fonseca, I. Saraiva, R.A.R. Boaventura, and V.J.P. Vilar, Biodegradability enhancement of a leachate after biological lagooning using a solar driven photo-Fenton reaction, and further combination with an activated sludge biological process, at pre-industrial scale Water Research, 2013. **47**: p. 3543-3557.

32. in *Decree-law no. 236/98, of 1$^{st}$ August*, P. Republic, Editor. 1998: Republic Diary - I Series - A.

33. Vogel, F., J. Harf, A. Hug, and P.R. von Rohr, The mean oxidation number of carbon (MOC) - A useful concept for describing oxidation processes. Water Research, 2000. **34**: p. 2689-2702.

34. Helms, J.R., A. Stubbins, J.D. Ritchie, E.C. Minor, D.J. Kieber, and K. Mopper, Absorption spectral slopes and slope ratios as indicators of molecular weight, source, and photobleaching of chromophoric dissolved organic matter. Limnology and Oceanography, 2008. **53**(3): p. 955-969.

35. Li, P. and J. Hur, Utilization of UV-Vis spectroscopy and related data analysis for dissolved organic matter (DOM) studies: A review. Critical Reviews in Environmental Science and Technology, 2017. **47**(6): p. 131-154.

36. Weishaar, J.L., G.R. Aiken, B.A. Bergamaschi, M.S. Fram, R. Fugii, and K. Mopper, Evaluation of specific ultraviolet absorbance as an indicator of the chemical composition and reactivity of dissolved organic carbon. Environmental Science & Technology, 2003. **37**: p. 4702-4708.

37. Peuravouri, J. and K. Pihlaja, Molecular size distribuition and spectroscopic properties of aquatic humic substances. Analytica Chimica Acta, 1997. **337**(2): p. 133-149.

38. Iskander, S.M., R. Zhao, A. Pathak, A. Gupta, A. Pruden, J.T. Novak, and Z. He, A review of landfill leachate induced ultraviolet quenching substances: Sources, characteristics, and treatment Water Research, 2018. **145**.

39. Gianguzza, A., E. Pelizzetti, and S. Sammartano, *Chemical processes in Marine Environments.* 2000: Springer.

# 9 Performance of ozone-driven processes for mature urban landfill leachate treatment under different pre-treatment scenarios

*In this last chapter, the performance of O₃ and O₃/UVC processes applied to landfill leachate after different pre-treatments was investigated. For bio-nitrified leachate (LN), mineralization was hindered since high amounts of ozone were consumed to oxidize nitrites to nitrates. In turn, the presence of carbonate/bicarbonate ions (alkalinity) in the bio-denitrified leachate (LD) inhibited the reaction rate due to the scavenging effect of •OH. For both bio-treated leachates, the O₃/UVC process led to a better performance than O₃, reaching a final COD of 205 and 167 mg/L, for LN and LD, respectively, after subsequent biological oxidation. Nonetheless, the estimated treatment cost for a treatment train combining Bio + O₃/UVC + Bio is not viable (> 30 €/m³). For the nitrified-coagulated leachate (LNC) and denitrified-coagulated leachate (LDC), although the differences in DOM composition revealed by fluorescence excitation-emission matrix, the amount of DOC and COD removed per gram of ozone was very similar. To reach COD < 150 mg/L (legal discharge limit) after a final biological process, the O₃ treatment applied to the LNC was the most cost-effective (5.7 €/m³). Nonetheless, a treatment train comprising: (i) a first biological stage for nitrification/denitrification (with addition of an external carbon source); (ii) coagulation with 300 mg Al³⁺/L and without pH adjustment; (iii) O₃/UVC advanced oxidation process, with transferred ozone dose of 2.1 g O₃/L and 12.2 kJ_{UVC}/L; and (iv) a final biological oxidation, allows to reach a final effluent able to simultaneously comply with the legal values for organic and nitrogen parameters, and not exceeding the discharge limits for other parameters affected by the addition of chemicals along the treatment train. Also, the treatment cost of this strategy was estimated as 8.9 €/m³, with the ozone-driven stage counting for 6.9 €/m³.*

## 9.1 Introduction

Previous work (Chapter 8), focused on the application of different ozone-driven processes for biologically nitrified and coagulated leachate treatment. The main findings of the research allowed to: (i) establish the best operational conditions and system setup; and (ii) demonstrate that the recalcitrant organic matter was successfully oxidized by $O_3$ and, in particular, by $O_3$/UVC (both treatments reached COD values < 150 mg/L, Portuguese legal limit for direct discharge (Table 2.6 of Chapter 2), at the end of a Zahn-Wellens biodegradability test). Despite the promising results for COD removal, the high nitrogen content (~ 0.56 g N/L) of the leachate was not addressed, although many countries present regulatory limits for both parameters (Table 2.5 of Chapter 2).

The usage of biological nitrification followed by coagulation with iron salts in acidic conditions, was proposed by Silva, *et al.* [1] as a preferential pre-treatment for mature landfill leachates when a photo-Fenton process is intended. This makes sense, as (i) biological nitrification leads to a leachate with very low alkalinity, decreasing acid requirements for the following selected physicochemical treatment stages, and (ii) PF is an iron catalysed reaction carried out at acidic pH (normally pH 2.8-3.0). So, by replacing the advanced photo-Fenton oxidation technique for an ozone-based process, it opens up the possibility of exploring different pre-treatments scenarios, not only more adequate to the ozonation process requirements (such as, basic pH conditions) but also able to comply with the legal discharge values for organic and nitrogen parameters.

The efficiency of a treatment train strategy for landfill leachate is usually assessed by measuring, at each stage of the treatment, chemical parameters such as dissolved organic carbon (DOC) and chemical oxygen demand (COD). However, these traditional parameters for measuring the organic components of leachate provide limited information about the nature of dissolved organic matter (DOM) and do not give a fingerprint of the different DOM components in the (treated) leachate [2]. Fluorescence spectroscopy is a simple, reagent-free, non-extractive and sensitive method with increasing reputation for DOM characterization [3]. It makes use of the fluorescent nature of DOM components with the added advantage of being able to distinguish between fluorophores absorbing at the same wavelengths [3]. By measuring fluorescence at several excitation (Ex) and emission (Em) wavelengths, a 3-dimensional excitation-emission matrix (3D-EEM) containing data about all the fluorophores is generated. So far, fluorescence EEM with peak identification methods have been used to characterize raw landfill leachate [4], to trace landfill leachate contamination of surface water [5] and ground water [6], to follow leachate treatment by coagulation-flocculation, activated carbon adsorption and ion exchange [2] and to track the changes in the nanofiltration membrane fouling potential after various pre-treatments [7].

In view of the above, the purpose of this work was to investigate the performance of $O_3$ and $O_3$/UVC processes applied to a pre-treated mature urban landfill leachate (with/without biological nitrogen removal and with/without coagulation, using Al or Fe salts). The efficiency of ozone-driven treatments was assessed by the removal of organic matter (in terms of DOC and COD) and colour, as well as the ability to enhance the effluent biodegradability (in view of a complete treatment train containing a subsequent and final biological oxidation). Moreover, this work aimed to examine the changes in the characteristics of organic matter in the leachate after different pre-treatment stages tested, before and after ozonation process, by means of fluorescence excitation-emission matrix spectroscopy. Finally, the treatment cost considering 6 treatment train scenarios was estimated.

## 9.2 Materials and methods

The mature urban leachate used in this work was pre-treated by: (i) biological nitrification (LN); (ii) biological nitrification/denitrification (LD); (iii) biological nitrification followed by coagulation (LNC); and (iv) biological nitrification/denitrification followed by coagulation (LDC). The main physicochemical characteristics of each pre-treated leachate are presented in Table 9.1.

Both nitrified leachates (LN and LNC) were collected at the full-scale facility (from Chapter 6) installed in a 20-year-old municipal landfill located in northern Portugal. LN was collected after the aerated biological treatment stage (nitrification), while LNC was collected at the end of the downstream coagulation stage (with $FeCl_3$ under acidic conditions, as described for Chapters 5 and 6).

To obtain the denitrified leachates (LD and LDC), part of the collected LN was placed in a biological reactor (10 L capacity) with biomass previously adapted, under anoxic conditions and mechanical agitation, at room temperature (22-25ºC), and with methanol as external carbon donor. After denitrification, part of LD was tested for coagulation with aluminium sulfate ($Al_2(SO_4)_3$), by means of *jar-test*, without pH adjustment.

All ozone-driven experiments were carried out by coupling a FluHelik photoreactor and bubble column reactor, using a Venturi injector at the inlet of the FluHelik, at the following operational conditions: leachate initial pH = 9.0, $[O_3]_{inlet}$ = 180 mg/L; $Q_{O_3}$ = 0.10 NL/min. For the experiments carried out with a bio-treated leachate (without coagulation stage), the treatment time was of 12 h and 10h, for tests using only $O_3$ and $O_3$/UVC, respectively; while for the bio-coagulated leachates, a treatment time of 3h was adopted for both ozone-driven processes.

All the chemicals used in this work, experimental units and respective procedures, as well as the analytical methods employed and calculations made, can be consulted, respectively, in sections 4.1, 4.3.4.2, 4.2 and 4.3.4.3 of Chapter 4.

**Table 9.1 –** Physicochemical characterization of the landfill leachate after different pre-treatment stages.

| Parameter | LN | LD | LNC | LDC | ELV |
|---|---|---|---|---|---|
| pH | 7.5 | 9.1 | 3.7 | 6.2 | 6.0 – 9.0 |
| DOC (mg/L) | 956 | 1149 | 430 | 574 | - |
| DIC (mg/L) | 89 | 464 | 7 | 143 | - |
| COD (mg/L) | 3479 | 3577 | 1174 | 1635 | 150 |
| $UV_{254}$ (cm$^{-1}$) | 27.1 | 24.9 | 6.8 | 4.1 | - |
| Colour[a] (Pt-Co) | 320 | 280 | 49 | 26 | Not visible[a] |
| $NH_4^+$ (mg N/L) | < 0.1 | < 0.1 | < 0.1 | < 0.1 | 8 |
| $NO_2^-$ (mg N/L) | 1034 | < 0.1 | < 0.1 | < 0.1 | - |
| $NO_3^-$ (mg N/L) | 19 | 14 | 523 | 12 | 10 |
| $Cl^-$ (mg/L) | 2723 | 2480 | 2639 | 2630 | - |
| $SO_4^{2-}$ (mg/L) | 247 | 319 | 1721 | 1903 | 2000 |
| Al (mg/L) | 1.8 | 2.0 | 2.2 | 2.4 | 10 |
| Cr (mg/L) | 1.5 | 1.2 | 0.7 | < 0.08 | 2.0 |
| Cu (mg/L) | < 0.01 | < 0.01 | 0.3 | 0.4 | 1.0 |
| Fe (mg/L) | 5.3 | 3.0 | 12.6 | 0.3 | 2.0 |
| Ni (mg/L) | n.d. | n.d. | < 0.25 | < 0.25 | 2.0 |
| Pb (mg/L) | < 0.25 | < 0.25 | < 0.25 | < 0.25 | 1.0 |
| Biodegradability (%) | 7 | 18 | 17 | 19 | - |

[a] Diluted 1:20.

## 9.3 Results and discussion

### 9.3.1 Bio-treated leachate samples

Observing the characteristics of the two bio-treated leachates (LN and LD, Table 9.1), the main differences were related to pH, inorganic carbon (DIC) and nitrogen content. This is related to the distinct biological metabolic processes involved in the nitrification and denitrification of the leachate. For biological nitrification (in this case partial nitrification, i.e. ammonium oxidation to nitrite), the autotrophic nitrifying bacteria consumed the inorganic carbon, thus reducing alkalinity and pH (theoretically, 7.14 mg of $CaCO_3$ are consumed per 1 mg of $NH_4^+$-N oxidized). In turn, biological denitrification led by heterotrophic bacteria recovered part of the inorganic carbon, raising alkalinity and pH (theoretically, each mg of $NO_3^-$-N reduced to $N_2$ causes an alkalinity increase of 3.57 mg $CaCO_3$). Consequently, LN effluent presents lower pH and DIC values, when compared to LD, and the nitrogen content was mainly in the form of nitrite ions. Since LD effluent resulted from denitrification of LN, both presented quite similar concentration values for chloride and sulfate ions, as for some selected heavy metals (Table 9.1). Nonetheless, LD effluent had slightly higher DOC and COD values, most likely some remnants of biodegradable organic matter from the addition of the external carbon donor. This was supported by the Zahn-Wellens biodegradability test results.

### 9.3.1.1 Efficiency of the ozone-driven processes

Taking the above, the effect of the LN and LD distinct features on the performance of $O_3$ and $O_3$/UVC treatment was assessed. A first glance at the results (Table 9.2), suggests that there were no significant differences between the efficiencies of the ozone-driven processes applied to LN and LD. For both bio-treated leachates, DOC and COD removals were very similar at the end of the ozonation treatment. Also, the combination of $O_3$/UVC further increased the organic matter oxidation, with LD presenting 10% less mineralization than LN. A closer look at the organic matter removal profiles (Figure 9.1 and Figure 9.2) reveals some particularities during the ozone-based treatments.

**Table 9.2 –** Main results and kinetic parameters, for DOC and COD degradation, of the $O_3$ and $O_3$/UVC processes applied to LN and LD.

| Parameters | $O_3$ | | $O_3$/UVC | |
|---|---|---|---|---|
| | LN | LD | LN | LD |
| $OD_I$[a] (g $O_3$/L) | 8.6 | 8.6 | 7.2 | 7.4 |
| $OD_T$[a] (g $O_3$/L) | 8.0 | 7.9 | 7.1 | 7.1 |
| DOC removal (%) | 50.5 | 49.3 | 73.2 | 62.9 |
| COD removal (%) | 64.8 | 68.7 | 79.4 | 82.9 |
| Colour removal (%) | 93.7 | 89.4 | 97.8 | 93.1 |
| Biodegradability (%) | 51 | 69 | 73 | 80 |
| *DOC Degradation Kinetics* | | | | |
| $k$[b]$\times 10^3$ (min$^{-1}$) | 2.0 ± 0.1 | 1.2 ± 0.1 | 4.7 ± 0.9 | 1.9 ± 0.2 |
| $R^{2,}$[c] | 0.997 | 0.995 | 0.990 | 0.994 |
| $t$[d] (min) | > 420 | > 240 | > 360 | > 120 |
| $k$[e]$\times 10^{-1}$ (mg DOC/g $OD_T$) | 12.0 ± 0.9 | 8.5 ± 0.5 | 19 ± 1 | 10.4 ± 0.7 |
| $R^{2,}$[c] | 0.997 | 0.997 | 0.997 | 0.994 |
| $OD_T$[d] (g $O_3$/L) | > 5.0 | > 2.9 | > 3.6 | > 0 |
| *COD Degradation Kinetics* | | | | |
| $k$[b]$\times 10^3$ (min$^{-1}$) | 1.7 ± 0.1 | 1.60 ± 0.08 | 2.7 ± 0.4 | 2.7 ± 0.2 |
| $R^{2,}$[c] | 0.991 | 0.994 | 0.994 | 0.995 |
| $t$[d] (min) | > 120 | > 0 | > 0 | > 0 |
| $k$[e]$\times 10^{-2}$ (mg COD/g $OD_T$) | 3.0 ± 0.2 | 4.0 ± 0.3    2.2 ± 0.2 | 3.7 ± 0.2 | 2.7 ± 0.1 |
| $R^{2,}$[c] | 0.994 | 0.997    0.994 | 0.998 | 0.998 |
| $OD_T$[d] (g $O_3$/L) | > 0 | < 3.6    > 3.6 | > 0 | > 1.4 |

[a] Inlet ($OD_I$) and transferred ($OD_T$) ozone dose per litre of leachate. [b] Pseudo-first-order rate constant for DOC and COD degradation in terms of reaction time. [c] Coefficient of determination. [d] Value or interval of time ($t$, min) or transferred ozone dose ($OD_T$), from which the kinetic parameters were calculated. [e] DOC and COD degradation reaction rates, expressed in terms of the transferred ozone dose ($OD_T$), whose values correspond to the slopes of Figure 9.1.
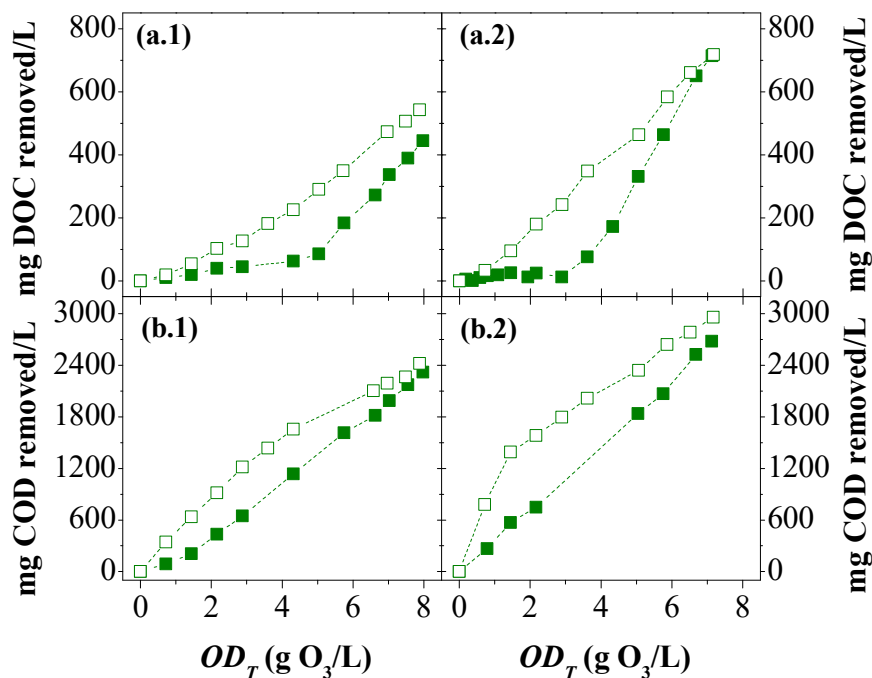


**Figure 9.1** – Representation of the amount of (a) DOC and (b) COD removed, as a function of the transferred ozone dose ($OD_T$), for (.1) $O_3$ and (.2) $O_3$/UVC treatments applied to the bio-treated leachates (■) LN and (□) LD.
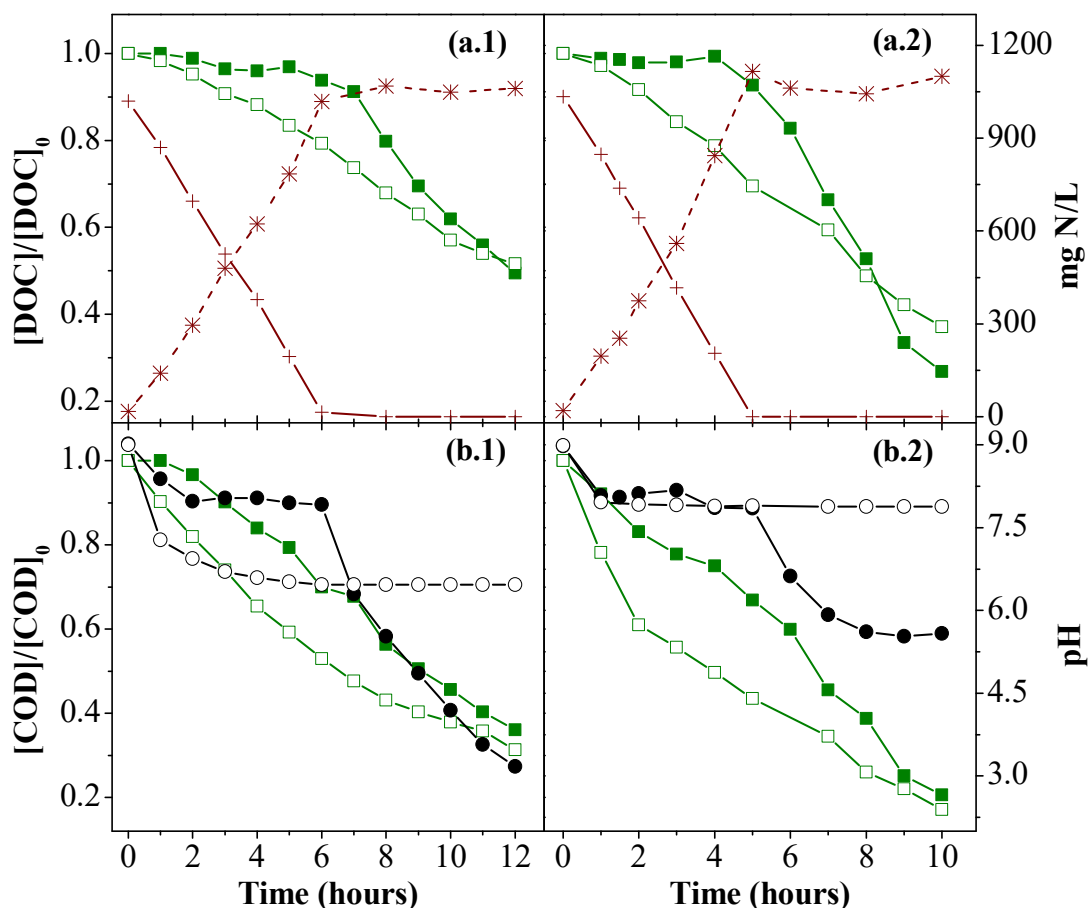
**Figure 9.2** – Evolution of the (a) DOC and (b) COD removals obtained for (.1) $O_3$ and (.2) $O_3$/UVC treatments applied to the bio-treated leachates (■) LN and (□) LD, including (×) nitrite and (✱) nitrate concentrations, for LN, and pH profile for (●) LN and (○) LD, as a function of treatment time.

For LN, there was an initial period up to about 7h, for $O_3$, and 5h, for $O_3$/UVC (corresponding to $OD_T$ of 5.0 and 3.6 g $O_3$/L, respectively), in which practically no mineralization was observed (Figure 9.2-a.1 and -a.2). This induction period coincided with the oxidation of nitrites to nitrates ($NO_2^- + O_3 \rightarrow NO_3^- + O_2$, $k = 1.8 \times 10^5$ M$^{-1}$ s$^{-1}$ [8], $k = 5.8 \times 10^5$ M$^{-1}$ s$^{-1}$ [9]) and did not appear to affect COD reduction. A clear linear relation was obtained between the $OD_T$ and the amount of nitrites oxidized (Figure 9.3), with an expected highest rate found for $O_3$/UVC treatment. This high ozone consumption hindered mineralization that started as soon as all the nitrite was converted to nitrate. Afterwards and until the end of the tests, the DOC reduction profile was followed by a significant drop in pH (down to pH 3.2 and 5.6, for $O_3$-only and $O_3$/UVC treatments, respectively, Figure 9.2-b.1 and -b.2). This acidification is associated with the oxidation of the leachate complex organic compounds into carboxylic acids and low weight organic acids, and with carbon dioxide and carbonic acids resulting from the mineralization of organic compounds (as observed and discussed in Chapter 8). The pH decay for LD was less pronounced due to its higher alkalinity

content, thus providing a pH buffer effect to this bio-effluent. Keeping in mind that, when applying $O_3$-only at pH < 6, the preferred oxidation mechanism will be the $O_3$ direct reaction, pseudo-first-order rate constants for DOC removal ($k$, min$^{-1}$) obtained for LN suggest a high affinity of ozone towards the bio-recalcitrant organic content of mature urban leachate.
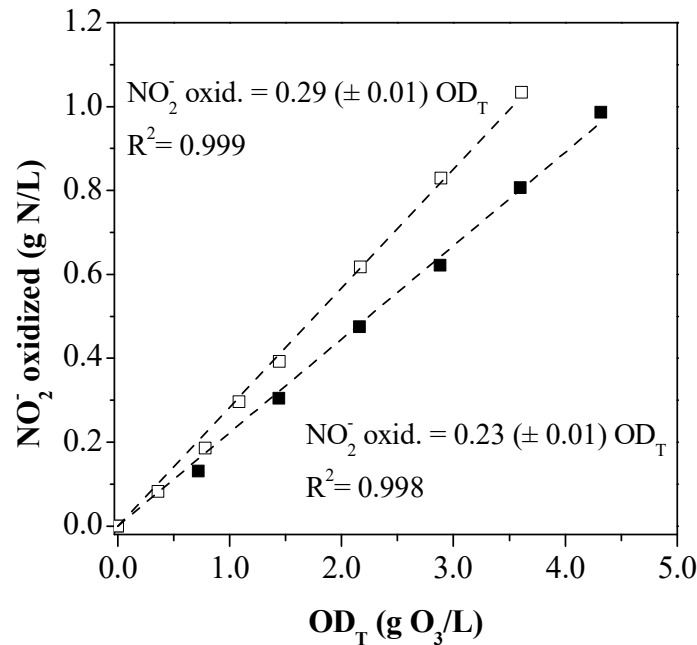


**Figure 9.3** – Relation between the amount of nitrite oxidized and the transferred ozone dose ($OD_T$) for the ozone-driven processes applied to LN: (■) $O_3$ and (□) $O_3$/UVC.

Concerning LD, although the DOC and COD removal was continuous throughout the tests, this was not reflected in an improvement when compared to the LN at the end of the trials. It would be expected that the buffer capacity of LD would contribute to a better performance of the ozonation processes. It is well known that at alkaline pH the ozone reaction pathway favours the production of $^{\bullet}$OH, boosting the oxidation reactions [10, 11]. So, observing the pH profiles (Figure 9.2-b.1 and -b.2) it is expected that hydroxyl radicals have predominate during the entire $O_3$ and $O_3$/UVC treatment (contrary to LN, as discussed above). On the other hand, it is also known that carbonate and bicarbonate ions may act as $^{\bullet}$OH scavengers, thus hindering the organic matter oxidation (Equations 3.27 and 3.28 of Chapter 3). In this case, this scavenging effect seems to have played a more important role than the neutral-basic pH that was maintained during the tests (Figure 9.2).

Ozone is highly recognized by its effectiveness in removing colour, with high affinity for chromophore groups [12, 13]. This was clearly seen by the colour evolution during the first hour of treatment (Figure 9.4). At the end of the ozone-driven treatments, the intense brown colour presented by both bio-treated leachate decreased to a very slight yellow. The colour values (for a

1:20 dilution) obtained at the end of the treatments by $O_3$ and $O_3$/UVC were, respectively, 28 and 9 units of Pt-Co, for LN, and 30 and 20 units of Pt-Co, for LD. Another indicator that can be employed to assess the effectiveness of ozone-driven processes is the change in biodegradability [14]. Therefore, prior to and after the ozonation treatments, the biodegradability of both leachate was evaluated by the Zahn-Wellens 28-day test and the following results were obtained: (i) LN = 7%, after $O_3$ = 51% and $O_3$/UVC = 73%, for LN, and; (ii) LD = 18%, after $O_3$ = 69% and $O_3$/UVC = 80%. Bearing in mind that for an effluent to be considered biodegradable, its organic carbon content must at least decrease by 70% after the 28-day test [15, 16], for both bio-treated leachates this only occurred after treatment with $O_3$/UVC. Also, in view of a target COD value < 150 mg/L (Portuguese legal limit for direct discharge), it is worth to mention that, although not achieved for any of the tested conditions, for the $O_3$/UVC treatments COD values of 205 and 167 mg/L were reached at the end of the biodegradability tests for LN and LD, respectively. Taking into consideration these results, the treatment of bio-treated leachate with $O_3$ alone will be disregarded as a possible treatment strategy.



t = 0       t = 30 min       t = 60 min
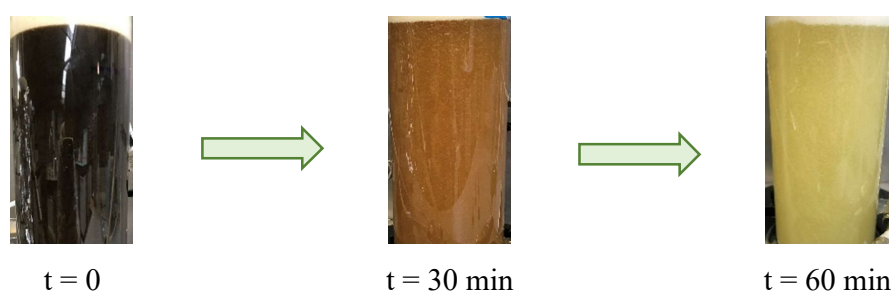
**Figure 9.4** – Evolution of colour for the bio-treated leachate during $O_3$ treatment.

### 9.3.1.2 Organic matter characterization

According to Chen, *et al.* [17], the fluorescence spectrum can be divided into five regions based on the type and location of fluorescent material: (i) region I – tyrosine-like aromatic protein (Ex < 250 nm, Em < 330 nm); (ii) region II – tryptophane-like aromatic protein (Ex < 250 nm, 330 nm < Em < 380 nm); (iii) region III – fulvic-like acids (Ex < 250 nm, Em > 380 nm); (iv) region IV – soluble microbial metabolic by-products (Ex > 250 nm, Em < 380 nm); and (v) region V – humic-like acids (Ex > 250 nm, Em > 380 nm). Observing the 3D-EEM spectra for LN and LD (Figure 9.5), it is possible to infer similarities in the nature of the organic content. This can be expected as LD was obtained from biological denitrification of LN effluent. For both bio-treated effluents, 3D-EEM

contours highlight two main regions responsible for more than 60% of total fluorescence intensity (Figure 9.5-a.1 and -b.1): (i) the fulvic acid-like matter (region III), representing 31.0% (LN) and 33.5% (LD), and (ii) humic acid-like matter (region V), corresponding to 35.5% (LN) and 33.1% (LD). This high fraction of fulvic- and humic-like acids is also an indication of the chemical stability of the leachate [2].
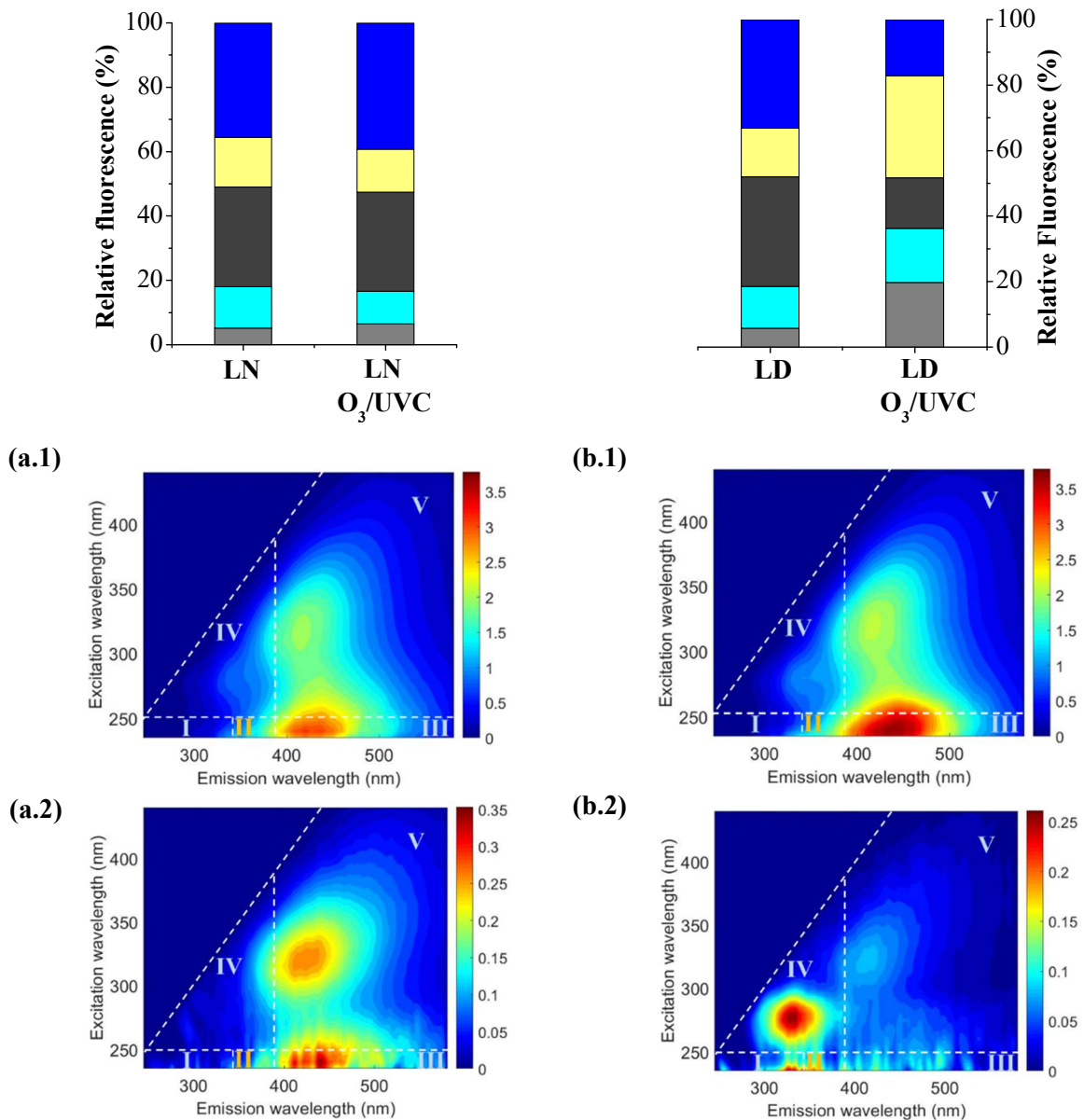


**Figure 9.5** – Relative fluorescence ( ▮ ▮ ▮ ▮ - regions I to V)  and 3D-EEM spectra for the bio-treated leachates (a) nitrified leachate – LN and (b) nitrified-denitrified leachate – LD, (.1) before and (.2) after O$_3$/UVC treatment (conditions: $V_L$ = 1.5 L; $Q_{O_3}$ = 0.1 NL/min; [O$_3$]$_{inlet}$ = 180 mg/L; $t$ = 10h; $Q_{UV}$ = 2.48 J/s).

After O$_3$/UVC treatment, the total fluorescence intensity largely decreased (95.8% and 97.6% for LN and LD, respectively), but major differences can be visualized in the 3D-EEM for both tested

leachates (Figure 9.5-a.2 and -b.2). While for the LN, the fulvic- and humic-like matter regions remained with high fluorescence (30.8% and 39.1%, respectively, of the total fluorescence), for LD the region with greater fluorescence intensity (representing 31.2% of the total fluorescence) was related to soluble microbial by product-like matter and likely responsible for the higher biodegradability obtained for this effluent.

### 9.3.2 Bio-coagulated leachates

Regarding the bio-coagulated leachates (LNC and LDC), and considering the distinct characteristics of the bio-treated leachates (Table 9.1), coagulation was performed: (i) using ferric salts at acidic conditions, for the nitrified leachate, and (ii) with aluminium salts at natural pH, in order to attain near-neutral pH conditions, for the denitrified leachate. While the LDC resulted from the coagulation of the LD (*jar-test* results are displayed in Table 9.3), attention should be drawn to the fact that the LNC was collected in the landfill, not corresponding to the coagulation of the LN effluent used for testing. Nonetheless, from previous coagulation tests under similar conditions, also using nitrified leachate from the same landfill [1], it can be assumed between 47% to 60% removal for both DOC and COD parameters. Moreover, in this case, aeration was applied to oxidize nitrites to nitrates (Table 9.1), eliminating its interference in the ozonation reactions towards the bio-recalcitrant organic content of the LNC. Total iron content of LNC was above the legal limit (but useful if a following iron-catalysed oxidation process is intended). To obtain LDC effluent, considering the *jar-test* results (50.5% and 54.4% of DOC and COD removal) and keeping in mind the sulfate legal limit compliance (see Table 8.2), a coagulant dose of 300 mg $Al^{3+}$/L was selected for LD coagulation.

**Table 9.3** – Main results from the jar-tests carried out with LD.

| Test | pH$_{final}$ | DOC | (%) | COD | (%) | Turbidity (NTU) |
|---|---|---|---|---|---|---|
| **LD** | 9.1 | 1158 | - | 3577 | - | 900 |
| **+ 100 mg Al/L** | 7.5 | 980 | 15.3 | 3165 | 11.6 | 670 |
| **+ 200 mg Al/L** | 6.9 | 765 | 33.9 | 2765 | 22.8 | 300 |
| **+ 300 mg Al/L** | **6.2** | **574** | **50.5** | **1635** | **54.4** | **330** |
| **+ 400 mg Al/L** | 5.5 | 524 | 54.7 | 1435 | 59.9 | 330 |
| **+ 600 mg Al/L** | 4.7 | 529 | 54.3 | 1449 | 59.6 | 330 |
| **+ 800 mg Al/L** | 4.4 | 531 | 54.2 | 1432 | 48.9 | 180 |

### 9.3.2.1 Efficiency of the ozone-driven processes

For LNC, as a result of the absence of nitrites, more oxidant species were available to react with the organic matter and, unlike LN, not only COD but also DOC has decreased continuously since the beginning of the ozone-driven treatments. This could explain, for both $O_3$ and $O_3$/UVC treatments, the higher percentages of DOC and COD removal presented by the LNC when compared to the LDC (Table 9.4). However, it can be misleading, as attention should be given to the differences of the organic content between the bio-coagulated leachates (lower organic content of LNC when compared to LDC, see Table 9.1). Thus, although LNC presents higher pseudo-first-order rate constants ($k$, min$^{-1}$) for DOC and COD removal, it is possible to verify that the amount of DOC and COD removed per gram of ozone is very similar for both bio-coagulated leachate effluents. This feature was valid for the two ozone-driven processes tested. Like for the bio-treated leachates, the pH decay for LDC was less pronounced due to its higher alkalinity content (pH buffer effect) (Figure 9.6-b.1 and -b.2). Also, for both bio-coagulated leachates, pH decay was slower for the $O_3$/UVC process.

**Table 9.4** – Main results and kinetic parameters, for DOC and COD degradation, of the $O_3$ and $O_3$/UVC processes applied to LNC and LDC.

| Parameters | $O_3$ | | $O_3$/UVC | |
|---|---|---|---|---|
| | LNC | LDC | LNC | LDC |
| $OD_I$[a] (g $O_3$/L) | 2.2 | 2.1 | 2.2 | 2.2 |
| $OD_T$[a] (g $O_3$/L) | 1.8 | 1.5 | 2.1 | 2.1 |
| DOC removal (%) | 36.2 | 26.1 | 54.5 | 43.3 |
| COD removal (%) | 53.1 | 36.4 | 69.9 | 60.0 |
| Colour removal (%) | 69.3 | 62.2 | 77.6 | 70.2 |
| Biodegradability (%) | 81 | 83 | 93 | 87 |
| *DOC Degradation Kinetics* | | | | |
| $k$[b]$\times 10^3$ (min$^{-1}$) | $2.5 \pm 0.2$ | $1.9 \pm 0.2$ | $4.2 \pm 0.4$ | $3.6 \pm 0.4$ |
| $R^{2,}$[c] | 0.996 | 0.996 | 0.991 | 0.992 |
| $t$[d] (min) | $> 0$ | $> 60$ | $> 30$ | $> 30$ |
| $k$[e]$\times 10^{-1}$ (mg DOC/g $OD_T$) | $7.8 \pm 0.8$ | $8.4 \pm 0.6$ | $11.8 \pm 0.8$ | $12.7 \pm 0.9$ |
| $R^{2,}$[c] | 0.994 | 0.996 | 0.995 | 0.994 |
| $OD_T$[d] (g $O_3$/L) | $> 0$ | $> 0$ | $> 0.2$ | $> 0.2$ |
| *COD Degradation Kinetics* | | | | |
| $k$[b]$\times 10^3$ (min$^{-1}$) | $4.2 \pm 0.8$ | $2.1 \pm 0.4$ | $6.5 \pm 0.8$ | $5.1 \pm 0.5$ |
| $R^{2,}$[c] | 0.990 | 0.991 | 0.993 | 0.996 |
| $t$[d] (min) | $> 0$ | $> 0$ | $> 0$ | $> 0$ |
| $k$[e]$\times 10^{-2}$ (mg COD/g $OD_T$) | $3.4 \pm 0.6$ | $3.3 \pm 0.5$ | $4.0 \pm 0.6$ | $4.6 \pm 0.8$ |
| $R^{2,}$[c] | 0.996 | 0.993 | 0.995 | 0.991 |
| $OD_T$[d] (g $O_3$/L) | $> 0$ | $> 0$ | $> 0$ | $> 0$ |

[a] Inlet ($OD_I$) and transferred ($OD_T$) ozone dose per litre of leachate. [b] Pseudo-first-order rate constant for DOC and COD degradation in terms of reaction time. [c] Coefficient of determination. [d] Value or interval of time ($t$, min) or transferred ozone dose ($OD_T$), from which the kinetic parameters were calculated. [e] DOC and COD degradation reaction rates, expressed in terms of the transferred ozone dose ($OD_T$), whose values correspond to the slopes of Figure 9.6.
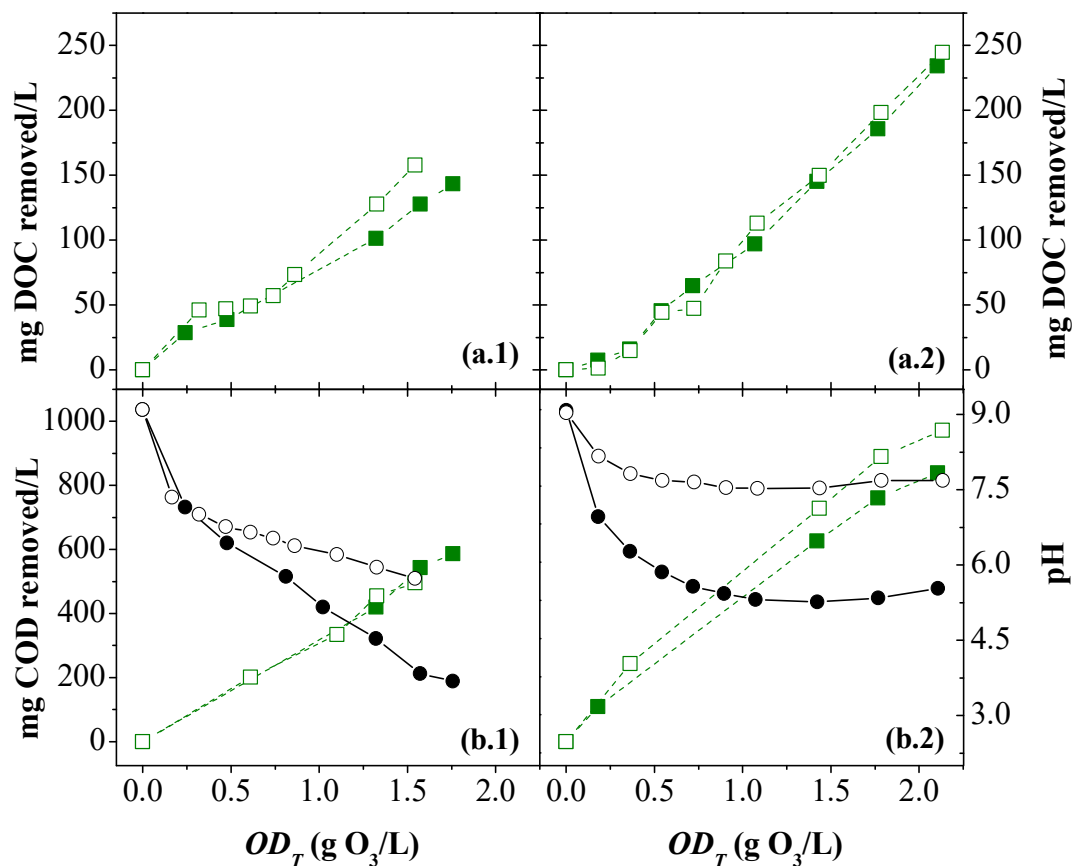
**Figure 9.6** – Representation of the amount of (a) DOC and (b) COD removed, as a function of the transferred ozone dose ($OD_T$), for (.1) $O_3$ and (.2) $O_3$/UVC treatments applied to the bio-coagulated leachates (■) LNC and (□) LDC, including the pH profile for (●) LNC and (○) LDC.

The colour values (for a 1:20 dilution) obtained at the end of the treatments (3h) by $O_3$ and $O_3$/UVC were, respectively, 13 and 9 units of Pt-Co, for LNC, and 12 and 9 units of Pt-Co, for LDC (Figure 9.7). In respect to the biodegradability before and after ozone-driven treatments, the following results were obtained: (i) LNC = 17%, and after $O_3$ = 81% and $O_3$/UVC = 93%; and (ii) LDC = 19%, and after $O_3$ = 83% and $O_3$/UVC = 87% (Table 9.4). Moreover, the COD values at the end of Zahn-Wellens test were of 123 mg/L ($O_3$) and 22 mg/L ($O_3$/UVC) for LNC, and 174 mg/L ($O_3$) and 144 mg/L ($O_3$/UVC) for LDC. In retrospect, all treatment scenarios, except for $O_3$ applied to LDC, reached a final COD < 150 mg/L at the end of the biodegradability test.
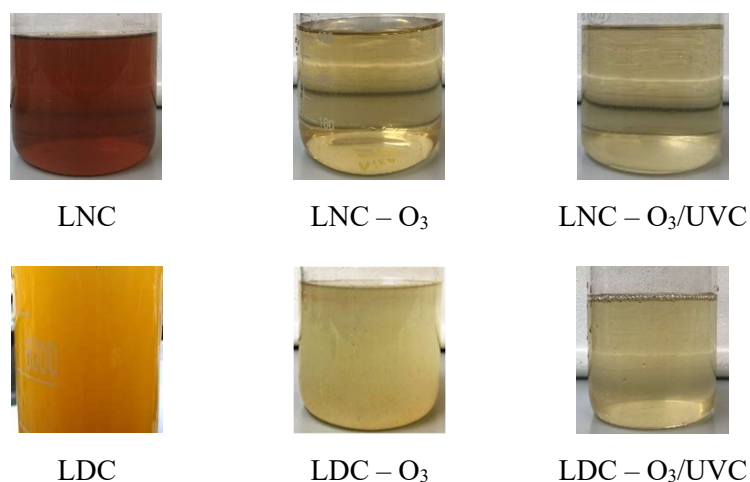
**Figure 9.7** – Colour before and after $O_3$ and $O_3/UVC$ treatment, for the bio-coagulated leachates.

### 9.3.2.2 Organic matter characterization

As expected, the coagulation stage reduced total fluorescence intensity by 61.5% and 60.3% for the nitrified and denitrified leachate, respectively (for practical purposes to discussion, LNC will be assumed as resulting from the coagulation of LN). Concerning the fluorescence intensity by region (I to V), there was a decrease of 46%, 54%, 63%, 58% and 67%, from LN to LNC, and 25%, 48%, 65%, 49% and 71%, from LD to LDC. Despite the similarity in the fluorescence intensity decrease (either total or by region, except for region I), as a result of the distinct biological and coagulation processes, different 3D-EEM patterns were obtained for the LNC and LDC effluents (Figure 9.8-a.1 and -b.1). Aftab and Hur [18] also reported higher removal of the humic-like (75%) versus the fulvic-like (~ 58%) acids for a coagulation treatment with an optimized dose of 300 mg $Al^{3+}/L$. The much lower removal of tyrosine-like protein (region I) was also verified in other studies [7, 19], having been attributed to the smaller molecular size of these compounds.

For LNC, after $O_3$ and $O_3/UVC$ treatment, total fluorescence intensity reduced by 98.1% and 98.7%, respectively (Figure 9.8-a.2 and -a.3). In both ozone-driven treatments, but more pronounced in $O_3/UVC$, the relative fluorescence intensity decreased in the regions associated with fulvic- and humic-like matter (from 60.2% to 48.1% after $O_3$, and to 38.9% after $O_3/UVC$), and increased in the regions related to tyrosine-like protein and microbial by-products (from 14.3% to 35.5% after $O_3$, and to 44.6% after $O_3/UVC$). Those regions (I and IV) reflect bioavailable substrates [3, 20], presenting a strong correlation with $BOD_5$ [21]. These changes in DOM composition are in line with the results obtained in the biodegradability tests.
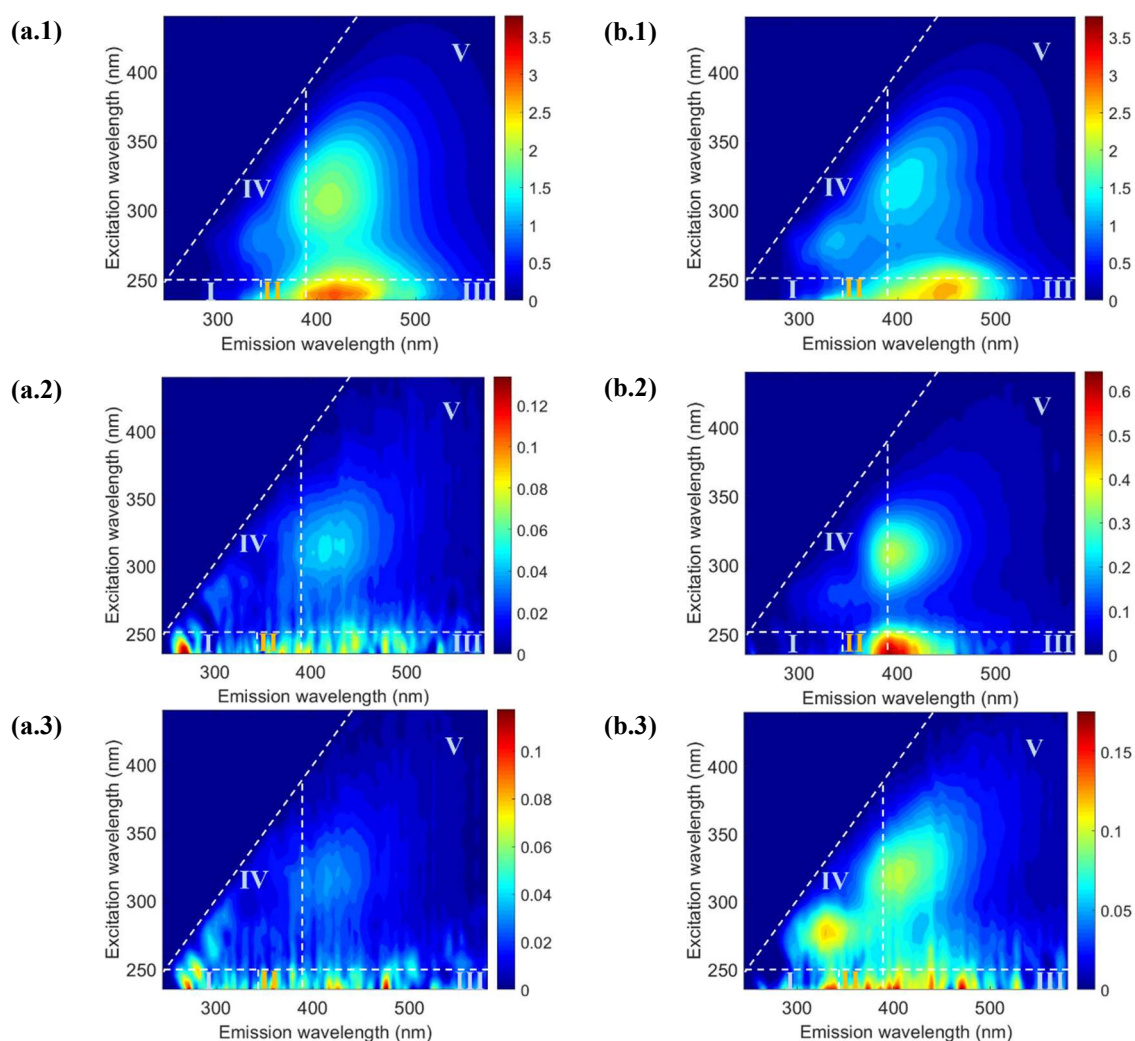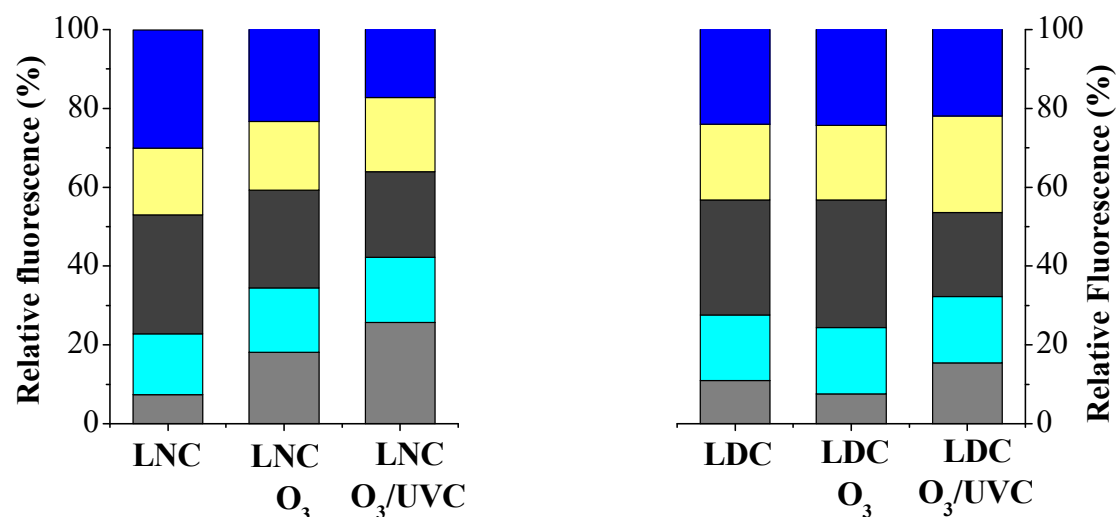
**Figure 9.8** – Relative fluorescence ( ▮▮▮▮▮ - regions I to V) and 3D-EEM spectra for the bio-coagulated leachates (a) nitrified-coagulated leachate – LNC (conditions: pH = 3.7 and $[Fe^{3+}]$ = 240 mg/L) and (b) nitrified-denitrified-coagulated leachate – LDC (conditions: pH = 9.2 and $[Al^{3+}]$ = 300 mg/L), (.1) before and (.2) after $O_3$ treatment (conditions: $V_L$ = 1.5 L; $Q_{O_3}$ = 0.1 L/min; $[O_3]_{inlet}$ = 180 mg/L; $t$ = 3h) or (.3) after $O_3$/UVC treatment (same conditions as for $O_3$, except for $Q_{UV}$ = 1.7 J/s).

In respect to LDC, total fluorescence intensity decreased 90.2% and 96.4%, respectively, after $O_3$ and $O_3$/UVC oxidation (Figure 9.8-b.2 and -b.3). Analysing the relative fluorescence, the application of $O_3$ did not significantly change the proportions of fulvic- and humic-like acids (in fact, there was a slight increase from 53.5% to 56.7%). In turn, after $O_3$/UVC treatment, not only the proportion of regions III and V in total fluorescence decreased, but also there was a significant increase (nearly two-fold) of the relative fluorescence intensity for tyrosine-like protein and microbial by-products. Again, these results are in good agreement with the biodegradability increase revealed by the Zhan-Wellens tests.

### 9.3.3 Treatment costs evaluation

Considering the results reported in this work and in view of simultaneous legal compliance for organic and nitrogen compounds, 6 possible treatment train strategies ((1) LN + $O_3$/UVC + bio-denitrification; (2) LD + $O_3$/UVC + bio-oxidation, (3;4) LN + iron-acidic coagulation (no nitrites) + $O_3$ or $O_3$/UVC + bio-denitrification, and (5;6) LD + aluminium-neutral coagulation + $O_3$ or $O_3$/UVC + bio-oxidation) were evaluated in terms of operating costs (Table 9.5). For the biological stages, to estimate the energy cost for aeration and the cost of the external carbon donor, theoretical values for oxygen and COD consumption were assumed. For the coagulation and ozone-driven stages, the operating costs were calculated taking into account the experimental conditions and data obtained, namely: (i) type and concentration of coagulant; (ii) amount of acid or base required for the pH adjustments; (iii) gas flow rate and ozone concentration and (iv) time required to achieve 85% (LN and LD) or 60% (LNC and LDC) of COD reduction (established according to the results obtained and calculated on the basis of the pseudo-first-order rate constants from Table 9.3 and Table 9.4). Furthermore, the following energy and reagents prices were considered: (i) 0.1276 €/kWh, energy market price in Portugal for industrial applications; (ii) 4.5 kg $O_2$/kWh for aeration carried out by fine bubble diffusers [22]; (iii) 15 kWh/kg $O_3$, for ozone energy consumption; (iv) 11W (LN and LD) or 6 W (LNC and LDC) for UVC lamp; (v) 0.48 €/kg for methanol; (vi) 0.08 €/m$^3$ for $O_2$; (vii) 0.24 €/kg for FeCl$_3$ 40% (w/w); (viii) 0.19 €/kg for Al$_2$(SO$_4$)$_3$ 48% (w/w), (ix) 0.16 €/kg for NaHO 30% (w/w), and (x) 0.10 €/kg for H$_2$SO$_4$ 98% (w/w). Regarding the sludge treatment and disposal costs, based on previous work (Chapter 6) an average value of 0.48 €/m$^3$ was assumed.

Analysing the estimated costs (Table 9.5), the main contribution comes, as expected, from the ozone-driven stage. Also, in the absence of the coagulation stage, the treatment train strategies (no.1

and no.2) are not economically viable. Regarding LN, if full nitrification (i.e. bio-oxidation of nitrite into nitrate) had occurred in the first biological reactor it would be possible to expect a cost-reduction of ~ 40% for the $O_3$-driven stage (to 20.5 €/m$^3$, but still not economically viable). As coagulation promotes a significant reduction of the leachate organic load (~ 50%), the required ozone dose to achieve a biodegradable effluent, able to reach COD < 150 mg/L after a subsequent biological oxidation step, is significantly lower, thus operational costs greatly reduce (treatment trains no.3 to 6). Considering the bio-coagulation pre-treatments, the strategies with LNC presented the lowest operational costs, particularly when the $O_3$/UVC advanced oxidation process is applied (as it showed the highest pseudo-first-order rate constant for COD removal, Table 9.4). Nonetheless, knowing that only partial nitrification occurs in the 1$^{st}$ biological reactor and, from previous experiences using similar bio-nitrified leachate and coagulation conditions (from Chapters 5 and 6), at the end of the C/S stage the leachate still presents part of the nitrogen content in the nitrite form (~ 70%). This is not desirable, as the presence of nitrites in a downstream advanced stage oxidation will inevitably lead to an increase in costs (total cost for the $O_3$ process were estimated to be of 9.4 and 12.3 €/m$^3$ considering a leachate with 500 and 1000 mg N/L of nitrite before coagulation). Therefore, the biological nitrogen removal should preferentially be performed at the first biological stage (strategies no. 5 and no. 6). Taking the reported costs (between 10 to 25 €/m$^3$, section 3.2.3 of Chapter 3) of landfills in Portugal whose leachate treatment complies with the legal limits for direct discharge into the environment (by means of reverse osmosis process), treatment train strategy no. 6 may be considered economically competitive. Furthermore, the problems arising from the concentrate that results from reverse osmosis are absent in ozone-based processes.

**Table 9.5** – Operating costs estimation for the different treatment train strategies.

| | | Un | Treatment train | | | | | |
|---|---|---|---|---|---|---|---|---|
| | | | $Bio_{NIT} + O_3/UVC +$ $Bio_{DESN}$ | $Bio_{NIT/DESN} +$ $O_3/UVC + Bio_{OXID.}$ | $Bio_{NIT} + C/S +$ $O_3 + Bio_{DESN}$ | $Bio_{NIT} + C/S +$ $O_3/UVC +$ $Bio_{DESN}$ | $Bio_{NIT/DESN} + C/S$ $+ O_3 + Bio_{OXID}$ | $Bio_{NIT/DESN} + C/S +$ $O_3/UVC + Bio_{OXID}$ |
| **1st Bio.** [a] | Aeration | €/m³ | 0.10 | 0.10 | 0.10 | 0.10 | 0.10 | 0.10 |
| | Methanol | €/m³ | - | 0.57 | - | - | 0.57 | 0.57 |
| | **(1) TOTAL** | **€/m³** | **0.10** | **0.67** | **0.10** | **0.10** | **0.67** | **0.67** |
| **Coagulation** [b] | $H_2SO_4$ | €/m³ | - | - | 0.08 | 0.08 | - | - |
| | $FeCl_3$ | €/m³ | - | - | 0.42 | 0.42 | - | - |
| | $Al_2(SO_4)_3$ | €/m³ | - | - | - | - | 0.75 | 0.75 |
| | Sludge | €/m³ | - | - | 0.48 | 0.48 | 0.48 | 0.48 |
| | **(2) TOTAL** | **€/m³** | **-** | **-** | **0.98** | **0.98** | **1.23** | **1.23** |
| **O₃-driven** [c] | NaHO | €/m³ | 0.18 | - | 0.43 | 0.34 | 0.50 | 0.28 |
| | $O_2$ | €/m³ | 4.07 | 3.75 | 1.16 | 0.78 | 1.95 | 0.96 |
| | Energy | €/m³ | 29.4 | 27.1 | 5.01 | 4.58 | 8.42 | 5.65 |
| | **(3) TOTAL** | **€/m³** | **33.7** | **30.8** | **6.61** | **5.69** | **10.88** | **6.89** |
| **2nd Bio.** [d] | Aeration | €/m³ | 0.03 | 0.06 | 0.03 | 0.03 | 0.06 | 0.06 |
| | Methanol | €/m³ | 0.86 | - | 0.81 | 0.81 | - | - |
| | **(4) TOTAL** | **€/m³** | **0.89** | **0.06** | **0.84** | **0.84** | **0.06** | **0.06** |
| **(1) + (2) + (3) + (4)** | | | **34.6** | **31.6** | **8.5** | **7.6** | **12.8** | **8.9** |

[a] The following theoretical values were assumed: 3.43 kg $O_2$ consumed per kg $N-NO_2^-$ formed (for nitritation) and 1.72 kg COD consumed per kg $N-NO_2^-$ reduced (for denitritation). [b] Conditions: 240 mg $Fe^{3+}$/L, pH ~ 4, requiring 0.42 L of $H_2SO_4$ per m³ of bio-nitrified leachate; and 300 mg $Al^{3+}$/L without pH adjustment, for the nitrified/denitrified leachate. [c] Conditions: initial pH adjusted to 9.0; $Q_g = 0.1$ L/min; $C_{O_3,I} = 180$ mg $O_3$/L. [d] The following theoretical value was assumed: 2.89 kg COD per g $N-NO_3^-$ reduced (for denitrification).

## 9.4 Conclusions

This work allowed to evaluate the performance of $O_3$ and $O_3$/UVC processes applied to different pre-treated leachates and to establish treatment train strategies potentially capable to originate an effluent that complies with both organic and nitrogen legal limits for discharge. In the absence of a coagulation stage, both bio-treated leachates (LN and LD) require an ozone dose ($OD_T$) of 7.1 g $O_3$/L combined with 59.5 kJ/L of UVC radiation, to obtain a biodegradable effluent. However, it is not certain that after a subsequent biological treatment the COD target value is attained, and the treatment cost exceeds 30 €/m$^3$. Therefore, the inclusion of a chemical coagulation process before the ozone-driven stage shows to be essential for the economic feasibility of a treatment train. The changes in DOM composition over the various treatment stages tested were consistent with the biodegradability presented by the respective effluents.

To deal with a mature urban landfill leachate, among the various treatment train strategies proposed, the most suitable is as follows: (i) first biological stage for nitritation/denitritation (with addition of an external carbon source), followed by (ii) coagulation, without pH adjustment and using 300 mg $Al^{3+}$/L, and (iii) advanced oxidation by means of $O_3$/UVC up to $OD_T$ of 2.1 g $O_3$/L and 12.2 kJ$_{UVC}$/L, prior to (iv) a final biological oxidation. This sequence allows to reach a final effluent able to simultaneously comply with the discharge legal values for organic and nitrogen parameters, and for other parameters whose concentration increases with the addition of chemicals along the treatment train (such as sulfate ions and aluminium). Furthermore, the operational cost for this treatment train is expected to be 8.9 €/m$^3$, with $O_3$/UVC process counting for 6.9 €/m$^3$, which is reasonable considering the costs for current membrane technology.

## 9.5 References

1.  Silva, T.F.C.V., P.A. Soares, D.R. Manenti, A. Fonseca, I. Saraiva, R.A.R. Boaventura, and V.J.P. Vilar, *An innovative multistage treatment system for sanitary landfill leachate depuration: Studies at pilot-scale.* Science of the Total Environment, 2017. **576**: p. 99-117.

2.  Oloibiri, V., S. Coninck, M. Chys, K. Demeestere, and S.W.H. Van Hulle, Characterisation of landfill leachate by EEM-PARAFAC-SOM during physical-chemical treatment by coagulation-flocculation, activated carbon adsorption and ion exchange. Chemosphere, 2017. **186**: p. 873-883.

3.  Henderson, R.K., A. Baker, K.R. Murphy, A. Hambly, R.M. Stuetz, and S.J. Khan, *Fluorescence as a potential monitoring tool for recycled water systems: a review.* Water Research, 2009. **43**: p. 863-881.

4.  Baker, A. and M. Curry, *Fluorescence of leachates from three contrasting landfills.* Water Research, 2004. **38**: p. 2605-2613.

5.  Baker, A., Fluorescence tracing of diffuse landfill leachate contamination in rivers. Water, Air & Soil Pollution, 2005. **163**: p. 229-244.

6.  Orecchio, S., D. Amorello, S. Barreca, A. Pace, S. Gambacurta, and M.G. Gulotta, Analytical method for monitoring micro trace of landfill leachate in groundwater using fluorescence excitation-emission matrix spectroscopy. Analytical Methods, 2016. **8**(17): p. 3475-3480.

7.  Aftab, B., J. Cho, H.S. Shin, and J. Hur, Using EEM-PARAFAC to probe NF membrane fouling potential of stabilized landfill leachate pretreated by various options. Waste Management, 2020. **102**: p. 260-269.

8.  Hoigné, J., H. Bader, W.R. Haag, and J. Staehelin, Rate constants of reactions of ozone with organic and inorganic compounds in water III. Inorganic compounds and radicals. Water Research, 1985. **19**: p. 993-1004.

9.  Liu, Q., L.M. Schurter, C.E. Muller, S. Aloisio, J.S. Francisco, and D.W. Margerum, *Kinetics and mechanisms of aqueous ozone reactions with bromide, sulfite, hydrogen sulfite, iodide, and nitrite Ions.* Inorganic Chemistry, 2001. **40**: p. 4436-4442.

10. Gardoni, D., A. Vailati, and R. Canziani, *Decay of ozone in water: A review.* Ozone: Science and Engineering, 2012. **34**(4): p. 233-242.

11. Rosenfeldt, E.J., K.G. Linden, S. Canonica, and U. Von Gunten, Comparison of the efficiency of $^\cdot$OH radical formation during ozonation and the advanced oxidation processes $O_3/H_2O_2$ and $UV/H_2O_2$. Water Research, 2006. **40**: p. 3695-3704.

12. Poznyak, T., G.L. Bautista, I. Chaírez, R.I. Córdova, and L.E. Ríos, *Decomposition of toxic pollutants in landfill leachate by ozone after coagulation.* Journal of Hazardous Materials, 2008. **152**: p. 1108-1114.

13. Chys, M., V.A. Oloibiri, W.T.M. Audenaert, K. Demeestere, and S.W.H. Van Hulle, *Ozonation of biologically treated landfill leachate: Efficiency and insights in organic conversions.* Chemical Engineering Journal, 2015. **277**: p. 104-111.

14. Chen, W., Z. Gu, P. Wen, and Q. Li, Degradation of refractory organic contaminants in membrane concentrates from landfill leachate by a combined coagulation-ozonation process. Chemosphere, 2019. **217**: p. 411-422.

15. Silva, T.F.C.V., M.E.F. Silva, A.C. Cunha-Queda, A. Fonseca, I. Saraiva, M.A. Sousa, C. Gonçalves, M.F. Alpendurada, R.A.R. Boaventura, and V.J.P. Vilar, *Multistage treatment system for raw leachate from sanitary landfill combining biological nitrification-denitrification/solar photo-Fenton/biological processes, at a scale close to industrial.* Water Research, 2013. **47**: p. 6167-6186.

16. Pluciennik-Koropczuk, E. and S. Myszograj, *Zahn-Wellens test in industrial wastewater biodegradability assessment.* Civil and Environmental Engineering Reports, 2018. **28**(1): p. 77-86.

17. Chen, W., P. Westerhoff, J.A. Leenheer, and K. Booksh, *Fluorescence Excitation-Emission matrix regional integration to quantify spectra for dissolved organic matter.* Environmental Science & Technology, 2003. **37**: p. 5701-5710.

18. Aftab, B. and J. Hur, Fast tracking the molecular weight changes of humic substances in coagulation/flocculation processes via fluorescence EEM-PARAFAC. Chemosphere, 2017. **178**: p. 317-324.

19. Wassink, J.K., R.C. Andrews, R.H. Peiris, and R.L. Legge, Evaluation of fluorescence excitation-emission and LC-OCD as methods of detecting removal of NOM and DBP precursors by enhanced coagulation. Water Supply, 2011. **11**(5): p. 621-630.

20. Hudson, N., A. Baker, and D. Reynolds, Fluorescence analysis of dissolved organic matter in natural, waste and polluted water - a review. River Research and Applications, 2007. **23**: p. 189.

21. Yang, L., H.S. Shin, and J. Hur, Estimating the concentration and biodegradability of organic matter in 22 wastewater treatment plants using fluorescence excitation emission matrices and parallel factor analysis. Sensors, 2013. **14**: p. 1771-1786.

22. Tchobanoglous, G., F. Burton, and H. Stensel, *Wastewater engineering: Treatment and reuse.* 2003: McGraw-Hill.

# 10 Final Remarks

*This last chapter presents the most relevant results and conclusions reported in the previous chapters, complemented with some suggestions for future work.*

## 10.1 Conclusions

Municipal solid waste production around the world continues to increase, with landfilling being the main waste management option in almost all countries, as it is expected to remain so in the coming years. Even with the various European initiatives to adopt a more circular economy towards a zero-waste program, it is still not possible to have a 'landfill-free' society. Inherent to landfills is the generation of leachate, which results from the percolation of rainwater through the deposited waste and biochemical reactions in waste cells, transferring contaminants from the solid to the liquid phase. The produced landfill leachate is usually characterized as a complex mixture of recalcitrant organic and inorganic compounds that depend on several factors (landfill age, type of disposed waste, climatic conditions, among others). So, it is difficult to define a unique treatment strategy to be efficient in any given situation. Additionally, to minimize the potential environmental impacts, legal authorities throughout the world have imposed maximum contaminants' levels in treated leachate prior to disposal. The strict implementation of environmental legislative demands and the ageing of existing landfills put pressure on managers and operators of landfills to implement more efficient processes.

The major challenges in treating mature landfill leachates are the: (i) variability, in composition and quantity, along the year and among landfills; (ii) high levels of ammonia, that may cause a toxic effect on the conventional biological processes; and (iii) rising presence of high molecular weight contaminants, i.e. bio-recalcitrant compounds, which leads to a very low biodegradability ($BOD_5/COD < 0.1$). To overcome this issue, especially during this last decade, most research targets the combination of two or more treatment technologies, normally including an advanced oxidation process (AOP), as efficient and effective way for landfill leachate treatment. In this sense, under the Advanced-LFT project (SI IDT – 33960/2012 F2), earlier research using leachate from the same urban landfill as that used in the present work, developed a multistage treatment system - combining biological processes, coagulation/sedimentation, and photo-Fenton oxidation - for leachates from mature municipal landfills (European Patent – EP 2784031A1). This strategy was partially tested at pilot-scale and proved to be effective for total ammonia nitrogen (TAN) and chemical oxidation demand (COD) removal up to legal values (according to the Portuguese legislation, Annex XVIII from Decree-Law no. 236/98). However, the removal of the high total nitrogen (TN) content of the leachate was not accomplished, nor the final biological reactor was fully assessed. Moreover, the photo-oxidation stage presented major drawbacks when aiming at a full-scale application, particularly with respect to the land area requirements and investment costs associated with the traditional compound parabolic collectors (CPCs), even when combining solar and artificial radiation.

## 10.1.1 Treatment train combining biological nitrogen removal, coagulation/sedimentation, photo-Fenton and final biological oxidation

First, based on the multistage strategy formerly proposed, optimization studies were carried out to include an additional denitrification step in the first biological stage, and its effects were evaluated in the following treatment stages. Thus, the tested treatment train comprised a: (i) sequential batch reactor (SBR), with nitrification/denitrification cycles; (ii) coagulation/sedimentation (C/S), using ferric salts at acidic conditions; (iii) photo-Fenton (PF) oxidation reaction ($Fe^{2+}/H_2O_2/UV$-Vis); and (iv) final biological oxidation. The mature urban leachate used for testing was collected at the aerated lagoon of a landfill treatment plant, and presented a high organic and nitrogen content (DOC = 1.1 g C/L; COD = 3.6 g $O_2$/L; TN = 2.0 g N/L) and low biodegradability ($BOD_5$/COD = 0.05).

In the first treatment stage, the SBR was operated to promote nitrification/denitrification while assessing the maximum daily nitrogen load that could be treated to comply with the TN legal discharge limit value. A final TN < 15 mg N/L and alkalinity values ~ 1.1 g $CaCO_3$/L were reached when the SBR was operated in a 24h-cycle mode, applying the following operational scheme: 15h aeration, with ~ 0.5 mg $O_2$/L, + 8.5h anoxic, with addition of methanol at COD/N mass ratio of 2.5, + 0.5h settling, and with volume exchange ratios of 14.3%, 16.4% and 21.4%, for operating temperatures of 20, 25 and 30 ºC, respectively. During all the SBR tests, only partial nitrification or "*nitritation*", i.e. oxidation of ammonium to nitrite, was attained whereas complete oxidation to nitrate was not observed. This is advantageous and even desirable, as nitritation/denitritation can save up to 25% of the oxygen uptake and 40% of the carbon needs, thus reducing operational costs involved in biological nitrogen removal.

To increase the efficiency of the subsequent photo-treatment stage, coagulation using $FeCl_3$ as the coagulant, dosed at 240 mg $Fe^{3+}$/L, with pH set at 3.0, was applied to precipitate humic substances (DOC decrease > 60%) and remove suspended and colloidal matter (residual turbidity ≈ 33 NTU). The jar-tests, comparing bio-nitrified (LN) and bio-nitrified/denitrified (LD) leachate, stressed the effect of the leachate alkalinity, generated during the denitrification reaction, on process efficiency. For the coagulated LD, with alkalinity of 1.1 g $CaCO_3$/L, the final concentration of sulfate was only slightly below the legal limit (< 2 g/L).

The photo-Fenton stage performed with a catalyst dosage of 60 mg $Fe^{2+}$/L and pH 2.8-3.0, promoted a significant enhancement on leachate biodegradability. Consuming 75 mM of $H_2O_2$ and 8.9 $kJ_{UV}$/L of accumulated energy, PF achieved an effluent (COD ~ 400 mg/L) that was further biologically treated reaching the COD discharge limit (150 mg/L). A final conventional activated sludge process,

operated in continuous mode, with an HRT of 12h, allowed to obtain COD and TSS values (107 ± 3 and 50 ± 2 mg/L, respectively) below the legal limits.

The above-mentioned results showed that legal compliance for mature landfill leachate direct discharge into waterbodies was successfully attained at lab-scale, using a treatment train combining biological nitrogen removal, coagulation/sedimentation (with iron salts at acidic conditions), photo-Fenton and a final biological oxidation. Afterward, the optimized treatment train strategy was applied at full-scale, in a compact facility located at an urban waste landfill comprising the following treatment units: (i) a first biological reactor (BR1); (ii) a coagulation and photo-treatment unit (C/P) and (iii) a final biological reactor (BR2). The treatment train facility also included a sludge tank (ST), a filter-press system and a drainage tank for the treatment of the produced sludge.

Each treatment sequence was applied to ca. 30 $m^3$ of urban leachate from an aerated lagoon, leading to global removal efficiencies of 98% for COD (from 8.30 to 0.15 g $O_2$/L), 97% for DOC (from 2.32 to 0.08 g C/L) and 85% for TN (from 2.65 to 0.41 g N/L). Glycerol, a by-product from biodiesel production, was successfully employed as an alternative and cost-effective external carbon source for denitrification purposes. Enabling a compact solution for the treatment train facility, coagulation/sedimentation (C/S) and photo-Fenton stages were carried out in the same tank, which was coupled to an innovative artificial photoreactor (4 FluHelik connected in series, each one using a 4.2 kW UV-Vis lamp). The FluHelik configuration, providing an helical movement of the fluid around the radiation source, generates (i) high velocities through the reactor but lower velocities near the lamp, (ii) high turbulence intensity, thus a high degree of mixing, and (iii) uniform radiation fluence inside the reactor. When compared with previous studies, where similar UV-Vis lamps were merely located inside the treatment tank, to achieve the same DOC goal, the usage of FluHelik photoreactors required 2 times less radiation energy.

Major operational difficulties were found in the: (i) coagulation/sedimentation stage, due to the production of dense foam that trapped the sludge; and (ii) photo-Fenton stage, for iron precipitation. These problems were overcome, respectively, with: (i) sludge removal after nitrite oxidation with hydrogen peroxide (intermediate step prior to PF); and (ii) maintenance of a residual amount of $H_2O_2$ before the neutralization step. Despite the efforts, achieving legal compliance with limits for direct discharge into waterbodies was not accomplished for all parameters. The balance between COD and TN removal, as well as sulfate content, revealed a challenge during operation and is a key element for the success of this strategy. TN removal in BR1 is advantageous for hydrogen peroxide saving during PF, however, it must be ensured that alkalinity is lower than 1.0 g $CaCO_3$/L so that the sulfate ion discharge limit is not exceeded. Promoting greater dilution and better alkalinity

control, BR1 could have benefited from operating with a lower volume exchange ratio. Moreover, some factors influenced the treatment efficiency, namely: (i) intense variations of the influent leachate; (ii) impossibility to operate the aerated lagoon upstream; (iii) occurrence of operational/technical problems that were not observed at pilot-scale; and (iv) difficulties to anticipate operational adjustments required as the treatment proceeded. Nevertheless, when consecutive treatment trials were performed under regular conditions, the overall efficiency of the system tended to increase. The sludge produced was also treated *in-situ* and compliance with legal disposal standards was achieved. The average total operational cost for the complete treatment sequence was 6.7 €/m$^3$, which included chemicals, energy consumption, sludge treatment and respective disposal.

Solar collectors' high investment cost, land area requirements, and loss of the photo-treatment efficiency over time (due to the soiled of the reflective surface) are some drawbacks that are blocking its use as light capture system to promote a photo-Fenton process at industrial scale. Therefore, aiming the application of the photo-Fenton process for the treatment of wastewaters with low transmissibility, e.g. sanitary landfill leachates, in a scale-up and cost saving perspective, solar collectors with different reflector materials (anodized aluminium with (MS) and without (R85) protective coating, soiled aluminium (R85s) and stainless steel (SS)) and geometries (flat (F), simple double parabola (SP) and traditional double parabola (DP)) were tested and their efficiency assessed.

Actinometric tests were carried out, as a simple and accurate method, to measure the total light dose reaching the photoreactors, which served as a performance indicator to compare the various photochemical reactors. In this sense, ferrioxalate actinometry was performed, at lab-scale under simulated sunlight, and the optical concentration ratio (CR$_O$) followed the sequence: SS-F (0.59) ≈ R85-F (0.60) < R85s-DP (0.67) ≈ SS-SP (0.70) ≈ SS-DP (0.72) < MS-DP (0.84) < R85-DP (0.93). These results agree with the ray-trace and specular reflectance analysis. In respect to the reflectors optical efficiency it was possible to conclude: (i) the major influence of the reflector geometry and specular reflectance of the materials; (ii) the impact of 8-years of outdoor exposure of the R85 anodized aluminium (loss of 38.7% of specular reflectance and a decrease of 26% in the optical efficiency); (iii) for flat geometry the difference in the material reflectance has a negligible influence on the optical efficiency; (iv) the inclusion of a simple reflective surface, such as SS-F, increases the optical efficiency up to 17% when compared to the absence of reflector.

The photo-Fenton system applied to an urban leachate showed that the process efficiency over time was mostly coherent with the optical efficiency of the different reflective surfaces. For the photo-

Fenton lab-trials using a pre-treated urban mature leachate (after biological and coagulation/sedimentation stages), the time required to achieve 60% mineralization decreased as follows: SS-F (158') > R85-F and R85s-DP (153') > SS-SP (141') > SS-DP (127') > R85-DP (121') > MS-DP (117'). Beyond that, at pilot-scale under natural sunlight, the SS-SP reflector presented a better performance, mainly due to the higher number of absorber tubes, i.e. higher illuminated volume. The SP geometry enables an increase of 30% of absorber tubes for approximately the same area as a collector using the DP traditional reflector, and further enhances the thermally induced reactions by a higher temperature increment.

According to the cost analysis, for the same investment required to build 100 m$^2$ of a conventional R85-DP collector, it is possible to construct 126 m$^2$ of an SS-F collector, containing 1.6 times more absorber tubes per square meter, which leads to a treatment rate increment of 51%. Considering that higher illuminated surface to volume ratios reduce the reactor dimensions and thereby, capital and operating costs, the flat geometry reflectors using a resistant material, such as the stainless steel, may be a cost-saving and effective solution in the treatment of wastewater with low transmissibility and presenting UV inner-filter effects, such as leachates, by the photo-Fenton process.

### 10.1.2 Treatment train using ozone-driven processes as an alternative to photo-Fenton oxidation

The application of ozone-driven processes for the treatment of mature landfill leachate started by testing different ozonation system setups, using a pre-treated leachate (after biological and coagulation/sedimentation stages). As a first approach, ozonation (O$_3$-only) was applied, using a porous ceramic diffuser combined with a bubble column (BC), and the best operational conditions were established for leachate treatment (initial pH = 9.0; inlet ozone dose = 18 mg O$_3$/min). Then, the FluHelik photoreactor was coupled in series with the bubble column, using a ceramic diffuser or a Venturi to inject ozone into the fluid stream. The FluHelik/BC-Venturi setup led to the highest efficiency, treating 50% more leachate than BC-alone using the same ozone dose and reaction time (3h). The helical motion of the fluid around the light source, promoting an intense radial mixing, may contribute for improving ozone dissolution and the contact between ozone molecules and UVC photons. The FluHelik/BC-Venturi was clearly the configuration that enhanced the ozone mass transfer from the gas phase to the liquid phase, resulting in lower amounts of O$_3$ in the off-gas, allowing for operational costs reduction of 41% when compared to the BC-alone.

Following, the oxidation ability of ozone combined with $H_2O_2$ and/or UVC for leachate treatment was assessed. The $O_3$/UVC oxidation process was the best among the ozone-based AOPs tested, leading to the highest synergistic effect (86% and 43%, for DOC and COD removals, respectively) and biodegradability enhancement (91%). Beyond that, the biodegradability tests have also emphasized that different oxidation mechanisms were involved, which were supported by UV-Vis spectra analysis (e.g. $SUVA_{254}$ and $Abs_{250}/Abs_{365}$ factors) and MOS. In this case, the addition of $H_2O_2$ was not beneficial in terms of biodegradability enhancement (especially for $O_3/H_2O_2$). To deal with this type of effluent, using a FluHelik/BC-Venturi system, the $O_3$/UVC oxidation process stands out as the most efficient and cost-effective (6.0 €/m³), ensuring an effluent that meets the discharge legal limit for COD (150 mg/L) after further biological oxidation.

Ultimately, to establish treatment train strategies potentially capable to originate an effluent that complies with both organic and nitrogen legal limits for discharge, the performance of $O_3$ and $O_3$/UVC processes applied to landfill leachate after different pre-treatments was investigated. In the absence of a coagulation stage, both bio-treated leachates (LN and LD) required an ozone dose ($OD_T$) of 7.1 g $O_3$/L combined with 59.5 kJ/L of accumulated UVC radiation energy, to obtain a biodegradable effluent. For bio-nitrified leachate (LN), mineralization was hindered since high amounts of ozone were consumed to oxidize nitrites to nitrates. In turn, the presence of carbonate/bicarbonate ions (alkalinity) in the bio-denitrified leachate (LD) inhibited the reaction due to the scavenging effect of •OH. For both bio-treated leachates, the $O_3$/UVC process led to a better performance than $O_3$, reaching a final COD of 205 and 167 mg/L, for LN and LD, respectively, after subsequent biological oxidation. Moreover, the estimated treatment cost for a treatment train combining Bio + $O_3$/UVC + Bio is not viable (> 30 €/m³). So, the inclusion of a chemical coagulation process before the ozone-driven stage shows to be essential for the economic feasibility of the treatment train.

For the nitrified-coagulated leachate (LNC) and denitrified-coagulated leachate (LDC), although the differences on DOM composition revealed by fluorescence excitation-emission matrix, the amount of DOC and COD removed per gram of ozone was very similar. To reach COD < 150 mg/L (legal discharge limit) after a final biological process, the $O_3$ treatment applied to the LNC was the most cost-effective (5.7 €/m³). Nonetheless, a treatment train comprising: (i) a first biological stage for nitrification/denitrification (with addition of an external carbon source); (ii) coagulation with 300 mg $Al^{3+}$/L and without pH adjustment; (iii) $O_3$/UVC advanced oxidation process, with transferred ozone dose of 2.1 g $O_3$/L and 12.2 $kJ_{UVC}$/L; and (iv) a final biological oxidation, allows to reach a final effluent able to simultaneously comply with the legal values for organic and nitrogen

parameters, and not exceeding the discharge limits for other parameters affected by the addition of chemicals along the treatment train. Also, the treatment cost of this strategy was estimated as 8.9 €/m$^3$, with the ozone-driven stage counting for 6.9 €/m$^3$.

## 10.2  Suggestions for future work

Some proposals for upcoming work regarding biological, coagulation and advanced oxidation processes applied to landfill leachates are presented below.

### 10.2.1 Biological nitrogen removal

Using the sequencing batch reactor (SBR) technology, the application of aerobic granular sludge (AGS) for simultaneous removal of organic carbon, nitrogen, phosphorus, and other contaminants, can be an interesting choice to explore. The AGS-SBR process advantages rely on the smaller land footprint (50-75%) and lower costs (20-25%) when compared to conventional activated sludge. The granular sludge presents distinct features from activated sludge in terms of compactness, particle size, settling velocities, extracellular polymeric substances (EPS) matrix and microbial community structure. Granules' layered structure, with aerobic outer layer and anaerobic/anoxic core enables the presence of diverse microbial populations, without need for supports. Besides, its strong and compact arrangement provides higher tolerance to toxic pollutants and the ability to withstand large load fluctuations, possibly with higher volume exchange ratios than those obtained in this work. This form of sludge promotes a better gravity-based separation of biomass from the bio-treated wastewater and other advantages such as, low requirements of external carbon sources for denitrification, high 'hard' COD elimination and nitrification/denitrification rates, lower residual alkalinity and low surplus sludge.

Nonetheless, AGS related research has been focused on carbon-nitrogen-phosphorus removal mainly from sanitary sewage, and literature is lacking for information regarding simultaneous nitrogen-carbon-sulphur removal or leachate treatment. So, there is a need to explore the potentials of AGS-SBR applied to leachate treatment, contributing to increase the technical-scientific knowledge, keeping in view nitrogen removal and further cost reductions of the biological treatment stage.

## 10.2.2 Coagulation

Electro-coagulation is a simple process in terms of equipment setup (compact treatment facility) and easy-to-handle with possible complete automation, high efficiency with less sludge production. The production of the coagulation agent is managed *in situ* by means of electro-oxidation of a sacrificial anode. In this case, there is no need for adding chemical coagulants or flocculants to perform the treatment. The mechanism of electrocoagulation process depends on the chemistry of the aqueous medium, especially the conductivity which makes landfill leachate a suitable candidate for a successful application of this treatment technique.

## 10.2.3 Ozone-driven processes

Ozone-driven processes showed to be well suited for the oxidation of landfill leachate, with high effectiveness in colour removal, affinity towards humic substances, and with great ability to enhance the effluent biodegradability. So, further ways to overcome the limitations presented by these processes, and already recognized in this work, should be explore by testing other reactional configurations. The incorporation of an inverted cone, or Speece cone (a very efficient oxygen contactor), as a down-flow gas-liquid contactor to enhance ozone mass transfer with efficiencies ~ 100%, resulting in a highly compact reaction vessel, can be an interesting choice to investigate. This system consists of a conical downflow contact vessel with a venturi injector located upstream of the cone's top, where ozone is fed. It is expected that the leachate-ozone mixture will enter at relatively high velocity, forcing $O_3$ bubbles downward and, as the cone cross-section area widens the leachate velocity decreases, until it becomes lower than the ozone-bubbles buoyancy velocity. This prevents $O_3$-bubbles from leaving at the cone's bottom, leading to a bubble-free $O_3$ enriched leachate stream.

Moreover, in view of cost-savings and environmental sustainability, there is an opportunity to make use of the off-gas released by the conventional bubble column reactor and recover (i) ozone, to be injected into a following contactor or, (ii) oxygen to re-feed the ozone generator or reused in the biological oxidation system.

### 10.2.4 Other process of interest

The electromagnetic radiation having wavelengths from 1 to 1000 mm (frequencies between 300 MHz and 300 GHz), known as microwave irradiation, is generally used for heating purposes in domestic use for cooking. In recent years, microwave technology has emerged in wastewater and leachate treatment due to its rapid and selective heating properties, better mineralization/degradation/solubilization effect on organic carbon and volatilization of ammonia nitrogen. Microwave can heat the substances rapidly, accelerate reaction rate, provide instant on/off control and higher energy efficiency owing to its selective heating (by interaction at molecular level) and non-thermal effect on pollutants (e.g. leading to the breakdown of hydrogen bonds). This type of irradiation can also activate a wide variety of photocatalysts (by formation of hotspots in the medium as a result of uneven heating) and can be used to generate UV irradiation from electrode-less discharge lamps (EDLs). The main drawback of microwave system is the high energy consumption (and consequent costs), however this could be rectified by incorporating solar powered microwave system. Moreover, it is suggested to test microwave combined with oxidants (such as persulfate and hydrogen peroxide), as free radicals are rapidly generated under this type of irradiation. The application of microwave technology is trifling due to lack of understanding in the coupling with other systems, reactor design and cost/economic analysis.